



Universitat Autònoma de Barcelona

**ADVERTIMENT.** L'accés als continguts d'aquesta tesi doctoral i la seva utilització ha de respectar els drets de la persona autora. Pot ser utilitzada per a consulta o estudi personal, així com en activitats o materials d'investigació i docència en els termes establerts a l'art. 32 del Text Refós de la Llei de Propietat Intel·lectual (RDL 1/1996). Per altres utilitzacions es requereix l'autorització prèvia i expressa de la persona autora. En qualsevol cas, en la utilització dels seus continguts caldrà indicar de forma clara el nom i cognoms de la persona autora i el títol de la tesi doctoral. No s'autoritza la seva reproducció o altres formes d'explotació efectuades amb finalitats de lucre ni la seva comunicació pública des d'un lloc aliè al servei TDX. Tampoc s'autoritza la presentació del seu contingut en una finestra o marc aliè a TDX (framing). Aquesta reserva de drets afecta tant als continguts de la tesi com als seus resums i índexs.

**ADVERTENCIA.** El acceso a los contenidos de esta tesis doctoral y su utilización debe respetar los derechos de la persona autora. Puede ser utilizada para consulta o estudio personal, así como en actividades o materiales de investigación y docencia en los términos establecidos en el art. 32 del Texto Refundido de la Ley de Propiedad Intelectual (RDL 1/1996). Para otros usos se requiere la autorización previa y expresa de la persona autora. En cualquier caso, en la utilización de sus contenidos se deberá indicar de forma clara el nombre y apellidos de la persona autora y el título de la tesis doctoral. No se autoriza su reproducción u otras formas de explotación efectuadas con fines lucrativos ni su comunicación pública desde un sitio ajeno al servicio TDR. Tampoco se autoriza la presentación de su contenido en una ventana o marco ajeno a TDR (framing). Esta reserva de derechos afecta tanto al contenido de la tesis como a sus resúmenes e índices.

**WARNING.** The access to the contents of this doctoral thesis and its use must respect the rights of the author. It can be used for reference or private study, as well as research and learning activities or materials in the terms established by the 32nd article of the Spanish Consolidated Copyright Act (RDL 1/1996). Express and previous authorization of the author is required for any other uses. In any case, when using its content, full name of the author and title of the thesis must be clearly indicated. Reproduction or other forms of for profit use or public communication from outside TDX service is not allowed. Presentation of its content in a window or frame external to TDX (framing) is not authorized either. These rights affect both the content of the thesis and its abstracts and indexes.



Doctoral Thesis

**A VISUAL PATHWAY STRUCTURE-FUNCTION  
RELATIONSHIP IN CENTRAL NERVOUS  
SYSTEM CONDITIONS MEDIATED BY  
ANTIBODIES (AQP4-IgG AND MOG-IgG)**

PhD in Medicine  
Department of Medicine

Adriana Roca Fernández

**Supervisors**

Dr Jaume Sastre Garriga  
Dr Matthew Craner

**Tutor**

Dr Albert Selva O'Callaghan

2022

*"Well, maybe it started that way, as a dream, but doesn't everything? Those buildings. These lights. This whole city. Somebody had to dream about it first. And maybe that is what I did. I dreamed about coming here, but then I did it."*

**Roald Dahl. *James and the Giant Peach***

To Dr Dan Lunn

# Acknowledgements

First and foremost, I would like to thank my supervisors Dr Jaume Sastre-Garriga and Dr Matthew Craner for this opportunity and for their guidance and mentorship in the production of this work and to my tutor, Professor Albert Selva O'Callaghan.

This thesis would not have been possible without the generous academic and financial support of Professor Jacqueline Palace who has allowed me to work with her patients, in her department at the University of Oxford, and has provided me with the logistic structure and endless advice to do this thesis.

I thank all the patients and all the staff who were involved in this research. In particular, to all the staff in the Neuromyelitis Optica Service (Professor Isabel Leite, Dr Giordani Passos, Rosie Everett) for their help with patient recruitment and project development, the Multiple Sclerosis Clinical Trials team (Chris Abarno, Ana Cavey, Helen Birmingham, Luisa Saldaña, Sadia Ahmed, Justin McKee and Joy Hodder) for helping me on the daily basis with my projects, with a special thanks to Alex Rubio, for being my friend and for all the fun in the endless days. The Eye clinic staff for their OCT support, and Pharmacology (Dr Ron Yeo and Dr Fay Probert) for their help with statistical modelling.

Big thanks to my PhD friends for all the shared breakfasts, lunches, dinners, parties, trips, laughs (and cries) and support: Ped, Silvia, Romina, Valentina, George, Maciej and specially to Martim, Tiago and Ricardo, for their endless proofreading and support in the final sprint of this thesis.

Thank you to Banjo, Matt, Helena and Andrea for their care, advice and patience, and all PD friends who coped with me while I was finishing this thesis.

Thank you to my friends Ana and Judith, for understanding all my moods, feeling this thesis as if it were theirs, giving me strength, and being always there for me. To Marzia, for being the best housemate and friend, and for providing the right life advice, always. To all my friends in Oxford, specially to Ludo; to Nick and Antonio; to Luismi and Ana; to Manolo, Celia and Andrea; to Amelia, Estefania, Toby, Lucas and Marcus; to Alberto del Carrizo for the huge support, to Javi and to my friends in Becerreá, for loving me regardless.

Finally, the most important acknowledgement is with no doubt to my parents and Abuela, for giving me the most unconditional love and support and for being responsible for the person that I am today. Gracias, os quiero.

# Abbreviations

**3D:** 3 dimensional

**ADEM:** Acute disseminated encephalomyelitis

**AQP4:** Aquaporin-4

**AQP4-NMOSD:** Neuromyelitis optica spectrum disorder aquaporin-4 seropositive

**AQP4-NMOSD-NON:** Eyes never affected by optic neuritis in neuromyelitis optica spectrum disorder Aquaporin-4 seropositive patients. Here we include (1) non-affected eyes whose contralateral eyes were previously affected by ON and (2) eyes from patients with no previous history of ON (both eyes never affected by previous ON). The latter will also be referred separately as “never affected” eyes (i.e., eyes from patients with no previous history of ON).

**AQP4-NMOSD-ON:** Eyes affected by optic neuritis in neuromyelitis optica spectrum disorder aquaporin-4 seropositive patients.

**BBB:** Blood brain barrier

**BrM:** Bruch’s membrane

**CBA:** Cell based assays

**CFT:** Central foveal thickness

**ChC:** Choriocapillaris

**CNS:** Central nervous system

**CRION:** Chronic relapsing inflammatory optic neuropathy

**CSF:** Cerebrospinal fluid

**CSF WCC:** White cell count in cerebrospinal fluid

**DRCP:** Deep retinal capillary plexus

**EAE:** Experimental autoimmune encephalomyelitis

**ELISA:** Enzyme-linked immunosorbent assay

**ELM:** External limiting membrane

**ETDRS:** retro-illuminated early treatment for diabetic retinopathy study charts

**FA:** Fractional anisotropy

**FAZ:** Foveal avascular zone

**FDA:** Food and Drug Administration

**FT:** Foveal thickness

**GCIP:** Combined ganglionar and inner plexiform layer

**GCL:** Ganglionar cell layer

**Gd:** Gadolinium

**GER:** Germany

**HC:** Healthy control

**HCVA:** High contrast visual acuity

**IFN-beta:** Interferon-beta

**IgG:** Immunoglobulin G

**IgM:** Immunoglobulin M

**ILM:** Inner limiting membrane

**INL:** Inner nuclear layer

**IPL:** Inner plexiform layer

**IVMP:** Intravenous methylprednisolone

**KO:** Knocked out

**LCVA:** Low contrast visual acuity

**LETM:** Longitudinally extensive transverse myelitis

**LGN:** Lateral geniculate nucleus (in the thalamus)

**MME:** Microcystic macular oedema

**MOG:** Myelin oligodendrocyte glycoprotein

**MOG-EM:** Myelin oligodendrocyte glycoprotein-IgG-associated encephalomyelitis (used only once, to paraphrase Jarius et al 2018)

**MOGAD:** Myelin oligodendrocyte glycoprotein antibody-associated disease

**MOGAD-NON:** Eyes never affected by optic neuritis in myelin oligodendrocyte glycoprotein antibody-associated disease seropositive patients. Here we include (1) non-affected eyes whose contralateral eyes were previously affected by ON and (2) eyes from patients with no previous history of ON (both eyes never affected by previous ON). The latter will also be referred separately as “never affected” eyes (i.e., eyes from patients with no previous history of ON).

**MOGAD-ON:** Eyes affected by optic neuritis in myelin oligodendrocyte glycoprotein antibody-associated disease seropositive patients.

**MRI:** Magnetic resonance imaging

**mRNFL:** Macular retinal nerve fibre layer

**MRZ reaction:** Measles rubella zoster reaction

**MS:** Multiple sclerosis

**ms:** Milliseconds

**MS-ON:** Eyes affected by optic neuritis in multiple sclerosis patients.

**NMOSD:** Neuromyelitis optica spectrum disorder (\* which in the experimental projects refers to seropositive patients only)

**OCT:** Optic coherence tomography

**OCT-A:** OCT angiography

**ON:** Optic neuritis

**ONL:** Outer nuclear layer

**OPL:** Outer plexiform layer

**OR:** Optic radiations

**PEV:** Potenciales evocados visuales

**PLEX:** Plasma exchange

**PMB:** Perimacular bundle

**PML:** Progressive multifocal leukoencephalopathy

**PPMS:** Primary progressive multiple sclerosis

**PRES:** Posterior reversible encephalopathy syndrome

**pRNFL:** Peripapillar retinal nerve fibre layer

**PRVEP:** Pattern reversal visual evoked potentials

**RCG:** Retinal ganglion cell

**RPE:** Retinal pigmented epithelium

**SD-OCT:** Spectral domain optic coherence tomography

**SPMS:** Secondary progressive multiple sclerosis

**SRCP:** Superficial retinal capillary plexus

**TD-OCT:** Time domain optic coherence tomography

**TM:** Transverse myelitis

**TMV:** Total macular volume

**UK:** United Kingdom

**VEP:** Visual evoked potentials

**WRCP:** Whole retinal capillary plexus

**µm:** Micrometres



# List of Tables

## 1. INTRODUCTION:

Table 1-1: AQP4-NMOSD diagnostic criteria.....	57
Table 1-2: International recommendations for the diagnosis of MOGAD .....	71
Table 1-3: Simplified diagnostic criteria for the diagnosis of MOGAD .....	72

## 5. METHODOLOGY:

Table 5-1: Cohorts used in this thesis' projects.....	82
---	----

## 6. RESULTS:

### Project 1:

Table 6-1: Cohort overview.....	105
Table 6-2: Baseline OCT measures.....	107
Table 6-3: Baseline OCT measures. Differences between disease groups and healthy controls.....	114
Table 6-4: Longitudinal changes in OCT parameters for the different eye categories .....	119

### Project 2:

Table 6-5: NMO tissue bank cohort overview .....	128
Table 6-6: Baseline measures of eyes with AQP4-NMOSD and MOGAD patients. 130	
Table 6-7: Baseline measures of eyes with AQP4-NMOSD and MOGAD patients. Differences between disease groups and healthy controls .....	131
Table 6-8: Macular sub-study cohort overview .....	133
Table 6-9: Structural tests in normal central visual function eyes in the research cohort.....	135
Table 6-10: Baseline OCT measures of the advanced research cohort.....	136
Table 6-11: Baseline OCT measures of the advanced research cohort in patients with normal HCVA.....	139

### Project 3:

Table 6-12: Cohort overview.....	148
Table 6-13: Baseline OCT measures for the retinal layers.....	148
Table 6-14: Baseline foveal parameters derived from the Cubic Bezier algorithm..	150

Table 6-15: Baseline OCT differences between disease group and healthy controls .....	150
Table 6-16: Baseline foveal shape parameters differences between disease group and healthy controls .....	154
Table 6-17: Annualized retinal layer changes in NON eyes .....	162
Table 6-18: Annualized foveal changes in NON eyes .....	163
Table 6-19: Assessment of baseline to follow-up changes in retinal layers .....	164
Table 6-20: Assessment of baseline to follow-up changes in foveal parameters ....	165
Table 6-21: Structural impairment in AQP4-NMOSD and MOGAD .....	170

# List of Figures

## 1. INTRODUCTION

Figure 1-1: Schematic view of the primary visual pathways .....	25
Figure 1-2 Schematic representation of the Eye.....	26
Figure 1-3: Representation of retinal layers in the human eye .....	27
Figure 1-4: Scheme of the retina on funduscopy .....	30
Figure 1-5: Macular OCT scan with a schematic representation of the fovea .....	32
Figure 1-6: Blood supply to the eye .....	33
Figure 1-7: The structure of the optic nerve.....	34
Figure 1-8: Schematic representation of the optic chiasm, fibre decussation and optic tracts .....	35
Figure 1-9: Scan types with Optical Coherence Tomography (OCT) .....	37
Figure 1-10: Light wave .....	38
Figure 1-11: Light waves in TD-OCT, SD-OCT and SS-OCT.....	38
Figure 1-12: Fast-Fourier transformation.....	40
Figure 1-13: Scheme of spectral-domain OCT mechanism.....	41
Figure 1-14: Schematic representation of the Cube model .....	43
Figure 1-15: Eugène Devic and Fernand Gault's doctoral thesis " <i>De la neuromyéélite optique aiguë</i> ".....	45
Figure 1-16: Pathophysiology of AQP4-NMOSD .....	47
Figure 1-17: Orbital MRI of an AQP4-NMOSD patient .....	50
Figure 1-18: Representation of an OCT scan from an AQP4-NMOSD patient.....	51
Figure 1-19: Spinal cord lesion of a patient with AQP4-NMOSD after an LETM.....	54
Figure 1-20 Brainstem lesion in a patient with AQP4-NMOSD.....	55
Figure 1-21: Pathophysiology of MOGAD.....	61
Figure 1-22: MRI of a patient with MOGAD .....	64
Figure 1-23: Example of cord involvement in a MOGAD patient.....	67
Figure 1-24: Example of brain lesions in a patient with MOGAD.....	69

## 5. METHODOLOGY:

Figure 5-1: Cohort Flowchart for project 1 .....	89
--	----

Figure 5-2: Cohort flowchart for project 2: NMO tissue bank.....	94
Figure 5-3: Cohort flowchart for project 2: Macular sub-study .....	95
Figure 5-4: Cohort flowchart for project 3: Study cohort and follow-up.....	100
Figure 5-5: The CuBe model.....	101
Figure 5-6: Orthogonal partial least squares analysis pipeline .....	103

## 6. RESULTS:

### Project 1:

Figure 6-1: QQ-plots of the dependent variables assessed before building the linear mixed effect model.....	109
Figure 6-2: QQ-plots of the dependent variables assessed after the transformations to normalize the data, used to build the final linear mixed effect model .....	111
Figure 6-3: Box plots of disc and macular baseline OCT values with overlaid LME results .....	116
Figure 6-4: Longitudinal LME predicted model graphs .....	120
Figure 6-5: Actual Vs predictive models .....	123
Figure 6-6: Residual plots of the longitudinal models .....	125

### Project 2:

Figure 6-7: Structural tests in normal central visual function eyes in the NMO tissue bank database cohort .....	129
Figure 6-8: Boxplots of pRNFL distributions between groups.....	132
Figure 6-9: Box plots of disc and macular baseline OCT and fovea in eyes with normal HCVA.....	141
Figure 6-10: Box plots of disc and macular baseline OCT and fovea for eyes with good HCVA divided by normal and abnormal VEP.....	144

### Project 3:

Figure 6-11: Box plots of disc and macular baseline OCT and foveal data .....	155
Figure 6-12: Foveal changes in NMOSD. OCT examples .....	157
Figure 6-13: Foveal changes in AQP4-NMOSD. Schematic model.....	158
Figure 6-14: OPLS-DA results .....	161
Figure 6-15: Significant longitudinal LME model graphs.....	167

## 9.FUTURE DIRECTIONS:

Figure 9-1: Anatomical scheme of the visual pathway.....	183
--	-----

Figure 9-2: Anatomical depiction of retrograde and anterograde transsynaptic degeneration in the visual pathway..... 184

# Table of contents

<b>ABSTRACT .....</b>	<b>18</b>
<b>RESUMEN .....</b>	<b>20</b>
<b>1. INTRODUCTION .....</b>	<b>22</b>
1.1. The retina and the optic nerve: a window into CNS antibody mediated disorders .....	23
1.2. The visual system .....	24
1.2.1. The retina.....	26
1.2.1.1. The macula: a trip from the outer to the inner layers.....	27
1.2.1.2. The fovea.....	31
1.2.1.3. Vascular structure of the macula .....	32
1.2.2. The optic nerve.....	34
1.2.3. The optic chiasm and optic tract.....	35
1.3. Assessment of the visual system.....	36
1.3.1. Basics of OCT .....	36
1.3.2. OCT modalities.....	37
1.3.3. The Cubic Bezier algorithm (CuBe).....	42
1.3.4. Visual evoked potentials (VEP).....	44
1.3.5. High contrast visual Acuity .....	44
1.4. AQP4-NMOSD.....	45
1.4.1. Pathophysiology .....	46
1.4.2. Epidemiology .....	48
1.4.3. AQP4 cell-based assay .....	48
1.4.4. Clinical and paraclinical findings .....	48
1.4.4.1. Visual System.....	49
1.4.4.1.1. Clinical manifestations derived from ON in AQP4-NMOSD .....	49
1.4.4.1.2. OCT findings .....	51

1.4.4.1.3. VEP findings.....	52
1.4.4.1.4. MRI findings .....	53
1.4.4.2. Spinal cord.....	54
1.4.4.3. Brainstem.....	55
1.4.5. Diagnostic criteria.....	56
1.4.6. Disease course.....	57
1.4.7. Treatment.....	58
1.5. MOGAD .....	60
1.5.1. Pathophysiology .....	60
1.5.2. Epidemiology.....	62
1.5.3. MOG cell-based assay .....	62
1.5.4. Clinical and paraclinical findings .....	63
1.5.4.1. Optic nerve .....	63
1.5.4.1.1. Clinical manifestations derived from ON in MOGAD.....	63
1.5.4.1.2. OCT findings .....	65
1.5.4.1.3. VEP findings.....	66
1.5.4.1.4. MRI findings .....	66
1.5.4.2. Spinal cord.....	67
1.5.4.3. Brain .....	68
1.5.4.3.1. The ADEM presentation.....	69
1.5.5. Diagnostic criteria.....	70
1.5.6. Disease Course.....	72
1.5.7. Treatment.....	73
1.6. Literature gaps .....	73
<b>2. RATIONALE OF THE THESIS .....</b>	<b>75</b>
<b>3. HYPOTHESIS .....</b>	<b>77</b>
<b>4. OBJECTIVES.....</b>	<b>79</b>
4.1. Main Objective .....	80
4.2. Secondary objectives.....	80

<b>5. METHODOLOGY .....</b>	<b>81</b>
5.1. Cohort descriptions .....	82
5.1.1. The NMO tissue bank [Projects 1, 2 and 3].....	83
5.1.2. The BABINSCI project [Projects 1,2 and 3].....	84
5.1.3. The NeuroCure-Charitè NMOSD cohort [Project 3]. .....	85
5.1.4. The VIMS study cohort [Project 3].....	86
5.2. Methodology by project: .....	87
5.2.1. PROJECT 1: <i>Structural retinal imaging in AQP4-NMOSD and MOGAD.</i> 87	
5.2.1.1. Study population .....	87
5.2.1.2. Optical Coherence Tomography .....	89
5.2.1.3. Statistical methods.....	90
5.2.2. PROJECT 2: <i>Structure-function relationship in the visual system of patients with AQP4- NMOSD and MOGAD disease</i> .....	93
5.2.2.1. Study population .....	93
5.2.2.1.1. NMO tissue bank study population .....	94
5.2.2.1.2. Macular sub-study population (BABINSCI cohort).....	95
5.2.2.2. Optical Coherence Tomography .....	96
5.2.2.3. Visual Evoked Potentials .....	97
5.2.2.4. High Contrast Visual Acuity (HCVA) assessment.....	97
5.2.2.5. Statistical methods.....	97
5.2.3. PROJECT 3: <i>Foveal changes in AQP4-NMOSD</i> .....	99
5.2.3.1. Study population .....	99
5.2.3.2. Optical Coherence Tomography .....	100
5.2.3.3. Fovea morphometry.....	101
5.2.3.4. Statistical methods.....	102
<b>6. RESULTS .....</b>	<b>104</b>
6.1. PROJECT 1: <i>Structural retinal imaging in AQP4-NMOSD and MOGAD</i> .....	105
6.1.1. Baseline results .....	106
6.1.2. Longitudinal results .....	116



6.2. PROJECT 2: <i>Structure-function relationship in the visual system of patients with AQP4- NMOSD and MOGAD disease</i> .....	126
6.2.1. The NMO tissue bank cohort.....	126
6.2.2. The macular sub-study cohort (BABINSCI cohort).....	133
6.2. PROJECT 3: <i>Foveal changes in AQP4-NMOSD</i> .....	146
6.2.1. Foveal changes .....	156
6.2.2. Discriminatory analysis.....	158
6.2.3. Longitudinal changes .....	162
6.3. Summary of the main structural findings: retinal impairment defined by OCT and foveal morphometry in AQP4-NOSD and MOGAD.....	168
<b>7. DISCUSSION .....</b>	<b>171</b>
<b>8. CONCLUSIONS .....</b>	<b>180</b>
<b>9. FUTURE DIRECTIONS .....</b>	<b>182</b>
<b>10. BIBLIOGRAPHY .....</b>	<b>186</b>
<b>11. APPENDIX .....</b>	<b>208</b>
11.1. Publications:.....	209
11.1.1. Publications directly related with this thesis:.....	209
11.1.1.1. Foveal changes in aquaporin-4 antibody seropositive neuromyelitis optica spectrum disorder are independent of optic neuritis and not overtly progressive .....	209
11.1.1.2. The use of OCT and VEPs in MOGAD and AQP4-NMOSD patients with normal visual acuity.....	224
11.1.2. Publications indirectly related with this thesis:.....	231
11.1.2.1. Clinical presentation and prognosis in MOG-antibody disease: A UK study	231
11.1.2.2. Retinal ganglion cell loss in neuromyelitis optica: A longitudinal study.	243

11.1.2.3. Quantitative spinal cord MRI in MOG-antibody disease, neuromyelitis optica and multiple sclerosis.....	251
11.1.2.4. Cohort profile: A collaborative multicentre study of retinal optical coherence tomography in 539 patients with neuromyelitis optica spectrum disorders (CROCTINO). .....	267
11.1.2.5. Contrasting the brain imaging features of MOG-antibody disease, with AQP4-antibody NMOSD and multiple sclerosis. ....	277
11.1.2.6. Retinal Optical Coherence Tomography in Neuromyelitis Optica...	289
11.1.2.7. Astrocytic outer retinal layer thinning is not a feature in AQP4-IgG seropositive neuromyelitis optica spectrum disorders. ....	303

# Abstract

Optic Neuritis (ON) is a common initial manifestation in Aquaporin-4 - Neuromyelitis Optica spectrum disease (AQP4-NMOSD) and Myelin oligodendrocyte glycoprotein (MOGAD), which are rare inflammatory antibody-mediated disorders of the central nervous system. Whether there is subclinical visual pathway damage and whether this accumulates overtime is unclear, especially in MOGAD. To address these questions, I have set up a cross-sectional study to interrogate two of the largest cohorts of AQP4-NMOSD and MOGAD in the world along with a matched healthy control population. Using optic coherence tomography (OCT), visual evoked potentials (VEP), detailed foveal morphometry and clinical outcomes I assessed the differential patterns of retinal damage in these two conditions. Longitudinal data was available in a subset of cases.

In AQP4-NMOSD, beyond the ON eye, I demonstrated that the retina was affected in fellow eyes and “never affected” eyes (from patients with no previous history of ON), this was characterised by total macular volume loss and significant thickening in inner nuclear layer (INL) respectively. To explore whether these observations could be attributed to subclinical inflammatory demyelinating events of the optic nerve, or to a foveal damage in AQP4-expressing Müller cells in the absence of clinically overt ON, microstructural changes in the retina of AQP4-NMOSD patients were assessed in detail with foveal morphometry analysis. I have shown that the parafoveal area is altered in AQP4-NMOSD patients who never experienced clinical inflammatory demyelinating events of the anterior visual pathway, while they are minor compared with those with ON events, these changes are likely to be independent from neuroaxonal damage related to subclinical inflammatory demyelinating events of the optic nerve, as macular and peripapillary layers appeared not to be affected in the subset of those without history of ON.

Recovery times after ON were studied in both AQP4-NMOSD and MOGAD; affected and fellow AQP4-NMOSD eyes showed a prolonged recovery after the acute phase in total macular volume (mean  $0.08\text{mm}^3$  and  $0.35\text{mm}^3$  per year respectively) while a significant decrease in foveal thickness (mean  $-0.06\ \mu\text{m}$  per year) was found in “never affected” eyes. In MOGAD macular volumes and foveal thickness were preserved

cross-sectionally and longitudinally in all eyes not affected by ON. Finally, I investigated subclinical visual pathway changes and pathophysiological mechanisms of retinal damage in AQP4-NMOSD and MOGAD patients with normal central visual function and its relation to visual function outcomes. I demonstrate that subclinical visual abnormalities (delayed VEP and inner retinal layers thinning) can occur without symptoms and although the relevance of the subclinical abnormalities is unknown, cumulative damage could well lead to clinical impairment, moreover, OCT has proved to have greater sensitivity than VEPs in detecting subclinical damage in MOGAD patients with normal visual function.

In conclusion, in this thesis I have shown different patterns of visual pathway involvement in AQP4-NMOSD and MOGAD and highlighted the importance of the use of OCT and foveal morphometry to determine subclinical retinal damage. This data may not only improve differential diagnosis and management but also contribute to the understanding of the underlying disease mechanisms and pathogenesis of these two disorders.

# Resumen

La neuritis óptica (ON) es una manifestación inicial común en el trastorno del espectro de la neuromielitis óptica (AQP4-NMOSD) y la enfermedad asociada a anticuerpos anti-MOG (MOGAD), que son enfermedades inflamatorias raras del sistema nervioso central mediadas por anticuerpos. A día de hoy, no está claro si estos pacientes presentan daño subclínico de la vía visual y si este se acumula con el tiempo, especialmente en MOGAD. Para abordar estas preguntas, esta tesis propone un estudio de línea base para interrogar a dos de las cohortes más grandes de AQP4-NMOSD y MOGAD disponibles, junto con una población de control sana emparejada, utilizando tomografía de coherencia óptica (OCT), potenciales evocados visuales (PEV), morfometría de la fóvea y pruebas clínicas para evaluar los patrones diferenciales de daño retiniano en estas dos enfermedades, con datos longitudinales para un subconjunto de casos.

En AQP4-NMOSD esta tesis demuestra, además del daño neuro axonal esperado en ojos con historia de ON, una afectación de los ojos contralaterales y de los ojos "nunca afectados" (de pacientes sin antecedentes de ON). Dicho daño se caracteriza por pérdida total del volumen macular y engrosamiento significativo en la capa nuclear interna (INL) respectivamente. Para explorar si estas observaciones podrían atribuirse a eventos desmielinizantes inflamatorios del nervio óptico o al daño a las células de Müller que expresan AQP4 en la fóvea en ausencia de una ON clínicamente evidente, se evaluaron en detalle los cambios microestructurales en la retina de pacientes con AQP4-NMOSD analizando la morfometría de la fóvea. Esta tesis demuestra que el área parafoveal está alterada en pacientes AQP4-NMOSD que nunca experimentaron eventos clínicos inflamatorios desmielinizantes de la vía visual anterior; siendo probable que estos cambios sean independientes del daño neuro axonal relacionado con eventos desmielinizantes inflamatorios del nervio óptico, ya que las capas macular y peripapilar parecen no estar afectadas en ojos sin historia de ON.

Los tiempos de recuperación post- ON se estudiaron tanto en AQP4-NMOSD como en MOGAD; Los ojos afectados (bilateral o unilateralmente) y sus contralaterales sanos en AQP4-NMOSD mostraron una recuperación prolongada después de la fase aguda en el volumen macular total (media de 0,08 mm<sup>3</sup> y 0,35 mm<sup>3</sup> por año, respectivamente) mientras que se encontró una disminución significativa en el grosor foveal (media -0,06 μm por año) en ojos de

pacientes sin previa historia de ON. En MOGAD, los volúmenes maculares y el grosor foveal se conservaron en línea base y longitudinalmente en todos los ojos no afectados por ON y no mostraron diferencias con aquellos de sujetos sanos. Finalmente, esta tesis investiga los cambios subclínicos de la vía visual en pacientes con AQP4-NMOSD y MOGAD con función visual central normal y su relación con los resultados de agudeza visual, demostrando que las anomalías visuales subclínicas (PEV retardado y pérdida de grosor de las capas internas de la retina) pueden ocurrir sin síntomas, y aunque se desconoce la relevancia de estas anomalías subclínicas, el daño acumulativo bien podría conducir al deterioro clínico. Además, esta tesis demuestra una mayor sensibilidad del OCT sobre los PEV en la detección de dicho daño subclínico en pacientes MOGAD con función visual normal.

En conclusión, en esta tesis he mostrado diferentes patrones de afectación de la vía visual en AQP4-NMOSD y MOGAD y resaltado la importancia del uso de la OCT y la morfometría de la fovea para determinar el daño retiniano asintomático. Estos datos pueden no solo mejorar el diagnóstico diferencial y el manejo de los pacientes, sino también contribuir a la comprensión de los mecanismos subyacentes de la enfermedad y la patogenia de estos dos trastornos.

# **1. INTRODUCTION**

## **1.1. The retina and the optic nerve: a window into CNS antibody mediated disorders**

Aquaporin-4 (AQP4) antibody-related Neuromyelitis Optica Spectrum Disorder (AQP4-NMOSD) and Myelin oligodendrocyte glycoprotein (MOG) antibody disease (MOGAD) are rare inflammatory antibody-mediated disorders of the central nervous system (CNS), which can mimic Multiple Sclerosis (MS). Unlike in MS, disability, and thus prognosis, in AQP4-NMOSD and MOGAD is thought to be exclusively a result of relapses and not from progression of neurological dysfunction independent of relapses (1,2).

Optic neuritis (ON) is a common initial manifestation of these three disorders. Access to reliable antibody tests (3,4) can help in determining the cause of ON; however the diagnosis can be challenging in some cases where the interpretation of clinical features is key to reach the diagnosis (5), and in consequence so the correct treatment/management is. The retina and optic nerve provide the clinician a window to the CNS through which paraclinical tests can reliably quantify changes in this structure providing useful biomarkers, not only for diagnosis but also treatment response and prognosis. It can also inform on disease mechanisms, as it can provide objective markers on neurodegeneration.

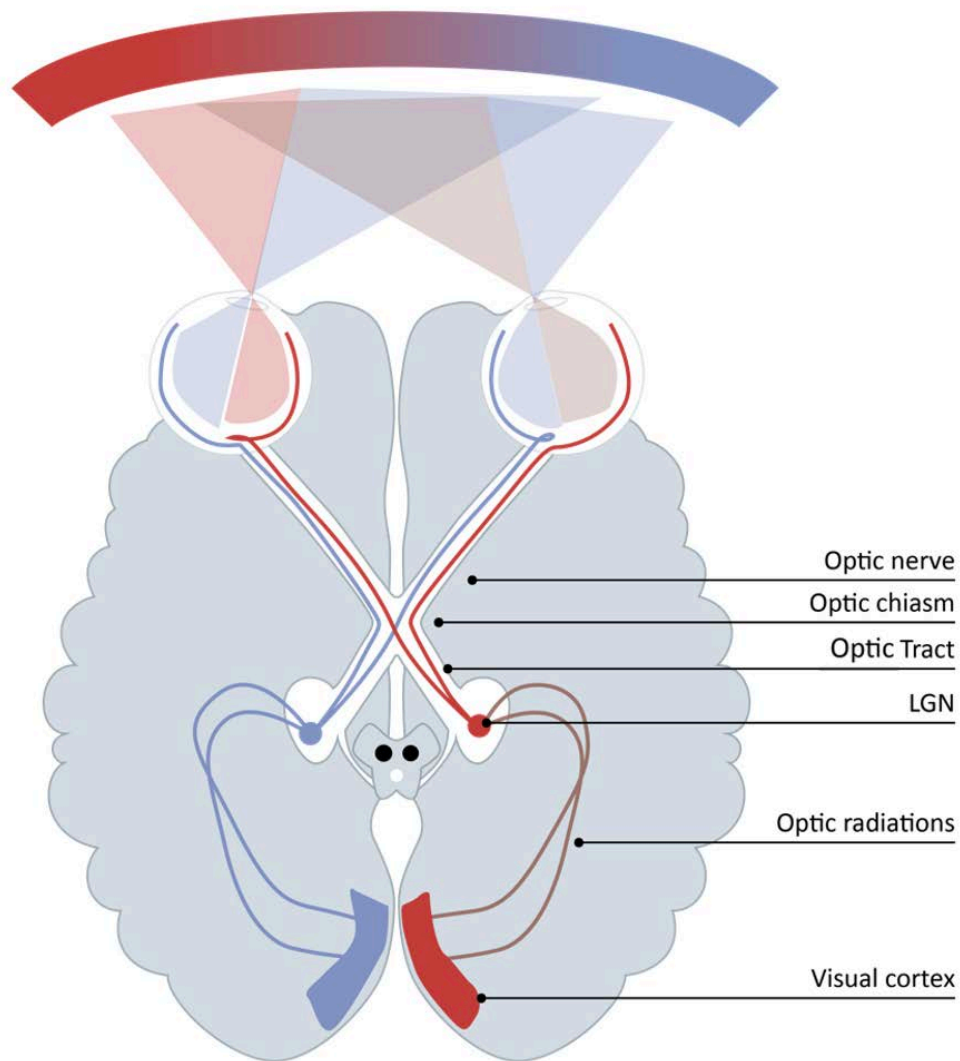
In this thesis introduction, I will review key aspects of the visual pathway neuroanatomy and advances in paraclinical tests used to assess its health and disease, focusing on the retina and ON. I will critically analyse the current literature on how AQP4-NMOSD and MOGAD can affect the visual system, highlighting some of the literature gaps, especially in MOGAD. This will serve as the background for the study of the visual pathways in one of the largest cohorts of AQP4-NMOSD and MOGAD in the world, presented in the following sections of this thesis.



## 1.2. The visual system

Vision is perhaps one of the most important of the perceptual senses. It helps us picture the surrounding environment and provides an essential context for the rest of the senses. The vision process starts in our eyes, where our retina converts information from visible light into a chemical signal.

The brain receives and processes the information arriving from the optic nerve and transmits this signal along the visual pathway, traveling along the optic nerves, chiasm, optic tracts, lateral geniculate nucleus (LGN) of the thalamus, superior colliculus, optic radiations, striate cortex, and extrastriate associative cortices (figure 1-1). Visual processing requires an enormous computational power in the brain, and takes over approximately 55% of the cortex in primates (6). A good understanding of the structure-function relationship in the visual system, combined with expert examinations, will allow a precise description of the pathological process in AQP4-NMOSD and MOGAD, and will be key for the clinical management of these diseases.




---

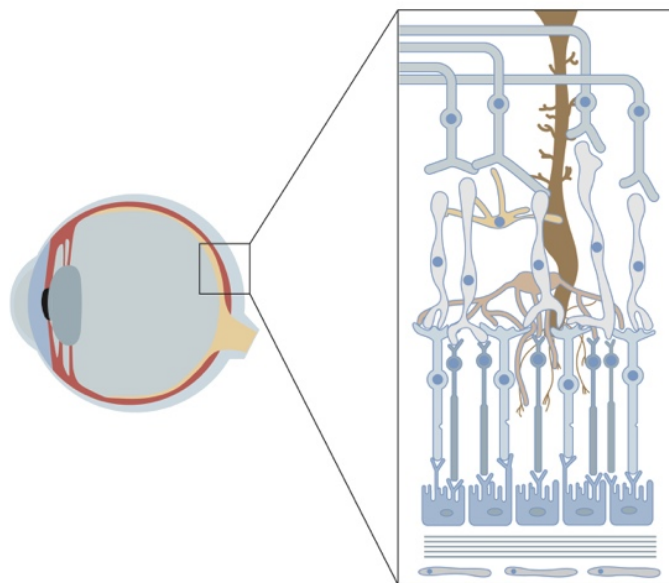
**Figure 1-1: Schematic view of the primary visual pathways**

Abbreviations: LGN, Lateral geniculate nucleus. Colours represent how the information from right and left visual fields is organised along the visual pathway (Original figure: Adobe Inc., 2019. Adobe Illustrator, Available at: <https://adobe.com/products/illustrator>)

---

## 1.2.1. The retina

The retina is a membrane that lines the inner surface of the eyeball. This sensory membrane is around 0.5 mm thick (7) , and it is composed by cells organized into layers that work cross-sectionally and in parallel for message encoding. The retina is divided between the central – also called “macula” – and the peripheral regions (figure 1-2). The landmark defining these two territories is the fovea, which is the eye’s maximum acuity point. This structure is considered the centre of the macula and extends across a circular area, spreading 6mm around its central point (7). Compared to the peripheral retina, the macula is particularly thick due to the high density of photoreceptors, particularly cones, and bipolar and ganglion cells. In this thesis, I will focus on the macular and foveal regions exclusively.



---

**Figure 1-2 Schematic representation of the Eye**

The square mark represents the macula, which is the central region of the retina.

(Original figure: Adobe Inc., 2019. Adobe Illustrator, Available at:

<https://adobe.com/products/illustrator>)

---

### 1.2.1.1. The macula: a trip from the outer to the inner layers

The cellular layers in the retina contain neurons, glial cells, vasculature and epithelial cells involved in the electrochemical process of vision. A scheme of the retinal cell organisation is provided in figure 1-3. Retinal layers are divided into two macrostructures: the inner and outer retina. The inner retina consists of all the layers between the internal limiting membrane and the external limiting membrane, and the outer retina contains the photoreceptor layers through to the choriocapillaris.

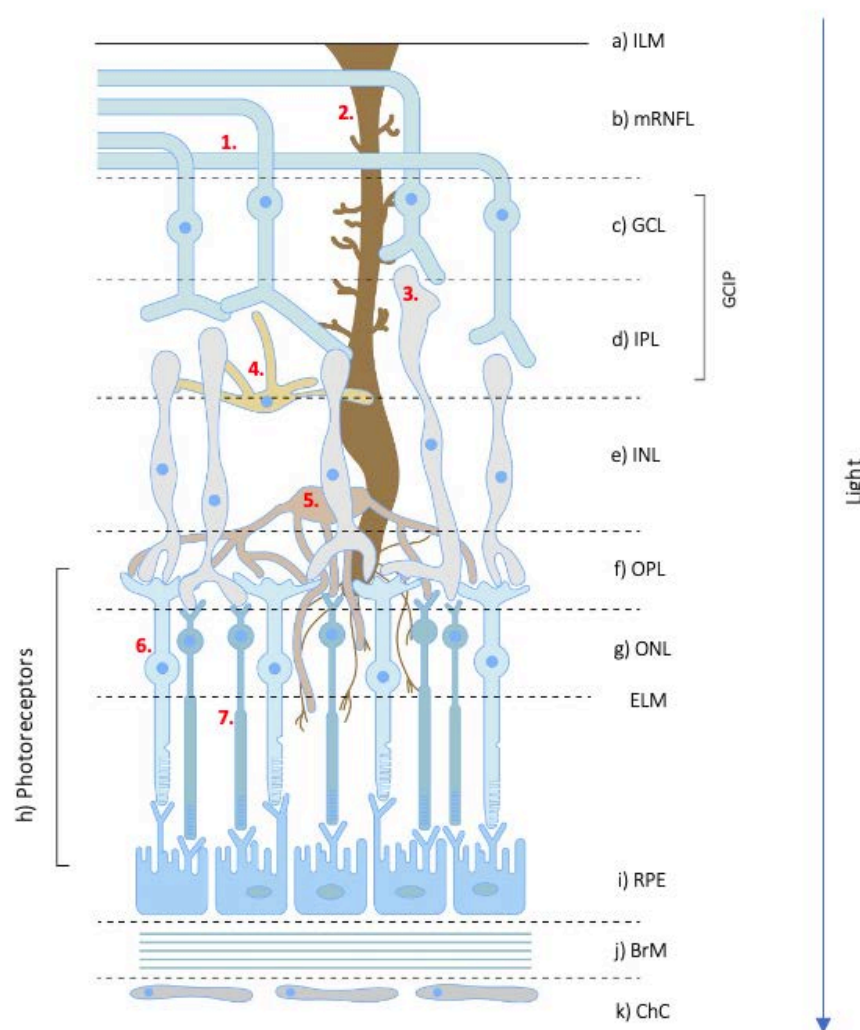


**Figure 1-3: Representation of retinal layers in the human eye**

Abbreviations: Retinal layers: a) Inner limiting membrane (ILM); b) Retinal nerve fibre layer (mRNFL); c) Ganglionar cell layer (GCL); d) Inner plexiform layer (IPL); Combined ganglionar and inner plexiform layer (GCIP); e) Inner nuclear layer (INL);

---

f) Outer plexiform layer (OPL); g) Outer nuclear layer (ONL); External limiting membrane (ELM); h) Retinal pigment epithelium (RPE); j) Bruch's membrane (BrM); k) choriocapillaris (ChC).

Retinal cells: 1. Ganglionar cells; 2. Müller cells; 3. Bipolar cells; 4. Amacrine Cells; 5. Horizontal cells; 6. Cones (photoreceptor); 7. Rods (photoreceptors).

(Original figure: Adobe Inc., 2019. Adobe Illustrator, Available at:

<https://adobe.com/products/illustrator>)

---

The eyeball is covered by **the sclera**; the function of this layer is to protect the eye and serve as an anchor point for the muscles controlling the eye movements.

Travelling from the outer to the inner structures, these layers are the following:

1. The **choriocapillaris (ChC)**, a layer of vasculature sitting in the sclera (figure 1-3, k), is responsible for nourishing the outer retinal layers and for discarding metabolic waste from the retinal pigment epithelium (8).
2. The **retinal pigment epithelium (RPE)** (figure 1-3, i) helps the photoreceptors (figure 1-3, cells numbered 6 and 7) to discard metabolic waste and contributes to giving support for pigment production (9).
3. **The Bruch's membrane (BrM)** (figure 1-3, j) is an elastic structure formed of five microlayers that is an integral part of the choroid. This structure is involved in the physiological process of transferring substances between the RPE cells, the vasculature and the inner retinal layers. It plays an important role in the mechanics of the eye, stretching in situations of intraocular pressure, accommodating changes in choroidal blood volume and acting like a spring that pulls the lens during the accommodation process (10,11).
4. **The photoreceptor layer** (figure 1-3, h) is formed by cones (figure 1-3, 6.) and rods (figure 1-3, 7.) which comprise an inner and an outer segment. While rods are involved in low-light vision, cones are responsible for colour vision during medium to bright-light conditions; there are 3 different subtypes of cones that are sensitive to different wavelengths (short (blue), middle (green), and long (red)). The inner segment of the photoreceptors is highly packed with mitochondria and is in charge of the metabolism and regulation of membrane potential. The outer segments contain disc membranes and receive the photons from the environment (12). These photons are absorbed by a protein called opsin, which changes its conformation from a resting state to a signalling state. This electrochemical process initiates to transmit the signal to the inner retina

starts (13–16). In low-light conditions, rods are continuously depolarized (transmitting signal). Instead, cones only start the depolarization process when their outer segment is excited by the photons.

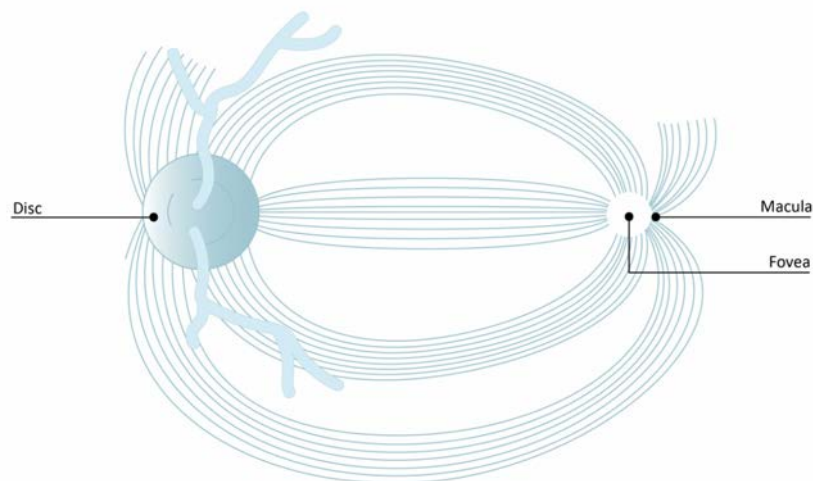
5. **The outer nuclear layer (ONL)** (figure 1-3, g) is where the cell bodies of the photoreceptors live.

6. **The outer plexiform layer (OPL)** (figure 1-3, f), comprises the axon terminals of photoreceptors synapsing with bipolar (figure 1-3, 3) and horizontal cells (figure 1-3, 5). There are different types of bipolar cells, depending on whether they connect with rods (1 type) or cones (around 12 types). Their main function is to do parallel transmission to start shaping stimulus properties, such as contrast, temporal profile and chromatic composition. They work as an assembly factory creating packages of information that then pass to the postsynaptic structures in a very good feature-oriented description of the visual environment (17). At the OPL level, bipolar cells are modulated by horizontal cells, which help them to integrate and regulate the input from multiple photoreceptors, increasing contrast via lateral inhibition and adapting to bright and low-light conditions, among other functions (18,19).

7. **The inner nuclear layer (INL)** (figure 1-3, e) is where the cellular bodies of bipolar and horizontal cells are located. This layer also contains amacrine cells (figure 1-3, 4.), involved in the regulation and integration of activity in bipolar and ganglion cells (19); and a particular subtype of glial cells called Müller cells (figure 1-3, 2.), these will be particularly important in the context of this thesis, as they play an important role in AQP4-NMOSD. Müller cells are in charge of regulating the extracellular space volume, the ion and water homeostasis, and of maintaining the integrity of the inner blood-retinal barrier. AQP4-water channels are accumulated in these cells and play a very important role in water and potassium homeostasis in the retina. Previous animal models have described neural hyperactivity and synaptic fatigue in AQP4 knock out mice before neurodegeneration becomes evident (20). AQP4 deficiency has been proven to disturb synaptic homeostasis and mitochondria metabolism, most likely through the dysregulation of potassium metabolism (21). These mechanisms are particularly relevant, as Müller glial dysfunction has been previously suggested to be present in AQP4-NMOSD patients (22–25).

8. **The inner plexiform layer (IPL)** (figure 1-3, d) is formed by interlaced dendrites of retinal ganglion cells and the inner nuclear layer cells. It contains the synapses between the second-order and third-order neuron in the visual pathway (26).

**9. Ganglion cell layer (GCL), retinal nerve fibre layer (mRNFL) and peripapillar retinal nerve fibre layer (pRNFL): The layer targeted by the downstream sequelae of inflammatory optic neuritis.** From the IPL, the signal is propagated to the retinal ganglion cells (figure 1-3, 1), located in the ganglion cell layer (GCL) (figure 1-3, c). Ganglionar cells have their dendrites in the IPL, and their cell bodies in the GCL, with their axons travelling along the vitreoretinal surface of the eye (figure 1-4) in a layer called the retinal nerve fibre layer (pRNFL: when the fibres are in the disc, mRNFL: same fibres at the macula) (figure 1-3, b). IPL and GCL are often combined and coined GCIP to improve analytic precision in OCT analysis. The inner limiting membrane (ILM) separates the retina and the vitreous body, formed by Type Ib astrocytes and the endfeet of Müller cells (27) (figure 1-3, a).



---

**Figure 1-4: Scheme of the retina on fundoscopy**

Representation of the retina on fundoscopy, showing the fovea, the macula (6mm circumference around the fovea), and the RNFL fibres travelling from the macula (mRNFL) to the disc (pRNFL) to form the optic nerve. (Original figure: Adobe Inc., 2019. Adobe Illustrator, Available at: <https://adobe.com/products/illustrator>)

---

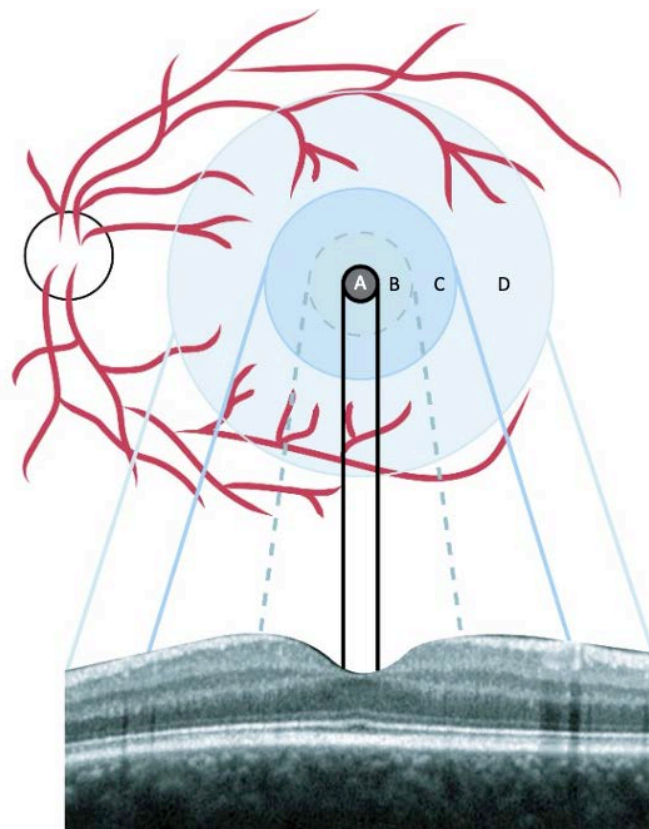
Each ganglionar cell sends a single output to a single axon. The mRNFL layer contains unmyelinated axons (28) that travel to the optic nerve head (also known as the optic disc) to form the optic nerve; from here, axons gain their myelin sheath and, for the

first time, this bunch of axons will be coined “optic nerve”. At the optic disc, which is located at a mean distance of 4.76 mm from the fovea (29), the retinal nerve fibre layer is thicker in the peripapillary area than in the macula. mRNFL, changes its name to “peripapillary retinal nerve fibre layer” (pRNFL) at the disc; here there are no rods or cones and is known to be a native blind spot (30).

After optic neuritis, the myelin in the optic nerve gets damaged (either by a direct (MOGAD) or indirect (AQP4-NMOSD) process, leading to atrophy of the optic nerve fibres at the level of the ganglion cell axons. These structures will be relevant for this research work; therefore, this thesis will be focusing on the macula (specifically, the inner macula), fovea and optic disc.

### 1.2.1.2. The fovea

The foveal area is divided into 4 sub-areas: foveola, fovea, parafovea and perifovea (figure 1-5).





---

**Figure 1-5: Macular OCT scan with a schematic representation of the fovea**

The shaded areas represent the macula. With the areas shaded in darker blue representing the foveal avascular zone (FAZ). A) Fovea, with its deepest point called Foveola; B) Parafovea; C) Perifovea, D) macula. (Original figure: Adobe Inc., 2019. Adobe Illustrator, Available at: <https://adobe.com/products/illustrator>)

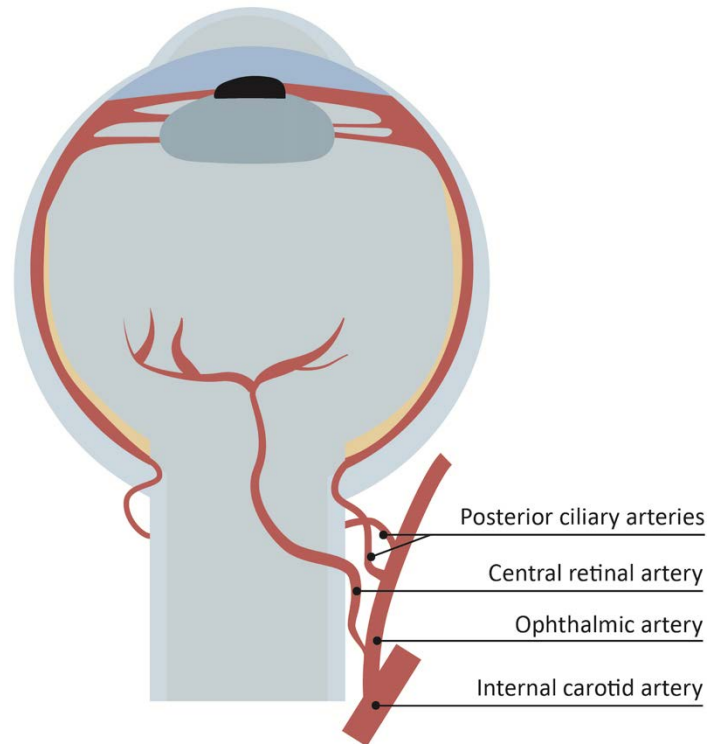
---

The **fovea** is the point of maximum acuity in the eye and its deepest point is called “**foveola**”. In the foveal depression, the inner retinal neurons are radially displaced relative to the foveola, providing a ‘V’ shape path for photons to create the highest acuity image without having to go through the inner retinal neurons. The fovea extends approximately with a diameter of 1.5 mm around the foveola. It contains the highest concentration of cones in the retina (31), with an estimation of around 199,000 to 300,000 cones per mm<sup>2</sup> (32,33) and a ratio between ganglionar cells and cones 1:1 (34). This area does not contain rods or capillaries (**foveal avascular zone (FAZ)** figure 1-4). The two consecutive circular rings surrounding the fovea are the parafoveal and perifoveal areas. The **parafoveal area** contains the highest concentration of bipolar and ganglionar cells (35), while the **perifoveal area** is characterized by a very thin layer of ganglionar cells.

### 1.2.1.3. Vascular structure of the macula

The retina gets blood supply from two main circulation pools: One arrives via the central retinal artery, which branches off the ophthalmic artery (figure 1-6) and is associated with the blood-retinal barrier (BRB). The other pool, supplied by the ophthalmic artery, sits under the photoreceptors and it is called the choriocapillaris (figure 1-3, k). This structure is responsible for the nutrition of the retinal pigment epithelium and the outer retinal layers. As they need to leak plasma proteins, vessels in the choriocapillaris are highly fenestrated (36) . The capillaries branching from the central retinal artery are characterized by a low blood flow and high oxygen consumption. In contrast, the choroidal circulation is characterized by a high blood flow and a low arteriovenous oxygen content, being the supplier for 85% of the total ocular

blood flow (37). Retinal arterioles, capillaries and venules complete the microcirculation circuit in the retina (38).



---

**Figure 1-6: Blood supply to the eye**

The ophthalmic artery supplies the anterior optic nerve, the choriocapillaris, retinal pigmented epithelium, an area of the choriocapillaris temporal to the macula as well as the iris and ciliary body through the posterior ciliary arteries. The central artery supplies the inner retina in the macular region. (Original figure: Adobe Inc., 2019. Adobe Illustrator, Available at: <https://adobe.com/products/illustrator>)

---

## 1.2.2. The optic nerve

The optic nerve is the second cranial nerve and it is considered part of the central nervous system as it has the same embryologic origin as the CNS (39). In the human anatomy, the optic nerve is formed by the ganglionic cells that exit the eye through the lamina cribrosa, which are little fenestrations within the sclera. Unlike the other axons inside of the eye, the optic nerve is formed by a bunch of myelinated fibres. These start at the lamina cribrosa and enter the skull through the optic foramen to travel through the optic canal until they meet with the contralateral optic nerve in the optic chiasm (40) (figure 1-7).

This differentiation between myelinated and unmyelinated fibres between the eye and the retina will become particularly important in the context of this thesis.

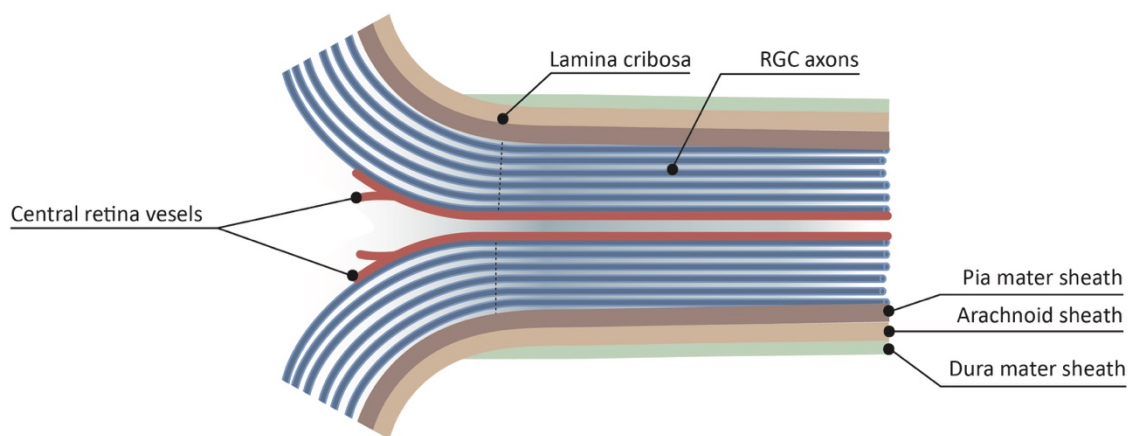


**Figure 1-7: The structure of the optic nerve**

The axons of the retinal ganglionic cells (RGC) gain myelin when they leave the eye. Fibre bundles are encapsulated by the three meningeal layers of the brain (dura, arachnoid, and pia mater). (Original figure: Adobe Inc., 2019. Adobe Illustrator, Available at: <https://adobe.com/products/illustrator>)

### 1.2.3. The optic chiasm and optic tract

At the optic chiasm, those fibres forming the optic tract that arrive from the temporal hemiretina will continue ipsilaterally towards the thalamus and those arriving from the nasal hemiretina will decussate to the contralateral side: at the optic chiasm (figure 1-8).

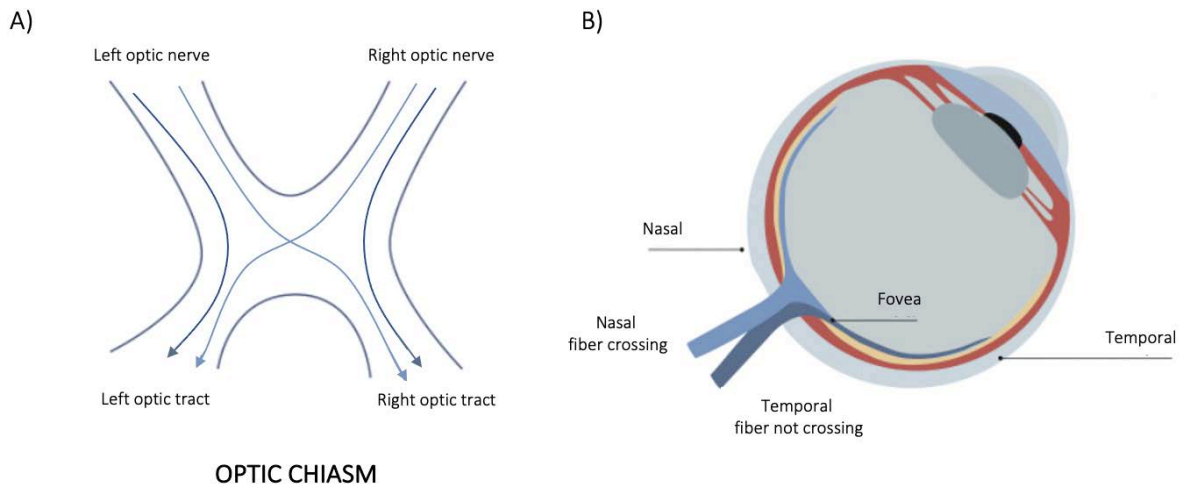


**Figure 1-8: Schematic representation of the optic chiasm, fibre decussation and optic tracts**

A) Schematic representation of the optic chiasm.

B) Distribution of crossed and uncrossed axons from the ganglionic retinal cells at the optic chiasm. (Original figure: Adobe Inc., 2019. Adobe Illustrator, Available at: <https://adobe.com/products/illustrator>)

This structure will be also important in the context of this thesis, as ON in AQP4-NMOSD tends to be posterior, sometimes affecting the chiasma, this may have implications on the visual acuity of the contralateral eye due to the transmission of the inflammation through the fibres in the optic chiasm.

## **1.3. Assessment of the visual system**

The eye offers a privileged window to the brain health. Direct access to neuronal structures is possible via fundoscopy at bedside; however, this technique has several limitations: lack of reproducibility, narrow field of view or monocularly of the measurement. Moreover, in some diseases where visual acuity can be compromised, the retina may look normal on fundoscopy, and disease activity/progression might be difficult to identify.

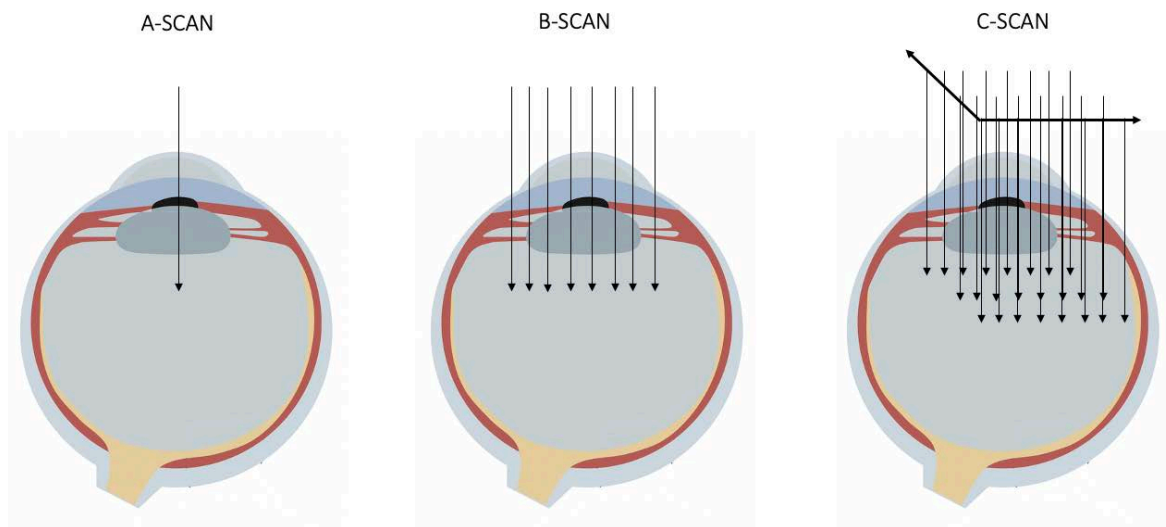
Since optical coherence tomography (OCT) imaging became part of the routine clinical practice, quantitative assessments of neuronal layers at the micron scale, both cross-sectionally and longitudinally have become possible with a high standard of repeatability, bringing the possibility to create direct associations between brain structures and retinal layers that help guiding clinical decisions. In MS, OCT has shown a huge potential over the years to investigate the relationship between retinal layers and CNS pathology (41). Several correlations between OCT markers and pathological processes have emerged: mRNFL and GCIP thickness seem to be good surrogates of brain atrophy measures, INL thickness has been found to be associated with inflammatory markers (e.g., T2 lesion volume) (42), and ONL thickness has been found by some to be a potential marker of progressive MS phenotypes (41).

### **1.3.1. Basics of OCT**

OCT stands for optical (which means light), coherence (which means light of a constant phase), and tomography (which means imaging by sections). OCT was first described in 1991 (43) and is a non-invasive transpupillary imaging technology that provides high-resolution, volumetric 3D histological images of the retinal microstructure, and imaging of the eye from the anterior segment to the posterior pole. This technology is the golden standard for histological imaging in ophthalmology and neuro-ophthalmology. It employs low coherence interferometry (830 nm wavelength), measuring the tissues through light reflection (44) with fast scanning rates, OCT improves patient experience, and allows quick signal processing, which results into a better quality of the image.

OCT technology produces three types of images: **A-Scans**, these axial scans are one-dimensional scans performed at several depths. Are used to create two-dimensional scans called **B-Scans**. These scans are often carefully examined one by one for the identification of macular abnormalities by the clinician. Consecutive B-scans can be aligned and transformed into volumetric images, called **C-Scans**, typically made with over 30,000 A-scans (45) (figure 1-9).

Quality control for OCT in this thesis follows OSCAR-IB criteria (46).



---

**Figure 1-9: Scan types with Optical Coherence Tomography (OCT)**

A-scan, axial; B-scans, 2-D; C-scans, volumetric scans (Original figure: Adobe Inc., 2019. Adobe Illustrator, Available at: <https://adobe.com/products/illustrator>)

---

### 1.3.2. OCT modalities

There are three different OCT modalities: time domain OCT (TD-OCT), spectral domain OCT (SD-OCT) and swept source OCT (SS-OCT). To be able to understand how the OCT works, it is important to understand how light behaves from a physical point of view. In figure 1-10 a light wave is represented (figure 1-10), the distance between peaks of a wave is a wavelength, and one complete oscillation is called a cycle. Any portion of a cycle is a phase and the fraction of a cycle by which one leads to another is known as phase-difference.

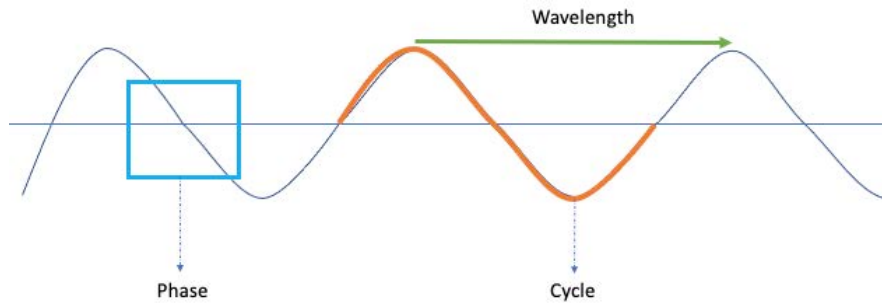
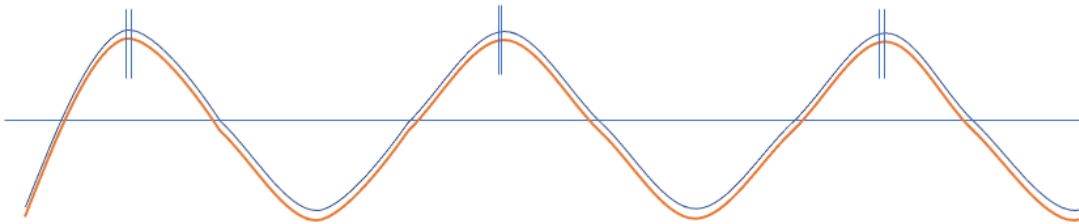


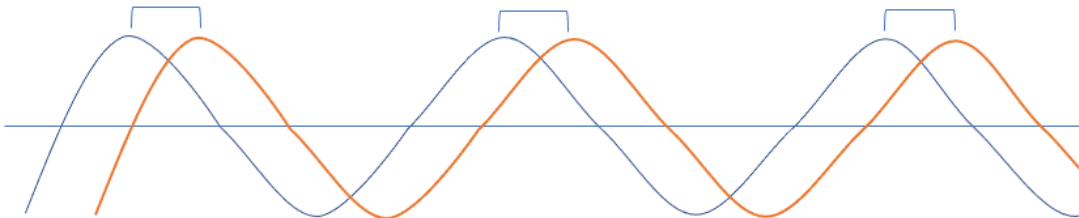
**Figure 1-10: Light wave**

In monochromatic systems (TD-OCT), the phase difference between waves is constant, while in broadband light systems (SD and SS-OCT) the phase difference between waves is variable due to the different wavelengths (figure 1-11)

**In phase. No phase difference**



**TD-OCT: Out of phase. Constant phase difference.**



**SD-OCT / SS-OCT: Out of phase. Variable phase difference.**

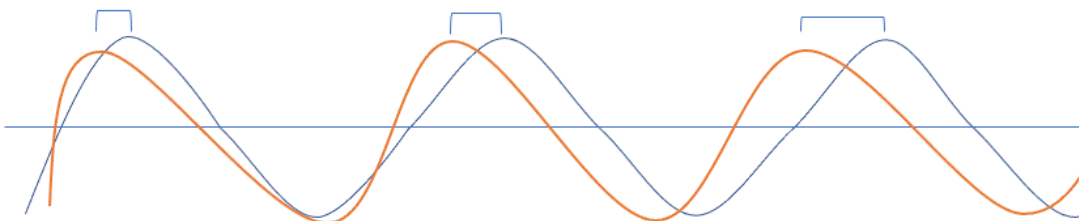
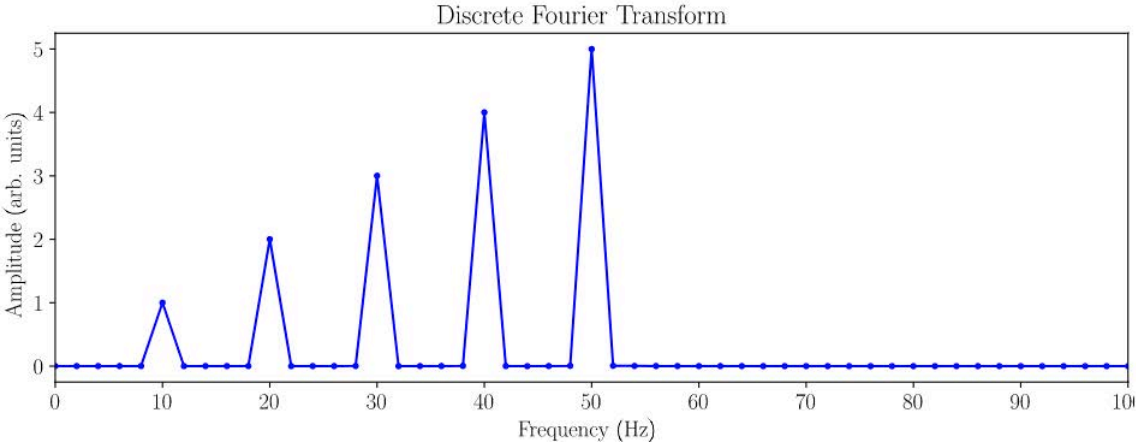
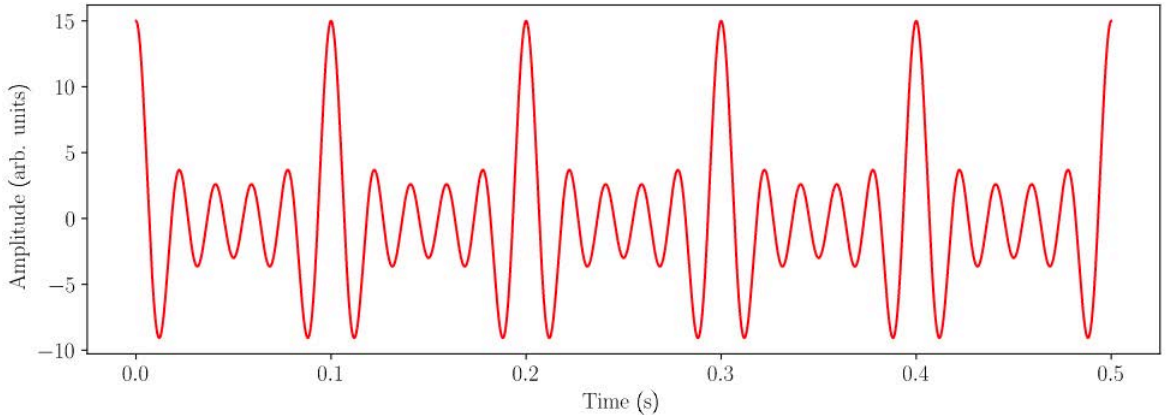


**Figure 1-11: Light waves in TD-OCT, SD-OCT and SS-OCT**

The first paper using in vivo time-domain OCT (TD-OCT) was published in 2000 (47), in TD-OCT the diode light (monochromatic light) reaches the beam splitter where half of the light goes to the eye and the other half goes into a mirror. Light comes back from both, and interfere together, reaching a detector (the design is the same as in figure 1-13, with a detector instead of a spectrometer). The mirror can be moved in order to get in focus the different retinal layers that will be interpreted by the detector due to the “destructive interference”, or said in different words, different out of phase wavelengths.

In 2002, Wojtkowsky et al. (48) published preliminary spectral-domain OCT results. SD-OCT, uses a broadband light and depends on fast Fourier transformation algorithms, it can also be called frequency domain. The fast Fourier transformation (figure 1-12) enables to transform one wave of phase difference (created by different wavelengths of light) into different waves and the reflection of each one.





---

**Figure 1-12: Fast-Fourier transformation**

This algorithm simplifies the wave, converting a signal from its original domain (time or space) to a representation in the frequency domain. Abbreviations: s, seconds; Hz, hertz.

Figure extracted from Wikipedia,

By AkanoToE - Own work, CC BY-SA 4.0,

<https://commons.wikimedia.org/w/index.php?curid=86139361>

---

SD-OCT devices include a spectrometer in the receiver that analyses the reflected light on the retina transforming it into information about the depth of the structures according to the Fourier principle (figure 1-13). This way, the operator does not depend on mirror movement. This technique is faster, as it only depends on velocity of light and not on the mechanical movement of the mirror.

However, the time domain is a slow process which allows time for the eye to move, and consequently, to create artifacts. While TD-OCT performs 400 scans per seconds, SD-OCT is able to scan 26000-40000 scans per seconds, this is faster than the eye movement and therefore scans are more stable. Moreover, the resolution is much better in SD-OCT (approximately 5  $\mu\text{m}$ ) compared to TD-OCT (approximately 10  $\mu\text{m}$ ). Automatic segmentation is also found to be better in SD-OCT. In a publication assessing a set of 104 patients with age-related macular degeneration by TD and SD-OCT significant differences in the accuracy of automatic segmentation were found, with TD-OCT failing in 69.2% of cases and SD-OCT in 25% (49). Automatic segmentations should always be checked by experienced clinicians/scientists in each B-scan.

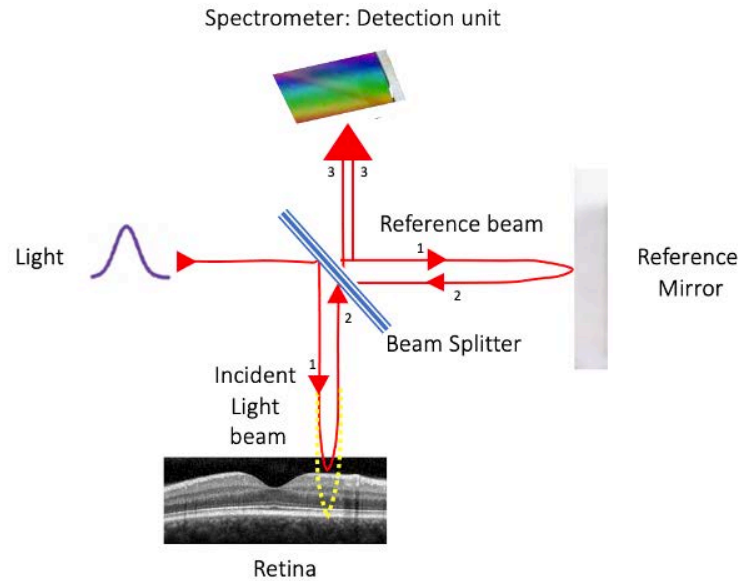


**Figure 1-13: Scheme of spectral-domain OCT mechanism**

The wavelength spectrum of the interference signal is recorded using a spectrometer located at the output of the interferometer. Echo reflections from different depths send different frequencies in the interference spectrum. This spectrum is rescaled and Fourier transformed to compute the A scan axial information. Unlike time-domain acquisitions, all echoes of light are detected simultaneously in SD-OCT. Numbers 1, 2 and 3 represent processes happening first (1), second (2) and third (3). (Original figure: Adobe Inc., 2019. Adobe Illustrator, Available at: <https://adobe.com/products/illustrator>)

In SS-OCT, the third modality, the separation of the waves is happening at the level of the beam splitter, (in the SD-OCT happens at the level of the spectrometer), this allows showing deeper structures as the lamina cribosa or the choroid.

SD-OCT will be used in the experimental projects of this thesis. It provides a high speed of data acquisition and increases the resolution, resulting in better visualization of the different intraretinal layers which allows to more accurate segmentation, both automatically and manually. Besides, this technology is less operator dependent, which increases the reliability of the scanned image and results can be easily translated into clinical practice.

### 1.3.3. The Cubic Bezier algorithm (CuBe)

As it was described in the previous section, OCT has been classically used to quantify macroscopic changes in the retina, however, recent advances in macular segmentation have allowed the quantification of microscopic structures as the retinal layers. Foveal shape, however appears still difficult to measure, due to the lack of built-in technology in the OCT available software, and the challenges on the modelling of this structure. Previous studies with data driven approaches (50–52) where segmentation lines from the OCT scan were used to compute parameters, assumed that the foveal pit shape is described by a Gaussian function. However, the use of the Gaussian function is imprecise to measure this structure as regions of this function are dependent on each other and on the standard deviation of the mean, while the different parameters of the foveal shape are independent to each other and therefore, cannot be modelled by Gaussian functions.

In this thesis, I have used a model-driven approach to assess the foveal structure, described by Yadav et al in 2017 (53): The “CuBe” model. The approach chosen by these authors to solve the issue of modelling independent parameters was to use cubic Bézier equations in order to account for all possible variations of the foveal shape. This equation uses invariant features of the fovea to be able to reconstruct the variations in the structure. This algorithm characterizes the foveal and parafoveal region by 19 parameters. The method first flattens the inner limiting membrane (ILM) surface taking the Bruch’s membrane as the reference (reference plane) and then radially reconstructs the ILM surface, from the centre of the fovea up to the points with maximum heights, which are called rim points using Cubic Bezier polynomials. Based on the reconstructed ILM surface and the reference plane, foveal morphometry parameters are defined. Twelve parameters are defined as area, average diameter, major length (the length in the dominant direction), and minor length (the length in the second dominant direction, perpendicular to the dominant direction) of three different surfaces; **pit flat disk**: a surface that captures the flatness of the foveal pit, **slope disk**: a surface that connects points with maximum slope, and **rim disk**: a surface that connects rim points. In addition to the parameters describing the defined surfaces, there are several other parameters describing the fovea: 1) Average pit depth: average height of the points on pit flat disk; 2) Central foveal thickness: minimum thickness of

the fovea; 3) Average rim height: average height of rim points; 4) Rim volume: volume between ILM surface and reference plane limited to rim points; 5) Inner rim volume: similar to rim volume but limited to 1-mm diameter around the centre of the fovea; 6) Pit volume: volume between ILM surface and rim disk; 7) Average maximum pit slope: average slope of points with maximum slope. Figure 1-14 shows an overview of the fovea morphometry method.

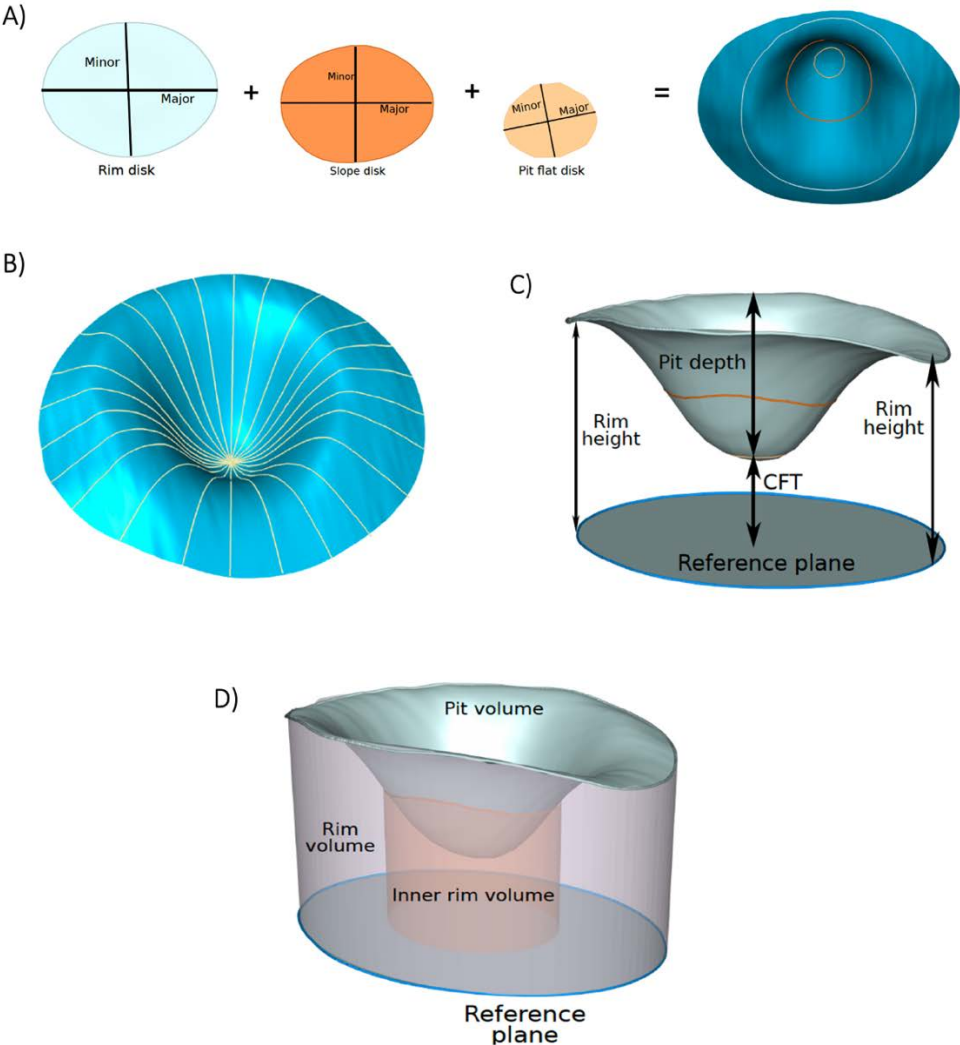


**Figure 1-14: Schematic representation of the Cube model**

A) Surfaces defined in the Cube method: rim disk, slope disk and pit flat disk. B) ILM surface smoothing and radial reconstruction using the cubic Bezier polynomial. C) The Rim height, average pit depth, and central foveal thickness reconstructed from

---

the cubic Bezier polynomials. D) Rim volume, pit volume, and inner rim volume reconstructed from the cubic Bezier polynomials. Abbreviations: CFT, central foveal thickness. (Original figure: MATLAB, 2010. version 7.10.0 (R2010a), Natick, Massachusetts: The MathWorks Inc.)

---

### **1.3.4. Visual evoked potentials (VEP)**

This technique is broadly used in clinical practice to study neuro-electric responses to sensory stimuli along the visual pathway. The standard stimulus for VEPs is a checkerboard pattern in which the squares alternate from black to white; it is called “pattern reversal VEP” (PRVEP) (54). Responses from PRVEP are recorded with three electrodes in the occipital region and one frontal reference electrode. Increases in latencies may be caused by processes such as demyelination, while abnormalities in the amplitude and waveform of the VEPs are more likely to be caused by the loss of axons in the pathway. These two parameters are enough to provide information about the conduction of the visual system, revealing subclinical involvement by silent lesions, particularly those inducing demyelination, and can help defining the anatomical distribution, being an excellent tool to monitor disease process and changes in clinical status (55).

### **1.3.5. High contrast visual Acuity**

High contrast visual acuity is assessed in this thesis using retro-illuminated Early Treatment for Diabetic Retinopathy Study (ETDRS) charts (56), measuring visual acuity in logMAR scores. LogMAR represents the logarithm of the minimum angle of resolution, and the scoring system provides a continuous statistical variable. These charts provide an equal number of letters per row, balanced for difficulty and equally spaced, which the only difference based on letter size between rows. Sloan charts at 100% contrast are equivalent to ETDRS. Low contrast visual acuity will not be discussed in the thesis.

## 1.4. AQP4-NMOSD

The first case of Neuromyelitis Optica dated from 1804 when the French pathologist Antoine Portal described a case of "Neuroencephalitis Optica". In this case, he reported a patient with intractable vomiting, relapsing visual loss, and spinal pain (57). In 1894, the French neurologists Eugène Devic and Fernand Gault described a syndrome combining optic neuritis and severe transverse myelitis, initially based on the observation of 16 patients (57) (figure 1-15).

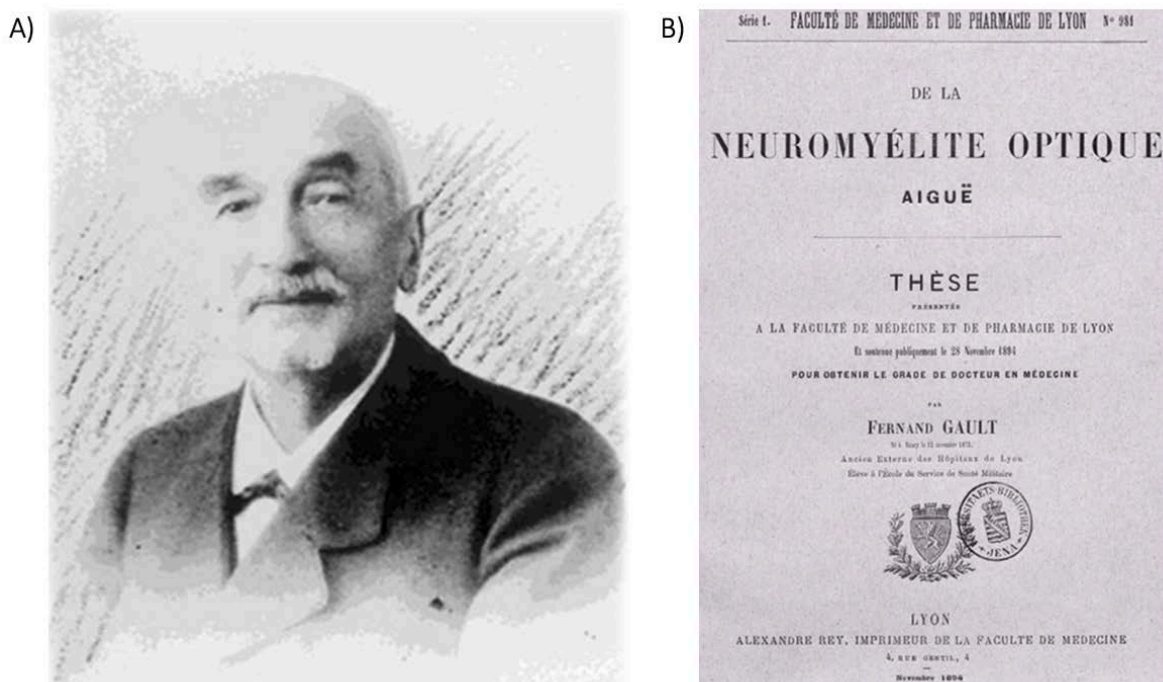


**Figure 1-15: Eugène Devic and Fernand Gault's doctoral thesis "De la neuromyéélite optique aiguë"**

A) Eugène Devic portrait. B) Doctoral thesis from Devic's student Fernand Gault, published in 1894 in Lyon (France). Extracted from Jarius, S., & Wildemann, B. (2013). *The history of neuromyelitis optica*. *Journal of Neuroinflammation* (57).

nsed under the terms of the Creative Commons

(<http://creativecommons.org/licenses/by/2.0>), which permits unrestricted use, distribution, and reproduction in any medium.

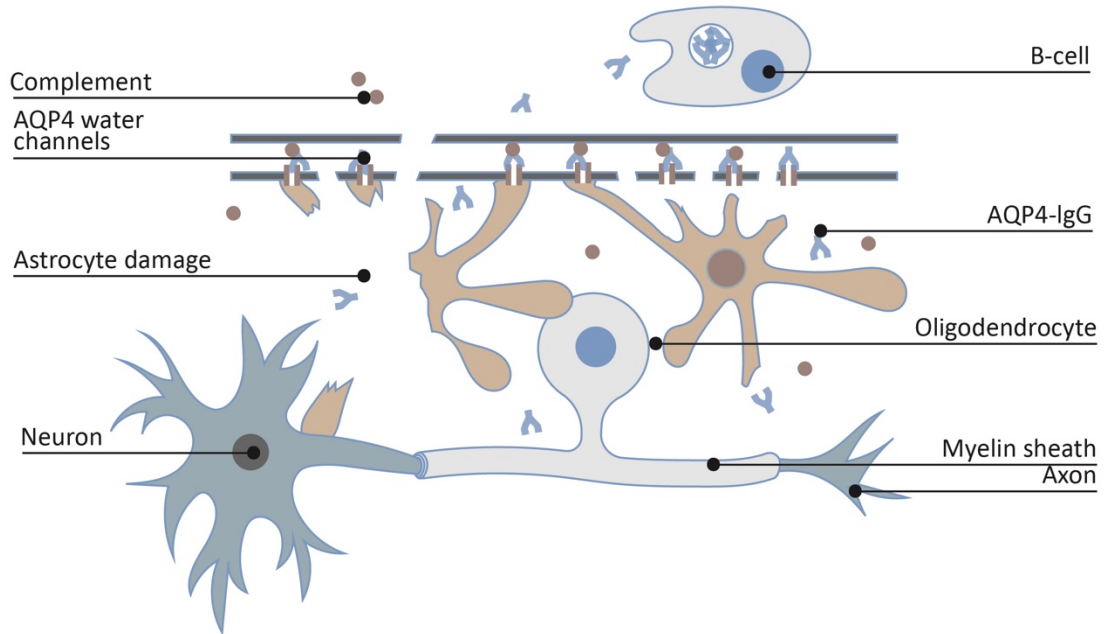
From this moment, more reports describing similar symptoms started to appear, with increasing interest among the neurological community. However, overlapping symptoms led to uncertainty as to whether Devic's Neuromyelitis Optica was a distinct syndrome or a subtype of MS. It was not until 1996 that this syndrome was reappraised; O'Riordan et al. used the term Devic's Neuromyelitis Optica and described the clinical features, cerebrospinal fluid (CSF) and magnetic resonance imaging (MRI) findings, and was then when this was acknowledged as a distinct disease (58,59). Eight years later, in 2004, Vanda Lennon and colleagues achieved an important milestone in the history of this syndrome: the auto-antibody Neuromyelitis Optica immunoglobulin G, which binds to the antigen (AQP4), was found in AQP4-NMOSD (60).

### **1.4.1. Pathophysiology**

AQP4 is part of a family of integral membrane proteins that conduct water in and out of the cells. AQP4 is expressed in the brain, spinal cord and optic nerve, within the white and grey matter, as well as in other parts of the body. In the brain, AQP4 water channels are localised to the endfoot processes of the astrocytes at the blood-brain barrier (BBB) (60) and are critical to the maintenance of water homeostasis.

There is some evidence to suggest that immune activation is initiated in the peripheral immune system, where pathogenic anti-AQP4 auto-antibodies are generated by plasmablasts (B-cells) (61). Initially, it was thought that these antibodies gained access to the astrocytic end-foot processes through portions of the BBB with relatively high permeability, such as some regions of the hypothalamus or the optic nerve head (62). However, later it was hypothesized that unknown humoral factor(s), present in the sera of diseased AQP4-NMOSD patients, would affect the integrity of the BBB (63,64). Indeed, recent investigations have found that serum or IgG from in AQP4-NMOSD patients was able to affect the integrity of the BBB (65,66). The lesion formation in AQP4-NMOSD starts with a breakdown of the BBB, which allows AQP4-IgG to invade the CNS and bind to AQP4 on the end-foot processes of astrocytes and activate complement-mediated astrocytic damage (67). The influx of neutrophils and eosinophils into the perivascular spaces cause astrocyte death. Damage to the

astrocytes causes oligodendrocyte death, leading to axonal degeneration and finally neuronal death (figure 1-16).



---

### Figure 1-16: Pathophysiology of AQP4-NMOSD

AQP4-IgG are produced by mature B-cells, and cross the blood-brain barrier causing astrocytic damage that may lead to myelin damage as a secondary process.

(Original figure: Adobe Inc., 2019. Adobe Illustrator, Available at: <https://adobe.com/products/illustrator>)

---

AQP4-NMOSD is a primary astrocytopathy with a secondary demyelination. Animal studies have supported primary astrocytopathy in AQP4-NMOSD outside of acute lesions, showing retraction of astrocytic endfeet and astrocytic death (23,66,68).



## **1.4.2. Epidemiology**

Population-based studies in AQP4-NMOSD are usually biased by the high number of patients misdiagnosed with MS (69), which is as high as 30-40% due to the lack of AQP4-IgG testing in some parts of the world. AQP4-NMOSD is considered a rare disease, and prevalence varies among different geographic areas and ethnicities. A recent prevalence review (70) has described a prevalence a 10/100 000 persons suffering this condition in the world. There is a female predominance in adults (9:1), mainly in the AQP4-NMOSD population; however, this gender difference is less remarkable at extremes of age. The incidence and prevalence appear to peak in middle-aged adults. African seems to appear the ethnicity with the highest incidence and prevalence of AQP4-NMOSD, whereas Caucasians have the lowest incidence and prevalence of this condition (71).

## **1.4.3. AQP4 cell-based assay**

The most widely used method to detect anti-AQP4 IgG in human serum, and the one used in this thesis, is the cell-based assay (CBA). With this method, the serum anti-AQP4 IgG is captured by the AQP4-transfected cell fixed in the biochip and is detected with high sensitivity and specificity by a fluorescein-labelled secondary antibody. In a multicentre comparison, researchers concluded that cell-based assays were most sensitive and specific overall (3); however, immunohistochemistry or flow cytometry could be equally accurate when performed in specialist centres. However, research on the associations between AQP4-IgG titres and clinical outcomes are inconclusive. Recent research has revealed that the level of AQP4-IgG titres does not reflect ongoing disease activity or neurological prognosis in AQP4-NMOSD (72).

## **1.4.4. Clinical and paraclinical findings**

Symptoms in AQP4-NMOSD are mainly the result of lesions in three primary CNS locations: visual symptoms are derived from retinal changes and optic nerve

lesions, sensorimotor symptoms result from spinal cord lesions, and a miscellaneous group of symptoms are usually a consequence of brainstem lesions. However, disability in AQP4-NMOSD is accepted to be relapse dependent and it does not come from progression of neurological dysfunction independent of relapses (2)

#### **1.4.4.1. Visual System**

Optic nerve susceptibility has been proposed to arise from, or to be due to the high AQP4 expression in the optic nerve compared to the brain (73). Other proposed theories for this predilection are:

- a. Regional differences in blood-brain barrier integrity (74).
- b. The presence of plasmablasts in the CSF secreting AQP4-IgG locally (75)
- c. Regional variations in regulators of complement (76)
- d. Low efficiency of the phagocytic process due to the particular morphology of the optic nerve and its restricted diffusion (77,78).

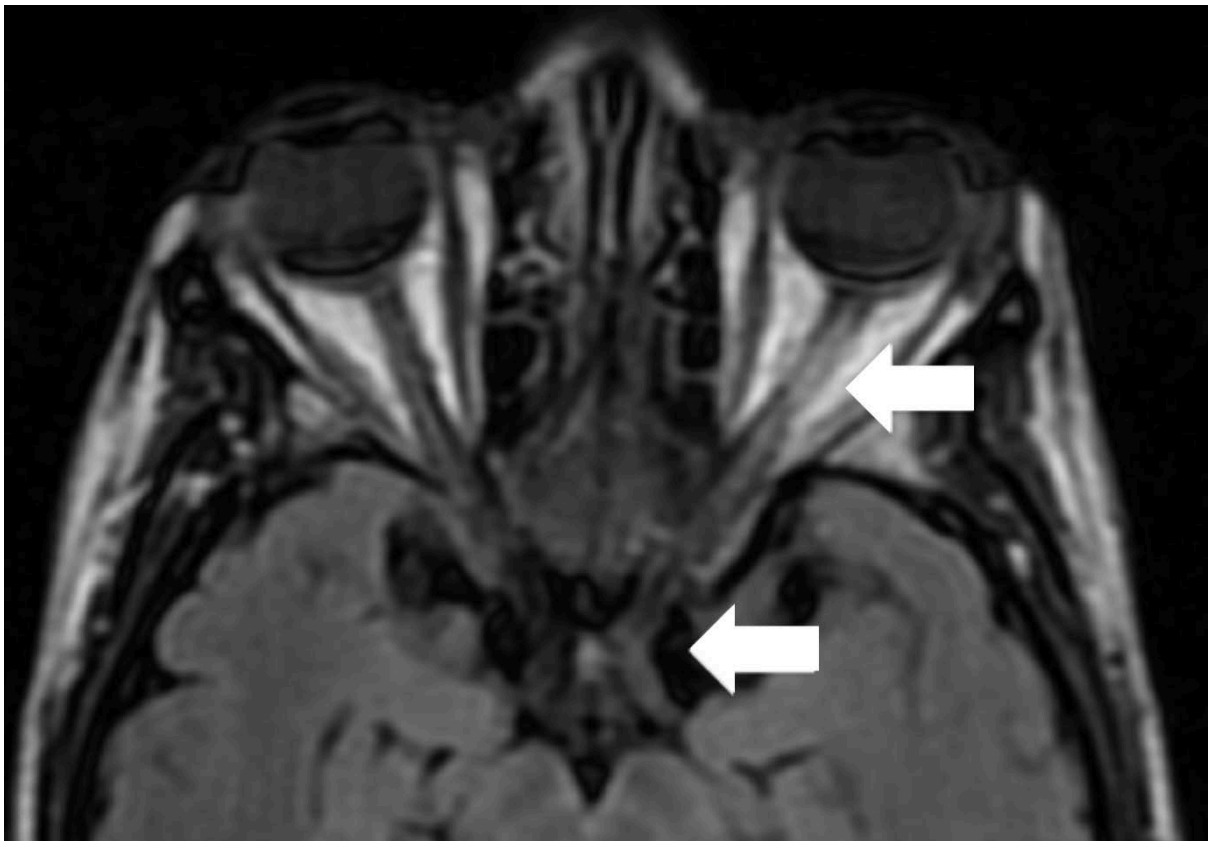
Inflammation in ON is not necessarily restricted to the anterior part of the optic nerves. In AQP4-NMOSD, ON attacks tend to occur in the posterior segments of the optic nerve, and they can often involve the optic chiasm (79). Moreover, in the last years, it has been broadly accepted that optic nerve damage is not the only source of visual impairment in AQP4-NMOSD patients. Thus, the retina has been identified as a second pathogenic target, where the osmotic water flux can be compromised, causing cellular death. This would be a result of the reduced osmotic process in the Müller cells (which express AQP4 water channels), the imbalance cause Müller cell damage and may ultimately lead to the death of ganglionar cells and compromised visual function (22).

##### **1.4.4.1.1. Clinical manifestations derived from ON in AQP4-NMOSD**

As it was stated previously, ON in AQP4-NMOSD often affects the posterior parts of the optic nerve - including the optic chiasma (80) - (figure 1-17); ON is a

common characteristic of AQP4-NMOSD patients, appearing as first manifestation in 64% of the cases (81).

Optic neuritis in AQP4-NMOSD tends to be severe, often leading to a significant neuroaxonal retinal damage after multiple relapses (82,83). Visual loss can be accompanied by pain evoked by eye movement due to the swelling of the intracranial section of the optic nerve (84). At the onset, almost half of the patients suffer from visual field defects. AQP4-NMOSD patients show a high incidence of non-central scotoma, often with altitudinal hemianopia (85). Altered colour vision is another common characteristic after ON in AQP4-NMOSD, as it is in MS. Patients with AQP4-NMOSD show poor visual recovery (86).



---

**Figure 1-17: Orbital MRI of an AQP4-NMOSD patient**

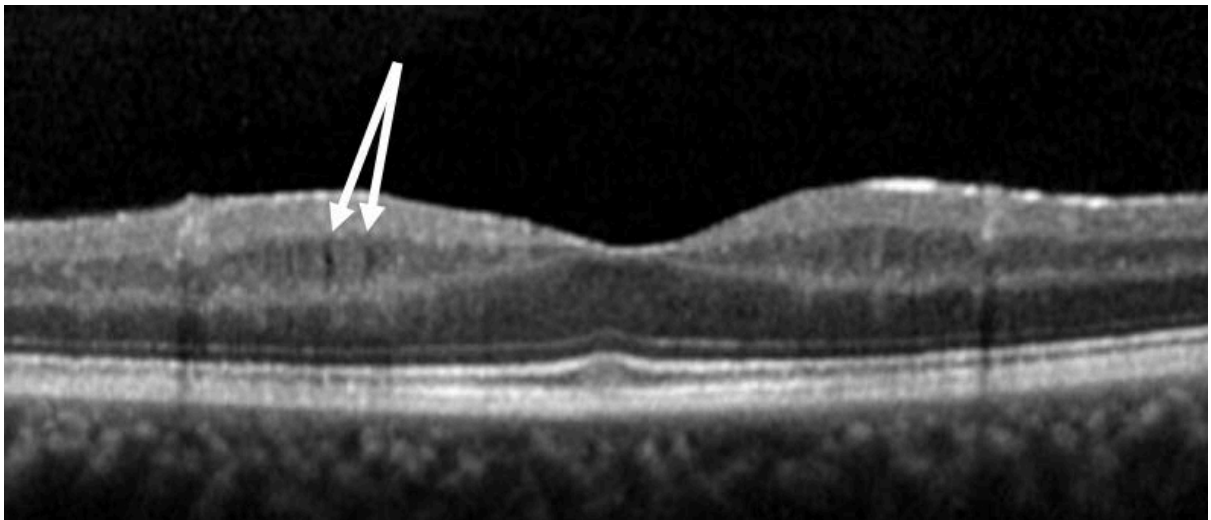
Arrows point to extensive ON lesion involving the optic chiasm

---

### 1.4.4.1.2. OCT findings

A marked retinal nerve fibre layer thinning (pRNFL in the disc and mRNFL in the macula) are often accompanied by a ganglionar-inner plexiform retinal layer (GCIP) loss which is observed after an ON in AQP4-NMOSD eyes. A recent population-based study (87) found significant thinning in all pRNFL quadrants compared to HC, with a predominant thinning of the temporal quadrants, similarly to what happens in MS. Profound foveal shape changes independent from ON have also been found in the affected eyes of these patients after an attack (88,89).

During the past few years, several studies have suggested that AQP4-NMOSD is associated with increased inner nuclear layer thickness, often accompanied by microcystic macular oedema (MME) (90) (figure 1-18).



---

**Figure 1-18: Representation of an OCT scan from an AQP4-NMOSD patient**

Arrows pointing to MME (Original figure: Oxford NMO tissue bank database)

---

In AQP4-NMOSD patients, these changes are not uniquely linked to ON eyes. Abnormal values in the GCIP layer and foveal thickness have also been reported in eyes without a history of ON. These abnormalities were associated with longitudinal changes in the GCIP layer that could be a result of primary retinopathy, drug-induced neurodegeneration or a retrograde neuroaxonal degeneration from other lesions in the brain (91–94). Previous studies have reported thresholds below which visual acuity is compromised (95,96). Using regression models, Costello et al (95) identified a

threshold of 75  $\mu\text{m}$  in mRNFL, whereby changes in mRNFL thickness above 75  $\mu\text{m}$  would be associated with a minimal and clinically insignificant increments of change in visual function. Ratchford et al (96) suggest a threshold of approximately 60  $\mu\text{m}$  below which visual acuity would become very poor. Other studies have reported that despite the profound changes in mRNFL after an ON, GCL thickness seems to be the stronger predictor of HCVA and LCVA (97). However, in some cases, visual acuity loss appears to follow an independent process from the retinal layer thinning in the retina, and this will be further explored in this thesis.

Dynamic changes (from oedema to retinal thinning) have been reported to stabilize in 7 to 12 months after optic neuritis however, this was not studied in depth. This is an important fact to take into account when planning research studies, as different time-frames may represent different stages of the disease process (i.e., acute vs chronic). In the task of exploring the chronic stage of the retina after an ON, it is crucial to determine how long does it take for the retina to transition from the oedema to the finalised process of retinal thinning, this will be addressed in the following sections of this thesis.

#### **1.4.4.1.3. VEP findings**

Visual pathways in patients with AQP4-NMOSD have been assessed using VEPs (98,99,82,100–102). Some studies have reported to have a pattern of VEP responses that is distinct from MS in AQP4-NMOSD patients, characterized by a reduced amplitude and normal latency, suggesting axonal damage rather than demyelination (99) (103,104).

However, the majority of publications, where several ethnicities have been represented, describe delays of P100 in AQP4-NMOSD patients, even if this process is less frequent in AQP4-NMOSD compared to MS. Watanabe et al. described delays of P100 in 17% of their AQP4-NMOSD eyes affected by ON (AQP4-NMOSD-ON) (98), while Neto et al. (99) reported this in 12.5% of AQP4-NMOSD-ON eyes. P100 delays were also found in AQP4-NMOSD eyes with no history of ON (AQP4-NMOSD-NON eyes) (100–102). In recent studies in Caucasian population, Ringelstein et al. describe delayed P100 waves in 49% of their AQP4-NMOSD cohort (100). In a longitudinal study, the same authors found a significant increase of P100 latencies and reduction

in amplitude in eyes with and without a history of ON. These abnormalities may be attributed to minor subclinical damage in the optic nerve impacting conduction speed or other changes of the retina, optic nerve, chiasm, optic tract, or optic radiation, or even cortical pathology (101,102). These results showing increase of P100 latencies in ON eyes are in line with a severe axonal loss in AQP4-NMOSD patients and consistent with the GCIP loss observed in OCT studies, consequently decreasing visual acuity in patients with severe ON (102). In spite of this, there is a lack of research on VEP in eyes not affected by ON in AQP4-NMOSD and the assessment of its sensitivity to structural damage as compared to OCT.

#### **1.4.4.1.4. MRI findings**

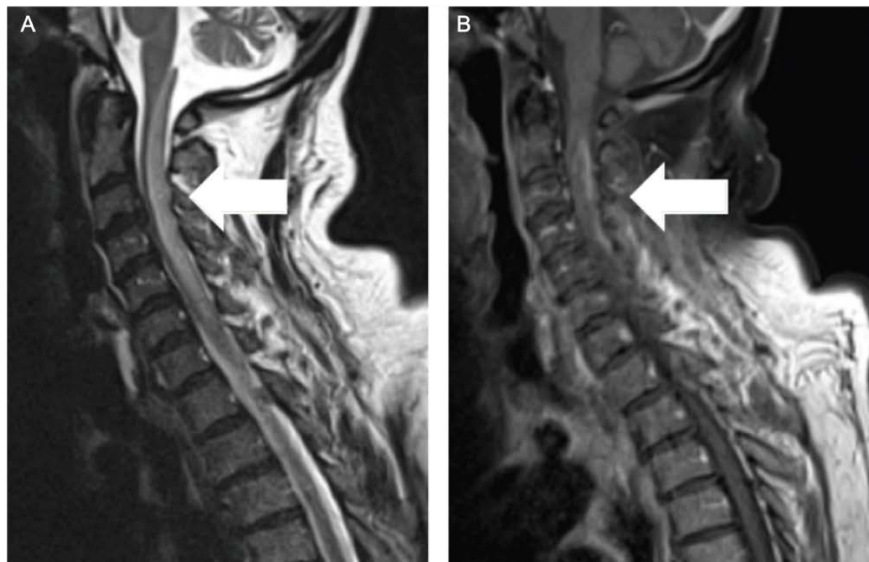
In AQP4-NMOSD, optic nerve lesions are often extensive, spanning greater than half of the length of the optic nerve and, in the acute stage, are associated with gadolinium- enhancement (105,106). AQP4-NMOSD patients with at least one ON showed significantly lower chiasmatic volumes, probably reflecting the recognised posterior location of ON in this disease and the severity of the ON or anterograde trans-synaptic degeneration (107,108). In a recent retrospective study, 20% of AQP4-NMOSD ON showed chiasmal involvement. In patients with chiasmal involvement, longitudinally extensive optic nerve enhancement (from the orbit extending to chiasm) was only identified in 7% of the patients (109).

Damage in the visual pathways was found in tract-based analysis in AQP4-NMOSD patients supporting remote damage (108,110,111). In 2017, Oertel et al., in a study with 25 patients, found microstructural white matter changes in the OR of AQP4-NMOSD patients without a history of ON (93). Reductions in fractional anisotropy (FA) in these patients did not correlate with any OCT biomarkers (pRNFL, GCIP or foveal thickness (FT)). Therefore, the authors suggested that these changes could be associated with a structural alteration independent from ON or subclinical activity not associated with symptoms. This hypothesis was supported by the fact that AQP4-NMOSD patients with previous ON showed positive correlations between the reduced FA in the OR and the GCIP layer. Shortly after, Tian et al. corroborated these results by reporting reductions in OR integrity in AQP4-NMOSD patients with no ON history. These authors also demonstrated bidirectional degeneration in patients with a history

of ON, showing significant reduction of pRNFL, inner and outer retinal thickness, LGN volume, decreased integrity of OR and primary visual cortex volume (94).

### 1.4.4.2. Spinal cord

Together with ON, the most distinct manifestation of AQP4-NMOSD is the inflammatory involvement of the spinal cord, mainly the grey matter, usually spanning over three or more contiguous vertebral segments (longitudinally extensive transverse myelitis - LETM) (figure 1-19). These attacks tend to be severe, and they usually involve the corticospinal tract, the cerebellar-spinal tract and sensory tracts (specially pain and temperature) (112). After a LETM, patients may present with symptoms that may vary in severity depending on the size of the lesion but typically present with walking difficulties and different degrees of sensory deficits, bladder and bowel, and sexual dysfunction. Symptoms will also vary depending on the spinal cord level in which the lesion has been formed. Up to 86 % of AQP4-NMOSD patients also report neuropathic pain (113,114) derived from spinal cord lesions (112,115,116).



---

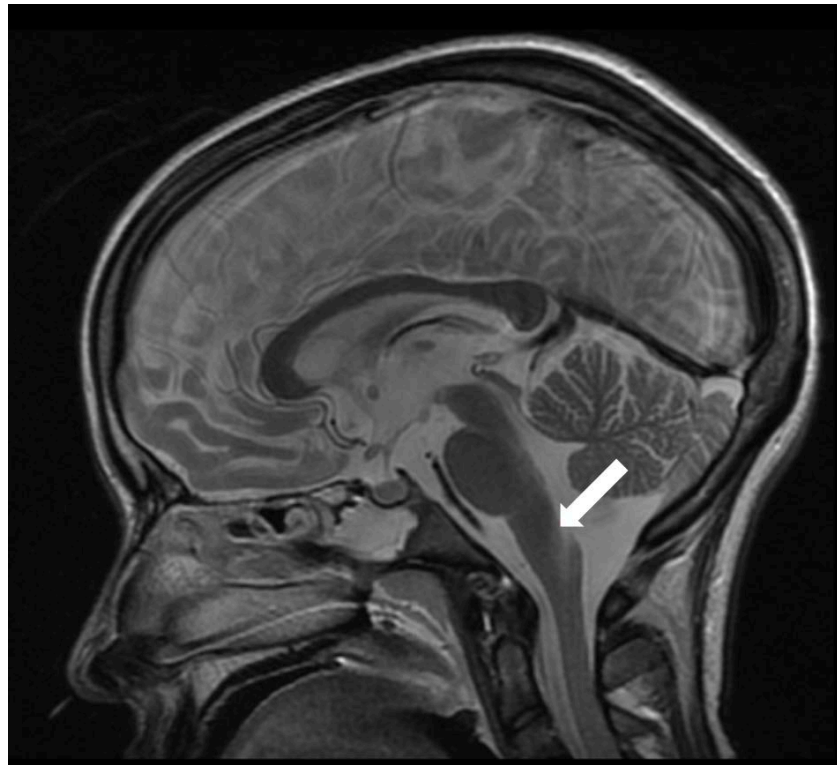
**Figure 1-19: Spinal cord lesion of a patient with AQP4-NMOSD after an LETM**  
A) Long lesion (>3 vertebral segments) on T2-weighted imaging B) the corresponding T1-weighted, gadolinium enhancement. (Original figure: Oxford NMO tissue bank database)

---

Bright spotty lesions, appear to be another spinal MRI feature that could be useful for differentiation of NMOSD from MS. These hyperintense lesions on axial T2-weighted images are sometimes associated with T1 low signal and appear to be highly sensitive and specific for the diagnosis of myelitis in patients with AQP4-NMOSD (117).

### 1.4.4.3. Brainstem

Brainstem lesions are frequent in AQP4-NMOSD (figure 1-20). These are often located in the dorsal part of the pons and may involve the cerebral peduncles.



---

**Figure 1-20 Brainstem lesion in a patient with AQP4-NMOSD**

Arrow points to T2-weighted hyperintensities in an MRI seen in the floor of the fourth ventricle, including area postrema. (Original figure: Oxford NMO tissue bank database)

---



The archetypal presentation of brainstem symptoms in NMOSD is what we know as “area postrema syndrome”, characterized by severe and protracted vomiting with or without hiccoughs for several days as a consequence of a lesion in this area (118,119) . This can be explained by the fact that the area postrema is particularly rich in AQP4, and therefore, a target of anti-AQP4.

### **1.4.5. Diagnostic criteria**

The latest criteria for the diagnosis of AQP4-NMOSD are those of Wingerchuk et al published in 2015 (119), these can be found in table 1-1.

**NOTE:** The following text in this table, formatted in *Italics*, is a literal copy from the diagnostic criteria in the publication, these criteria have been reproduced in the table below with the permission of the publishers of *Neurology*.

**a. Diagnostic criteria for NMOSD with AQP4-IgG**

1. *At least 1 core clinical characteristic.*
2. *Positive test from AQP4-IgG using best available detection method (cell-based assay strongly recommended).*
3. *Exclusion of alternative diagnoses.*

**b. Diagnostic criteria for NMOSD without AQP4-IgG or NMOSD with unknown AQP4-IgG status**

1. *At least 2 core clinical characteristics occurring as a result of one or more clinical attacks and meeting all of the following requirements:*
  - i. *At least 1 core clinical characteristic must be optic neuritis, acute myelitis with LETM, or area postrema syndrome.*
  - ii. *Dissemination in space (2 or more different core clinical characteristics).*
  - iii. *Fulfilment of additional MRI requirements, as applicable.*
2. *Negative tests for AQP4-IgG using best available detection method, or testing unavailable.*
3. *Exclusion of alternative diagnoses.*

---

**Table 1-1: AQP4-NMOSD diagnostic criteria**

---

### **1.4.6. Disease course**

The typical disease course of NMOSD is characterized by multiple relapses leading to increasing disability. Relapses are alternated with remissions of variable duration with no known degenerative component. However, subclinical damage has been previously reported in AQP4-NMOSD, and although this hypothesis still leads to controversy, the role of OCT, together with other assessment techniques such as MRI are key on the monitoring and treatment of the disease - even in asymptomatic patients

- to evaluate potential persistent inflammation and re-assess treatment strategies when is required (120).

In a collaborative international research with 449 AQP4-NMOSD patients (121), the spinal cord appeared to be the most prevalent attack location for these patients, followed by optic neuritis and brainstem. As described above, attacks in AQP4-NMOSD tend to be severe. Transverse myelitis is also the most prevalent overall attack, but also the most prevalent form of onset, with around half of the patients with this presentation being left with significant motor disability after this episode. Patients presenting with ON as first attack, were described to be left with around 20% less disability that those presenting with TM (82). The number of subsequent relapses varies, and a good treatment management has shown efficacy in delaying or preventing relapses in AQP4-NMOSD, for this reason, research published presents a wide range of relapsing prevalence that varies from 40-80% depending on the publication (82,122). However, in a recent study (122) researchers have shown relapse rates in AQP4-NMOSD that double the ones in MS.

Recently, several authors have discussed whether independent subclinical damage can occur in the eyes of patients with AQP4-NMOSD independently from ON attacks (89,91–93,97). The hypothesis states that a local astrocytopathy occurs as a consequence of the AQP4-IgG and this could lead to changes in retinal integrity and impairment of visual outcomes; however, this hypothesis needs to be further investigated.

### **1.4.7. Treatment**

As mentioned in the previous sections, relapses in AQP4-NMOSD are usually severe, and the occurrence of multiple subsequent relapses may leave the patient with a high degree of disability. For this reason, the main strategy when it comes to treatment in these patients is to aggressively manage the acute stage, followed up by long-term immunosuppressive treatments to prevent further relapses (123).

The **acute treatment** aims to reduce active inflammation, accelerate recovery, and avoid irreversible damage. The typical starting strategy for treating an AQP4-NMOSD attack is methylprednisolone (1000 mg) intravenously for five days. This initial

approach is usually followed by an oral steroid dose that tapers depending on the severity of the attack (124,125). However, there are cases when intravenous methylprednisolone is not enough to improve the patient's condition, and the lead physician may decide to start the use of plasma exchange (PLEX) (126). PLEX has been demonstrated to be effective in managing acute attacks in AQP4-NMOSD (127–129).

Three drugs have been approved by the FDA for the **chronic treatment of AQP4-NMOSD**: 1) Eculizumab: Approved in June 2019. Monoclonal antibody, anti-human complement component 5 (130), 2) Inebilizumab: Approved in June 2020. Monoclonal antibody, anti-CD19-positive B-cells (131) and 3) Satralizumab: Approved in August 2020. Monoclonal antibody anti- Interleukin-6 (IL-6) (132) Prior to the approval of these drugs, other off label drugs were extensively available and are still in use for the management of AQP4-NMOSD: mainly rituximab (now approved as a second line treatment), but also azathioprine, mycophenolate mofetil, oral prednisolone and tocilizumab (125,133–135). Other immunosuppressive therapies have been also used: methotrexate (136), mitoxantrone (137), and cyclophosphamide (138) .

## 1.5. MOGAD

Myelin oligodendrocyte glycoprotein associated disease (MOGAD) is a recently recognised distinct demyelinating disease of the central nervous system. Despite MOG-IgG being studied for many years, and due to the overlapping clinical and MRI features with MS, as it happened with AQP4-NMOSD patients, MOGAD patients were historically included in the same group as MS patients (139–143).

It was not until 2007 when MOG-IgG were reported for the first time in a cohort of patients diagnosed with acute disseminated encephalomyelitis, affecting mainly children (144) with very classical overlapping clinical characteristics with AQP4-NMOSD. Since then, and until very recently, patients with MOG antibodies who had a negative AQP4 antibody test started to be broadly categorised as seronegative NMOSD (82,83,145,146)

In the last years, the development of CBAs and a better understanding of the differential characteristics of MOGAD patients from AQP4-NMOSD have led to accept MOGAD as a new disease entity, although interesting controversies remain (147). MOGAD is understood as a disease where disability is associated with relapses and not with neurodegeneration in between relapse, as it happens in MS (148,149). However, this is a relatively new disease entity, and more longitudinal studies are needed to prove this concept.

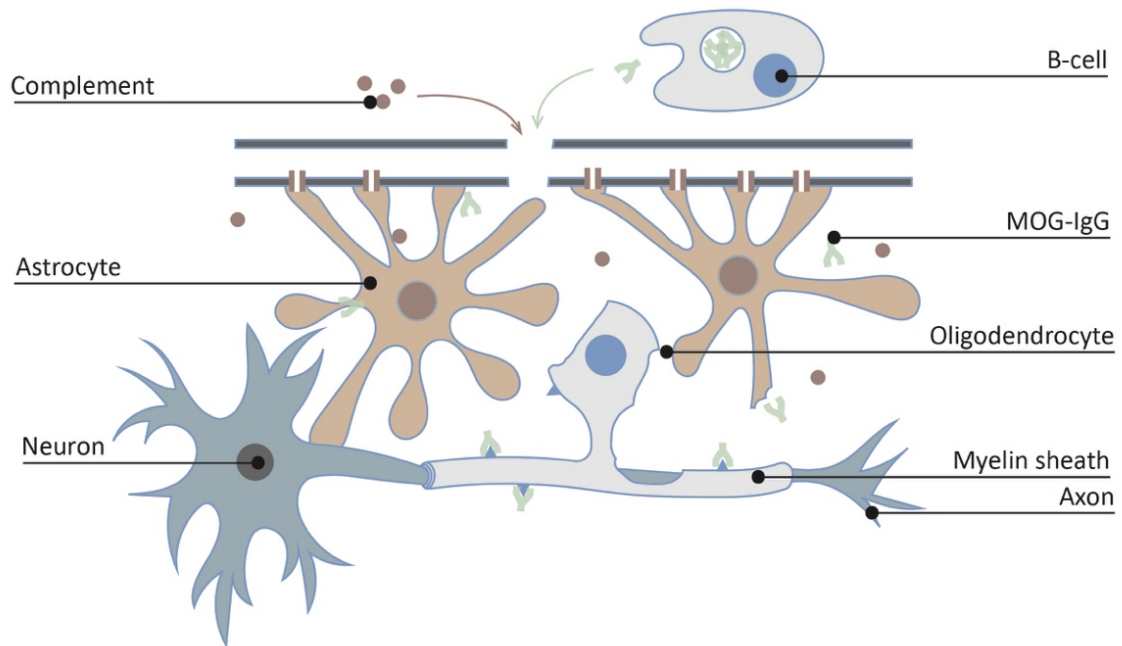
### 1.5.1. Pathophysiology

Myelin oligodendrocyte glycoprotein (MOG) is located mainly at the external lamellae of myelin sheaths on the oligodendrocyte membrane's surface in the CNS. However, in the last decade, low protein expressions have been also found in the periphery of the CNS (150,151).

The main role of MOG is the formation, maintenance and disintegration of myelin sheaths (152) by regulating oligodendrocyte microtubule stability, maintaining the structural integrity of the myelin sheath and mediating the interactions between myelin and the immune system (153). Moreover, MOG may also play a role in the adhesion

between neighbouring myelinated fibres acting as a binder in maintaining axon bundles in the CNS (152,153).

Although MOG antibodies are a marker for MOGAD, the exact pathogenic role of these antibodies is not yet well established. MOG experimental autoimmune encephalomyelitis (EAE) model in rodents has been broadly used as an animal model of MS (154). The EAE model has allowed the study of the combination of pathogenic T-cells and Ab-dependant mechanisms (155). The use of this model in MS is not at all random, as MOG antibody-positive patients often develop MS pattern II active lesions with infiltration of T cells and deposition of IgG as well as activated complement at the sites of ongoing demyelination (156). (Figure 1-21).



---

### Figure 1-21: Pathophysiology of MOGAD

MOG-IgG are produced by mature B-cells, and cross the blood-brain barrier causing myelin damage, by binding to MOG on the surface of the oligodendrocytes.

(Original figure: Adobe Inc., 2019. Adobe Illustrator, Available at: <https://adobe.com/products/illustrator>)

---

## 1.5.2. Epidemiology

The epidemiology of MOGAD worldwide is unknown. In a study performed in the Netherlands between 2014 and 2017, the incidence rate of MOGAD was set to 1.6/1,000,000 persons, with a higher rate in children (157). In the UK population (158) a higher incidence rate of 3.4/1,000,000 person-years was observed, noting an increase in incidence year by year. These changes in incidence are likely to be driven by the recognition of MOGAD as a separate disease entity and its clinical phenotypes. The rise in the number of detected MOGAD cases is also likely to reflect the broader availability of antibody testing.

MOGAD can occur in both young and older populations. However, there is a slight predominance in women with a median onset age in the early thirties (81,159–163). There is a higher prevalence of disease in women (1.8:1) in the UK population, which is nevertheless significantly lower than what it has been observed in AQP4-NMOSD patients.

## 1.5.3. MOG cell-based assay

MOG-IgG were initially measured by western blot or ELISA; however, both tests were associated with low sensitivity and specificity, carrying a high probability for false positives. The CBA employs a full-length human MOG as the target antigen (4) and associated with IgG1 is deemed as the gold standard for testing. To avoid misdiagnosis, testing for the presence of MOG antibody should only be undertaken in selected cases presenting with clinical and paraclinical features of MOGAD (164). MOG antibody titres are higher in relapse than in remission (159), in opposite with what it was described in AQP4-NMOSD. In MOGAD the monophasic course is often associated with decreasing titre levels (81,159,161), followed by a conversion to antibody negativity. However, it is not unusual for antibodies to become positive again.

## **1.5.4. Clinical and paraclinical findings**

In this section we will separately discuss symptoms resulting from the 3 main lesion locations in MOGAD: brain, optic nerve and spinal cord. Acute disseminated encephalomyelitis will be reviewed separately in this section.

### **1.5.4.1. Optic nerve**

The mechanism of ON in MOGAD is a primary inflammatory event with demyelination which induces conduction block, often involving the anterior aspect of the optic nerve with associated disc oedema (165).

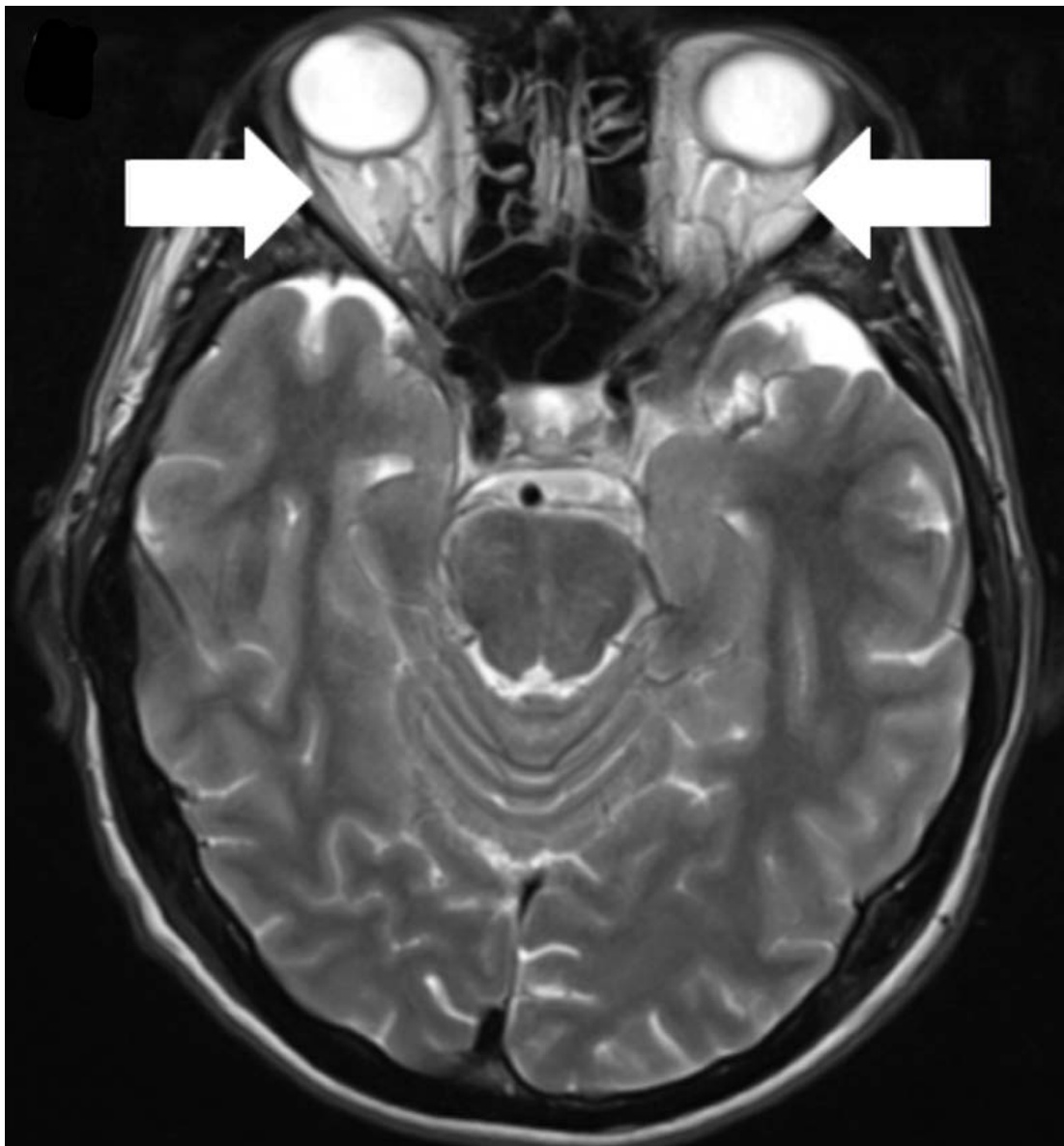
#### **1.5.4.1.1. Clinical manifestations derived from ON in MOGAD**

Acute ON in MOGAD is often simultaneous, bilateral in ~50% of the cases (81). Is associated with optic nerve swelling and often localised in the anterior optic nerve; these features lead to severe and characteristic retinal oedema (papilledema) during the acute phase (165), with neuroaxonal damage accumulating over the post-acute stage and subsequently when new ON attacks occur (166). ON is the most frequent presenting feature, and even more common in relapsing cases. Previous studies have reported that 44-60% of initial attacks (81,167,168) in MOGAD being ON. In the UK cohort, to which part of the population studied in this thesis belongs, 55% presented with optic neuritis: 31% unilateral and 24% bilateral, with 9% of the cohort presenting with simultaneous optic neuritis and transverse myelitis (81).

Previous cohorts have reported up to 88% of patients having had an acute ON at least once (167). Optic neuritis in MOGAD tends to be monophasic, with severe visual loss at onset and good visual recovery. Despite a similar severity of pRNFL and GCIP thinning in AQP4-NMOSD and MOGAD ON visual outcomes diverged; in cases with an identical extent of damage, MOGAD ON eyes presented with better functional visual outcomes than AQP4-NMOSD (169). Such structure/function discordance remains relatively unexplored in MOGAD. Since the retina does not contain myelin, mRNFL and GCIP thinning is expected to result from retrograde degeneration derived from



lesions in the optic nerve, rather than from direct MOG-IgG related injury in the retina, as it may happen in AQP4-NMOSD.



---

**Figure 1-22: MRI of a patient with MOGAD**

Arrows point to bilateral anterior optic nerve involvement. (Original figure: Oxford NMO tissue bank database)

---

### 1.5.4.1.2. OCT findings

The OCT pattern in MOGAD-ON is characterised by severe loss in pRNFL, GCIP and total macular volume (TMV). The extent of the damage in these patients is comparable to the one found in AQP4-NMOSD-ON patients (166,170) (Figure 1-22). A recent systematic review and meta-analysis (169) has revealed that the pooled mean difference for MOGAD-ON eyes compared to HC was  $-35.7 \mu\text{m}$  (95% CI:  $-43.1$  to  $-28.4 \mu\text{m}$ ) for pRNFL and  $-26.7 \mu\text{m}$  (95% CI:  $-32.6$  to  $-20.8 \mu\text{m}$ ) for GCIP. This study found no differences in OCT measures between AQP4-NMOSD-ON and MOGAD-ON eyes (pRNFL:  $-1.9 \mu\text{m}$ ; 95% CI:  $-9.1$  to  $5.4 \mu\text{m}$ ; GCIP:  $-2.6 \mu\text{m}$ ; 95% CI:  $-8.9$  to  $3.8 \mu\text{m}$ ). In eyes without a history of ON, Havla et al. (171) found a reduction in pRNFL and GCIP compared to HC. However, in a different cohort, Oertel et al. (170) did not confirm a significant reduction in pRNFL. Due to the lack of myelin in the retina, these changes in eyes without a history of ON cannot be associated with primary retinal damage and are more likely to be associated with a subclinical inflammatory event of the optic nerve. This hypothesis needs further investigation in larger cohorts of patients never experiencing ON.

The damage accrual in MOGAD patients seems to be associated with higher relapse rates instead than attack severity (166). Several studies suggest that besides the neuroaxonal damage due to the effect of ON relapses, visual impairment would accumulate due to subclinical inflammatory events in these patients (166,171). However, whether there is neurodegeneration independent of clinical attacks in these patients is something that remains to be proven with larger longitudinal studies (172)

Longitudinal studies in MOGAD patients have shown progressive pRNFL thinning (170). However, currently available studies on MOGAD visual system included small cohorts, used heterogeneous/non reproducible methods and show conflicting results. Larger cohorts and more standardized protocols are needed to reliably characterize retinal changes in MOGAD patients (83,166,170,171).

### **1.5.4.1.3. VEP findings**

The field of VEP in MOGAD has been relatively unexplored. A multicentric study published in 2016 with 16 MOGAD patients reported 60% of ON eyes with abnormal P100 latencies, 10% of them despite having normal pRNFL, while 10% of fellow eyes showed reduced pRNFL but normal VEPs. All eyes without previous history of ON presented with normal P100 latencies (166). However, these results were only partially confirmed by a recent study with 39 MOGAD adults, where VEP latencies were found only moderately prolonged, with no significant differences between affected and unaffected eyes. A significant reduction of the VEP amplitudes was observed in the affected eyes (173). Several case reports have been published, including VEP as a clinical feature; however, bigger clinical cohort studies will be needed to understand the extent of damage in the afferent visual system in MOGAD patients both with and without ON.

### **1.5.4.1.4. MRI findings**

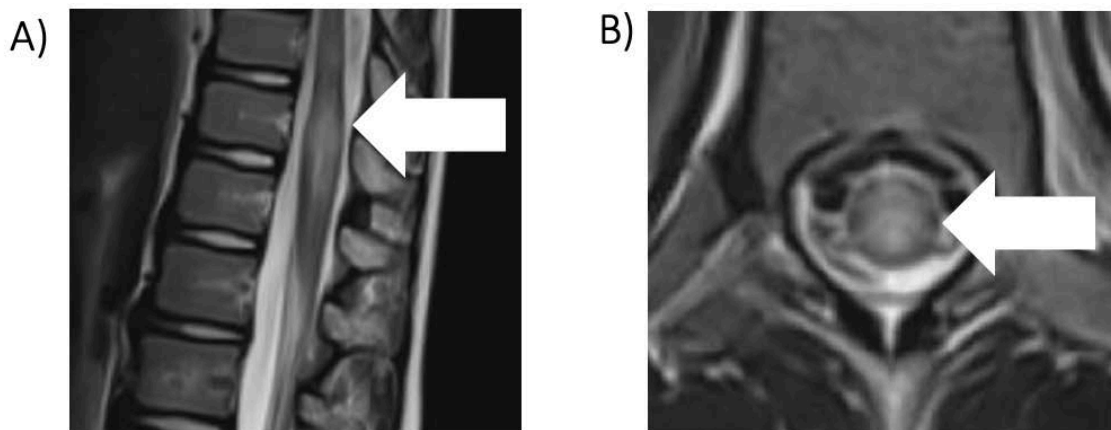
As I mentioned in previous sections, lesions derived from ON in MOGAD patients are generally bilateral, characterized by affected long sections in the anterior part of the optic nerve with periorbital enhancement (more than half of the pre-chiasmatic optic nerve length) (106). After an ON, optic nerve lesions are characterized by extensive T2-weighted image (T2WI)/short tau inversion recovery (STIR) orbital MRI with contrast enhancement and perineural oedema in the anterior sections with no optic chiasm involvement as it happens in AQP4-NMOSD or MS (Kitley et al., 2014; Sato, Callegaro, Lana-Peixoto, Waters, de Haidar Jorge, et al., 2014). In 2018, Chen et al. published an observational study where perineural enhancement was reported in 50% of the patients, and longitudinally extensive involvement in 80% (107). One year later, Song et al. investigated 110 MOGAD patients (where 52.7% were paediatric), confirming the previous results and showing optic nerve peri-neural enhancement in 52.0% of patients, with extensive longitudinal involvement in 87.7% of the patients. Moreover, intracranial optic nerve involvement was significantly more prevalent in the paediatric population than in adults in this study

(174). A year later, Schmidt et al. reported decreased parallel diffusivity within the optic nerves of MOGAD patients after acute ON, suggesting that parallel diffusivity may be associated with various mechanisms of axonal damage, such as Wallerian degeneration and diffuse axonal injury (175). In a recent study with 80 MOGAD patients, 16% showed chiasmal involvement, and of those, 54% presented with longitudinally extensive optic nerve enhancement, from orbit extending to chiasm (109).

### 1.5.4.2. Spinal cord

Spinal cord lesions in MOGAD can be characterized by multiple long and short lesions (more or less than 3 segments), with a tendency to appear in the lower spinal cord segments, including the conus (82,83).

A recent study describing the 'H' sign seen on acute axial T2 imaging in MOGAD adds new information to the central cord involvement in patients with MOGAD, that may be limited to the grey matter (176) (figure 1-23). MOGAD myelitis shows a predilection for involvement of the lower spinal cord, including the medullary cone (177).



---

**Figure 1-23: Example of cord involvement in a MOGAD patient**

A) conus lesions and B) central grey matter involvement. (Original figure: Oxford NMO tissue bank database)

---

In the UK cohort, LETM was the initial presentation of MOGAD in 14% of the patients, with 4% presenting with short transverse myelitis and 9% presenting with simultaneous optic neuritis and transverse myelitis (81). These different presentations are thought to be age-related, with large inflammatory lesions (LETM) being more characteristic of younger age and short TM being associated with older age (81,159). Acute myelitis in MOGAD commonly manifests with sensory or motor deficits that can cause bladder and sexual dysfunction (due to the sacral involvement) (160). Other myelitis symptoms can be tetra/paraparesis, dysesthesia and pain (153). Symptoms typically progress over days to varying degrees of dysfunction.

### **1.5.4.3. Brain**

Brainstem lesions are a common feature in MOGAD (figure 1-24) and are present in around one-third of MOGAD patients with ON and/or myelitis. Lesions within the dorsal medulla oblongata may cause symptoms that resemble AQP4-NMOSD (intractable nausea, vomiting, hiccup and cough symptoms of the area-postrema syndrome), however, intractable vomiting and hiccups occur less commonly in MOGAD than in AQP4-NMOSD, and these patients do not normally present with area postrema symptoms (115). In contrast, other locations may cause symptoms that resemble MS (dysarthria, dysphagia, internuclear ophthalmoplegia, third nerve palsy with diplopia, nystagmus, trigeminal hypesthesia or facial nerve paresis) (178). The hypothalamic area is not normally affected in MOGAD, as it happens in AQP4-NMOSD. The cerebellum, which is often involved in MS, is normally not involved in MOGAD associated lesions.

In the last years, cerebral cortical lesions have also been described in these patients mostly associated with epileptic seizures (179,180). This phenotype of MOGAD has been recently described, and although rare, acute epilepsy attacks seem to be 20 times more frequent in MOGAD than in AQP4-NMOSD (181).

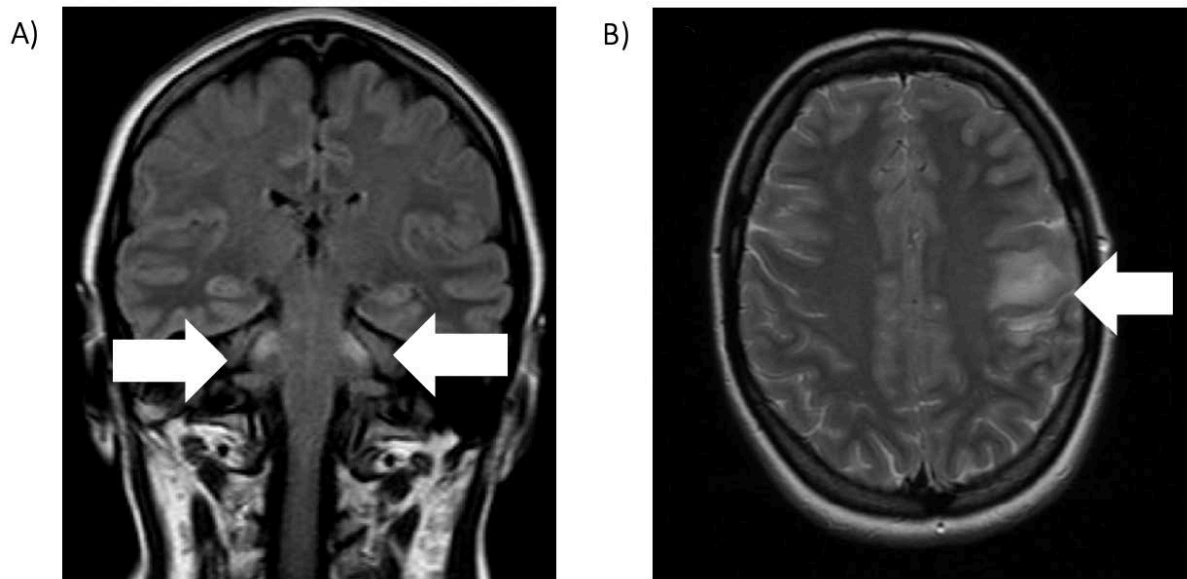


**Figure 1-24: Example of brain lesions in a patient with MOGAD**

A) Bilateral cerebellar peduncle lesions and B) cortical involvement. (Original figure: Oxford NMO tissue bank database)

#### 1.5.4.3.1. The ADEM presentation

ADEM is a widespread inflammation of the white matter that affects the brain and spinal cord, and is the most common presentation in the paediatric MOGAD population (144). Symptoms include systemic manifestations (fever, headache, nausea, vomiting, malaise, altered mental status) and other more specific, which vary based upon the locations of the lesions within the CNS (vision impairment, ataxia, hemiparesis, hemisensory loss) (153). MOGAD ADEM/brainstem lesions carried a risk of permanent cognitive impairment of 40% (81).

In children, MOGAD tends to present with ADEM-like onset attacks in a younger population compared to AQP4-NMOSD. Young children have been shown to have the best recovery among the MOGAD population (159).

### 1.5.5. Diagnostic criteria

There are no current diagnostic criteria for MOGAD; however, in May 2018, a group of experts (182) outlined the first international recommendations for the indication of MOG-IgG testing in patients presenting with acute CNS demyelination of putative autoimmune aetiology (table 1-2).

1. *Monophasic or relapsing acute optic neuritis, myelitis, brainstem encephalitis, encephalitis, or any combination, **and***
2. *radiological or, only in patients with a history of optic neuritis, electrophysiological (VEP) findings compatible with CNS demyelination, **and***
3. *at least one of the following findings:*

#### **MRI:**

- a. *Longitudinally extensive spinal cord lesion ( $\geq 3$  VS, contiguous) on MRI (so-called LETM)*
- b. *Longitudinally extensive spinal cord atrophy ( $\geq 3$  VS, contiguous) on MRI in patients with a history compatible with acute myelitis*
- c. *Conus medullaris lesions, especially if present at onset*
- d. *Longitudinally extensive optic nerve lesion (e.g.,  $>1/2$  of the length of the pre-chiasmal optic nerve, T2 or T1/Gd)*
- e. *Perioptic Gd enhancement during acute ON*
- f. *Normal supratentorial MRI in patients with acute ON, myelitis and/or brainstem encephalitis*
- g. *Brain MRI abnormal but no lesion adjacent to a lateral ventricle that is ovoid/round or associated with an inferior temporal lobe lesion and no Dawson's finger-type or juxtacortical U fibre lesion (Matthews- Juryńczyk criteria (183))*
- h. *Large, confluent T2 brain lesions suggestive of ADEM*

#### **Fundoscopy**

- i. *Prominent papilledema/papillitis/optic disc swelling during acute ON CSF*

#### **CSF**

- j. *Neutrophilic CSF pleocytosis or CSF WCC  $> 50/\mu\text{l}$*

- k. No CSF-restricted OCB as detected by IEF at first or any follow-up examination (applies to continental European patients only)

**Histopathology**

- l. Primary demyelination with intralesional complement and IgG deposits  
m. Previous diagnosis of “pattern II MS”

**Clinical findings**

- n. Simultaneous bilateral acute ON  
o. Unusually high ON frequency or disease mainly characterized by recurrent ON  
p. Particularly severe visual deficit/blindness in one or both eyes during or after acute ON  
q. Particularly severe or frequent episodes of acute myelitis or brainstem encephalitis  
r. Permanent sphincter and/or erectile disorder after myelitis  
s. Patients diagnosed with “ADEM”, “recurrent ADEM”, “multiphasic ADEM” or “ADEM-ON”  
t. Acute respiratory insufficiency, disturbance of consciousness, behavioural changes, or epileptic seizures (radiological signs of demyelination required)  
u. Disease started within 4 days to ~ 4 weeks after vaccination  
v. Otherwise unexplained intractable nausea and vomiting or intractable hiccups (compatible with area postrema syndrome)  
w. Co-existing teratoma or NMDAR encephalitis (low evidence)

**Treatment response**

- x. Frequent flare-ups after IVMP, or steroid-dependent symptoms (including CRION)  
y. Clear increase in relapse rate following treatment with IFN-beta or natalizumab in patients diagnosed with MS (low evidence)

---

**Table 1-2: International recommendations for the diagnosis of MOGAD**

Reproduced under the terms of the Creative Commons Attribution 4.0 International License

---



---

(<http://creativecommons.org/licenses/by/4.0/>), which permits unrestricted use, distribution, and reproduction in any medium).

---

In November 2018, researchers from the Mayo Clinic suggested simplified criteria for the diagnosis of MOGAD (184) (table 1-3).

1. *Laboratory findings based on a MOG-IgG positive cell-based assay.*
2. *Clinical findings. Any of the following:*
  - a. *ADEM.*
  - b. *Optic neuritis, including chronic relapsing optic neuropathy.*
  - c. *Transverse myelitis (short or long segments).*
  - d. *Brain or brainstem syndrome, compatible with demyelination.*
  - e. *Any combination of the above.*
3. *Exclusion of any other alternative diagnosis.*

---

**Table 1-3: Simplified diagnostic criteria for the diagnosis of MOGAD**

---

## 1.5.6. Disease Course

The most common onset feature in MOGAD is optic neuritis (ON), followed by myelitis and ADEM or ADEM-like attacks (81,159,161,167).

Between 44%-83% of the patients with MOGAD follow a relapsing course (81,159,161) with most of these relapses happening in the first two years of the disease (81,159). The monophasic course is associated with decreasing titre levels (81,159,161), suggesting that patients who become seronegative may be less likely to relapse in the future. Further relapses, following the common ON onset tendency, usually involve the optic nerve (81,159), with up to 80% of patients with an initial episode of optic neuritis developing at least one more optic neuritis attack (107). Despite having a significantly higher ON relapse rate than AQP4-NMOSD patients, MOGAD tends to accrue less disability and have better visual outcomes (169,185).

Disability in MOGAD seems to be relapse-related and appears to be driven by the degree of recovery from the initial attack. Although some studies report no difference between monophasic and relapsing disease courses (186), it is likely that disability is also related to the overall number of attacks (81).

Irreversible motor disability is rare in MOGAD, with only 10% of the patients requiring walking assistance (159). It is important to note that the most prevalent disability associated with myelitis is the bladder, bowel, or erectile dysfunction, happening in almost 30% of patients, due to the relatively frequent conus involvement in TM (81,176).

### **1.5.7. Treatment**

To my knowledge, no clinical trials have been conducted in MOGAD, and there is still no consensus on the therapeutic recommendations after the initial attack. For this reason, treatment strategies have been commonly shared with AQP4-NMOSD patients, being the severity of the onset attack, the clinical course of the disease, the persistence of positive antibodies or the occurrence of relapses essential factors in the decision of the most accurate treatment algorithm for each patient.

Relapses, even if mild, must be treated early and aggressively in antibody-mediated conditions. MOGAD patients experience a good clinical recovery after acute treatment with steroids, and the need for a chronic treatment option might be arguable (162). However, recent research has reported a proportion of 76.5% of patients developing relapses in the absence of chronic treatment (167), hypothesising that premature corticosteroid tapering may at least partially explain this phenomenon. To prevent this, it has been recommended to use oral steroids for at least three months and tapering gradually after this (162). The same authors suggest using a chronic immunosuppressive treatment in cases where the initial episode was severe and accrued significant disability.

## **1.6. Literature gaps**

In summary, there are several gaps in the literature that this thesis will aim to address.

*Better understanding of AQP4-NMOSD and MOGAD disease process:* To date there are few longitudinal studies on MOGAD. Those are mostly multicentric, carrying the limitation of potential variability in scanning protocols and QC process. Moreover, eyes from patients who never suffered from ON attacks (so called in this thesis “never affected” eyes) and fellow eyes from contralateral ON have often been treated as a single entity, while the underlying pathological process might be different.

*Help defining the optimal clinical management:* it is crucial to understand how long the post-acute stage lasts in both AQP4-NMOSD and MOGAD ON eyes while in those with no clinical events, subclinical damage needs more sensitive testing.

These gaps will be addressed in the following sections using one of the biggest cohorts currently available with two longitudinal and one cross-sectional study using OCT, VEP and foveal morphometry.

## **2. RATIONALE OF THE THESIS**

As highlighted in the introduction of this thesis, there is uncertainty regarding anterior visual pathways (retina and ON) changes overtime in patients with AQP4-NMOSD and very few studies have investigated the visual pathways in the relatively newly defined MOGAD. In a collaborative work with Charité – Universitätsmedizin Berlin (92), we have found ganglionar cell loss over time independently of ON attacks in small group of AQP4-NMOSD patients. This finding suggested that retinal damage was occurring independently of ON in these patients. Confirming these results would be important to the understanding of AQP4-NMOSD pathology and course. Was the ganglion fibre loss due to ongoing neurodegeneration or due to a primary retinopathy? Is there retinal/optic nerve damage independently of ON events? To answer these questions, I have investigated and quantified retinal and optic nerve changes in a cohort of AQP4-NMOSD patients and healthy controls.

Furthermore, as previously summarized, retinal changes and their longitudinal evolution in MOGAD patients have not been systematically described in the literature, and the existing studies have very small sample sizes. Further, direct comparisons between visual pathway changes between AQP4-NMOSD and MOGAD are scarce, and bigger sample size comparisons are needed. Therefore, the second general aim of this thesis was to characterize retinal disease in ON and NON-ON eyes in a large cohort of MOGAD patients.

## **3. HYPOTHESIS**

The conduction of this thesis will be based on the following hypothesis:

1. Retinal damage after ON is permanent in AQP4-NMOSD and MOGAD however, this does not have a neurodegenerative progressive component. In AQP4-NMOSD, changes after ON affect the foveal shape but these are not evolving outside the relapses.
2. Fellow eyes (from contralateral affected ON eyes) are affected in AQP4-NMOSD due to the nature of posterior lesions, but not in MOGAD.
3. Eyes “never affected” (from patients with no history of ON) do not present with macular or foveal changes in AQP4-NMOSD or MOGAD.
4. After ON, there is structure-function concordance in AQP4-NMOSD but not in MOGAD, in eyes not affected by ON, there is structure-function concordance in both disease groups.

## **4. OBJECTIVES**



## **4.1. Main Objective**

This thesis aims to explore, cross-sectionally and longitudinally, the structure-function of the retina in patients affected with AQP4-NMOSD and MOGAD.

## **4.2. Secondary objectives**

1. To describe retinal changes in AQP4-NMOSD and MOGAD eyes, particularly in eyes never affected by ON.
2. To describe subclinical retinal damage in AQP4-NMOSD and MOGAD patients with normal central visual function and its relation to outcomes in paraclinical tests.
3. To describe parafoveal involvement and changes in foveal change in AQP4-NMOSD and its potential diagnostic implications.

# **5. METHODOLOGY**

To address the hypothesis and objectives stated in the previous sections, I conducted 3 different research projects that helped me defining the structural integrity in AQP4-NMOSD and MOGAD patients (project 1) with a special focus on the foveal changes in AQP4-NMOSD (project 3), and to understand the relationship between structure and function (project 2) in both diseases.

## 5.1. Cohort descriptions

In this thesis, four different cohorts from two different centres were studied (table 5-1). These cohorts and their recruitment ethics numbers will be explained in this section. In table 1, each project is associated with the cohorts used for the specific analysis. All research in this thesis has been conducted in accordance with the current version of the Declaration of Helsinki and the applicable British and German laws. All participants gave written informed consent. The inclusion criteria described in this section for each project are cohort specific, and project specific inclusion criteria will be described in the following pages (sections 5.2.1., 5.2.2. and 5.2.3.)

Project	Disease population	Healthy controls
<b>Project 1</b> <i>Structural retinal imaging in AQP4-NMOSD and MOGAD</i>	- NMO Tissue Bank (UK)	- Babinski Project (UK)
<b>Project 2</b> <i>Structure-function relationship in the visual system of patients with AQP4- NMOSD and MOGAD disease</i>	- NMO Tissue Bank (UK) - Babinski Project (UK)	- Babinski Project (UK)
<b>Project 3</b> <i>Foveal changes in AQP4-NMOSD</i>	- NMO Tissue Bank (UK) -NeuroCure-Charité NMOSD cohort (GER)	- Babinski Project (UK) - VIMS study (GER)

---

**Table 5-1: Cohorts used in this thesis' projects**

---

## 5.1.1. The NMO tissue bank [Projects 1, 2 and 3]

**Ethics number:** 16/SC/0224

**Informed consent:** Yes

**Description:** Study of Neuromyelitis Optica Spectrum Disorders (NMOSD), Myelin oligodendrocyte glycoprotein antibody disease (MOGAD): clinical, genetic and immunological studies.

**Site of recruitment:** Oxford University Hospitals-University of Oxford in the United Kingdom.

**Inclusion criteria:**

- Patients with neurological syndromes suspected of NMOSD or MOGAD
- Adult willing and able to give informed consent for participation in all or part of the study.
- Child under 16 whom parents or guardian has provided informed consent.

**Exclusion Criteria:**

The tissue may not be collected if ANY of the following apply:

- In the investigator's opinion taking part may cause distress to participants and or families.
- In the investigator's opinion, participation in the study would be detrimental to the patient.
- Unwilling to provide informed consent
- Unable to give informed consent

**Data collection relevant to this thesis:** Data was collected directly from patients attending clinics for regular outpatient appointments or as inpatients and from their clinic notes, including any retrospective relevant information, GP information, investigation results and imaging.

Participants were asked to complete a questionnaire which collected the following information: demographics, past medical history and family medical history. All participants undergo an OCT assessment in the Eye Clinic- John Radcliffe Hospital in Oxford under the following protocol: optic disc assessment and macula assessment 25° x 30°, 61 vertical B-scans ART 11-22. In difficult cases where the patient may have fixation problems, this protocol may be altered. All OCTs are assessed by an ophthalmologist in weekly multidisciplinary team meetings.

## 5.1.2. The BABINSCI project [Projects 1,2 and 3].

**Ethics number:** 17/EE/0246

**Informed consent:** Yes

**Description:** This study aims to investigate three neurological disorders characterised by inflammation and demyelination: Neuromyelitis Optica Spectrum Disorders (NMOSD), Myelin oligodendrocyte glycoprotein antibody disease (MOGAD) and Multiple sclerosis (MS).

**Site of recruitment:** Oxford University Hospitals and WIN Centre, both at the University of Oxford in the United Kingdom.

### **Inclusion criteria:**

- Participant is willing and able to give informed consent for participation in the study.
- Fluency in the English language in order to complete the consent form and MRI safety questionnaire.
- Male or Female, aged 16 years or above.
- Diagnosed with AQP4-IgG positive NMO, MOG-Ab disease or MS (as specified above) or, if healthy volunteer study participant should be in good health.

### **Exclusion Criteria:**

The participant may not enter the study if ANY of the following apply:

- Any contraindication to MRI scanning
- Participant unwilling to sign consent; or unable to fully understand consent or MRI safety questionnaire
- Pregnancy
- A concurrent disease/disorder that, as determined by the specialist neurologist, may confound the data or lead to an undue risk to the patient.

**Data collection relevant to this thesis:** optic disc assessment and macula assessment 25° x 30°, 61 vertical B-scans ART 11-22. In complicated cases where the subject may have a fixation problem or difficulties keeping the eyes opened, this protocol may be slightly altered. All the OCTs have been reviewed by me. All the OCTs not following OSCAR-IB and APOSTEL criteria were discarded after the initial assessment. Automatic segmentation of the macular layers, followed by a manual correction by me, was performed.

### **5.1.3. The NeuroCure-Charité NMOSD cohort [Project 3].**

**Ethics number:** EA1/131/09

**Informed consent:** Yes

**Description:** Study of Neuromyelitis Optica Spectrum Disorders (NMOSD), Myelin oligodendrocyte glycoprotein antibody disease (MOGAD): clinical, MRI and ophthalmological data.

**Site of recruitment:** NeuroCure Clinical Research Centre (NCRC) – Charité Universitätsmedizin Berlin in Germany.

**Inclusion criteria:** All NMOSD and MOGAD patients attending to NeuroCure Clinical Research Centre (NCRC) – Charité Universitätsmedizin Berlin were included in this cohort.

**Exclusion criteria:** Patients not diagnosed with NMOSD or MOGAD.

**Data collection relevant to this thesis:** Data was collected directly from patients attending clinics for regular outpatient appointments or as inpatients and from their clinic notes, including any retrospective relevant information, GP information, investigation results and imaging. In addition, cohort study recruits EDSS, cognitive assessment, MRI and visual assessments annually. Data is collected and stored via RedCap.

## 5.1.4. The VIMS study cohort [Project 3].

**\*\* NOTE:** although this cohort is formed by patients and healthy controls. In this thesis I will only include healthy controls from the VIMS project.

**Ethics number:** EA1/182/10

**Informed consent:** Yes

**Description:** OCT examination loss of nerve cells and fibres and measurable longitudinal changes that can be detected that reflecting disease activity, disease progression, and disease severity in patients with MS and its comparison with a HC cohort.

**Site of recruitment:** NeuroCure Clinical Research Centre (NCRC) – Charité Universitätsmedizin Berlin in Germany.

**Inclusion criteria:**

- Male or Female, aged 20-69
- Signed informed consent
- Diagnosis of Multiple sclerosis (RRMS, PPMS, SPMS)
- Healthy control

**Exclusion criteria:**

- Eye disease that could interfere with OCT (e.g., glaucoma, diabetic retinopathy)

Data collection relevant to this thesis: Data is being collected yearly in 10 years follow up examination. This cohort study recruits EDSS, cognitive assessment and visual assessments annually. Data is collected and stored via RedCap.

## 5.2. Methodology by project:

### 5.2.1. PROJECT 1: Structural retinal imaging in AQP4-NMOSD and MOGAD

#### 5.2.1.1. Study population

Retrospectively collected data of AQP4-NMOSD patients and MOGAD patients with no other ophthalmologic or neurological disease was extracted from the Diagnostic and Advisory Service for Neuromyelitis Optica OCT database in Oxford (NMO Tissue Bank (UK)) (see section 5.1.1 in this thesis). Healthy controls data was acquired prospectively as part of a different research ethics project (BABINSCI project (UK)) (see section 5.1.2 in this thesis).

Specific inclusion criteria for all the patients for this project were:

1. Clinic diagnosis of AQP4-IgG seropositive NMOSD according to the 2015 diagnostic criteria with a positive IgG test (119) or clinical diagnosis of MOGAD (182).
2. A minimum of 1 year since last ON to OCT.
3. No ON between timepoints.
4. Minimum age, 16 years old.

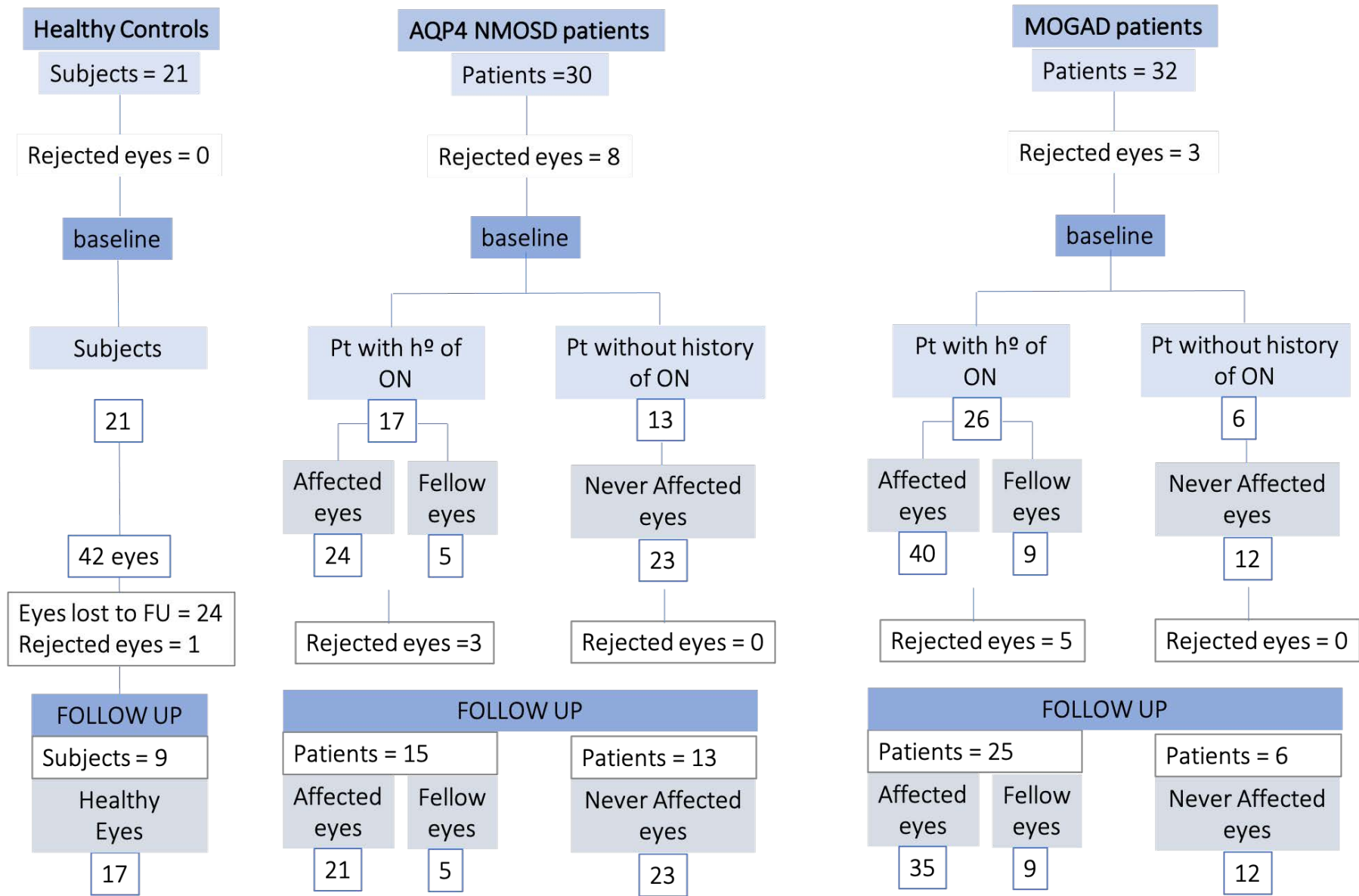
Specific inclusion criteria for the healthy population in this project were:

1. Minimum age, 16 years old.
2. No ocular nor systemic diseases
3. Absence of abnormalities that might affect visual functions or refractive development
4. Absence of eye pathology and conditions

Exclusion criteria were: ophthalmological or other neurological comorbidities potentially influencing OCT results.

A flow diagram of the clinical cohort is presented in Figure 5-1.





---

**Figure 5-1: Cohort Flowchart for project 1**

Flowchart of participants and eyes from the study cohort. Abbreviations: AQP4-NMOSD, aquaporin-4 antibody positive, neuromyelitis optica spectrum disease; MOGAD IgG seropositive, Myelin oligodendrocyte glycoprotein antibody; Pt, patients; h<sup>o</sup>, history; ON, optic neuritis eyes; NON eyes, eyes without a history of ON. At baseline, in the AQP4-NMOSD 8 eyes were excluded from the analysis, 7 eyes due to poor image quality or technical issues and 1 eye due to amblyopia. In the MOGAD group, 3 eyes were excluded from the analysis due to poor image quality or technical issues. In addition, in the follow-up scans, three AQP4-NMOSD eyes and 5 MOGAD eyes were lost to follow up due to poor imaging quality.

---

**5.2.1.2. Optical Coherence Tomography**

All patients were retrospectively scanned, healthy controls were prospectively scanned on Spectralis spectral-domain devices (SD-devices) (Heidelberg Engineering, Heidelberg, Germany) with automatic real-time (ART) function for image averaging. All clinical disc scans have been acquired with an activated eye tracker using 3.4mm ring scans around the optic nerve (12°, 1536 A-scans, 1≤ART≤ 99). Combined ganglion cell layer and inner plexiform layer volume (GCIP), macular volume (TMV), inner nuclear layer (INL) and retinal nerve fibre layer in the macula (mRNFL) were calculated as a 3mm diameter cylinder around the fovea for a macular volume scan (30° x 25°, 61 vertical B-scans, 7≤ART≤ 22). Foveal thickness (FT) was measured as the mean thickness of a 1mm diameter cylinder around the fovea for the macular scan between the internal limiting membrane and the Bruch's membrane.

Intraretinal semi-automatic segmentation was performed for all data with HEYEX software (version 1.10.4.0 with viewing module 1.0.16.0., Heidelberg Engineering, Germany). The images were checked to correct segmentation errors and discard scans of insufficient quality. OCT data presented in this study follows OSCAR-IB quality criteria (46) and APOSTEL recommendations (187).

It is important to note that, to the best of my knowledge, there are no published results on repeatability coefficient of Heidelberg machines, and the longitudinal variation in the results must be interpreted with caution.

### 5.2.1.3. Statistical methods

Group differences between AQP4-NMOSD, MOGAD and HC were calculated with one-way ANOVA for age and the chi-squared test for multiple groups for sex. Shapiro test was performed to assess whether the dependent variables followed a normal distribution. A quantile-quantile (Q-Q) plot in which two sets of quantiles were plotted against one another was used to support this, acting as a graphical tool to help assessing this phenomenon. If both sets of quantiles come from the same distribution, the points forming a line will be plotted straight and, therefore, will indicate a normal distribution. The package 'quantile' from R (version 3.6.2) was used in this analysis.

When data was not shown to be normal, the package 'BestNormalize' was used to find the best calculation to normalise the variable. This package contains a suite of transformation-estimating functions that can be used to normalise data. The normalisation transformations options available were: Lambert W x F transformation, Box-Cox transformation, Yeo-Johnson transformation, Ordered Quantile technique, logarithmic, exponential, inverse hyperbolic sine function. The 'BestNormalize' function selects the best transformation according to the Pearson P statistic. For this chapter, the chosen transformations were: The ordered quantile technique (ORQ) for pRNFL, GCIP, INL and mRNFL; exponential transformation for TMV and square root transformation for INL. The ORQ is based on the linear interpolation between two of the original data points. On new data outside the original data range, this transformation uses a shifted logit approximation of the ranks to the original data, this approximation is often relatively minimal since we should not expect to see many observations outside the observed range. The exponential transformation is performed by calculating the exponential function of  $x$ , which is the inverse function of the logarithm; and the square root transformation  $x^{(1/2)} = \text{sqrt}(x)$  reduces the right skewness and can be applied to zero values. It is commonly applied in very low values. After selecting and transforming the variable with the correct function, the Shapiro test and QQ-plots were repeated to re-assess the process.

Multivariate linear mixed-effects models (LME) adjusted by sex and age were performed to analyse differences in baseline OCT parameters (pRNFL, GCIP, TMV, FT, INL and mRNFL). In addition, random effects in the LME models were applied to account for inter-eye correlations of monocular measurements. Finally, group

comparisons were established by obtaining estimated marginal means (EMMs) for the mixed effect model. The first challenge in the cross-sectional and longitudinal study of the eyes is the existence of inter-eye correlation, which means that each data point (each eye) does not represent an independent observation (one person = two eyes). Therefore, most of the standard statistical methods assume the independence of data points.

Including two eyes in the same comparison group and assuming that they are independent observations would bias the estimation of variance, leading to unreliably small p-values with narrow confidence intervals. Including two eyes in different comparison groups assuming that they are independent observations would bias the estimation of the variance, leading to unreliably large p-values with too wide confidence intervals, making this analysis unreliable and meaningless. One possible way to overcome this problem would be to use one eye per subject, or the average of both eyes. However, these methods would significantly reduce sample size - particularly dramatic when studying a rare disease - leading to a loss of information depending on the degree of inter-eye correlation in each patient (188).

For this reason, this thesis proposes the use of linear mixed-effects models (189) which allow us to account for inter-class correlations of monocular measurements together with the use of nested random effects to account for the repeated measures of non-independent observations in the longitudinal context.

LME models in the cross-sectional context aim nothing but to express the relationships in the data in terms of a function. Each person contributes with two eyes to the analysis, which would violate the independence assumption of a linear model; therefore, this design takes into account that each subject will contribute with data twice to the analysis, where every pair of eyes has an idiosyncratic factor that will affect all responses from the same subject, making these different responses inter-dependent rather than independent. LME models deal with this situation by adding random effect for each subject, which will allow resolving the non-independence violation. Moreover, this approach would allow modelling any individual differences by assuming different random intercepts for each subject, for example, if there were clear gender differences. Essentially, the linear mixed models divide the world into things that we understand or that are systematic (exploratory variables, also called fixed effects) and things that we cannot control for (standard error, also called random effects). However, unlike the linear models, where the general standard error exists too, LME models add one more

random effect by giving structure to the error term, which informs the model which factor in the analysis is more likely to be introducing the error. In the case of this thesis will be “Patient ID”, The combination of fixed and random effects is what makes a mixed model.

Longitudinal analysis was performed using the LME model described above, including an interaction term for follow up (Time) to explore the longitudinal component and a nested component in the random effects for “Patient ID/Eye ID”. In addition, the model was adjusted for age and sex. The nesting structure assumes that there is some hierarchy in the grouping of the observations. Each data point of one group (Eye ID) is contained entirely within a single unit of another group (Patient ID). The nesting allows the model to recognise that each patient will appear more than once in the analysis (repeated measures), and for each time point, that patient will appear twice (2 eyes per timepoint). Therefore, in this case, apart from correcting for inter-class correlation of monocular measurements, the model will account for the correlations over time for each patient (190).

The second more obvious modification is the introduction of the ‘Time’ variable. For the experiments contained in this thesis, timepoints were variable between subjects. It was presupposed that the effect of time could be different in each one of the possible disease-group combinations. “Status” was a variable with different factor levels (AQP4-NMOSD eyes with ON (“affected eyes”), eyes without ON in neither eye (“never affected eyes”), eyes without ON with an ON in the contralateral eye (“fellow eyes”), and the same for MOGAD eyes). For this reason, I chose to use the interaction effect, where time interacts with the variable ‘Status’, to show the explanatory variable interaction with another explanatory variable on the effect of the response variable (Time interacts with Status on the retinal thickness outcome). This is the opposite to the “main effect”, which is the action of a single independent variable on the dependent variable. These results provided information about changes over time compared to a HC reference factor.

**NOTE:** For transparency and reproducibility, this section reports detailed explanation of statistical methods which includes LME rationale, variable preparation and model accuracy checking. These are steps that have been also followed for project 2 and 3, however, details will be avoided in further sections to improve clarity and readability.

## **5.2.2. PROJECT 2: *Structure-function relationship in the visual system of patients with AQP4- NMOSD and MOGAD disease***

### **5.2.2.1. Study population**

Two cohorts were analysed:

- 1) A cohort extracted from the Tissue bank at the diagnostic and Advisory Service for Neuromyelitis Optica in Oxford (see section 5.1.1.); and
- 2) A macular sub-study (from the BABINSCI cohort - see section 5.1.2.), where also healthy controls (HC) have been included.

For both cohorts, inclusion criteria for this specific project was:

1. Clinical diagnosis of AQP4-NMOSD according to the 2015 diagnostic criteria (119) or clinical diagnosis of MOGAD;
2. Positive antibody tests based on AQP4-IgG (191) and MOG-IgG (4) cell based assays;
3. No ON between tests (OCT, VEP or HCVA);
4. Normal central visual function defined as LogMAR  $\leq 0$ ;
5. Full ophthalmological assessment (OCT+VEP+HCVA).

For the macular sub-study, the inclusion criteria for healthy control were that they must had HCVA defined as LogMAR  $\leq 0$ .

Inclusion criteria for the healthy population were:

1. Minimum age, 16 years old.
2. No ocular and systemic diseases
3. Absence of abnormalities that might affect visual functions or refractive development
4. Absence of eye pathology and conditions

For all participants, exclusion criteria were:

1. Ophthalmological or neurological comorbidities potentially influencing OCT results
2. HCVA defined as LogMAR  $> 0$ .

### 5.2.2.1.1. NMO tissue bank study population

Retrospectively collected data of MOGAD or AQP4-NMOSD at the hospital routine clinical visits from patients with both clinical OCTs (peripapillary retinal nerve fiber layer, pRNFL) and VEP measurements were included. A flow diagram of the selection process and the final cohort is presented in figure 5-2.

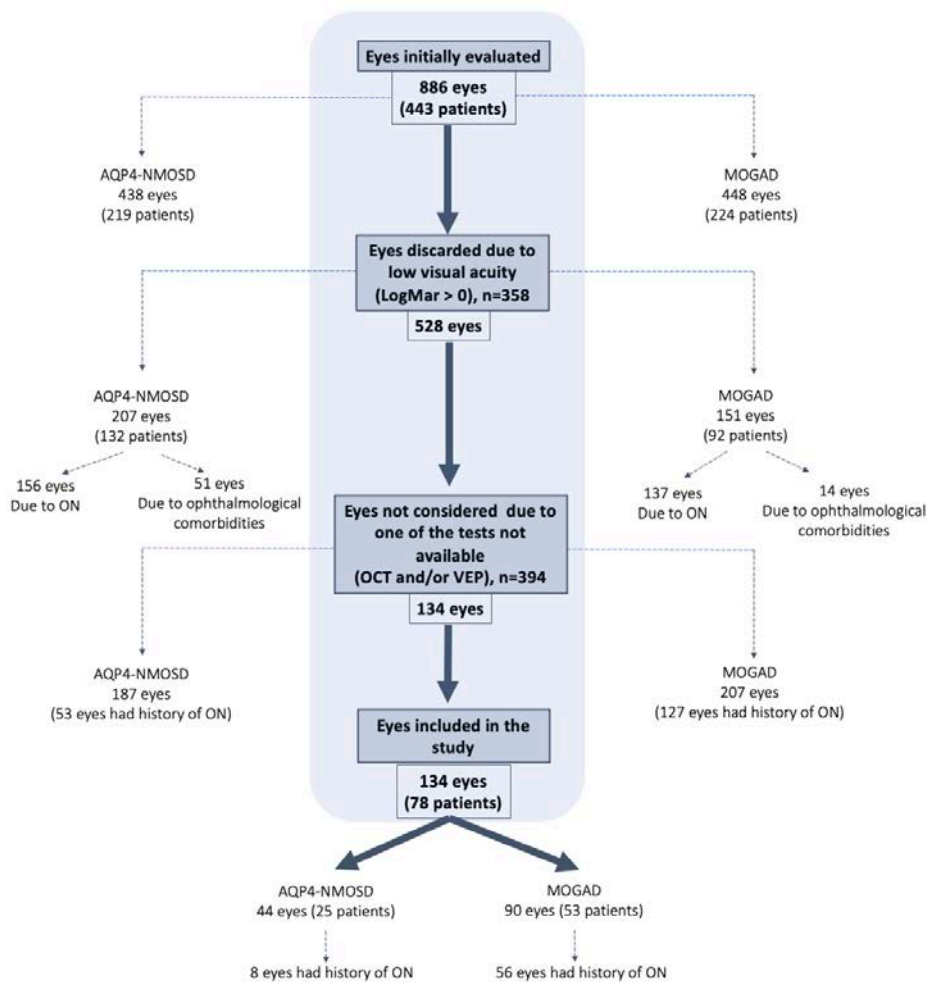


**Figure 5-2: Cohort flowchart for project 2: NMO tissue bank**

Flow chart of cohort selection (blue shade). Exclusions for each group are detailed on the sides of the flowchart (dashed lines). Abbreviations: AQP4-NMOSD, aquaporin-4 antibody positive NMOSD patients; MOGAD, myelin oligodendrocyte glycoprotein associated disease patients; HC, Healthy control participants; ON, optic neuritis eyes; NON eyes, eyes without a history of ON.

### 5.2.2.1.2. Macular sub-study population (BABINSCI cohort)

Prospectively collected data on AQP4-NMOSD and MOGAD patients. A flow diagram of the cohort is presented in figure 5-3.

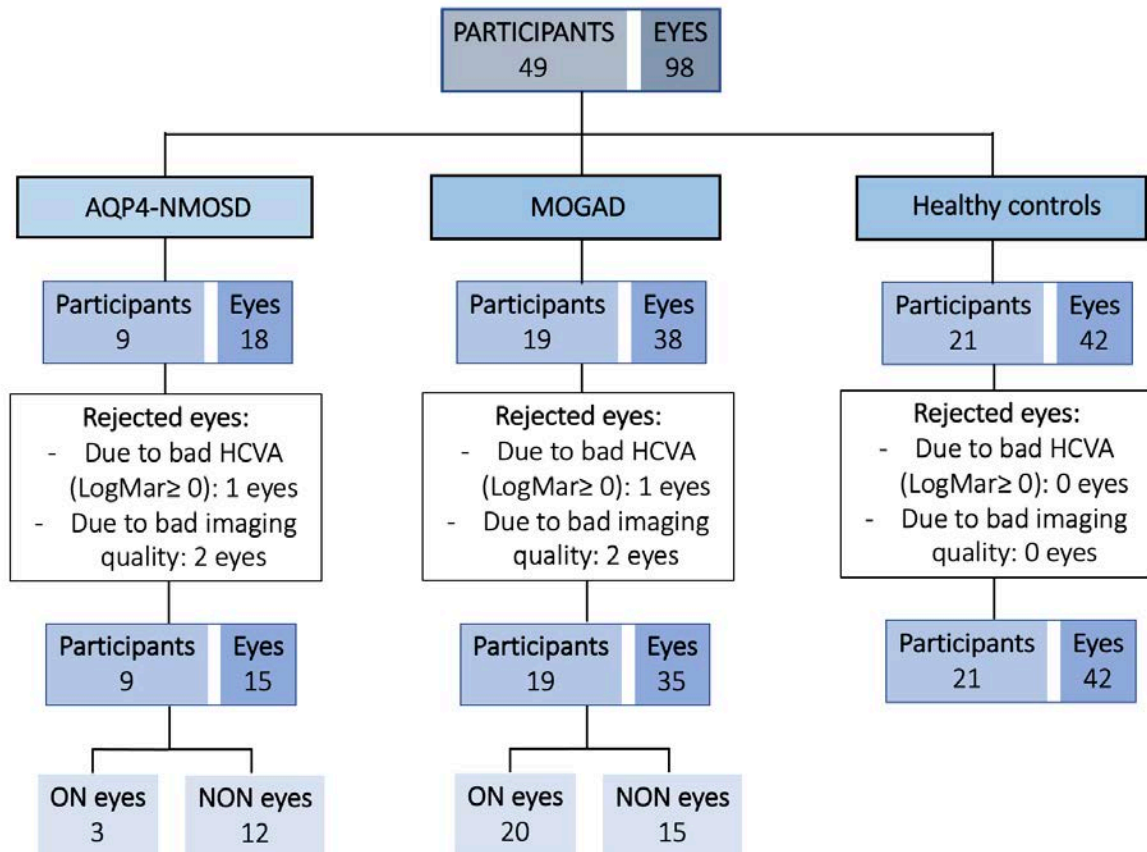


**Figure 5-3: Cohort flowchart for project 2: Macular sub-study**

Flow chart of participants in the advanced research cohort study. Abbreviations: AQP4-NMOSD, aquaporin-4 antibody positive NMOSD patients; MOGAD, myelin oligodendrocyte glycoprotein patients associated disease; HC, Healthy control participants; ON, optic neuritis eyes; NON eyes, eyes without a history of ON.



### 5.2.2.2. Optical Coherence Tomography

All participants and healthy controls were scanned on the same Spectralis spectral-domain device (SD-OCT) (Heidelberg Engineering, Heidelberg, Germany) with automatic real-time (ART) function for image averaging.

Intraretinal semi-automatic segmentation was performed for all data with HEYEX software (version 1.10.4.0 with viewing module 1.0.16.0., Heidelberg Engineering, Germany). The images were checked to correct segmentation errors and discard scans of insufficient quality. OCT data presented in this study follows OSCAR-IB quality criteria (46) and APOSTEL recommendations (187)

**Acquisitions for the NMO tissue bank cohort:** OCT acquisitions for all patients were performed at the Eye Clinic at the John Radcliffe hospital under the same scanning protocol. The peripapillary retinal nerve fiber layer (pRNFL) was measured with an activated eye tracker using 3.4-mm ring scans around the optic nerve (12°, 1536 A-scans,  $1 \leq \text{ART} \leq 99$ ). Definition of abnormality was taken from the Heidelberg Spectralis reports.

**Acquisitions for the macular sub-study cohort:** same Spectralis spectral-domain devices available at the Eye clinic in the John Radcliffe hospital were used (Heidelberg Engineering, Heidelberg, Germany) with automatic real-time function for image averaging to measure disc (pRNFL) and OCT macular volumes. All disc scans were acquired with activated eye tracker using a 3.4mm ring around the optic nerve (12°, 1536 A-scans,  $1 \leq \text{ART} \leq 99$ ). For the macula, combined ganglion cell layer and inner plexiform layer volume (GCIP), macular volume (TMV), inner nuclear layer (INL) and retinal nerve fibre layer in the macula (mRNFL) were calculated as a 3mm diameter cylinder around the fovea for a macular volume scan (30° x 25°, 61 vertical B-scans,  $7 \leq \text{ART} \leq 24$ ). Foveal thickness (FT) was measured as the mean thickness of a 1mm diameter cylinder around the fovea for the macular scan between the internal limiting membrane and the Bruch's membrane. Two AQP4-NMOSD and 2 MOGAD eyes were discarded in this cohort due to bad imaging quality. The fifth percentile in HC research population was calculated for pRNFL, mRNFL, GCIP layers and it was used to define abnormality in OCT. This value was then used in the research population to define abnormality, using a composite biomarker defined by the 5<sup>th</sup> percentile of pRNFL ( $\leq 80 \mu\text{m}$ ) + GCIP ( $\leq 0.55 \text{ mm}^3$ ) + mRNFL ( $\leq 0.12 \text{ mm}^3$ ).

### 5.2.2.3. Visual Evoked Potentials

For both cohorts VEPs were performed during clinical appointments in different clinical laboratories for the NMO tissue bank cohort and at the John Radcliffe hospital in Oxford for the macular sub-study cohort. P100-N140 peak-to-peak amplitudes were measured. Abnormal VEP latency has been defined as per electrophysiology clinical report following in house standard operating procedure. Where no peak or dispersal is seen, VEP is considered clearly abnormal. There was no amplitude recorded in the database. VEPs for HC were not available.

### 5.2.2.4. High Contrast Visual Acuity (HCVA) assessment

High contrast visual acuity was assessed during clinical appointments for AQP4-NMOSD patients and MOGAD patients. Snellen and retro-illuminated Early Treatment for Diabetic Retinopathy Study (ETDRS) were used. HCVA for HC was assessed with Sloan charts at 100% contrast. Both Snellen and Sloan scores were converted into logarithm of the minimum angle of resolution (LogMar) for the purpose of the statistical analysis.

### 5.2.2.5. Statistical methods

In the **NMO tissue bank cohort analysis**, group differences are analysed by Fisher's exact tests for sex and by Mann Whitney U test for age.

**In the macular sub-study analysis**, group differences at baseline between AQP4-NMOSD, MOGAD and HC were calculated with one-way ANOVA for age and chi-squared test for multiple groups for sex.

To calculate differences between groups I performed LME models adjusting for age, sex and race (described in section 5.2.1.3. in more detail). Estimated regression coefficients (B), standard errors (SE) and P values are provided in the results section. Random effects in this model were used to account for inter-eye correlations of monocular measurements and group comparisons were established by obtaining estimated marginal means (EMMs) for the mixed effect logistic model. In the macular sub-study analysis, the number of eyes with normal central visual function and

abnormal VEP was too low to be able to perform any reliable statistical analysis so only descriptions are provided.

These multivariate LME models adjusted were used to analyze differences in baseline OCT parameters both in the NMO tissue bank and macular sub-study cohort. Visual evoked potentials were analyzed in the NMO tissue bank cohort with a mixed effects logistic regression (similar to the linear regression but with a binary outcome variable (VEP: normal/abnormal) adjusted by age, sex and race.

## **5.2.3. PROJECT 3: *Foveal changes in AQP4-NMOSD***

### **5.2.3.1. Study population**

In this retrospective study, patients and controls were followed up in two longitudinal observational studies in Oxford (section 5.1.1.) and Berlin (section 5.1.3.).

Inclusion criteria for patients this study was:

- 1) clinic diagnosis of AQP4-NMOSD according to the 2015 diagnostic criteria (192)
- 2) follow-up examinations with a minimum longitudinal clinical and OCT imaging data of one year
- 3) minimum age of 18 at baseline
- 4) minimum of one year from ON to baseline
- 5) macular OCT scan characteristics to ensure inter-centre compatibility: 61 B-Scans with 768 A-Scans

Exclusion criteria for patients were: ophthalmological or neurological comorbidities potentially influencing OCT results, insufficient OCT image quality, acute ON attacks in the last twelve months, or ON attacks during follow-up.

Inclusion criteria for the healthy population were:

1. Minimum age, 16 years old.
2. No ocular and systemic diseases
3. Absence of abnormalities that might affect visual functions or refractive development
4. Absence of eye pathology and conditions

Data from healthy age and sex matched controls were selected from both centres' image databases (sections 5.1.2 and 5.1.4.), longitudinal OCT data for HC was only available from the Berlin site. A flow diagram of the study cohort is presented in figure 5-4.

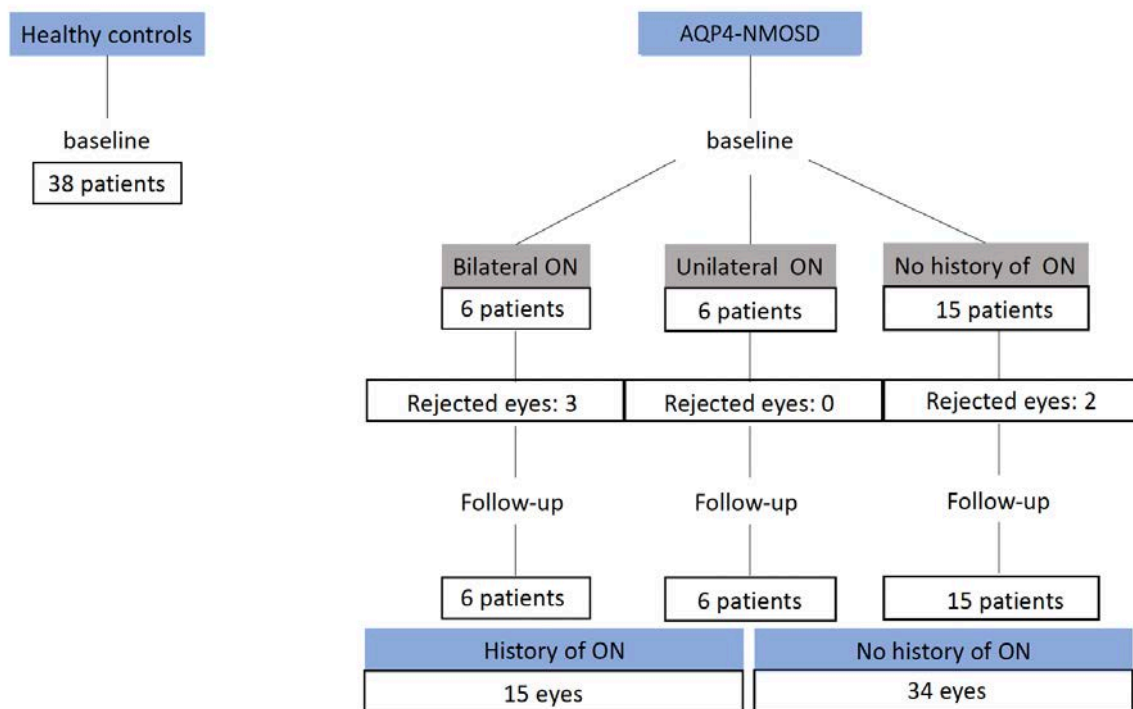


**Figure 5-4: Cohort flowchart for project 3: Study cohort and follow-up**

Flow chart of participants in cohort study. Abbreviations: NMOSD, neuromyelitis optica spectrum disorders; AQP4-NMOSD, aquaporin-4 antibody positive neuromyelitis optica spectrum disease; ON, optic neuritis.

### 5.2.3.2. Optical Coherence Tomography

All participants were scanned during routine clinical visits by experienced retinal photographers on Spectralis spectral-domain devices (SD-devices) (Heidelberg Engineering, Heidelberg, Germany) with automatic real-time (ART) function for image averaging. Peripapillary retinal nerve fibre layer (pRNFL) was measured with an activated eye tracker using 3.4mm ring scans around the optic nerve (Berlin and Oxford: 12°, 1536 A-scans, 1≤ART≤ 99). Combined ganglion cell layer and inner plexiform layer volume (GCIP), macular volume (TMV), inner nuclear layer (INL) and retinal nerve fibre layer in the macula (mRNFL) were calculated as a 3mm diameter cylinder around the fovea for a macular volume scan (Berlin: 25°x30°, 61 vertical B-

scans,  $11 \leq \text{ART} \leq 18$ ; Oxford:  $30^\circ \times 25^\circ$ , 61 vertical B-scans,  $17 \leq \text{ART} \leq 22$ ). Foveal thickness (FT) was measured as the mean thickness of a 1mm diameter cylinder around the fovea for the macular scan between the internal limiting membrane and the Bruch's membrane. Intraretinal semi-automatic segmentation was performed for all data with HEYEX software (version 1.10.4.0 with viewing module 1.0.16.0., Heidelberg Engineering, Germany) to correct segmentation errors and discard scans of insufficient quality. OCT data presented in this chapter follows OSCAR-IB quality criteria (46) and APOSTEL recommendations (187).

### 5.2.3.3. Fovea morphometry

To characterize the foveal shape, a 3D modelling algorithm was applied to macular OCT scans, applying parametric modelling of the fovea using cubic Bèzier equations for foveal morphometry described in section 1.3.3. (53). The method extracts foveal measurements as depth, diameter, slope, pit and areas and volumes of different regions (Figure 5-5).

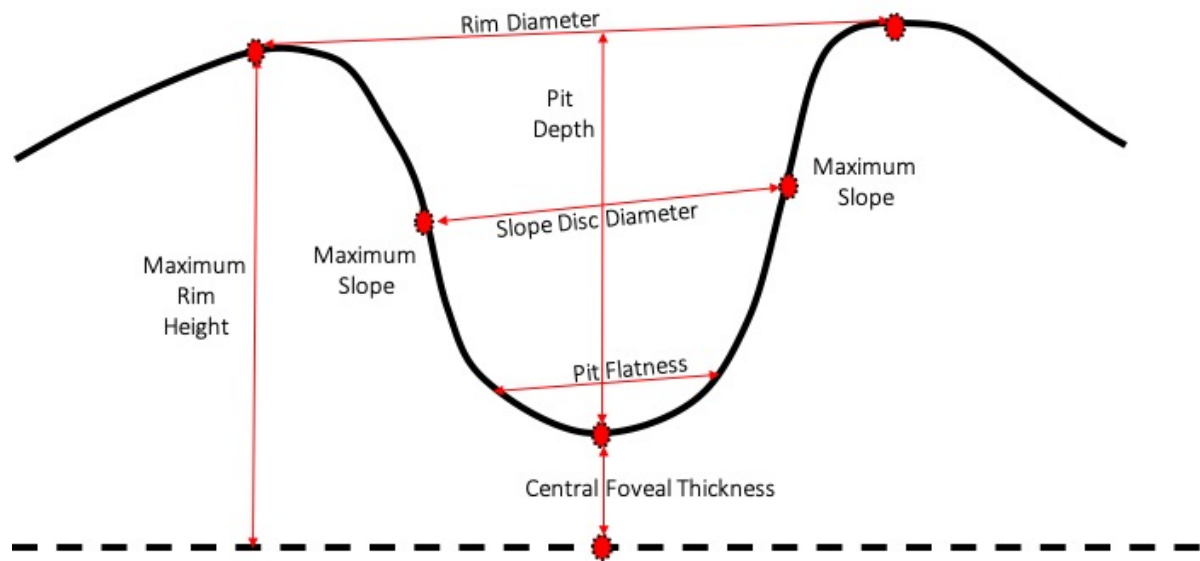


**Figure 5-5: The CuBe model**

Cross-sectional, 2D illustration on a central B-scan of foveal region parameters extracted with CuBe algorithm

#### 5.2.3.4. Statistical methods

Group differences between AQP4- NMOSD and HC were tested by Fisher's exact tests for sex and by Wilcoxon test for age. Multivariate analysis was used to analyse baseline and longitudinal differences for OCT and foveal shape parameters. Linear mixed effects (LME) models were applied to account for inter-eye correlations of monocular measurements: The initial model used for all the parameters was 'OCT ~ Age at baseline + Sex + Site + Group, random= ~1|Eye' for baseline and a nested LME model described as 'OCT ~ Age at baseline + Sex + Site + Group \* time since baseline, random= ~1|Patient/Eye' for the longitudinal analysis. From the initial models, simpler models were built by discarding not significant fixed effects, to avoid overfitting the model.

Group comparisons were established both at baseline and longitudinally by obtaining estimated marginal means (EMMs) for the mixed effect model and contrasts of EMMs were computed of all pairwise comparisons of least-squares means.

After this, orthogonal partial-least square discriminant analysis (OPLS-DA) was applied to identify the best combination of foveal and macular measure to discriminate the AQP4-NMOSD patients from HC. OPLS-DA is a method that has been widely used in metabolomic studies. Following the CuBe method, the foveal shape project presented the challenge of multicollinearity across variables and the need for meaningful variable reduction.

OPLSA-DA is a supervised multivariate analysis approach used to investigate the variables responsible for class discrimination between disease groups (193), for this reason, this was selected as the preferred method for variable reduction.

The performance of the model starts correcting for unequal class sizes with a 10-fold external cross-validation, this entails splitting the data into a training set (using 90% of data) and a test set (using 10% of data) a total of ten times to ensure that each sample appears in the test set exactly once. The test set is applied to the OPLS-DA model (generated using only the training set) to determine the predictive accuracy of independent (previously unseen) data. This process was repeated 100 times to produce 1000 models in total. If these models perform better than models produced by random class assignments (50%), then separation of the two groups has not occurred by chance, and the model is statistically significant (194,195) (figure 5-6)

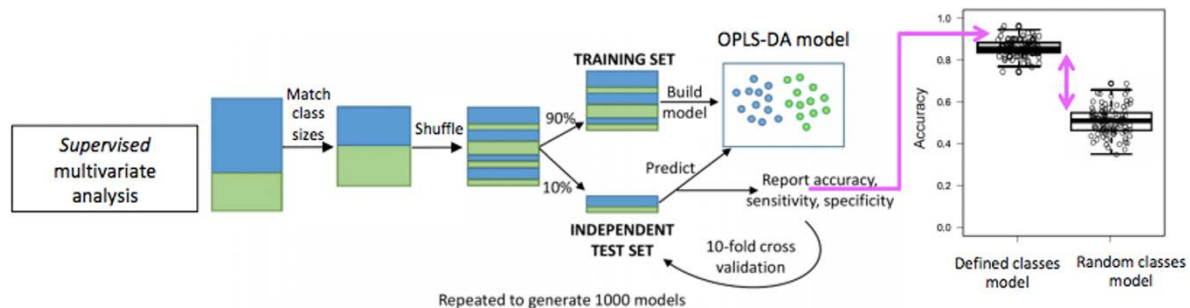


**Figure 5-6: Orthogonal partial least squares analysis pipeline**

Figure reproduced with the authorisation of Dr Fay Probert.

To identify the most critical parameters responsible for separating patient groups, variable importance in projection (VIP) scores were generated. A VIP score measures a parameter's importance to the OPLS-DA model; the higher the VIP score, the more critical the parameter contributes to separating patient groups.

Statistical significance was established at  $p < 0.05$ . All tests and graphical representations were performed in R 3.6.2 with packages, nlme, ropls, ggplot2 and emmeans.



## **6. RESULTS**

## 6.1. PROJECT 1: *Structural retinal imaging in AQP4-NMOSD and MOGAD*

Thirty AQP4-NMOSD patients and 32 MOGAD patients were included in the analysis (Table 6-1).

	HC	AQP4-NMOSD	MOGAD
Subjects (N)	21	30	32
Baseline eyes (N)	42	52	61
Sex (female (%))	15 (71.42%)	23 (76.7%)	23 (71.9%)
Age at first OCT (years, median (range))	44.82 (23.96- 71.45)	47.12 (16.90-81.48)	37.75 (18.02-71.05)
Disease duration at OCT (years, median (range))*	-	6.5 (0.28- 25.54)	2.8 (0.22-32.95)
Eyes with history of ON (N (%))*	-	24 (46.15%)	40 (65.57%)
Number of ON in the Affected eye median (range) - [%monophasic]*	-	1 (1-6) – [62.5%]	1 (1-9) – [75%]
Number of other attacks (TM or BS) median (range)	-	2 (0-14)	1 (0-9)
Time from last ON to OCT (months, median (range))*	-	2.1 (1.18-19.15)	2.8 (1-7.98)
Time between OCT examinations (years, median (range))	2.45 (1.46-2.98)	2.14 (0.69-7.76)	1.15 (0.28- 5)

**Table 6-1: Cohort overview**

Age, sex and disease duration group differences between AQP4-NMOSD, MOGAD and HC participants were not significant. Abbreviations: AQP4-NMOSD,

---

neuromyelitis optica spectrum disease aquaporin-4 seropositive patients; MOG-IgG seropositive, Myelin oligodendrocyte glycoprotein antibody positive; N, number; OCT, Optic coherence tomography; ON, optic neuritis eyes; SD, standard deviation. No significant differences were found between the three groups for age ( $p=0.315$ ), sex ( $p=0.75$ ) or, in case of the disease groups, disease duration ( $p=0.2214$ ), age ( $p=0.08$ ) or sex ( $p=0.37$ ). \*rejected eyes were not included in this table

---

At baseline, in the AQP4-NMOSD group, 28 eyes never had a history of ON (NON - includes 5 fellow eyes of ON eyes, and 23 eyes from 13 patients with no previous history of ON, so called “never affected eyes”), and 24 had a history of ON. Eight eyes were excluded from the analysis, 7 eyes due to poor image quality or technical issues and 1 eye due to amblyopia. At baseline, in the MOGAD group, 21 eyes never had a history of ON (NON - includes 9 fellow eyes of ON eyes, and 12 eyes from six patients with no previous history of ON, so called “never affected eyes”), and 40 had a history of ON. Three eyes were excluded from the analysis due to poor image quality or technical issues. In addition, in the follow-up scans, three AQP4-NMOSD eyes and 5 MOGAD eyes were lost to follow up due to poor imaging quality. (see flowchart on figure 6-1).

### **6.1.1. Baseline results**

This cohort did not present with significant differences between the three groups for age ( $p=0.32$ ), sex ( $p=0.75$ ) or, in case of the disease groups, disease duration ( $p=0.22$ ). None of the patients experienced any clinical relapse since baseline to the completion of this project. In the majority of ON cases (62.5%, of AQP4-NMOSD and 75% in MOGAD) participants presented with monophasic ON.

Mean and standard deviations of retinal thickness are presented in table 6-2. A detailed analysis of group differences at baseline was investigated using multivariate linear mixed-effects models with estimated marginal means, adjusted for age at baseline and sex while accounting for inter-eye correlations. These results are presented in detail in table 6-3 and figure 6-3.

	HC	AQP4-NMOSD			MOGAD		
Eye status	HC	Affected	Fellow	Never Affected	Affected	Fellow	Never Affected
	Mean (SD)	Mean (SD)	Mean (SD)	Mean (SD)	Mean (SD)	Mean (SD)	Mean (SD)
<b>pRNFL (<math>\mu\text{m}</math>)</b>	98.64 (10.93)	56.84 (25.78)	97.40 (11.80)	97.04 (7.68)	64.91 (18.77)	93.77 (7.74)	89.41 (11.55)
<b>GCIP (<math>\text{mm}^3</math>)</b>	0.617 (0.075)	0.363 (0.11)	0.598 (0.057)	0.603 (0.053)	0.432 (0.101)	0.612 (0.031)	0.598 (0.036)
<b>TMV (<math>\text{mm}^3</math>)</b>	2.33 (0.097)	2.12 (0.140)	2.15 (0.212)	2.31 (0.098)	2.19 (0.108)	2.404 (0.076)	2.352 (0.097)
<b>INL (<math>\text{mm}^3</math>)</b>	271.85 (19.668)	265.37 (14.796)	268.80 (14.618)	273.13 (24.454)	264.77 (16.212)	289.11 (20.176)	268.16 (20.184)
<b>FT (<math>\mu\text{m}</math>)</b>	0.266 (0.015)	0.308 (0.032)	0.292 (0.029)	0.282 (0.020)	0.288 (0.026)	0.279 (0.018)	0.267 (0.023)
<b>mRNFL (<math>\text{mm}^3</math>)</b>	0.142 (0.019)	0.116 (0.019)	0.144 (0.016)	0.151 (0.014)	0.120 (0.014)	0.147 (0.017)	0.145 (0.010)

**Table 6-2: Baseline OCT measures**

This table contains mean and standard deviations for baseline retinal imaging metrics. Abbreviations: AQP4-NMOSD, Aquaporin Neuromyelitis Spectrum Disorder eyes; MOGAD, Myelin oligodendrocyte glycoprotein associated disease eyes; HC, Healthy controls eyes; Affected, eyes with history of optic neuritis; Fellow, eyes without a history of optic neuritis but with a contralateral eye with a history of optic neuritis; Never affected, eyes from patients who do not have a history of optic neuritis in any of the eyes; pRNFL, peripapillary retinal nerve fibre layer; GCIP,

---

ganglionar and inner plexiform layer; TMV, total macular volume; FT, foveal thickness; INL, Inner nuclear layer; mRNFL, macular retinal nerve fibre layer; SD, standard deviation.

---

Linear mixed effects models, performed to assess changes in retinal thickness of disease eyes compared to HC (accounting from the absence of monocular measurements), required some assumptions that had to be fulfilled before the model fitting. One of these assumptions was the normal distribution of the dependent variables (the retinal layers in this case). To assess normality Shapiro tests and Q-Q plots were performed after and before normalization to assess the distribution of these variables.

Initial Shapiro test determined that none of the dependent variables followed a normal distribution (pRNFL,  $p \leq 0.001$ ; GCIP,  $p \leq 0.001$ ; TMV  $p=0.02188$ ; FT,  $p=0.03238$ ; INL,  $p \leq 0.001$ ; mRNFL=0.0002). Confirmatory Q-Q plots for the variables previous to the transformation can be found in figure 6-1.

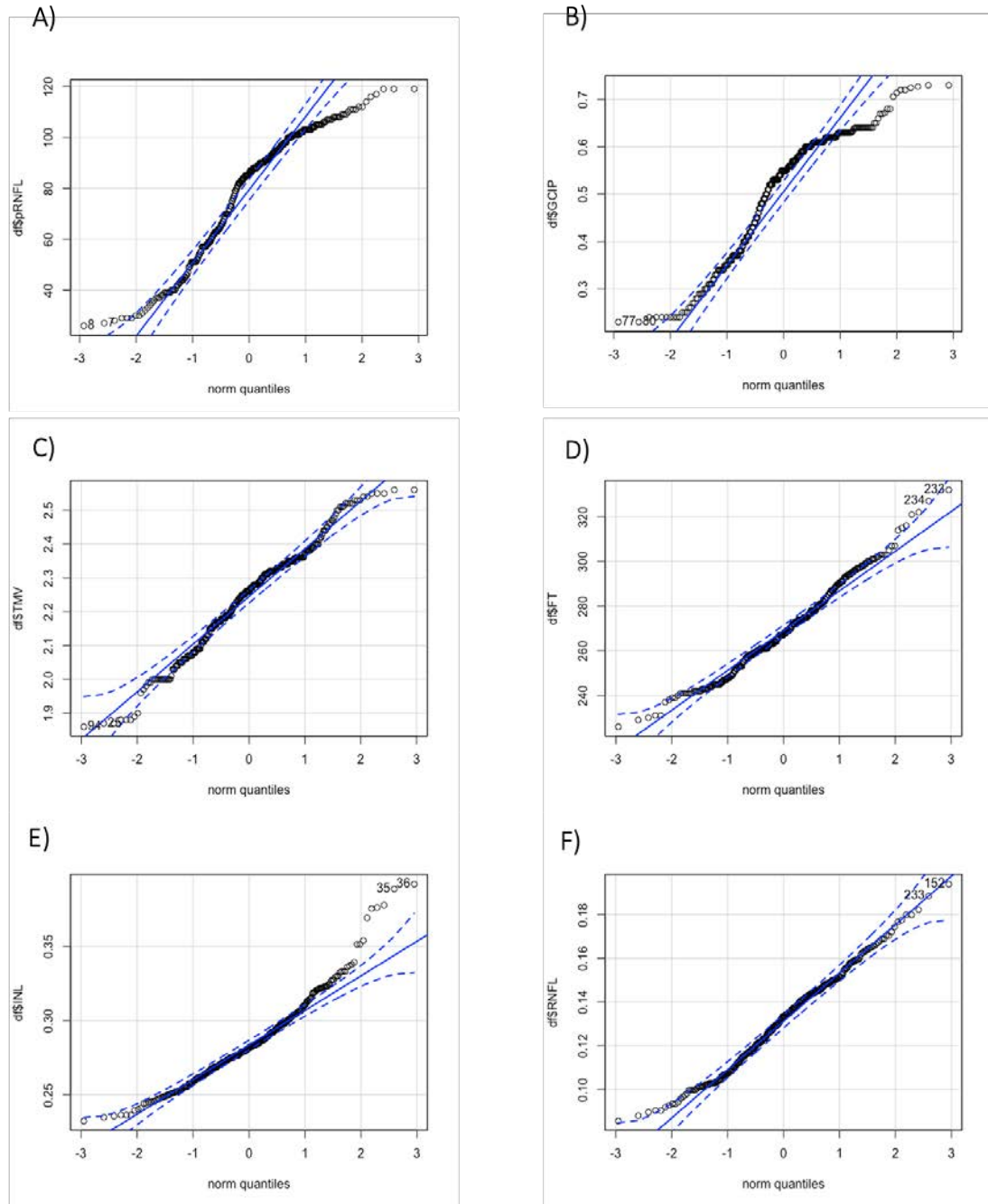


**Figure 6-1: QQ-plots of the dependent variables assessed before building the linear mixed effect model**

Plot of the quantiles of the dependent variable data set (retinal layer) against the quantiles of the second data set from a theoretical standard normal distribution. A) pRNFL, peripapillary retinal nerve fibre layer at the disc; B) GCIP, combined ganglion cell and inner plexiform layer; C) TMV: total macular volume; D) FT, foveal thickness; E) INL: Inner nuclear layer; F) mRNFL: retina nerve fibre layer at macula.

The order quantile was applied to normalize pRNFL, GCIP, INL and mRNFL variables, while exponential transformation and square-root transformation were applied to the TMV and the INL variables, respectively.

After all distributions were adjusted, normalization was re-assessed by Shapiro test and Q-Q confirmatory plots. Shapiro results were the following: pRNFL,  $p= 0.9993$ ; GCIP,  $p=1$ ; TMV,  $p= 0.1653$ ; FT,  $p= 0.08893$ ; INL,  $p=1$ ; mRNFL=1 indicating successful normalization. Q-Q plots for the variables after the transformation confirm this and can be observed in figure 6-2.

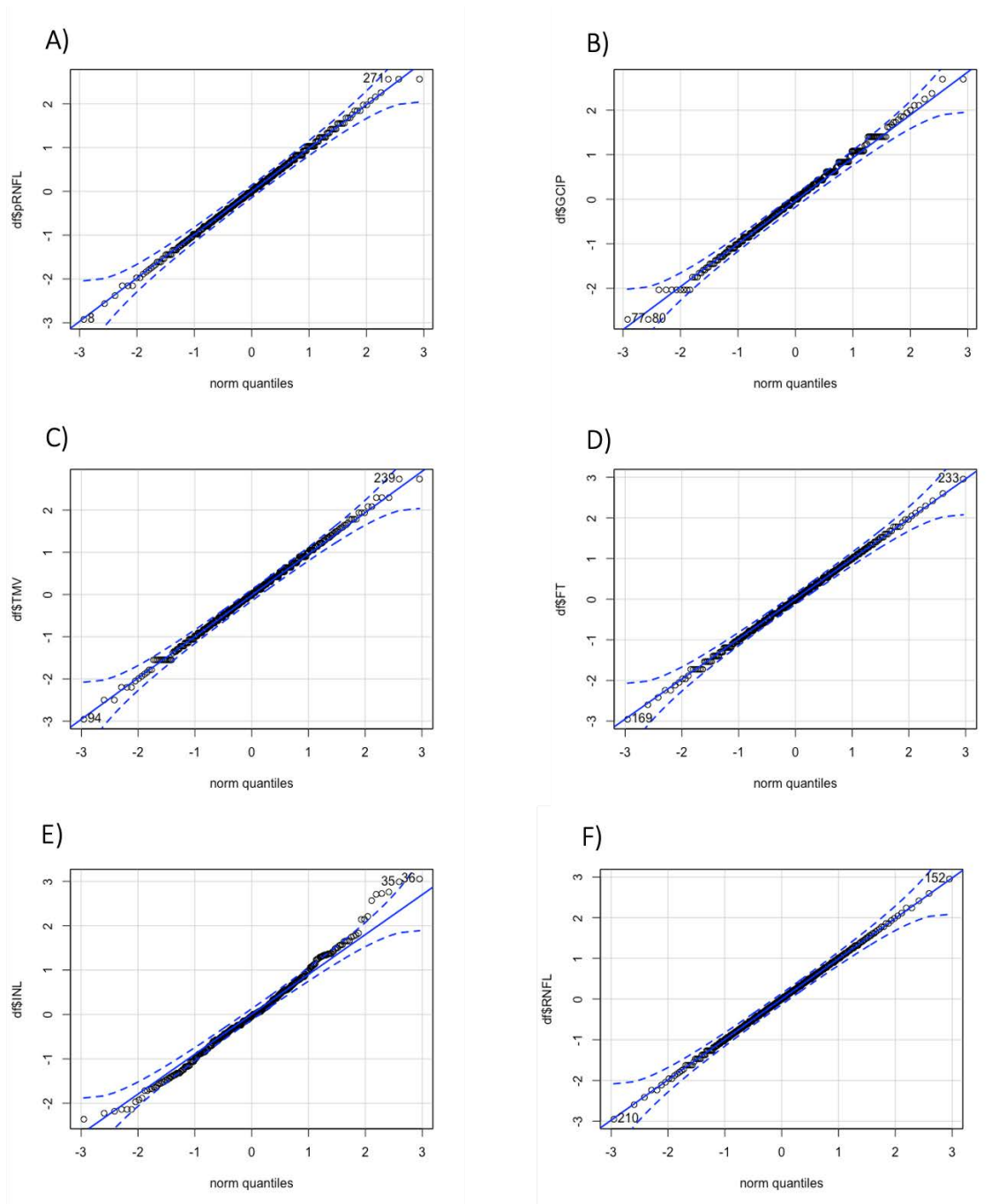


**Figure 6-2: QQ-plots of the dependent variables assessed after the transformations to normalize the data, used to build the final linear mixed effect model**

Plot of the quantiles of the dependent variable data set (retinal layers) against the quantiles of the second data set from a theoretical standard normal distribution. A) pRNFL, peripapillary retinal nerve fibre layer at the disc; B) GCIP, combined ganglion cell and inner plexiform layer; C) TMV: total macular volume; D) FT, foveal thickness; E) INL: Inner nuclear layer; F) mRNFL: retina nerve fibre layer at macula.



### **Retinal changes in AQP4-NMOSD-ON and MOGAD-ON**

Linear mixed-effect models showed significant thinning in affected eyes compared to HC eyes in both conditions for pRNFL, GCIP, TMV, INL, and mRNFL (no differences were found for FT), suggesting profound neuroaxonal damage after ON in both conditions. Fellow eyes in AQP4-NMOSD patients showed significant thinning only in TMV that cannot be attributed to any of the studied inner retinal structures, as pRNFL, GCIP, FT, INL and mRNFL present with no difference in thickness from HC (table 6-3). In AQP4-NMOSD “never affected” eyes (from patients with no history of ON) a significant thickening of INL was found (B= 0.020, SD= 0.007, p=0.0103). This thickening was not observed in the same group of MOGAD patients (figure 6-3, table 6-3).

### **Are fellow eyes from contralateral affected ON eyes affected in AQP4-NMOSD and MOGAD? And are there retinal changes in AQP4-NMOSD-NON and MOGAD-NON eyes independent of ON?**

Fellow eyes in MOGAD eyes did not show significant differences with healthy controls. “Never affected” eyes (from patients with no history of ON) did not show remarkable differences characteristic of neuroaxonal damage in any of the two diseases compared to HC.

	pRNFL ( $\mu\text{m}$ )		GCIP ( $\text{mm}^3$ )		TMV ( $\text{mm}^3$ )		FT ( $\mu\text{m}$ )		INL ( $\text{mm}^3$ )		mRNFL ( $\text{mm}^3$ )	
	B (SE)	p value	B (SE)	p value	B (SE)	p value	B (SE)	p value	B (SE)	p value	B (SE)	p value
<b>A-AQP4</b>	-41.39 (5.05)	<0.0001	-0.249 (0.02)	<0.0001	-0.194 (0.03)	<0.0001	-4.93 (5.88)	0.4049	0.043 (0.007)	<0.0001	-0.023 (0.005)	<0.0001
<b>A-MOG</b>	-34.22 (4.38)	<0.0001	-0.186 (0.02)	<0.0001	-0.130 (0.03)	0.0001	-4.17 (5.62)	0.4599	0.022 (0.006)	0.0009	-0.020 (0.004)	<0.0001
<b>F-AQP4</b>	3.68 (6.93)	0.5976	-0.003 (0.03)	0.9281	-0.103 (0.04)	0.0285	7.056 (6.45)	0.2783	0.019 (0.010)	0.061	0.007 (0.007)	0.3243
<b>F-MOG</b>	-3.65 (5.64)	0.5196	-0.004 (0.03)	0.8747	0.047 (0.03)	0.2274	9.96 (5.93)	0.0979	0.010 (0.008)	0.1977	0.005 (0.006)	0.3871
<b>N-AQP4</b>	-5.51 (5.18)	0.2914	-0.019 (0.02)	0.467	-0.033 (0.03)	0.3833	0.32 (6.22)	0.9585	0.020 (0.007)	0.0103	0.006 (0.005)	0.2402
<b>N-MOG</b>	-8.09 (6.81)	0.2384	-0.024 (0.035)	0.4833	0.013 (0.05)	0.7961	0.07 (9.01)	0.9934	0.0001 (0.010)	0.9893	0.004 (0.006)	0.511

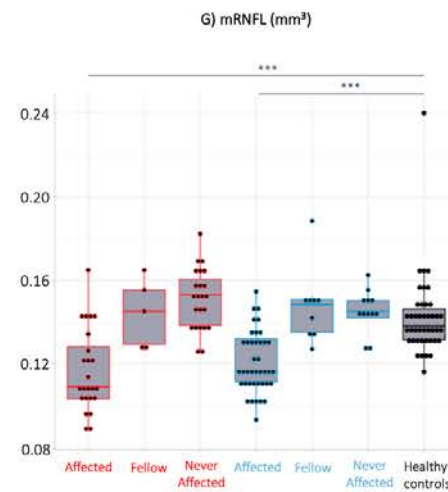
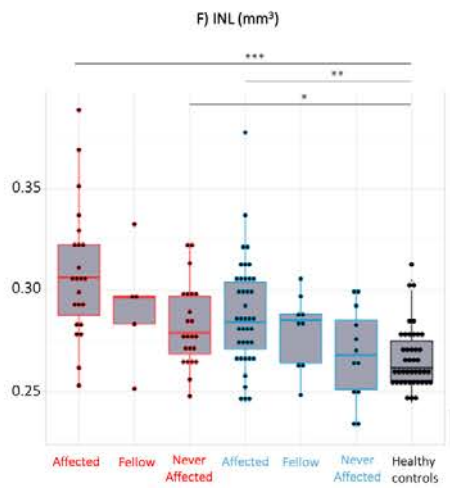
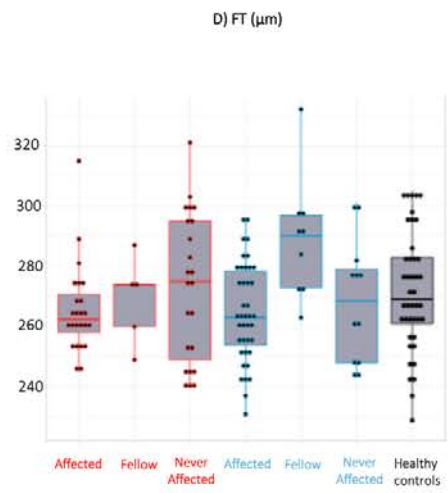
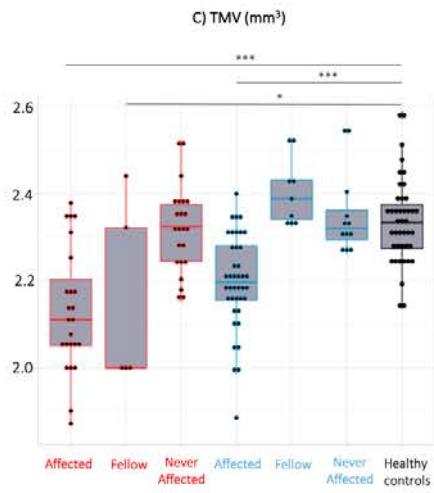
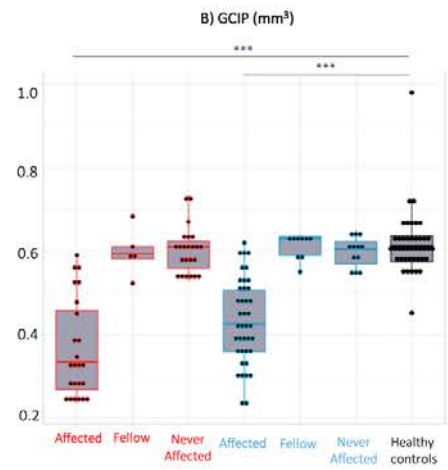
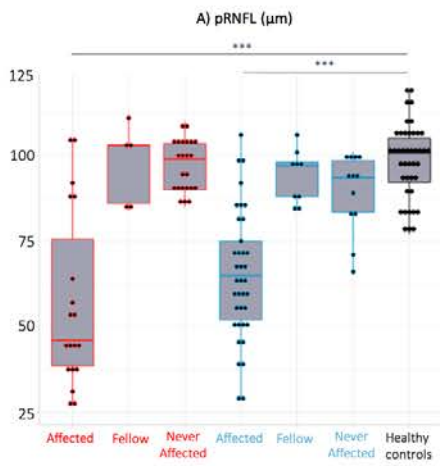
---

**Table 6-3: Baseline OCT measures. Differences between disease groups and healthy controls**

Maximum likelihood was used for the estimation of p-values. Abbreviations: A-AQP4, Aquaporin-4 NMOSD eyes with a history of ON; F-AQP4, Aquaporin-4 NMOSD eyes without a history of ON but with a contralateral eye with a history of ON; N-AQP4, Aquaporin-4 NMOSD eyes from patients who do not have a history of ON in any of the eyes. A-MOG, MOGAD eyes with a history of ON; F-MOG, MOGAD eyes without a history of ON but with a contralateral eye with a history of ON; N-MOG, MOGAD eyes from patients who do not have a history of ON in any of the eyes (“never affected”); pRNFL, peripapillary retinal nerve fibre layer; GCIP, ganglionar and inner plexiform layer; TMV, total macular volume; FT, foveal thickness; INL, inner nuclear layer; mRNFL, retinal nerve fibre layer; B, estimate; SE, standard error. Boxes in red establish the significance at  $p < 0.05$ .

---

A summary of raw OCT values with median, 25<sup>th</sup> and 75<sup>th</sup> percentile for each variable and each group is shown in figure 6-3 , note that significance bars with LME models results have been overlayed for a more comprehensive understanding of the real differences (accounting for inter eye correlations of monocular measurements and adjusted by sex and age) between groups and eye categories



---

**Figure 6-3: Box plots of disc and macular baseline OCT values with overlaid LME results**

A) pRNFL, peripapillary retinal nerve fibre layer at the disc; B) GCIP, combined ganglion cell and inner plexiform layer; C) TMV: total macular volume; D) FT, foveal thickness; E) INL: Inner nuclear layer; F) mRNFL: retinal nerve fibre layer at macula; Boxplot show median and 25<sup>th</sup> and 75<sup>th</sup> percentile. Significance bars refer to LMS results from table 4-3. Abbreviations: AQP4-NMOSD, Aquaporin-4 Neuromyelitis Optica Spectrum Disorder. MOGAD, Myelin Oligodendrocyte Glycoprotein Associated Disease.

---

## 6.1.2. Longitudinal results

To assess each of the inner retinal structures (pRNFL, GCIP, TMV, FT, INL and mRNFL) over time for each group of eyes and disease categories compared to HC, LME models were built accounting for time as an interaction factor and adjusting by age and sex.

### **Is retinal damage after the acute stage in AQP4-NMOSD and MOGAD eyes permanent or does it evolve? Are there longitudinal changes in NON-ON eyes?**

Longitudinal results suggest that TMV increases after the acute stage in AQP4-NMOSD patients compared to HC in affected and fellow eyes, for the observed time of this study (median [min-max]) 2.14 [0.69-7.76] years). In “never affected” eyes (from patients with no history of ON) of AQP4-NMOSD patients, changes in foveal thickness are observed with a significant thinning over time as compared to HC. Eyes from MOGAD patients did not show any difference over time compared with HC eyes. Full results are presented in table 6-4 and predictive graphs for the described models above are shown in figure 6-4.

### **How does retinal damage evolve over time?**

The estimates from the LME models show a mean increase of 0.08mm<sup>3</sup> in TMV per year in affected eyes of AQP4-NMOSD patients and of 0.35mm<sup>3</sup> per year in fellow

eyes of AQP4-NMOSD patients; as it was explained in the methods section, it is not possible to know whether longitudinal variations are or not within the coefficient of repeatability of the metric, for that reason, the variation over time presented in this section, refers to a comparison against a HC group, which was used as a reference in this analysis (i.e., variation is compared against HC trajectory and not against themselves). These changes in TMV could not be however attributed to any specific retinal structure, as pRNFL, GCIP, FT, INL and mRNFL did not show any significant longitudinal change compared to HC for these group of eyes (table 6-4). A decrease in foveal thickness is estimated over time at minus 0.06  $\mu\text{m}$  per year in in “never affected” eyes (from patients with no history of ON) of AQP4-NMOSD patients.

	pRNFL ( $\mu\text{m}$ )		GCIP ( $\text{mm}^3$ )		TMV ( $\text{mm}^3$ )		FT ( $\mu\text{m}$ )		INL ( $\text{mm}^3$ )		mRNFL ( $\text{mm}^3$ )	
	B (SE)	p value	B (SE)	p value	B (SE)	p value	B (SE)	p value	B (SE)	p value	B (SE)	p value
<b>A- AQP4</b>	0.0267 (0.023)	0.2512	0.0276 (0.021)	0.191	0.0834 (0.033)	0.012	-0.0071 (0.03)	0.8113	0.062 (0.056)	0.266	-0.0411 (0.061)	0.5008
<b>A-MOG</b>	0.0219 (0.024)	0.3697	0.0093 (0.022)	0.6756	-0.0073 (0.037)	0.8415	-0.0425 (0.033)	0.2033	-0.0185 (0.062)	0.764	0.1284 (0.068)	0.0594
<b>F- AQP4</b>	0.0156 (0.031)	0.6129	-0.0053 (0.028)	0.8506	0.3479 (0.048)	<0.0001	0.0027 (0.044)	0.9505	-0.1335 (0.081)	0.0995	-0.023 (0.089)	0.7956
<b>F-MOG</b>	0.0109 (0.055)	0.8433	-0.0439 (0.05)	0.3804	-0.086 (0.086)	0.3196	-0.1349 (0.078)	0.0865	-0.0153 (0.145)	0.9162	-0.0148 (0.16)	0.926
<b>N- AQP4</b>	0.0146 (0.023)	0.5308	0.001 (0.021)	0.9629	-0.0227 (0.036)	0.5325	-0.0662 (0.033)	0.0463	0.0874 (0.061)	0.1551	-0.0801 (0.067)	0.2355
<b>N-MOG</b>	0.0861 (0.046)	0.0602	-0.0773 (0.041)	0.063	0.0002 (0.071)	0.9973	-0.0883 (0.065)	0.1755	0.1588 (0.121)	0.1898	-0.1706 (0.133)	0.2006

---

**Table 6-4: Longitudinal changes in OCT parameters for the different eye categories**

Maximum likelihood was used for the estimation of p values. Abbreviations: A-AQP4, Aquaporin-4 NMOSD eyes with a history of ON; F-AQP4, Aquaporin-4 IgG NMOSD eyes without a history of ON but with a contralateral eye with a history of ON; N-AQP4, Aquaporin-4 IgG NMOSD eyes from patients who do not have a history of ON in any of the eyes. A-MOG, MOGAD eyes with a history of ON, so called “affected eyes”; F-MOG, MOGAD eyes without a history of ON but with a contralateral eye with a history of ON, so called “fellow eyes”; N-MOG, MOGAD eyes from patients who do not have a history of ON in any of the eyes, so called “never affected eyes”; pRNFL, peripapillary retinal nerve fibre layer; GCIP, ganglionar and inner plexiform layer; TMV, total macular volume; FT, foveal thickness; INL, inner nuclear layer; mRNFL, retinal nerve fibre layer; B, estimate; SE, standard error. Boxes in red establish the significance at  $p < 0.05$ .

---



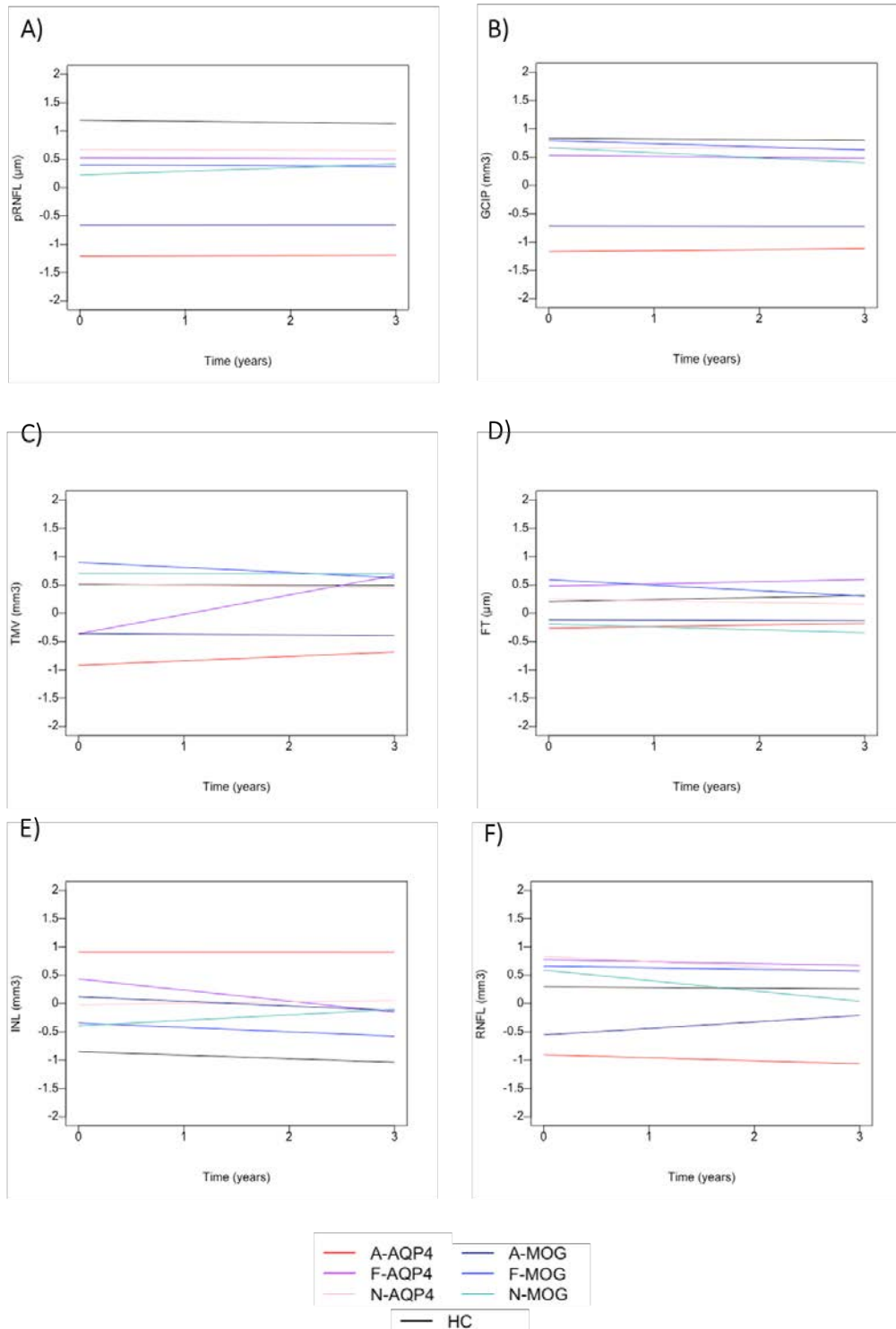
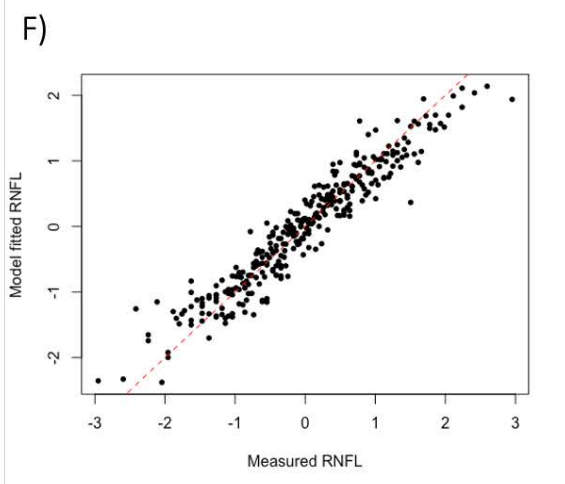
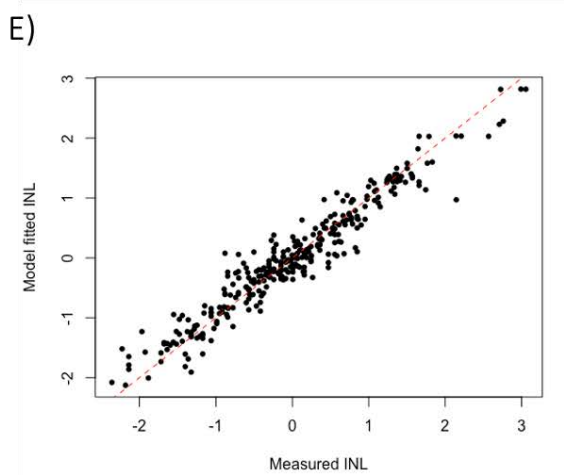
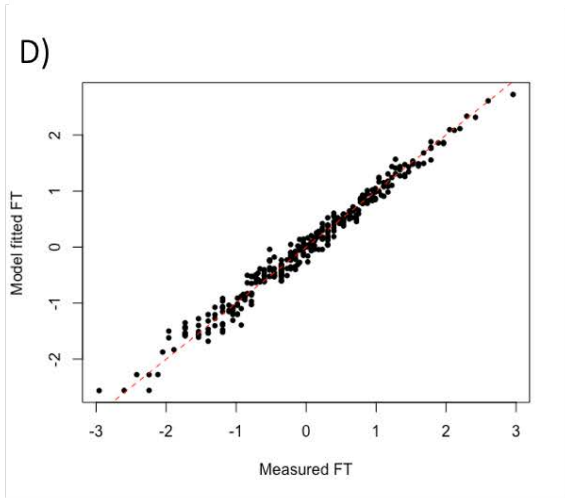
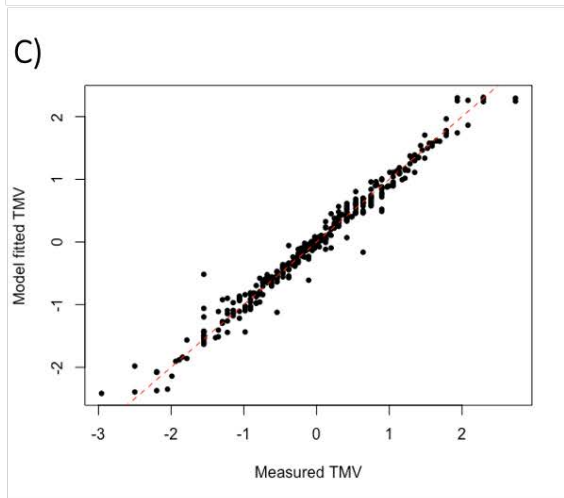
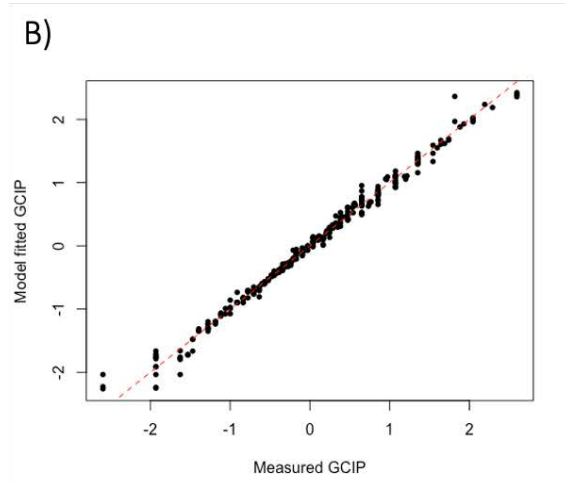
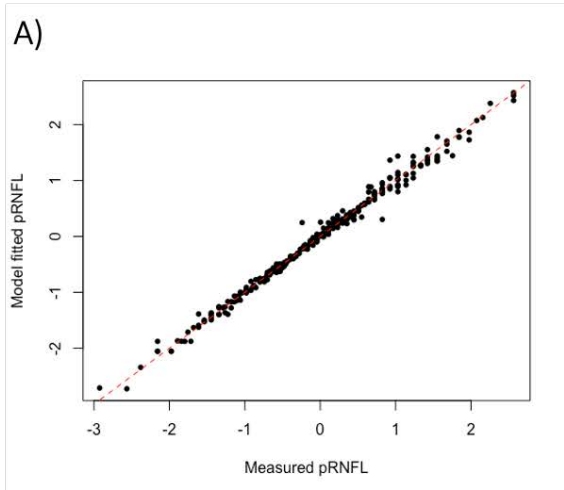


**Figure 6-4: Longitudinal LME predicted model graphs**

A) pRNFL, peripapillary retinal nerve fibre layer; B) GCIP, ganglionar and inner plexiform layer; C) TMV, total macular volume; D) FT, foveal thickness; E) INL, Inner nuclear layer; F) mRNFL, retinal nerve fibre layer

After extracting these longitudinal results, a few additional steps were needed to determine the accuracy of the models, and therefore, the validity of the results stated. For that purpose, models were assessed in two ways: one by calculating marginal and conditional R squared values (accompanied by a visual representation plotting actual values against predicted (figure 6-5)), and other by assessing the residuals of the model.

Marginal R squared values (R2m-associated to fixed effects) and conditional R squared values (R2c-associated to fixed effects plus the random effects) were calculated to understand whether the variance was explained only by fixed effects or also by random effects from the model (pRNFL: R2m=57%, R2c= 99%; GCIP: R2m=64%, R2c= 98%; TMV: R2m=40%, R2c= 97%; FT: R2m=7%, R2c= 98%; INL: R2m=27%, R2c= 90%; mRNFL: R2m=48%, R2c= 88%). To interpret these percentages, it is important to understand that a R2m close to zero tells us that the fixed effects (age + sex + status + time: status) are not explaining much variation, and a R2c close to 1 tells us that most of the unexplained variation is between groups rather than between observations within groups (pairs of eyes). In this case, these R2m and R2c indicate that the variation of these models is associated to the fixed effects and the unexplained variation is due to the differences between groups (except for INL and mRNFL where there is a certain amount of unexplained variation coming from the inter-individual differences within groups – which could be explained by the presence of MME in some patients).



---

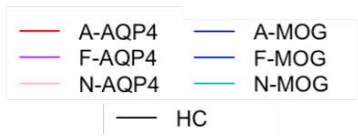
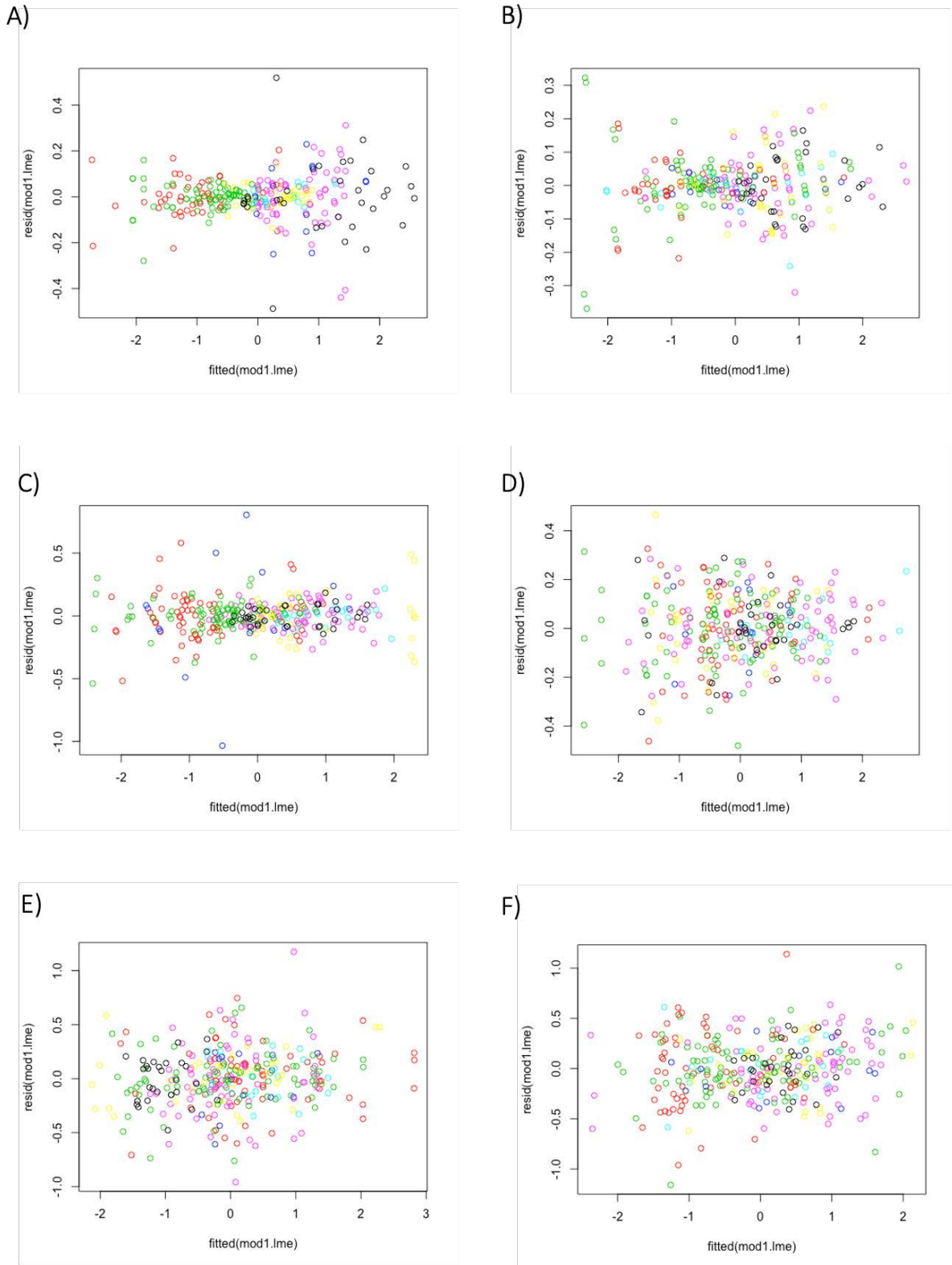
**Figure 6-5: Actual Vs predictive models**

This figure graphically illustrates different R-squared values for the different linear mixed-effects models presenting the residuals on the  $y$ -axis and the fitted values from the model on the  $x$ -axis and indicates a deviation from the residual that is close to the 0 line, sharing the same pattern as their deviation from the estimated regression line.

A) pRNFL, peripapillary retinal nerve fibre layer; B) GCIP, ganglionar and inner plexiform layer; C) TMV, total macular volume; D) FT, foveal thickness; E) INL, Inner nuclear layer; F) mRNFL, retinal nerve fibre layer.

---

The best way to assess goodness of the fit is assessing the residuals, which are plotted in figure 6-5. This suggests that the relationship is linear. To assess heteroscedasticity, residuals were plotted against the fitted values. Heteroscedasticity refers to situations where the variance of the residuals is unequal over a range of measured values and it tends to appear when there is a large difference among the sizes of the observations. Error terms demonstrate to have a constant variance in this analysis and therefore, satisfies the regression assumption (figure 6-6).



---

**Figure 6-6: Residual plots of the longitudinal models**

Error terms demonstrate to have a constant variance in this analysis and therefore, they satisfy the regression assumption. A) pRNFL, peripapillary retinal nerve fibre layer; B) GCIP, ganglionar and inner plexiform layer; C) TMV, total macular volume; D) FT, foveal thickness; E) INL, Inner nuclear layer; F) mRNFL, macular retinal nerve fibre layer. A- AQP4, Aquaporin-4 NMOSD eyes with history of ON; F-AQP4, Aquaporin-4 NMOSD eyes without a history of ON but with a contralateral eye with a history of ON; N-AQP4, Aquaporin-4 IgG NMOSD eyes from patients who do not have a history of ON in any of the eyes. A- MOG, MOGAD eyes with history of ON; F-MOG, MOGAD eyes without a history of ON but with a contralateral eye with a history of ON; N-MOG, MOGAD eyes from patients who do not have a history of ON in any of the eyes.

---

In summary, this analysis suggests retinal damage after ON in both disease groups in affected eyes. While fellow eyes in AQP4-NMOSD showed significant total macular volume loss with individual inner structures preserved, “never affected” eyes (from patients with no history of ON) in AQP4-NMOSD showed a significant thickening in INL, which could suggest inflammatory activity. None of these changes were observed in fellow or “never affected” eyes (from patients with no history of ON) MOGAD eyes. Longitudinal results show a mean increase thickness in total macular volume during the chronic period in affected (mean 0.08mm<sup>3</sup> per year) and fellow (mean 0.35mm<sup>3</sup>) AQP4-NMOSD-affected eyes compared to healthy controls as well as a significant decrease in foveal thickness (mean 0.06 µm per year) in AQP4-NMOSD “never affected” eyes (from patients with no history of ON) eyes. Models have a good fit and therefore results are reliable to draw conclusions.

## **6.2. PROJECT 2: *Structure-function relationship in the visual system of patients with AQP4- NMOSD and MOGAD disease***

### **6.2.1. The NMO tissue bank cohort**

Twenty-five AQP4-NMOSD patients and 53 MOGAD patients are included in the analysis (Table 6-5).

	<b>MOGAD</b>			<b>AQP4-NMOSD</b>		
Number patients	53			25		
Males / Females	20/33			21/4		
Age years median (range)	35 (11 – 73)			57 (17 – 83)		
Ethnicity	43 White (81.1%) 0 African-Caribbean (0%) 3 Asian (5.7%) 1 Mixed race (1.9%) 6 Prefer not to say (11.3%)			16 White (64%) 8 African-Caribbean (32%) 1 Asian (4%)		
No. Patients with past history of optic neuritis	28			5		
Time from ON to OCT, median (range) in months	32 (6-124)			44 (17-98)		
No. Patients with no past history of optic neuritis	25			20		
<b>OCT &amp; VEP test results (number of eyes)</b>						
	<b>MOGAD</b>			<b>AQP4-NMOSD</b>		
	TOTAL	ON	NON-ON	TOTAL	ON	NON-ON
Eyes with both OCT and VEP examination normal, N	37	9	28	35	5	30
Eyes with only OCT examination abnormal, N	21	18	3	4	2	2
Eyes with only VEP examination abnormal, N	6	3	3	1	0	1
Eyes with both OCT and VEP examination abnormal, N	26	26	0	4	1	3



---

**Table 6-5: NMO tissue bank cohort overview**

Note: Age and sex group differences between MOGAD and AQP4-NMOSD patients were significant (Fisher's exact tests for sex,  $p=0.007$ ; Wilcoxon test for age,  $p=0.001$ ). Differences between normal vs abnormal ophthalmic examinations were assessed with Fisher's exact test and significant between MOGAD and AQP4-NMOSD for the Total number of eyes ( $p\leq 0.001$ ) and ON eyes ( $p=0.009$ ).

Abbreviations: N, number; MOGAD, Myelin oligodendrocyte glycoprotein; AQP4-NMOSD, AQP4 seropositive Neuromyelitis optica spectrum disease; OCT, Optic coherence tomography; VEP, Visual evoked potentials; VA, central visual acuity.

\* Indicates significant difference.

---

Data was available for analysis on 53 MOGAD patients with 90 good VA eyes and 25 AQP4-NMOSD patients with 44 good VA eyes. Of these, 56/90 MOGAD eyes (62%) and 8/44 AQP4-NMOSD eyes (18%) had history of one or more ON episodes (median number of ON, 1.5 for AQP4-NMOSD, 1 for MOGAD) (table 6-5) (figure 6-7). A summary of all results of clinical OCT and VEP measurements are shown in figure 6-7 (table 6-5).

**Is there a correlation in severity between structure and function of the anterior optic pathways in eyes of AQP4-NMOSD and MOGAD patients with normal visual acuity?**

Whereas the majority (80%) of AQP4-NMOSD eyes with good VA had normal VEP and OCT examinations, only 41% of MOGAD eyes with normal VA had normal findings, the remainder having abnormal OCT, VEP or both ( $p\leq 0.001$ ) (figure 6-7). This difference between the two diseases was most apparent in those with normal VA and a previous ON (figure 6-7); only 16% of MOGAD eyes compared with 63% of AQP4-NMOSD eyes had normal investigations ( $p=0.003$ ) (table 6-5).

Notably, OCT abnormalities were found in 79% MOGAD-ON patients compared to 38% of AQP4-NMOSD-ON patients ( $p= 0.01$ ) and these were more common than VEP abnormalities in both conditions (52% vs 12% respectively).

**Is there subclinical damage in “never affected” eyes (from patients with no history of ON). from AQP4-NMOSD and MOGAD patients?**

Abnormalities were also noted in some eyes without a previous history of ON but without a difference between MOGAD (18%) of which 4/6 had a contralateral ON and AQP4-NMOSD (17%) of which none had a contralateral ON (p=0.91) (figure 6-7).

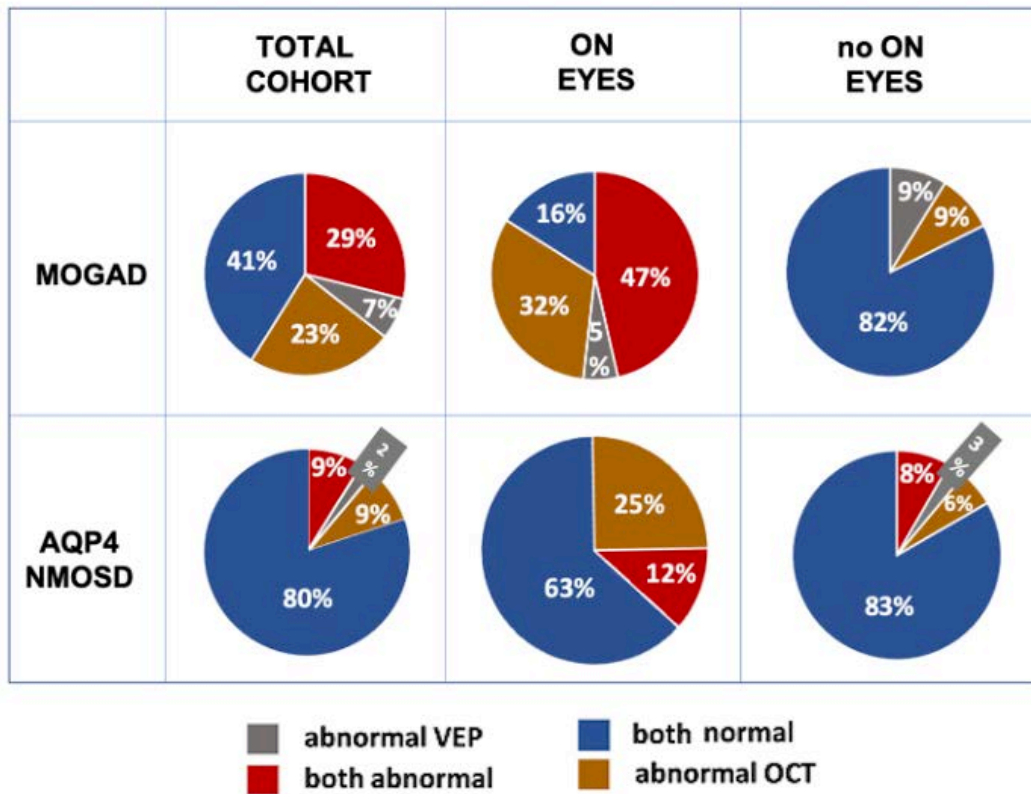


**Figure 6-7: Structural tests in normal central visual function eyes in the NMO tissue bank database cohort**

NMO tissue bank cohort grouped according abnormal optic coherence tomography (OCT), Abnormal OCT= pRNFL  $\leq 80(\mu\text{m})$ ; abnormal visual evoked potentials (VEP), VEP= latency  $>112\text{ms}$ ; both tests abnormal or both tests normal. A) Total Cohort (B) Only eyes that have had previous history of optic neuritis (ON) (C) Only eyes with no history of optic neuritis (NON).

**Are OCT and VEP measures related to visual outcomes?**

Baseline characteristics for HCVA, pRNFL and VEP are presented in table 6-6. Group differences were analysed using multivariate mixed effects models for HCVA and pRNFL adjusted for age at OCT, sex and race while accounting for inter-eye correlations. VEP differences were analysed with logistic mixed effects model adjusted for age at VEP, sex, and race accounting as well for inter-eye correlations.

	<b>AQP4-NMOSD- ON eyes</b>	<b>AQP4-NMOSD- NON eyes</b>	<b>MOGAD- ON eyes</b>	<b>MOGAD- NON eyes</b>
<b>HCVA (LogMAR) (median (IQR))</b>	-0.1 (0.1)	-0.1 (0.1)	-0.1 (0.1)	-0.1 (0)
<b>pRNFL (µm) (mean (SD))</b>	83 (24.9)	97.4 (11.8)	66.5 (16.1)	92.41 (12.5)
<b>VEP (delayed) N (%)</b>	1 (11.1%)	3 (8.3%)	29 (51.78%)	3 (8.82%)

**Table 6-6: Baseline measures of eyes with AQP4-NMOSD and MOGAD patients**

Baseline characteristics and differences between the two disease groups. Abbreviations: AQP4-NMOSD, aquaporin-4 antibody positive Neuromyelitis Optica Spectrum Disease; MOGAD, Myelin oligodendrocyte glycoprotein antibody positive associated disease; VEP, visual evoked potentials; LogMar, logarithm of the minimum angle of resolution; pRNFL, peripapillary retinal nerve fibre layer; µm, micrometre; N, Number; ON eyes, eyes with a history of ON; NON eyes, eyes without a history of ON.

All eyes included in this study had normal HCVA (LogMAR ≥0), and as it was expected, there were no significant differences between groups for this metric. There were no differences in the risk of having a VEP delayed status (table 6-7).

	HCVA		pRNFL		VEP	
	B (SE)	P value	B (SE)	P value	B (SE)	P value
AQP4-NMOSD-NON vs MOGAD-NON	0.002 (0.01)	1	9.88 (4.49)	0.19	4.35 (4.75)	1
AQP4-NMOSD-NON vs AQP4-NMOSD-ON	-0.006 (0.02)	1	13.73 (6.53)	0.24	6.88 (7.14)	1
AQP4-NMOSD-NON vs MOGAD-ON	-0.01 (0.01)	1	31.01 (4.21)	<0.0001	16.04 (7.66)	0.22
MOGAD-NON vs AQP4-NMOSD-ON	-0.008 (0.02)	1	3.85 (6.45)	1	2.53 (6.02)	1
MOGAD-NON vs MOGAD-ON	-0.02 (0.008)	0.12	21.12 (3.17)	<0.0001	11.69 (4.71)	0.07
AQP4-NMOSD-ON vs MOGAD-ON	-0.014 (0.022)	1	17.27 (6.24)	0.04	9.15 (6.61)	0.99

**Table 6-7: Baseline measures of eyes with AQP4-NMOSD and MOGAD patients. Differences between disease groups and healthy controls**

Baseline characteristics and differences between the two disease groups. Abbreviations: AQP4-NMOSD, aquaporin-4 antibody positive Neuromyelitis Optica; MOGAD, Myelin oligodendrocyte glycoprotein antibody positive associated disease; VEP, visual evoked potentials; LogMar, logarithm of the minimum angle of resolution; pRNFL, peripapillary retinal nerve fibre layer; SD, standard deviation; N, Number; B, estimate; SE, standard error. Red shading establishes significance at  $p < 0.05$

However, the peripapillary retinal nerve fibre layer of MOGAD eyes with previous history of ON appears to be more affected than any other eyes, presenting significant differences with AQP4-NMOSD eyes with previous history of ON ( $p=0.04$ ), AQP4-NMOSD eyes without previous history of ON ( $p < 0.001$ ), and MOGAD without previous history of ON ( $p < 0.001$ ) (table 6-7). These results indicate a dissonance between

structure and function in MOGAD eyes with previous history of ON, where despite patients preserving their visual acuity, they present a significant thinning in pRNFL compared to other disease groups (figure 6-8).

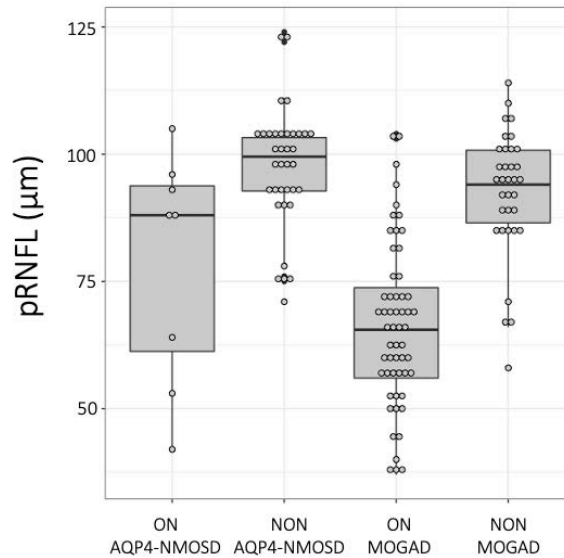


**Figure 6-8: Boxplots of pRNFL distributions between groups**

pRNFL in AQP4-NMOSD and MOGAD patients. Abbreviations: AQP4-NMOSD-ON, aquaporin-4 antibody positive NMOSD eyes with history of optic neuritis; AQP4-NMOSD-NON, aquaporin-4 antibody positive NMOSD eyes with no history of optic neuritis; MOGAD-ON, Myelin oligodendrocyte glycoprotein antibody positive associated disease eyes with history of optic neuritis; MOGAD-NON, Myelin oligodendrocyte glycoprotein antibody positive associated disease eyes with no history of optic neuritis; pRNFL, peripapillary retinal nerve fibre layer.

## 6.2.2. The macular sub-study cohort (BABINSCI cohort)

Twenty-one HC, 9 AQP4-NMOSD patients and 19 MOGAD patients were included in the analysis (table 6-8).

	AQP4-NMOSD	MOGAD	Healthy controls
Subjects (N)	9	19	21
Eyes (N)	15	35	42
Sex (female (%))	7 (77.8%)	15 (78.9%)	15 (71.4%)
Age at OCT (years, median (range))	46 (12-82)	35 (19-72)	45 (24-72)
Disease duration at OCT (years, median (range))*	7 (1-25)	3 (0-32)	-
Eyes with history of ON (N (%))	3 (20%)	20 (57.1%)	-
Time from last ON to OCT (months, median (range)) *	20 (17-25)	37 (10-384)	-

**Table 6-8: Macular sub-study cohort overview**

Age group differences between AQP4-NMOSD and MOGAD participants were not significant (One-way ANOVA test for age,  $p=0.339$ ). Sex differences tested by multiple groups chi-squared,  $X$ -statistic=0.34,  $p=0.84$ . Differences in disease duration and time since last ON to OCT were significant between the disease groups (Mann Whitney test  $p=0.04$ ,  $p=0.01$  respectively). Abbreviations: AQP4-NMOSD, aquaporin-4 antibody positive Neuromyelitis Optica; MOGAD, Myelin oligodendrocyte glycoprotein antibody positive associated disease; N, number;

---

OCT, Optic coherence tomography; ON, optic neuritis eyes; SD, standard deviation.

\* Indicates significant difference between MOGAD and AQP4-NMOSD.

---

Due to the small sample size, the numbers and percentages of eyes with normal and abnormal structural tests are presented in table 6-9 rather than in percentages only. This cohort adopts a stricter definition of OCT abnormality. While in the previous cohort OCT abnormality was defined based uniquely on the peripapillary retinal nerve fibre layer (pRNFL), this cohort adds the macula in the definition of abnormality, with a composite biomarker of impairment composed by pRNFL + GCIP + mRNFL for a better understanding of the macular pathology.

AQP4-NMOSD eyes with previous history of ON are characterized by delayed VEP values (67%) while eyes with no previous history of ON present with normal OCT and only 1 presents with abnormal VEP.

In MOGAD eyes with previous history of ON, only 20% recover completely at a structural and functional level, while 73% of patients with no history of ON show both normal OCT and VEP (Table 6-9).

<b>Eyes Normal HCVA (N(%))</b>	<b>Normal VEP &amp; Normal OCT</b>	<b>Abnormal VEP &amp; Abnormal OCT</b>	<b>Normal VEP &amp; Abnormal OCT</b>	<b>Abnormal VEP &amp; Normal OCT</b>
<b>AQP4-NMOSD eyes</b>				
<b>TOTAL (n=15)</b>	12 (80%)	0 (0%)	0 (0%)	3 (20%)
<b>ON (n=3)</b>	1 (33%)	0 (0%)	0 (0%)	2 (67%)
<b>NON (n=12)</b>	11 (92%)	0 (0%)	0 (0%)	1 (8%)
<b>MOGAD eyes</b>				
<b>TOTAL (n=35)</b>	15 (43%)	6 (17%)	5 (14%)	9 (26%)
<b>ON (n=20)</b>	4 (20%)	6 (30%)	5 (25%)	5 (25%)
<b>NON (n=15)</b>	11 (73%)	0 (0%)	0 (0%)	4 (27%)

**Table 6-9: Structural tests in normal central visual function eyes in the research cohort**

Distribution between normal and abnormal structural tests for eyes with normal central visual function. Abnormal VEP= latency >112ms. Abnormal OCT= pRNFL  $\leq 80 \mu\text{m}$  + GCIP  $\leq 0.55 \text{ mm}^3$  + mRNFL  $\leq 0.12 \text{ mm}^3$ . Abbreviations: AQP4-NMOSD, aquaporin-4 antibody positive Neuromyelitis Optica; MOGAD, Myelin oligodendrocyte glycoprotein antibody positive associated disease; VEP, visual evoked potentials; OCT, optic coherence tomography.



A description of baseline retinal thickness of the research cohort can be found in table 6-10.

	<b>AQP4- NMOSD ON eyes Mean (SD)</b>	<b>MOGAD ON eyes Mean (SD)</b>	<b>AQP4- NMOSD NON eyes Mean (SD)</b>	<b>MOGAD NON eyes Mean (SD)</b>	<b>HC eyes Mean (SD)</b>
<b>pRNFL (<math>\mu\text{m}</math>)</b>	93.6 (9.86)	69.1 (16.49)	98.8 (6.29)	95.2 (5.54)	98.6 (10.9)
<b>GCIP (<math>\text{mm}^3</math>)</b>	0.51 (0.04)	0.45 (0.08)	0.61 (0.05)	0.60 (0.03)	0.61 (0.075)
<b>TMV (<math>\text{mm}^3</math>)</b>	2.26 (0.10)	2.21 (0.08)	2.32 (0.10)	2.37 (0.09)	2.33 (0.09)
<b>FT (<math>\mu\text{m}</math>)</b>	272.3 (10.96)	267.1 (16.5)	266.5 (26.6)	276.2 (21.6)	271.8 (19.6)
<b>INL (<math>\text{mm}^3</math>)</b>	0.29 (0.03)	0.28 (0.02)	0.27 (0.022)	0.27 (0.02)	0.26 (0.015)
<b>mRNFL (<math>\text{mm}^3</math>)</b>	0.137 (0.012)	0.121 (0.015)	0.15 (0.014)	0.14 (0.015)	0.14 (0.019)

**Table 6-10: Baseline OCT measures of the advanced research cohort**

This table contains eyes with good HCVA (HCVA LogMAR  $\leq 0$ ). Abbreviations: AQP4 ON, Aquaporin-4 IgG seropositive eyes with a history of ON; MOG ON, Myelin oligodendrocyte glycoprotein IgG seropositive eyes with a history of ON; AQP4 NON, Aquaporin-4 IgG seropositive eyes without a history of ON; MOG NON, Myelin oligodendrocyte glycoprotein IgG seropositive eyes without a history of ON; HC, healthy control eyes; pRNFL, peripapillary retinal nerve fibre layer; GCIP, ganglionar and inner plexiform layer; TMV, total macular volume; FT, foveal thickness; INL, Inner nuclear layer; mRNFL, retinal nerve fibre layer; SD, standard deviation.

A more comprehensive distribution of the data is presented in figure 6-9. Linear mixed effects models were performed in ON vs HC, NON vs HC and ON vs NON to assess baseline differences in the macular sub-study cohort in the two diseases. LME models were adjusted by sex, age at the time of the OCT and race while accounting for inter-eye correlations of monocular measurements. AQP4- NMOSD-ON eyes with recovered visual function show no differences in any of the retinal layers or pRNFL with HC, however, MOGAD-ON eyes, despite of having recovered the central visual function, remain with a significant impairment in all their inner retinal layers and pRNFL compared to HC (pRNFL,  $p < 0.0001$ ; GCIP,  $p < 0.0001$ ; TMV,  $p = 0.0132$ ; INL,  $p = 0.0491$ ; mRNFL,  $p = 0.0179$ ) and show a significant thinning in their pRNFL compared to AQP4-NMOSD-ON eyes. In the case of MOGAD-NON eyes, they show no significant differences compared to HC or AQP4-NMOSD eyes (table 6-11).

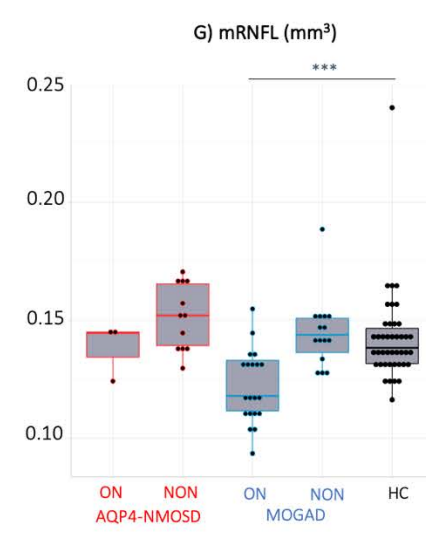
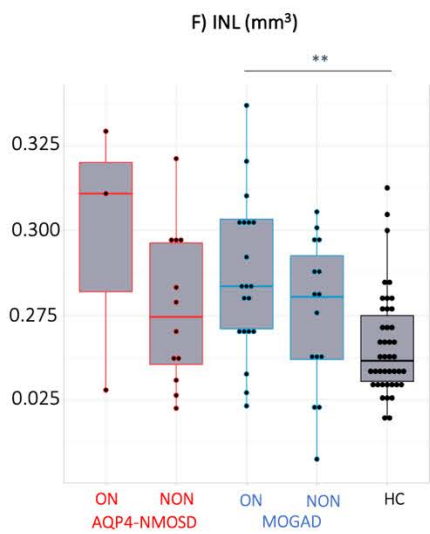
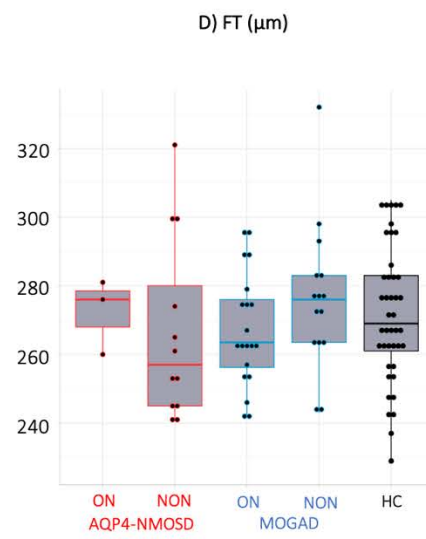
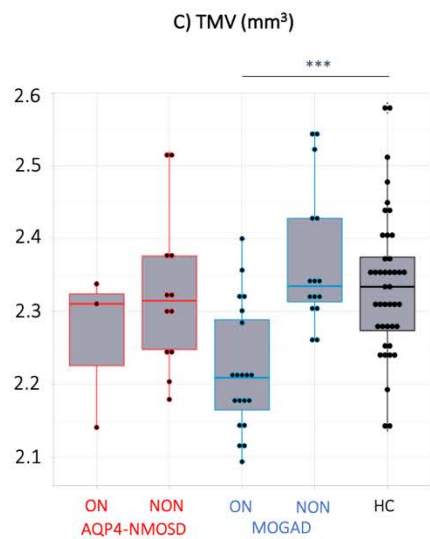
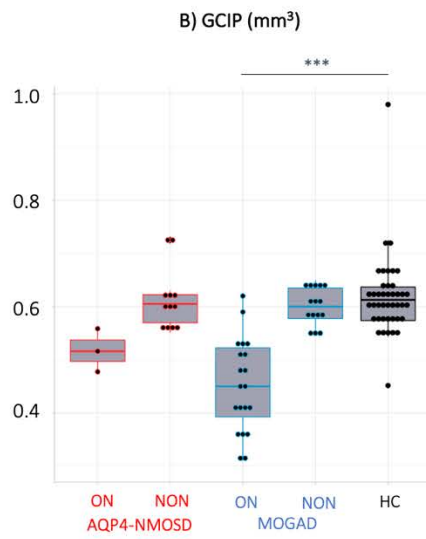
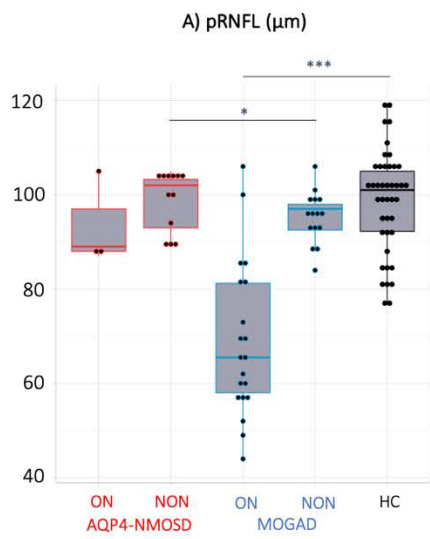
	AQP4-NMOSD ON eyes Vs HC		MOGAD ON eyes Vs HC		AQP4-NMOSD NON eyes Vs HC		MOGAD NON eyes Vs HC		<u>ON eyes:</u> AQP4-NMOSD Vs MOGAD		<u>NON eyes:</u> AQP4-NMOSD Vs MOGAD	
	B(SE)	P value	B(SE)	P value	B(SE)	P value	B(SE)	P value	B(SE)	P value	B(SE)	P value
<b>pRNFL</b>	-4.18 (8.30)	0.6164	-33.1 (3.77)	≤0.001	0.057 (4.77)	0.9904	-1.31 (3.91)	0.739	1.37 (5.22)	1	28.96 (8.45)	0.0141
<b>GCIP</b>	-0.09 (0.04)	0.0507	-0.18 (0.02)	≤0.001	-0.003 (0.02)	0.8862	-0.012 (0.02)	0.6067	0.008 (0.03)	1	0.08 (0.05)	0.8933
<b>TMV</b>	-0.10 (0.07)	0.1655	-0.12 (0.03)	≤0.001	-0.012 (0.042)	0.7613	0.046 (0.032)	0.1632	-0.05 (0.04)	1	0.02 (0.07)	1
<b>FT</b>	-4.54 (14.98)	0.7632	-4.68 (6.56)	0.4799	-1.64 (8.74)	0.8513	8.55 (6.62)	0.2034	-10.20 (9.11)	1	0.13 (15.08)	1
<b>INL</b>	0.021 (0.01)	0.1677	0.020 (0.006)	0.0039	0.010 (0.008)	0.241	0.007 (0.007)	0.3211	0.003 (0.009)	1	0.0004 (0.015)	1
<b>mRNFL</b>	-0.007 (0.01)	0.5485	-0.020 (0.005)	≤0.001	0.008 (0.006)	0.2208	0.003 (0.005)	0.5259	0.004 (0.007)	1	0.013 (0.012)	1

---

**Table 6-11: Baseline OCT measures of the advanced research cohort in patients with normal HCVA**

Abbreviations: AQP4-NMOSD ON, Aquaporin-4 NMOSD seropositive eyes with a history of ON; MOGAD ON, Myelin oligodendrocyte glycoprotein associated disease seropositive eyes with a history of ON; AQP4-NMOSD NON, Aquaporin-4 NMOSD seropositive eyes without a history of ON; MOG NON, Myelin oligodendrocyte glycoprotein associated disease seropositive eyes without a history of ON; HC, healthy control eyes; pRNFL, peripapillary retinal nerve fibre layer; GCIP, ganglionar and inner plexiform layer; TMV, total macular volume; FT, foveal thickness; INL, Inner nuclear layer; mRNFL, retinal nerve fibre layer; B, estimate; SE, standard error. Red shading stablishes significance at  $p < 0.05$ .

---



---

**Figure 6-9: Box plots of disc and macular baseline OCT and fovea in eyes with normal HCVA**

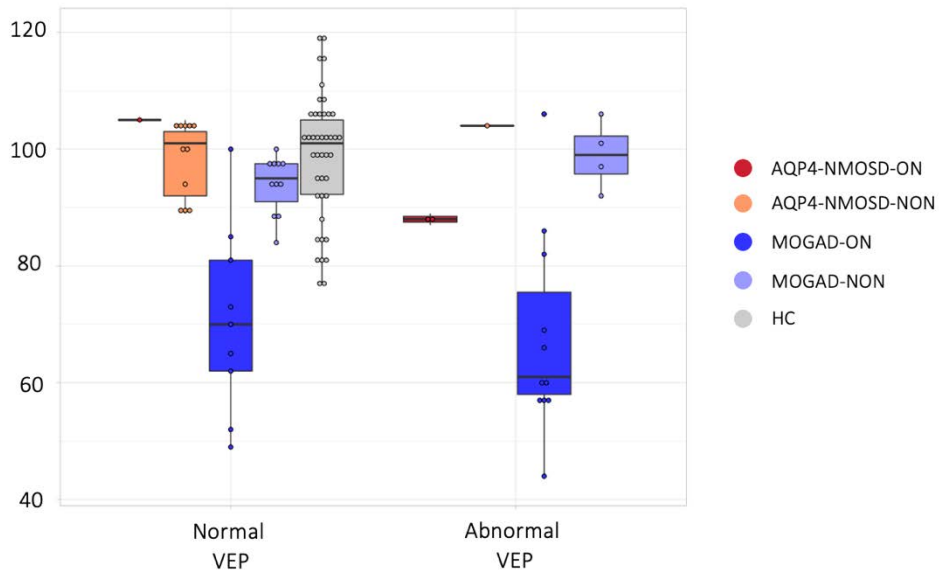
A) pRNFL, peripapillary retinal nerve fibre layer at the disc; B) GCIP, combined ganglion cell and inner plexiform layer; C) TMV: total macular volume; D) FT, foveal thickness; E) INL: Inner nuclear layer; F) mRNFL: retina nerve fibre layer at macula; Boxplot show median and 25<sup>th</sup> and 75<sup>th</sup> percentile. Abbreviations: ON AQP4, Aquaporin-4 IgG seropositive eyes with a history of ON; ON MOG, Myelin oligodendrocyte glycoprotein IgG seropositive eyes with a history of ON; NON AQP4, Aquaporin-4 IgG seropositive eyes without a history of ON; NON MOG, Myelin oligodendrocyte glycoprotein IgG seropositive eyes without a history of ON; HC, healthy control eyes.

Significance of LME model comparison is shown in this boxplot:  $<0.05$  &  $\geq 0.01$  (\*);  $<0.01$  &  $>0.001$  (\*\*);  $\leq 0.001$  (\*\*\*)

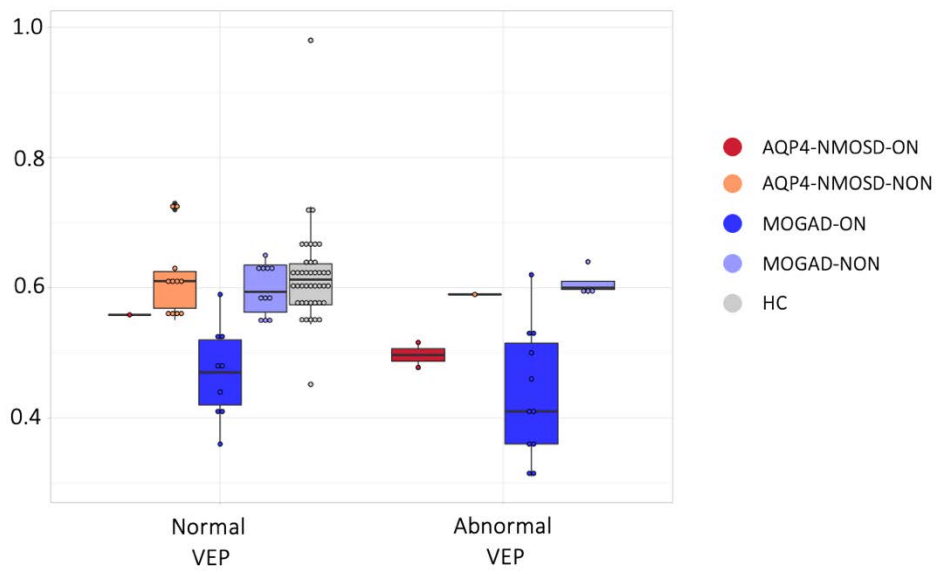
---

The number of eyes with abnormal VEP and normal HCVA is not big enough in this cohort to be able to perform any statistical analysis. However, as it can be observed in figure 6-10, abnormalities in VEP are more frequent in MOGAD eyes previously affected by ON as compared to MOGAD eyes not previously affected by ON or in all AQP4-NMOSD eyes.

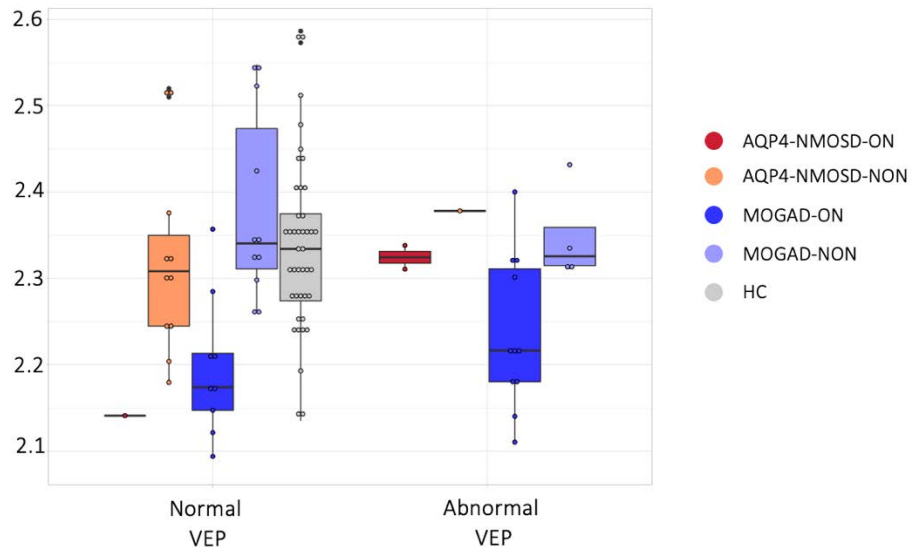
A) pRNFL ( $\mu\text{m}$ )



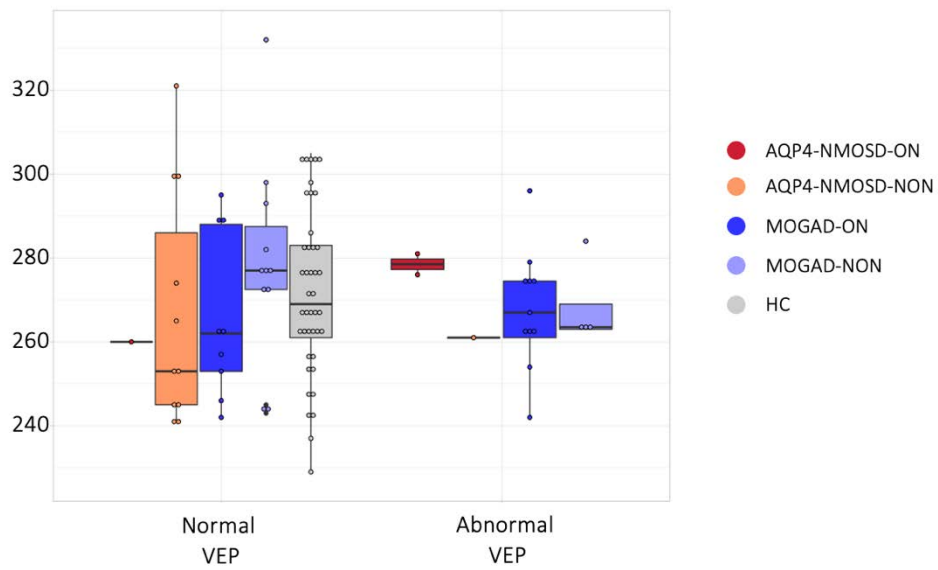
B) GCIP ( $\text{mm}^3$ )



C) TMV (mm<sup>3</sup>)



D) FT (μm)





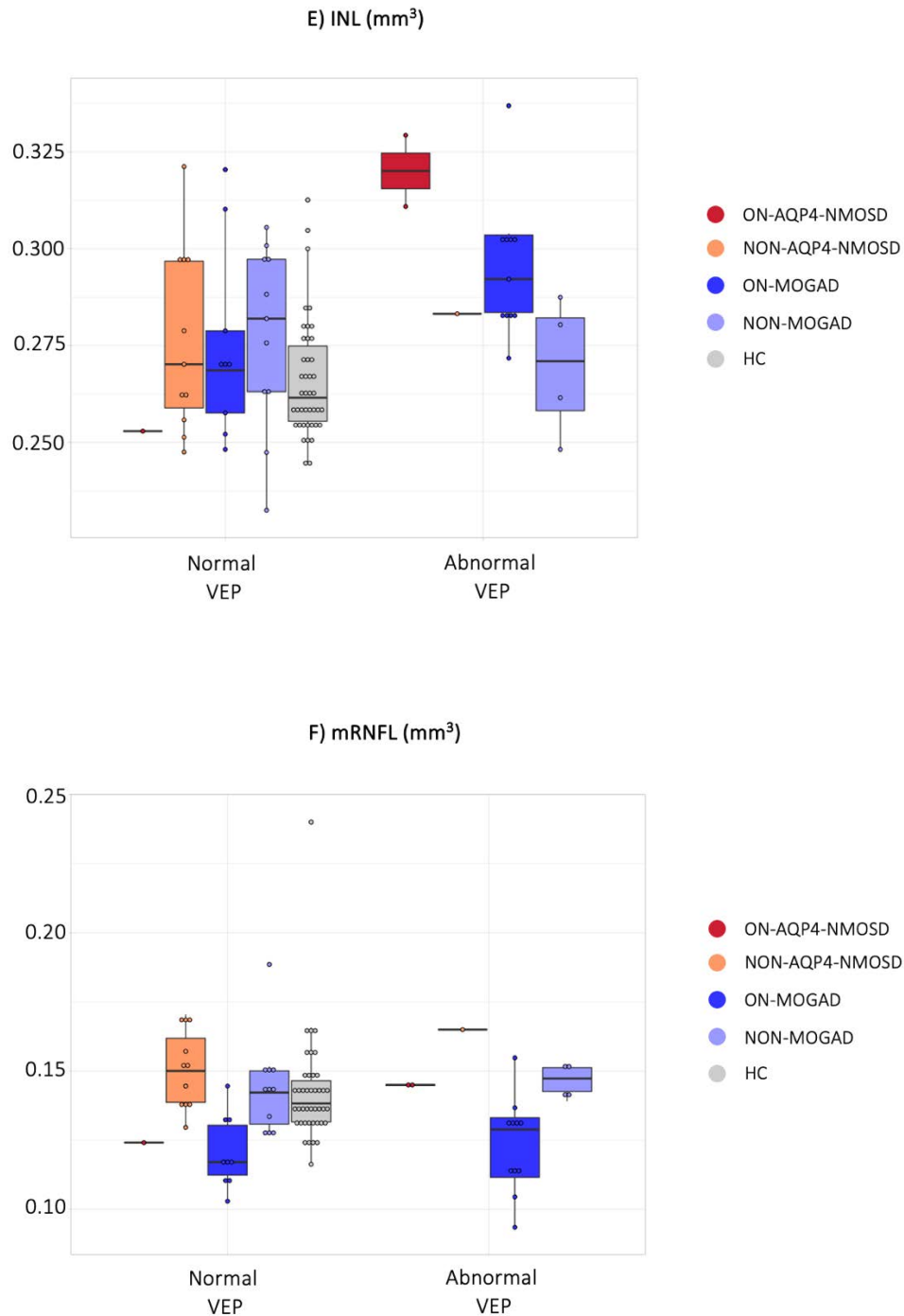


**Figure 6-10: Box plots of disc and macular baseline OCT and fovea for eyes with good HCVA divided by normal and abnormal VEP**

A) pRNFL, peripapillary retinal nerve fibre layer at the disc; B) GCIP, combined ganglion cell and inner plexiform layer; C) TMV: total macular volume; D) FT, foveal thickness; E) INL: Inner nuclear layer; F) mRNFL: retina nerve fibre layer at macula;

---

Boxplot show median and 25<sup>th</sup> and 75<sup>th</sup> percentile. Abbreviations: VEP, visual evoked potentials; ON AQP4, Aquaporin-4 NMOSD seropositive eyes with a history of ON; ON MOG, Myelin oligodendrocyte glycoprotein associated disease seropositive eyes with a history of ON; NON AQP4, Aquaporin-4 NMOSD seropositive eyes without a history of ON; NON MOG, Myelin oligodendrocyte glycoprotein associated disease seropositive eyes without a history of ON; HC, healthy control eyes.

---

## **6.2. PROJECT 3: *Foveal changes in AQP4-NMOSD***

Thirty-eight HC and 27 AQP4-NMOSD patients were included in the analysis (Table 6-12).

PATIENT CHARACTERISTICS		HC	AQP4-NMOSD		
			Unilateral ON	Bilateral ON	No history of ON
Number of participants		38	6	6	15
Sex	female n (%)	27(74%)	5 (83%)	5 (83%)	15 (100%)
Age at baseline (years)	median (IQR)	42.60 (30.65-51.77)	34.4 (18.1)	45.8 (27.0)	46.6 (15.5)
F/U time (years)	median (IQR)	1.95 (1.83-2.54)	3.16 (0.66)	1.54 (1.98)	2.19 (1.6)
Race	African/Caribbean n (%)	NA	1 (17%)	1 (17%)	2 (7%)
	Asian n (%)		1 (17%)	0 (0%)	1 (13%)
	Caucasian n (%)		4 (66%)	4 (66%)	12 (80%)
	Mix n (%)		0 (0%)	1 (17%)	0 (0%)
Disease Duration (years)	median (IQR)	-	4.4 (6.7)	6.6 (8.4)	1.44 (2.2)
EYE CHARACTERISTICS		HC	AQP4-NMOSD		
			ON	NON	
Number of eyes		76	15	34	
Time from last ON (years)	median (IQR)	-	4.21 (5.30)	-	

---

**Table 6-12: Cohort overview**

Age and sex group differences between HC and AQP4-NMOSD patients were not significant (Fisher's exact tests for sex, [AQP4 vs HC p=0.1020] Wilcoxon test for age [AQP4 vs HC p=0.3796] and follow up time, [AQP4 vs HC p=0.1712]. Abbreviations: AQP4-NMOSD, neuromyelitis optica spectrum disorder AQP4 ab positive; F/U, Follow-up; HC, Healthy controls; ON, Optic neuritis; NON, Non-optic neuritis; SD, standard deviation.

---

Of the AQP4-NMOSD group, 34 eyes had no previous history of ON (NON), and 15 had previous history of ON. Four eyes were excluded from the analysis due to poor image quality or technical issues, one eye due to amblyopia. There were no significant differences between the HC and the AQP4-NMOSD group in baseline demographic features, indicating successful matching.

Baseline characteristics for retinal layers and foveal parameters are described in table 6-13 and table 6-14 respectively.

	HC	NMOSD	
		ON	NON
	mean (SD)	mean (SD)	mean (SD)
pRNFL( $\mu\text{m}$ )	99.10 (10.35)	61.86 (21.72)	98.17 (10.86)
GCIP ( $\text{mm}^3$ )	0.62 (0.04)	0.40 (0.11)	0.57 (0.05)
TMV ( $\text{mm}^3$ )	2.36 (0.09)	2.1 (0.13)	2.28 (0.07)
INL ( $\text{mm}^3$ )	0.27 (0.02)	0.28 (0.02)	0.25 (0.02)
FT( $\mu\text{m}$ )	275.10 (19.58)	268.13 (19.39)	264 (18.61)
mRNFL( $\text{mm}^3$ )	0.14 (0.01)	0.12 (0.03)	0.14 (0.01)

---

**Table 6-13: Baseline OCT measures for the retinal layers**

This table contains baseline retinal imaging metrics. Abbreviations: AQP4-NMOSD, Aquaporin Neuromyelitis Spectrum Disorder eyes; HC, Healthy controls eyes; ON,

---

Optic neuritis; NON, Non-optic neuritis; pRNFL, peripapillary retinal nerve fibre layer; GCIP, ganglionar and inner plexiform layer; TMV, total macular volume; FT, foveal thickness; INL, Inner nuclear layer; mRNFL, retinal nerve fibre layer in the macula; SD, standard deviation.

	HC	NMOSD	
		ON	NON
	mean (SD)	mean (SD)	mean (SD)
Average Pit Depth (mm)	0.11 (0.02)	0.08 (0.01)	0.11 (0.02)
Central Foveal Thickness (mm)	0.23 (0.01)	0.23 (0.01)	0.22 (0.01)
Average Rim Height (mm)	0.34 (0.01)	0.31 (0.02)	0.33 (0.01)
Average Rim Diameter (mm)	2.19 (0.12)	2.02 (0.05)	2.17 (0.13)
Rim Disc Area (mm <sup>2</sup> )	3.75 (0.40)	3.20 (0.17)	3.67 (0.44)
Major Rim Disc Length (mm)	0.63 (0.069)	0.54 (0.03)	0.62 (0.07)
Minor Rim Disc Length (mm)	0.62 (0.068)	0.53 (0.02)	0.61 (0.07)
Major Slope Disc Length (mm)	0.07 (0.02)	0.06 (0.021)	0.08 (0.03)
Minor Slope Disc Length (mm)	0.05 (0.02)	0.05 (0.02)	0.07 (0.02)
Slope Disc Area (mm <sup>2</sup> )	0.40 (0.15)	0.366 (0.12)	0.48 (0.18)
Average Slope Disc Diameter (mm)	0.69 (0.14)	0.66 (0.12)	0.76 (0.15)
Pit Disc Area (mm <sup>2</sup> )	0.03(0.01)	0.044 (0.015)	0.04 (0.01)
Average Pit Flat disc diameter (mm)	0.21 (0.03)	0.23 (0.04)	0.24 (0.03)
Major Pit Flat disc length (mm)	0.006 (0.002)	0.008 (0.002)	0.008 (0.002)
Minor pit flat disc length (mm)	0.005 (0.001)	0.0068 (0.002)	0.007 (0.002)
Rim Volume (mm <sup>3</sup> )	1.04 (0.15)	0.79 (0.10)	0.97 (0.15)
Pit Volume (mm <sup>3</sup> )	0.26 (0.04)	0.21 (0.032)	0.26 (0.04)
Inner Rim Volume (mm <sup>3</sup> )	0.10 (0.01)	0.09 (0.01)	0.09 (0.01)
Av Max Pit slope degree (°)	11.67 (3.38)	7.87 (2.57)	11.02 (2.88)

**Table 6-14: Baseline foveal parameters derived from the Cubic Bezier algorithm**

Baseline descriptive and comparisons of foveal results for patients with NMOSD (ON and NON) and HC. Abbreviations: AQP4-NMOSD, neuromyelitis optica spectrum disorder with AQP4 Ab positive; ON, optic neuritis eyes; NON, eyes without a history of optic neuritis; HC, healthy control eyes; SD, standard deviation.

Group differences at baseline analysed using multivariate linear mixed effects models with estimated marginal means adjusted for age at baseline, sex and site while accounting for inter-eye correlations is presented in detail in table 6-15 for the retinal layers and in table 6-16 for the foveal parameters.

	ON Vs HC		NON Vs HC		ON Vs NON	
	B (SE)	P values	B(SE)	P values	B (SE)	P values
pRNFL ( $\mu\text{m}$ )	-37.23 (3.48)	<0.0001	-0.929 (2.54)	1	-36.310 (3.82)	<0.0001
GCIP ( $\text{mm}^3$ )	-0.2099 (0.0170)	<0.0001	-0.0539 (0.0124)	0.0001	-0.1561 (0.0189)	<0.0001
TMV ( $\text{mm}^3$ )	-0.1901 (0.0262)	<0.0001	-0.0863 (0.0192)	<0.0001	-0.1038 (0.0291)	0.0016
INL ( $\text{mm}^3$ )	0.009 (0.006)	0.4456	-0.01 (0.004)	0.0072	0.02 (0.007)	0.0028
FT ( $\mu\text{m}$ )	-5.56 (5.39)	0.9121	-12.46 (3.96)	0.0062	6.90 (6)	0.7570
mRNFL( $\text{mm}^3$ )	-0.01874 (0.00440)	0.0001	-0.00267 (0.00323)	1	-0.01606 (0.00490)	0.0041

**Table 6-15: Baseline OCT differences between disease group and healthy controls**

---

Maximum likelihood was used for the estimation of p-values. Abbreviations: ON, optic neuritis eyes; NON, eyes without a previous history of optic neuritis; HC, healthy control eyes; B, estimate, SE, standard error. pRNFL, peripapillary retinal nerve fibre layer; GCIP, ganglionar and inner plexiform layer; TMV, total macular volume; FT, foveal thickness; INL, inner nuclear layer; mRNFL, retinal nerve fibre layer. Boxes in red establish the significance at  $p < 0.05$ .

---



	LME					
	ON Vs HC		NON Vs HC		ON Vs NON	
	B (SE)	P values	B(SE)	P values	B (SE)	P values
Average Pit Depth (mm)	-0.04371 (0.00622)	<0.0001	-0.0062 (0.0045)	0.5230	-0.0309 (0.00682)	<0.0001
Central Foveal Thickness (mm)	0.001(0.005)	1	-0.004(0.003)	0.407	0.007(0.005)	0.656
Average Rim Height (mm)	-0.0344 (0.0398)	<0.0001	- 0.0133 (0.00292)	<0.0001	-0.0211 (0.00443)	<0.0001
Average Rim Diameter (mm)	-0.1649 (0.0344)	<0.0001	- 0.0232 (0.0244)	1	-0.1417 (0.0376)	0.0008
Rim Disc Area (mm <sup>2</sup> )	-0.5507 (0.1162)	<0.0001	-0.0765 (0.0824)	1	-0.4742 (0.1268)	0.0009
Major Rim Disc Length (mm)	-0.0953 (0.0198)	<0.0001	-0.0136 (0.0140)	0.9988	-0.0817 (0.0216)	0.0007
Minor Rim Disc Length (mm)	-0.0896 (0.0194)	<0.0001	-0.0121 (0.0137)	1	-0.0775 (0.021)	0.0011
Major Slope Disc Length (mm)	-0.007(0.008)	1	0.013(0.006)	0.1003	-0.021(0.009)	0.075
Minor Slope Disc Length (mm)	-0.00496 (0.00668)	1	0.01625 (0.00490)	0.0036	-0.2121 (0.00743)	0.0152
Slope Disc Area (mm <sup>2</sup> )	-0.0338 (0.448)	1	0.0854 (0.0327)	0.0304	-0.1192 (0.0491)	0.0502
Average Slope Disc Diameter (mm)	-0.274 (0.0407)	1	0.0719 (0.0297)	0.0514	-0.0993 (0.0447)	0.0842
Pit Disc Area (mm <sup>2</sup> )	0.00639 (0.00371)	0.261	0.00936 (0.00271)	0.0023	-0.00296 (0.00407)	1
Average Pit Flat disc diameter (mm)	0.01721 (0.01039)	0.3006	0.02597 (0.00759)	0.0025	-0.00876 (0.01140)	1
Major Pit Flat disc length (mm)	0.00121 (0.000669)	0.2216	0.00158 (0.000488)	0.0048	-0.00037 (0.000734)	1

Minor pit flat disc length (mm)	0.000937 (0.000586)	0.3378	0.001540 (0.000428)	0.0014	-0.000603 (0.000643)	0.3378
Rim Volume (mm <sup>3</sup> )	-0.25 (0.043)	< 0.0001	-0.07(0.031)	0.0662	-0.183(0.043)	0.0006
Pit Volume (mm <sup>3</sup> )	-0.05250 (0.01307)	0.0003	0.00148 (0.00955)	1	0.05398 (0.01434)	0.0008
Inner Rim Volume (mm <sup>3</sup> )	0.00409 (0.00539)	1	-0.00967 (0.00394)	0.0464	0.00559 (0.00592)	1
Av Max Pit slope degree (°)	-3.798 (0.896)	0.0001	-0.652 (0.654)	0.9639	-3.146 (0.983)	0.0053

---

**Table 6-16: Baseline foveal shape parameters differences between disease group and healthy controls**

Maximum likelihood was used for the estimation of p-values. Abbreviations: ON, optic neuritis eyes; NON, eyes without a history of optic neuritis; HC, healthy control eyes; B, estimate, SE, standard error. Boxes in red establish the significance at  $p < 0.05$ .

---

As expected, the models showed significant thinning in pRNFL, GCIP, TMV, and mRNFL in ON eyes compared to HC eyes and to NON eyes, suggesting profound neuroaxonal damage. NON versus HC eyes showed significantly thinner GCIP, TMV, INL and FT in NON eyes (figure 6-11).

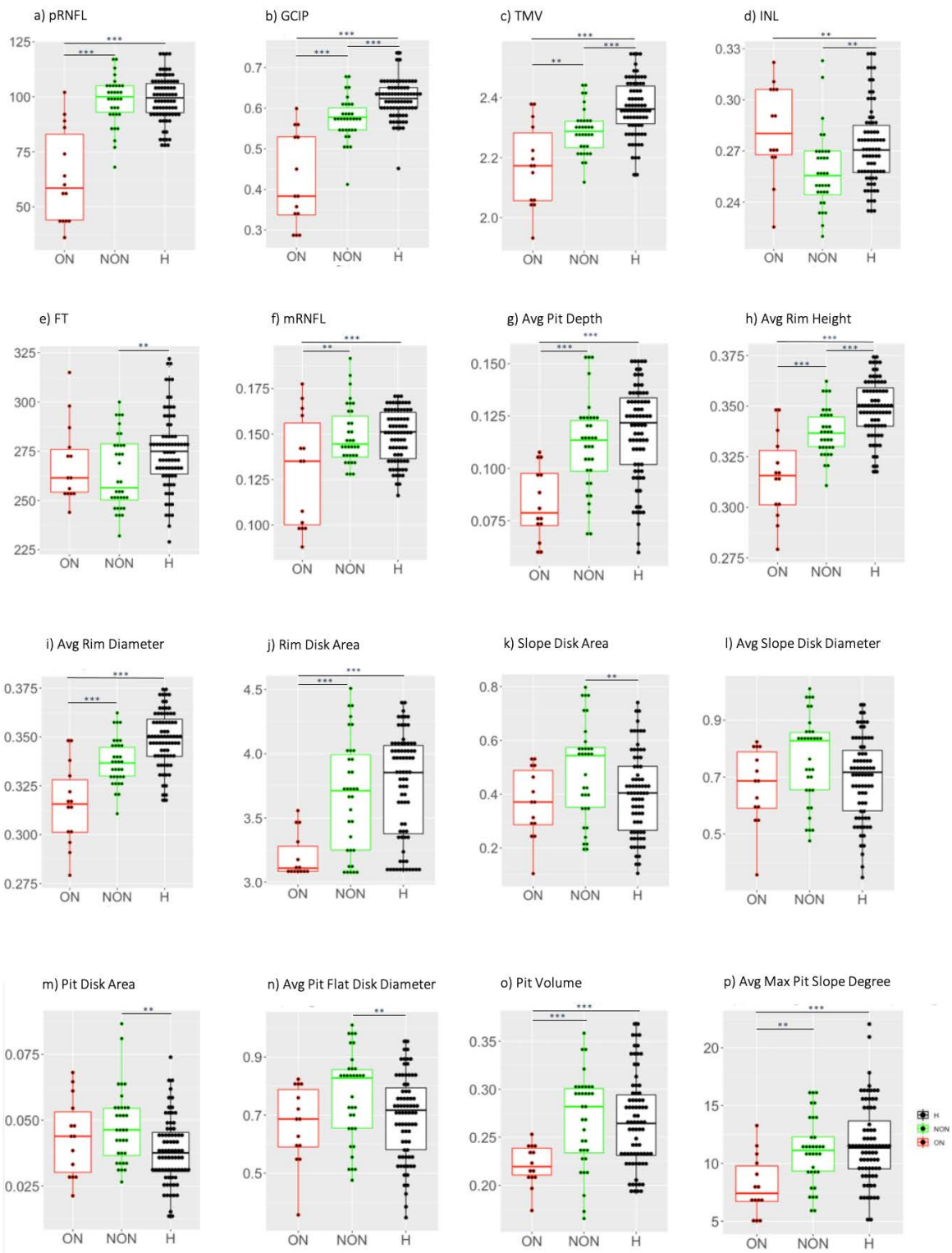


**Figure 6-11: Box plots of disc and macular baseline OCT and foveal data**

a) pRNFL: peripapillary retinal nerve fibre layer at the disc; b) GCIP: combined ganglion cell and inner plexiform layer; c) TMV: total macular volume; d) INL: Inner

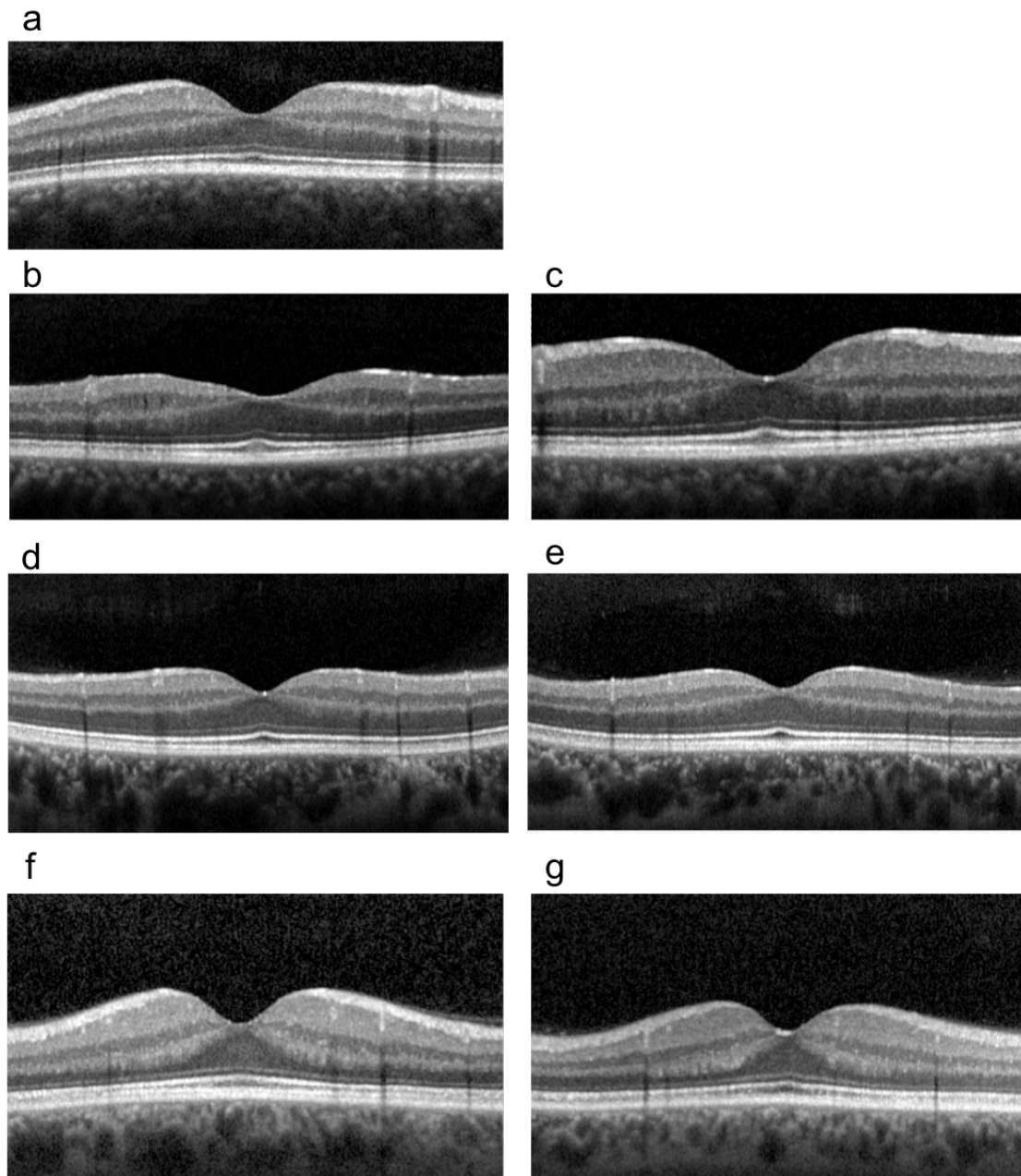
---

nuclear layer; e) FT: foveal thickness; f) mRNFL: retina nerve fibre layer at macula; g) Average Pit Depth; h) Average rim height; i) Average rim diameter; j) Rim disc area; k) Slope disc area; l) Average slope disc diameter; m) Pit disc area; n) average pit flat disc diameter; o) Pit volume; and p) Average maximum pit slope degree. Boxplot show median and 25<sup>th</sup> and 75<sup>th</sup> percentile. Significance of LME model comparison is shown in this boxplot: <0.05 & ≥0.01 (\*); <0.01 & >0.001 (\*\*); ≤0.001 (\*\*\*).

---

### 6.2.1. Foveal changes

Fovea morphometry quantifies several metrics of the fovea (figure 5-5). Visually, ON-related changes in the fovea/parafoveal area can be interpreted as flattening of this area (figure 6-12 b,d,e), whereas NON changes appear can be interpreted as widening of this area (figure 6-12 c,f,g), already suggesting different mechanisms causing the change (figure 6-13 a and b).




---

**Figure 6-12: Foveal changes in NMOSD. OCT examples**

**a:** Healthy eye, **b:** Optic neuritis (ON) right eye from a unilateral ON patient, **c:** Fellow left eye from a unilateral ON patient, **d:** ON right eye from a bilateral ON patient, **e:** ON left eye from a bilateral ON patient, **f:** NON right eye from a patient “never affected” (from patients with no history of ON) by ON, **g:** NON left eye from a patient “never affected” (from patients with no history of ON) by ON.

---

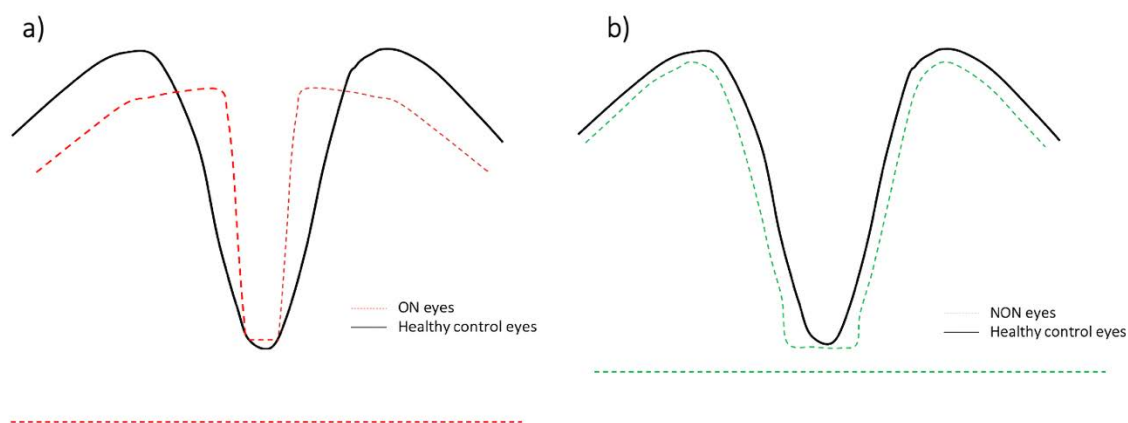


**Figure 6-13: Foveal changes in AQP4-NMOSD. Schematic model**

**a:** eyes with a history of ON (ON eyes) and **b:** eyes without a history of ON (NON-eyes). Both horizontal dashed lines in figures **a** and **b** refer to the central foveal thickness distance, defined as the minimum height of fovea at the centre of the pit. Abbreviations: NMOSD, Neuromyelitis optica spectrum disorders; HC, Healthy controls; ON, optic neuritis eyes; NON, non-optic neuritis eyes.

Lower values for ON versus HC were found in the following parameters: average pit depth, average rim height, average rim diameter, rim disc area, major and minor rim disc length, pit volume and average maximum pit slope degree. ON versus NON-eyes showed significantly lower values for average pit depth, average rim height, average rim diameter, minor slope disc length, slope disc area, rim disc area, major and minor rim disc length, pit volume and average maximum pit slope degree. Conversely, NON versus HC showed significantly lower values for average rim height and higher values for minor slope disc length, slope disc area, average slope disc diameter, pit disc area, average pit flat disc diameter, and major and minor pit flat disc length (table 6-17).

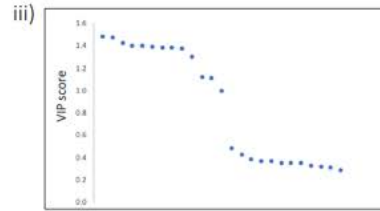
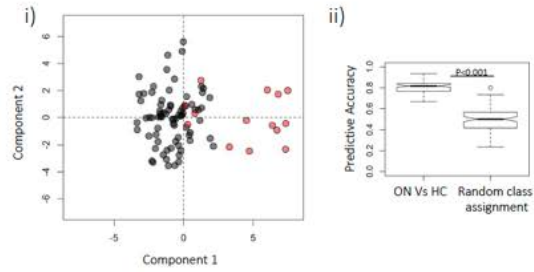
## 6.2.2. Discriminatory analysis

OPLS-DA identifies a linear combination of measures to separate two groups. This method reduces the weight of tightly correlated values that do not give an

additional benefit. OPLS-DA was employed as a supervised statistical method to discriminate ON from HC, ON versus NON, and NON-eyes from HC



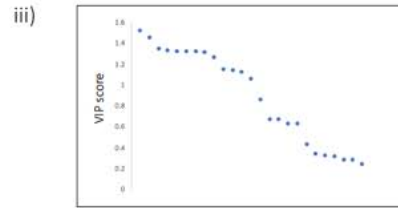
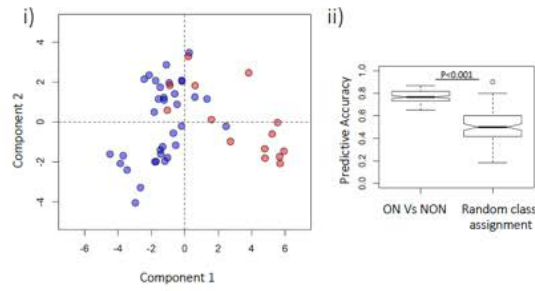
A



iv)

Parameter	VIP score
pRNFL( $\mu\text{m}$ )	1.469
GCIPL( $\text{mm}^2$ )	1.460
Rim Volume ( $\text{mm}^3$ )	1.413
Major Rim Disc Length (mm)	1.384
Average Rim Diameter (mm)	1.383
Rim Disc Area ( $\text{mm}^2$ )	1.381
Minor Rim Disc Length (mm)	1.369
Average Pit Depth (mm)	1.366
Average Rim Height (mm)	1.365

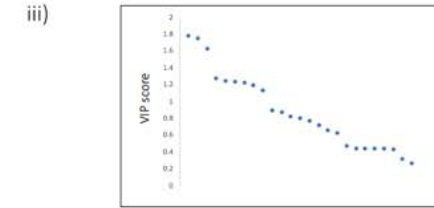
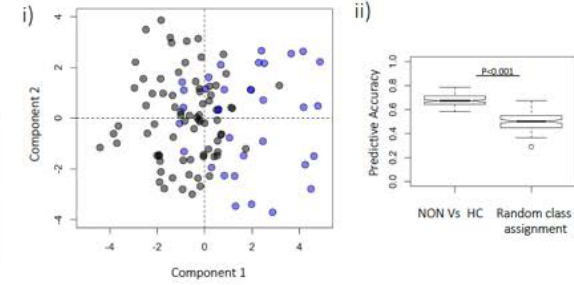
B



iv)

Parameter	VIP score
pRNFL( $\mu\text{m}$ )	1.508
GCIPL( $\text{mm}^2$ )	1.443
Average Pit Depth (mm)	1.335
Average Rim Diameter (mm)	1.316
Rim Disc Area ( $\text{mm}^2$ )	1.314
Major Rim Disc Length (mm)	1.310
Minor Rim Disc Length (mm)	1.308
Rim Volume ( $\text{mm}^3$ )	1.300
Average Rim Height (mm)	1.255

C



iv)

Parameter	VIP score
TMV( $\text{mm}^3$ )	1.769
Average Rim Height (mm)	1.733
GCIPL( $\text{mm}^2$ )	1.611
Average Pit Flat disc diameter (mm)	1.258
Minor pit flat disc length (mm)	1.235
Pit Disc Area ( $\text{mm}^2$ )	1.218
INL( $\text{mm}^3$ )	1.209
Major Pit Flat disc length (mm)	1.178
FT( $\mu\text{m}$ )	1.119

● ON ● NON ● HC

---

**Figure 6-14: OPLS-DA results**

**Ai:** OPLS-DA, ON vs HC - eyes comparison (Accuracy = 81,16%), **Aii:** OPLS-DA ON Vs HC model validation, **Aiii:** VIP scores from all parameters used in the model for each comparison, **Aiv:** Values of the most important parameters for ON vs HC. **Bi:** OPLS-DA, ON Vs NON - eyes comparison (Accuracy = 76,48%). **Bii:** OPLS-DA ON vs NON-eyes model validation, **Biii:** VIP scores from all parameters used in the model for each comparison. **Biv:** Values of the most important parameters for ON vs NON. **Ci:** OPLS-DA, NON vs HC-eyes comparison (Accuracy = 67,71%). **Cii:** OPLS-DA NON vs HC model validation, **Ciii:** VIP scores from all parameters used in the model for each comparison. **Civ:** Values of the most important parameters for NON vs HC. Abbreviations: OPLS-DA: orthogonal partial least squares discriminatory analysis; VIP, variable importance in projection; ON, optic neuritis eyes; NON, non-optic neuritis eyes; HC: healthy control eyes; pRNFL, peripapillary retinal nerve fibre layer; GCIP, ganglion cell and inner plexiform layer; INL inner nuclear layer; FT, foveal thickness.

---

Notably, the top nine most discriminatory variables contributing to the separation of ON eyes from HC and NON-eyes are pRNFL, GCIP, rim volume, major and minor rim disc length, average rim diameter, rim disc area, average pit depth and average rim height. In the separation between NON-eyes from HC, the top nine most discriminatory variables were TMV, average rim height, GCIP, average pit flat disc diameter, major and minor pit flat disc length, pit disc area, INL and FT (Figure 6-14). The selection of largely different morphometrical factors in ON and NON-eyes suggest that while NON-eyes show some evidence of neuroaxonal damage, this damage cannot explain the foveal shape changes. The variables that better describe the difference between HC and NON-eyes are not at the retinal or peripapillary level but at the foveal level, indicating an unlikely effect of subclinical inflammatory events in the optic nerve and/or a chiasmal crossover effect from a contralateral ON, but being more in line with a primary astrocytopathy effect.

### 6.2.3. Longitudinal changes

After OPLS-DA indicated that foveal shape changes in NON eyes are unlikely to be attributable to neuroaxonal damage to the optic nerve, potential longitudinal changes were also investigated. The analysis was limited to NON eyes to not overlay ON-unrelated changes with potential changes from ON. Annualized changes from baseline to last follow up for the NON eyes are summarized in table 6-17 for retinal layers and in table 6-18 for the foveal parameters.

	AQP4-NMOSD-NON
	Annualized change, Mean (SD)
pRNFL( $\mu\text{m}$ )	-0.611 (1.85)
GCIP ( $\text{mm}^3$ )	-0.009 (0.0044)
TMV ( $\text{mm}^3$ )	-0.004 (0.013)
INL ( $\text{mm}^3$ )	0.003 (0.001)
FT( $\mu\text{m}$ )	-0.43 (2.19)
mRNFL ( $\text{mm}^3$ )	-0.0003 (0.006)

---

**Table 6-17: Annualized retinal layer changes in NON eyes**

Abbreviations: NON, eyes without a history of optic neuritis. pRNFL, peripapillary retinal nerve fibre layer; GCIP, ganglionar and inner plexiform layer; TMV, total macular volume; FT, foveal thickness; INL, inner nuclear layer; mRNFL, retinal nerve fibre layer.

---

	AQP4-NMOSD-NON
	Annualized change, Mean (SD)
Average Pit Depth (mm)	0.00012 (0.002)
Central Foveal Thickness (mm)	-0.0005 (0.0001)
Average Rim Height (mm)	-0.00038 (0.0023)
Average Rim Diameter (mm)	-0.00088 (0.01)
Rim Disc Area (mm <sup>2</sup> )	-0.0029 (0.04)
Major Rim Disc Length (mm)	2.38 E-05 (0.009)
Minor Rim Disc Length (mm)	-0.0009 (0.007)
Major Slope Disc Length (mm)	-0.001 (0.005)
Minor Slope Disc Length (mm)	-0.001 (0.004)
Slope Disc Area (mm <sup>2</sup> )	-0.01 (0.026)
Average Slope Disc Diameter (mm)	-0.006 (0.02)
Pit Disc Area (mm <sup>2</sup> )	-0.0002 (0.002)
Average Pit Flat disc diameter (mm)	-0.0008537 (0.006)
Major Pit Flat disc length (mm)	-7.97 E-05 (0.0004)
Minor pit flat disc length (mm)	1.25 E-05 (0.0005)
Rim Volume (mm <sup>3</sup> )	0.000333 (0.017)
Pit Volume (mm <sup>3</sup> )	-0.0020 (0.008)
Inner Rim Volume (mm <sup>3</sup> )	0.00022 (0.002)
Av Max Pit slope degree (°)	0.0034 (0.41)

**Table 6-18: Annualized foveal changes in NON eyes**

Abbreviations: NON, eyes without a history of optic neuritis.

Longitudinal analysis using linear mixed effects models identified no significant retinal changes (table 6-19) or foveal parameter changed (table 6-20) at follow-up compared to baseline in eyes with no previous history of ON in AQP4-NMOSD.

	AQP4-NMOSD-NON. F/U vs baseline	
	B (SE)	P values
pRNFL( $\mu\text{m}$ )	-0.11563 (0.276813)	0.6767
GCIP (mm <sup>3</sup> )	-0.0007202 (0.000816)	0.3788
TMV (mm <sup>3</sup> )	-0.0028363 (0.002249)	0.2090
INL (mm <sup>3</sup> )	-0.00044411 (0.000955)	0.6427
FT ( $\mu\text{m}$ )	-0.61538 (0.429695)	0.1538
mRNFL (mm <sup>3</sup> )	-0.00122806 (0.000881)	0.1653

---

**Table 6-19: Assessment of baseline to follow-up changes in retinal layers**

Significant p values are shown in red. Maximum likelihood was used for the estimation of p values. Abbreviations: F/U, Follow-up; SD, standard deviation; B, estimate; SE, standard error; AQP4-NMOSD-NON, neuromyelitis optica spectrum disease eyes from AQP4 ab positive, with no history of optic neuritis.

---

	AQP4-NMOSD-NON. F/U vs baseline	
	B (SE)	P values
Average Pit Depth (mm)	0.0004 (0.0004)	0.3149
Central Foveal Thickness (mm)	-0.0004 (0.0004)	0.3891
Average Rim Height (mm)	-0.0000040 (0.00039)	0.9918
Average Rim Diameter (mm)	-0.00059 (0.002)	0.8039
Rim Disc Area (mm <sup>2</sup> )	-0.001 (0.007)	0.8040
Major Rim Disc Length (mm)	0.0000439 (0.0013)	0.9746
Minor Rim Disc Length (mm)	-0.00067 (0.0016)	0.6194
Major Slope Disc Length (mm)	-0.001(0.0008)	0.157
Minor Slope Disc Length (mm)	-0.00017(0.0006)	0.803
Slope Disc Area (mm <sup>2</sup> )	-0.004(0.004)	0.35
Average Slope Disc Diameter (mm)	-0.002(0.003)	0.49
Pit Disc Area (mm <sup>2</sup> )	-0.0002 (0.0006)	0.6445
Average Pit Flat disc diameter (mm)	-0.001 (0.00146)	0.4528
Major Pit Flat disc length (mm)	-0.00008 (0.00011)	0.4782
Minor pit flat disc length (mm)	-0.000016 (0.00008)	0.8469
Rim Volume (mm <sup>3</sup> )	0.00010 (0.0030)	0.9721
Pit Volume (mm <sup>3</sup> )	-0.0003(0.001)	0.77
Inner Rim Volume (mm <sup>3</sup> )	-0.00002(0.0004)	0.96
Av Max Pit slope degree (°)	-0.041(0.079)	0.599

**Table 6-20: Assessment of baseline to follow-up changes in foveal parameters**

Significant p values are shown in red. Maximum likelihood was used for the estimation of p values. Abbreviations: F/U, Follow-up; SD, standard deviation; B, estimate; SE, standard error; AQP4-NMOSD-NON, neuromyelitis optica spectrum disease eyes from AQP4 ab positive, with no history of optic neuritis.

In eyes with previous attacks of ON, changes with a positive trend towards significance in foveal thickness [B(SE): 0.89(0.49); p=0.0753] were observed, as well as a significant increase in central foveal thickness [B(SE): 0.0014(0.00054); p=0.0098] and average rim height [B(SE): 0.0012 (0.002); p=0.0064]. Predicted changes are plotted in figure 6-15.

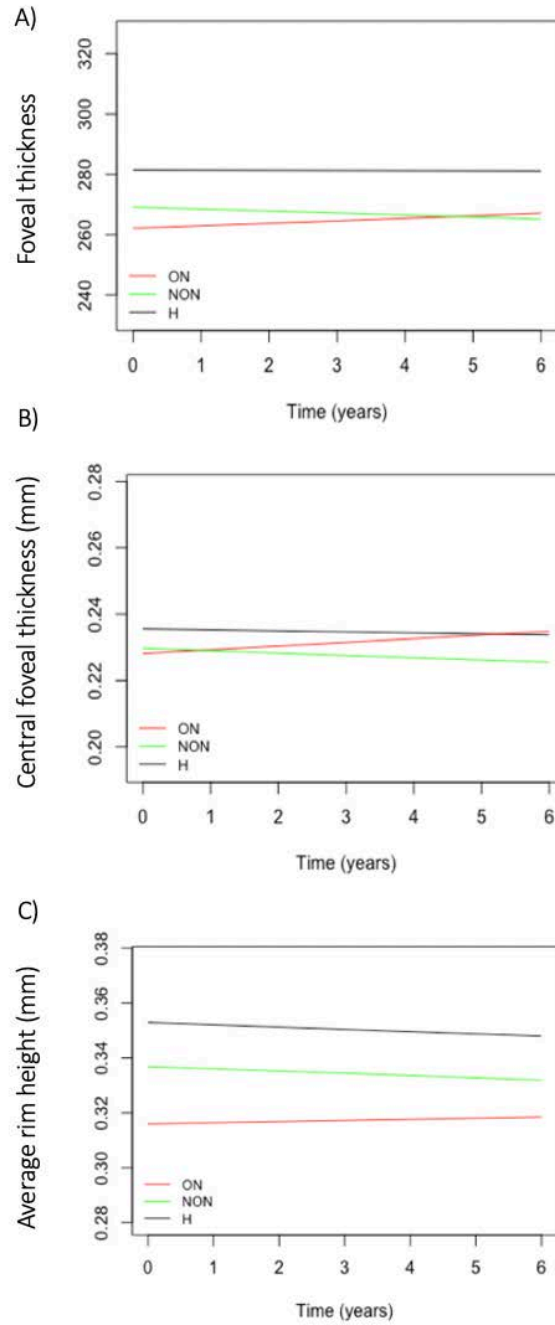


**Figure 6-15: Significant longitudinal LME model graphs**

a) FT: foveal thickness; b) Central foveal thickness and c) Average rim height significant for ON eyes compared to baseline.



### 6.3. Summary of the main structural findings: retinal impairment defined by OCT and foveal morphometry in AQP4-NOSD and MOGAD.

The following table (table 6-21) summarizes the structural impairments (note, not longitudinal evolution) in AQP4-NMOSD and MOGAD. Fellow and “never affected eyes” (from patients never affected by ON) were considered one single category for the study of the foveal shape. Red share indicates impairment.

	AQP4-NMOSD			MOGAD		
Eyes	ON	Fellow*	Never Affected*	ON	Fellow	Never Affected
DISC						
pRNFL						
MACULA						
GCIP						
TMV						
INL						
mRNFL						
FOVEA						
FT				NA	NA	NA
Average Pit Depth (mm)				NA	NA	NA
Central Foveal Thickness (mm)				NA	NA	NA

Average Rim Height (mm)			NA	NA	NA
Average Rim Diameter (mm)			NA	NA	NA
Rim Disc Area (mm <sup>2</sup> )			NA	NA	NA
Major Rim Disc Length (mm)			NA	NA	NA
Minor Rim Disc Length (mm)			NA	NA	NA
Major Slope Disc Length (mm)			NA	NA	NA
Minor Slope Disc Length (mm)			NA	NA	NA
Slope Disc Area (mm <sup>2</sup> )			NA	NA	NA
Average Slope Disc Diameter (mm)			NA	NA	NA
Pit Disc Area (mm <sup>2</sup> )			NA	NA	NA
Average Pit Flat disc diameter (mm)			NA	NA	NA
Major Pit Flat disc length (mm)			NA	NA	NA
Minor pit flat disc length (mm)			NA	NA	NA
Rim Volume (mm <sup>3</sup> )			NA	NA	NA
Pit Volume (mm <sup>3</sup> )			NA	NA	NA
Inner Rim Volume (mm <sup>3</sup> )			NA	NA	NA

Av Max Pit slope degree (°)			NA	NA	NA
--------------------------------	--	--	----	----	----

---

**Table 6-21: Structural impairment in AQP4-NMOSD and MOGAD**

Abbreviations: AQP4-NMOSD-NON, neuromyelitis optica spectrum disease eyes from AQP4 ab positive; MOGAD, Myelin Oligodendrocyte Glycoprotein spectrum disorder; ON, Optic neuritis; pRNFL, peripapillar retinal nerve fiber layer; GCIP, Ganglionar and inner plexiform retinal nerve fibre layer; TMV, total macular volume; INL, Inner nuclear layer; FT, Foveal thickness; mRNFL, macular retinal nerve fibre layer; NA, not available.

---

## 7. DISCUSSION

The study of the neuro-ophthalmological consequences of MOGAD and AQP4-NMOSD is a rapidly evolving field. This thesis complements other work published in the last years, adding a significant contribution to the knowledge needed to provide an appropriate clinical management and to provide clinical trials a valuable information regarding clinical endpoints; in this thesis I provide a comprehensive overview of structural damage, recovery and structural changes in affected, fellow and “never affected” eyes in AQP4-NMOSD and MOGAD patients.

The study of longitudinal retinal changes after ON in AQP4-NMOSD and MOGAD has been a hot topic in the last years. However, the current literature still presents with several gaps, being the most important: the definition of damage in function of time after an ON, whether the fellow eyes from affected ON eyes present with neuroaxonal damage, and whether eyes from patients with no history of ON (so called “never affected eyes”) present with damage not patently related with ON.

### **ON eyes in AQP4-NMOSD and MOGAD suffer from neuroaxonal damage, but what else?**

In this thesis, I support previous studies describing thinning of inner retinal layers after ON in affected eyes of AQP4-NMOSD and MOGAD patients. The results included in this thesis shows damage in pRNFL, mRNFL, GCIP, TMV and INL in both AQP4-NMOSD and MOGAD eyes previously affected by ON compared to HC. These findings have been observed in previous research in both conditions, particularly in AQP4-NMOSD (82,97,166,196,197) but also in MOGAD eyes (170,171). Thinning in pRNFL, mRNFL and GCIP demonstrates profound neuroaxonal damage after ON, that is consequently reflected in the global TMV (198). INL has been broadly described in MS as a marker of global inflammatory disease activity (199–202), and the occurrence of clinical relapses in any functional system was found to be significantly associated with a subsequent increase in INL in MS patients (201). But studies employing OCT in MS have demonstrated a spectrum of abnormalities of the INL that include not only thickening but also thinning associated with progressive disease (203). An increase in INL thickness in AQP4-NMOSD eyes (97,197) and MOGAD affected eyes (170,171) has been previously described, but has not been yet associated with relapses outside the visual system and, in the context of this research, it appears in relapse-free cohorts. An explanation to this

can be due to the high density of inflammatory cells in the INL (204), which may cause residual inflammation due to previous ON or, in the case of AQP4-NMOSD eyes, due to an ongoing local inflammatory activity. Thinning of INL was not found in any of these 2 conditions, supporting the current knowledge of AQP4-NMOSD and MOGAD being not degenerative.

At the same time, in AQP4-NMOSD longitudinal observations focusing on the recovery window in absence of new relapses, I show for the first time increases in macular volume (that could be interpreted as recovery) in the chronic phase. This has been observed in a time window of 2 years after the acute event. This minimal increase in TMV, with an estimated variation of  $+0.08 \text{ mm}^3$  per year, may be attributed to an extreme neuroaxonal damage that in some cases might limit the magnitude of recovery. This increase might not be clinically meaningful, but is statistically significant in this population compared to healthy controls indicating dynamic changes in the post-acute phase. These findings could be related with several hypotheses: The first hypothesis being related with a more profound damage after ON in AQP4-NMOSD after the first attack that would result in a longer recovery. A second hypothesis could also reflect an additional process, independent from ON, which in AQP4-NMOSD would be related with a subclinical antibody activity affecting retinal Müller cells, or even to subclinical inflammatory events. Finally, the third hypothesis could be related with molecular changes in the extracellular environment, led by intercellular interactions between synaptic and non-synaptic cells and ganglionar cells, that could help promoting axon regeneration (205). These 3 scenarios are not independent, and all three could play a role at different stages of the process.

No changes over time have been observed longitudinally in MOGAD-ON eyes where the retina appears stable 1 year after the ON.

### **Eyes with no history of ON in APQ4-NMOSD and MOGAD, shall we pay attention?**

In AQP4-NMOSD, this thesis highlights the importance of the separation of NON-ON eyes into 2 different categories: fellow eyes from contralateral ON eyes, and eyes from patients never affected by ON (so called “never affected eyes”) suggesting that a differential pattern of damage is observed in these 2 categories of eyes.

While previous studies have found a reduction in pRNFL and GCIP in patients with no history of ON compared to HC in the MOGAD population (where fellow and “never

affected eyes” were grouped together) (170,171), my results indicate that retinal integrity is preserved in MOGAD-NON eyes (cross-sectionally and longitudinally) both in fellow and “never affected” category.

### **Unilateral ON in AQP4-NMOSD, really unilateral? The fellow contralateral eyes speak**

Findings from project 1 indicate that AQP4-NMOSD fellow eyes from contralateral affected ON eyes show significantly lower total macular volume than healthy controls and this seems not to be attributable to the thickness of any of the individual retinal layers. A possible explanation for this finding is due to the posterior nature of ON in AQP4-NMOSD patients. Inflammation may transfer across the crossing fibres in the optic chiasm and affect less severely the contralateral eye with a similar pattern of damage. Another plausible explanation could be the presence of subclinical inflammatory activity in the fellow eye, either in the optic nerve or locally in the retina. It is important to note that a subtle ON event may be unnoticed by the patient when a severe attack is happening in the contralateral eye or elsewhere in the body, and might be under-reported.

Over follow up, these eyes show increases in total macular volume that are not attributable to changes in any of the inner retinal structures either. However, the longitudinal variability estimated by linear mixed-effects model suggest that neuroaxonal damage did not happen in this cohort in the fellow eye, and thinning in TMV could be a transient inflammatory process. This increase over time in TMV, estimated at a mean rate of  $+0.35 \text{ mm}^3$  per year in a time window of 2 years after the acute event, may indicate a recovery from an inflammation that was neither local nor too severe, or as it was described for the affected eyes, due to a compensation of the extracellular environment or foveal remodelling resulting from Müller cells death. This evidence reinforces the hypothesis of a contralateral crossover inflammation through the optic chiasm. However, larger sample sizes are needed to make more robust conclusions in these fellow eyes.

Fellow eyes from MOGAD patients did not show any difference compared with healthy control eyes.

### **AQP4-NMOSD patients with no history of ON, your eyes have something to say**

A differential pattern of damage was found in “never affected eyes” from AQP4-NMOSD patients. In this category, TMV appears preserved, but INL shows a significant increase

in thickness. As I mentioned above for the ON eyes, this increase in INL thickness could be linked to an active inflammation and this is especially important in this group of eyes, where no contralateral affection is present.

In the last years, some publications have opened a new debate discussing attack-independent neuroaxonal damage in AQP4-NMOSD eyes (90,93,97,197,206–210), and experimental scientists have described underlying astrocytopathy in animal models (211,212), with further publications demonstrating attack independent damage in AQP4-NMOSD cohorts (91–94,210).

While changes in INL found cross-sectionally did not seem to evolve over time, these categories of eyes showed a significant foveal thinning over time. Taken this, I hypothesise that both might be part of the same process, related to an attack-independent loss of AQP4-expressing Müller cells in these patients, confined to the retina, where the disruption of osmotic and ionic homeostasis due to circulating antibodies (linked or not to other attacks elsewhere in the CNS) would result in the dysregulation of Müller cells, causing INL oedema that could potentially result in neuronal loss and foveal remodelling over time (22,213–215).

This hypothesis would be supported by the findings in a recent publication describing patterns of microvascular damage in AQP4-NMOSD patients (216); where the authors found a significantly smaller foveal avascular zone in affected and unaffected eyes compared with healthy controls, and propose that this reduction in microvasculature could be associated to the process described above.

Interestingly, where fellow and “never affected eyes” were treated as a single entity in project 3, OPLS-DA selected GCIP but not pRNFL as one of the most robust parameters discriminating NON-eyes from HC. This adds a piece of information that potentially suggests that GCIP changes may reflect a neurodegenerative reaction of ganglion cells to Müller cell affection or that GCIP thinning is caused by changes to Müller cell processes itself. The discrepancy between pRNFL and GCIP differences in NON-eyes is interesting and warrants further investigation. Future studies with bigger sample size and higher power are required to address this issue.

The results presented in the post-acute setting in this work are novel and have not been found previously in other research, where either a plateau effect was suggested (92), or



in case of multicentric research, the variability in the data coming from different centres and different protocols did not allow to state robust conclusions (217). The annual changes reported in this study, albeit not clinically meaningful, may serve as the basis for sample size calculations.

### **The fovea in AQP4-NMOSD patients, diving into a black hole**

At this point, after all the stated above, my hypothesis supports that different process might be happening at the same time in AQP4-NMOSD eyes. The study of fellow eyes and “never affected eyes” was particularly important as it helped shedding light into the different mechanisms of retinal damage. While changes in fellow eyes might be attributed to inflammatory chiasmal crossover or retinal astrocytopathy, the study of “never affected eyes” helped me isolating the second effect. Foveal shape changes had been previously reported AQP4-NMOSD patients after ON (89,91,93) and foveal morphometry had also identified foveal shape differences between MS patients and HC (89). Other authors had also reported FT thickness on OCT in AQP4-NMOSD patients (91,93). All these clues lead this research to investigate further the importance of the fovea and the Müller cells in this disease, and foveal shape changes in AQP4-NMOSD patients never affected by ON (fellow + “never affected” jointly) were further investigated in this thesis. For the first time, foveal morphometry was performed to describe the parafoveal involvement and the parafoveal changes in AQP4-NMOSD NON-eyes. My results, provided with evidence that the parafoveal area, which is rich in AQP4-expressing Müller cells, is altered in AQP4-NMOSD patients who never experienced a clinical ON, and suggested that these changes are likely to be independent of neuroaxonal damage from subclinical inflammatory events in the optic nerve, as macular and peripapillary layers were not affected in this subset. In this thesis, the fovea of NON-eyes was found to be characterized by wider pits and more pronounced slopes, best described as foveal widening compared to ON eyes. OPLS-DA selected parameters helped successfully differentiating ON and NON-eyes, lending strong support to the hypothesis that the observed foveal changes in NON-eyes are not caused by neuroaxonal damage to the optic nerve.

Foveal changes were also found in ON eyes, which can best be described as *flattening* of the parafoveal ring: OPLS-DA selected primarily parameters of neuroaxonal damage

(pRNFL, GCIP) as well as parameters describing the volume and flatness of the fovea. Some of these changes can be due to the fact that ON causes neuroaxonal damage in AQP4-NMOSD, and this damage, that is reflected by pRNFL thickness loss reflecting axonal damage and GCIP loss reflecting neuronal ganglion cell loss (92,93,166,218) can also affect the foveal shape.

My thesis, as well as previous clinical studies did not address the underlying aetiology of foveal involvement in AQP4-NMOSD, however, we can hypothesise: The parafoveal area is rich in Müller cells, the principal astrocytic glia of the retina, which expresses AQP4 in their end feet adjacent to retinal vessels (219). In an animal model of retinal damage in NMOSD, AQP4-IgG injection into the vitreous resulted in reactive changes and loss of Müller cells without complement activation (211). Previous studies have demonstrated a lack of complement reactivity in the area postrema (220), This could also be the case in the fovea, where AQP4-IgG would still bind the retinal AQP4-expressing cells but would fail to activate the complement, and therefore would not cause mediated damage in the retinal cell integrity but still would be able to affect foveal morphometry.

This thesis did not found evidence for overt progressiveness of foveal shape changes, neither in ON nor NON-eyes. Given the sample size limitation, it is unclear whether this sub-study is simply underpowered or whether changes to the fovea are indeed not progressive.

While these findings are limited to the retina, the observation that slight AQP4-related damage in NMOSD is also relevant for other CNS areas, secondary symptoms in NMOSD like cognitive dysfunction (221), fatigue (222), pain (116) and mood disorders (223) are yet mostly unexplained. Imaging studies have so far been inconclusive regarding focal damage to brain structures in NMOSD, which is outside of attack-related areas or potential subject to secondary axonal or transsynaptic neurodegeneration (208,224,225). An independent recent study, has identified the nucleus accumbens as a potentially interesting target with functional relevance of AQP4 expressing cells for neural plasticity (226).

### **Structure-function in AQP4-NMOSD and MOGAD: correlation or dissociation?**

Finally, after defining the retinal structure in affected, fellow, and never affected eyes in AQP4-NMOSD and MOGAD and foveal changes in AQP4-NMOSD patients, a further

step was needed to investigate the relationship between structure-function in these patients.

Previous research had demonstrated that ON in AQP4-NMOSD is often associated with severe visual function loss (227), presenting with worse visual outcomes compared to multiple sclerosis (MS) patients and to patients with MOGAD (90). In this regard, it is well known that MOGAD patients present with better recovery rates than AQP4-NMOSD (169), however structure-function relationships in eyes in absence of functional problems were not explored before.

In this thesis, where the majority of patients followed a monophasic ON course AQP4-NMOSD eyes accounted for more severe thinning than MOGAD eyes. In patients with no problems in their central vision, I demonstrate that there are fewer occasions where subclinical damage happens in patients with AQP4-NMOSD, since residual damage is proven to impact the function. Even so, there may be cases of subclinical damage without visual impact, and in patients with a previous history of optic neuritis, this would indicate better recovery mechanisms.

In MOGAD, given the much lower prevalence of abnormal tests (18%) from eyes who had never had ON compared to 84% of MOGAD ON eyes, it is likely that the abnormal OCT and VEP results are mainly a direct consequence of an ON attack rather than an unrelated disease process. It is important to note that the retina is an unmyelinated zone, and for that reason, changes in MOGAD eyes are highly likely to come from optic nerve defects. However, abnormalities still occurred in a few eyes without previous history of ON. In AQP4-NMOSD disease, patients who do recover normal vision are more likely to have normal investigations than MOGAD-ON patients. Based on this finding, I hypothesize that astrocyte damage in AQP4-NMOSD attacks might be more of an 'all or nothing' event affecting the optic nerve and those that recover may not have secondary demyelination. For this reason, assessment with OCT and VEPs appear to be sensitive (as previously demonstrated in MS), for detecting primary demyelinating pathology.

These findings are important because it could lead to an adjustment in the on-going immunosuppression therapy. In addition, as subclinical abnormalities can occur without symptoms, it is important to repeat the tests after each MOGAD relapse to provide comparison data should future visual symptoms occur.

This thesis not only contributes to demonstrate the structure-function concordance in AQP4-NMOSD, and dissonance in MOGAD but also shows that OCT, rather than VEPs, is able to detect subclinical damage in eyes of patients with MOGAD with normal visual acuity in spite of a previous ON.

The **conclusions** of this work need to be considered in light of the **limitations**, such as small sample size and differences in demographic and treatment characteristics that, although accounted for in all statistical analyses, cannot be matched entirely. However, this work demonstrates distinctive **strengths** with respect to the current literature: diagnosis was consistent and accurate across participants, including only those with an antibody positive test, unlike many other studies which include heterogenous phenotypes; this thesis investigates one of the biggest cohorts currently available with two longitudinal and one cross-sectional study (two of those, single-centre) using routine (OCT, VEP) and advance (foveal morphometry) paraclinical tests; finally each stage of the analysis pipeline was designed with high standards paying special attention to statistical design and QC process.

In **summary**, sub-clinical abnormalities can occur due to silent ON (MOGAD) or antibody activity leading to retinal astrocytopathy (AQP4-NMOSD) therefore, monitoring subclinical activity and the post-acute recovery window is crucial. The data presented in the previous sections of this thesis supports the importance of repeating visual tests after each ON relapse, or yearly, in the absence of those.

This is an exciting field and if the standardization of protocols and analysis methods across centers can be achieved, OCT and foveal morphometry imaging will prove to be important tools to inform personalized treatment strategies within the clinical pathway, for the study and monitoring of disease and to measure outcomes for clinical trials.

## 8. CONCLUSIONS

- After the ON patients with **AQP4-NMOSD and MOGAD show different retinal integrity recovery times**, with AQP4-NMOSD taking longer to stabilise after an ON, this process is still dynamic 2 years after the acute attack, as the ongoing recovery in TMV demonstrates. MOGAD-ON eyes reach a stable retinal thickness 1 year after the acute attack.
- **Fellow eyes from contralateral ON present with signs of inflammation in AQP4-NMOSD** that can be attributed to inflammatory chiasmal crossover or ON-independent retinal astrocytopathy. However, this is not accompanied by neuroaxonal damage (inner retinal structures are preserved). As its contralateral ON eyes, fellow eyes present with ongoing TMV recovery beyond 1 year post-acute. Fellow eyes in MOGAD do not show any difference with HC eyes.
- **Retinal damage independent from ON occurs in AQP4-NMOSD but not in MOGAD, as shown by “never affected” eyes** (from patients with no history of ON), and is associated with INL thickening and foveal shape changes in the OCT examination. “Never affected eyes” in MOGAD patients do not present any different with HC.
- **Foveal shape changes in AQP4-NMOSD are independent from ON but not progressive**. Parafoveal area of AQP4-NMOSD eyes presents with structural changes in both eyes affected and not affected by ON. These changes are characterized by flattening of the parafoveal area in ON eyes and wider pits, and more pronounced slopes in NON eyes. Foveal shape changes suggest that this retinal process is independent from ON, and might be associated with local antibody activity in the parafoveal area. Changes in foveal morphometry are not overtly progressive.
- **Structure-function discordance in MOGAD may be associated with subclinical inflammatory events in the optic nerve**, as retinal damage often occurs in patients with good central vision. In AQP4-NMOSD the degree of retinal damage appears to be directly associated with central visual function.

## 9. FUTURE DIRECTIONS

The visual system is formed by three chain neurons (228) (figure 9-1). In this thesis, two main techniques were used: OCT to investigate the retrograde retinal degeneration from lesions in the optic nerve, as well as the ON independent changes affecting the retinal integrity; and VEP to assess the demyelination of the visual pathway.

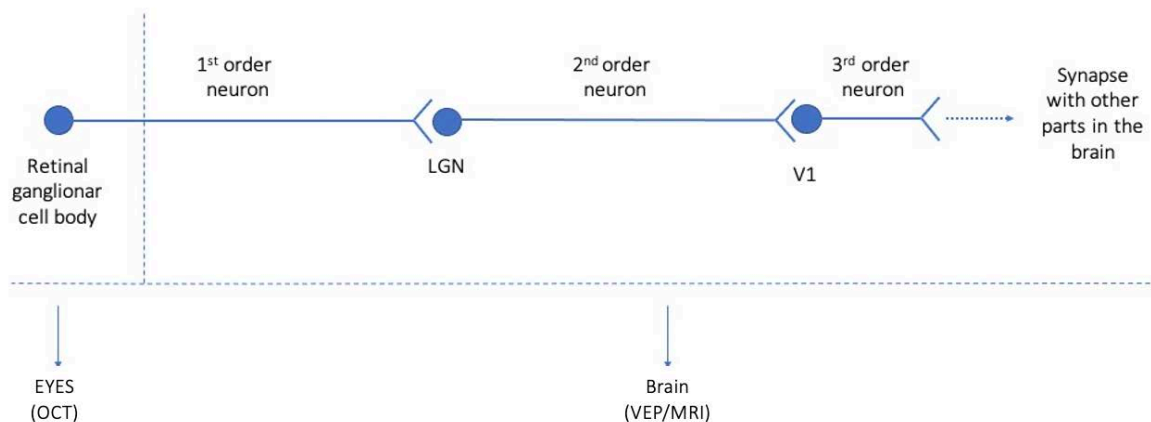


**Figure 9-1: Anatomical scheme of the visual pathway**

The retinal ganglion cell (RGC), visualised with spectral-domain optical coherence tomography (SD-OCT), projects to the lateral geniculate nucleus (LGN) in the midbrain. The axon of the 2<sup>nd</sup> order neuron in the LGN projects through the optic radiations (ORs), assessed using diffusion tensor imaging, to the primary visual cortex.

The injury induced by the inflammation of the optic nerve in CNS antibody mediated diseases often leads to degeneration of the axon (229), however the occurrence of degeneration is not always dependent on the inflammation (230), and a local degeneration can be spread through the neurons and result in an atrophy elsewhere. Anterograde and retrograde degeneration have been described in depth in the literature (231–235). Retrograde degeneration is the damage of the retinal layers in the eye that is caused by a damage in the optic nerve due to an ON while anterograde degeneration is the damage of the posterior visual pathway due to an ON (figure 9-2).



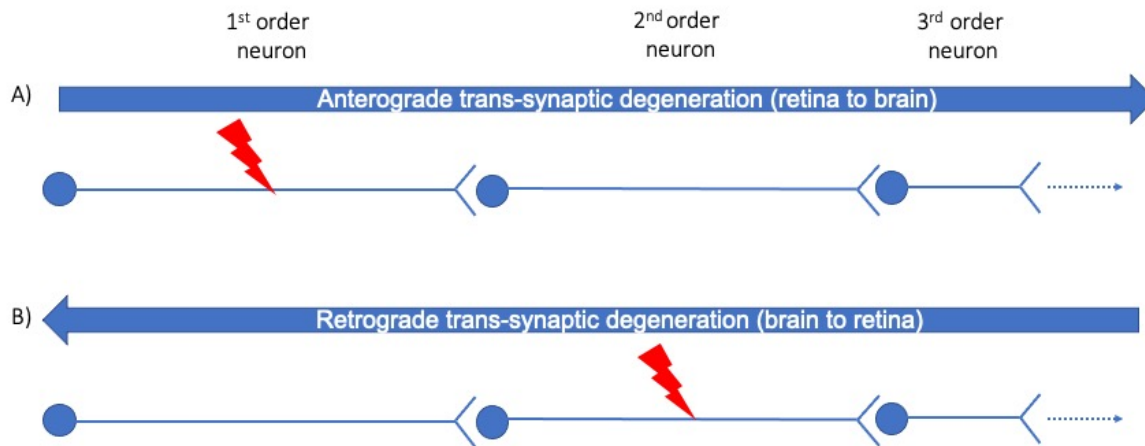


**Figure 9-2: Anatomical depiction of retrograde and anterograde transsynaptic degeneration in the visual pathway**

A) Anterograde trans-synaptic degeneration (retina to brain), B) Retrograde trans-synaptic degeneration (brain to retina).

In AQP4-NMOSD previous studies have suggested that the thinning in the mRNFL layer and the GCIP complex were associated to a decreased integrity of the optic radiation and volume in the primary visual cortex (236) and others have suggested the existence of trans-synaptic degeneration in the anterior and posterior visual pathway that would demonstrate the existence of bidirectional degeneration in AQP4-NMOSD (94,236,237) It is known, that anterior visual pathway damage is often more severe than posterior visual pathway damage and in previous research, associations between macular thickness and atrophy of the posterior visual pathway has not been found in AQP4-NMOSD (94). In the same study, the largest to date in AQP4-NMOSD (n=36, only 22 of those were AQP4-IgG seropositive), they have identified ganglionic cell layer in the retina and OR as the most vulnerable structures to degeneration.

Retrograde degeneration has been clearly demonstrated in those patients with an ON, however the decreased integrity in the OR and V1 could be a caused by lesions in the OR and more advanced methods are needed.

**Future steps:**

1. To validate Tian et al 2018 findings including exclusively AQP4-IgG seropositive NMSOD and to further investigate the posterior structural damage relationship with visual outcomes.
2. To describe posterior visual pathway damage in MOGAD and assess a potential anterograde degeneration from ON and its relationship with visual outcomes.
3. To investigate a potential cortical reorganization in the visual networks in MOGAD that could explain why these patients have preserved visual function despite the retinal impairment after ON.

**Methods:**

To address these points, I would use OCT to assess retinal integrity, diffusion tensor MRI to assess demyelination and axonal loss of the OR, volumetric analysis from brain structural MRI to assess atrophy of the LGN and resting state functional MRI to assess cortical reorganization of the visual networks.

The standardisation of protocols together with bigger sample sizes and more advanced imaging analysis could rapidly expand the knowledge. The deployment in clinical routine of new analysis methods as foveal shape morphometry can be achieved, as they prove to be important tools for the study of disease and could play a role in measuring outcomes for clinical trials.

## **10. BIBLIOGRAPHY**

1. Gheraldes R, Ciccarelli O, Barkhof F, De Stefano N, Enzinger C, Filippi M, et al. The current role of MRI in differentiating multiple sclerosis from its imaging mimics. *Nat Rev Neurol*. 2018 Apr;14(4):199–213.
2. Juryńczyk M, Craner M, Palace J. Overlapping CNS inflammatory diseases: differentiating features of NMO and MS. *J Neurol Neurosurg Psychiatry*. 2015 Jan;86(1):20–5.
3. Waters P, Reindl M, Saiz A, Schanda K, Tuller F, Kral V, et al. Multicentre comparison of a diagnostic assay: aquaporin-4 antibodies in neuromyelitis optica. *J Neurol Neurosurg Psychiatry*. 2016 Sep 1;87(9):1005–15.
4. Waters P, Woodhall M, O'Connor KC, Reindl M, Lang B, Sato DK, et al. MOG cell-based assay detects non-MS patients with inflammatory neurologic disease. *Neurol Neuroimmunol Neuroinflammation*. 2015 Jun;2(3):e89.
5. Rodríguez-Acevedo B, Rovira A, Vidal-Jordana A, Moncho D, Pareto D, Sastre-Garriga J. [Optic neuritis: aetiopathogenesis, diagnosis, prognosis and management]. *Rev Neurol*. 2022 Feb 1;74(3):93–104.
6. Felleman DJ, Van Essen DC. Distributed hierarchical processing in the primate cerebral cortex. *Cereb Cortex N Y N* 1991. 1991 Feb;1(1):1–47.
7. Kolb H. Simple Anatomy of the Retina. In: Kolb H, Fernandez E, Nelson R, editors. *Webvision: The Organization of the Retina and Visual System* [Internet]. Salt Lake City (UT): University of Utah Health Sciences Center; 1995 [cited 2021 May 2]. Available from: <http://www.ncbi.nlm.nih.gov/books/NBK11533/>
8. Pemp B, Schmetterer L. Ocular blood flow in diabetes and age-related macular degeneration. *Can J Ophthalmol J Can Ophtalmol*. 2008 Jun;43(3):295–301.
9. Strauss O. The retinal pigment epithelium in visual function. *Physiol Rev*. 2005 Jul;85(3):845–81.
10. Booij JC, Baas DC, Beisekeeva J, Gorgels TGMF, Bergen A a. B. The dynamic nature of Bruch's membrane. *Prog Retin Eye Res*. 2010 Jan;29(1):1–18.
11. Curcio CA, Johnson M. Structure, Function, and Pathology of Bruch's Membrane. In: *Retina* [Internet]. Elsevier; 2013 [cited 2021 Jun 6]. p. 465–81. Available from: <https://linkinghub.elsevier.com/retrieve/pii/B9781455707379000205>
12. Baker SA, Kerov V. Chapter Seven - Photoreceptor Inner and Outer Segments. In: Bennett V, editor. *Current Topics in Membranes* [Internet]. Academic Press; 2013 [cited 2021 May 3]. p. 231–65. (Functional Organization of Vertebrate Plasma Membrane; vol. 72). Available from: <https://www.sciencedirect.com/science/article/pii/B9780124170278000076>

13. Arshavsky VY, Burns ME. Photoreceptor signaling: supporting vision across a wide range of light intensities. *J Biol Chem*. 2012 Jan 13;287(3):1620–6.
14. Fain GL, Matthews HR, Cornwall MC, Koutalos Y. Adaptation in vertebrate photoreceptors. *Physiol Rev*. 2001 Jan;81(1):117–51.
15. Kefalov VJ. Rod and cone visual pigments and phototransduction through pharmacological, genetic, and physiological approaches. *J Biol Chem*. 2012 Jan 13;287(3):1635–41.
16. Palczewski K. Chemistry and Biology of Vision \*. *J Biol Chem*. 2012 Jan 13;287(3):1612–9.
17. Euler T, Haverkamp S, Schubert T, Baden T. Retinal bipolar cells: elementary building blocks of vision. *Nat Rev Neurosci*. 2014 Aug;15(8):507–19.
18. Masland RH. The Neuronal Organization of the Retina. *Neuron*. 2012 Oct 18;76(2):266–80.
19. Demb JB, Singer JH. Functional Circuitry of the Retina. *Annu Rev Vis Sci*. 2015 Nov 18;1(1):263–89.
20. Ozawa Y, Toda E, Kawashima H, Homma K, Osada H, Nagai N, et al. Aquaporin 4 Suppresses Neural Hyperactivity and Synaptic Fatigue and Fine-Tunes Neurotransmission to Regulate Visual Function in the Mouse Retina. *Mol Neurobiol*. 2019 Dec 1;56(12):8124–35.
21. Goodyear MJ, Crewther SG, Junghans BM. A role for aquaporin-4 in fluid regulation in the inner retina. *Vis Neurosci*. 2009 Apr;26(2):159–65.
22. You Y, Zhu L, Zhang T, Shen T, Fontes A, Yiannikas C, et al. Evidence of Müller Glial Dysfunction in Patients with Aquaporin-4 Immunoglobulin G-Positive Neuromyelitis Optica Spectrum Disorder. *Ophthalmology*. 2019 Jun;126(6):801–10.
23. Zeka B, Lassmann H, Bradl M. Müller cells and retinal axons can be primary targets in experimental neuromyelitis optica spectrum disorder. *Clin Exp Neuroimmunol*. 2017 Jan;8(Suppl Suppl 1):3–7.
24. Bradl M, Reindl M, Lassmann H. Mechanisms for lesion localization in neuromyelitis optica spectrum disorders. *Curr Opin Neurol*. 2018 Jun;31(3):325–33.
25. Akiba R, Yokouchi H, Mori M, Oshitari T, Baba T, Sawai S, et al. Retinal Morphology and Sensitivity Are Primarily Impaired in Eyes with Neuromyelitis Optica Spectrum Disorder (NMOSD). *PLOS ONE*. 2016 dic;11(12):e0167473.

26. Clinical Anatomy and Physiology of the Visual System [Internet]. Elsevier; 2012 [cited 2021 May 3]. Available from: <https://linkinghub.elsevier.com/retrieve/pii/C20090561089>
27. Mac Nair CE, Nickells RW. Chapter Twenty - Neuroinflammation in Glaucoma and Optic Nerve Damage. In: Hejtmancik JF, Nickerson JM, editors. Progress in Molecular Biology and Translational Science [Internet]. Academic Press; 2015 [cited 2021 May 3]. p. 343–63. (Molecular Biology of Eye Disease; vol. 134). Available from: <https://www.sciencedirect.com/science/article/pii/S187711731500112X>
28. Salazar J, Ramírez A, Hoz RD, Salobar-García E, Rojas P, Fernández-Albarral JA, et al. Anatomy of the Human Optic Nerve: Structure and Function. In 2018.
29. Jonas RA, Wang YX, Yang H, Li JJ, Xu L, Panda-Jonas S, et al. Optic Disc - Fovea Distance, Axial Length and Parapapillary Zones. The Beijing Eye Study 2011. PLoS ONE [Internet]. 2015 Sep 21 [cited 2021 May 3];10(9). Available from: <https://www.ncbi.nlm.nih.gov/pmc/articles/PMC4577126/>
30. Meyer JH, Guhlmann M, Funk J. Blind spot size depends on the optic disc topography: a study using SLO controlled scotometry and the Heidelberg retina tomograph. Br J Ophthalmol. 1997 May;81(5):355–9.
31. Remington LA. Chapter 4 - Retina. In: Remington LA, editor. Clinical Anatomy and Physiology of the Visual System (Third Edition) [Internet]. Saint Louis: Butterworth-Heinemann; 2012 [cited 2021 May 3]. p. 61–92. Available from: <https://www.sciencedirect.com/science/article/pii/B9781437719260100049>
32. Ahnelt PK. The photoreceptor mosaic. Eye. 1998 May;12(3):531–40.
33. Curcio CA, Sloan KR, Kalina RE, Hendrickson AE. Human photoreceptor topography. J Comp Neurol. 1990 Feb 22;292(4):497–523.
34. Adler's Physiology of the Eye - 11th Edition [Internet]. [cited 2021 May 3]. Available from: <https://www.elsevier.com/books/adlers-physiology-of-the-eye/levin/978-0-323-05714-1>
35. Wybar K. Wolff's Anatomy of the Eye and Orbit. Br J Ophthalmol. 1977 Apr;61(4):302.
36. Foulds WS. The choroidal circulation and retinal metabolism—An overview. Eye. 1990 Mar;4(2):243–8.
37. Alm A, Bill A. Ocular and optic nerve blood flow at normal and increased intraocular pressures in monkeys (*Macaca irus*): a study with radioactively labelled microspheres including flow determinations in brain and some other tissues. Exp Eye Res. 1973 Jan 1;15(1):15–29.

38. Riva CE, Cranstoun SD, Grunwald JE, Petrig BL. Choroidal blood flow in the foveal region of the human ocular fundus. *Invest Ophthalmol Vis Sci.* 1994 Dec;35(13):4273–81.
39. Elshazzly M, Lopez MJ, Reddy V, Caban O. Embryology, Central Nervous System. In: StatPearls [Internet]. Treasure Island (FL): StatPearls Publishing; 2022 [cited 2022 Mar 20]. Available from: <http://www.ncbi.nlm.nih.gov/books/NBK526024/>
40. Smith AM, Czyz CN. Neuroanatomy, Cranial Nerve 2 (Optic). In: StatPearls [Internet]. Treasure Island (FL): StatPearls Publishing; 2021 [cited 2021 May 3]. Available from: <http://www.ncbi.nlm.nih.gov/books/NBK507907/>
41. Saidha S, Sotirchos ES, Oh J, Syc SB, Seigo MA, Shiee N, et al. Relationships between retinal axonal and neuronal measures and global central nervous system pathology in multiple sclerosis. *JAMA Neurol.* 2013 Jan;70(1):34–43.
42. Sotirchos ES, Saidha S. OCT is an alternative to MRI for monitoring MS – YES. *Mult Scler J.* 2018 May 1;24(6):701–3.
43. Huang D, Swanson EA, Lin CP, Schuman JS, Stinson WG, Chang W, et al. Optical coherence tomography. *Science.* 1991 Nov 22;254(5035):1178–81.
44. Drexler W, Fujimoto JG. State-of-the-art retinal optical coherence tomography. *Prog Retin Eye Res.* 2008 Jan;27(1):45–88.
45. Costa RA, Skaf M, Melo LAS, Calucci D, Cardillo JA, Castro JC, et al. Retinal assessment using optical coherence tomography. *Prog Retin Eye Res.* 2006 May;25(3):325–53.
46. Tewarie P, Balk L, Costello F, Green A, Martin R, Schippling S, et al. The OSCAR-IB consensus criteria for retinal OCT quality assessment. *PloS One.* 2012;7(4):e34823.
47. Morgner U, Drexler W, Kärtner FX, Li XD, Pitris C, Ippen EP, et al. Spectroscopic optical coherence tomography. *Opt Lett.* 2000 Jan 15;25(2):111–3.
48. Wojtkowski M, Leitgeb R, Kowalczyk A, Bajraszewski T, Fercher AF. In vivo human retinal imaging by Fourier domain optical coherence tomography. *J Biomed Opt.* 2002 Jul;7(3):457–63.
49. Krebs I, Falkner-Radler C, Hagen S, Haas P, Brannath W, Lie S, et al. Quality of the Threshold Algorithm in Age-Related Macular Degeneration: Stratus versus Cirrus OCT. *Invest Ophthalmol Vis Sci.* 2009 Mar 1;50(3):995–1000.
50. Tick S, Rossant F, Ghorbel I, Gaudric A, Sahel JA, Chaumet-Riffaud P, et al. Foveal shape and structure in a normal population. *Invest Ophthalmol Vis Sci.* 2011 Jul 29;52(8):5105–10.

51. Chui TYP, VanNasdale DA, Elsner AE, Burns SA. The Association Between the Foveal Avascular Zone and Retinal Thickness. *Invest Ophthalmol Vis Sci*. 2014 Oct;55(10):6870–7.
52. Hammer DX, Iftimia NV, Ferguson RD, Bigelow CE, Ustun TE, Barnaby AM, et al. Foveal Fine Structure in Retinopathy of Prematurity: An Adaptive Optics Fourier Domain Optical Coherence Tomography Study. *Invest Ophthalmol Vis Sci*. 2008 May;49(5):2061–70.
53. Yadav SK, Motamedi S, Oberwahrenbrock T, Oertel FC, Polthier K, Paul F, et al. CuBe: parametric modeling of 3D foveal shape using cubic Bézier. *Biomed Opt Express*. 2017 Aug 22;8(9):4181–99.
54. Emmerson-Hanover R, Shearer DE, Creel DJ, Dustman RE. Pattern reversal evoked potentials: gender differences and age-related changes in amplitude and latency. *Electroencephalogr Clin Neurophysiol*. 1994 Mar;92(2):93–101.
55. Walsh P, Kane N, Butler S. The clinical role of evoked potentials. *J Neurol Neurosurg Psychiatry*. 2005 Jun 1;76(suppl 2):ii16–22.
56. Kaiser PK. Prospective evaluation of visual acuity assessment: a comparison of snellen versus ETDRS charts in clinical practice (An AOS Thesis). *Trans Am Ophthalmol Soc*. 2009 Dec;107:311–24.
57. Jarius S, Wildemann B. The history of neuromyelitis optica. *J Neuroinflammation*. 2013 Jan 15;10:8.
58. O’Riordan JI, Gallagher HL, Thompson AJ, Howard RS, Kingsley DP, Thompson EJ, et al. Clinical, CSF, and MRI findings in Devic’s neuromyelitis optica. *J Neurol Neurosurg Psychiatry*. 1996 Apr;60(4):382–7.
59. Wingerchuk DM, Hogancamp WF, O’Brien PC, Weinshenker BG. The clinical course of neuromyelitis optica (Devic’s syndrome). *Neurology*. 1999 Sep 22;53(5):1107–14.
60. Lennon VA, Wingerchuk DM, Kryzer TJ, Pittock SJ, Lucchinetti CF, Fujihara K, et al. A serum autoantibody marker of neuromyelitis optica: distinction from multiple sclerosis. *Lancet Lond Engl*. 2004 Dec 11;364(9451):2106–12.
61. Hoshino Y, Noto D, Sano S, Tomizawa Y, Yokoyama K, Hattori N, et al. Dysregulated B cell differentiation towards antibody-secreting cells in neuromyelitis optica spectrum disorder. *J Neuroinflammation*. 2022 Jan 6;19(1):6.
62. Tso MO, Shih CY, McLean IW. Is there a blood-brain barrier at the optic nerve head? *Arch Ophthalmol Chic Ill 1960*. 1975 Sep;93(9):815–25.



63. Shimizu F, Schaller KL, Owens GP, Cotleur AC, Kellner D, Takeshita Y, et al. Glucose-regulated protein 78 autoantibody associates with blood-brain barrier disruption in neuromyelitis optica. *Sci Transl Med*. 2017 05;9(397).
64. Brimberg L, Mader S, Fujieda Y, Arinuma Y, Kowal C, Volpe BT, et al. Antibodies as Mediators of Brain Pathology. *Trends Immunol*. 2015 Nov 1;36(11):709–24.
65. Magaña SM, Matiello M, Pittock SJ, McKeon A, Lennon VA, Rabinstein AA, et al. Posterior reversible encephalopathy syndrome in neuromyelitis optica spectrum disorders. *Neurology*. 2009 Feb 24;72(8):712–7.
66. Misu T, Fujihara K, Kakita A, Konno H, Nakamura M, Watanabe S, et al. Loss of aquaporin 4 in lesions of neuromyelitis optica: distinction from multiple sclerosis. *Brain J Neurol*. 2007 May;130(Pt 5):1224–34.
67. Hinson SR, Pittock SJ, Lucchinetti CF, Roemer SF, Fryer JP, Kryzer TJ, et al. Pathogenic potential of IgG binding to water channel extracellular domain in neuromyelitis optica. *Neurology*. 2007 Dec 11;69(24):2221–31.
68. Kurosawa K, Misu T, Takai Y, Sato DK, Takahashi T, Abe Y, et al. Severely exacerbated neuromyelitis optica rat model with extensive astrocytopathy by high affinity anti-aquaporin-4 monoclonal antibody. *Acta Neuropathol Commun*. 2015 Dec 4;3(1):82.
69. Sepúlveda M, Aldea M, Escudero D, Llufríu S, Arrambide G, Otero-Romero S, et al. Epidemiology of NMOSD in Catalonia: Influence of the new 2015 criteria in incidence and prevalence estimates. *Mult Scler Houndmills Basingstoke Engl*. 2018 Dec;24(14):1843–51.
70. Papp V, Magyari M, Aktas O, Berger T, Broadley SA, Cabre P, et al. Worldwide Incidence and Prevalence of Neuromyelitis Optica. *Neurology*. 2021 Jan 12;96(2):59–77.
71. Kim SH, Mealy MA, Levy M, Schmidt F, Ruprecht K, Paul F, et al. Racial differences in neuromyelitis optica spectrum disorder. *Neurology*. 2018 Nov 27;91(22):e2089–99.
72. Akaishi T, Takahashi T, Nakashima I, Abe M, Ishii T, Aoki M, et al. Repeated follow-up of AQP4-IgG titer by cell-based assay in neuromyelitis optica spectrum disorders (NMOSD). *J Neurol Sci*. 2020 Mar 15;410:116671.
73. Saini H, Fernandez G, Kerr D, Levy M. Differential expression of aquaporin-4 isoforms localizes with neuromyelitis optica disease activity. *J Neuroimmunol*. 2010 Apr 15;221(1–2):68–72.
74. Hofman P, Hoyng P, vanderWerf F, Vrensen GF, Schlingemann RO. Lack of blood-brain barrier properties in microvessels of the prelaminar optic nerve head. *Invest Ophthalmol Vis Sci*. 2001 Apr;42(5):895–901.

75. Bennett JL, Lam C, Kalluri SR, Saikali P, Bautista K, Dupree C, et al. Intrathecal pathogenic anti-aquaporin-4 antibodies in early neuromyelitis optica. *Ann Neurol*. 2009 Nov;66(5):617–29.
76. Levin MH, Bennett JL, Verkman AS. OPTIC NEURITIS IN NEUROMYELITIS OPTICA. *Prog Retin Eye Res*. 2013 Sep;36:159–71.
77. Ludwin SK. Phagocytosis in the rat optic nerve following Wallerian degeneration. *Acta Neuropathol (Berl)*. 1990;80(3):266–73.
78. Hickman SJ, Toosy AT, Jones SJ, Altmann DR, Miszkiel KA, MacManus DG, et al. Serial magnetization transfer imaging in acute optic neuritis. *Brain J Neurol*. 2004 Mar;127(Pt 3):692–700.
79. Kim HJ, Paul F, Lana-Peixoto MA, Tenenbaum S, Asgari N, Palace J, et al. MRI characteristics of neuromyelitis optica spectrum disorder. *Neurology*. 2015 Mar 17;84(11):1165–73.
80. Pittock SJ, Lucchinetti CF. Neuromyelitis optica and the evolving spectrum of autoimmune aquaporin-4 channelopathies: a decade later. *Ann N Y Acad Sci*. 2016;1366(1):20–39.
81. Jurynczyk M, Messina S, Woodhall MR, Raza N, Everett R, Roca-Fernandez A, et al. Clinical presentation and prognosis in MOG-antibody disease: a UK study. *Brain J Neurol*. 2017 01;140(12):3128–38.
82. Kitley J, Waters P, Woodhall M, Leite MI, Murchison A, George J, et al. Neuromyelitis optica spectrum disorders with aquaporin-4 and myelin-oligodendrocyte glycoprotein antibodies: a comparative study. *JAMA Neurol*. 2014 Mar;71(3):276–83.
83. Sato DK, Callegaro D, Lana-Peixoto MA, Waters PJ, Jorge FM de H, Takahashi T, et al. Distinction between MOG antibody-positive and AQP4 antibody-positive NMO spectrum disorders. *Neurology*. 2014 Feb 11;82(6):474–81.
84. Kawachi I. Clinical characteristics of autoimmune optic neuritis. *Clin Exp Neuroimmunol*. 2017;8(S1):8–16.
85. Nakajima H, Hosokawa T, Sugino M, Kimura F, Sugasawa J, Hanafusa T, et al. Visual field defects of optic neuritis in neuromyelitis optica compared with multiple sclerosis. *BMC Neurol*. 2010 Jun 18;10:45.
86. Huda S, Whittam D, Bhojak M, Chamberlain J, Noonan C, Jacob A, et al. Neuromyelitis optica spectrum disorders. *Clin Med*. 2019 Mar;19(2):169–76.
87. Ashtari F, Ataei A, Kafieh R, Khodabandeh Z, Barzegar M, Raei M, et al. Optical Coherence Tomography in Neuromyelitis Optica spectrum disorder and Multiple Sclerosis: A population-based study. *Mult Scler Relat Disord*. 2021 Jan;47:102625.

88. Yamamura T, Nakashima I. Foveal thinning in neuromyelitis optica: A sign of retinal astrocytopathy? *Neurol Neuroimmunol Neuroinflammation*. 2017 May;4(3):e347.
89. Motamedi S, Oertel FC, Yadav SK, Kadas EM, Weise M, Havla J, et al. Altered fovea in AQP4-IgG-seropositive neuromyelitis optica spectrum disorders. *Neurol - Neuroimmunol Neuroinflammation*. 2020 Sep;7(5):e805.
90. Sotirchos ES, Filippatou A, Fitzgerald KC, Salama S, Pardo S, Wang J, et al. Aquaporin-4 IgG seropositivity is associated with worse visual outcomes after optic neuritis than MOG-IgG seropositivity and multiple sclerosis, independent of macular ganglion cell layer thinning: *Mult Scler J* [Internet]. 2019 Jul 31 [cited 2020 May 13]; Available from: <https://journals.sagepub.com/doi/10.1177/1352458519864928>
91. Jeong IH, Kim HJ, Kim NH, Jeong KS, Park CY. Subclinical primary retinal pathology in neuromyelitis optica spectrum disorder. *J Neurol*. 2016 Jul;263(7):1343–8.
92. Oertel FC, Havla J, Roca-Fernández A, Lizak N, Zimmermann H, Motamedi S, et al. Retinal ganglion cell loss in neuromyelitis optica: a longitudinal study. *J Neurol Neurosurg Psychiatry*. 2018;89(12):1259–65.
93. Oertel FC, Kuchling J, Zimmermann H, Chien C, Schmidt F, Knier B, et al. Microstructural visual system changes in AQP4-antibody-seropositive NMOSD. *Neurol Neuroimmunol Neuroinflammation* [Internet]. 2017 Feb 22 [cited 2020 Dec 28];4(3). Available from: <https://www.ncbi.nlm.nih.gov/pmc/articles/PMC5322864/>
94. Tian DC, Su L, Fan M, Yang J, Zhang R, Wen P, et al. Bidirectional degeneration in the visual pathway in neuromyelitis optica spectrum disorder (NMOSD). *Mult Scler J*. 2018 Oct 1;24(12):1585–93.
95. Costello F, Hodge W, Pan Y, Eggenberger E, Coupland S, Kardon R. Tracking retinal nerve fiber layer loss after optic neuritis: a prospective study using optical coherence tomography. *Mult Scler J*. 2008 Aug 1;14(7):893–905.
96. Ratchford JN, Quigg ME, Conger A, Frohman T, Frohman E, Balcer LJ, et al. Optical coherence tomography helps differentiate neuromyelitis optica and MS optic neuropathies. *Neurology*. 2009 Jul 28;73(4):302–8.
97. Schneider E, Zimmermann H, Oberwahrenbrock T, Kaufhold F, Kadas EM, Petzold A, et al. Optical Coherence Tomography Reveals Distinct Patterns of Retinal Damage in Neuromyelitis Optica and Multiple Sclerosis. *PLOS ONE*. 2013 Jun 21;8(6):e66151.
98. Watanabe A, Matsushita T, Doi H, Matsuoka T, Shigeto H, Isobe N, et al. Multimodality-evoked potential study of anti-aquaporin-4 antibody-positive and -negative multiple sclerosis patients. *J Neurol Sci*. 2009 Jun 15;281(1–2):34–40.

99. Neto SP, Alvarenga RMP, Vasconcelos CCF, Alvarenga MP, Pinto LC, Pinto VLR. Evaluation of pattern-reversal visual evoked potential in patients with neuromyelitis optica. *Mult Scler Houndmills Basingstoke Engl.* 2013 Feb;19(2):173–8.
100. Ringelstein M, Kleiter I, Ayzenberg I, Borisow N, Paul F, Ruprecht K, et al. Visual evoked potentials in neuromyelitis optica and its spectrum disorders. *Mult Scler Houndmills Basingstoke Engl.* 2014 Apr;20(5):617–20.
101. Vabanesi M, Pisa M, Guerrieri S, Moiola L, Radaelli M, Medaglini S, et al. In vivo structural and functional assessment of optic nerve damage in neuromyelitis optica spectrum disorders and multiple sclerosis. *Sci Rep.* 2019 Jul 17;9(1):10371.
102. Ringelstein M, Harmel J, Zimmermann H, Brandt AU, Paul F, Haarmann A, et al. Longitudinal optic neuritis-unrelated visual evoked potential changes in NMO spectrum disorders. *Neurology.* 2020 28;94(4):e407–18.
103. Niklas A, Sebraoui H, Hess E, Wagner A, Then Bergh F. Outcome measures for trials of remyelinating agents in multiple sclerosis: retrospective longitudinal analysis of visual evoked potential latency. *Mult Scler Houndmills Basingstoke Engl.* 2009 Jan;15(1):68–74.
104. Barton JL, Garber JY, Klistorner A, Barnett MH. The electrophysiological assessment of visual function in Multiple Sclerosis. *Clin Neurophysiol Pract.* 2019 May 8;4:90–6.
105. Khanna S, Sharma A, Huecker J, Gordon M, Naismith RT, Van Stavern GP. Magnetic resonance imaging of optic neuritis in patients with neuromyelitis optica versus multiple sclerosis. *J Neuro-Ophthalmol Off J North Am Neuro-Ophthalmol Soc.* 2012 Sep;32(3):216–20.
106. Ramanathan S, Prelog K, Barnes EH, Tantsis EM, Reddel SW, Henderson APD, et al. Radiological differentiation of optic neuritis with myelin oligodendrocyte glycoprotein antibodies, aquaporin-4 antibodies, and multiple sclerosis. *Mult Scler Houndmills Basingstoke Engl.* 2016 Apr;22(4):470–82.
107. Chen JJ, Flanagan EP, Jitrapaikulsan J, López-Chiriboga A (Sebastian) S, Fryer JP, Leavitt JA, et al. Myelin Oligodendrocyte Glycoprotein Antibody–Positive Optic Neuritis: Clinical Characteristics, Radiologic Clues, and Outcome. *Am J Ophthalmol.* 2018 Nov;195:8–15.
108. Messina S, Mariano R, Roca-Fernandez A, Cavey A, Jurynczyk M, Leite MI, et al. Contrasting the brain imaging features of MOG-antibody disease, with AQP4-antibody NMOSD and multiple sclerosis. *Mult Scler Houndmills Basingstoke Engl.* 2021 May 28;13524585211018988.
109. Tajfirouz D, Padungkiatsagul T, Beres S, Moss HE, Pittock S, Flanagan E, et al. Optic chiasm involvement in AQP-4 antibody-positive NMO and MOG antibody-

- associated disorder. *Mult Scler Houndmills Basingstoke Engl.* 2021 May 12;13524585211011450.
110. Kim SH, Kwak K, Hyun JW, Joung A, Lee SH, Choi YH, et al. Diffusion tensor imaging of normal-appearing white matter in patients with neuromyelitis optica spectrum disorder and multiple sclerosis. *Eur J Neurol.* 2017 Jul;24(7):966–73.
  111. Matthews L, Kolind S, Brazier A, Leite MI, Brooks J, Traboulsee A, et al. Imaging Surrogates of Disease Activity in Neuromyelitis Optica Allow Distinction from Multiple Sclerosis. *PloS One.* 2015;10(9):e0137715.
  112. Asseyer S, Cooper G, Paul F. Pain in NMOSD and MOGAD: A Systematic Literature Review of Pathophysiology, Symptoms, and Current Treatment Strategies. *Front Neurol [Internet].* 2020 [cited 2022 Mar 28];11. Available from: <https://www.frontiersin.org/article/10.3389/fneur.2020.00778>
  113. Qian P, Lancia S, Alvarez E, Klawiter EC, Cross AH, Naismith RT. Association of Neuromyelitis Optica With Severe and Intractable Pain. *Arch Neurol.* 2012 Nov;69(11):1482–7.
  114. Zhao S, Mutch K, Elson L, Nurmikko T, Jacob A. Neuropathic pain in neuromyelitis optica affects activities of daily living and quality of life. *Mult Scler Houndmills Basingstoke Engl.* 2014 Oct;20(12):1658–61.
  115. Mariano R, Messina S, Roca-Fernandez A, Leite MI, Kong Y, Palace JA. Quantitative spinal cord MRI in MOG-antibody disease, neuromyelitis optica and multiple sclerosis. *Brain J Neurol.* 2020 Nov 18;
  116. Asseyer S, Schmidt F, Chien C, Scheel M, Ruprecht K, Bellmann-Strobl J, et al. Pain in AQP4-IgG-positive and MOG-IgG-positive neuromyelitis optica spectrum disorders. *Mult Scler J - Exp Transl Clin.* 2018 Jul 1;4(3):2055217318796684.
  117. Salama S, Levy M. Bright spotty lesions as an imaging marker for neuromyelitis optica spectrum disorder. *Mult Scler Houndmills Basingstoke Engl.* 2021 Feb 26;1352458521994259.
  118. Misu T, Fujihara K, Nakashima I, Sato S, Itoyama Y. Intractable hiccup and nausea with periaqueductal lesions in neuromyelitis optica. *Neurology.* 2005 Nov 8;65(9):1479–82.
  119. Wingerchuk DM, Banwell B, Bennett JL, Cabre P, Carroll W, Chitnis T, et al. International consensus diagnostic criteria for neuromyelitis optica spectrum disorders. *Neurology.* 2015 Jul 14;85(2):177–89.
  120. Carnero Contentti E, Correale J. Spinal cord and brain MRI should be routinely performed during follow-up in patients with NMOSD – Yes. *Mult Scler J.* 2021 Jan 1;27(1):13–5.

121. Cook LJ, Rose JW, Alvey JS, Jolley AM, Kuhn R, Marron B, et al. Collaborative International Research in Clinical and Longitudinal Experience Study in NMOSD. *Neurol - Neuroimmunol Neuroinflammation*. 2019 Sep;6(5):e583.
122. Khalilidehkordi E, Clarke L, Arnett S, Bukhari W, Jimenez Sanchez S, O’Gorman C, et al. Relapse Patterns in NMOSD: Evidence for Earlier Occurrence of Optic Neuritis and Possible Seasonal Variation. *Front Neurol* [Internet]. 2020 Jun 16 [cited 2021 May 16];11. Available from: <https://www.ncbi.nlm.nih.gov/pmc/articles/PMC7308484/>
123. Kessler RA, Mealy MA, Levy M. Treatment of Neuromyelitis Optica Spectrum Disorder: Acute, Preventive, and Symptomatic. *Curr Treat Options Neurol*. 2016 Jan;18(1):2.
124. Kimbrough DJ, Fujihara K, Jacob A, Lana-Peixoto MA, Leite MI, Levy M, et al. Treatment of Neuromyelitis Optica: Review and Recommendations. *Mult Scler Relat Disord*. 2012 Oct;1(4):180–7.
125. Sherman E, Han MH. Acute and Chronic Management of Neuromyelitis Optica Spectrum Disorder. *Curr Treat Options Neurol*. 2015 Nov;17(11):48.
126. Bonnan M, Valentino R, Olindo S, Mehdaoui H, Smadja D, Cabre P. Plasma exchange in severe spinal attacks associated with neuromyelitis optica spectrum disorder. *Mult Scler Houndmills Basingstoke Engl*. 2009 Apr;15(4):487–92.
127. Shemin D, Briggs D, Greenan M. Complications of therapeutic plasma exchange: a prospective study of 1,727 procedures. *J Clin Apheresis*. 2007;22(5):270–6.
128. Weinshenker BG, O’Brien PC, Petterson TM, Noseworthy JH, Lucchinetti CF, Dodick DW, et al. A randomized trial of plasma exchange in acute central nervous system inflammatory demyelinating disease. *Ann Neurol*. 1999 Dec;46(6):878–86.
129. Abboud H, Petrak A, Mealy M, Sasidharan S, Siddique L, Levy M. Treatment of acute relapses in neuromyelitis optica: Steroids alone versus steroids plus plasma exchange. *Mult Scler Houndmills Basingstoke Engl*. 2016 Feb;22(2):185–92.
130. Wingerchuk DM, Fujihara K, Palace J, Berthele A, Levy M, Kim HJ, et al. Long-Term Safety and Efficacy of Eculizumab in Aquaporin-4 IgG-Positive NMOSD. *Ann Neurol*. 2021 Feb 14;
131. Cree BA, Bennett JL, Kim HJ, Weinshenker BG, Pittock SJ, Wingerchuk D, et al. Sensitivity analysis of the primary endpoint from the N-MOMentum study of inebilizumab in NMOSD. *Mult Scler Houndmills Basingstoke Engl*. 2021 Feb 4;1352458521988926.
132. Yamamura T, Kleiter I, Fujihara K, Palace J, Greenberg B, Zakrzewska-Pniewska B, et al. Trial of Satralizumab in Neuromyelitis Optica Spectrum Disorder. *N Engl J Med*. 2019 Nov 28;381(22):2114–24.

133. Watanabe S, Misu T, Miyazawa I, Nakashima I, Shiga Y, Fujihara K, et al. Low-dose corticosteroids reduce relapses in neuromyelitis optica: a retrospective analysis. *Mult Scler Houndmills Basingstoke Engl.* 2007 Sep;13(8):968–74.
134. Lotan I, Charlson RW, Ryerson LZ, Levy M, Kister I. Effectiveness of subcutaneous tocilizumab in neuromyelitis optica spectrum disorders. *Mult Scler Relat Disord* [Internet]. 2020 Apr 1 [cited 2021 May 17];39. Available from: [https://www.msard-journal.com/article/S2211-0348\(19\)30991-5/abstract](https://www.msard-journal.com/article/S2211-0348(19)30991-5/abstract)
135. Zhang C, Zhang M, Qiu W, Ma H, Zhang X, Zhu Z, et al. Safety and efficacy of tocilizumab versus azathioprine in highly relapsing neuromyelitis optica spectrum disorder (TANGO): an open-label, multicentre, randomised, phase 2 trial. *Lancet Neurol.* 2020 May;19(5):391–401.
136. Kitley J, Elson L, George J, Waters P, Woodhall M, Vincent A, et al. Methotrexate is an alternative to azathioprine in neuromyelitis optica spectrum disorders with aquaporin-4 antibodies. *J Neurol Neurosurg Psychiatry.* 2013 Aug;84(8):918–21.
137. Weinstock-Guttman B, Ramanathan M, Lincoff N, Napoli SQ, Sharma J, Feichter J, et al. Study of mitoxantrone for the treatment of recurrent neuromyelitis optica (Devic disease). *Arch Neurol.* 2006 Jul;63(7):957–63.
138. Yaguchi H, Sakushima K, Takahashi I, Nishimura H, Yashima-Yamada M, Nakamura M, et al. Efficacy of intravenous cyclophosphamide therapy for neuromyelitis optica spectrum disorder. *Intern Med Tokyo Jpn.* 2013;52(9):969–72.
139. Tomassini V, De Giglio L, Reindl M, Russo P, Pestalozza I, Pantano P, et al. Anti-myelin antibodies predict the clinical outcome after a first episode suggestive of MS. *Mult Scler Houndmills Basingstoke Engl.* 2007 Nov;13(9):1086–94.
140. Pelayo R, Tintoré M, Montalban X, Rovira A, Espejo C, Reindl M, et al. Antimyelin antibodies with no progression to multiple sclerosis. *N Engl J Med.* 2007 Jan 25;356(4):426–8.
141. Kuhle J, Pohl C, Mehling M, Edan G, Freedman MS, Hartung HP, et al. Lack of association between antimyelin antibodies and progression to multiple sclerosis. *N Engl J Med.* 2007 Jan 25;356(4):371–8.
142. Kaushansky N, Eisenstein M, Zilkha-Falb R, Ben-Nun A. The myelin-associated oligodendrocytic basic protein (MOBP) as a relevant primary target autoantigen in multiple sclerosis. *Autoimmun Rev.* 2010 Feb;9(4):233–6.
143. Berger T, Rubner P, Schautzer F, Egg R, Ulmer H, Mayringer I, et al. Antimyelin antibodies as a predictor of clinically definite multiple sclerosis after a first demyelinating event. *N Engl J Med.* 2003 Jul 10;349(2):139–45.

144. O'Connor KC, McLaughlin KA, De Jager PL, Chitnis T, Bettelli E, Xu C, et al. Self-antigen tetramers discriminate between myelin autoantibodies to native or denatured protein. *Nat Med*. 2007 Feb;13(2):211–7.
145. Kitley J, Woodhall M, Waters P, Leite MI, Devenney E, Craig J, et al. Myelin-oligodendrocyte glycoprotein antibodies in adults with a neuromyelitis optica phenotype. *Neurology*. 2012 Sep 18;79(12):1273–7.
146. Kitley J, Leite MI, Küker W, Quaghebeur G, George J, Waters P, et al. Longitudinally extensive transverse myelitis with and without aquaporin 4 antibodies. *JAMA Neurol*. 2013 Nov;70(11):1375–81.
147. Cobo-Calvo A, Marignier R. MOG-antibody-associated disease is different from MS and NMO and should be considered as a distinct disease entity - No. *Mult Scler Houndmills Basingstoke Engl*. 2020 Mar;26(3):274–6.
148. Leite MI, Sato DK. MOG-antibody-associated disease is different from MS and NMOSD and should be considered as a distinct disease entity - Yes. *Mult Scler Houndmills Basingstoke Engl*. 2020 Mar;26(3):272–4.
149. Fujihara K. MOG-antibody-associated disease is different from MS and NMOSD and should be classified as a distinct disease entity - Commentary. *Mult Scler Houndmills Basingstoke Engl*. 2020 Mar;26(3):276–8.
150. Vazquez Do Campo R, Stephens A, Marin Collazo IV, Rubin DI. MOG antibodies in combined central and peripheral demyelination syndromes. *Neurol Neuroimmunol Neuroinflammation*. 2018 Nov;5(6):e503.
151. Pagany M, Jagodic M, Schubart A, Pham-Dinh D, Bachelin C, Baron van Evercooren A, et al. Myelin oligodendrocyte glycoprotein is expressed in the peripheral nervous system of rodents and primates. *Neurosci Lett*. 2003 Oct 30;350(3):165–8.
152. Quarles RH. Myelin sheaths: glycoproteins involved in their formation, maintenance and degeneration. *Cell Mol Life Sci CMLS*. 2002 Nov;59(11):1851–71.
153. Ambrosius W, Michalak S, Kozubski W, Kalinowska A. Myelin Oligodendrocyte Glycoprotein Antibody-Associated Disease: Current Insights into the Disease Pathophysiology, Diagnosis and Management. *Int J Mol Sci [Internet]*. 2020 Dec 24 [cited 2021 May 24];22(1). Available from: <https://www.ncbi.nlm.nih.gov/pmc/articles/PMC7795410/>
154. Becquart P, Vilariño-Güell C, Quandt JA. Enhanced expression of complement and microglial-specific genes prior to clinical progression in the MOG-experimental autoimmune encephalomyelitis model of multiple sclerosis. *Brain Res Bull*. 2020 Dec;165:63–9.



155. Gold R, Linington C, Lassmann H. Understanding pathogenesis and therapy of multiple sclerosis via animal models: 70 years of merits and culprits in experimental autoimmune encephalomyelitis research. *Brain J Neurol.* 2006 Aug;129(Pt 8):1953–71.
156. Jarius S, Metz I, König FB, Ruprecht K, Reindl M, Paul F, et al. Screening for MOG-IgG and 27 other anti-glia and anti-neuronal autoantibodies in 'pattern II multiple sclerosis' and brain biopsy findings in a MOG-IgG-positive case. *Mult Scler Houndmills Basingstoke Engl.* 2016 Oct;22(12):1541–9.
157. de Mol CL, Wong Y, van Pelt ED, Wokke B, Siepman T, Neuteboom RF, et al. The clinical spectrum and incidence of anti-MOG-associated acquired demyelinating syndromes in children and adults. *Mult Scler Houndmills Basingstoke Engl.* 2020 Jun;26(7):806–14.
158. O'Connell K, Hamilton-Shield A, Woodhall M, Messina S, Mariano R, Waters P, et al. Prevalence and incidence of neuromyelitis optica spectrum disorder, aquaporin-4 antibody-positive NMOSD and MOG antibody-positive disease in Oxfordshire, UK. *J Neurol Neurosurg Psychiatry.* 2020 Oct 1;91(10):1126–8.
159. Cobo-Calvo A, Ruiz A, Maillart E, Audoin B, Zephir H, Bourre B, et al. Clinical spectrum and prognostic value of CNS MOG autoimmunity in adults: The MOGADOR study. *Neurology.* 2018 May 22;90(21):e1858–69.
160. Jarius S, Ruprecht K, Kleiter I, Borisow N, Asgari N, Pitarokoili K, et al. MOG-IgG in NMO and related disorders: a multicenter study of 50 patients. Part 2: Epidemiology, clinical presentation, radiological and laboratory features, treatment responses, and long-term outcome. *J Neuroinflammation.* 2016 Sep 27;13(1):280.
161. Mariotto S, Ferrari S, Monaco S, Benedetti MD, Schanda K, Alberti D, et al. Clinical spectrum and IgG subclass analysis of anti-myelin oligodendrocyte glycoprotein antibody-associated syndromes: a multicenter study. *J Neurol.* 2017 Dec;264(12):2420–30.
162. Cobo-Calvo A, Vukusic S, Marignier R. Clinical spectrum of central nervous system myelin oligodendrocyte glycoprotein autoimmunity in adults. *Curr Opin Neurol.* 2019 Jun;32(3):459–66.
163. Ramanathan S, Mohammad S, Tantsis E, Nguyen TK, Merheb V, Fung VSC, et al. Clinical course, therapeutic responses and outcomes in relapsing MOG antibody-associated demyelination. *J Neurol Neurosurg Psychiatry.* 2018 Feb;89(2):127–37.
164. Woodhall M, Mgbachi V, Fox H, Irani S, Waters P. Utility of Live Cell-Based Assays for Autoimmune Neurology Diagnostics. *J Appl Lab Med.* 2022 Jan 5;7(1):391–3.
165. Vicini R, Brügger D, Abegg M, Salmen A, Grabe HM. Differences in morphology and visual function of myelin oligodendrocyte glycoprotein antibody and multiple sclerosis associated optic neuritis. *J Neurol.* 2021 Jan;268(1):276–84.

166. Pache F, Zimmermann H, Mikolajczak J, Schumacher S, Lacheta A, Oertel FC, et al. MOG-IgG in NMO and related disorders: a multicenter study of 50 patients. Part 4: Afferent visual system damage after optic neuritis in MOG-IgG-seropositive versus AQP4-IgG-seropositive patients. *J Neuroinflammation*. 2016 01;13(1):282.
167. Ciotti JR, Eby NS, Wu GF, Naismith RT, Chahin S, Cross AH. Clinical and laboratory features distinguishing MOG antibody disease from multiple sclerosis and AQP4 antibody-positive neuromyelitis optica. *Mult Scler Relat Disord*. 2020 Oct 1;45:102399.
168. Armangue T, Olivé-Cirera G, Martínez-Hernandez E, Sepulveda M, Ruiz-Garcia R, Muñoz-Batista M, et al. Associations of paediatric demyelinating and encephalitic syndromes with myelin oligodendrocyte glycoprotein antibodies: a multicentre observational study. *Lancet Neurol*. 2020 Mar 1;19(3):234–46.
169. Filippatou AG, Mukharesh L, Saidha S, Calabresi PA, Sotirchos ES. AQP4-IgG and MOG-IgG Related Optic Neuritis—Prevalence, Optical Coherence Tomography Findings, and Visual Outcomes: A Systematic Review and Meta-Analysis. *Front Neurol* [Internet]. 2020 [cited 2020 Dec 28];11. Available from: <https://www.frontiersin.org/articles/10.3389/fneur.2020.540156/full>
170. Oertel FC, Outteryck O, Knier B, Zimmermann H, Borisow N, Bellmann-Strobl J, et al. Optical coherence tomography in myelin-oligodendrocyte-glycoprotein antibody-seropositive patients: a longitudinal study. *J Neuroinflammation*. 2019 Jul 25;16(1):154.
171. Havla J, Kümpfel T, Schinner R, Spadaro M, Schuh E, Meinl E, et al. Myelin-oligodendrocyte-glycoprotein (MOG) autoantibodies as potential markers of severe optic neuritis and subclinical retinal axonal degeneration. *J Neurol*. 2017 Jan;264(1):139–51.
172. Molazadeh N, Filippatou AG, Vasileiou ES, Levy M, Sotirchos ES. Evidence for and against subclinical disease activity and progressive disease in MOG antibody disease and neuromyelitis optica spectrum disorder. *J Neuroimmunol*. 2021 Nov 15;360:577702.
173. Havla J, Pakeerathan T, Schwake C, Bennett JL, Kleiter I, Felipe-Rucián A, et al. Age-dependent favorable visual recovery despite significant retinal atrophy in pediatric MOGAD: how much retina do you really need to see well? *J Neuroinflammation* [Internet]. 2021 May 29 [cited 2021 Jun 6];18. Available from: <https://www.ncbi.nlm.nih.gov/pmc/articles/PMC8164737/>
174. Song H, Zhou H, Yang M, Wang J, Liu H, Sun M, et al. Different Characteristics of Aquaporin-4 and Myelin Oligodendrocyte Glycoprotein Antibody-Seropositive Male Optic Neuritis in China [Internet]. Vol. 2019, *Journal of Ophthalmology*. Hindawi; 2019 [cited 2020 Dec 28]. p. e4015075. Available from: <https://www.hindawi.com/journals/joph/2019/4015075/>

175. Schmidt FA, Chien C, Kuchling J, Bellmann-Strobl J, Ruprecht K, Siebert N, et al. Differences in Advanced Magnetic Resonance Imaging in MOG-IgG and AQP4-IgG Seropositive Neuromyelitis Optica Spectrum Disorders: A Comparative Study. *Front Neurol* [Internet]. 2020 [cited 2021 Jun 6];11. Available from: <https://www.frontiersin.org/articles/10.3389/fneur.2020.499910/full#F5>
176. Dubey D, Pittock SJ, Krecke KN, Morris PP, Sechi E, Zaleski NL, et al. Clinical, Radiologic, and Prognostic Features of Myelitis Associated With Myelin Oligodendrocyte Glycoprotein Autoantibody. *JAMA Neurol*. 2019 Mar 1;76(3):301–9.
177. Mariano R, Flanagan EP, Weinshenker BG, Palace J. A practical approach to the diagnosis of spinal cord lesions. *Pract Neurol*. 2018 Jun;18(3):187–200.
178. Jarius S, Kleiter I, Ruprecht K, Asgari N, Pitarokoili K, Borisow N, et al. MOG-IgG in NMO and related disorders: a multicenter study of 50 patients. Part 3: Brainstem involvement - frequency, presentation and outcome. *J Neuroinflammation*. 2016 Nov 1;13(1):281.
179. Ogawa R, Nakashima I, Takahashi T, Kaneko K, Akaishi T, Takai Y, et al. MOG antibody-positive, benign, unilateral, cerebral cortical encephalitis with epilepsy. *Neurol Neuroimmunol Neuroinflammation*. 2017 Mar;4(2):e322.
180. Reindl M, Waters P. Myelin oligodendrocyte glycoprotein antibodies in neurological disease. *Nat Rev Neurol*. 2019 Feb;15(2):89–102.
181. Shen CH, Zheng Y, Cai MT, Yang F, Fang W, Zhang YX, et al. Seizure occurrence in myelin oligodendrocyte glycoprotein antibody-associated disease: A systematic review and meta-analysis. *Mult Scler Relat Disord*. 2020 Jul;42:102057.
182. Jarius S, Paul F, Aktas O, Asgari N, Dale RC, de Seze J, et al. MOG encephalomyelitis: international recommendations on diagnosis and antibody testing. *J Neuroinflammation*. 2018 May 3;15(1):134.
183. Juryńczyk M, Tackley G, Kong Y, Geraldine R, Matthews L, Woodhall M, et al. Brain lesion distribution criteria distinguish MS from AQP4-antibody NMOSD and MOG-antibody disease. *J Neurol Neurosurg Psychiatry*. 2017 Feb;88(2):132–6.
184. López-Chiriboga AS, Majed M, Fryer J, Dubey D, McKeon A, Flanagan EP, et al. Association of MOG-IgG Serostatus With Relapse After Acute Disseminated Encephalomyelitis and Proposed Diagnostic Criteria for MOG-IgG-Associated Disorders. *JAMA Neurol*. 2018 Nov 1;75(11):1355–63.
185. Stiebel-Kalish H, Lotan I, Brody J, Chodick G, Bialer O, Marignier R, et al. Retinal Nerve Fiber Layer May Be Better Preserved in MOG-IgG versus AQP4-IgG Optic Neuritis: A Cohort Study. *PloS One*. 2017;12(1):e0170847.

186. Nave KA. Myelination and support of axonal integrity by glia. *Nature*. 2010 Nov 11;468(7321):244–52.
187. Cruz-Herranz A, Balk LJ, Oberwahrenbrock T, Saidha S, Martinez-Lapiscina EH, Lagreze WA, et al. The APOSTEL recommendations for reporting quantitative optical coherence tomography studies. *Neurology*. 2016 Jun 14;86(24):2303–9.
188. Moezzi AM, Hutchings N, Fonn D, Simpson TL. Mixed Model Analysis of Between-Subject Variability in Overnight Corneal Swelling and Deswelling With Silicone Hydrogel Lenses. *Invest Ophthalmol Vis Sci*. 2018 May 1;59(6):2576–85.
189. Vazquez AI, Bates DM, Rosa GJM, Gianola D, Weigel KA. Technical note: an R package for fitting generalized linear mixed models in animal breeding. *J Anim Sci*. 2010 Feb;88(2):497–504.
190. Verbeke G. Linear Mixed Models for Longitudinal Data. In: Verbeke G, Molenberghs G, editors. *Linear Mixed Models in Practice: A SAS-Oriented Approach* [Internet]. New York, NY: Springer; 1997 [cited 2021 Jun 14]. p. 63–153. (Lecture Notes in Statistics). Available from: [https://doi.org/10.1007/978-1-4612-2294-1\\_3](https://doi.org/10.1007/978-1-4612-2294-1_3)
191. Waters PJ, McKeon A, Leite MI, Rajasekharan S, Lennon VA, Villalobos A, et al. Serologic diagnosis of NMO: a multicenter comparison of aquaporin-4-IgG assays. *Neurology*. 2012 Feb 28;78(9):665–71; discussion 669.
192. Wingerchuk DM, Banwell B, Bennett JL, Cabre P, Carroll W, Chitnis T, et al. International consensus diagnostic criteria for neuromyelitis optica spectrum disorders. *Neurology*. 2015 Jul 14;85(2):177–89.
193. Worley B, Powers R. PCA as a Practical Indicator of OPLS-DA Model Reliability [Internet]. 2016 [cited 2019 Oct 21]. Available from: <https://www.ingentaconnect.com/content/ben/cmb/2016/00000004/00000002/art0004>
194. Jurynczyk M, Probert F, Yeo T, Tackley G, Claridge TDW, Cavey A, et al. Metabolomics reveals distinct, antibody-independent, molecular signatures of MS, AQP4-antibody and MOG-antibody disease. *Acta Neuropathol Commun*. 2017 Dec 6;5(1):95.
195. Yeo T, Probert F, Jurynczyk M, Sealey M, Cavey A, Claridge TDW, et al. Classifying the antibody-negative NMO syndromes: Clinical, imaging, and metabolomic modeling. *Neurol Neuroimmunol Neuroinflammation*. 2019 Nov;6(6):e626.
196. Oertel FC, Zimmermann H, Paul F, Brandt AU. Optical coherence tomography in neuromyelitis optica spectrum disorders: potential advantages for individualized monitoring of progression and therapy. *EPMA J*. 2017 Dec 22;9(1):21–33.
197. Bennett J, de Seze J, Lana-Peixoto M, Palace J, Waldman A, Schippling S, et al. Neuromyelitis optica and multiple sclerosis: Seeing differences through optical

- coherence tomography. *Mult Scler* Houndmills Basingstoke Engl. 2015 May;21(6):678–88.
198. Burkholder BM, Osborne B, Loguidice MJ, Bisker E, Frohman TC, Conger A, et al. Macular Volume Determined by Optical Coherence Tomography as a Measure of Neuronal Loss in Multiple Sclerosis. *Arch Neurol* [Internet]. 2009 Nov 1 [cited 2021 Apr 6];66(11). Available from: <http://archneur.jamanetwork.com/article.aspx?doi=10.1001/archneurol.2009.230>
  199. Gelfand JM, Nolan R, Schwartz DM, Graves J, Green AJ. Microcystic macular oedema in multiple sclerosis is associated with disease severity. *Brain J Neurol*. 2012 Jun;135(Pt 6):1786–93.
  200. Saidha S, Sotirchos ES, Ibrahim MA, Crainiceanu CM, Gelfand JM, Sepah YJ, et al. Microcystic macular oedema, thickness of the inner nuclear layer of the retina, and disease characteristics in multiple sclerosis: a retrospective study. *Lancet Neurol*. 2012 Nov;11(11):963–72.
  201. Balk LJ, Coric D, Knier B, Zimmermann HG, Behbehani R, Alroughani R, et al. Retinal inner nuclear layer volume reflects inflammatory disease activity in multiple sclerosis; a longitudinal OCT study. *Mult Scler J - Exp Transl Clin* [Internet]. 2019 Sep 5 [cited 2021 Jan 10];5(3). Available from: <https://www.ncbi.nlm.nih.gov/pmc/articles/PMC6728683/>
  202. Knier B, Schmidt P, Aly L, Buck D, Berthele A, Mühlau M, et al. Retinal inner nuclear layer volume reflects response to immunotherapy in multiple sclerosis. *Brain J Neurol*. 2016 Nov 1;139(11):2855–63.
  203. Sotirchos ES, Caldito NG, Filippatou A, Fitzgerald KC, Murphy OC, Lambe J, et al. Progressive multiple sclerosis is associated with faster and specific retinal layer atrophy. *Ann Neurol*. 2020 Jun;87(6):885–96.
  204. Green AJ, McQuaid S, Hauser SL, Allen IV, Lyness R. Ocular pathology in multiple sclerosis: retinal atrophy and inflammation irrespective of disease duration. *Brain J Neurol*. 2010 Jun;133(Pt 6):1591–601.
  205. Zhang Q, Li Y, Zhuo Y. Synaptic or Non-synaptic? Different Intercellular Interactions with Retinal Ganglion Cells in Optic Nerve Regeneration. *Mol Neurobiol*. 2022 May;59(5):3052–72.
  206. Ong Chin Feng W, Wan Hitam WH. Evaluation of retinal nerve fiber layer thickness and optic nerve functions in fellow eye of neuromyelitis optica with unilateral optic neuritis. *Taiwan J Ophthalmol*. 2020 Jun 20;10(3):189–96.
  207. Akaishi T, Kaneko K, Himori N, Takeshita T, Takahashi T, Nakazawa T, et al. Subclinical retinal atrophy in the unaffected fellow eyes of multiple sclerosis and neuromyelitis optica. *J Neuroimmunol*. 2017 Dec 15;313:10–5.

208. Finke C, Zimmermann H, Pache F, Oertel FC, Chavarro VS, Kramarenko Y, et al. Association of Visual Impairment in Neuromyelitis Optica Spectrum Disorder With Visual Network Reorganization. *JAMA Neurol.* 2018 Mar;75(3):296–303.
209. Saji E, Arakawa M, Yanagawa K, Toyoshima Y, Yokoseki A, Okamoto K, et al. Cognitive impairment and cortical degeneration in neuromyelitis optica. *Ann Neurol.* 2013;73(1):65–76.
210. Sinha PK, Joshi D, Singh VP, Deshmukh S, Singh U, Pathak A, et al. Optical Coherence Tomography and Subclinical Optical Neuritis in Longitudinally Extensive Transverse Myelitis. *Ann Indian Acad Neurol.* 2017;20(4):358–62.
211. Felix CM, Levin MH, Verkman AS. Complement-independent retinal pathology produced by intravitreal injection of neuromyelitis optica immunoglobulin G. *J Neuroinflammation.* 2016 20;13(1):275.
212. Lucchinetti CF, Guo Y, Popescu BFG, Fujihara K, Itoyama Y, Misu T. The pathology of an autoimmune astrocytopathy: lessons learned from neuromyelitis optica. *Brain Pathol Zurich Switz.* 2014 Jan;24(1):83–97.
213. Bringmann A, Pannicke T, Grosche J, Francke M, Wiedemann P, Skatchkov SN, et al. Müller cells in the healthy and diseased retina. *Prog Retin Eye Res.* 2006 Jul;25(4):397–424.
214. Iandiev I, Pannicke T, Biedermann B, Wiedemann P, Reichenbach A, Bringmann A. Ischemia-reperfusion alters the immunolocalization of glial aquaporins in rat retina. *Neurosci Lett.* 2006 Nov 13;408(2):108–12.
215. Nagelhus EA, Mathiisen TM, Ottersen OP. Aquaporin-4 in the central nervous system: Cellular and subcellular distribution and coexpression with KIR4.1. *Neuroscience.* 2004 Jan 1;129(4):905–13.
216. Zhang X, Xiao H, Liu C, Zhao L, Wang J, Li H, et al. Comparison of macular structural and vascular changes in neuromyelitis optica spectrum disorder and primary open angle glaucoma: a cross-sectional study. *Br J Ophthalmol.* 2021 Mar;105(3):354–60.
217. Manogaran P, Traboulssee AL, Lange AP. Longitudinal Study of Retinal Nerve Fiber Layer Thickness and Macular Volume in Patients With Neuromyelitis Optica Spectrum Disorder. *J Neuroophthalmol.* 2016 Dec;36(4):363–8.
218. Pisa M, Ratti F, Vabanesi M, Radaelli M, Guerrieri S, Muiola L, et al. Subclinical neurodegeneration in multiple sclerosis and neuromyelitis optica spectrum disorder revealed by optical coherence tomography. *Mult Scler J.* 2019 Aug 8;135245851986160.
219. Gleiser C, Wagner A, Fallier-Becker P, Wolburg H, Hirt B, Mack AF. Aquaporin-4 in Astroglial Cells in the CNS and Supporting Cells of Sensory Organs—A

- Comparative Perspective. *Int J Mol Sci* [Internet]. 2016 Aug 26 [cited 2020 May 13];17(9). Available from: <https://www.ncbi.nlm.nih.gov/pmc/articles/PMC5037691/>
220. Bennett JL, Owens GP. Neuromyelitis Optica: Deciphering a Complex Immune-Mediated Astrocytopathy. *J Neuro-Ophthalmol Off J North Am Neuro-Ophthalmol Soc.* 2017 Sep;37(3):291–9.
  221. Oertel FC, Schließert J, Brandt AU, Paul F. Cognitive Impairment in Neuromyelitis Optica Spectrum Disorders: A Review of Clinical and Neuroradiological Features. *Front Neurol* [Internet]. 2019 [cited 2020 May 13];10. Available from: <https://www.frontiersin.org/articles/10.3389/fneur.2019.00608/full>
  222. Penner IK, Paul F. Fatigue as a symptom or comorbidity of neurological diseases. *Nat Rev Neurol.* 2017 Nov;13(11):662–75.
  223. Chavarro VS, Mealy MA, Simpson A, Lacheta A, Pache F, Ruprecht K, et al. Insufficient treatment of severe depression in neuromyelitis optica spectrum disorder. *Neurol Neuroimmunol Neuroinflammation* [Internet]. 2016 Oct 24 [cited 2020 May 13];3(6). Available from: <https://www.ncbi.nlm.nih.gov/pmc/articles/PMC5079380/>
  224. Liu Y, Duan Y, He Y, Yu C, Wang J, Huang J, et al. A tract-based diffusion study of cerebral white matter in neuromyelitis optica reveals widespread pathological alterations. *Mult Scler Houndmills Basingstoke Engl.* 2012 Jul;18(7):1013–21.
  225. Papadopoulou A, Oertel FC, Gaetano L, Kuchling J, Zimmermann H, Chien C, et al. Attack-related damage of thalamic nuclei in neuromyelitis optica spectrum disorders. *J Neurol Neurosurg Psychiatry.* 2019 Oct;90(10):1156–64.
  226. Xiao M, Hu G. Involvement of Aquaporin 4 in Astrocyte Function and Neuropsychiatric Disorders. *CNS Neurosci Ther.* 2014 Apr 8;20(5):385–90.
  227. Schmidt F, Zimmermann H, Mikolajczak J, Oertel FC, Pache F, Weinhold M, et al. Severe structural and functional visual system damage leads to profound loss of vision-related quality of life in patients with neuromyelitis optica spectrum disorders. *Mult Scler Relat Disord.* 2017 Jan;11:45–50.
  228. Martínez de Lapiscina E, Sánchez-Dalmau B, Fraga-Pumar E, Ortiz-Perez S, Tercero A, Torres R, et al. The visual pathway as a model to understand brain damage in multiple sclerosis. *Mult Scler.* 2014 Nov 20;20:1678–85.
  229. Bankston AN, Mandler MD, Feng Y. Oligodendroglia and neurotrophic factors in neurodegeneration. *Neurosci Bull.* 2013 Apr 5;29(2):216–28.
  230. Bermel R, Inglese M. Neurodegeneration and inflammation in MS The eye teaches us about the storm. *Neurology.* 2013 Jan 1;80:19–20.

231. Panneman EL, Coric D, Tran LMD, de Vries-Knoppert W a. EJ, Petzold A. Progression of Anterograde Trans-Synaptic Degeneration in the Human Retina Is Modulated by Axonal Convergence and Divergence. *Neuro-Ophthalmol* Aeolus Press. 2019 Dec;43(6):382–90.
232. Pawlitzki M, Horbrügger M, Loewe K, Kaufmann J, Opfer R, Wagner M, et al. MS optic neuritis-induced long-term structural changes within the visual pathway. *Neurol Neuroimmunol Neuroinflammation*. 2020 05;7(2).
233. Dinkin M. Trans-synaptic Retrograde Degeneration in the Human Visual System: Slow, Silent, and Real. *Curr Neurol Neurosci Rep*. 2017 Feb 22;17(2):16.
234. Al-Louzi O, Button J, Newsome SD, Calabresi PA, Saidha S. Retrograde trans-synaptic visual pathway degeneration in multiple sclerosis: A case series. *Mult Scler* Houndmills Basingstoke Engl. 2017 Jun;23(7):1035–9.
235. You Y, Gupta VK, Graham SL, Klistorner A. Anterograde Degeneration along the Visual Pathway after Optic Nerve Injury. *PLoS ONE* [Internet]. 2012 Dec 26 [cited 2020 Nov 22];7(12). Available from: <https://www.ncbi.nlm.nih.gov/pmc/articles/PMC3530579/>
236. Manogaran P, Vavasour IM, Lange AP, Zhao Y, McMullen K, Rauscher A, et al. Quantifying visual pathway axonal and myelin loss in multiple sclerosis and neuromyelitis optica. *NeuroImage Clin*. 2016 May 26;11:743–50.
237. von Glehn F, Jarius S, Cavalcanti Lira RP, Alves Ferreira MC, von Glehn FHR, Costa e Castro SM, et al. Structural brain abnormalities are related to retinal nerve fiber layer thinning and disease duration in neuromyelitis optica spectrum disorders. *Mult Scler J*. 2014 Aug 1;20(9):1189–97.



# 11. APPENDIX

## 11.1. Publications:

### 11.1.1. Publications directly related with this thesis:

#### 11.1.1.1. Foveal changes in aquaporin-4 antibody seropositive neuromyelitis optica spectrum disorder are independent of optic neuritis and not overtly progressive

Citation: **Roca-Fernández A**, Oertel FC, Yeo T, Motamedi S, Probert F, Craner MJ, Sastre-Garriga J, Zimmermann HG, Asseyer S, Kuchling J, Bellmann-Strobl J, Ruprecht K, Leite MI, Paul F, Brandt AU, Palace J. *Foveal changes in aquaporin-4 antibody seropositive neuromyelitis optica spectrum disorder are independent of optic neuritis and not overtly progressive*. Eur J Neurol. 2021 Jul;28(7):2280-2293. doi: 10.1111/ene.14766. Epub 2021 Mar 23. IF: 6.089

# Foveal changes in aquaporin-4 antibody seropositive neuromyelitis optica spectrum disorder are independent of optic neuritis and not overtly progressive

Adriana Roca-Fernández<sup>1,2</sup> | Frederike Cosima Oertel<sup>3,4</sup> | Tianrong Yeo<sup>5,6</sup> |  
Seyedamirhosein Motamedi<sup>3,4</sup> | Fay Probert<sup>5</sup> | Matthew J. Craner<sup>1</sup> |  
Jaume Sastre-Garriga<sup>2</sup> | Hanna G. Zimmermann<sup>3,4</sup> | Susanna Assejer<sup>3,4</sup> |  
Joseph Kuchling<sup>3,4,7,8</sup> | Judith Bellmann-Strobl<sup>3,4</sup> | Klemens Ruprecht<sup>7</sup> |  
Maria Isabel Leite<sup>1</sup> | Friedemann Paul<sup>3,4,7</sup> | Alexander Ulrich Brandt<sup>3,4,9</sup> | Jacqueline Palace<sup>1</sup>

<sup>1</sup>Nuffield Department of Clinical Neurosciences, University of Oxford, Oxford, UK

<sup>2</sup>Department of Neurology/Neuroimmunology, Multiple Sclerosis Centre of Catalonia (Cemcat), Hospital Universitari Vall d'Hebron, Universitat Autònoma de Barcelona, Barcelona, Spain

<sup>3</sup>Experimental and Clinical Research Center, Max Delbrück Center for Molecular Medicine and Charité – Universitätsmedizin Berlin, Corporate Member of Freie Universität Berlin, Humboldt-Universität zu Berlin, and Berlin Institute of Health, Berlin, Germany

<sup>4</sup>NeuroCure Clinical Research Center, Charité – Universitätsmedizin Berlin, Corporate Member of Freie Universität Berlin, Humboldt-Universität zu Berlin, and Berlin Institute of Health, Berlin, Germany

<sup>5</sup>Department of Pharmacology, University of Oxford, Oxford, UK

<sup>6</sup>Department of Neurology, National Neuroscience Institute, Singapore, Singapore

<sup>7</sup>Department of Neurology, Charité – Universitätsmedizin Berlin, Corporate member of Freie Universität Berlin, Humboldt-Universität zu Berlin, and Berlin Institute of Health, Berlin, Germany

<sup>8</sup>Berlin Institute of Health (BIH), Berlin, Germany

<sup>9</sup>Department of Neurology, University of California Irvine, Irvine, CA, USA

## Correspondence

Alexander Ulrich Brandt, Translational Neuroimaging Group, Clinical Neuroimmunology, Experimental and Clinical Research Center, Charité – Universitätsmedizin Berlin, Laboradresse: Sauerbruchweg 5, Charitéplatz 1, 10117 Berlin, Germany.  
Emails: alexander.brandt@charite.de; aubrandt@uci.edu

## Funding information

Supported by the Einstein Foundation Berlin (Einstein Junior Scholarship to S.M.), the German Federal Ministry of

## Abstract

**Background and purpose:** Foveal changes were reported in aquaporin-4 antibody (AQP4-Ab) seropositive neuromyelitis optica spectrum disorder (NMOSD) patients; however, it is unclear whether they are independent of optic neuritis (ON), stem from sub-clinical ON or crossover from ON in fellow eyes. Fovea morphometry and a statistical classification approach were used to investigate if foveal changes in NMOSD are independent of ON and progressive.

**Methods:** This was a retrospective longitudinal study of 27 AQP4-IgG + NMOSD patients (49 eyes; 15 ON eyes and 34 eyes without a history of ON [NON eyes]), follow-up median (first and third quartile) 2.32 (1.33–3.28), and 38 healthy controls (HCs) (76 eyes),

**Abbreviations:** AQP4-Ab, aquaporin-4 antibody; ART, automatic real-time; FT, foveal thickness; GCIP, combined ganglion cell and inner plexiform layer volume; HC, healthy control; INL, inner nuclear layer; LME, linear mixed effects; NMOSD, neuromyelitis optica spectrum disorder; NON, eyes without history of optic neuritis; OCT, optical coherence tomography; ON, optic neuritis; OPLS-DA, orthogonal partial least squares discriminant analysis; pRNFL, peripapillary retinal nerve fibre layer; TMV, total macular volume; VIP, variable importance in projection. Adriana Roca-Fernández and Frederike Cosima Oertel are equally contributing first authors.

Alexander Ulrich Brandt and Jacqueline Palace are equally contributing senior authors.

[Correction added on 21 April 2021, after first online publication: The author name Sedamirhosein Motamedi has been corrected to Seyedamirhosein Motamedi.]

This is an open access article under the terms of the Creative Commons Attribution-NonCommercial-NoDerivs License, which permits use and distribution in any medium, provided the original work is properly cited, the use is non-commercial and no modifications or adaptations are made.

© 2021 The Authors. *European Journal of Neurology* published by John Wiley & Sons Ltd on behalf of European Academy of Neurology.

Economic Affairs and Energy (BMWl EXIST 03EFE079 to A.U.B.), German Research Foundation (DFG Exc. 257 to F.P. and A.U.B.), German Federal Ministry of Education and Research (BMBF Neu2 ADVISIMS to F.P. and A.U.B.) and Novartis (research grant to H.G.Z.) and Ministry of Health, Singapore, through the National Medical Research Council Research Training Fellowship (NMRC/Fellowship/0038/2016) (grant to T.Y.).

follow-up median (first and third quartile) 1.95 (1.83–2.54). The peripapillary retinal nerve fibre layer thickness and the volume of combined ganglion cell and inner plexiform layer as measures of neuroaxonal damage from ON were determined by optical coherence tomography. Nineteen foveal morphometry parameters were extracted from macular optical coherence tomography volume scans. Data were analysed using orthogonal partial least squares discriminant analysis and linear mixed effects models.

**Results:** At baseline, foveal shape was significantly altered in ON eyes and NON eyes compared to HCs. Discriminatory analysis showed 81% accuracy distinguishing ON vs. HCs and 68% accuracy in NON vs. HCs. NON eyes were distinguished from HCs by foveal shape parameters indicating widening. Orthogonal partial least squares discriminant analysis discriminated ON vs. NON with 76% accuracy. In a follow-up of 2.4 (20.85) years, no significant time-dependent foveal changes were found.

**Conclusion:** The parafoveal area is altered in AQP4-Ab seropositive NMOSD patients suggesting independent neuroaxonal damage from subclinical ON. Longer follow-ups are needed to confirm the stability of the parafoveal structure over time.

#### KEYWORDS

aquaporin-4 antibodies (AQP4-IgG), foveal morphometry, neuromyelitis optica spectrum disorders (NMOSD), optic neuritis, retinal neuroaxonal damage

## INTRODUCTION

Neuromyelitis optica spectrum disorders (NMOSDs) are relapsing inflammatory diseases of the central nervous system with a predilection for optic nerves, brainstem and spinal cord [1]. The discovery of pathogenic antibodies to astrocytic aquaporin-4 (AQP4) water channels [2] in the majority of patients [3,4] has led to NMOSD being categorized as a primary astrocytopathy, in which AQP4 antibodies (AQP4-Abs) cause complement-mediated damage to AQP4-expressing astrocytes [3].

Aquaporin-4 antibody seropositive NMOSD is defined by a relapsing course, but without chronic clinical progression or chronic lesion activity [5]. Acute optic neuritis (ON) is a frequent manifestation of AQP4-Ab seropositive NMOSD and is typically characterized by severe visual impairment [6], posterior involvement of the optic nerve on magnetic resonance imaging, severe damage neuropathologically [7] and neuroaxonal loss in the retina measured by optical coherence tomography (OCT) [8].

An increasing number of studies have reported retinal changes in NMOSD patient eyes with no known history of clinical ON [9–11]. This is supported by data from animal models of NMOSD, in which rats injected with AQP4-Abs show complement-independent Müller cell loss in the retina [12]. Müller cells are glial cells that extend longitudinally through the retina [13] and that express AQP4 in end feet covering retinal blood vessels [14,15]. Müller cell density is high in the parafoveal area, but it decreases in the central avascular foveal zone [16]. To specifically target this area in OCT a fovea morphometry on 3D macular OCT images was developed, which can reliably describe the foveal/parafoveal shape [17]. Using this approach, specific foveal changes in NMOSD were previously reported, which are distinct to

changes in multiple sclerosis patients, a disorder also leading to ON but without AQP4-Abs [18].

An alternative hypothesis is that foveal changes stem from ON attacks that do not reach clinical threshold or from chiasmal cross-over during an ON in the contralateral eye. Whilst the focus of this research has been on the fovea, previous studies also reported some degree of neuroaxonal damage in eyes without clinical ON [10]. When excluding patients with a history of ON, evidence for retinal neuroaxonal damage was still found [9] and neuronal loss in the ganglion cell layer may even be progressive [10] lending support to this hypothesis.

The aim of this study was to longitudinally describe parafoveal changes and their diagnostic potential in AQP4-Ab seropositive NMOSD.

## METHODS

### Study population

In this retrospective study of patients and controls followed in two longitudinal observational studies in Oxford and Berlin, NMOSD AQP4-Ab seropositive patients with no other ophthalmological or neurological disease and a minimum of 1 year clinical and OCT follow-up were included. Inclusion criteria were (1) a clinic diagnosis of AQP4-Ab seropositive NMOSD according to the 2015 diagnostic criteria [19]; (2) follow-up examinations with minimum longitudinal clinical and OCT imaging data of 1 year; (3) minimum age of 18 at baseline; (4) minimum of 1 year from ON to baseline; (5) macular OCT scan characteristics, 61 B-scans with 768 A-scans. Exclusion

criteria were ophthalmological or neurological comorbidities potentially influencing OCT results, insufficient OCT image quality, acute ON attacks in the last 12 months or ON attacks during follow-up. Data from healthy age and sex matched controls were selected from both centres' image databases; longitudinal OCT data for healthy controls (HCs) was only available from the Berlin site. A flow diagram of the study cohort is presented in Figure 1.

### Optical coherence tomography

All participants were scanned on Spectralis spectral domain devices (Heidelberg Engineering, Heidelberg, Germany) with automatic real-time (ART) function for image averaging. The peripapillary retinal nerve fibre layer (pRNFL) was measured with an activated eye tracker using 3.4-mm ring scans around the optic nerve (Berlin and Oxford: 12°, 1536 A-scans, 1 ≤ ART ≤ 99). Combined ganglion cell layer and inner plexiform layer volume (GCIP), total macular volume (TMV), inner nuclear layer (INL) and retinal nerve fibre layer at the macula were calculated as a 3-mm diameter cylinder around the fovea for a macular volume scan (Berlin, 25° × 30°, 61 vertical B-scans, 11 ≤ ART ≤ 18; Oxford, 30° × 25°, 61 vertical B-scans, 17 ≤ ART ≤ 22). Foveal thickness (FT) was measured as the mean thickness of a 1-mm diameter cylinder around the fovea for the macular scan between the internal limiting membrane and the Bruch's membrane. Intraretinal semi-automatic segmentation was performed by the same experienced rater (FCO) for all data with HEYEX software (version 1.10.4.0 with viewing module 1.0.16.0., Heidelberg Engineering) to correct segmentation errors and discard scans of insufficient quality. OCT data presented in this study follow OSCAR-IB quality criteria [20] and APOSTEL recommendations [21]

### Fovea morphometry

To characterize the foveal shape, a 3D modelling algorithm was applied to macular OCT scans, applying parametric modelling of the

fovea using cubic Bèzier equations for foveal morphometry [17]. The method extracts foveal measurements such as depth, diameter, slope, pit and areas and volumes of different regions (Figure 2a). A detailed parameter overview is provided in Appendix A.

### Statistical methods

Group differences between AQP4-Ab seropositive NMOSD patients and HCs were tested by Fisher's exact tests for sex and by the Mann-Whitney *U* test for age. Multivariate analysis was used to analyse baseline and longitudinal differences for OCT and foveal shape parameters. Linear mixed effects (LME) models were applied to account for inter-eye correlations of monocular measurements. The initial model used for all the parameters was 'OCT ~ Age at baseline + Sex + Site + Group, random = ~1|Eye' for baseline and a nested LME model described as 'OCT ~ Age at baseline + Sex + Site + Group × time since baseline, random = ~1|Patient/Eye' for the longitudinal analysis. From the initial models, simpler models were built by discarding not significant fixed effects, to avoid overfitting the model.

Group comparisons were established both at baseline and longitudinally by obtaining estimated marginal means for the mixed effects model and contrasts of estimated marginal means were computed of all pairwise comparisons of least squares means.

After this, orthogonal partial least squares discriminant analysis (OPLS-DA) was applied to identify the best combination of foveal and macular measure to discriminate the NMOSD AQP4-Ab seropositive patients from HCs. OPLS-DA is a supervised multivariate analysis approach used to investigate the variables that are responsible for class discrimination between disease groups [22]. Nineteen foveal and six macular parameters from each patient were included in the model. In brief, after correction for unequal class sizes, 10-fold external cross-validation was performed; this entails splitting the foveal and macular data into a training set (using 90% of data) and a test set (using 10% of data) a total of 10 times to ensure that each sample appears in the test set exactly once. The test set is applied

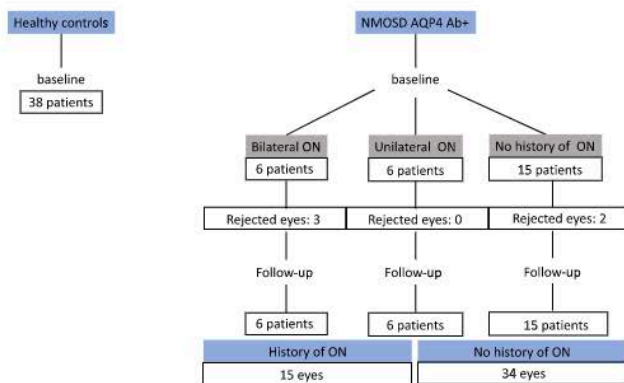


**FIGURE 1** Study cohort and follow-up flowchart. Flowchart of participants in the cohort study. NMOSD, neuromyelitis optica spectrum disorders; AQP4-ab+, aquaporin-4 antibody positive; ON, optic neuritis eyes [Colour figure can be viewed at [wileyonlinelibrary.com](http://wileyonlinelibrary.com)]

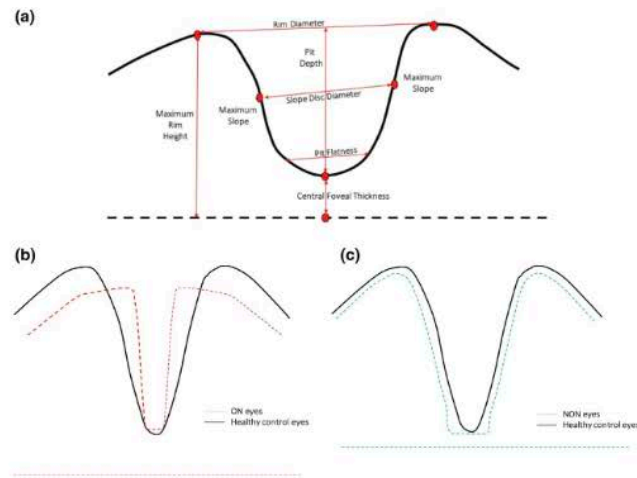


**FIGURE 2** Foveal changes in NMOSD. (a) Cross-sectional, 2D illustration on a central B-scan of foveal region parameters extracted with the CuBe algorithm [17]. (b) Eyes with a history of ON (ON eyes) and (c) eyes without a history of ON (NON eyes). Both horizontal dashed lines in (b) and (c) refer to the central foveal thickness distance, defined as the minimum height of the fovea at the centre of the pit. ON, optic neuritis; NON, non-optic neuritis [Colour figure can be viewed at [wileyonlinelibrary.com](http://wileyonlinelibrary.com)]

to the OPLS-DA model (generated using only the training set) to determine the predictive accuracy on independent (previously unseen) data. This process was repeated 100 times to produce 1000 models in total. If these models perform better than models produced by random class assignments (50%) then separation of the two groups has not occurred by chance and the model is statistically significant [23,24]. To identify the most important foveal/macular parameters responsible for the separation between patient groups, variable importance in projection (VIP) scores were generated. A VIP score is a measure of a parameter's importance to the OPLS-DA model: the higher the VIP score, the more importantly the parameter contributes towards the separation of patient groups. OPLS-DA was performed using in-house scripts and the *ropls* package in R software [23,25].

Statistical significance was established at  $p < 0.05$ . All tests and graphical representations were performed in R 3.6.2 with packages *nlme*, *ropls*, *ggplot2* and *emmeans*.

## RESULTS

### Cohort overview

Thirty-eight HCs and 27 AQP4-Ab seropositive NMOSD patients were included in the analysis (Table 1). Of the AQP4-Ab seropositive NMOSD group, 34 eyes never had a history of ON (NON), and 15 had a history of ON. Four eyes were excluded from the analysis due to poor image quality or technical issues, one eye due to amblyopia.

There were no significant differences between the HCs and the NMOSD group in the baseline demographic.

Group differences at baseline analysed using multivariate LME models with estimated marginal means adjusted for age at baseline, sex and site whilst accounting for inter-eye correlations are presented in detail in Table 2. As expected, the models showed significant thinning in pRNFL, GCIP, TMV and retinal nerve fibre layer at the macula in ON eyes compared to HC eyes, suggesting profound neuroaxonal damage. NON vs. HC eyes showed significantly thinner GCIP, TMV, INL and FT, but changes were less severe than in the ON eyes (Table 2).

### Foveal changes

Fovea morphometry quantifies several metrics of the fovea (Figure 2a). Visually, ON-related changes in the fovea/parafoveal area appear as flattened, whereas NON changes appear to be widened, already suggesting different mechanisms causing the change (Figure 2b,c). Lower values for ON vs. HC eyes were found in the following parameters: average pit depth, average rim height, average rim diameter, rim disc area, major and minor rim disc length, pit volume and average maximum pit slope degree. ON vs. NON eyes showed significantly lower values for average pit depth, average rim height, average rim diameter, minor slope disc length, slope disc area, rim disc area, major and minor rim disc length, pit volume and average maximum pit slope degree. NON vs. HC eyes showed significantly lower values for average rim height and higher values for minor slope disc length, slope disc area, average slope disc diameter,

pit disc area, average pit flat disc diameter, and major and minor pit flat disc length (Table 2 and Appendix A, Figure A2).

### Discriminatory analysis

Orthogonal partial least squares discriminant analysis identifies a linear combination of measures to separate two groups, with the aim of being able to classify individual patients. This method reduces the weight of tightly correlated values that do not give additional benefit. OPLS-DA was employed as a supervised statistical method to discriminate ON from HCs, ON vs. NON and NON eyes from HCs. The mean predictive accuracy of the OPLS-DA models distinguishing ON vs. HC eyes was  $81.16\% \pm 5.39\%$  ( $p < 0.0001$ ), whilst the mean predictive accuracies of the OPLS-DA models separating ON vs. NON eyes and ON eyes vs. HCs were  $76.48\% \pm 5.33\%$  ( $p < 0.0001$ ) and  $67.71\% \pm 4.77\%$  ( $p < 0.0001$ ) respectively (Figure 3).

Importantly, the top nine most discriminatory variables contributing to the separation of ON eyes from HC and NON eyes are pRNFL, GCIP, rim volume, major and minor rim disc length, average rim diameter, rim disc area, average pit depth and average rim height. In the case of the separation between NON eyes and HCs, the top nine most discriminatory variables were TMV, average rim height, GCIP, average pit flat disc diameter, major and minor pit flat disc length, pit disc area, INL and FT (Figure 3). The selection of largely different morphometrical factors in ON and NON eyes clearly suggest that, whilst NON eyes show some evidence of neuroaxonal damage, this damage cannot explain the foveal shape changes. The variables that better describe the difference between HC and NON eyes are not at the retinal or peripapillary level but at foveal level, indicating an unlikely effect of a subclinical ON and/or a chiasmal crossover effect from a contralateral ON, but being more in line with a primary astrocytopathy effect.

	HCs	NMOSD	
		ON	NON
Number of participants	38	12 <sup>a</sup>	21 <sup>a</sup>
Number of eyes	76	15 <sup>b</sup>	34 <sup>b</sup>
Sex			
Female n (%)	27 (74%)	10 (83%)	20 (95%)
Age at baseline (years)			
Median (1st–3rd quartile)	42.60 (30.65–51.77)	38.75 (25.65–49.17)	46.00 (38.60–52.40)
F/U time (years)			
Median (1st–3rd quartile)	1.95 (1.83–2.54)	2.765 (1.022–3.280)	2.44 (1.76–3.28)
Race			
African/Caribbean n (%)	Not available	2 (17%)	3 (14%)
Asian n (%)		1 (8%)	2 (10%)
Caucasian n (%)		8 (67%)	16 (76%)
Mix n (%)		1 (8%)	
Disease duration (years)			
Median (1st–3rd quartile)	Not applicable	1.16 (0.39–3.70)	1.90 (0.54–5.80) <sup>c</sup>
Time from last ON (years)			
Median (1st–3rd quartile)		4.21 (1.94–9.27)	3.66 (2.15–8.35) <sup>c</sup>

TABLE 1 Cohort overview

Note: Age and sex group differences between HCs and NMOSD patients were not significant (Fisher's exact tests for sex, estimate 4.37,  $p = 0.1020$ ; Mann-Whitney test for age, estimate 3.19,  $p = 0.3796$ ; follow-up time, estimate  $-0.33$ ,  $p = 0.17$ ).

Abbreviations: F/U, follow-up; HCs, healthy controls; NMOSD, neuromyelitis optica spectrum disorder; NON, non-optic neuritis; ON, optic neuritis.

<sup>a</sup>Six patients with bilateral ON, six patients with unilateral ON and 15 patients with no history of ON. ON = 6 + 6 and NON = 6 + 15.

<sup>b</sup>Eyes counted after the exclusion of five eyes.

<sup>c</sup>Based on unilateral ON eyes.

TABLE 2 Baseline OCT measurements

	NMOSD		LME					
	HCs	NON	ON vs. HCs		NON vs. HCs			
	Mean (SD)	Mean (SD)	B (SE)	p value	B (SE)	p value		
pRNFL (µm)	99.10 ± 10.35	61.86 ± 21.72	98.17 ± 10.86	<0.0001	-37.23 (3.48)	-0.929 (2.54)	-36.310 (3.82)	<0.0001
GCIPL (mm <sup>3</sup> )	0.62 ± 0.04	0.40 ± 0.11	0.57 ± 0.05	<0.0001	-0.2099 (0.0170)	-0.0539 (0.0124)	-0.1561 (0.0189)	<0.0001
TMV (mm <sup>3</sup> )	2.36 ± 0.09	2.1 ± 0.13	2.28 ± 0.07	<0.0001	-0.1901 (0.0262)	-0.0863 (0.0192)	-0.1038 (0.0291)	0.0016
INL (mm <sup>3</sup> )	0.27 ± 0.02	0.28 ± 0.02	0.25 ± 0.02	0.4456	0.009 (0.006)	-0.01 (0.004)	0.02 (0.007)	0.0028
FT (µm)	275.10 ± 19.58	268.13 ± 19.39	264 ± 18.61	0.9121	-5.56 (5.39)	-12.46 (3.96)	6.90 (6)	0.7570
mRNFL (mm <sup>3</sup> )	0.14 ± 0.01	0.12 ± 0.03	0.14 ± 0.01	0.0001	-0.01874 (0.00440)	-0.00267 (0.00323)	-0.01606 (0.00490)	0.0041
Average pit depth (mm)	0.11 ± 0.02	0.08 ± 0.01	0.11 ± 0.02	<0.0001	-0.0371 (0.00622)	-0.0062 (0.0045)	-0.0309 (0.00682)	<0.0001
Central foveal thickness (mm)	0.23 ± 0.01	0.23 ± 0.01	0.22 ± 0.01	1	0.001(0.005)	-0.004(0.003)	0.007(0.005)	0.656
Average rim height (mm)	0.34 ± 0.01	0.31 ± 0.02	0.33 ± 0.01	<0.0001	-0.0344 (0.0398)	-0.0133 (0.00292)	-0.0211 (0.00443)	<0.0001
Average rim diameter (mm)	2.19 ± 0.12	2.02 ± 0.05	2.17 ± 0.13	<0.0001	-0.1649 (0.0344)	-0.0232 (0.0244)	-0.1417 (0.0376)	0.0008
Rim disc area (mm <sup>2</sup> )	3.75 ± 0.40	3.20 ± 0.17	3.67 ± 0.44	<0.0001	-0.5507 (0.1162)	-0.0765 (0.0824)	-0.4742 (0.1268)	0.0009
Major rim disc length (mm)	0.63 ± 0.069	0.54 ± 0.03	0.62 ± 0.07	<0.0001	-0.0953 (0.0198)	-0.0136 (0.0140)	-0.0817 (0.0216)	0.0007
Minor rim disc length (mm)	0.62 ± 0.068	0.53 ± 0.02	0.61 ± 0.07	<0.0001	-0.0896 (0.0194)	-0.0121 (0.0137)	-0.0775 (0.021)	0.0011
Major slope disc length (mm)	0.07 ± 0.02	0.06 ± 0.021	0.08 ± 0.03	1.000	-0.007(0.008)	0.013(0.006)	-0.021(0.009)	0.075
Minor slope disc length (mm)	0.05 ± 0.02	0.05 ± 0.02	0.07 ± 0.02	1	-0.00496 (0.00668)	0.01625 (0.00490)	-0.2121 (0.00743)	0.0152
Slope disc area (mm <sup>2</sup> )	0.40 ± 0.15	0.366 ± 0.12	0.48 ± 0.18	1	-0.0338 (0.448)	0.0854 (0.0327)	-0.1192 (0.0491)	0.0502
Average slope disc diameter (mm)	0.69 ± 0.14	0.66 ± 0.12	0.76 ± 0.15	1	-0.274 (0.0407)	0.0719 (0.0297)	-0.0993 (0.0447)	0.0842
Pit disc area (mm <sup>2</sup> )	0.03 ± 0.01	0.044 ± 0.015	0.04 ± 0.01	0.261	0.00639 (0.00371)	0.00936 (0.00271)	-0.00296 (0.00407)	1
Average pit flat disc diameter (mm)	0.21 ± 0.03	0.23 ± 0.04	0.24 ± 0.03	0.3006	0.01721 (0.01039)	0.02597 (0.00759)	-0.00876 (0.01140)	1
Major pit flat disc length (mm)	0.006 ± 0.002	0.008 ± 0.002	0.008 ± 0.002	0.2216	0.00121 (0.000669)	0.00158 (0.000488)	-0.00037 (0.000734)	1
Minor pit flat disc length (mm)	0.005 ± 0.001	0.0068 ± 0.002	0.007 ± 0.002	0.3378	0.000937 (0.000586)	0.001540 (0.000428)	-0.000603 (0.000643)	0.3378

(Continues)



TABLE 2 (Continued)

	NMOSD		LME						
	HCs	ON	NON	ON vs. HCs		NON vs. HCs		ON vs. NON	
	Mean (SD)	Mean (SD)	Mean (SD)	B (SE)	p value	B (SE)	p value	B (SE)	p value
Rim volume (mm <sup>3</sup> )	1.04 ± 0.15	0.79 ± 0.10	0.97 ± 0.15	-0.25 (0.043)	<0.0001	-0.07(0.031)	0.0662	-0.183(0.043)	0.0006
Pit volume (mm <sup>3</sup> )	0.26 ± 0.04	0.21 ± 0.032	0.26 ± 0.04	-0.05250 (0.01307)	0.0003	0.00148 (0.00955)	1	0.05398 (0.01434)	0.0008
Inner rim volume (mm <sup>3</sup> )	0.10 ± 0.01	0.09 ± 0.01	0.09 ± 0.01	0.00409 (0.00539)	1	-0.00967 (0.00394)	<b>0.0464</b>	0.00559 (0.00592)	1
Average maximum pit slope degree (°)	11.67 ± 3.38	7.87 ± 2.57	11.02 ± 2.88	-3.798 (0.896)	<b>0.0001</b>	-0.652 (0.654)	0.9639	-3.146 (0.983)	<b>0.0053</b>

Notes: Baseline OCT and foveal results and baseline comparisons for patients with NMOSD (ON and NON) and HCs. Maximum likelihood was used for the estimation of p values. Abbreviations: B, estimate; FT, foveal thickness; GCIP, combined ganglion cell and inner plexiform layer volume; HCs, healthy controls; INL, inner nuclear layer; LME, linear mixed effects; mRNFL, retinal nerve fibre layer at the macula; NMOSD, neuromyelitis optica spectrum disorder; NON, eyes without a history of optic neuritis; OCT, optical coherence tomography; ON, eyes with a history of optic neuritis; pRNFL, peripapillary retinal nerve fibre layer at the disc; SE, standard error; TMV, total macular volume. Bold values indicate significant result ( $p \leq 0.05$ ).

## Longitudinal changes

After OPLS-DA indicated that foveal shape changes in NON eyes are unlikely to be attributable to neuroaxonal damage to the optic nerve, potential longitudinal changes were then investigated. The analysis was limited on NON eyes to not overlay ON-unrelated changes with potential changes from ON. Annualized changes from baseline to last follow-up for the NON eyes are summarized in Table 3. In summary, longitudinal analysis using LME models identified no significant changes in any of the foveal parameters at follow-up compared to baseline (Table 3). Standard ring scan and macular parameters also did not change significantly in comparison to HCs (not shown).

## DISCUSSION

Our study provides evidence that the parafoveal area, which is rich in AQP4-expressing Müller cells, is altered in AQP4-Ab seropositive NMOSD patients who never experienced clinical ON, and suggests that these changes are likely to be independent of neuroaxonal damage from subclinical ON, as macular and peripapillary layers were not affected in this subset. No evidence was found that these foveal changes are progressive in a longitudinal follow-up.

## Neuroaxonal damage and foveal/parafoveal changes from optic neuritis

Optic neuritis causes neuroaxonal damage in NMOSD, and this damage is reflected by pRNFL thickness loss reflecting axonal damage and GCIP loss reflecting neuronal ganglion cell loss [9,10,26,27] ON in NMOSD typically affects posterior segments of the optic nerve, often with involvement of the optic chiasm [28]. Consequently, in some cases, inflammatory activity due to chiasmal crossover fibres from an ON eye may have partial involvement of the contralateral side, which may be overlooked in clinical assessment [29]. Our study shows that ON also leads to foveal changes, which can best be described as flattening of the parafoveal ring: OPLS-DA selected primarily parameters of neuroaxonal damage (pRNFL, GCIP) as well as parameters describing the volume and flatness of the fovea, namely a decrease in rim volume, major rim disc length, average rim diameter, rim disc area and others.

## Are foveal changes independent of optic neuropathy?

Eyes without a history of ON also showed significant GCIP but not pRNFL loss in our study, which is in line with previous studies showing ON-independent retinal changes in NMOSD [9,11] This could be explained by the fact that GCIP measurements were performed in the parafoveal area, whilst pRNFL reflects the neuroaxonal content of the whole eye. Hence, pRNFL measures may not be as proportionally damaged as GCIP measured regionally. GCIP loss was much less

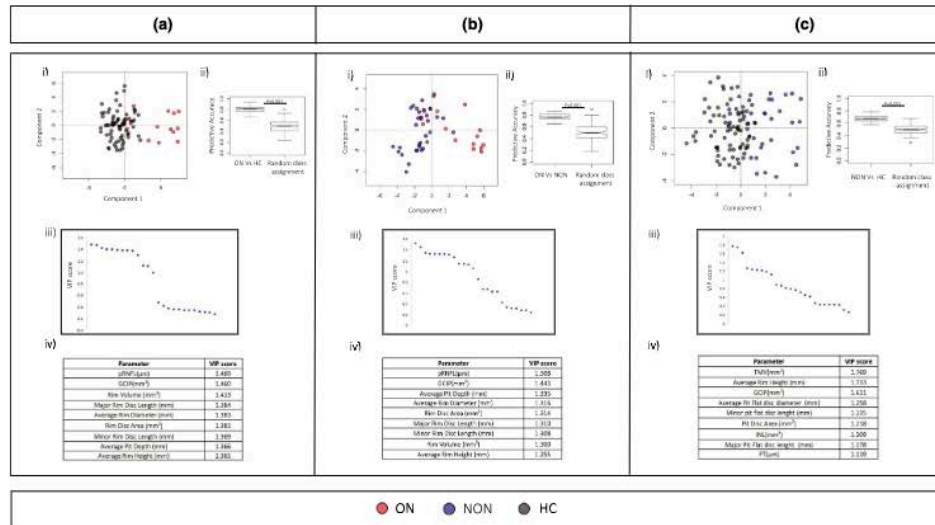


**FIGURE 3** OPLS-DA results. (ai) OPLS-DA, ON vs. HC eyes comparison (accuracy 81.16%); (aii) OPLS-DA, ON vs. HC eyes model validation; (aiii) VIP scores from all parameters used in the model for each comparison; (aiv) values of the most important parameters for ON vs. HC eyes. (bi) OPLS-DA, ON vs. NON eyes comparison (accuracy 76.48%); (bii) OPLS-DA, ON vs. NON eyes model validation; (biii) VIP scores from all parameters used in the model for each comparison; (biv) values of the most important parameters for ON vs. NON eyes. (ci) OPLS-DA, NON vs. HC eyes comparison (accuracy 67.71%); (cii) OPLS-DA, NON vs. HC eyes model validation; (ciii) VIP scores from all parameters used in the model for each comparison; (civ) values of the most important parameters for NON vs. HC eyes. OPLS-DA, orthogonal partial least squares discriminatory analysis; VIP, variable importance in projection; ON, optic neuritis; NON, non-optic neuritis; HC, healthy control; pRNFL, peripapillary retinal nerve fibre layer; GCIP, ganglion cell and inner plexiform layer volume; INL, inner nuclear layer; FT, foveal thickness [Colour figure can be viewed at [wileyonlinelibrary.com](http://wileyonlinelibrary.com)]

pronounced than in ON eyes. In a previous study potential progressive GCIP loss in NMOSD patients was reported regardless of ON [10]. Previously, FT changes on OCT in NMOSD AQP4-Ab seropositive patients were also reported [9,11]. Fovea morphometry changes were also identified not only comparing against HCs but also when compared to multiple sclerosis patients [18]. Here it is shown that, in contrast to ON eyes, the fovea of NON eyes was characterized by wider pits and more pronounced slopes, best described as foveal widening. OPLS-DA selected parameters TMV, average rim height, average pit flat disc diameter, minor pit flat disc length, pit disc area and others as best discriminatory against HCs. Importantly, OPLS-DA selected parameters differed significantly between ON and NON eyes, lending strong support to the hypothesis that the observed foveal changes in NON eyes are not caused by neuroaxonal damage to the optic nerve.

Ours and previous clinical studies did not address the underlying aetiology of foveal involvement in AQP4-Ab seropositive NMOSD. The parafoveal area is rich in Müller cells, the principal astrocytic glia of the retina, which express AQP4 in their end feet adjacent to retinal vessels [30]. In an animal model of retinal damage in NMOSD, AQP4-Ab injection into the vitreous resulted in reactive changes and loss of Müller cells without complement activation [12]. Previous studies have demonstrated lack of

complement reactivity in the area postrema [31] this could also be the case in the retina, where AQP4-Ab would still bind the retinal AQP4-expressing cells but would fail to activate the complement, and therefore would not cause mediated damage in the retinal cell integrity but still would make the changes in the foveal morphometry.

### Longitudinal observations

In a previous study progressive GCIP loss in AQP4-Ab seropositive NMOSD regardless of ON was reported [10]. In contrast, in the current study no evidence for overt progressiveness of foveal shape changes in NON eyes was found. Given the sample size limitation of this study, it is unclear whether it was simply underpowered or whether changes to the fovea are indeed not progressive. Interestingly, OPLS-DA selected GCIP but not pRNFL as one of the strongest parameters discriminating NON eyes from HCs. It is possible that GCIP changes reflect a neurodegenerative reaction of ganglion cells to Müller cell affection, it is possible that GCIP changes reflect a neurodegenerative reaction of ganglion cells to Müller cell affection. The discrepancy between pRNFL and GCIP differences in NON eyes is interesting and warrants further investigation. Future studies with greater sample size and higher power

TABLE 3 Annualized foveal changes

	NMOSD-NON	NMOSD-NON F/U vs baseline	
	Annualized change, mean (SD)	B (SE)	p value
<b>Macular parameters</b>			
pRNFL ( $\mu\text{m}$ )	-0.611 $\pm$ 1.85	-0.11563 (0.276813)	0.6767
GCIPL ( $\text{mm}^3$ )	-0.009 $\pm$ 0.0044	-0.0007202 (0.000816)	0.3788
TMV ( $\text{mm}^3$ )	-0.004 $\pm$ 0.013	-0.0028363 (0.002249)	0.2090
INL ( $\text{mm}^3$ )	0.003 $\pm$ 0.001	-0.00044411 (0.000955)	0.6427
FT ( $\mu\text{m}$ )	-0.43 $\pm$ 2.19	-0.61538 (0.429695)	0.1538
RNFL ( $\text{mm}^3$ )	-0.0003 $\pm$ 0.006	-0.00122806 (0.000881)	0.1653
<b>Foveal parameters</b>			
Average pit depth (mm)	0.00012 $\pm$ 0.002	0.0004 (0.0004)	0.3149
Central foveal thickness (mm)	-0.0005 $\pm$ 0.0001	-0.0004 (0.0004)	0.3891
Average rim height (mm)	-0.00038 $\pm$ 0.0023	-0.0000040 (0.00039)	0.9918
Average rim diameter (mm)	-0.00088 $\pm$ 0.01	-0.00059 (0.002)	0.8039
Rim disc area ( $\text{mm}^2$ )	-0.0029 $\pm$ 0.04	-0.001 (0.007)	0.8040
Major rim disc length (mm)	2.38 E-05 $\pm$ 0.009	0.0000439 (0.0013)	0.9746
Minor rim disc length (mm)	-0.0009 $\pm$ 0.007	-0.00067 (0.0016)	0.6194
Major slope disc length (mm)	-0.001 $\pm$ 0.005	-0.001 (0.0008)	0.157
Minor slope disc length (mm)	-0.001 $\pm$ 0.004	-0.00017 (0.0006)	0.803
Slope disc area ( $\text{mm}^2$ )	-0.01 $\pm$ 0.026	-0.004 (0.004)	0.35
Average slope disc diameter (mm)	-0.006 $\pm$ 0.02	-0.002 (0.003)	0.49
Pit disc area ( $\text{mm}^2$ )	-0.0002 $\pm$ 0.002	-0.0002 (0.0006)	0.6445
Average pit flat disc diameter (mm)	-0.0008537 $\pm$ 0.006	-0.001 (0.00146)	0.4528
Major pit flat disc length (mm)	-7.97E-05 $\pm$ 0.0004	-0.00008 (0.00011)	0.4782
Minor pit flat disc length (mm)	1.25 E-05 $\pm$ 0.0005	-0.000016 (0.00008)	0.8469
Rim volume ( $\text{mm}^3$ )	0.000333 $\pm$ 0.017	0.00010 (0.0030)	0.9721
Pit volume ( $\text{mm}^3$ )	-0.0020 $\pm$ 0.008	-0.0003 (0.001)	0.77
Inner rim volume ( $\text{mm}^3$ )	0.00022 $\pm$ 0.002	-0.00002 (0.0004)	0.96
Average maximum pit slope degree ( $^\circ$ )	0.0034 $\pm$ 0.41	-0.041 (0.079)	0.599

Note: Significant p values are shown in bold. Maximum likelihood was used for the estimation of p values.

Abbreviations: B, estimate; FT, foveal thickness; F/U, follow-up; GCIPL, combined ganglion cell and inner plexiform layer volume; INL, inner nuclear layer; NMOSD-NON, neuromyelitis optica spectrum disease eyes with no history of optic neuritis; pRNFL, peripapillary retinal nerve fibre layer; SE, standard error; TMV, total macular volume.

are required to address this. The annual changes reported in this study, albeit not significant, may serve as a basis for sample size calculations.

clinical relevance and to identify potential avenues for symptomatic treatment.

## Functional relevance

The fovea is the most important region for functional vision in the retina [32]. Due to the high concentration of cones, the fovea is responsible for central vision and involved in high-resolution image formation [33]. ON in NMOSD is associated with often severe visual function loss [6]. A recent study found that patients with AQP4-Ab seropositive NMOSD had worse visual outcomes compared to multiple sclerosis patients and patients with myelin oligodendrocyte glycoprotein antibody seropositive disease in relation to their actual ganglion cell loss [34]. Further studies are warranted to confirm the

## Relevance for other central nervous system areas

Whilst our findings are limited to the retina, the observation that there may be subtle AQP4-related damage in NMOSD is also relevant for other central nervous system areas. Secondary symptoms in NMOSD like cognitive dysfunction [35] fatigue [36] pain [37] and mood disorders [38] are yet mostly unexplained. Imaging studies have so far been inconclusive regarding focal damage to brain structures in NMOSD. Imaging studies have so far been inconclusive regarding focal damage to brain structures in NMOSD happening outside of attack-related areas or potentially caused by a secondary axonal or transsynaptic

neurodegeneration [39–41]. A recent independent study has identified the nucleus accumbens as a potentially interesting target with functional relevance of AQP4-expressing cells for neural plasticity [42].

### Limitations and strengths

An important limitation of our study is the small number of NON eyes, which prevents us from separately analysing patients with contralateral ON and those never having ON. Additionally, most patients presenting with an acute long extensive transverse myelitis and no visual symptoms will not have extensive visual and OCT testing to investigate subtle ON. A recent publication [43] investigating latency delay and amplitude reduction in visual evoked potentials in patients with no history of ON suggests that attack-unrelated subclinical disease activity may be happening in the visual system; one of the limitations of this study is the lack of visual evoked potential data that could shed light on how this process happens.

A major strength of this paper is the use of a novel parametric modelling of the 3D foveal shape using cubic Bèzier equations [17]. This has allowed us to describe the fovea and parafoveal area in an objective and reproducible way. Our cohort, constituted only of AQP4-Ab seropositive patients, sets the first step on clinical significance ensuring the examination of only one disease process. Further, our results suggest that foveal morphometry may offer clinical diagnostic utility. However, broad application would require further validation across alternative platforms and protocols.

### CONCLUSION

In summary, evidence is provided that the fovea is wider in NON eyes in patients with NMOSD, whereas ON eyes typically present with a flatter fovea compared to HCs and NON eyes. Discriminatory analysis strongly suggests that changes in NON eyes are not caused by subclinical optic neuropathy or ON. Our study supports a model in which AQP4-Abs affect antigen-expressing glial cells in NMOSD, in this case Müller cells, without complement involvement. This has relevance for the pathological understanding of NMOSD as well as potential clinical implications.

### ACKNOWLEDGEMENTS

To Dr Sunil Yadav for foveal morphometry model definitions. Open Access funding enabled and organized by Projekt DEAL. WOA Institution: Charite Universitätsmedizin Berlin Blended DEAL: Projekt DEAL

### CONFLICT OF INTEREST

A Roca-Fernandez has no competing interests. FC Oertel was employed by Nocturne, unrelated to this project. T Yeo has received travel grants from UCB, Merck and PACTRIMS, and travel awards from ACTRIMS and Orebro University. S Motamedi is named as co-inventor on the patent application for the fovea

morphometry method used in this paper ('Method for estimating shape parameters of the fovea by optical coherence tomography', International Publication Number WO 2019/016319 A1), related to this work. F Probert has no competing interests. MJ Craner has received honoraria for educational events and/or consultancy from Biogen, Merck, Roche, AbbVie and Novartis. J Sastre-Garriga declares grants and personal fees from Genzyme, personal fees from Almirall, Biogen, Celgene, Merck, Bayer, Biopass, Bial, Novartis, Roche and Teva, outside the submitted work; he is Associate Editor of *Multiple Sclerosis Journal* and Scientific Director of *Revista de Neurologia*, outside the submitted work. HG Zimmermann received research grants from Novartis and speaking honoraria from Bayer Healthcare. S Asseger received travel grants from Celgene GmbH, unrelated to this project. J Kuchling received congress registration fees from Biogen, speaker honoraria from Sanofi Genzyme and Bayer Schering, and research support from Krankheitsbezogenes Kompetenznetz, Multiple Sklerose (KKNMS), not related to this work. JK is a participant in the BIH-Charité Junior Clinician Scientist Program funded by the Charité – Universitätsmedizin Berlin and Berlin Institute of Health. J Bellmann-Strobl has received travel grants and speaking honoraria from Bayer Healthcare, Biogen Idec, Merck Serono, Sanofi Genzyme, Teva Pharmaceuticals, Roche and Novartis, none of them related to preparing this paper. K Ruprecht was supported by the German Ministry of Education and Research (BMBF/KKNMS, Competence Network Multiple Sclerosis) and has received research support from Novartis and Merck Serono as well as speaking fees and travel grants from Guthy Jackson Charitable Foundation, Bayer Healthcare, Biogen Idec, Merck Serono, sanofi-aventis/Genzyme, Teva Pharmaceuticals, Roche and Novartis. MI Leite reports funding from NHS National Specialised Commissioning Group for Neuromyelitis Optica, UK, and the NIHR Oxford Biomedical Research Centre, UK; and speaker honoraria or travel grants from Biogen Idec, Novartis and the Guthy-Jackson Charitable Foundation. F Paul is named as co-inventor on the patent application for the fovea morphometry method used in this paper ('Method for estimating shape parameters of the fovea by optical coherence tomography', International Publication Number WO 2019/016319 A1), related to this work; Dr Paul is cofounder and holds shares in technology start-up Nocturne GmbH, which has commercial interest in OCT applications in neurology and declares that he has received research grants and speaker's honoraria from Bayer Healthcare, Teva Pharmaceuticals, Genzyme, Merck and Co., Novartis and MedImmune. He is also a member of the steering committee for the OCTIMS study (run by Novartis). AU Brandt is named as co-inventor on the patent application for the fovea morphometry method used in this paper ('Method for estimating shape parameters of the fovea by optical coherence tomography', International Publication Number WO 2019/016319 A1), related to this work. Dr Brandt is cofounder and shareholder of technology start-ups Motognosis and Nocturne. He is named as inventor on several patent applications describing multiple sclerosis serum biomarkers, perceptive visual computing for motor function assessment and retinal image analysis. J Palace reported receiving grants from the National Health Service to

conduct a national congenital myasthenia service and neuromyelitis service, the Multiple Sclerosis Society, Guthrie Jackson Foundation, Chugai, and MedImmune; personal fees from Teva, Novartis, Roche, MedDay and ARGENX; and grants and personal fees from Merck Serono, Biogen, Alexion, and ABIDE, Genzyme and MedImmune. No other disclosures were reported.

#### AUTHOR CONTRIBUTIONS

Adriana Roca-Fernandez: Conceptualization (equal); data curation (lead); formal analysis (lead); funding acquisition (equal); investigation (lead); methodology (lead); visualization (equal); writing original draft (lead). Frederike Cosima Oertel: Conceptualization (equal); data curation (equal); investigation (equal); methodology (equal); supervision (equal); writing original draft (equal); writing review and editing (equal). Tianrong Yeo: Formal analysis (equal); supervision (supporting); writing review and editing (equal). Seyedamirhosein Motamedi: Data curation (supporting); formal analysis (equal); investigation (equal); methodology (equal); software (equal); visualization (equal); writing review and editing (equal). Fay Probert: Methodology (equal); software (equal); visualization (equal); writing review and editing (equal). Matthew Craner: Conceptualization (equal); investigation (equal); methodology (equal); resources (equal); supervision (equal); writing review and editing (equal). Jaume Sastre-Garriga: Investigation (equal); resources (equal); writing review and editing (equal). Hanna Zimmermann: Conceptualization (equal); data curation (equal); investigation (equal); methodology (equal); software (equal); supervision (equal); writing review and editing (equal). Susanna Asseyer: Data curation (equal); validation (equal); writing review and editing (equal). Joseph Kuchling: Data curation (equal); investigation (equal); supervision (equal); writing review and editing (equal). Judith Bellmann-Strobl: Data curation (equal); writing review and editing (equal). Klemens Ruprecht: Data curation (equal); investigation (equal); writing review and editing (equal). Maria Isabel Leite: Funding acquisition (equal); investigation (equal); supervision (equal); writing review and editing (equal). Friedemann Paul: Conceptualization (equal); funding acquisition (equal); investigation (equal); methodology (equal); project administration (equal); resources (equal); supervision (equal); writing review and editing (equal). Alexander U Brandt: Conceptualization (equal); data curation (equal); funding acquisition (equal); investigation (equal); methodology (equal); project administration (equal); resources (equal); supervision (equal); validation (equal); writing review and editing (equal). Jacqueline Palace: Conceptualization (equal); data curation (equal); funding acquisition (equal); investigation (equal); methodology (equal); project administration (equal); resources (equal); supervision (equal); validation (equal); writing review and editing (equal).

#### ETHICAL APPROVAL

Patients were recruited and consented from ongoing cohort studies of patients with AQP4-Ab seropositive NMOSD at Oxford University Hospital (REC 16/SC/0224) and Charité – Universitätsmedizin Berlin (EA1/131/09). Healthy controls from the University of Oxford were

recruited under ethics 17/EE/0246 and EA1/182/10 at Charité – Universitätsmedizin Berlin. The study was conducted in accordance with the current version of the Declaration of Helsinki and the applicable British and German laws. All participants gave written informed consent.

#### CONSENT FOR PUBLICATION

Consent for publication was included in consent forms submitted to ethics.

#### DATA AVAILABILITY STATEMENT

The datasets during and/or analysed during the current study are available from the corresponding author on reasonable request.

#### ORCID

Adriana Roca-Fernández  <https://orcid.org/0000-0002-8720-9397>

Jaume Sastre-Garriga  <https://orcid.org/0000-0002-1589-2254>

Susanna Asseyer  <https://orcid.org/0000-0001-6289-1791>

#### REFERENCES

- Pittock SJ, Lucchinetti CF. Neuromyelitis optica and the evolving spectrum of autoimmune aquaporin-4 channelopathies: a decade later. *Ann N Y Acad Sci.* 2016;1366(1):20-39.
- Lennon VA, Wingerchuk DM, Kryzer TJ, et al. A serum autoantibody marker of neuromyelitis optica: distinction from multiple sclerosis. *Lancet Lond Engl.* 2004;364(9451):2106-2112.
- Zekeridou A, Lennon VA. Aquaporin-4 autoimmunity. *Neurol Neuroimmunol Neuroinflammation.* 2015;2(4):e110.
- Waters P, Jarius S, Littleton E, et al. Aquaporin-4 antibodies in neuromyelitis optica and longitudinally extensive transverse myelitis. *Arch Neurol.* 2008;65(7):913-919.
- Wingerchuk DM, Pittock SJ, Lucchinetti CF, Lennon VA, Weinschenker BG. A secondary progressive clinical course is uncommon in neuromyelitis optica. *Neurology.* 2007;68(8):603-605.
- Schmidt F, Zimmermann H, Mikolajczak J, et al. Severe structural and functional visual system damage leads to profound loss of vision-related quality of life in patients with neuromyelitis optica spectrum disorders. *Mult Scler Relat Disord.* 2017;11:45-50.
- Hokari M, Yokoseki A, Arakawa M, et al. Clinicopathological features in anterior visual pathway in neuromyelitis optica. *Ann Neurol.* 2016;79(4):605-624.
- Oertel FC, Zimmermann H, Paul F, Brandt AU. Optical coherence tomography in neuromyelitis optica spectrum disorders: potential advantages for individualized monitoring of progression and therapy. *EPMA J.* 2017;9(1):21-33.
- Oertel FC, Kuchling J, Zimmermann H, et al. Microstructural visual system changes in AQP4-antibody-seropositive NMOSD. *Neurol Neuroimmunol Neuroinflammation [Internet].* 2017;4(3):e334.
- Oertel FC, Havla J, Roca-Fernández A, et al. Retinal ganglion cell loss in neuromyelitis optica: a longitudinal study. *J Neurol Neurosurg Psychiatry.* 2018;89(12):1259-1265.
- Jeong IH, Kim HJ, Kim N-H, Jeong KS, Park CY. Subclinical primary retinal pathology in neuromyelitis optica spectrum disorder. *J Neurol.* 2016;263(7):1343-1348.
- Felix CM, Levin MH, Verkman AS. Complement-independent retinal pathology produced by intravitreal injection of neuromyelitis optica immunoglobulin G. *J Neuroinflammation.* 2016;13(1):275.

13. Bringmann A, Pannicke T, Grosche J, et al. Müller cells in the healthy and diseased retina. *Prog Retin Eye Res.* 2006;25(4):397-424.
14. Bringmann A, Reichenbach A, Wiedemann P. Pathomechanisms of cystoid macular edema. - PubMed - NCBI [Internet]. [cited 2019 Oct 21]. <https://www.ncbi.nlm.nih.gov/pubmed/15583429>.
15. Goodyear MJ, Crewther SG, Junghans BM. A role for aquaporin-4 in fluid regulation in the inner retina. *Vis Neurosci.* 2009;26(2):159-165.
16. Nishikawa S, Tamai M. Müller cells in the human foveal region. *Curr Eye Res.* 2001;22(1):34-41.
17. Yadav SK, Motamedi S, Oberwahrenbrock T, et al. CuBe: parametric modeling of 3D foveal shape using cubic Bézier. *Biomed Opt Express.* 2017;8(9):4181-4199.
18. Motamedi S, Oertel FC, Yadav SK, et al. Altered fovea in AQP4-IgG-seropositive neuromyelitis optica spectrum disorders. *Neurol Neuroimmunol Neuroinflammation.* 2020;7(5):e805.
19. Wingerchuk DM, Banwell B, Bennett JL, et al. International consensus diagnostic criteria for neuromyelitis optica spectrum disorders. *Neurology.* 2015;85(2):177-189.
20. Tewarie P, Balk L, Costello F, et al. The OSCAR-IB consensus criteria for retinal OCT quality assessment. *PLoS One.* 2012;7(4):e34823.
21. Cruz-Herranz A, Balk LJ, Oberwahrenbrock T, et al. The APOSTEL recommendations for reporting quantitative optical coherence tomography studies. *Neurology.* 2016;86(24):2303-2309.
22. Worley B, Powers R. PCA as a Practical Indicator of OPLS-DA Model Reliability [Internet]. 2016 [cited 2019 Oct 21]. <https://www.ingen-taconnect.com/content/ben/cmb/2016/00000004/00000002/art00004>.
23. Jurynczyk M, Probert F, Yeo T, et al. Metabolomics reveals distinct, antibody-independent, molecular signatures of MS, AQP4-antibody and MOG-antibody disease. *Acta Neuropathol Commun.* 2017;5(1):95.
24. Yeo T, Probert F, Jurynczyk M, et al. Classifying the antibody-negative NMO syndromes: clinical, imaging, and metabolomic modeling. *Neurol Neuroimmunol Neuroinflammation.* 2019;6(6):e626.
25. Thévenot EA, Roux A, Xu Y, Ezan E, Junot C. Analysis of the human adult urinary metabolome variations with age, body mass index, and gender by implementing a comprehensive workflow for univariate and OPLS statistical analyses. *J Proteome Res.* 2015;14(8):3322-3335.
26. Pisa M, Ratti F, Vabanesi M, et al. Subclinical neurodegeneration in multiple sclerosis and neuromyelitis optica spectrum disorder revealed by optical coherence tomography. *Mult Scler J.* 2019;26(10):1197-1206.
27. Pache F, Zimmermann H, Mikolajczak J, et al. MOG-IgG in NMO and related disorders: a multicenter study of 50 patients. Part 4: Afferent visual system damage after optic neuritis in MOG-IgG-seropositive versus AQP4-IgG-seropositive patients. *J Neuroinflammation.* 2016;13(1):282.
28. Ramanathan S, Prelog K, Barnes EH, et al. Radiological differentiation of optic neuritis with myelin oligodendrocyte glycoprotein antibodies, aquaporin-4 antibodies, and multiple sclerosis. *Mult Scler J.* 2016;22(4):470-482.
29. Petzold A, Wattjes MP, Costello F, et al. The investigation of acute optic neuritis: a review and proposed protocol. *Nat Rev Neurol.* 2014;10(8):447-458.
30. Gleiser C, Wagner A, Fallier-Becker P, Wolburg H, Hirt B, Mack AF. Aquaporin-4 in astroglial cells in the CNS and supporting cells of sensory organs—a comparative perspective. *Int J Mol Sci [Internet].* 2016;17(9):1411. <https://www.ncbi.nlm.nih.gov/pmc/articles/PMC5037691/>.
31. Bennett JL, Owens GP. Neuromyelitis optica: deciphering a complex immune-mediated astrocytopathy. *J Neuro-Ophthalmol Off J North Am Neuro-Ophthalmol Soc.* 2017;37(3):291-299.
32. Provis JM, Penfold PL, Cornish EE, Sandercoe TM, Madigan MC. Anatomy and development of the macula: specialisation and the vulnerability to macular degeneration. *Clin Exp Optom.* 2005;88(5):269-281.
33. Artal P. Image formation in the living human eye. *Annu Rev Vis Sci.* 2015;1:1-17.
34. Sotirchos ES, Filippatou A, Fitzgerald KC, et al. Aquaporin-4 IgG seropositivity is associated with worse visual outcomes after optic neuritis than MOG-IgG seropositivity and multiple sclerosis, independent of macular ganglion cell layer thinning. *Mult Scler J [Internet].* 2020. 26(11):1360-1371. <https://journals.sagepub.com/doi/10.1177/1352458519864928>.
35. Oertel FC, Schließeit J, Brandt AU, Paul F. Cognitive impairment in neuromyelitis optica spectrum disorders: a review of clinical and neuroradiological features. *Front Neurol [Internet].* 2019. 10. <https://doi.org/10.3389/fneur.2019.00608>.
36. Penner I-K, Paul F. Fatigue as a symptom or comorbidity of neurological diseases. *Nat Rev Neurol.* 2017;13(11):662-675.
37. Asseyer S, Schmidt F, Chien C, et al. Pain in AQP4-IgG-positive and MOG-IgG-positive neuromyelitis optica spectrum disorders. *Mult Scler J Exp Transl Clin.* 2018;4(3). <https://doi.org/10.1177/2055217318796684>.
38. Chavarro VS, Mealy MA, Simpson A, et al. Insufficient treatment of severe depression in neuromyelitis optica spectrum disorder. *Neurol Neuroimmunol Neuroinflammation [Internet].* 2016;3(6):e286. <https://www.ncbi.nlm.nih.gov/pmc/articles/PMC5079380/>.
39. Liu Y, Duan Y, He Y, et al. A tract-based diffusion study of cerebral white matter in neuromyelitis optica reveals widespread pathological alterations. *Mult Scler J.* 2012;18(7):1013-1021.
40. Finke C, Zimmermann H, Pache F, et al. Association of visual impairment in neuromyelitis optica spectrum disorder with visual network reorganization. *JAMA Neurol.* 2018;75(3):296-303.
41. Papadopoulou A, Oertel FC, Gaetano L, et al. Attack-related damage of thalamic nuclei in neuromyelitis optica spectrum disorders. *J Neurol Neurosurg Psychiatry.* 2019;90(10):1156-1164.
42. Xiao M, Hu G. Involvement of aquaporin 4 in astrocyte function and neuropsychiatric disorders. *CNS Neurosci Ther.* 2014;20(5):385-390.
43. Ringelstein M, Harmel J, Zimmermann H, et al. Longitudinal optic neuritis-unrelated visual evoked potential changes in NMO spectrum disorders. *Neurology.* 2020;94(4):e407-e418.

**How to cite this article:** Roca-Fernández A, Oertel FC, Yeo T, et al. Foveal changes in aquaporin-4 antibody seropositive neuromyelitis optica spectrum disorder are independent of optic neuritis and not overtly progressive. *Eur J Neurol.* 2021;28:2280-2293. <https://doi.org/10.1111/ene.14766>

## APPENDIX A

### FOVEA MORPHOMETRY

The fovea morphometry method is described in detail by Yadav et al. [17]. Fovea morphometry characterizes the foveal and parafoveal region by 19 parameters. The method first flattens the inner limiting membrane (ILM) surface according to Bruch's membrane as the reference (reference plane) and then radially reconstructs the ILM surface, from the centre of the fovea up to the points with maximum heights which are called rim points, using cubic Bézier polynomials. Based on the reconstructed ILM surface and the reference plane, foveal morphometry parameters are defined. Twelve parameters are defined as area, average diameter, major length (the length in the dominant direction) and minor length (the length in the second dominant direction,

perpendicular to the dominant direction) of three different surfaces: pit flat disc, a surface that captures the flatness of the foveal pit; slope disc, a surface that connects points with maximum slope; and rim disc, a surface that connects rim points. In addition to the parameters describing the defined surfaces, there are several other parameters describing the fovea: average pit depth, average height of the points on the pit flat disc; central foveal thickness, minimum thickness of the

fovea; average rim height, average height of rim points; rim volume, volume between the ILM surface and the reference plane limited to rim points; inner rim volume, similar to rim volume but limited to 1-mm diameter around the centre of the fovea; pit volume, volume between the ILM surface and the rim disc; and average maximum pit slope, average slope of points with maximum slope. Figure A1 shows an overview of the fovea morphometry method.

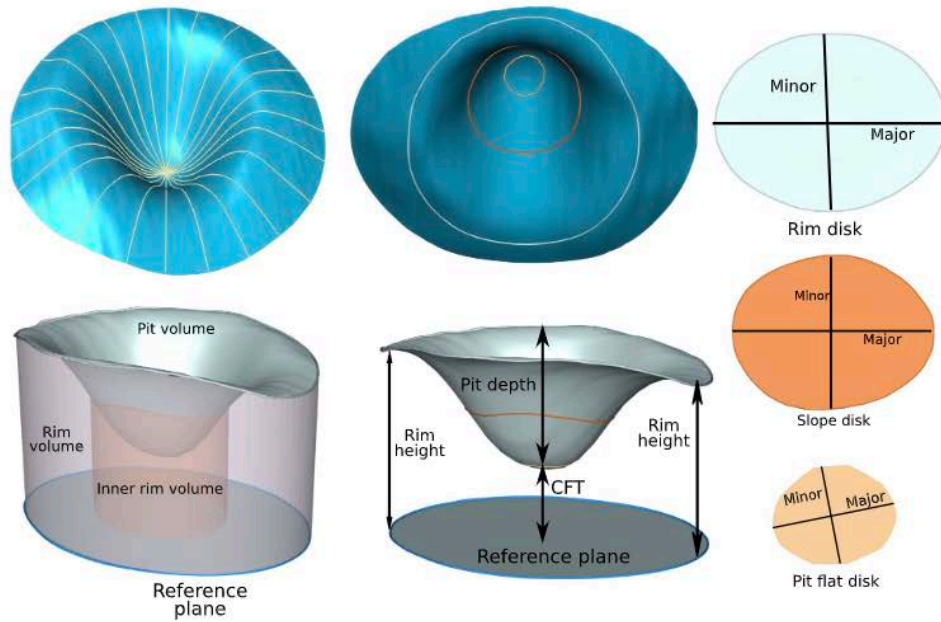
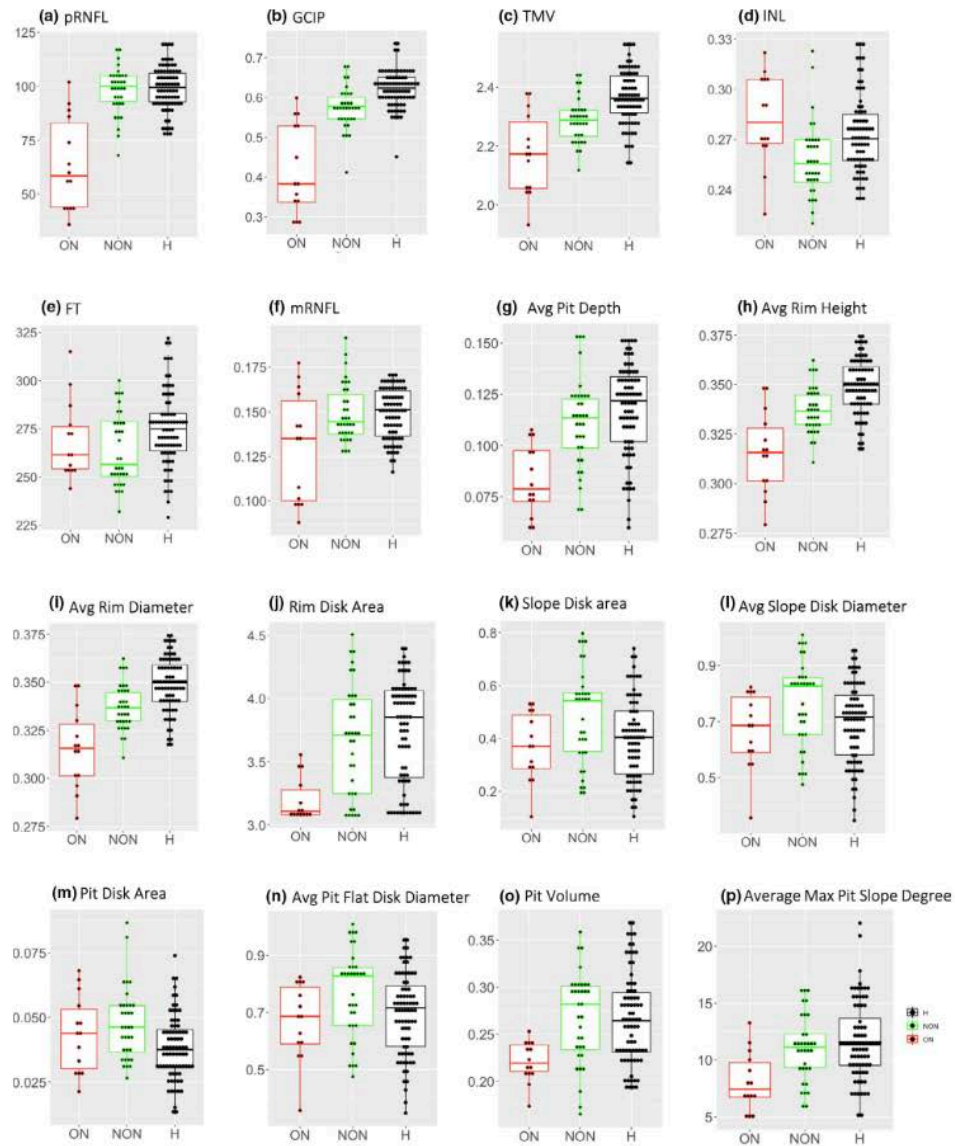


FIGURE A1 3D representation of the foveal shape. [Colour figure can be viewed at [wileyonlinelibrary.com](http://wileyonlinelibrary.com)]



**FIGURE A2** Box plots of disc and macular baseline OCT and foveal data where there are significant differences between at least one group: (a) peripapillary retinal nerve fibre layer (pRNFL) at the disc; (b) combined ganglion cell and inner plexiform layer volume (GCIP); (c) total macular volume (TMV); (d) inner nuclear layer (INL); (e) foveal thickness (FT); (f) retinal nerve fibre layer at the macula (mRNFL); (g) average pit depth; (h) average rim height; (i) average rim diameter; (j) rim disc area; (k) slope disc area; (l) average slope disc diameter; (m) pit disc area; (n) average pit flat disc diameter; (o) pit volume; (p) average maximum pit slope degree. The boxplots show the median and 25th and 75th percentiles [Colour figure can be viewed at [wileyonlinelibrary.com](http://wileyonlinelibrary.com)]



### **11.1.1.2. The use of OCT and VEPs in MOGAD and AQP4-NMOSD patients with normal visual acuity.**

Citation: **Roca-Fernández, A.**, Camera, V., Whitacker, G., Messina, S., Mariano, R., Sharma, S.M., Leite, M.I., Palace, J. (2021). *The use of OCT and VEPs in MOGAD and AQP4-NMOSD patients with normal visual acuity*. Mult Scler J Exp Transl Clin. 2021 Dec22;7(4):20552173211066446. doi: 10.1177/20552173211066446. IF: not yet available

# The use of OCT in good visual acuity MOGAD and AQP4-NMOSD patients; with and without optic neuritis

A Roca-Fernández , V Camera\*, G Loncarevic-Whitaker\*  
S Messina , R Mariano, A Vincent, S Sharma, MI Leite and J Palace

Multiple Sclerosis Journal—  
Experimental, Translational  
and Clinical

October–December 2021,  
1–6

DOI: 10.1177/  
20552173211066446

© The Author(s), 2021.  
Article reuse guidelines:  
sagepub.com/journals-  
permissions

## Abstract

Myelin oligodendrocyte-antibody-associated disease (MOGAD) often presents with severe optic neuritis (ON) but tends to recover better than in aquaporin-4 antibody neuromyelitis optica spectrum disorder (AQP4-NMOSD). We measured OCT and VEP in MOGAD and AQP4-NMOSD eyes with good visual function, with or without previous ON episodes. Surprisingly, OCT and/or VEPs were abnormal in 84% MOGAD-ON versus 38% AQP4-NMOSD-ON eyes ( $p=0.009$ ) with good vision, compared with 18% and 17% respectively of eyes with no previous ON. A sub-group with macular OCT performed as part of a research study confirmed both retinal and macular defects in visually-recovered MOGAD eyes. These findings have implications for investigation and management of MOGAD patients.

**Keywords:** Neuromyelitis Optica spectrum disorder (NMOSD), myelin oligodendrocyte glycoprotein antibody disease (MOGAD) optic coherence tomography (OCT), visual evoked potentials (VEP), Visual function, Optic Neuritis

Date received: 13 August 2021; accepted: 25 November 2021

## Introduction

Aquaporin-4 antibody neuromyelitis optica spectrum disorder (AQP4-NMOSD) and myelin-oligodendrocyte glycoprotein antibody disease (MOGAD) often present with recurrent attacks of optic neuritis (ON) but visual recovery is generally better in MOGAD-ON than in AQP4-NMOSD ON.<sup>1,2</sup> It is assumed that optic coherence tomography (OCT) and visual evoked potentials (VEPs) reflects visual recovery, however, our observations are that some MOGAD patients with good visual recovery from ON had very abnormal clinical OCT results.<sup>3</sup> This study was designed to review systematically this observation comparing MOGAD with AQP4-NMOSD patients to see if OCT (and VEPs) were more sensitive in MOGAD in those with good vision

## Methods

Patients where OCT had occurred at least 6 months post ON attack were recruited from the Oxford NMO nationally commissioned service. Only results from eyes with

good central visual acuity (VA) defined as LogMar  $\leq 0$  (best corrected score on the retro-illuminated ETDRS chart) were included, and OCT and visual evoked potentials (VEP) results were analysed.

(a) For the clinical study MOGAD or AQP4-NMOSD patients with both clinical OCTs (peripapillary retinal nerve fiber layer, pRNFL) and VEP measurements were included. OCT scans for all patients were performed on Heidelberg Spectralis OCT machines at the Eye Clinic at the John Radcliffe hospital under the same scanning protocol. The peripapillary retinal nerve fibre layer (pRNFL) was measured with an activated eye tracker using 3.4 mm ring scans around the optic nerve ( $12^\circ$ , 1536 A-scans,  $1 \leq \text{ART} \leq 99$ ). Definition of abnormality was taken from the Heidelberg Spectralis reports. VEPs were performed in different clinical laboratories, in different hospitals and on different machines; therefore, abnormality was

Correspondence to:  
Jacqueline Palace,  
Nuffield Department of  
Clinical Neurosciences, West  
Wing, John Radcliffe Hospital,  
University of Oxford, Oxford  
OX3 9DU, UK  
Jacqueline.palace@ndcn.  
ox.ac.uk

\* Authors equally contributed.

**A Roca-Fernández**,  
Nuffield Department of  
Clinical Neurosciences,  
University Of Oxford, UK  
Department of Neurology/  
Neuroimmunology, Multiple  
Sclerosis Centre of Catalonia  
(CEMCAT), Hospital  
Universitari Vall d'Hebron,  
Universitat Autònoma de  
Barcelona, Spain

**V Camera**,  
Nuffield Department of  
Clinical Neurosciences,  
University Of Oxford, UK

**G Loncarevic-Whitaker**,  
University of Oxford Clinical  
Medical School, Medical  
Science Division, University of  
Oxford, UK

S Messina,  
R Mariano,  
A Vincent,  
Nuffield Department of  
Clinical Neuroscience,  
University Of Oxford, UK

S Sharma,  
Department of  
Ophthalmology, Oxford  
University Hospitals, National  
Health Service Trust, Oxford,  
UK

MI Leite,  
J Palace,  
Nuffield Department of  
Clinical Neuroscience,  
University Of Oxford, UK

defined according to the local neurophysiology laboratory definition.

- (b) In order to validate the clinical cohort, allowing for validation and quality control, as well as the relation with macular data we carried out a macular sub-study. For this analysis we used the same Spectralis spectral-domain devices (Heidelberg Engineering, Heidelberg, Germany) with automatic real-time function for image averaging to measure disc (pRNFL) and OCT macular volumes calculated as a 3 mm diameter cylinder around the fovea. Segmentation of all layers was performed semi-automatically using Eye explorer (version 1.10.4.0. with viewing module 1.0.16.0. Heidelberg Engineering). One experienced rater adriana roca-fernandez (ARF) carefully checked all scans for sufficient quality and segmentation errors and corrected when necessary. OCT data in this study are reported according to the APOSTEL recommendations. The QC process discarded 2 AQP4-NMOSD and 2 MOGAD eyes due to bad imaging quality. The reference range for abnormality in these scans has been defined as the 5th quantile of the healthy controls (HC) cohort. To calculate differences between groups we performed linear mixed effect (LME) models, accounting for inter-eye correlations of monocular measurements, and adjusting by age and sex. Estimated regression coefficients (B), standard errors (SE) and p values are provided in the results section.

Consent obtained under ethics 16/SC/0224 and 17/EE/0246.

## Results

### Clinical cohort

From our service of 219 AQP4 patients and 224 MOGAD patients, 358 eyes were discarded due to reduced visual acuity ( $\log\text{MAR} > 0$ ): 293 due to ON (137 in MOGAD patients, 156 in AQP4-NMOSD patients) and 65 were discarded due to other comorbid eyes diseases (age related eye disorders and systemic autoimmune diseases with ophthalmological involvement – the majority in AQP4-NMOSD patients) (Figure 1). Only patients with both clinical Oxford OCT and any VEPs performed (where an ON attack occurred  $> 6$  months after onset) were included. Data was available for analysis on 53 MOGAD patients with 90 good VA eyes and 25 AQP4-NMOSD patients with 44 good VA eyes. Of these, 56/90 MOGAD eyes (62%) and 8/44 AQP4-NMOSD eyes (18%) had history of one or

more ON episodes (median number of ON, 1.5 for AQP4-NMOSD, 1 for MOGAD) (Table 1) (Figure 1).

A summary of all results of clinical OCT and VEP measurements are shown in Fig 2A (Table 1). Whereas, the majority (80%) of AQP4-NMOSD eyes with good VA had normal VEP and OCT examinations, only 41% of MOGAD eyes with normal VA had normal findings, the remainder having abnormal OCT, VEP or both ( $p \leq 0.001$ ) (Figure 2A).

This difference between the two diseases was most apparent in those with normal VA and a previous ON (Figure 2A); only 16% of MOGAD eyes compared with 63% of AQP4-NMOSD eyes had normal investigations ( $p = 0.003$ ) (Table 1). Notably, OCT abnormalities were more common than VEP abnormalities, with 79% MOGAD-ON patients having abnormal OCTs compared to 38% of AQP4-NMOSD-ON patients ( $p = 0.01$ ).

Abnormalities were also noted in some eyes without a previous history of ON but without a difference between MOGAD (18%) of which 4/6 had a contralateral ON and AQP4-NMOSD (17%) of which none had a contralateral ON ( $p = 0.91$ ) (Figure 2A).

### Macular sub-study cohort

To further investigate these unexpected observations, we performed a macular sub-study in a subgroup of the above; 19 MOGAD patients (35/38 normal VA eyes), 9 AQP4-NMOSD (15/18 normal VA eyes), and 21 healthy individuals (42/42 normal VA eyes). From those, 20 MOGAD eyes and 3 AQP4-NMOSD eyes had histories of a median of 1 or 2 ON episodes respectively. Figure 2B(1–3) shows the pRNFL, macular retinal nerve fibre layer (RNFL) and ganglionar and inner plexiform retinal layer (GCIP) values for each group. The results confirmed a significant reduction in OCT values in the MOGAD ON group compared to HC not only in the pRNFL ( $B(SE) = -33.1(3.77)$ ,  $p \leq 0.001$ ), but also in the macular GCIP ( $B(SE) = -0.18(0.02)$ ,  $p \leq 0.001$ ) and RNFL ( $B(SE) = -0.020(0.005)$ ,  $p = \leq 0.001$ ) parameters Figure 2B(1–3).

## Discussion

This observational study demonstrates the sensitivity of OCT, greater than that of VEPs, in detecting subclinical damage in MOGAD-ON patients. Our macular sub-study OCT cohort demonstrated a similar pattern in macular OCT measurements, and confirmed our clinic observations where the majority of

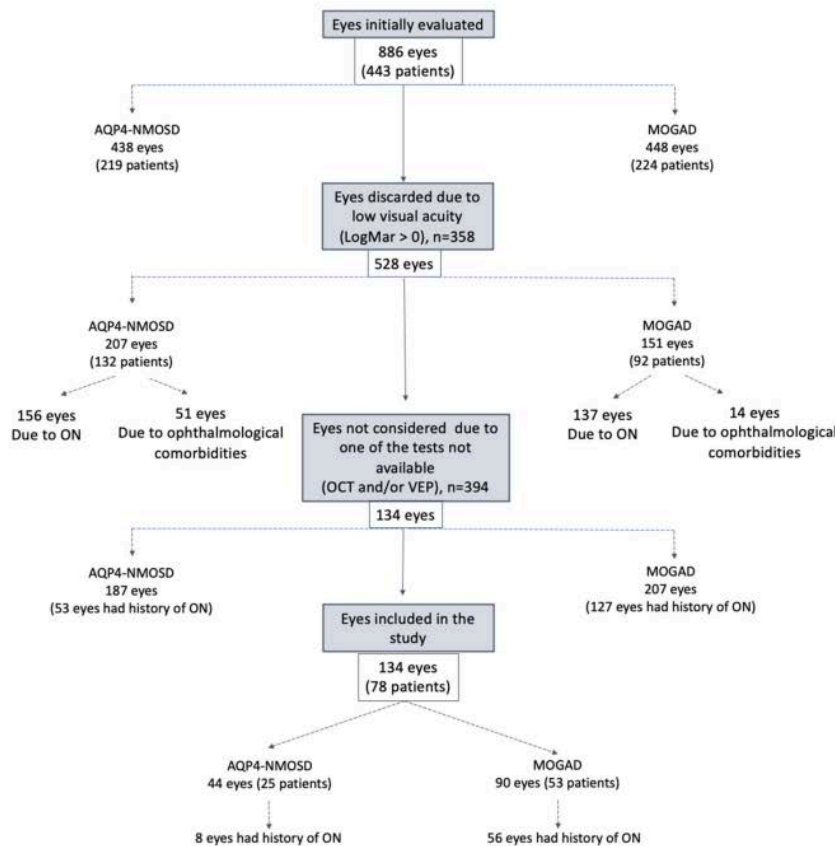


Figure 1. Flowchart of cohort selection.

MOGAD patients continue to have abnormal tests despite recovering vision after an ON attack.

Given the much lower prevalence of abnormal tests (18%) in MOGAD patients who have never had ON compared to 84% of MOGAD ON patients, it is likely that the abnormal OCT and VEP results are mainly a direct consequence of an ON attack rather than an unrelated disease process. However, abnormalities still occurred in a moderate number of non-ON eyes.

Although we previously showed that AQP4-NMOSD-ON is associated with a worse visual outcome than MOGAD ON<sup>1,4,5</sup> here we note that those patients who do recover good vision are

more likely to have normal investigations than MOGAD-ON patients. Thus, by studying only patients with good visual recovery, we selected a smaller subgroup of AQP4-NMOSD patients than MOGAD patients because of the better clinical recovery in MOGAD. We excluded those with poor vision because OCT would be expected to be abnormal and thus has less diagnostic value. Sotirchos et al.<sup>6</sup> found worse visual recovery in AQP4-NMOSD with similar severity of macular GCIP thinning. We hypothesize that astrocyte damage in AQP4-NMOSD attacks might be more of an 'all or nothing' event and those that recover may have no secondary demyelination. Moreover, knowing that OCT and VEPs are also sensitive markers in MS, we have demonstrated that OCT (as done at a clinical level) and VEPs appear better at

**Table 1.** Demographics and clinical characteristics.

	MOGAD			AQP4-NMOSD		
Number patients	53			25		
Males / Females	33/29			21/4		
Age years median (range)	35 (11–73)			57 (17–83)		
Ethnicity	43 White (81.1%) 0 African-Caribbean (0%) 3 Asian (5.7%) 1 Mixed race (1.9%) 6 Prefer not to say (11.3%)			16 White (64%) 8 African-Caribbean (32%) 1 Asian (4%)		
No. Patients with past history of optic neuritis	28			5		
- Time from ON to OCT, median (range) in months	32 (6–124)			44 (17–98)		
No. Patients with no past history of optic neuritis	25			20		
	OCT examination					
Both eyes examined (patients)	74 (37)			38 (19)		
Patients with concordant OCT result in both eyes	26			18		
Patients with discordant OCT result in both eyes	11			1		
One eye only examined -other eye poor VA post ON (patients)	16(16)			6 (6)		
	Ophthalmic test results					
	TOTAL	ON	No-ON	TOTAL	ON	No-ON
OCT and VEP examination normal, N	37	9	28	35	5	30
OCT examination abnormal, N	21	18	3	4	2	2
VEP examination abnormal, N	6	3	3	1	0	1
OCT and VEP examination abnormal, N	26	26	0	4	1	3

Note: Age and sex group differences between MOGAD and AQP4-NMOSD patients were significant (Fisher's exact tests for sex,  $p = 0.007$ ; Wilcoxon test for age,  $p = 0.001$ ). Differences between normal Vs abnormal ophthalmic examinations were assessed with Fisher's exact test and significant between MOGAD and AQP4-NMOSD for the Total number of eyes ( $p \leq 0.001$ ) and ON eyes ( $p = 0.009$ ).

Abbreviations: ARF, Adriana Roca-Fernandez; BMOMRW, Bruch's membrane opening based minimum rim width; ETDRS, Early Treatment Diabetic Retinopathy Study; GCIP, ganglionar and inner plexiform retinal layer; HC, healthy control; IS, immunosuppression; MOGAD, Myelin Oligodendrocyte glycoprotein antibody disease; MRI, magneticresonance imaging; MS, multiple sclerosis; NMO, Neuromyelitis Optica; NMOSD, neuromyelitis optica spectrum disorder; NON, no history of optic neuritis; OCTs, optic coherence tomography (in plural); QC, quality control; RNFL, retinal nerve fibre layer; N, number; AQP4-NMOSD, AQP4 seropositive Neuromyelitis optica spectrum disease; OCT, Optic coherence tomography; VEP, Visual evoked potentials; VA, central visual acuity.

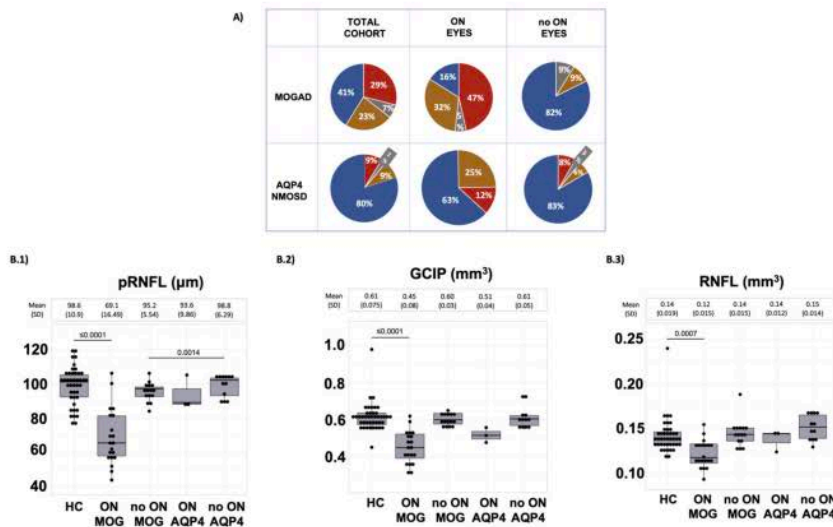


**Figure 2. Comparisons between AQP4-NMOSD (AQP4) and MOGAD patients**

\*AQP4-NMOSD is referred in this table as AQP4 for simplicity.

(A) **Clinical cohort** grouped according abnormal OCT (orange); abnormal VEP (grey), both tests abnormal (red) or both tests normal (blue).

(B) **Macular sub-study cohort** grouped according disease group or HC group and ON or NON group, boxplot shows median, 25<sup>th</sup> and 75<sup>th</sup> percentile (B.1) *pRNFL* (B.2) *GCIP* (B.3) macular *RNFL*. Maximum likelihood was used for the estimation of p values.

Abbreviations: MOGAD, Myelin oligodendrocyte glycoprotein; AQP4, AQP4 seropositive Neuromyelitis optica spectrum disease; OCT, Optic coherence tomography; ON, Only eyes that have had previous ON; no ON, Only eyes not have previous ON; *pRNFL*, peripapillary retinal nerve fibre layer; *GCIP*, ganglionar and inner plexiform layer; *RNFL*, macular retinal nerve fibre layer.

detecting primary demyelinating pathology as occurs in MOGAD. Although more AQP4-NMOSD patients overall were on IS the patients with normal vision post ON who had normal OCT were not on treatment as their attacks were prior to diagnosis and there was no evidence their attacks were milder.

This retrospective analysis has limitations. The diagnosis of ON in this study, as in routine clinical practice, was based on clinical signs and symptoms. We did not use the other eye as the normal control because many patients had bilateral ON and even in those without ON in the other eye a subset had abnormal OCT. Orbital magnetic resonance imaging (MRI) was not routinely performed although it was used where the diagnosis was in doubt. Mild ON could have been missed and ON could have been diagnosed incorrectly but the NMOSD clinicians reviewed the patients' symptoms and signs with the relevant neurologists/ophthalmologists and it is likely these errors would be small. Additionally, more AQP4-NMOSD patients were on

immunosuppressive medication than MOGAD patients. However, we do not think these factors would not cause the observed differences between the two diseases noted. VEPs were performed at different centres with different reference ranges and equipment. Likewise, for the clinical cohort, we used the Heidelberg BMO-MRW Reference Database which includes only subjects of European descent. Retinal thickness variability between races, and the use of a single threshold in OCT could have underestimated abnormalities in the AQP4-Ab group with a greater proportion of patients of Afro-Caribbean origin. However, this aims to be pragmatic in order to be easily translated into clinical practice. We defined good visual function based upon central visual acuity, and visual fields were not systematically performed. We analysed all eyes measured whether or not they had paired observations, and did not distinguish between those with concordant ON eyes or those where only one eye was affected. A major strength is the use of a single centre for the clinical OCT tests performed under the same protocol and, in the

case of the macular sub-study OCT analysis, segmented by the same person.

Our observations support the use of VEPs and OCT to determine the likelihood of previous visual symptoms being due to a MOGAD-ON. This is important because it could lead to an adjustment in the on-going immunosuppression. In addition, as sub-clinical abnormalities can occur without symptoms and although the relevance of the subclinical abnormalities is unknown, cumulative damage could well lead to clinical impairment and so close monitoring where it is noted is important. Hence, it is important to repeat the tests after each MOGAD relapse (i.e. to re-baseline the results) to provide comparison data should future visual symptoms occur.

#### Acknowledgements

NHS England for funding the Highly Specialized Diagnostic and Advisory Service for Neuromyelitis Optica



#### Declaration of conflicting interests

The author(s) declared no potential conflicts of interest with respect to the research, authorship, and/or publication of this article.

#### Funding

The author(s) received no financial support for the research, authorship and/or publication of this article.

#### ORCID iDs

A Roca-Fernández  <https://orcid.org/0000-0002-8720-9397>  
S Messina  <https://orcid.org/0000-0002-1134-5771>

#### References

1. Juryńczyk M, Messina S, Woodhall MR, et al. Clinical presentation and prognosis in MOG-antibody disease: a UK study. *Brain J Neurol* 2017; 01): 3128–3138.
2. Fujihara K, Mitsu T, Nakashima I, et al. Neuromyelitis optica should be classified as an astrocytopathic disease rather than a demyelinating disease. *Clin Exp Neuroimmunol* 2012; 3: 58–73.
3. Filippatou AG, Mukharesh L, Saidha S, et al. AQP4-IgG And MOG-IgG related optic neuritis—prevalence, optical coherence tomography findings, and visual outcomes: a systematic review and meta-analysis. *Front Neurol [Internet]*, 2020 Oct 8; 11:540156. doi: 10.3389/fneur.2020.540156.
4. Cobo-Calvo A, Ruiz A, Maillart E, et al. Clinical spectrum and prognostic value of CNS MOG autoimmunity in adults: the MOGADOR study. *Neurology* 2018 May 22; 90: e1858–e1869.
5. Kitley J, Leite MI, Nakashima I, et al. Prognostic factors and disease course in aquaporin-4 antibody-positive patients with neuromyelitis optica spectrum disorder from the United Kingdom and Japan. *Brain J Neurol* 2012 Jun; 135: 1834–1849.
6. Sotirchos ES, Filippatou A, Fitzgerald KC, et al. Aquaporin-4 IgG seropositivity is associated with worse visual outcomes after optic neuritis than MOG-IgG seropositivity and multiple sclerosis, independent of macular ganglion cell layer thinning. *Mult Scler J* 2020 Oct 1; 26: 1360–1371.

## 11.1.2. Publications indirectly related with this thesis:

### 11.1.2.1. Clinical presentation and prognosis in MOG-antibody disease: A UK study

Citation: Jurynczyk, M., Messina, S., Woodhall, M. R., Raza, N., Everett, R., **Roca-Fernández, A.**, ... Waters, P., & Palace, J. (2017). *Clinical presentation and prognosis in MOG-antibody disease: A UK study*. *Brain: A Journal of Neurology*, 140(12), 3128–3138.  
IF: 13.501



## Clinical presentation and prognosis in MOG-antibody disease: a UK study

Maciej Jurynczyk,<sup>1,\*</sup> Silvia Messina,<sup>1,\*</sup> Mark R. Woodhall,<sup>1,\*</sup> Naheed Raza,<sup>1</sup> Rosie Everett,<sup>1</sup> Adriana Roca-Fernandez,<sup>1</sup> George Tackley,<sup>1</sup> Shahd Hamid,<sup>2</sup> Angela Sheard,<sup>1</sup> Gavin Reynolds,<sup>1</sup> Saleel Chandratre,<sup>1</sup> Cheryl Hemingway,<sup>3</sup> Anu Jacob,<sup>2</sup> Angela Vincent,<sup>1</sup> M. Isabel Leite,<sup>1,#</sup> Patrick Waters<sup>1,#</sup> and Jacqueline Palace<sup>1,#</sup>

\*:#These authors contributed equally to this work.

See de Seze (doi:10.1093/brain/awx292) for a scientific commentary on this article.

A condition associated with an autoantibody against MOG has been recently recognized as a new inflammatory disease of the central nervous system, but the disease course and disability outcomes are largely unknown. In this study we investigated clinical characteristics of MOG-antibody disease on a large cohort of patients from the UK. We obtained demographic and clinical data on 252 UK patients positive for serum immunoglobulin G1 MOG antibodies as tested by the Autoimmune Neurology Group in Oxford. Disability outcomes and disease course were analysed in more detail in a cohort followed in the Neuromyelitis Optica Oxford Service ( $n = 75$ ), and this included an incident cohort who were diagnosed at disease onset ( $n = 44$ ). MOG-antibody disease affects females (57%) slightly more often than males, shows no ethnic bias and typically presents with isolated optic neuritis (55%, bilateral in almost half), transverse myelitis (18%) or acute disseminated encephalomyelitis-like presentations (18%). In the total Oxford cohort after a median disease duration of 28 months, 47% of patients were left with permanent disability in at least one of the following: 16% patients had visual acuity  $\leq 6/36$  in at least one eye, mobility was limited in 7% (i.e. Expanded Disability Status Scale  $\geq 4.0$ ), 5% had Expanded Disability Status Scale  $\geq 6.0$ , 28% had permanent bladder issues, 20% had bowel dysfunction, and 21% of males had erectile dysfunction. Transverse myelitis at onset was a significant predictor of long-term disability. In the incident cohort 36% relapsed after median disease duration of 16 months. The annualized relapse rate was 0.2. Immunosuppression longer than 3 months following the onset attack was associated with a lower risk of a second relapse. MOG-antibody disease has a moderate relapse risk, which might be mitigated by medium term immunosuppression at onset. Permanent disability occurs in about half of patients and more often involves sphincter and erectile functions than vision or mobility.

1 Nuffield Department of Clinical Neurosciences, John Radcliffe Hospital, University of Oxford, Oxford, UK

2 NMO Clinical Service, The Walton Centre, Liverpool, UK

3 Department of Neurology, Great Ormond Street Hospital for Children, London, UK

Correspondence to: Jacqueline Palace

Nuffield Department of Clinical Neurosciences, West Wing, John Radcliffe Hospital, University of Oxford, Oxford OX3 9DU, UK

E-mail: jacqueline.palace@ndcn.ox.ac.uk

**Keywords:** demyelination; neuroinflammation; multiple sclerosis; neuromyelitis optica; acute disseminated encephalomyelitis

**Abbreviations:** ADEM = acute demyelinating encephalomyelitis; EDSS = Expanded Disability Status Scale; LETM = longitudinally extensive transverse myelitis; NMO = neuromyelitis optica; NMOSD = neuromyelitis optica spectrum disorders

Received June 8, 2017. Revised August 9, 2017. Accepted August 22, 2017. Advance Access publication November 9, 2017

© The Author (2017). Published by Oxford University Press on behalf of the Guarantors of Brain. All rights reserved.

For Permissions, please email: journals.permissions@oup.com

## Introduction

A condition associated with the presence of serum anti-MOG antibodies has been recently proposed as a new inflammatory disease of the CNS driven by antibodies of the IgG1 class, which target MOG expressed on myelin sheaths and promote demyelination (Reindl *et al.*, 2013). MOG-antibody disease is increasingly recognized as distinct from multiple sclerosis as typical multiple sclerosis patients test negative for the presence of MOG antibodies when novel assays with conformationally intact MOG are used (Waters *et al.*, 2015). Moreover, MOG-antibody disease clinically and radiologically resembles AQP4-antibody neuromyelitis optica spectrum disorders (NMOSD) and acute demyelinating encephalomyelitis (ADEM) rather than multiple sclerosis (Brilot *et al.*, 2009; Mader *et al.*, 2011; Kitley *et al.*, 2012b, 2014; Jurynczyk *et al.*, 2017). Although MOG-antibody disease is considered milder and less relapsing than AQP4-antibody NMOSD (Kitley *et al.*, 2014; Sato *et al.*, 2014), the clinical course, predictors of relapses and clinical outcomes remain largely unknown due to a relatively small number of patients included in previous studies and biases towards recruiting relapsing patients because monophasic patients could not be diagnosed at onset until the recent discovery of the disease (Kitley *et al.*, 2014; Jarius *et al.*, 2016a).

In this study we examined demographics, disease presentation, disease course and clinical outcomes in a large cohort of patients from the UK ( $n = 252$ ), who tested positive for serum IgG1 MOG antibodies. Clinical outcomes and predictors of relapses were studied in more detail in a cohort followed-up in the neuromyelitis optica (NMO) Specialist Clinic in Oxford ( $n = 75$ ), including patients who were diagnosed with MOG-antibody disease at onset ( $n = 44$ ).

## Materials and methods

### Ethics

All patients followed in Oxford signed written consent of the NMO Tissue Bank (Oxford Research Ethics Committee C Ref: 10/H0606/56) and the audit of the MOG antibody-positive patients was registered under the Oxford University Hospitals Trust policy.

### MOG antibody testing

Testing for the presence of serum MOG antibodies was performed in the Autoimmune Neurology laboratory in Oxford using a cell-based assay (M.W.) as described previously (Waters *et al.*, 2015). All MOG antibody-positive patients were negative for AQP4 antibodies.

### Cohorts

We selected three different cohorts to analyse: the 'UK Cohort', which was the largest but least detailed and objective

dataset; the 'Oxford Total Cohort' with more detailed uniformly and prospectively collected data; and an 'Oxford Incident Cohort' where only those diagnosed at onset were included.

### UK cohort

Questionnaires on 494 samples positive for MOG antibodies were sent out to hospitals, or requesting clinicians (where they were identifiable), which included 12 basic questions on year of birth, ethnicity (Caucasian, Asian, Afro-Caribbean, Mixed or Other), date of onset attack, onset attack type [unilateral optic neuritis, bilateral optic neuritis, short transverse myelitis, longitudinally extensive transverse myelitis (LETM), ADEM, other], recovery from first attack (full, good, moderate or poor), maintenance prednisolone or immunosuppression treatment (none, yes for <3 months, 3–6 months, >6 months), number of attacks, date of first relapse, date of last relapse, end date of follow-up, disability at last follow-up (none, mild, moderate, severe) and current diagnosis (the questionnaire is shown in the Supplementary material). Clinicians were asked to specify if the onset attack was in the 'other' category. ADEM-like presentations (e.g. brainstem attack) were merged with ADEM attacks and analysed as one group. Complete questionnaires were returned on 252 patients.

### Oxford total cohort

More extensive prospectively collected data from 75 patients seen within the specialist Neuromyelitis Optica Clinic in Oxford were available and included treatment, disability outcomes, disease course and phenotype. We selected disability outcomes that were prevalent enough in the MOG-antibody cohort: visual acuity  $\leq 6/36$  in at least one eye, Expanded Disability Status Scale (EDSS)  $\geq 4.0$  (ambulatory without aid or rest for <500 m), neurogenic bladder dysfunction (urinary incontinence and/or urgency), neurogenic bowel dysfunction (faecal incontinence and/or constipation) and erectile dysfunction. Outcomes were considered in the analysis if they persisted for at least 6 months and were present at last follow-up. Cognitive problems were noted when reported but were not systematically assessed and thus not analysed.

### Oxford incident cohort

Because MOG-antibody disease is a recent discovery and thus the diagnosis was not possible until the past 5 years, patients captured in prevalence cohorts with longer follow-up are likely to have been diagnosed if they present with relapses. To avoid this relapse risk bias, a 44-patient incident cohort from the Oxford cohort were identified where the diagnosis was made shortly after onset and before the second relapse. The onset dates were all after January 2012, once the diagnostic MOG-IgG1 assay became available.

### Statistical analysis

Statistical analysis was performed using R. Unpaired *t*-tests or Mann-Whitney *U*-tests were used when comparing two groups. ANOVA or Kruskal-Wallis tests were used when comparing multiple groups (e.g. patients with distinct onset presentations). The Kaplan-Meier method was used for estimating relapse risk and disability outcomes. Binomial and logistic regression was used to identify predictors of relapses and

disability. K-means clustering was used to identify patient subgroups according to age of onset.

## Results

### Demographic data

The demographics of the UK cohort, the Oxford total cohort and Oxford incident cohort are shown in Table 1.

There were no obvious differences between the three cohort sets except for shorter follow-up periods and lower relapse rate in the Oxford incident cohort.

In the UK cohort, the ethnic breakdown was as expected in the general population. There was a slight female predominance of 57% and a broad onset age range of 1–81 years with a trimodal appearing distribution identified from the modelling analysis, with the age clusters being <20 years, 20–45 years and >45 years at disease onset (Fig. 1A and Supplementary Fig. 1A). Male and female patients

**Table 1** Comparison of basic demographics, clinical features between the UK cohort, Oxford total cohort and Oxford incident cohort (diagnosis after the onset attack)

	Total cohort	Oxford	
		Total	Incident
Patients, n	252	75	44
Mean age at onset $\pm$ SD	30.1 $\pm$ 18.3	29.0 $\pm$ 16.5	32.0 $\pm$ 17.6
Female, %	57	56	48
Onset attack, %			
Unilateral ON	31	25	18
Bilateral ON	24	27	27
Transverse myelitis	18	20	21
ADEM or ADEM-like	18	20	25
Simultaneous ON and TM	9	8	9
With short TM	4	1	0
With LETM	5	7	9
Disease course, %			
Monophasic	56	41	64
Relapsing	44	59	36
Phenotype at follow-up, %			
ON	NA	37	36
TM	NA	12	18
ADEM/ADEM-like	NA	24	32
ON + TM	NA	27	14
Median disease duration in months (range)	26 (0–492)	28 (1–437)	15.5 (1–57)
Time until relapse, months			
1st quartile	14	7	5
Median	40*	27	44*
Reaching endpoints			
VA $\leq$ 6/36 in one or both eyes, %	NA	16	7
Limited walking distance, EDSS $\geq$ 4, %	NA	7	9
Permanent bladder dysfunction, %	NA	28	34
Self or <i>in situ</i> catheterization, %	NA	17	25
Permanent bowel dysfunction, %	NA	20	27
Permanent erectile dysfunction, % males	NA	21	26
CSF findings		Oxford total cohort	
Normal WBC (< 10/ $\mu$ l)		29/47	
WBC 10–50/ $\mu$ l		12/47	
WBC 50–100/ $\mu$ l		3/47	
WBC $\geq$ 100/ $\mu$ l (range)		3/47 (100–300)	
Normal protein		27/50	
CSF protein, 0.5–1 g/l		18/50	
CSF protein, $\geq$ 1 g/l (range)		5/50 (1–2.9)	
Elevated protein with normal WBC (protein range)		4/39 (0.6–1.7)	
Unmatched OCB		7/57	

\*Estimated from Kaplan-Meier curves.

OCB = oligoclonal bands; ON = optic neuritis; TM = transverse myelitis; VA = visual acuity; WBC = white blood cells.

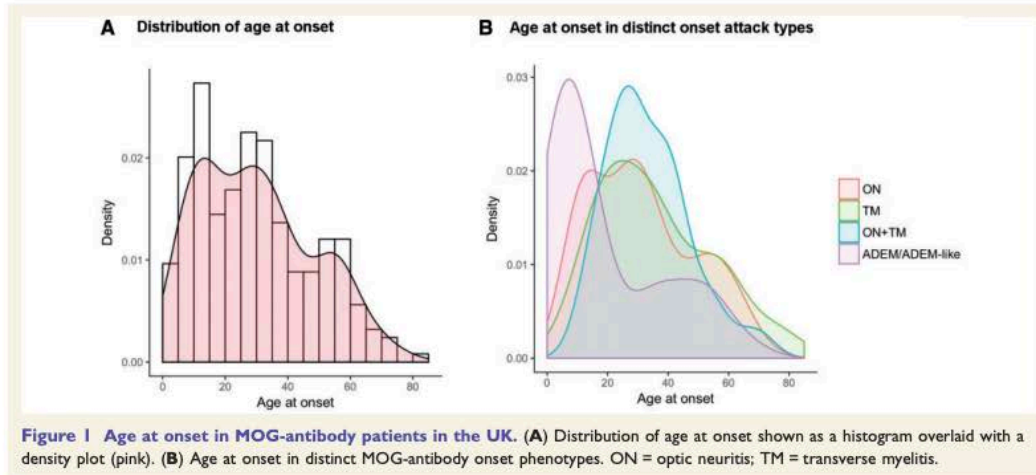


**Figure 1** Age at onset in MOG-antibody patients in the UK. (A) Distribution of age at onset shown as a histogram overlaid with a density plot (pink). (B) Age at onset in distinct MOG-antibody onset phenotypes. ON = optic neuritis; TM = transverse myelitis.

**Table 2** Basic clinical information on patients with different onset attack phenotypes in the UK and Oxford incident cohorts

	Unilateral ON	Bilateral ON	LETM	Short TM	ON + TM	ADEM/ADEM-like
<b>UK cohort (n = 252)</b>						
Patients, %	31	24	14	4	9	18
Mean age at onset in years $\pm$ SD (range)	28 $\pm$ 16 (7–68)	36 $\pm$ 18 (6–74)	31 $\pm$ 17 (6–73)	53 $\pm$ 16 (22–81)	33 $\pm$ 14 (15–69)	19 $\pm$ 19 (1–67)
Median disease duration in months (range)	27 (2–432)	17 (1–355)	26 (0–287)	28 (5–108)	24 (3–312)	26 (8–492)
Relapsing, %	53	43	31	22	39	46
<b>Oxford incident cohort (n = 44)</b>						
Patients, %	18	27	18	2	9	25
Median disease duration in months (range)	25 (2–43)	10 (3–20)	6.5 (1–57)	9	31 (11–37)	37 (8–53)
Relapsing, %	50	42	12	0	50	36

ON = optic neuritis; SD = standard deviation; TM = transverse myelitis.

had comparable general characteristics with similar mean onset age, ethnicity and similar disease duration although there were more onset optic neuritis + transverse myelitis in males (14% versus 6%, not significant, Supplementary Table 1). There was a trend towards higher proportion of female patients and younger age at onset in non-Caucasian patients when compared with Caucasians (Supplementary Table 2).

### Disease presentation

In the UK cohort the majority of patients (55%) presented with optic neuritis: 24% bilateral, 18% had isolated transverse myelitis; 14% were longitudinally extensive and 4% short-segment; 9% had simultaneous optic neuritis and transverse myelitis; and 18% had an ADEM or ADEM-

like presentation (including brainstem attacks). Patients with ADEM/ADEM-like presentations were younger than the other groups (Fig. 1B and Table 2) and in patients with disease onset <20 years of age it was the most prevalent presentation (36% of patients). Patients with disease onset between 20 and 45 years of age most often presented with unilateral optic neuritis (36%), while patients with disease onset above 45 years of age presented with bilateral optic neuritis (39%). Short transverse myelitis was more common than LETM in patients older than 45 years at onset (14% versus 9%), but was exceptional in younger patients. Onset presentations in different age groups are shown on Supplementary Fig. 1B.

In the Oxford Total cohort, where more detailed history was available, 11/75 patients experienced symptoms in keeping with area postrema syndrome (nausea, vomiting,

hiccup), most of them (91%) at onset attacks. In 5/11 patients, area postrema symptoms preceded the recognized onset attack symptoms. Vomiting was the most frequent symptom (nine patients), followed by hiccup (one), and cough (one). Five had ADEM/ADEM-like presentations, four had transverse myelitis  $\pm$  optic neuritis and two had bilateral optic neuritis. Brain MRI scans were performed at the time of symptoms in 9/11 patients; three had brainstem lesions adjacent to fourth ventricle (Supplementary Fig. 2), one had cerebellar lesions, three had brain lesions without brainstem or cerebellar involvement and two had normal brain MRI.

### Recovery from relapses

In the UK cohort, recovery from the onset attack was full or good in 78%, with full recovery more frequent in patients with unilateral optic neuritis and ADEM-like presentations (Fig. 2A). Younger patients were more likely to fully recover than older adults (Fig. 2B). Patients with optic neuritis at onset tended to relapse more frequently than those with transverse myelitis or ADEM (Table 2).

### Disease course in the Oxford incident cohort

Time taken until 25% of patients relapsed was 5 months (Fig. 3A), with 36% relapsing at final follow-up. In those who were followed-up for at least 24 months ( $n = 16$ ), the annualized relapse rate (excluding the onset attack) was 0.2. There was a tendency for more relapses in younger patients (Fig. 3B).

Patients presenting with optic neuritis and classic Devic's phenotype were more likely to relapse than those with isolated transverse myelitis or ADEM-like presentation (Fig. 3C and Table 2). The same phenomenon was observed in the total UK cohort (Supplementary Fig. 3).

### Second attacks in the Oxford total cohort

Second attacks were predominantly optic neuritis (35/44 relapsing patients, 24/26 among those with isolated optic neuritis onset and 4/7 among those with isolated transverse myelitis at onset).

### NMOSD, ADEM and multiple sclerosis criteria in the Oxford total cohort

Of the 53 adults (>16 years), 47 fulfilled either the NMO 2006 (Wingerchuk *et al.*, 2006) or NMOSD 2007 (Wingerchuk *et al.*, 2007) criteria but only 17 fulfilled the NMOSD 2015 (Wingerchuk *et al.*, 2015) criteria (because of the requirement for more than one area to be involved if AQP4 antibody-negative), two of whom fulfilled the ADEM criteria defined primarily for children (Krupp *et al.*, 2013). Six patients did not fulfil any of the aforementioned criteria: five had monophasic unilateral optic neuritis with normal brain MRI and one patient had short-segment transverse myelitis with a single non-specific brain white matter lesion. Assuming LETM attacks do not count as multiple sclerosis relapses, only one patient fulfilled the McDonald 2010 multiple sclerosis criteria

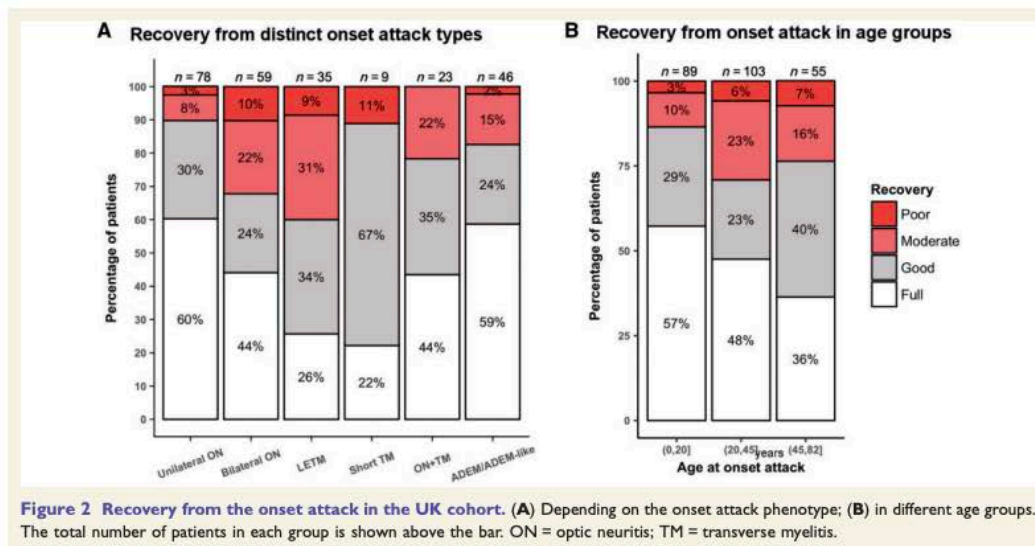
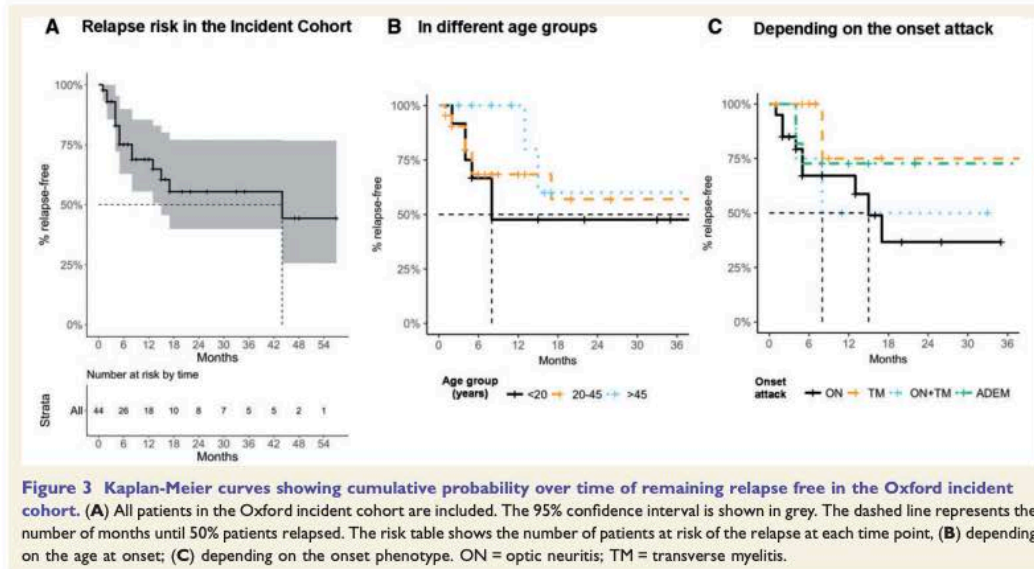


**Figure 2** Recovery from the onset attack in the UK cohort. (A) Depending on the onset attack phenotype; (B) in different age groups. The total number of patients in each group is shown above the bar. ON = optic neuritis; TM = transverse myelitis.



(Polman *et al.*, 2011) but with red flags: bilateral optic neuritis followed within weeks by a short lateral transverse myelitis with a low thoracic lesion and typical NMO-like brain lesions (thalamic and brainstem). These lesions resolved (multiple sclerosis patients would be expected to increase lesion load over time) and oligoclonal bands were not detected in the CSF.

Of the 22 paediatric patients, 19 fulfilled the 2006 NMO or 2007 NMOSD criteria but only 13 fulfilled the 2015 NMOSD criteria, two of whom fulfilled the ADEM criteria. A further two fulfilled the ADEM criteria alone and another two had a diagnosable ADEM attack but because of other relapses these could not be diagnosed as ADEM at follow-up.

A detailed breakdown of how MOG-antibody patients fulfilled distinct disease criteria is shown in Supplementary Fig. 5A and B (adults and children, respectively).

### Treatment duration and relapse risk

In the UK cohort, 40% did not receive long-term immunosuppression after the first attack, 34% were treated for less than 3 months, 11% from 3–6 months and 15% for more than 6 months. The risk of relapse was higher in those who were not immunosuppressed or immunosuppressed for less than 3 months (53% and 47%, respectively) when compared with those treated for 3 to 6 months or longer than 6 months (22% and 26%, respectively).

We then assessed this in more detail in the Oxford total cohort. Forty-five of 75 patients received long-term immunosuppression after their onset attack. Of those, 38 were treated with oral prednisolone, six with oral

prednisolone and azathioprine and one with oral prednisolone and methotrexate. The risk of relapse was significantly lower in patients who were treated for more than 3 months in comparison to those treated for less than 3 months ( $P = 0.005$ , Cox regression, Fig. 4A). It was clear that relapses tended to occur early and often shortly after stopping corticosteroids (Fig. 4B).

### Disability outcome in the UK cohort

In the UK cohort, where disability was subjectively scored by the referring clinician, 41% of patients did not have any disability at last follow-up but approximately a quarter had moderate to severe disability. Logistic regression showed that disability at last follow-up was significantly worse with number of attacks ( $P < 0.01$ ) and worse recovery from the onset attack ( $P < 0.01$ ), but was not significantly influenced by age at onset ( $P = 0.07$ ), gender ( $P = 0.7$ ), ethnicity ( $P = 0.37$ ) or disease duration ( $P = 0.8$ ).

### Disability outcomes in the Oxford total cohort

Thirty-five of 75 patients in the Oxford total cohort had permanent visual (visual acuity  $\leq 6/36$  in at least one eye), motor (EDSS  $\geq 4.0$ ), sphincter or erectile dysfunction at the last follow-up. Twenty-five became disabled from the onset attack (33%) and 10 from subsequent attacks (20% of 50 who recovered fully from the onset attacks). We detail these outcomes below.

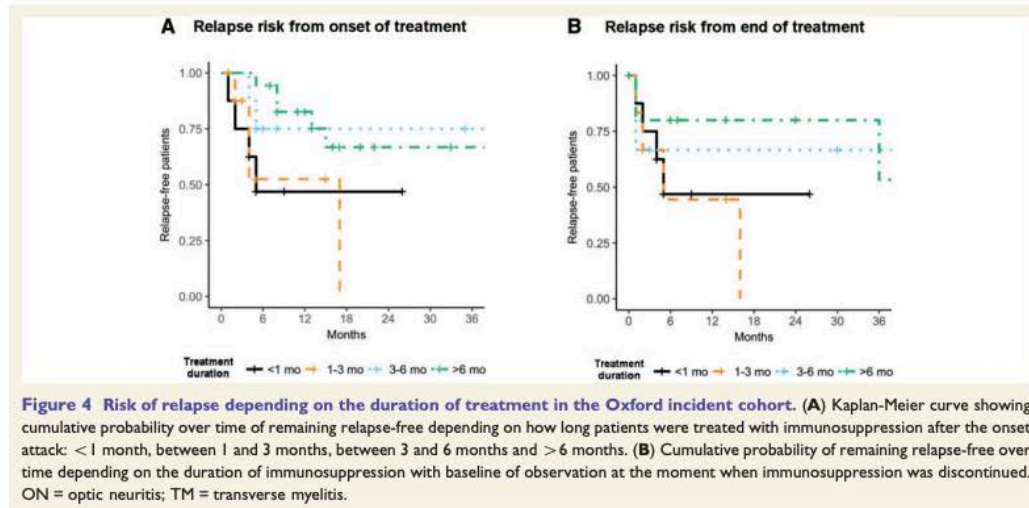


**Figure 4** Risk of relapse depending on the duration of treatment in the Oxford incident cohort. (A) Kaplan-Meier curve showing cumulative probability over time of remaining relapse-free depending on how long patients were treated with immunosuppression after the onset attack: <1 month, between 1 and 3 months, between 3 and 6 months and >6 months. (B) Cumulative probability of remaining relapse-free over time depending on the duration of immunosuppression with baseline of observation at the moment when immunosuppression was discontinued. ON = optic neuritis; TM = transverse myelitis.

### Visual disability

Twelve of 75 patients reached the permanent visual outcome of visual acuity 6/36 or worse in at least one eye at last follow-up and all of them had optic neuritis during the onset attack ( $\pm$  transverse myelitis or ADEM.) In nine, this was a consequence of the first attack, i.e. 9 of 48 patients who had optic neuritis at onset became visually disabled from the onset attack (four had unilateral optic neuritis, three bilateral optic neuritis and two had optic neuritis + ADEM). Seven of the nine were treated at acute attack with intravenous methylprednisolone, one with dexamethasone and one was not treated.

Of the remaining 39 patients with optic neuritis onset ( $\pm$  transverse myelitis or ADEM), three became visually impaired from subsequent attacks of isolated (uni- or bilateral) optic neuritis attacks. These three patients all recovered fully from the onset optic neuritis attacks. At the time of subsequent disabling attacks, two of them were not on background immunosuppression, and one was on a reducing dose of prednisolone and methotrexate. In the acute phase of the subsequent disabling optic neuritis attacks one patient received intravenous methylprednisolone, one had an increase in the dose of oral prednisolone and one was not treated.

Two of 75 patients had visual acuity 6/36 or worse in the best eye at last follow-up. Older patients were less likely to develop permanent visual disability at follow-up (Supplementary Table 3 and Supplementary Fig. 4A). Accordingly, patients who reached the visual disability endpoint were younger at disease onset than those who did not (mean  $20.8 \pm 11.3$  versus  $30.6 \pm 17.0$ ,  $P = 0.06$ ). Of all patients who had optic neuritis at onset ( $\pm$  transverse myelitis or ADEM,  $n = 48$ ) visual disability occurred in 12/39

(31%) patients younger than 45, and 0/9 (0%) older than 45 years of age. Cumulative probability of remaining free from visual disability is shown on Supplementary Fig. 4A and B.

### Motor disability

All permanent motor disability (EDSS  $\geq 4.0$ ) at follow-up was associated with transverse myelitis attacks ( $\pm$  optic neuritis) and occurred in five patients only (three males, two females). Four of the five had EDSS  $\geq 6$  at last follow-up (5%). In three of five patients, disability was related to the onset attack and these three were of 30 patients with transverse myelitis at onset, 14 females, 16 males (15 transverse myelitis alone, nine ADEM + transverse myelitis, six optic neuritis + transverse myelitis). Of these three patients, two were treated at acute onset attack with intravenous methylprednisolone, plasma exchange and intravenous immunoglobulins and one was treated with intravenous methylprednisolone only. Two patients became disabled from subsequent transverse myelitis attacks and initially presented with optic neuritis or ADEM onset phenotypes. Both had stopped short courses of steroids just prior to the disabling transverse myelitis attack. In the acute transverse myelitis attack one of them was treated with intravenous methylprednisolone followed by oral prednisolone and the other had no acute treatment, but was started on interferon- $\beta$ .

Those who had limited walking distance at last follow-up were slightly older than those without walking disability ( $36.3 \pm 22.7$  versus  $28.6 \pm 15.9$ , not significant). However, age of onset was not a significant predictor of final motor disability, neither was gender, disease duration or type of onset attack (Supplementary Table 3).

Cumulative probability of remaining free from motor disability is shown in Supplementary Fig. 4C and >D.

### Bladder disability

Permanent bladder dysfunction at follow-up occurred in 21 patients, all related to transverse myelitis (with or without other features). Males were affected more frequently than females (12/33 versus 9/42), which was likely to be related to the higher proportion of males having transverse myelitis ( $\pm$  optic neuritis or ADEM) than females (16/33 versus 14/42 onset attacks, respectively). All of these patients had lesions affecting the thoracic cord or conus. Fifteen patients had bladder dysfunction from the onset attack. Six were treated with intravenous methylprednisolone only, five with intravenous methylprednisolone and plasma exchange, two with intravenous methylprednisolone, plasma exchange and intravenous immunoglobulins and two with oral steroids.

Six patients were disabled from further attacks (two from transverse myelitis onset phenotype, two from ADEM onset phenotype and two from optic neuritis onset attacks). Three were not on background immunosuppression, two stopped steroids within the last 2 weeks and one was on a reducing dose of prednisolone. During the attack that left them with bladder disability, five were treated with intravenous methylprednisolone and one with oral methylprednisolone.

Thirteen patients required long-term catheterization (5/42 females and 8/33 males) at last follow-up. Only two of these patients had ambulation problems (EDSS  $\geq$  4.0) at the same time.

Overall bladder outcome was not significantly affected by age of onset, disease duration or gender (Supplementary Table 3). Cumulative probability of remaining free from bladder disability is shown in Supplementary Fig. 4E and F.

### Bowel and erectile dysfunction

Bowel and erectile dysfunction only occurred in those with bladder disability. Bowel dysfunction occurred in 15 patients (six females and nine males). Erectile dysfunction occurred in 21% of males, or 44% of males presenting with transverse myelitis at onset.

### Cognitive problems

Six of 15 (40%) patients with ADEM/ADEM-like onset presentations were left with cognitive problems, three had paediatric and three had adult onset. Within the ADEM/ADEM-like group, age at onset was similar between those left with and without residual cognitive problems. Cognition was not affected in patients with other onset presentations. Of the paediatric patients, one showed poor concentration, one learning difficulties and one psychiatric (mania, hallucinations) and memory problems. In particular, the last patient was also positive for NMDAR-antibody encephalitis. Among adult patients, one showed memory impairment and low mood, one poor concentration and one drowsiness.

## Poor outcome predictors in the Oxford total cohort

Onset attack involving transverse myelitis was a predictor of poor outcome (visual, motor, bladder, bowel or erectile) in the Oxford cohort ( $P = 0.02$ ). This was not the case for the age at onset, gender or Caucasian ethnicity.

Importantly, when taking the 50 patients who did not reach poor outcome from the onset attack and looking for predictors of a subsequent poor outcome we found none among onset attack type, age at onset, gender, Caucasian ethnicity and poor recovery from onset attack.

## Test positivity over time and relapse risk

We assessed whether the persistence of MOG antibodies on follow-up testing might be correlated with the risk of further relapses. We obtained information on 57 patients who had at least two MOG antibody tests over time, at least 6 months apart (all patients included in the group who showed persistence of the antibody in the serum had testing performed at least 6 months apart). Forty-one (72%) remained positive over time (median disease duration 37 months, range 17–57), 14 (25%) became negative on follow-up testing and two (3%) turned negative and then again positive (median disease duration 9 months, range 1–16, Fig. 5). Twenty-four of 41 (59%) patients in whom the antibody remained positive over time had further relapses. All patients who became negative over time remained relapse-free. Two patients who became negative and then positive (Fig. 5) did not have further attacks.

Patients who became antibody-negative over time more often presented with simultaneous optic neuritis and transverse myelitis, and ADEM-like phenotypes when compared with those who remained antibody-positive, and were more likely to be monophasic (58% versus 36%), but the differences were not statistically significant (Supplementary Table 4). The duration of immunosuppression after the onset attack did not seem to predict the antibody status.

## Discussion

This is the largest MOG-antibody study reported and incorporates a national unselected patient cohort, the largest single centre cohort with more detailed clinical data and also a large incident cohort. We show that MOG-antibody disease can present at any age, most commonly with optic neuritis, shows slight female preponderance and no ethnic bias. It is often a relapsing disease with the risk of relapse affected by the duration of immunosuppression initiated after the onset attack. The prognosis is typically favourable, but patients can be left with significant sphincter and erectile dysfunction, cognitive impairment and poor visual acuity. The majority of this disability originates from the onset attack.



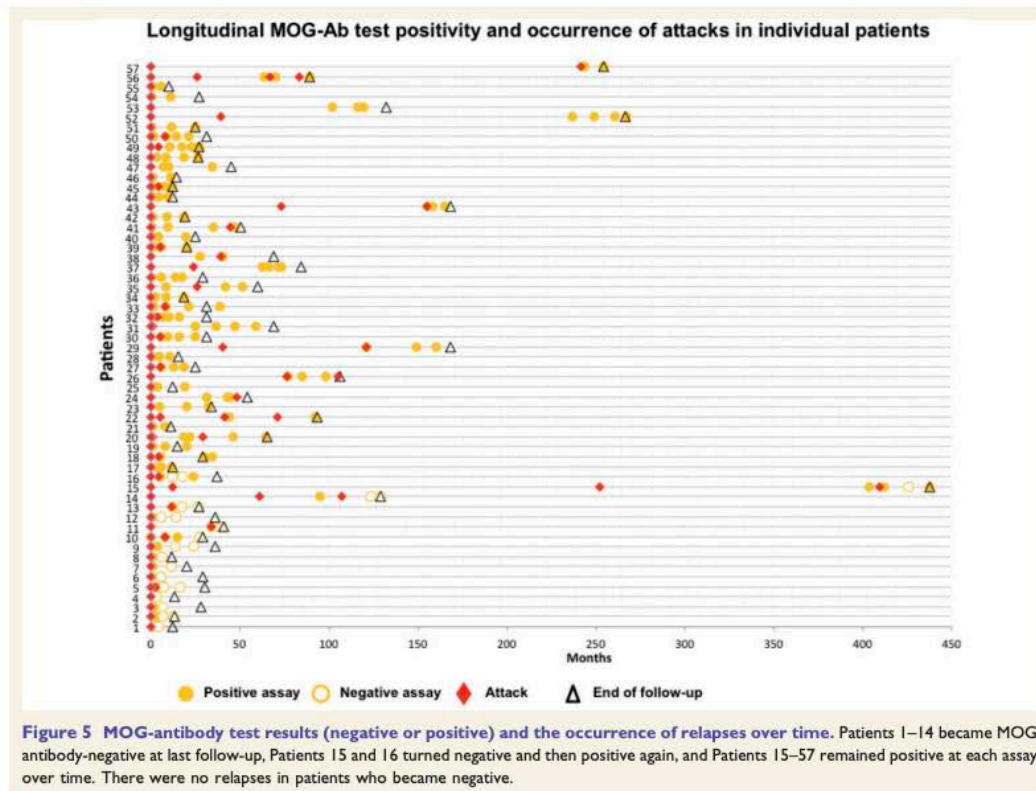


**Figure 5** MOG-antibody test results (negative or positive) and the occurrence of relapses over time. Patients 1–14 became MOG antibody-negative at last follow-up, Patients 15 and 16 turned negative and then positive again, and Patients 15–57 remained positive at each assay over time. There were no relapses in patients who became negative.

Initial reports indicated that the presence of MOG antibody typically predicts a monophasic disease but focused on patients presenting with both optic neuritis and LETM (Kitley *et al.*, 2012b, 2014); however, the phenotype is clearly broader and includes a relapsing disorder (Sato *et al.*, 2014; Höftberger *et al.*, 2015). High risk of relapse over time (~80%) and high annualized relapse risk (0.92) recently reported (Jarius *et al.*, 2016a) may be overestimated because patients with onset prior to the availability of the antibody test will ordinarily only re-present and thus be diagnosed, if they relapse. Additionally, there is likely to be a bias towards testing patients with relapses. Our study, using an incident cohort with our policy of treating patients at onset with >6 months prednisolone (which appears to reduce the risk of relapse), may explain the lower risk of relapse of ~50% over 2 years (Fig. 3A) and lower annual relapse rates. However, it is still likely that some monophasic patients were not referred and thus the true risk of relapse may be even lower. It is also worth mentioning that none of the patients who turned antibody-negative on repetitive testing experienced further relapses during follow-

up, which is in line with a recent report (Hyun *et al.*, 2017).

The prognosis in MOG-antibody disease has been a question of debate. In a recent study including 50 MOG-antibody patients, severe visual impairment was present at last follow-up in 36% (defined as visual acuity <0.5 in one or both eyes) and markedly impaired ambulation in 25% patients (Jarius *et al.*, 2016b). Another study reported a more favourable outcome with 19% patients with optic neuritis visually impaired (sustained visual acuity <0.2) at last follow-up (Sepúlveda *et al.*, 2016), which compares with our figure of 16%. Only 11% patients had EDSS ≥4 (Sepúlveda *et al.*, 2016). In a study including 17 MOG-antibody patients only one had EDSS ≥6 at last follow-up (Kim *et al.*, 2015). Analysis of our Oxford cohort showed that permanent visual disability affected only patients with optic neuritis at onset and typically was a consequence of the onset attack but could also result from subsequent optic neuritis attacks. Motor disability was rarer and might result either from onset or further transverse myelitis attacks. Interestingly, permanent bladder and

erectile dysfunction was more prevalent than motor disability at follow-up (28% and 21%, respectively), and this observation may be an important indicator to test for MOG antibodies, as in multiple sclerosis the occurrence of urogenital symptoms is considered similar to that of lower limb dysfunction (Miller *et al.*, 1965). Importantly our study indicates that patients with good recovery from the onset attacks are still potentially at risk of disabling attacks and that although it is difficult to predict who will have a future disabling attack, longer-term immunosuppression could be considered in patients presenting with optic neuritis because even among those who recovered there was an 8% risk of developing visual disability over the next 28 months. It is also worth noting that MOG-antibody ADEM/brainstem disease carried a risk of permanent cognitive impairment (40%).

When compared with our previous work MOG-antibody disease is clearly less disabling than AQP4-antibody NMOSD in terms of visual function and ambulation. After 25 months from onset permanent bilateral visual disability and reduced mobility as defined by EDSS  $\geq 6.0$  occurred in 1% and 4% of MOG-antibody patients, respectively, as compared with 20% and 25% of AQP4-antibody patients from the UK (Kitley *et al.*, 2012a). Sphincter dysfunction was not assessed in the AQP4-antibody cohort, but from our experience it is typically associated with motor disability rather than stand alone. It is also worth noting that a sizeable proportion (roughly 15%) of MOG-antibody patients presented with symptoms suggestive of area postrema syndrome, which has been thought to be highly specific for AQP4-antibody NMOSD.

Previous studies reported the presence of serum MOG antibodies in rare cases of paediatric and adult multiple sclerosis (Hacohen *et al.*, 2015; Spadaro *et al.*, 2016) although the paediatric cases have had their diagnoses revised to ADEM-optic neuritis, a known MOG-antibody phenotype (personal communication, Hacohen) and the adults had atypical multiple sclerosis phenotypes. In our UK cohort, 17/252 patients were diagnosed with multiple sclerosis by the referring clinicians but all had typical MOG-antibody disease features such as bilateral optic neuritis, LETM, ADEM-like presentation including brainstem involvement, lack of progressive disease, and brain MRI not typical of multiple sclerosis, including the absence of silent brain lesions. Assuming that LETM is not considered as a multiple sclerosis attack, only one adult patient in the Oxford cohort fulfilled McDonald criteria but with red flags such as NMO-typical brain imaging and absent oligoclonal bands in the CSF.

There are several strengths and limitations to our study. The main limitation of the study is the lack of information from all clinicians who requested testing. This was mainly due to the difficulty in identifying the responsible clinicians from the request forms because their in-house laboratories transpose request details when sending samples for external testing. However, we cannot think of a likely bias towards completing questionnaires for some phenotypes over others.

The strength is that this is by far the largest national MOG-antibody cohort reported and the UK cohort was very similar to the Oxford cohort suggesting the obtained data were representative of the whole. Additionally, auditing results obtained from a single UK assay service allowed a wider range of patients to be assessed, thus included paediatric and adult populations, ADEM as well as NMOSD phenotypes, and we were able to identify the not uncommon presentation of short transverse myelitis. Further strengths of our study include: an incident cohort to reduce the risk of bias towards relapsing patients in those with onset before the availability of the antibody test and the largest single centre cohort ( $n = 75$ ) ensuring homogeneous detailed data collection.

In conclusion, MOG-antibody disease is a newly identified CNS inflammatory condition, distinct from multiple sclerosis and is associated with attacks involving the optic nerve, spinal cord, brainstem and the brain. The risk of a relapsing disease is moderate and might be mitigated by prolonged immunosuppression. The prognosis is typically good, but a subset of patients might be left with some degree of sphincter, erectile, cognitive or visual dysfunction.

## Acknowledgements

We would like to thank all UK clinicians who provided us with the patient data.

## Funding

We gratefully acknowledge the Highly Specialised Commissioning Team for funding the Neuromyelitis Optica service in Oxford. Dr Maciej Jurynczyk received research fellowship from the Polish Ministry of Science and Higher Education programme Mobilnosc Plus (1070/MOB/B/2013/0).

## Supplementary material

Supplementary material is available at *Brain* online.

## References

- Brirot F, Dale RC, Selter RC, Grummel V, Kalluri SR, Aslam M, et al. Antibodies to native myelin oligodendrocyte glycoprotein in children with inflammatory demyelinating central nervous system disease [Internet]. *Ann Neurol* 2009; 66: 833–42.
- Hacohen Y, Absoud M, Deiva K, Hemingway C, Nytrova P, Woodhall M, et al. Myelin oligodendrocyte glycoprotein antibodies are associated with a non-MS course in children [Internet]. *Neuro Immunol Neuroinflamm* 2015; 2: e81.
- Höftberger R, Sepulveda M, Armangue T, Blanco Y, Rostásy K, Calvo AC, et al. Antibodies to MOG and AQP4 in adults with neuromyelitis optica and suspected limited forms of the disease [Internet]. *Mult Scler J* 2015; 21: 866–74.

- Hyun J-W, Woodhall MR, Kim S-H, Jeong IH, Kong B, Kim G, et al. Longitudinal analysis of myelin oligodendrocyte glycoprotein antibodies in CNS inflammatory diseases. *J Neurol Neurosurg Psychiatry* 2017; 88: 811–17.
- Jarius S, Ruprecht K, Kleiter I, Borisow N, Asgari N, Pitarokoili K, et al. MOG-IgG in NMO and related disorders: a multicenter study of 50 patients. Part 1: frequency, syndrome specificity, influence of disease activity, long-term course, association with AQP4-IgG, and origin. *J Neuroinflammation* 2016a; 13: 279.
- Jarius S, Ruprecht K, Kleiter I, Borisow N, Asgari N, Pitarokoili K, et al. MOG-IgG in NMO and related disorders: a multicenter study of 50 patients. Part 2: epidemiology, clinical presentation, radiological and laboratory features, treatment responses, and long-term outcome. *J Neuroinflammation* 2016b; 13: 280.
- Jurynczyk M, Geraldes R, Probert F, Woodhall MR, Waters P, Tackley G, et al. Distinct brain imaging characteristics of antibody-mediated CNS conditions and multiple sclerosis. *Brain* 2017; 140: 617–27.
- Kim S-M, Woodhall MR, Kim J-S, Kim S-J, Park KS, Vincent A, et al. Antibodies to MOG in adults with inflammatory demyelinating disease of the CNS. *Neurol Neuroimmunol Neuroinflamm* 2015; 2: e163.
- Kitley J, Leite MI, Nakashima I, Waters P, McNeill B, Brown R, et al. Prognostic factors and disease course in aquaporin-4 antibody-positive patients with neuromyelitis optica spectrum disorder from the UK and Japan. *Brain* 2012a; 135: 1834–49.
- Kitley J, Waters P, Woodhall M, Leite MI, Murchison A, George J, et al. Neuromyelitis optica spectrum disorders with aquaporin-4 and myelin-oligodendrocyte glycoprotein antibodies: a comparative study. *JAMA Neurol* 2014; 1–8.
- Kitley J, Woodhall M, Waters P, Leite MI, Devenney E, Craig J, et al. Myelin-oligodendrocyte glycoprotein antibodies in adults with a neuromyelitis optica phenotype. *Neurology* 2012b; 79: 1273–7.
- Krupp LB, Tardieu M, Amato MP, Banwell B, Chitnis T, Dale RC, et al. International Pediatric Multiple Sclerosis Study Group criteria for pediatric multiple sclerosis and immune-mediated central nervous system demyelinating disorders: revisions to the 2007 definitions. *Mult Scler J* 2013; 19: 1261–7.
- Mader S, Gredler V, Schanda K, Rostasy K, Dujmovic I, Pfaller K, et al. Complement activating antibodies to myelin oligodendrocyte glycoprotein in neuromyelitis optica and related disorders. *J Neuroinflamm* 2011; 8: 184.
- Miller H, Simpson CA, Yeates WK. Bladder dysfunction in multiple sclerosis. *BMJ* 1965; 1: 1265–9.
- Polman CH, Reingold SC, Banwell B, Clanet M, Cohen J a, Filippi M, et al. Diagnostic criteria for multiple sclerosis: 2010 revisions to the McDonald criteria. *Ann Neurol* 2011; 69: 292–302.
- Reindl M, Di Pauli F, Rostásy K, Berger T. The spectrum of MOG autoantibody-associated demyelinating diseases. *Nat Rev Neurol* 2013; 9: 455–61.
- Sato DK, Callegaro D, Lana-Peixoto MA, Waters PJ, Jorge FMDH, Takahashi T, et al. Distinction between MOG antibody-positive and AQP4 antibody-positive NMO spectrum disorders. *Neurology* 2014; 82: 474–81.
- Sepúlveda M, Armangue T, Martínez-Hernández E, Arrambide G, Sola-Valls N, Sabater L, et al. Clinical spectrum associated with MOG autoimmunity in adults: significance of sharing rodent MOG epitopes [Internet]. *J Neurol* 2016; 263: 1349–60.
- Spadaro M, Gerdes LA, Krumbholz M, Ertl-Wagner B, Thaler FS, Schuh E, et al. Autoantibodies to MOG in a distinct subgroup of adult multiple sclerosis [Internet]. *Neurol Neuroimmunol Neuroinflamm* 2016; 3: e257.
- Waters P, Woodhall M, O'Connor KC, Reindl M, Lang B, Sato DK, et al. MOG cell-based assay detects non-MS patients with inflammatory neurologic disease. *Neurol Neuroimmunol Neuroinflamm* 2015; 2: e89.
- Wingerchuk DM, Banwell B, Bennett JL, Cabre P, Carroll W, Chitnis T, et al. International consensus diagnostic criteria for neuromyelitis optica spectrum disorders. *Neurology* 2015; 85: 177.
- Wingerchuk DM, Lennon VA, Lucchinetti CF, Pittock SJ, Weinschenker BG. The spectrum of neuromyelitis optica [Internet]. *Lancet Neurol* 2007; 6: 805–15.
- Wingerchuk DM, Lennon VA, Pittock SJ, Lucchinetti CF, Weinschenker BG. Revised diagnostic criteria for neuromyelitis optica. *Neurology* 2006; 66: 1485–9.

### 11.1.2.2. Retinal ganglion cell loss in neuromyelitis optica: A longitudinal study.

Citation: Oertel, F. C., Havla, J., Roca-Fernández, A., ... Paul, F., & Brandt, A. U. (2018). *Retinal ganglion cell loss in neuromyelitis optica: A longitudinal study*. Journal of Neurology, Neurosurgery, and Psychiatry, 89(12), 1259–1265. IF: 10.283

(doi:10.1136/jnnp-2018-318382)

(doi:10.1136/jnnp-2018-318382)

(doi:10.1136/jnnp-2018-318382)

(doi:10.1136/jnnp-2018-318382)



(doi:10.1136/jnnp-2018-318382)

(doi:10.1136/jnnp-2018-318382)

(doi:10.1136/jnnp-2018-318382)

### **11.1.2.3. Quantitative spinal cord MRI in MOG-antibody disease, neuromyelitis optica and multiple sclerosis.**

Citation: Mariano, R., Messina, S., **Roca-Fernández, A.**, Leite, M. I., Kong, Y., & Palace, J. A. (2020). *Quantitative spinal cord MRI in MOG-antibody disease, neuromyelitis optica and multiple sclerosis*. Brain J Neurol. 2021 Feb 12;144(1):198–212. IF: 13.501

## Quantitative spinal cord MRI in MOG-antibody disease, neuromyelitis optica and multiple sclerosis

Romina Mariano,<sup>1</sup> Silvia Messina,<sup>1</sup> Adriana Roca-Fernandez,<sup>1</sup> Maria I. Leite,<sup>1</sup> Yazhuo Kong<sup>2,3,4</sup> and Jacqueline A. Palace<sup>1</sup>

Spinal cord involvement is a hallmark feature of multiple sclerosis, neuromyelitis optica with AQP4 antibodies and MOG-antibody disease. In this cross-sectional study we use quantitative spinal cord MRI to better understand these conditions, differentiate them and associate with relevant clinical outcomes. Eighty participants (20 in each disease group and 20 matched healthy volunteers) underwent spinal cord MRI (cervical cord: 3D T<sub>1</sub>, 3D T<sub>2</sub>, diffusion tensor imaging and magnetization transfer ratio; thoracic cord: 3D T<sub>2</sub>), together with disability, pain and fatigue scoring. All participants had documented spinal cord involvement and were at least 6 months post an acute event. MRI scans were analysed using publicly available software. Those with AQP4-antibody disease showed a significant reduction in cervical cord cross-sectional area ( $P = 0.038$ ), thoracic cord cross-sectional area ( $P = 0.043$ ), cervical cord grey matter ( $P = 0.011$ ), magnetization transfer ratio ( $P \leq 0.001$ ), fractional anisotropy ( $P = 0.004$ ) and increased mean diffusivity ( $P = 0.008$ ). Those with multiple sclerosis showed significantly increased mean diffusivity ( $P = 0.001$ ) and reduced fractional anisotropy ( $P = 0.013$ ), grey matter volume ( $P = 0.002$ ) and magnetization transfer ratio ( $P = 0.011$ ). In AQP4-antibody disease the damage was localized to areas of the cord involved in the acute attack. In multiple sclerosis this relationship with lesions was absent. MOG-antibody disease did not show significant differences to healthy volunteers in any modality. However, when considering only areas involved at the time of the acute attack, a reduction in grey matter volume was found ( $P = 0.023$ ). This suggests a predominant central grey matter component to MOG-antibody myelitis, which we hypothesize could be partially responsible for the significant residual sphincter dysfunction. Those with relapsing MOG-antibody disease showed a reduction in cord cross-sectional area compared to those with monophasic disease, even when relapses occurred elsewhere ( $P = 0.012$ ). This suggests that relapsing MOG-antibody disease is a more severe phenotype. We then applied a principal component analysis, followed by an orthogonal partial least squares analysis. MOG-antibody disease was discriminated from both AQP4-antibody disease and multiple sclerosis with moderate predictive values. Finally, we assessed the clinical relevance of these metrics using a multiple regression model. Cervical cord cross-sectional area associated with disability scores ( $B = -0.07$ ,  $P = 0.0440$ ,  $R^2 = 0.20$ ) and cervical cord spinothalamic tract fractional anisotropy associated with pain scores ( $B = -19.57$ ,  $P = 0.016$ ,  $R^2 = 0.55$ ). No spinal cord metric captured fatigue. This work contributes to our understanding of myelitis in these conditions and highlights the clinical relevance of quantitative spinal cord MRI.

- 1 Nuffield Department of Clinical Neurosciences, University of Oxford, Oxford, UK
- 2 CAS Key Laboratory of Behavioral Science, Institute of Psychology, Chinese Academy of Sciences, Beijing 100101, China
- 3 Department of Psychology, University of Chinese Academy of Sciences, Beijing 100049, China
- 4 Wellcome Centre for Integrative Neuroimaging, University of Oxford, Oxford, UK

Correspondence to: Jacqueline A. Palace  
 Level 3, West Wing, John Radcliffe Hospital, Headley Way, Oxford, OX3 9DU, UK  
 E-mail: jacqueline.palace@ndcn.ox.ac.uk

Received April 19, 2020. Revised July 2, 2020. Accepted August 11, 2020. Advance access publication November 18, 2020  
 © The Author(s) (2020). Published by Oxford University Press on behalf of the Guarantors of Brain. All rights reserved.  
 For permissions, please email: journals.permissions@oup.com

Correspondence may also be addressed to: Yazhuo Kong  
16 Lincui Road, Chaoyang District, Beijing 100101, China  
E-mail: kongyz@psych.ac.cn

**Keywords:** neuromyelitis optica; multiple sclerosis; transverse myelitis; neuroinflammation; white matter lesion

**Abbreviations:** Ab = antibody; CSA = cross-sectional area; EDSS = Expanded Disability Status Scale; MTR = magnetization transfer ratio; NMOSD = neuromyelitis optica spectrum disorder

## Introduction

The most well-described inflammatory demyelinating CNS disease is multiple sclerosis, a T-cell predominant immunological disorder of unknown aetiology (Olsson *et al.*, 2016). More recently, two further diseases caused by antibodies have been described. Aquaporin-4 antibodies (AQP4-Ab) target the AQP4 water channels situated on astrocyte foot processes and cause a primary astrocytopathy with secondary demyelination and the clinical phenotype of neuromyelitis optica spectrum disorders (NMOSD) (Lucchinetti *et al.*, 2014). Myelin oligodendrocyte glycoprotein antibodies (MOG-Ab) target myelin and are associated with a primary demyelinating disease with a wider clinical phenotype (Kitley *et al.*, 2014).

Although there is clinical overlap, the underlying pathogenesis for each is unique causing important phenotype differences. Most notable is that multiple sclerosis is associated with chronic disease activity and progressive disability outside of relapse whereas the two antibody diseases cause a relapsing course with more severe relapses and stability in between relapses (Tan *et al.*, 2016). The presence of AQP4-Ab is an independent predictor for relapses and so all patients require long-term immunosuppression therapy to prevent relapses (Weinshenker *et al.*, 2006; Jarius *et al.*, 2012). In MOG-Ab disease, relapses occur in 34–46% of patients (Jurynczyk *et al.*, 2017b; Cobo-Calvo *et al.*, 2018; Senanayake *et al.*, 2018). Differences between the monophasic and relapsing cohorts of this condition are not yet understood. Understanding what drives the differences between and within these disease groups would offer essential information to our understanding of these conditions and to therapeutic development and outcome prediction.

Spinal cord involvement is a hallmark feature of all three conditions and spinal cord lesions are important because they are a major driver of clinical symptoms and may cause substantial disability (Ciccarelli *et al.*, 2019). The classically described MRI findings are short, asymmetrical lesions in multiple sclerosis and longitudinally extensive central lesions ( $\geq 3$  vertebral segments) in both NMOSD and MOG-Ab disease (Ciccarelli *et al.*, 2019) with involvement of the conus being noted particularly in those with MOG-Ab (Mariano *et al.*, 2019). However, short lesions are being reported more commonly in MOG-Ab disease (Dubey *et al.*, 2019; Mariano *et al.*, 2019) and both short and asymptomatic lesions have been reported in patients with AQP4-Ab disease (Flanagan *et al.*, 2015a, b). Although clinical MRI

has provided sound guidelines for an approach to these conditions, there are limitations (Filippi *et al.*, 2019). The use of quantitative and non-conventional imaging gives more insight into the pathogenic process than conventional imaging. Spinal cord MRI is notably more challenging and has been most applied predominantly in multiple sclerosis but recent developments in improved acquisition and analysis have made more widespread application possible (Stroman *et al.*, 2015a, b).

In multiple sclerosis, measurements of spinal cord cross-sectional area (CSA), diffusion metrics and magnetization transfer ratio (MTR) have shown clinical relevance in terms of disability, prognosis and progression (Moccia *et al.*, 2019). In particular, CSA has been shown to be a highly relevant outcome (Casserly *et al.*, 2018) and as having potential as a primary outcome in clinical trials for progressive multiple sclerosis (Cawley *et al.*, 2018; Prados and Barkhof, 2018). Furthermore, it has been shown that diffusion imaging in specific tracts within the cord demonstrate a strong relationship with the relevant clinical outcomes (Naismith *et al.*, 2013). Few studies have shown that these imaging techniques are also applicable in NMOSD (Benedetti *et al.*, 2006; Klawiter *et al.*, 2012; Pessôa *et al.*, 2012; Liu *et al.*, 2015; Matthews *et al.*, 2015; Chien *et al.*, 2019). Finally, one study has looked at atrophy measurements in MOG-Ab disease but none to our knowledge have explored the use of other quantitative measures (Chien *et al.*, 2019). No standardized comparative study has been conducted using these non-conventional methods in the spinal cord across the three diseases and including healthy volunteers.

In this study we used multimodal MRI to study spinal cord involvement in AQP4-Ab-positive NMOSD and MOG-Ab disease and compared it to multiple sclerosis and healthy volunteers. MRI sequences that have shown clinical relevance were selected and clinical data were collected using established measures. We aim to assess if these markers can be used to differentiate these conditions, provide a better understanding of the underlying condition outside of an acute episode, and if they are clinically relevant.

## Materials and methods

### Ethics

All participants signed informed, written consent specific to this study, which was approved the Research Ethics Committee of Cambridge South and was obtained according to the

Declaration of Helsinki. The reporting of this research was done in conjunction with the STROBE supporting guidelines.

## Diagnosis

Testing for MOG-Abs and AQP4-Abs was performed in the autoimmune neurology laboratory at the University of Oxford using cell-based assays, as previously described (Wingerchuk *et al.*, 2014; Waters *et al.*, 2015). In particular, the MOG-Ab assay was to full-length MOG with an IgG1-specific secondary antibody, which increases specificity. All those positive for MOG-Ab were negative for AQP4-Ab and vice versa. The diagnosis of relapsing-remitting multiple sclerosis was made by a trained neurologist according to the 2010 McDonald criteria and confirmed by a second trained neurologist prior to approaching the patient to participate. None of the patients with multiple sclerosis had atypical features.

## Subjects

Our clinic database was screened for adult patients either positive for AQP4-Ab or MOG-Ab and at least one possible episode of cord involvement. Adult multiple sclerosis patients, recruited as a disease control, were approached at consecutive clinic visits if they were confirmed to be relapsing-remitting and to have spinal cord involvement (either symptomatic or asymptomatic). Healthy volunteers were recruited by advertising, as per our ethics regulations. We age and sex-matched these participants as closely as possible to the disease groups. Recruitment ran from January 2018 to March 2019.

Patients in any disease cohort were excluded if they were unwilling to participate, had any contraindication to MRI scanning, including claustrophobia, or had been diagnosed with a confounding neurological comorbidity.

Sample size considerations included the rarity of the diseases being studied and selecting only those with spinal cord involvement. Spinal cord disease occurs in roughly 27% of those with MOG-Ab disease (Jurynczyk *et al.*, 2017b) and 40% of those with AQP4-Ab disease (Pandit *et al.*, 2015), which further limits availability but it was important for the objectives of our study that we included only those with documented cord involvement. We designed the study to have the power to detect group differences in metrics based on data from previous studies (Benedetti *et al.*, 2006; Klawiter *et al.*, 2012; Pessôa *et al.*, 2012; Liu *et al.*, 2015; Matthews *et al.*, 2015; Chien *et al.*, 2019) using G\*power (Faul *et al.*, 2007) as well as recommendations for imaging studies based on evidence from multiple sclerosis (Altmann *et al.*, 2014; Reich *et al.*, 2015).

## Severity and treatment of acute attacks

The severity at nadir for the antibody mediated conditions was the same: median (range) 6.0 (3–9) in MOG-Ab disease and 6.0 (3–8) in AQP4-Ab disease.

In the antibody-mediated conditions, treatment of the acute attack is particularly important (Kleiter *et al.*, 2016). In the AQP4-Ab cohort, all patients were treated acutely in a range of 1–10 days from the onset of symptoms. A total of 45 myelitis attacks occurred in this cohort. Five (from three patients) were treated with intravenous methylprednisolone, followed by

plasma exchange; one was treated with high dose oral prednisolone and the remaining were all treated with intravenous methylprednisolone. In all cases the acute treatment was followed by a tapering dose of oral prednisolone and all of these patients were put on long-term immunosuppression thereafter. In the MOG-Ab cohort, all patients were treated acutely in a range of 1–9 days from the symptom onset. A total of 31 myelitis attacks occurred in this cohort. Twenty-five were treated with intravenous methylprednisolone. Five were treated with high dose oral prednisolone and one was untreated and resolved spontaneously. All those in the MOG-Ab cohort then received tapering oral prednisolone which continued for a range of 6 months to 1 year after their attack. Six of the relapsing MOG-Ab patients were started on an additional long-term immunosuppressant.

## Cervical cord

The clinical scans were reviewed and compared to the research scans collected for this study and patients were categorized as follows: (i) lesion present in cervical cord on clinical scan and on follow-up research scan (persistent); (ii) lesion present on clinical scan but no longer identifiable on follow-up research scan (resolved); or (iii) no lesion in the cervical cord (no cervical).

## Thoracic cord

In the thoracic cord, patients were categorized as either having had thoracic involvement (thoracic involvement) or not (no thoracic). The thoracic images were not further categorized into persistent or not as the axial imaging sequences were not applied in this region.

## Study visit

This research study visit was conducted at least 6 months outside of an acute event in any disease cohort.

During the study visit we collected demographic characteristics (i.e. age at onset of the disease, sex, and self-reported race/ethnicity), date of onset of the disease (disease duration was then calculated from the onset to the date of the research study visit), current treatment, and relapse history, in particular the specific location of any episode of spinal cord involvement.

During the same visit, participants completed a Brief Pain Inventory and a Modified Fatigue Impact Scale (MFIS). An Expanded Disability Status Scale (EDSS) was conducted and each patient underwent a 1-h multimodal spinal cord MRI, described in detail below. Healthy volunteers underwent the same MRI scan.

## MRI data acquisition

MRI scans were acquired on a 3 T Siemens Prisma at the Oxford Centre for Functional MRI of the Brain (FMRIB) with a 64-channel head and neck coil and additional spine array.

The protocol included cervical cord 3D T<sub>1</sub> MPRAGE (repetition time: 2.3 s; echo time: 3.57 ms; flip angle 9°; phase encoding: A ≫ P; res: 0.8 × 0.8 × 0.8 mm<sup>3</sup>), 3D T<sub>2</sub> SPACE (repetition time: 1.5 s; echo time: 95 ms; GRAPPA 2; phase encoding: H ≫ F; res: 0.9 × 0.9 × 0.9 mm<sup>3</sup>), 2D T<sub>2</sub>\* MEDIC (repetition time: 5.6 s; echo time: 71 ms; GRAPPA 2; phase encoding: R ≫ L; res: 0.4 × 0.4 × 3 mm<sup>3</sup>, six echoes), DTI AP/

PA (repetition time: 2.9 s; echo time: 79 s; flip angle 80°; phase encoding: AP and PA; res:  $1.5 \times 1.5 \times 4 \text{ mm}^3$ ,  $b = 1000$ , 32 directions), MT on/off (repetition time: 600 ms; echo time: 8.6 ms; res:  $0.4 \times 0.4 \times 4 \text{ mm}^3$ ) and thoracic cord 3D T<sub>2</sub> (repetition time: 1.5 s; echo time: 136 ms; GRAPPA 2; phase encoding: A  $\gg$  P; res:  $0.8 \times 0.8 \times 0.8 \text{ mm}^3$ ).

A standard operation procedure was developed to ensure uniform acquisition in terms of participant positioning and sequence set-up. As far as possible, scans were done at the same time of day and all participants were encouraged to be remain well hydrated in the 24 h preceding the scan. The same researcher was present at all scans to ensure uniformity (R.M.).

## MRI data processing and analysis

Data were processed with tools from Spinal Cord Toolbox (SCT) v4.0 (De Leener *et al.*, 2017) and FMRIB Software Library (FSL) 6.0 (Jenkinson *et al.*, 2012). See Fig. 1 for illustration of quantitative analysis.

## Structural imaging

### Cervical cord atrophy and lesion measurements

Cervical cord images were analysed to obtain mean CSA, number of lesions and lesion volume. 3D T<sub>1</sub> images were automatically segmented to generate a cord mask using the DeepSeg (Gros *et al.*, 2019) tool in SCT and manually adjusted, when necessary, using the FSL viewer FSleyes (McCarthy, 2019) in slices presenting low contrast between cord and CSF. T<sub>1</sub> images were labelled per segment and straightened before being registered to the PAM-50-T<sub>1</sub> spinal cord template from SCT using a

multi-step registration method based on non-linear transformations. Quality of registration was visually inspected using the quality control mechanism provided by SCT (De Leener *et al.*, 2017). CSA was calculated per vertebral level and the mean CSA from C1–C7 was used for statistical analysis.

Binary lesion masks were manually generated using both axial MEDIC and sagittal T<sub>2</sub>-weighted images, which were co-registered and then confirmed by a blinded rater. In cases of discrepancy, a third rater reviewed the image.

### Thoracic cord atrophy measurements

Thoracic cord images were analysed to obtain the mean CSA. 3D T<sub>2</sub> images were segmented to generate a cord mask using DeepSeg (De Leener *et al.*, 2017) and manually adjusted, when necessary, using the FSL viewer FSleyes (McCarthy, 2019) in slices presenting low contrast between cord and CSF. A multi-step registration method based on non-linear transformations was used to register each magnetic resonance scan to the PAM-50-T<sub>1</sub> spinal cord template (De Leener *et al.*, 2017). Quality of registration was visually inspected using the quality control mechanism provided by SCT (De Leener *et al.*, 2017). CSA was calculated per vertebral level to encompass the whole thoracic cord but excluding the conus, therefore the mean CSA for each participant was taken from T<sub>1</sub> to one level above the conus.

### Cervical cord diffusion tensor imaging

Diffusion data were acquired in two phase encoding directions: AP and PA and merged. FSL tools topup (Andersson *et al.*, 2003; Smith *et al.*, 2004) and eddy (Andersson and Sotiropoulos, 2016) were used for distortion correction. Diftit (Jenkinson *et al.*, 2012) was then used to generate fractional

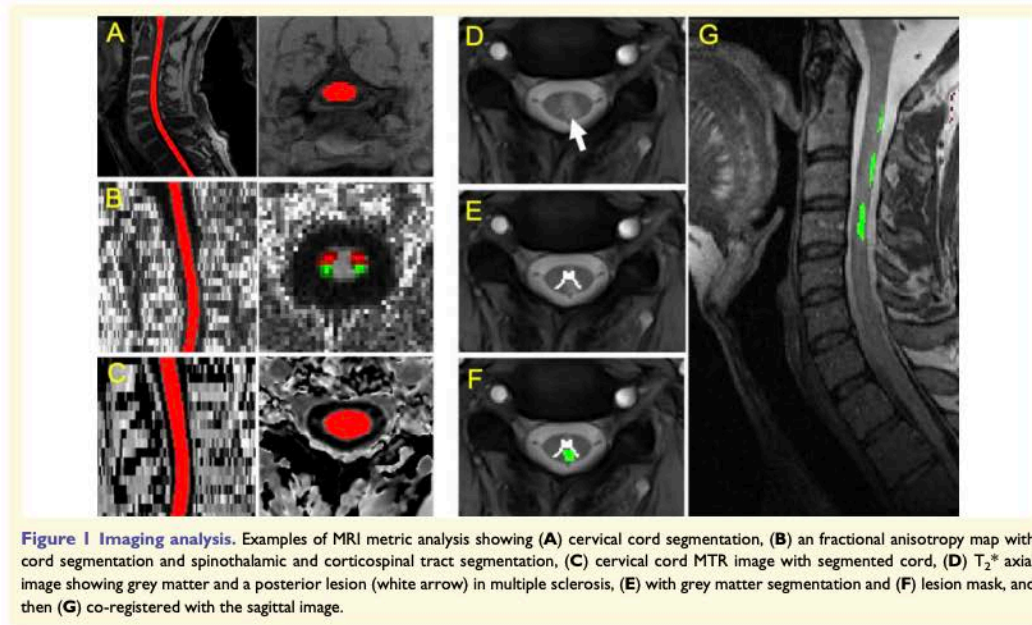


**Figure 1** Imaging analysis. Examples of MRI metric analysis showing (A) cervical cord segmentation, (B) an fractional anisotropy map with cord segmentation and spinothalamic and corticospinal tract segmentation, (C) cervical cord MTR image with segmented cord, (D) T<sub>2</sub>\* axial image showing grey matter and a posterior lesion (white arrow) in multiple sclerosis, (E) with grey matter segmentation and (F) lesion mask, and then (G) co-registered with the sagittal image.



anisotropy and mean diffusivity maps. The cord was segmented within the native DTI space and this mask was applied to each quantitative map. A multi-step registration method based on non-linear transformations was used to register the fractional anisotropy/mean diffusivity image to the PAM-50 spinal cord template via the previously registered anatomical references with SCT tool `register_multimodal` (De Leener *et al.*, 2017). The template was then warped into fractional anisotropy/mean diffusivity image and metrics (whole cord, grey matter, white matter, lesional areas and normal-appearing cord) were then extracted per slice using `sct_extract_metric` (De Leener *et al.*, 2017). Tract-based analysis was done using the PAM-50 probability atlas, which includes the corticospinal and spinothalamic tracts.

#### Cervical cord magnetization transfer ratio

Magnetization transfer (MT)-on image was registered to MT-off image and MTR was computed using SCT. The MTR image was registered to the PAM-50 spinal cord template using the SCT tool `register_multimodal`, (De Leener *et al.*, 2017) as described above for the DTI analysis. The template was then warped into the map and metrics were extracted per slice using `sct_extract_metric` (De Leener *et al.*, 2017).

#### Statistical analysis

Statistical analysis was performed using SPSS v26.0 and GraphPad Prism version 6.0c. Mann-Whitney U-tests were used when comparing continuous variables. A chi-square test was used for comparing frequencies. Between-group comparisons were done using ANCOVA (general linear model in SPSS with age and sex as covariates) with *post hoc* Bonferroni. Within-group comparisons were done using ANOVA with *post hoc* Tukey or Kruskal-Wallis with *post hoc* Dunn test. Binomial logistic and multivariate regression models were used to identify factors associated with disability, pain and fatigue. *P*-values were two-tailed and statistical significance was set at 0.05. Principal component analysis was run using SIMCA v14.0.0.1359 (MKS Data Analytics Solutions, Sweden) with all MRI metrics that showed differences between groups to assess for spontaneous, unsupervised clustering. Thereafter a predictive regression analysis was run and an orthogonal partial least square analysis (OPLS-DA) model with seven cross-validation rounds and 200 iterations, comparing the three conditions in pairs (MOG-Ab versus AQP4-Ab, MOG-Ab versus multiple sclerosis, and AQP4-Ab versus multiple sclerosis). Each model was assessed for total variation in X (R2X), the total variation in Y (R2Y) and the accuracy of the prediction (q2). An R2Y of 100% suggests the model can explain all variation between groups. A higher R2Y and q2 mean a better separation. A q2 of 0.4 is generally accepted as the threshold for significance (Waterman *et al.*, 2010).

#### Data availability

All data were collected and stored in accordance with GDPR guidelines. Its availability is dependent on specific collaboration and data sharing agreements made with the host organization. Analysis software and methods are publicly available.

## Results

### Demographics

The study consisted of 80 participants (20 in each of the four groups). Where possible, key baseline characteristics were matched; however, there are important differences between these diseases that made complete matching impossible and this was handled by adjusting for differences in the statistical analysis (see below). The demographics of each group are represented in Table 1. Patients with AQP4-Ab tended to be older and with a female and non-Caucasian predominance, in keeping with demographics described in the literature (Kitley *et al.*, 2012) and the MOG-Ab group had the shortest disease duration.

### Spinal cord involvement throughout disease course

All patients in the three disease cohorts were selected if they had spinal cord involvement during the course of their disease. In keeping with the recognized differences in the antibody diseases versus multiple sclerosis, patients with MOG-Ab and AQP4-Ab myelitis all had symptomatic transverse myelitis, and those with multiple sclerosis myelitis included both symptomatic and asymptomatic transverse myelitis lesions. The distribution of sagittal areas of the cord involved (cervical, thoracic and/or conus) is shown in Fig. 2 and highlights more conus involvement and lack of isolated cervical cord involvement in MOG-Ab disease, and more isolated cervical involvement in multiple sclerosis. The axial location of the lesions was central in 16/20 (80%) of the patients with MOG-Ab disease and 17/20 (85%) of those with AQP4-Ab. In the multiple sclerosis group, more than one lesion was present in each person with a total of 48 lesions noted. Nineteen of 48 (40%) were posterior and 29/48 (60%) were lateral; and none were central.

### Clinical data

#### Motor

The median EDSS scores did not differ significantly between the three groups and are as follows: MOG-Ab 1.5 (0–8), AQP4-Ab 3.0 (0–8) and multiple sclerosis 2 (0–6). However, in patients with MOG-Ab, there was a single patient with an EDSS of 8, the remainder of the patients were all  $\leq 3$  (Table 1).

#### Sphincter

When considering long-term sphincter dysfunction, this occurred predominantly in those with MOG-Ab disease (13 with sphincter dysfunction, four requiring catheterization) when compared to AQP4-Ab (nine with sphincter dysfunction, two requiring catheterization) and multiple sclerosis (six with sphincter dysfunction, one requiring catheterization).

**Table 1 Demographics and clinical features**

	MOG	AQP4	Multiple sclerosis	Healthy volunteers	P-values
<i>n</i>	20	20	20	20	–
Mean age ± SD	43.4 ± 10.9	52.9 ± 12.5	45.3 ± 6.9	44.5 ± 14.3	0.010
Sex, female:male	10:10	13:7	11:9	12:8	0.796
Ethnicity (%)					0.001
Caucasian	20 (100)	11 (55)	20 (100)	18 (90)	
Afro-Caribbean	0 (0)	5 (25)	0 (0)	1 (5)	
Asian	0 (0)	4 (20)	0 (0)	1 (5)	
Phenotype (%)					<0.001
Isolated TM	4 (20)	10 (50)	0 (0)	–	
TM + ON	10 (50)	4 (20)	0 (0)	–	
TM + BS/BR	5 (25)	4 (20)	8 (40)	–	
TM + BS/BR + ON	1 (5)	2 (10)	12 (60)	–	
Median disease duration in months (range)	40.1 (8.5–239.9)	141.5 (8.5–297.7)	147.1 (10.4–252.1)	–	0.015
Mean total number of attacks	2	3	3	–	0.949
Mean number of myelitis attacks	1.1	2.3	0.75 <sup>a</sup>	–	0.045
Median EDSS (range)	1.5 (0–8)	3 (0–8)	2 (0–6)	–	0.109
Sphincter dysfunction (number requiring catheter)	13 (4)	9 (2)	6 (1)	–	0.084
Mean BPI score ± SD	2.04 ± 4.16	5.66 ± 4.19	2.28 ± 3.45	0	0.009
Mean MFIS score ± SD	27.4 ± 18.92	35.26 ± 20.8	36.05 ± 14.27	8.9 ± 7.2	0.260

<sup>a</sup>This is the number of clinically symptomatic attacks.

BPI = Brief Pain Inventory; BR = brain; BS = brainstem; MFIS = Modified Fatigue Impact Scale; ON = optic neuritis; SD = standard deviation; TM = transverse myelitis.

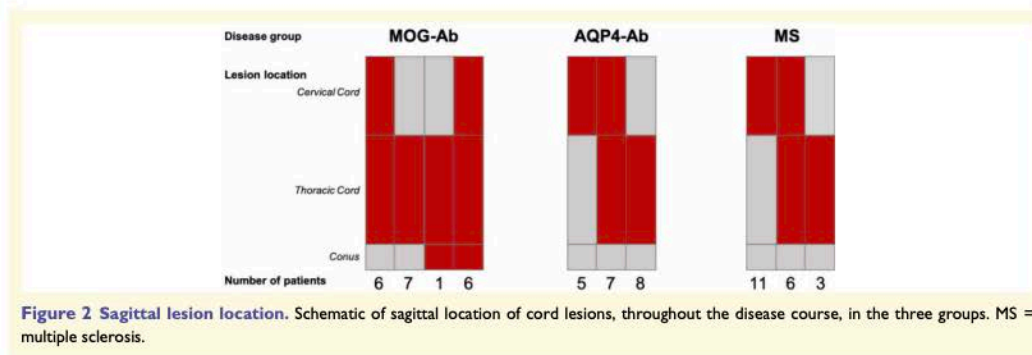


**Figure 2 Sagittal lesion location.** Schematic of sagittal location of cord lesions, throughout the disease course, in the three groups. MS = multiple sclerosis.

### Pain

Those with AQP4-Abs had significantly higher scores than those with MOG-Ab ( $P = 0.006$ ) and multiple sclerosis ( $P = 0.045$ ) [ $\chi^2(2) = 10.18$ ,  $P = 0.006$ ].

### Fatigue

Five patients with MOG-Abs, nine patients with AQP4-Abs, eight patients with multiple sclerosis and 0 healthy volunteers reached the diagnostic score of 38 on the MFIS. The mean MFIS scores in all three disease groups ( $P = 0.006$ ,  $<0.001$ ,  $<0.001$ , respectively) were significantly higher than healthy volunteers [ $\chi^2(3) = 29.13$ ,  $P \leq 0.001$ ].

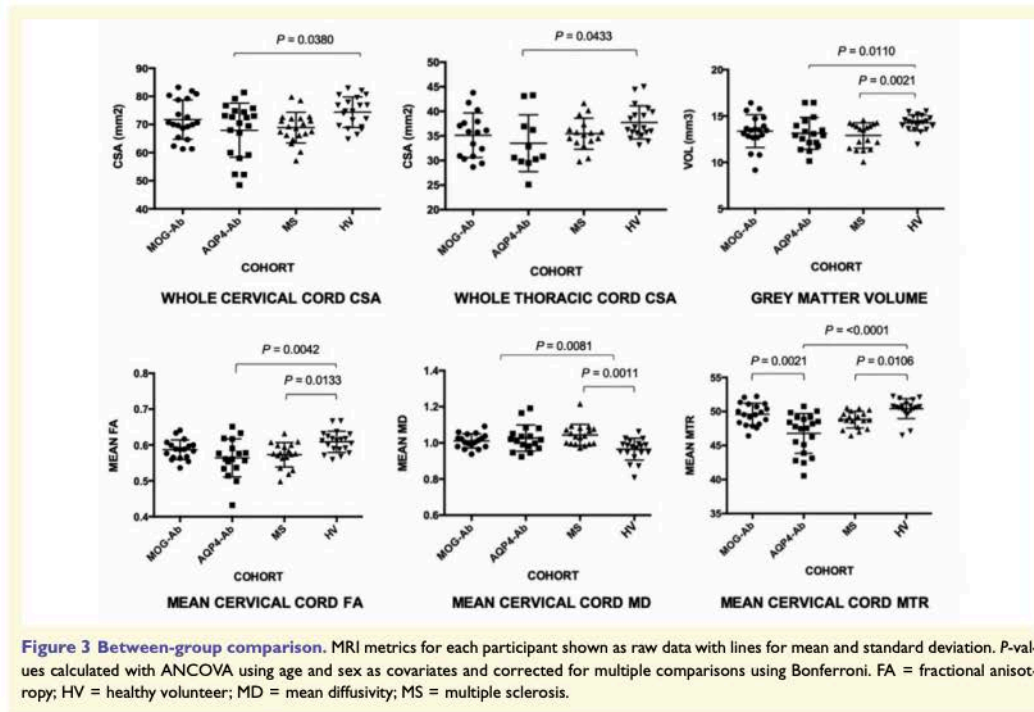
### Imaging results

Of the five imaging modalities for each of the 80 subjects, a total of 34 individual scans were not included because of

either poor quality or incomplete acquisition (six diffusion, 18 thoracic, four MTR, six grey matter segmentations). **Supplementary Table 1** shows all raw data means ± standard deviation (SD) as well as the estimated marginal means, after age and sex correction. The imaging results are shown graphically in **Fig. 3**, the between-group comparison, and **Fig. 4**, the within-group comparison based on whether there is a persistent lesion, a previous lesion that has now resolved on MRI or no lesion ever affecting that area. Key features of interest are highlighted below.

### Cervical cord lesions

Nine of 12 AQP4-Abs and 14 of 17 multiple sclerosis cervical cord lesions were persistent, all 12 cervical cord lesions in MOG patients had resolved on structural imaging.



Mean cervical lesion volume did not differ between AQP4-Ab and multiple sclerosis (247.78 mm<sup>3</sup> versus 305.56 mm<sup>3</sup>,  $P = 0.853$ ); however, the mean number of lesions was significantly different with a greater number of lesions occurring in patients with multiple sclerosis ( $1 \pm 0$  versus  $3 \pm 2$ ,  $P = 0.007$ ), in keeping with the expected single, long lesions in AQP4-Ab disease.

### Cervical cord cross-sectional area

The patients with AQP4-Abs showed a significant reduction in mean cervical cord CSA compared to the healthy volunteers ( $P = 0.038$ ) [ $F(3,76) = 3.234$ ,  $P = 0.027$ ] with those with lesions driving this difference. This is evidenced by the significant difference between those with persistent lesions when compared to those without cervical cord involvement ( $P = 0.035$ ) [ $F(2,17) = 3.788$ ,  $P = 0.035$ ]. The mean CSA of those without a history of cervical cord lesions being almost equivalent to healthy volunteers (73.86 mm<sup>2</sup> versus 74.38 mm<sup>2</sup>,  $P = 0.815$ ).

In those with multiple sclerosis there was a significant reduction compared to the healthy volunteers on direct comparison (68.96 mm<sup>2</sup> versus 74.71 mm<sup>2</sup>,  $P = 0.005$ ), not significant when comparing all groups. Additionally, the relationship with the lesion status was not significant (Fig. 4).

In those with MOG-Abs, there was no significant reduction in CSA overall compared to healthy volunteers or when comparing those with previous lesions in the cervical cord to those without (Fig. 4).

### Thoracic cord cross-sectional area

Patients with AQP4-Abs just reached significance reduction in thoracic cord CSA compared to the healthy volunteers ( $P = 0.043$ ) [ $F(3,46) = 3.252$ ,  $P = 0.032$ ]. This was driven by involvement of the thoracic cord with those that had never been affected by thoracic cord lesions having values comparable to the healthy volunteers group (37.11 mm<sup>2</sup> versus 37.91 mm<sup>2</sup>,  $P = 0.677$ ). This pattern is not evident in the multiple sclerosis group. There were no patients with MOG-Ab disease that did not have thoracic cord involvement and no thoracic lesions were persistent. The group mean did not differ statistically from the healthy volunteers; however, the only patient to reach EDSS > 6 in the MOG-Ab group had the smallest thoracic CSA (28.69 mm<sup>2</sup>).

### Cervical cord grey matter volume

The patients with AQP4-Ab disease ( $P = 0.011$ ) and with multiple sclerosis ( $P = 0.002$ ) showed a significant

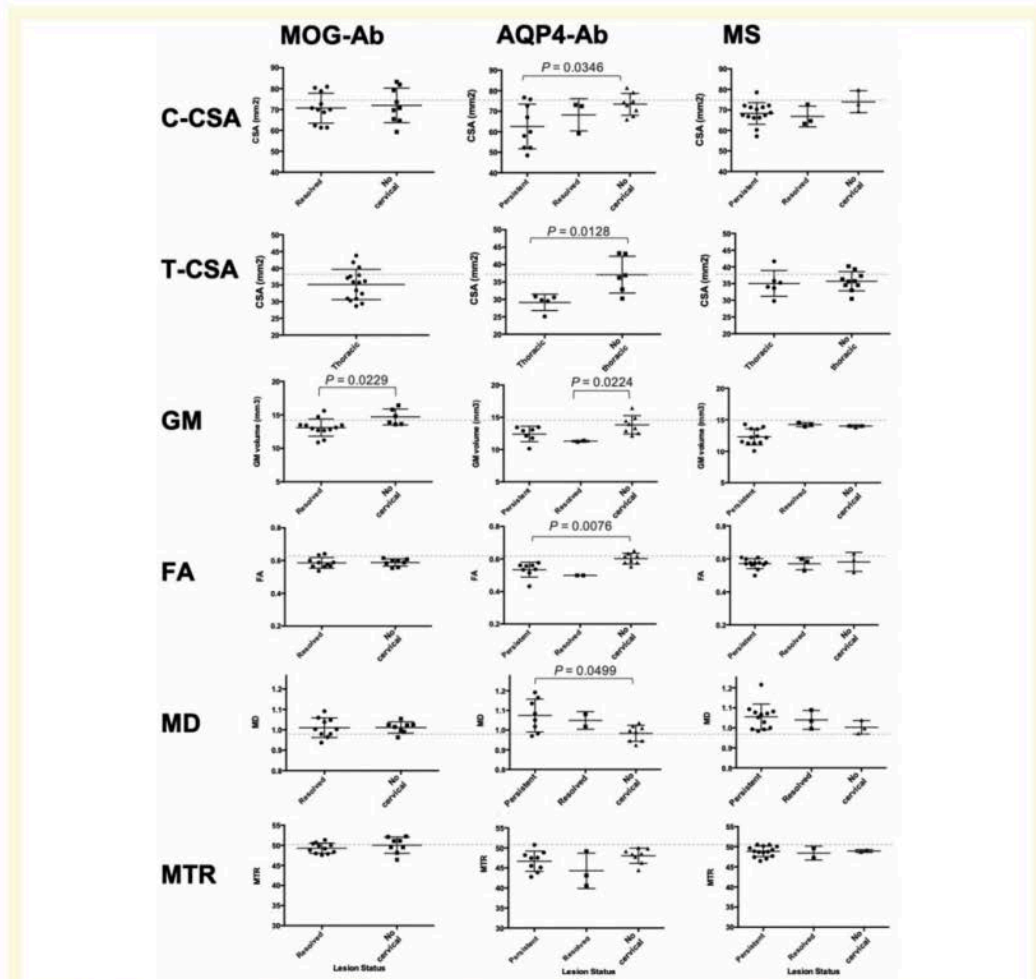


**Figure 4** Within-group comparison. ANOVA (with *post hoc* Tukey) or Kruskal Wallis (with *post hoc* Dunn) results for within-group comparisons in each cohort, dividing patients by lesion status (*x*-axis) in the cervical cord (persistent, resolved or no cervical) and in the thoracic cord (thoracic or no thoracic). No patients with MOG-Ab had persistent cervical cord lesions. The dotted line represents the healthy volunteer (HV) mean for each modality. C-CSA = cervical cross-sectional area; FA = fractional anisotropy; GM = grey matter; MD = mean diffusivity; MS = multiple sclerosis; T-CSA = thoracic cross-sectional area.

reduction in mean cervical cord grey matter volume compared to the healthy volunteers [ $F(3,74) = 3.984$ ,  $P = 0.011$ ], but not in those with MOG-Ab. This effect was related to lesions in the AQP4 group (Fig. 4) and lower but not significantly so in persistent lesions in the multiple sclerosis group.

Patients with MOG-Ab and affected cervical cords had significantly reduced grey matter volume when compared to MOG-Ab without cervical cord lesions ( $P = 0.023$ ) and

compared to the healthy volunteers ( $P = 0.010$ ) [ $\chi^2(1) = 11.01$ ,  $P = 0.004$ ].

### Cervical cord DTI

The mean fractional anisotropy in both those with AQP4-Ab ( $P = 0.004$ ) and multiple sclerosis ( $P = 0.013$ ) was significantly reduced compared to the healthy volunteers [ $F(3,73) = 5.323$ ,  $P = 0.002$ ]. This difference appeared to be

driven by the lesions in AQP4-Ab (Fig. 4). In MOG-Ab disease, the mean fractional anisotropy was comparable to healthy volunteers whether the cervical cord had been involved or not (Fig. 4).

Cervical lesional fractional anisotropy was significantly reduced compared to the normal-appearing spinal cord in both AQP4-Ab ( $0.46 \pm 0.10$  versus  $0.56 \pm 0.04$ ,  $P = 0.037$ ) and multiple sclerosis ( $0.43 \pm 0.06$  versus  $0.59 \pm 0.02$ ,  $P \leq 0.001$ ), and the mean lesional fractional anisotropy did not differ between groups ( $0.46$  versus  $0.43$ ,  $P = 0.539$ ). MOG-Ab patients had fractional anisotropy values comparable to healthy control subjects whether previous lesions affected the cervical cord or not (Fig. 4).

The mean mean diffusivity was increased in those with AQP4-Ab ( $P = 0.008$ ) and in multiple sclerosis ( $P = 0.001$ ) compared to healthy volunteers [ $F(3,73) = 6.794$ ,  $P \leq 0.001$ ].

### Cervical cord magnetization transfer ratio

Cervical cord MTR showed very similar patterns. Mean MTR was reduced in both AQP4-Ab ( $P \leq 0.001$ ) and multiple sclerosis ( $P = 0.011$ ) groups compared to healthy volunteers; as well as in AQP4-Ab when compared to the MOG-Ab group ( $P = 0.002$ ) [ $F(3,76) = 7.336$ ,  $P \leq 0.001$ ]. Those with MOG-Ab showed no difference in mean MTR whether they had cervical cord involvement or not and, in both subsets, the mean MTR was comparable with healthy volunteers (49.28, 50.02 and 50.41, respectively).

Cervical lesional MTR was significantly reduced compared to the normal-appearing spinal cord in both AQP4-Ab ( $41.43 \pm 2.08$  versus  $47.70 \pm 4.85$ ,  $P = 0.003$ ) and multiple sclerosis ( $43.10 \pm 1.03$  versus  $49.40 \pm 3.82$ ,  $P \leq 0.001$ ) and the mean lesional values did not differ significantly between groups ( $41.43 \pm 2.08$  versus  $43.10 \pm 1.03$ ,  $P = 0.269$ ). Supplementary Fig. 1 shows all lesional metrics compared to surrounding normal-appearing spinal cord in patients with persistent lesions.

### Monophasic versus relapsing disease in MOG-Ab disease

These results are shown in Supplementary Fig. 2.

In those with MOG-Ab disease, volumetric measures of cervical cord area, thoracic cord area, as well as grey matter volume were lower in the 14 relapsing patients and lower values occurred in both those with relapsing myelitis ( $n = 3$ ) as well as those whose relapses occurred elsewhere ( $n = 11$ ). This reached significance in the thoracic cord, the location that was affected in all MOG-Ab patients, ( $33.60 \pm 3.75$  versus  $40.75 \pm 3.86$ ,  $P = 0.002$ ) and held when comparing the monophasic to relapsing myelitis ( $40.75 \pm 3.86$  versus  $29.48 \pm 0.81$ ,  $P = 0.003$ ) and those with non-myelitis relapses ( $40.75 \pm 3.86$  versus  $34.96 \pm 3.27$ ,  $P = 0.012$ ). Additionally, when comparing thoracic cord volumes of those with relapsing MOG-Ab disease to healthy volunteers there was a significant difference ( $33.60 \pm 3.75$  versus  $37.86 \pm 3.22$ ,  $P = 0.003$ ) but not when

comparing monophasic MOG-Ab disease to healthy volunteers ( $40.75 \pm 3.86$  versus  $37.86 \pm 3.22$ ,  $P = 0.100$ ). Age and sex were included as covariates in all models.

### Clinical association of cervical cord imaging metrics

We built a multiple regression model for each of the three clinical outcomes: EDSS, pain and fatigue (Supplementary Table 2). We included age, sex, disease duration and disease type and then included significantly associated MRI metrics using a stepwise regression model. Due to anatomical and physiological *a priori* hypotheses, we assessed associations between EDSS and corticospinal tract fractional anisotropy, and pain spinothalamic tract fractional anisotropy.

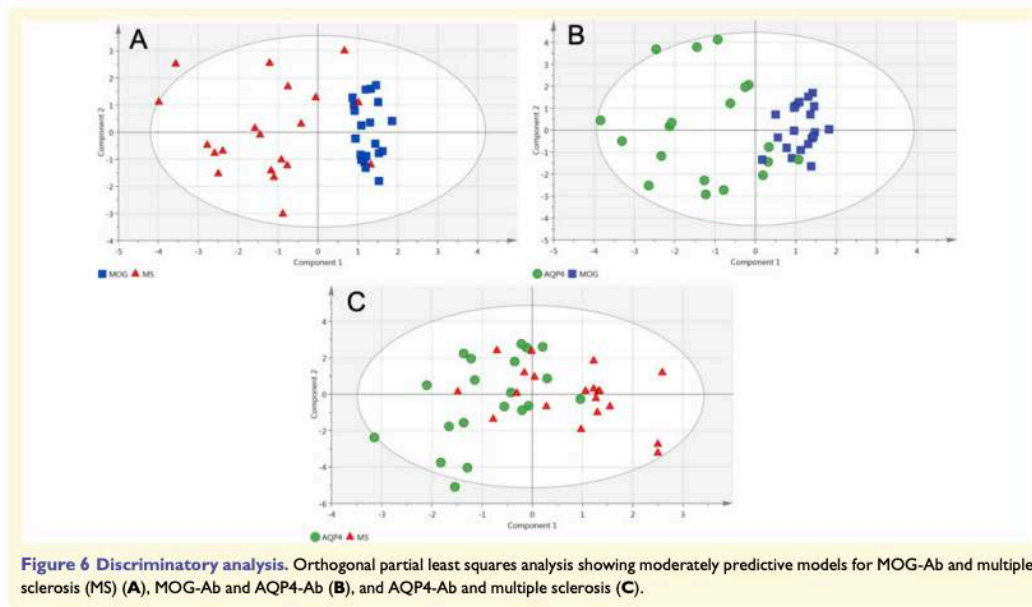
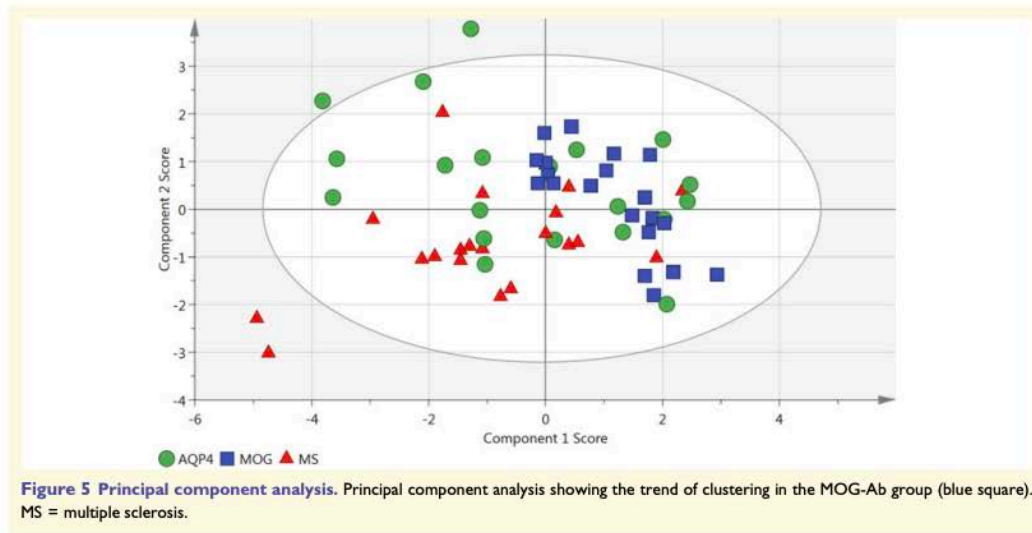
In the EDSS model, the mean cervical cord CSA was the only significant variable ( $B = -0.07$ ,  $P = 0.0440$ , overall model  $R^2 = 0.20$ ).

In the pain model, the fractional anisotropy in the spinothalamic tract ( $B = -19.57$ ,  $P = 0.016$ ), the presence of AQP4-Ab ( $B = 14.08$ ,  $P = 0.010$ ) and EDSS score ( $B = 0.46$ ,  $P = 0.002$ ) were significant predictors (overall model  $R^2 = 0.55$ ). As no MRI metrics associated with fatigue, only clinical factors were included.

As disability and fatigue showed a significant relationship in the univariate analysis, we conducted a logistic regression using the cut-off of  $\geq 38$  to represent clinically significant fatigue. The odds ratio (OR) was 1.5 for every 1-point increase in EDSS [OR = 1.5, confidence interval (CI) = 1.05–2.15,  $P = 0.038$ ].

### Discriminatory analysis

To test the ability of these MRI measures to discriminate between diseases and predict the disease type, we used the MRI metrics in a principal component analysis. Variables included were as follows: mean cervical CSA, whole cervical cord MTR, whole cervical cord fractional anisotropy, whole cervical cord mean diffusivity, number of lesions, sagittal lesion location and length, cervical cord grey matter volume and thoracic cord volume. Patients with MOG-Ab tended to spontaneously separate (Fig. 5). We therefore applied discriminatory models to each pair separately using OPLS-DA). A moderately predictive model was created to distinguish MOG-Ab from multiple sclerosis ( $q^2 = 0.43$ , R2Y 68%) (Fig. 6A). The most important classifiers between MOG-Ab and multiple sclerosis were number of persistent lesions, sagittal lesion location (thoracic more predictive of MOG-Ab), whole cervical cord mean diffusivity and mean cervical cord CSA. A model was also built to distinguish MOG-Ab from AQP4-Ab ( $q^2 = 0.51$ , R2Y 59%) (Fig. 6B). The most important classifiers between MOG-Ab and AQP4-Ab were number of persistent lesions, sagittal lesion location (thoracic predictive of MOG-Ab) and whole cervical cord MTR. AQP4-Ab could not be distinguished significantly from multiple sclerosis ( $q^2 = 0.37$ , R2Y = 49%) (Fig. 6C).



## Discussion

This is the first paper, to our knowledge, that uses quantitative MRI methods to study spinal cord involvement in MOG-Ab disease and compare it with AQP4-Ab-positive NMOSD and multiple sclerosis. In particular, we highlight

that both patients with MOG-Ab and AQP4-Ab disease show changes only in the area of the cord affected by the lesion. In MOG-Ab there is evidence of atrophy in some cases, and this appears to more significantly involve the grey matter. However, it is milder than AQP4-Ab disease and in addition, in keeping with their good clinical recovery, those with

MOG-Ab show no difference to healthy volunteers in quantitative measures using diffusion and magnetization-weighted imaging after recovery from the myelitis. Additionally, these spinal cord MRI metrics show clinical relevance in terms of pain and disability, but not fatigue. Our results suggest that cervical cord CSA associates with EDSS and spinothalamic fractional anisotropy may be predictive of pain scores.

To understand the evolution of spinal cord involvement in these conditions it is important to consider findings throughout the disease course. Therefore, the results of our research MRI scans, conducted at least 6 months after an acute event, are presented in a way that is informed by the earlier presentations. None of the patients with MOG-Ab had persistent cord lesions. This is a clinically relevant finding as the imaging protocol is one used in clinical practice in many centres and may be useful diagnostically where a reliable MOG-Ab test is unavailable or gives a low positive and thus less specific result. Those with AQP4-Ab had single, predominantly central, long lesions as is typical of this disease (Tackley *et al.*, 2014a). Patients with multiple sclerosis had multiple small asymmetrical lesions, in keeping with the literature (Eden *et al.*, 2019).

Those with AQP4-Ab showed the greatest atrophy in the cervical and thoracic cord and grey matter as well as the most tissue damage as represented by the quantitative MRI metrics (fractional anisotropy, mean diffusivity and MTR). This damage was localized to areas of the cord involved during the acute attack. Those with persistent lesions had the worst metrics while areas of the cord that had never been involved were comparable to healthy volunteers. Lesions in AQP4-Ab disease therefore appeared to cause more localized damage than in multiple sclerosis and MOG-Ab disease. The involvement of the grey matter is expected in AQP4-Ab disease as it typically involves the central cord (Tackley *et al.*, 2014b).

In those with multiple sclerosis the overall mean metrics were abnormal when compared to healthy volunteers in grey matter volume, mean diffusivity, fractional anisotropy and MTR. However, there were no clear differences between those with lesions and those without. This suggests abnormalities in the normal-appearing spinal cord. This is an expected finding due to the background neurodegeneration and the findings of quantitative abnormalities in normal-appearing brain tissue in multiple sclerosis (Moll *et al.*, 2011). However, it must be taken into consideration that in multiple sclerosis because subclinical lesion activity is typical, and frequent enough MRI scans cannot be performed, normal-appearing tissue on MRI could include previous 'MRI resolved' lesions. Although in multiple sclerosis, lesions are not typically central, grey matter damage is well described in pathology (Geurts and Barkhof, 2008) and brain grey matter volume loss is predominant even in the early stages of multiple sclerosis (Calabrese *et al.*, 2007).

In MOG-Ab patients all reported metrics were normal except that of the grey matter volume in those with previous lesions. The findings in the MOG-Ab group are consistent with the clinical recovery in MOG-Ab patients, where in our

clinical practice we also see normalization of sensory and visual evoked potentials. This is not expected in multiple sclerosis or AQP4-Ab disease.

As mentioned, central cord involvement is well reported in those with AQP4-Ab and in MOG-Ab disease (Mariano *et al.*, 2019) and a recent study (Dubey *et al.*, 2019) described the 'H' sign seen on acute axial T<sub>2</sub> imaging where involvement of the cord appears to be limited to the grey matter. Grey matter involvement in MOG-Ab disease is proving to be increasingly important with a cortical phenotype now recognized (Ogawa *et al.*, 2017), documented grey matter involvement in ADEM-like disease (Hacohen *et al.*, 2017) and reports of acute flaccid myelitis associated with MOG-Ab (Dubey *et al.*, 2018; Wang *et al.*, 2018). Our finding of a reduction in grey matter volume in the MOG-Ab affected cord area further supports this and is the first quantitative evidence of long-term damage of grey matter. As measures such as fractional anisotropy and MTR are thought to better represent myelination and axonal integrity, (Miller *et al.*, 1998), the fact that they are unaffected may represent either that white matter is less affected or recovers better in the course of MOG-Ab disease but this grey matter involvement also requires further research into the underlying pathogenesis of MOG-Ab disease and the location of MOG expression within the CNS. The degree of grey matter atrophy in the cervical cord did not correlate with any clinical outcomes. However, as the predominant area involved in MOG-Ab disease is the thoracic cord and the most common symptoms that persist after an attack of myelitis are related to sphincter dysfunction, it may be the cervical cord does not capture this. We recently described the outcomes in myelitis in MOG-Ab disease (Mariano *et al.*, 2019) and found an association with conus lesions and long-term catheter requirements. However, conus involvement does not fully explain sphincter dysfunction in all patients with MOG-Ab. Given the importance of the grey matter in micturition pathways and sphincter control mechanisms (Fowler *et al.*, 2008), we hypothesize that this may be due to grey matter involvement in the lower cord and that improvements in thoracic cord imaging techniques would assist in studying this. Additionally, although our limited thoracic cord measurements did not correlate with disability outcomes, it must be noted that they only patient who reached EDSS 8 in the MOG-Ab cohort had the smallest thoracic cord volume and so the variability in the CSA values in the thoracic cord in MOG-Ab may suggest variable levels of tissue loss during the acute attack.

We then looked at the effect of relapses in the MOG-Ab disease group. It has been established that the presence of AQP4-Ab is predictive of relapsing disease and so it is recommended that all patients be treated with immunosuppressive treatment to prevent relapses (Weinshenker *et al.*, 2006; Jarius *et al.*, 2012). However, in MOG-Ab disease relapse rates of 34–46% (Jurynczyk *et al.*, 2017b; Cobo-Calvo *et al.*, 2018; Senanayake *et al.*, 2018) have been reported and so many patients may remain monophasic in their disease course and this has important treatment implications.

We compared those with relapsing disease and found that volumetric cord measures were lower in those with relapsing disease, even if the relapse occurred outside of the cord. It has been argued that if followed-up for long enough, all patients with MOG-Ab disease may eventually have a relapse and it is a continuum. However, our findings suggest that relapsing MOG-Ab disease may be distinct from monophasic disease.

We then considered the clinical relevance of the MRI metrics with regard to our three outcomes: disability, pain and fatigue. Our findings suggested that mean cervical cord area associates with disability independent of the disease type. It has already been suggested as an outcome measure for clinical trials in primary progressive multiple sclerosis (Cawley *et al.*, 2018) and has also been shown to be clinically useful in HTLV-1-associated neurological disease (Azodi *et al.*, 2017). Our hypothesis was that this measure would show an association with disability in our total cohort, independent of disease type. It was the only imaging metric that correlated with disability in a univariate analysis in each disease and, when combining diseases, it was the metric that built the strongest model using a stepwise regression. However, only 20% of disability is accounted for by this model and this is in keeping with other studies that have assessed cervical cord atrophy as measures of disability in multiple sclerosis (Tsagkas *et al.*, 2018; Song *et al.*, 2020). Correlations of disability with imaging outcomes is complex because disability scoring is imperfect and usually non-linear and imaging markers need to capture total pathology (volume loss and damage in remaining tissue) and account for the eloquence of different areas affected (although spinal cord is likely to be eloquent). Studies have largely only considered brain imaging markers as spinal cord imaging is notoriously difficult, particularly to standardize across centres to allow for larger cohorts. Future work may identify feasible methods for validating and incorporating these spinal cord measures into AQP4-Ab and MOG-Ab clinical trials together with brain imaging markers. Having an episode of myelitis in the context of NMOSD with AQP4-Abs is an independent predictor of pain separate to EDSS. Additionally, independent of disease type, we have shown for the first time, fractional anisotropy scores in the spinothalamic tracts associate with pain scores. We show that tract-specific analysis may be a useful tool when studying spinal cord involvement.

No spinal cord metric used in this study was able to capture sphincter dysfunction, particularly prominent in those with MOG-Ab. However, as described above, we feel that the thoracic cord would be more useful in the study of sphincter dysfunction as lower cord involvement is more common in MOG-Ab disease.

The final outcome that we studied was fatigue. There was no measure within the spinal cord that was able to explain fatigue and it is possible that fatigue is mainly driven by brain pathology although this may depend on the type of fatigue. It is a symptom that was experienced in all three conditions. Fatigue is a complex symptom with pathways that are still unclear (Braley and Chervin, 2010). It may be that

studies of functionality, such as resting state functional MRI, are more useful in better understanding this symptom. There is some evidence of its use in the brain (Jaeger *et al.*, 2019) but functional MRI of the spinal cord is an emerging field that may be useful in better understanding the complexity of such symptoms (Powers *et al.*, 2018).

Finally, we considered whether or not these metrics are able to discriminate these conditions. Our models showed a moderate ability to differentiate MOG-Ab disease cords from those with AQP4-Ab or multiple sclerosis, by using cord metrics alone, but the model for AQP4-Ab versus multiple sclerosis was not significant. In the brain it has been shown that clinical features of acute brain scans were able to differentiate the antibody-mediated conditions from multiple sclerosis (Jurynczyk *et al.*, 2017a). If we consider the acute spinal cord MRI features of AQP4-Ab and MOG-Ab myelitis, we have shown in a previous study that while there are notable differences i.e. predominance of the conus and multiple lesions in MOG-Ab, that 76% of patients with MOG-Ab and 89% of patients with AQP4-Ab had a long central lesion on their acute scan and so there is overlap in the acute setting between the antibody conditions. However, when we consider the features at follow-up, as we have shown in this study, the MOG-Ab group becomes distinct due to the significant recovery of both clinical MRI features and of the quantitative measures used in our study. While the predictive strength may not be adequate for individual patient diagnostic precision, these findings further support the evidence that MOG-Ab disease appears to be different from both AQP4-Ab disease and multiple sclerosis, which may be related to its milder phenotype with good recovery. In this cross-sectional comparison, AQP4-Ab and multiple sclerosis could not be accurately differentiated. Therefore, a prospective longitudinal study would be necessary to explore these conditions as one would expect worsening of all metrics in multiple sclerosis independent of relapse.

## Limitations

We acknowledge the limitations of this study being sample size, where subtle differences may not be evident, and differences between the recognized disease characteristics within the groups that cannot be totally matched e.g. predominance of female sex, higher mean number of myelitis attacks and greater disability in AQP4-Ab disease and predominance of cervical cord involvement in multiple sclerosis as compared to the lower cord in antibody-mediated conditions. However, our groups were fairly well matched across many characteristics and we adjusted for those that were not in our analyses. Additionally, the homogeneity of a single-centre study where imaging is done on the same scanner (especially because obtaining reliable quantitative spinal cord imaging is challenging), and where consistency and accuracy of diagnosis is maximized (using the same highly specific assays and clinicians) is an advantage. The findings can then be used to build hypotheses and decide which protocols need to be aligned when taking observations forward into



multi-centre studies. Finally, technical limitations prevented the use of the quantitative MRI sequences in the thoracic cord.

### Future perspectives

A longitudinal study would be important to see if the groups can be differentiated by the presence or absence of silent disease pathology and by combining brain, spinal cord and optical coherence tomography findings to capture the full spectrum of CNS involvement.

### Conclusion

In this study we show that multimodal MRI provides us with valuable information about the spinal cord involvement in three different inflammatory demyelinating conditions. The conclusions of this study are based on the results of between-group and within-group comparisons that show consistent patterns, regardless of imaging metric, making the overall findings more compelling. This establishes a more robust understanding of these disorders. Myelitis with AQP4-Abs shows the most severe, localized damage in areas involved during the acute episode. In multiple sclerosis, metrics show significant change in comparison to healthy volunteers; however, the relationship with lesion location is not as pronounced. Finally, in MOG-Ab disease, metrics are comparable with healthy volunteers in all measures except that there is significant localized grey matter atrophy in affected areas of the cord. MOG-Ab disease is also moderately discriminated from AQP4-Ab disease and multiple sclerosis based on these quantitative metrics due to good recovery. Finally, we show that these metrics have clinical significance in their generic association with disability and pain scores.

### Acknowledgements

We gratefully acknowledge all those who participated in this study. We thank Ms Ana Cavey for her assistance with participant recruitment. We thank Mr Michael Sanders, Mr Jon Campbell, Mr David Parker and all the staff at the Wellcome Centre for Integrative Neuroimaging. We thank Dr Maciej Jurynczyk for his insight on the use of discriminatory analysis.

### Funding

We thank the Highly Specialised Commissioning Team for funding the Neuromyelitis Optica service in Oxford. R.M. is undertaking graduate studies funded by scholarships from the Rhodes Trust and the Oppenheimer Memorial Trust. MRI scans were funded by a Research and Development Fund belonging to the principal investigator, J.A.P. Y.K. was supported by the National Natural Science Foundation of China (No. 81871436) and the Informatization Special

Project of Chinese Academy of Sciences (No. XXH13506–306).

### Competing interests

The authors report no competing interests.

### Supplementary material

Supplementary material is available at *Brain* online.

### References

- Altmann D, Button T, Schmierer K, Hunter K, Tozer D, Wheeler-Kingshott C, et al. Sample sizes for lesion magnetisation transfer ratio outcomes in remyelination trials for multiple sclerosis. *Mult Scler Relat Disord* 2014; 3: 237–43.
- Andersson JLR, Skare S, Ashburner J. How to correct susceptibility distortions in spin-echo echo-planar images: application to diffusion tensor imaging. *Neuroimage* 2003; 20: 870–88.
- Andersson JLR, Sotiropoulos SN. An integrated approach to correction for off-resonance effects and subject movement in diffusion MR imaging. *Neuroimage* 2016; 125: 1063–78.
- Azodi S, Nair G, Enose-Akahata Y, Charlip E, Vellucci A, Cortese I, et al. Imaging spinal cord atrophy in progressive myelopathies: HTLV-1-associated neurological disease (HAM/TSP) and multiple sclerosis. *Ann Neurol* 2017; 82: 719–28.
- Benedetti B, Valsasina P, Judica E, Martinelli V, Ghezzi A, Capra R, et al. Grading cervical cord damage in neuromyelitis optica and MS by diffusion tensor MRI. *Neurology* 2006; 67: 161.
- Bralley TJ, Chervin RD. Fatigue in multiple sclerosis: mechanisms, evaluation, and treatment. *Sleep* 2010; 33: 1061.
- Calabrese M, Atzori M, Bernardi V, Morra A, Romualdi C, Rinaldi L, et al. Cortical atrophy is relevant in multiple sclerosis at clinical onset. *J Neurol* 2007; 254: 1212–20.
- Casserly C, Seyman EE, Alcaide-Leon P, Guenette M, Lyons C, Sankar S, et al. Spinal cord atrophy in multiple sclerosis: a systematic review and meta-analysis. *J Neuroimaging* 2018; 28: 556–586.
- Cawley N, Tur C, Prados F, Plantone D, Kearney H, Abdel-Aziz K, et al. Spinal cord atrophy as a primary outcome measure in phase II trials of progressive multiple sclerosis. *Mult Scler J* 2018; 24: 932–41.
- Chien C, Scheel M, Schmitz-Hübsch T, Borisow N, Ruprecht K, Bellmann-Strobl J, et al. Spinal cord lesions and atrophy in NMOSD with AQP4-IgG and MOG-IgG associated autoimmunity. *Mult Scler J* 2019; 25: 1926–36.
- Ciccharelli O, Cohen JA, Reingold SC, Weinshenker BG, Amato MP, Banwell B, et al. Spinal cord involvement in multiple sclerosis and neuromyelitis optica spectrum disorders. *Lancet Neurol* 2019; 18: 185–97.
- Cobo-Calvo A, Ruiz A, Maillart E, Audoin B, Zephir H, Bourre B, et al. Clinical spectrum and prognostic value of CNS MOG autoimmunity in adults. *Neurology* 2018; 90: e1858–e1869.
- De Leener B, Lévy S, Dupont SM, Fonov VS, Stikov N, Louis Collins D, et al. SCT: spinal Cord Toolbox, an open-source software for processing spinal cord MRI data. *Neuroimage* 2017; 145: 24–43.
- Dubey D, Pittock SJ, Krecke KN, Morris PP, Sechi E, Zalewski NL, et al. Clinical, radiologic, and prognostic features of myelitis associated with myelin oligodendrocyte glycoprotein autoantibody. *JAMA Neurol* 2018; 55905: 1–9.
- Dubey D, Pittock SJ, Krecke KN, Morris PP, Sechi E, Zalewski NL, et al. Clinical, radiologic, and prognostic features of myelitis

- associated with myelin oligodendrocyte glycoprotein autoantibody. *JAMA Neurol* 2019; 76: 301–9.
- Eden D, Gros C, Badji A, Dupont SM, De Leener B, Maranzano J, et al. Spatial distribution of multiple sclerosis lesions in the cervical spinal cord. *Brain* 2019; 142: 633–46.
- Faul F, Erdfelder E, Lang A-G, Buchner A. GPower 3: a flexible statistical power analysis program for the social, behavioral, and biomedical sciences. *Behav Res Methods* 2007; 39: 175.
- Filippi M, Preziosa P, Banwell BL, Barkhof F, Ciccarelli O, De Stefano N, et al. Assessment of lesions on magnetic resonance imaging in multiple sclerosis: practical guidelines. *Brain* 2019; 142: 1858–75.
- Flanagan EP, Weinschenker BG, Krecke KN, Lennon VA, Lucchinetti CF, McKeon A, et al. Short myelitis lesions in aquaporin-4-IgG-positive neuromyelitis optica spectrum disorders. *JAMA Neurol* 2015a; 72: 81–7.
- Flanagan EP, Weinschenker BG, Krecke KN, Pittock SJ. Asymptomatic myelitis in neuromyelitis optica and autoimmune aquaporin-4 channelopathy. *Neurol Clin Pract* 2015b; 5: 175–7.
- Fowler C, Griffiths D, De Groat W. The neural control of micturition. *Nat Rev Neurosci* 2008; 9: 453.
- Geurts JJ, Barkhof F. Grey matter pathology in multiple sclerosis. *Lancet Neurol* 2008; 7: 841–51.
- Gros C, De Leener B, Badji A, Maranzano J, Eden D, Dupont SM, et al. Automatic segmentation of the spinal cord and intramedullary multiple sclerosis lesions with convolutional neural networks. *Neuroimage* 2019; 184: 901–915.
- Hacohen Y, Mankad K, Chong WK, Barkhof F, Vincent A, Lim M, et al. Diagnostic algorithm for relapsing demyelinating syndromes of the CNS in children including myelin oligodendrocyte glycoprotein. *Lancet* 2017; 389: S41.
- Jaeger S, Paul F, Scheel M, Brandt A, Heine J, Pach D, et al. Multiple sclerosis-related fatigue: altered resting-state functional connectivity of the ventral striatum and dorsolateral prefrontal cortex. *Mult Scler J* 2019; 25: 554–64.
- Jarius S, Rupprecht K, Wildemann B, Kuempfel T, Ringelstein M, Geis C, et al. Contrasting disease patterns in seropositive and seronegative neuromyelitis optica: a multicentre study of 175 patients. *J Neuroinflammation* 2012; 9: 14.
- Jenkinson M, Beckmann CF, Behrens TE, Woolrich MW, Smith SM. FSL. *Neuroimage* 2012; 62: 782–90.
- Jurynczyk M, Geraldes R, Probert F, Woodhall MR, Waters P, Tackley G, et al. Distinct brain imaging characteristics of autoantibody-mediated CNS conditions and multiple sclerosis. *Brain* 2017a; 140: 617–27.
- Jurynczyk M, Messina S, Woodhall MR, Raza N, Everett R, Rocaferrandez A, et al. Clinical presentation and prognosis in MOG-antibody disease: a UK study. *Brain* 2017b; 140: 3128–38.
- Kitley J, Leite MI, Nakashima I, Waters P, McNeill B, Brown R, et al. Prognostic factors and disease course in aquaporin-4 antibody-positive patients with neuromyelitis optica spectrum disorder from the United Kingdom and Japan. *Brain* 2012; 135: 1834–49.
- Kitley J, Waters P, Woodhall M, Leite MI, Murchison A, George J, et al. Neuromyelitis optica spectrum disorders with aquaporin-4 and myelin-oligodendrocyte glycoprotein antibodies: a comparative study. *JAMA Neurol* 2014; 71: 276–83.
- Klawiter EC, Xu J, Naismith RT, Benzinger TL, Shimony JS, Lancia S, et al. Increased radial diffusivity in spinal cord lesions in neuromyelitis optica compared with multiple sclerosis. *Mult Scler J* 2012; 18: 1259–68.
- Kleiter I, Gahlen A, Borisow N, Fischer K, Wernecke KD, Wegner B, et al. Neuromyelitis optica: evaluation of 871 attacks and 1,153 treatment courses. *Ann Neurol* 2016; 79: 206–16.
- Liu Y, Wang J, Daams M, Weiler F, Hahn HK, Duan Y, et al. Differential patterns of spinal cord and brain atrophy in NMO and MS. *Neurology* 2015; 84: 1465 LP–72.
- Lucchinetti CF, Guo Y, Popescu BFG, Fujihara K, Itoyama Y, Misu T. The pathology of an autoimmune astrocytopathy: lessons learned from neuromyelitis optica. *Brain Pathol* 2014; 24: 83–97.
- Mariano R, Messina S, Kumar K, Kuker W, Leite MI, Palace J. Comparison of clinical outcomes of transverse myelitis among adults with myelin oligodendrocyte glycoprotein antibody vs aquaporin-4 antibody disease. *JAMA Netw Open* 2019; 2: e1912732.
- Matthews L, Kolind S, Brazier A, Leite MI, Brooks J, Traboulsee A, et al. Imaging surrogates of disease activity in neuromyelitis optica allow distinction from multiple sclerosis. *PLoS One* 2015; 10: 1–19.
- McCarthy P. FSLeyes. 2019. [https://doi.org/10.5281/zenodo.3403671#.XbAuog\\_Uj0t](https://doi.org/10.5281/zenodo.3403671#.XbAuog_Uj0t) (23 October 2019, date last accessed).
- Miller DH, Grossman RI, Reingold SC, McFarland HF. The role of magnetic resonance techniques in understanding and managing multiple sclerosis. *Brain* 1998; 121: 3–24.
- Moccia M, Ruggieri S, Ianniello A, Toosy A, Pozzilli C, Ciccarelli O. Advances in spinal cord imaging in multiple sclerosis. *Ther Adv Neurol Disord* 2019; 12: 1756286419840593.
- Moll NM, Rietsch AM, Thomas S, Ransohoff AJ, Lee JC, Fox R, et al. Multiple sclerosis normal-appearing white matter: pathology-imaging correlations. *Ann Neurol* 2011; 70: 764–73.
- Naismith RT, Xu J, Klawiter EC, Lancia S, Tutlam NT, Wagner JM, et al. Spinal cord tract diffusion tensor imaging reveals disability substrate in demyelinating disease. *Neurology* 2013; 80: 2201.
- Ogawa R, Nakashima I, Takahashi T, Kaneko K, Akaishi T, Takai Y, et al. MOG antibody-positive, benign, unilateral, cerebral cortical encephalitis with epilepsy. *Neurol Neuroimmunol Neuroinflamm* 2017; 4.
- Olsson T, Barcellos LF, Alfredsson L. Interactions between genetic, lifestyle and environmental risk factors for multiple sclerosis. *Nat Rev Neurol* 2016; 13: 26–36.
- Pandit L, Asgari N, Apiwattanakul M, Palace J, Paul F, Leite M, et al. Demographic and clinical features of neuromyelitis optica: a review. *Mult Scler J* 2015; 21: 845–53.
- Pessôa FMC, Lopes FCR, Costa JVA, Leon SVA, Domingues RC, Gasparetto EL. The cervical spinal cord in neuromyelitis optica patients: a comparative study with multiple sclerosis using diffusion tensor imaging. *Eur J Radiol* 2012; 81: 2697–701.
- Powers JM, Ioachim G, Stroman PW. Ten key insights into the use of spinal cord fmri. *Brain Sci* 2018; 8: 173.
- Prados F, Barkhof F. Spinal cord atrophy rates: ready for prime time in multiple sclerosis clinical trials? *Neurology* 2018; 91: 157–8.
- Reich DS, White R, Cortese IC, Vuolo L, Shea CD, Collins TL, et al. Sample-size calculations for short-term proof-of-concept studies of tissue protection and repair in multiple sclerosis lesions via conventional clinical imaging. *Mult Scler J* 2015; 21: 1693–704.
- Senanayake B, Jitrapaikulsan J, Aravinthan M, Wijesekera JC, Ranawaka UK, Riffy MT, et al. Seroprevalence and clinical phenotype of MOG-IgG-associated disorders in Sri Lanka. *J Neurol Neurosurg Psychiatry* 2018; 90: 1381.
- Smith SM, Jenkinson M, Woolrich MW, Beckmann CF, Behrens TE, Johansen-Berg H, et al. Advances in functional and structural MR image analysis and implementation as FSL. *Neuroimage* 2004; 23: S208–19.
- Song X, Li D, Qiu Z, Su S, Wu Y, Wang J, et al. Correlation between EDSS scores and cervical spinal cord atrophy at 3T MRI in multiple sclerosis: a systematic review and meta-analysis. *Mult Scler Relat Disord* 2020; 37: 101426.
- Stroman PW, Bacon M, Schwab JM, Bosma R, Cadotte D, Carlstedt T, et al. The current state-of-the-art of spinal cord imaging: methods. *Neuroimage* 2015a; 84: 1070–81.
- Stroman PW, Schwab JM, Bacon M, Bosma R, Cadotte DW, Carlstedt T, et al. The current state-of-the-art of spinal cord imaging: applications. *Neuroimage* 2015b; 1082–93.
- Tackley G, Kuker W, Palace J. Magnetic resonance imaging in neuromyelitis optica. *Mult Scler* 2014; 1153–64.
- Tan CT, Mao Z, Wingerchuk DM, Qiu W, Hu X, Weinschenker BG. International consensus diagnostic criteria for neuromyelitis optica spectrum disorders. *Neurology* 2016; 86: 491–2.
- Tsagkas C, Magon S, Gaetano L, Pezold S, Naegelin Y, Amann M, et al. Spinal cord volume loss. *Neurology* 2018; 91: e349–358.

- Wang C, Narayan R, Greenberg B. Anti-myelin oligodendrocyte glycoprotein antibody associated with gray matter predominant transverse myelitis mimicking acute flaccid myelitis: a presentation of two cases. *Pediatr Neurol* 2018; 86: 42–5.
- Waterman CL, Currie RA, Cottrell LA, Dow J, Wright J, Waterfield CJ, et al. An integrated functional genomic study of acute phenobarbital exposure in the rat. *BMC Genomics* 2010; 11: 9.
- Waters P, Woodhall M, O'Connor KC, Reindl M, Lang B, Sato DK, et al. MOG cell-based assay detects non-MS patients with inflammatory neurologic disease. *Neurol Neuroimmunol Neuroinflamm* 2015; 2: e89.
- Weinshenker BG, Wingerchuk DM, Vukusic S, Linbo L, Pittock SJ, Lucchinetti CF, et al. Neuromyelitis optica IgG predicts relapse after longitudinally extensive transverse myelitis. *Ann Neurol* 2006; 59: 566–569.
- Wingerchuk DM, Pittock SJ, Waters PJ, Weinshenker BG, Bennett JL, Jarius S. Evaluation of aquaporin-4 antibody assays. *Clin Exp Neuroimmunol* 2014; 5: 290–303.

#### **11.1.2.4. Cohort profile: A collaborative multicentre study of retinal optical coherence tomography in 539 patients with neuromyelitis optica spectrum disorders (CROCTINO).**

Citation: Specovius, S., Zimmermann, H. G., Oertel, F. C., Chien, C., Bereuter, C., Cook, L. J., Peixoto, M. A. L., Fontenelle, M. A., Kim, H. J., Hyun, J.-W., Jung, S.-K., Palace, J., **Roca-Fernández, A.**, ... Paul, F. (2020). *Cohort profile: A collaborative multicentre study of retinal optical coherence tomography in 539 patients with neuromyelitis optica spectrum disorders (CROCTINO)*. *BMJ Open*, 10(10), e035397. IF: 2.692

# BMJ Open Cohort profile: a collaborative multicentre study of retinal optical coherence tomography in 539 patients with neuromyelitis optica spectrum disorders (CROCTINO)

Svenja Specovius <sup>1,2</sup>, Hanna G Zimmermann,<sup>1,2</sup> Frederike Cosima Oertel,<sup>1,2</sup> Claudia Chien,<sup>1,2</sup> Charlotte Bereuter,<sup>1,2</sup> Lawrence J Cook,<sup>3</sup> Marco Aurélio Lana Peixoto,<sup>4</sup> Mariana Andrade Fontenelle,<sup>4</sup> Ho Jin Kim,<sup>5</sup> Jae-Won Hyun,<sup>5</sup> Su-Kyung Jung,<sup>6</sup> Jacqueline Palace,<sup>7</sup> Adriana Roca-Fernandez,<sup>8</sup> Alejandro Rubio Diaz,<sup>7</sup> Maria Isabel Leite,<sup>7</sup> Srilakshmi M Sharma,<sup>9</sup> Fereshte Ashtari,<sup>10</sup> Rahele Kafieh,<sup>11</sup> Alireza Dehghani,<sup>12</sup> Mohsen Pourazizi,<sup>12</sup> Lekha Pandit,<sup>13</sup> Anitha Dcunha,<sup>13</sup> Orhan Aktas,<sup>14</sup> Marius Ringelstein,<sup>14,15</sup> Philipp Albrecht <sup>14</sup>, Eugene May,<sup>16</sup> Caryl Tongco,<sup>16</sup> Letizia Leocani,<sup>17</sup> Marco Pisa,<sup>17</sup> Marta Radaelli,<sup>17</sup> Elena H Martinez-Lapiscina,<sup>18</sup> Hadas Stiebel-Kalish,<sup>19,20</sup> Mark Hellmann,<sup>19</sup> Itay Lotan,<sup>19</sup> Sasitorn Siritho,<sup>21</sup> Jérôme de Seze,<sup>22</sup> Thomas Senger,<sup>22</sup> Joachim Havla,<sup>23</sup> Romain Marignier,<sup>24</sup> Caroline Tilikete,<sup>25</sup> Alvaro Cobo Calvo,<sup>24</sup> Denis Bernardi Bichueti,<sup>26</sup> Ivan Maynard Tavares <sup>27</sup>, Nasrin Asgari,<sup>28,29</sup> Kerstin Soelberg,<sup>28,29</sup> Ayse Altintas,<sup>30</sup> Rengin Yildirim,<sup>31</sup> Uygur Tanriverdi,<sup>32</sup> Anu Jacob,<sup>33</sup> Saif Huda,<sup>33</sup> Zoe Rimler,<sup>34</sup> Allyson Reid,<sup>34</sup> Yang Mao-Draayer,<sup>35</sup> Ibis Soto de Castillo,<sup>36</sup> Michael R Yeaman,<sup>37,38</sup> Terry J Smith,<sup>39,40</sup> Alexander U Brandt,<sup>1,2,41</sup> Friedemann Paul,<sup>1,2,42</sup> On behalf of the GJCF International Clinical Consortium for NMOSD

**To cite:** Specovius S, Zimmermann HG, Oertel FC, et al. Cohort profile: a collaborative multicentre study of retinal optical coherence tomography in 539 patients with neuromyelitis optica spectrum disorders (CROCTINO). *BMJ Open* 2020;**10**:e035397. doi:10.1136/bmjopen-2019-035397

► Prepublication history and additional material for this paper is available online. To view these files, please visit the journal online (<http://dx.doi.org/10.1136/bmjopen-2019-035397>).

AUB and FP contributed equally.

Received 30 October 2019  
Revised 29 April 2020  
Accepted 14 July 2020



© Author(s) (or their employer(s)) 2020. Re-use permitted under CC BY-NC. No commercial re-use. See rights and permissions. Published by BMJ.

For numbered affiliations see end of article.

**Correspondence to**  
Friedemann Paul;  
friedemann.paul@charite.de

## ABSTRACT

**Purpose** Optical coherence tomography (OCT) captures retinal damage in neuromyelitis optica spectrum disorders (NMOSD). Previous studies investigating OCT in NMOSD have been limited by the rareness and heterogeneity of the disease. The goal of this study was to establish an image repository platform, which will facilitate neuroimaging studies in NMOSD. Here we summarise the profile of the Collaborative OCT in NMOSD repository as the initial effort in establishing this platform. This repository should prove invaluable for studies using OCT to investigate NMOSD.

**Participants** The current cohort includes data from 539 patients with NMOSD and 114 healthy controls. These were collected at 22 participating centres from North and South America, Asia and Europe. The dataset consists of demographic details, diagnosis, antibody status, clinical disability, visual function, history of optic neuritis and other NMOSD defining attacks, and OCT source data from three different OCT devices.

**Findings to date** The cohort informs similar demographic and clinical characteristics as those of previously published NMOSD cohorts. The image repository platform and centre network continue to be available for future prospective neuroimaging studies in NMOSD. For the conduct of the study, we have refined OCT image quality criteria and developed a cross-device intraretinal segmentation pipeline.

## Strengths and limitations of this study

- The Collaborative OCT in neuromyelitis optica spectrum disorders repository cohort comprises the largest number of retinal optical coherence tomography (OCT) images from patients with a neuromyelitis spectrum disorder, a rare autoimmune disease of the central nervous system.
- Besides imaging data, information on clinical and functional scores as well as laboratory parameters were assessed.
- We collect OCT images as original files, allowing for a detailed quality reading and standardised, device-independent OCT analysis.
- Despite standardised image analysis, the image heterogeneity due to different OCT machines and scan protocols remains a challenge.

**Future plans** We are pursuing several scientific projects based on the repository, such as analysing retinal layer thickness measurements, in this cohort in an attempt to identify differences between distinct disease phenotypes, demographics and ethnicities. The dataset will be available for further projects to interested, qualified parties, such as those using specialised image analysis or artificial intelligence applications.



## INTRODUCTION

Neuromyelitis optical spectrum disorders (NMOSD) are rare autoimmune neuroinflammatory diseases spanning a broad age range. They are clinically characterised by recurrent attacks of optic neuritis (ON), myelitis and less frequently by the brainstem and cerebral attacks, and profoundly impact patients' quality of life.<sup>1–4</sup> The current concepts of NMOSD are rapidly changing. An international panel of experts published the latest NMOSD diagnostic criteria in 2015.<sup>5</sup> Pathogenic serum autoantibodies against aquaporin-4 (AQP4-IgG), an astrocytic water channel protein, can be detected in 60%–80% of patients with NMOSD.<sup>6,7</sup> The diagnostic criteria differentiate patients with positive or negative/unknown AQP4-IgG status. In the latter case, strict rules apply to the clinical presentation and paraclinical findings, in particular those from MRI for diagnosing NMOSD.<sup>5,8</sup> In some AQP4-IgG seronegative patients within the NMO disease spectrum, for example with isolated recurrent ON or myelitis, serum antibodies against myelin oligodendrocyte glycoprotein (MOG) can be detected.<sup>9–12</sup> As a different cellular target is involved, most experts consider MOG-IgG autoimmunity, or MOG-IgG-associated encephalomyelitis, as a separate disease entity, pathogenetically distinct from classic AQP4-IgG-associated NMOSD.<sup>13–15</sup> The term myelin oligodendrocyte glycoprotein antibody disease has recently been proposed for this disorder.<sup>16</sup>

ON is one of the most common clinical manifestation of NMOSD. It frequently results in severe structural optic nerve damage and visual impairment, often occurs bilaterally, with common relapses.<sup>3,17,18</sup> Patients often develop a visual disability as a result of decreased high-contrast visual acuity (HCVA) and low-contrast visual acuity, as well as colour and visual field defects. These functional limitations result in impaired vision-related quality of life and a high incidence of legal blindness.<sup>19–21</sup>

Optical coherence tomography (OCT) acquires high-resolution retinal images and plays an important role in assessing ON-associated damage in NMOSD<sup>22</sup> and other neuroinflammatory disorders associated with ON.<sup>23–24</sup> After transection of optic nerve axons following acute ON, retrograde neurodegeneration leads to neuroaxonal damage in the retina.<sup>25</sup>

Retinal post-inflammatory neuroaxonal degeneration typically progresses for about 6 months after the onset of acute idiopathic ON. It can be assessed by OCT as peripapillary retinal nerve fibre layer thickness (pRNFL) or ganglion and inner plexiform layer thickness (GCIP).<sup>26</sup> Due to the rarity of NMOSD, adequate disease-specific studies on temporal ON dynamics are scant.<sup>27</sup> Thus, it remains uncertain which time frame accurately reflects the disease. For example, in a recent population-based study of all acute ON in Southern Denmark, there was not a single AQP4-IgG seropositive case and only two with MOG-IgG in the 50 patients presenting with de novo acute ON during study duration.<sup>28</sup> In MOG-IgG seropositive patients, ON appears to be milder than in patients with detectable AQP4-IgG<sup>29</sup> and leads to a better outcome

despite equally severe retinal thinning.<sup>30</sup> However, MOG-IgG seropositive patients display a higher relapse frequency, potentially leading to comparable cumulative retinal damage and loss of vision in the two subgroups.<sup>31,32</sup> Furthermore, MOG-IgG seropositive patients have a more pronounced pRNFL thinning in the temporal quadrant, while temporal and nasal quadrants are equally affected in AQP4-IgG positive disease.<sup>19,33</sup> It is currently unclear, to what extent the retina and vision are affected by NMOSD independently of ON.<sup>22</sup> In multiple sclerosis (MS), disease-associated and progressive neurodegeneration can occur in eyes unaffected by ON.<sup>34,35</sup> Studies of NMOSD have led to conflicting results. ON in NMOSD tends to be more posterior and closer to the chiasm than that occurring in MS, and chiasmal affection could lead to carry-over effects in the less affected companion eye.<sup>36,37</sup> However, recently described microstructural changes in the retina also suggest a primary retinopathy in NMOSD.<sup>38–41</sup> This is potentially mediated by AQP4-expressing retinal Müller cells and could be independent of ON. Longitudinal data demonstrating progressive GCIP loss in AQP4-IgG positive patients with NMOSD independent of ON further supports this notion.<sup>42,43</sup> These observations remain to be independently confirmed. In contrast, a recent exploratory longitudinal study in MOG-IgG seropositive patients suggested only progressive RNFL loss but not longitudinal GCIP reduction.<sup>44</sup>

Besides neuroaxonal damage, macroscopic retinal findings have been reported in NMOSD. Macular microcysts occur in the inner nuclear layer and are associated with severe ON in approximately 20% of patients with NMOSD.<sup>45–47</sup> Pathology and clinical significance of macular microcysts, sometimes called microcystic macular oedema, remain unclear; however, macular processes appear to occur more frequently than other processes such as vitreous traction, which was found in one MOG-IgG positive patient with microcysts.<sup>48</sup>

Investigating OCT for clinically and pathologically meaningful information is hampered by the rareness and heterogeneity of NMOSD.<sup>49</sup> In 2015, the Guthy Jackson Charitable Foundation International Clinical Consortium (GJCF-ICC) agreed to establish an image repository platform (neuromyelitis optical imaging repository (NOIR)), the purpose of which is to facilitate multinational and multicentre neuroimaging studies in NMOSD. NOIR is intended to help identify imaging pitfalls in NMOSD, develop and clinically validate imaging biomarkers of the disease, clinical disability and to define imaging endpoints for clinical trials. Here we report the outcome of the Collaborative OCT in NMOSD repository study (CROCTINO) as the initial effort in establishing a platform for investigating retinal abnormalities using OCT in NMOSD.

## COHORT DESCRIPTION

### Study design

The study was designed as a multinational and multicentre repository study collecting longitudinal OCT data as well

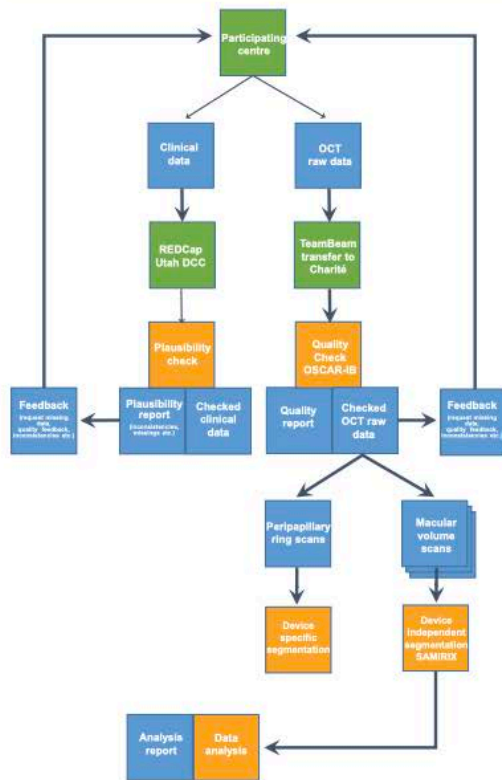


**Figure 1** Flow chart explaining the overall study design and information technology (IT) infrastructure. DCC, Data Coordinating Center; OCT, optical coherence tomography; REDCap, Research Electronic Data Capture; SAMIRIX is a custom-developed intraretinal segmentation pipeline<sup>55</sup>. OSCAR-IB are validated consensus quality criteria for retinal OCT reading<sup>53</sup>.

as relevant clinical data from patients with NMOSD and healthy controls (HCs). Participating centres were asked to contribute both retrospective and prospective data that was collected over a defined period extending from 2000 to 2018. Scientific coordination and OCT reading were performed at the Charité—Universitätsmedizin Berlin Translational Neuroimaging Group. Participating centres were mainly recruited from the GJCF-ICC, which includes international researchers and clinicians focusing on NMOSD. Additional experts who had previously published studies using OCT in NMOSD but who were not members of the GJCF-ICC were contacted and invited to participate. For this purpose, a questionnaire screening each centre for the number of eligible patients and the type of OCT instruments used at their site was sent to the entire GJCF-ICC and to other identified experts. Centres giving a positive response to the recruitment questionnaire received further instructions

on how to contribute OCT images and the associated demographical and clinical data of their patients and HCs. The overall study design—including the workflow—is illustrated in figure 1.

#### Inclusion and exclusion criteria

Subjects were included with (a) a diagnosis of NMOSD as specified by the 2015 International Panel criteria<sup>5</sup> or (b) longitudinal extensive transverse myelitis and/or (c) recurrent ON or (d) HCs (without matching requirements). OCT source data, demographic and clinical metadata from patients and HCs were required, including age, sex, disease subtype, autoantibody status and clinical history including details of ON.

#### Data collection and workflow

All demographic and clinical data were assessed in an electronic repository based on Research Electronic Data Capture (REDCap),<sup>50</sup> located at the University of Utah Data Coordination Center. OCT images were transferred by participating centres via TeamBeam (Skalio GmbH, Hamburg, Germany), a commercial web-based medical data exchange service certified for secure data transfer. OCT images were then stored and analysed using a secure server at Charité—Universitätsmedizin Berlin, Berlin, Germany.

Study preparation began in January 2016 by identifying potential participating centres, setting up the information technology (IT) infrastructure and developing the electronic case report forms (eCRFs) in REDCap. eCRFs were sent to all participants for review and were revised accordingly. The data collection was launched on 1 September 2016, when the final repository was released, and centres received REDCap accounts for data entry. Data collection officially closed on 30 September 2018. After a detailed plausibility check, identified missing data could be submitted until 31 December 2018. A detailed timeline is illustrated in figure 2.

#### Collected dataset

The data elements that were collected are listed in online supplemental file 1 (including indications of which data elements were mandatory or optional) and are summarised as follows:

#### Demographic and clinical data

In addition to age and sex, ethnicity was assessed based on published NIH categories (<https://grants.nih.gov/grants/guide/notice-files/not-od-15-089.html>). Possible selections comprised 'American Indian or Alaska Native', 'Asian', 'Black or African American', 'Hispanic or Latino', 'Native Hawaiian or Other Pacific Islander', 'White' and 'Other'; up to two selections were possible. Height and weight were collected. Information concerning the presence of ophthalmological comorbidities other than those related to NMOSD was requested. The possible answers were: 'Unknown', 'No (excluded by examination)', 'No (excluded by history taking)' and 'Yes'. In case of 'Yes', the condition had to be specified. Furthermore,

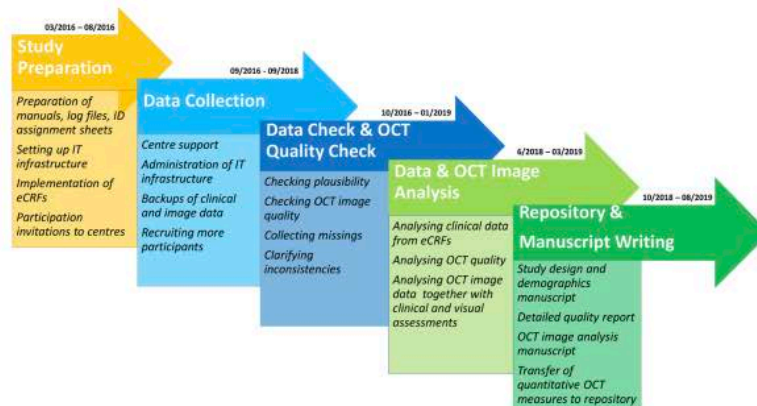


**Figure 2** Detailed study timeline including all study phases with start and end dates, as well as a brief description of each phase. eCRFs, electronic case report forms; OCT, optical coherence tomography.

the presence of other comorbidities was assessed. Information about NMOSD diagnosis was mandatory, with possible selections of ‘NMO (2006 criteria)’, ‘AQP4-IgG seropositive NMOSD (2015 criteria)’, ‘AQP4-IgG seronegative NMOSD (2015 criteria)’, ‘MOG-IgG-associated encephalomyelitis/NMOSD’, ‘RON/CRION (Recurrent Optic Neuritis)’, ‘LETM (Longitudinal Extensive Transverse Myelitis)’. We inquired about the AQP4 and MOG antibody statuses separately (both mandatory) with possible answers ‘Seropositive’, ‘Currently seronegative, but at least one previous test was positive’, ‘Seronegative’, ‘Not known/ Never assessed’. Patients were considered to be seropositive for AQP4-IgG or MOG-IgG if antibodies were detected in at least one assay. Centres were also asked which assay they used for antibody testing. Provision of the Expanded Disability Status Scale (EDSS) score was optional.<sup>51</sup> History of clinical attacks was requested with a focus on ON. Information concerning each eye was recorded separately as was the number of ON attacks and date of last episode. History of other NMOSD defining attacks, such as transverse myelitis, area postrema syndrome, brainstem syndromes, symptomatic narcolepsy or acute diencephalic clinical syndrome with NMOSD-typical diencephalic MRI lesions, and symptomatic cerebral syndrome with NMOSD-typical brain lesions was requested without dates and with the option ‘unknown’. Immunotherapy was assessed with a selection of common NMOSD treatments<sup>52</sup> and possible selections ‘Current’ and ‘Previous use’.

#### Optical coherence tomography

Scans from all common OCT machines were accepted, resulting in scans from three different types of machines: (a) Spectralis SD-OCT (Heidelberg Engineering, Heidelberg, Germany), (b) Cirrus HD-OCT (Carl Zeiss Meditec, Dublin, California, USA) and (c) Topcon 3D OCT-1 (Topcon, Tokyo, Japan). We requested that centres upload two scan types per eye from each visit:

- ▶ A peripapillary ring scan with 12° or approximately 3.4 mm diameter around the optic disc. For those using Cirrus and Topcon, an optic disc volume scan was uploaded since peripapillary data are extracted from this scan.
- ▶ A macular volume scan, centred on the fovea, with a minimum size of 20°×20° (approximately 6 mm×6 mm).

There were no restrictions regarding OCT image averaging or quality. At least one scan per visit was required to be included in the repository. After images were transferred, their quality was assessed based on modified OSCAR-IB criteria.<sup>53–54</sup> Modifications were made for better applicability to macular scans (see online supplemental file 2). pRNFL segmentation was performed with device-internal algorithms, intraretinal layer segmentation with a device-independent segmentation pipeline.<sup>55</sup>

#### Visual function

HCVA was requested with a selection menu ranging from 20/10 (−0.3 logMAR) to ‘no light perception’. Information on the method of testing was not requested, but details of whether testing was performed best corrected, habitually corrected or uncorrected were recorded. Monocular HCVA was mandatory while binocular HCVA was optional. Additionally, low contrast letter acuity (LCLA) from 2.5% contrast Sloan charts, normal/abnormal classifications of visual evoked potentials (VEP) P100 latencies and mean deficit and pattern standard deviation from visual fields could be entered as optional information.

#### Statistical analysis

Cohort and statistical description for this cohort profile were performed with R V.3.4.4<sup>56</sup> in R Markdown and RStudio (RStudio, Boston, Massachusetts, USA).



**Table 1** Participating centres with number of patients, number of HCs and used OCT device

Centre	Patients	HC	OCT device
Bangkok, Thailand	25	0	Cirrus
Barcelona, Spain	13	13	Spectralis or Cirrus
Belo Horizonte, Brazil	57	0	Spectralis
Berlin, Germany	76	39	Spectralis
Duesseldorf, Germany	11	28	Spectralis
Goyang-si, Korea	50	0	Topcon OCT
Isfahan, Iran	40	18	Spectralis
Istanbul, Turkey	8	0	Cirrus
Liverpool, UK	8	0	Spectralis
Lyon, France	10	0	Spectralis
Mangalore, India	40	16	Spectralis
Maracaibo, Venezuela	3	0	Spectralis
Michigan, USA	5	0	Spectralis
Milan, Italy	30	0	Spectralis
Munich, Germany	11	0	Spectralis
New York, USA	6	0	Spectralis and Cirrus
Odense, Denmark	9	0	Spectralis
Oxford, UK	48	0	Spectralis
Petah-Tikva, Israel	25	0	Cirrus
Sao Paulo, Brazil	9	0	Spectralis
Seattle, USA	30	0	Cirrus
Strasbourg, France	25	0	Spectralis

HC, healthy control; OCT, optical coherence tomography.

### Cohort overview

Centres from North and South America, Asia and Europe participated in CROCTINO. In total, data from 539 patients from 22 centres and 114 HCs from 5 centres were

collected. Centres and the size of their patient and HC cohorts are listed alphabetically in [table 1](#).

In total, we collected 1868 peripapillary ring scans/optic nerve volume scans and 1672 macular volume scans fulfilling defined specifications. Only scans with corresponding clinical data were considered. Device and scan specifications are depicted in [table 2](#).

A cohort characterisation is depicted in [table 3](#). The mean patient age (mean±SD) was 43.1±14.8 years with 444 (82%) women. The age of HCs (mean±SD) was 32.1±9.8 years with 72 (63%) women. The majority of patients were White or Middle Eastern (n=315), followed by Asian (n=128) and Black or African American (n=27).

Among all patients, 515 (95.5%) fulfilled the 2015 diagnostic criteria for NMOSD.<sup>5</sup> Of those not meeting the 2015 criteria, 21 (3.9%) carried the diagnosis of LETM, and 3 (0.6%) recurrent ON. Among those fulfilling NMOSD diagnostic criteria, 369 (72%) were AQP4-IgG seropositive, leaving 146 (28%) with negative or unknown AQP4-IgG status. Among the AQP4-IgG seronegative patients, 54 (37%) were MOG-IgG seropositive, 34 (23%) were double-negative for AQP4-IgG and MOG-IgG and 58 (40%) had an unknown antibody status. In the entire cohort, 369 (68%) were AQP4-IgG seropositive, 54 (10%) MOG-IgG seropositive, 52 (10%) had double negative and 64 (12%) had an unknown antibody status. There were 400 (74%) patients with at least one episode of ON, and 410 (76%) patients with a history of myelitis. The mean time since disease onset (mean±SD) was 5.47±19.47 years and mean age at initial symptom onset (mean±SD) was 36.18±15.05 years. Information about current N,N-Dimethyltryptamine (DMT) was available in 398 (74%) patients. Ninety-seven patients (18.0%) received a combination of multiple DMTs. Most frequent DMT options comprised rituximab (n=128; 24%), azathioprine (n=121; 22%), oral prednisolone (n=98; 18%), mycophenolate mofetil (n=77; 14%) and methotrexate (n=11; 2%).

**Table 2** Technical and scan specifications

Protocol*	Axial resolution (µm)	Acquisition (A-scans/s)	n	B-scans	A-scans per B-scan	Size (mm)†
Spectralis Mac-1	3.9 <sup>62</sup>	40 000 <sup>62</sup>	651	61	768	6×6
Spectralis Mac-2			240	25	512	6×6
Spectralis Mac-3			225	25	1024	7.5×9
Spectralis Ring-1			1143	1	1536	3.4
Spectralis Ring-2			226	1	768	3.5
Cirrus Mac	5.0 <sup>63</sup>	27 000 <sup>63</sup>	293	128	512	6×6
Cirrus Ring			388	200	200	6×6/3.4‡
Topcon Mac	6.0 <sup>64</sup>	50 000 <sup>64</sup>	263	128	512	6×6
Topcon Ring			111	128	512	6×6/3.4‡

\*Only protocols making up more than 5% of the total macular scan rates were considered.

†Scan size can vary as it depends on the eye length.

‡Peripapillary ring scan extracted from optic nerve head volume scan. Mac, macular volume.



Table 3 Cohort description

	Healthy controls	Patients
Subjects (n)	114	539
Centres (n)	5	22
Age (years; mean±SD)	32.1±9.8	43.1±14.8
Sex (woman; n (%))	72 (63.2)	444 (82.4)
Time since disease onset (years; mean±SD)	–	5.5±19.5
Age at initial symptom onset (years; mean±SD)	–	36.2±15.1
Ethnicity (n (%))		
White or Middle Eastern	96 (84.2)	315 (58.4)
Asian	17 (14.9)	128 (23.7)
Black or African American	0 (0)	27 (5.0)
Hispanic or Latino	1 (0.9)	11 (2.0)
Other	0 (0)	23 (4.3)
Not reported	0 (0)	35 (6.5)
Patients fulfilling the 2015 diagnostic criteria for NMOSD (fulfilled; n (%))	–	515 (95.5)
AQP4-IgG seropositive NMOSD (n (%))	–	369 (68.5)
MOG-IgG seropositive NMOSD (n (%))	–	54 (10.0)
Double-negative NMOSD (n (%))	–	34 (6.3)
NMOSD with unknown antibody-status (n (%))	–	58 (11.0)
Patients with a history of optic neuritis (n (%))	–	400 (74.2)
Patients with a history of myelitis (n (%))	–	410 (76.1)

AQP4-IgG, aquaporin-4 IgG antibodies; MOG-IgG, myelin oligodendrocyte glycoprotein IgG antibodies; NMOSD, neuromyelitis optica spectrum disorders.

The majority of the centres provided OCT source data from a Spectralis machine (17 centres), followed by Cirrus (6 centres) and one centre contributed Topcon OCT images (table 1).

HCVA was available for 529 (98%) patients and 83 (73%) HCs. Most of the patients received best-corrected HCVA (47%), 28% were habitually corrected and 25% not corrected. LCLA was obtained from 99 (18%) patients and 40 (35%) HCs. VEP were available for 177 (33%), and visual fields for 90 (17%) patients applying devices at the discretion of each centre.

Longitudinal data were available for 157 (29%) patients from 11 centres. Mean follow-up time (mean±SD) was 27±17 months.

#### Patient and public involvement

Patients and the Public were not explicitly involved in the design or conduct of this study. However, the results

of this study will be presented on a Guthy-Jackson Charitable Foundation's International NMO Patient Day, giving patients, relatives and researchers the opportunity to share ideas for projects based on this cohort.

#### Findings to date

To our knowledge, the CROCTINO repository comprises the largest dataset on retinal OCT in NMOSD. Cohort demographics are in line with previous epidemiological NMOSD studies: gender ratio, age at symptom onset and prevalence of AQP4-IgG and MOG-IgG antibodies are similar to previously published studies and suggest a cohort that is representative of the disease spectrum.<sup>57–59</sup> OCT quality and quantitative analyses are currently being investigated as first scientific derivatives of the work and will be published in the near future. During the study, many challenges in conducting an investigator-driven academic repository study were experienced. First, this study was implemented without centre reimbursement. While we are unaware of specific guidelines in this regard, we felt that data quality would potentially be higher when centres receive no reimbursement. Although without reimbursement we expected a lower motivation for interested centres to participate at all, we reckoned that data quality might be higher from participating centres contributing out of sole scientific interest. Despite the absence of financial compensation, centre motivation was excellent, and we were able to include substantially more datasets (n=539) than initially anticipated (n=200). Lack of reimbursement did preclude the participation of some centres, particularly in North America. Sharing of data requires legal compliance, including the conclusion of data transfer agreements (DTA). Although we provided an initial DTA template for this study, almost all centres required modifications, the consequence of different legal systems in this multinational setting. This process resulted in a substantially delayed data collection. On the other hand, the DTA templates for each of the involved centres in combination with concluded DTA for this repository now provide a powerful platform and network for future studies in NMOSD.

During the conduct of this study, we developed several technical solutions, which will be made available beyond the scope of this repository. First, the technical infrastructure and newly established workflows will be instrumental in conducting future neuroimaging studies in NMOSD. We further developed a device-independent intraretinal layer segmentation pipeline based on an established segmentation algorithm.<sup>60</sup> This pipeline is capable of importing and segmenting OCT scans from all devices included in the study and will presumably lead to better comparability of OCT data obtained from different devices.<sup>55</sup> Finally, we modified the widely used OSCAR-IB criteria<sup>53</sup> for assessing OCT image quality to be applicable to macular volume scans and all OCT devices. The modified criteria will be validated using data from our repository.



### Strengths and limitations

With 539 patients, CROCTINO comprises the largest dataset of OCT images from patients with NMOSD that we are aware of. The cohort resembles epidemiological studies published earlier and includes relevant demographic and clinical data. Further, the autoantibody status is available for many datasets, including not only AQP4-IgG but also MOG-IgG, thus distinguishing this cohort from many earlier studies where MOG-IgG was either unknown or unavailable. Inclusion of different ethnicities and geographical regions should allow analysis and comparison with patients with NMOSD in different cohorts, who are usually investigated only in smaller separate analyses from one or few centres. Finally, this study collected raw OCT imaging data thereby allowing detailed quality reading and image analysis, also with advanced technologies in the future.

The study has several limitations, many of which are inherent to multicentre settings. First, the inclusion of retrospective data precluded application of a standardised, homogeneous imaging protocol. Heterogeneity in the dataset is further caused by (a) use of different OCT machines, (b) different scan protocols and (c) no homogeneous visual function measures. Several geographic regions are not represented in the repository (eg, Australia, Africa), and HC scans are not matched demographically and are only available for some ethnicities and from certain regions. Although great care was taken in collecting, completing and verifying the data, we could not ensure complete individual data set validity. For example, different methods for antibody testing<sup>61</sup> with often uncertain sensitivity and specificity and a non-standardised documentation of patient-reported information could lead to some noise in respective analyses.

### Collaboration and future directions

The study coordinating centre is pursuing several scientific projects based on the repository in collaboration with the participating centres, such as the analysis of pRNFL and intramacular layer thickness measurements in this cohort in an attempt to identify differences between distinct disease phenotypes, demographics and ethnicities. We encourage collaboration with interested researchers in additional scientific projects. The CROCTINO dataset will be made available to all participating centres and to qualified investigators on request (details see below). The study coordinators are also interested in further expanding the repository by including (a) additional data from currently underrepresented geographic regions, (b) additional HC data to provide expanded ethnicity comparators and (c) more prospective, longitudinal data, also extending already existing follow-up periods of the included patients. The established NOIR platform and the CROCTINO cohort will serve to investigate retinal imaging biomarkers in NMOSD in the future.

### Author affiliations

- <sup>1</sup>Experimental and Clinical Research Center, Max Delbrück Center for Molecular Medicine and Charité—Universitätsmedizin Berlin, Corporate Member of Freie Universität Berlin, Humboldt-Universität zu Berlin, and Berlin Institute of Health, Berlin, Germany
- <sup>2</sup>NeuroCure Clinical Research Center, Charité—Universitätsmedizin Berlin, Corporate Member of Freie Universität Berlin, Humboldt-Universität zu Berlin, and Berlin Institute of Health, Berlin, Germany
- <sup>3</sup>Department of Pediatrics, University of Utah, Salt Lake City, Utah, USA
- <sup>4</sup>CIEM MS Research Center, University of Minas Gerais, Medical School, Belo Horizonte, Brazil
- <sup>5</sup>Department of Neurology, National Cancer Center, Goyang, Republic of Korea
- <sup>6</sup>Department of Ophthalmology, National Cancer Center, Goyang, Republic of Korea
- <sup>7</sup>Department of Neurology, Oxford University Hospitals, National Health Service Trust, Oxford, UK
- <sup>8</sup>Nuffield Department of Clinical Neurosciences, University of Oxford, Oxford, UK
- <sup>9</sup>Department of Ophthalmology, Oxford University Hospitals, National Health Service Trust, Oxford, UK
- <sup>10</sup>Kashani MS Center, Isfahan University of Medical Sciences, Isfahan, Iran
- <sup>11</sup>School of Advanced Technologies in Medicine, Isfahan University of Medical Sciences, Isfahan, Iran
- <sup>12</sup>Department of Ophthalmology, Isfahan Eye Research Center, Isfahan University of Medical Sciences, Isfahan, Iran
- <sup>13</sup>Department of Neurology, KS Hegde Medical Academy, Nitte University, Mangalore, India
- <sup>14</sup>Department of Neurology, Medical Faculty, Heinrich Heine University Düsseldorf, Düsseldorf, Germany
- <sup>15</sup>Department of Neurology, Center for Neurology and Neuropsychiatry, LVR-Klinikum, Heinrich Heine University Düsseldorf, Düsseldorf, Germany
- <sup>16</sup>Swedish Neuroscience Institute Neuro-Ophthalmology, Seattle, Washington, USA
- <sup>17</sup>Neurological Department and Institute of Experimental Neurology (INSPE) Scientific Institute, Hospital San Raffaele; and University Vita-Salute San Raffaele, Milan, Italy
- <sup>18</sup>Hospital Clinic of Barcelona-Institut d'Investigacions, Biomèdiques August Pi Sunyer (IDIBAPS), Barcelona, Spain
- <sup>19</sup>Sackler School of Medicine, Tel Aviv University, Tel Aviv, Israel
- <sup>20</sup>Neuro-Ophthalmology Division, Department of Ophthalmology, Rabin Medical Center, Petah Tikva, Israel
- <sup>21</sup>Division of Neurology, Department of Medicine, Siriraj Hospital and Bumrungrad International Hospital, Bangkok, Thailand
- <sup>22</sup>Neurology Service, University Hospital of Strasbourg, Strasbourg, France
- <sup>23</sup>Institute of Clinical Neuroimmunology, University Hospital, Ludwig Maximilians University, Munich, Germany
- <sup>24</sup>Neurology, Multiple Sclerosis, Myelin Disorders and Neuroinflammation, Pierre Wertheimer Neurological Hospital, Hospices Civils de Lyon, Lyon, France
- <sup>25</sup>Department of Neuro-Ophthalmology, Hospices Civils de Lyon, Lyon, France
- <sup>26</sup>Departamento de Neurologia e Neurocirurgia, Escola Paulista de Medicina, Universidade Federal de São Paulo, São Paulo, Brazil
- <sup>27</sup>Department of Ophthalmology and Visual Sciences, Escola Paulista de Medicina, Universidade Federal de São Paulo, São Paulo, Brazil
- <sup>28</sup>Departments of Neurology, Slagelse Hospital, Slagelse, Denmark
- <sup>29</sup>Institutes of Regional Health Research and Molecular Medicine, University of Southern Denmark, Odense, Denmark
- <sup>30</sup>Neurology Department, School of Medicine, Koc University and Istanbul University - Cerrahpasa School of Medicine, Istanbul, Turkey
- <sup>31</sup>Department of Ophthalmology, Cerrahpasa Medical Faculty, Istanbul University, Istanbul, Turkey
- <sup>32</sup>Neurology Department Istanbul, Istanbul University, Cerrahpasa School of Medicine, Istanbul, Turkey
- <sup>33</sup>Department of Neurology, The Walton Centre NHS Foundation Trust, Liverpool, UK
- <sup>34</sup>Department of Neurology, NYU Multiple Sclerosis Comprehensive Care Center, NYU School of Medicine, New York, New York, USA
- <sup>35</sup>Department of Neurology, University of Michigan Medical School, Ann Arbor, Michigan, USA
- <sup>36</sup>Department of Neurology, Hospital Clínico de Maracaibo, Maracaibo, Venezuela
- <sup>37</sup>Department of Medicine, Los Angeles Biomedical Research Institute at Harbor-University of California at Los Angeles (UCLA) Medical Center, Torrance, California, USA



<sup>38</sup>Department of Medicine, David Geffen School of Medicine at UCLA, Los Angeles, California, USA  
<sup>39</sup>Departments of Ophthalmology and Visual Sciences, Kellogg Eye Center, Ann Arbor, Michigan, USA  
<sup>40</sup>Division of Metabolism, Endocrine and Diabetes, Department of Internal Medicine, University of Michigan Medical School, Ann Arbor, Michigan, USA  
<sup>41</sup>Department of Neurology, University of California, Irvine, California, USA  
<sup>42</sup>Department of Neurology, Charité—Universitätsmedizin Berlin, corporate member of Freie Universität Berlin, Humboldt-Universität zu Berlin, and Berlin Institute of Health, Berlin, Germany

**Twitter** Ivan Maynard Tavares @imaynard

**Acknowledgements** The authors would like to thank all who contributed to data assessment and collection at the participating centres.

**Collaboration and future directions** The study coordinating centre is pursuing several scientific projects based on the repository in collaboration with the participating centres, such as the analysis of pRNFL and intramacular layer thickness measurements in this cohort in an attempt to identify differences between distinct disease phenotypes, demographics and ethnicities. We encourage collaboration with interested researchers in additional scientific projects. The CROCTINO dataset will be made available to all participating centres and to qualified investigators upon request (details see below). The study coordinators are also interested in further expanding the repository by including (a) additional data from currently underrepresented geographic regions, (b) additional healthy control data to provide expanded ethnicity comparators and (c) more prospective, longitudinal data, also extending already existing follow-up periods of the included patients. The established NOIR platform and the CROCTINO cohort will serve to investigate retinal imaging biomarkers in NMOSD in the future.

**Funding** The creation of this repository was supported by a grant from the Guthy Jackson Charitable Foundation.

**Patient consent for publication** Not required.

**Provenance and peer review** Not commissioned; externally peer reviewed.

**Data availability statement** All data collected will be electronically stored in a repository and can be accessed by all participants for research purposes upon request. GJCF-ICC and the principal investigators of the repository will coordinate projects and access. Investigators not involved in CROCTINO data collection who desire access to the data should approach the corresponding author or the GJCF-ICC for access.

**Supplemental material** This content has been supplied by the author(s). It has not been vetted by BMJ Publishing Group Limited (BMJ) and may not have been peer-reviewed. Any opinions or recommendations discussed are solely those of the author(s) and are not endorsed by BMJ. BMJ disclaims all liability and responsibility arising from any reliance placed on the content. Where the content includes any translated material, BMJ does not warrant the accuracy and reliability of the translations (including but not limited to local regulations, clinical guidelines, terminology, drug names and drug dosages), and is not responsible for any error and/or omissions arising from translation and adaptation or otherwise.

**Open access** This is an open access article distributed in accordance with the Creative Commons Attribution Non Commercial (CC BY-NC 4.0) license, which permits others to distribute, remix, adapt, build upon this work non-commercially, and license their derivative works on different terms, provided the original work is properly cited, appropriate credit is given, any changes made indicated, and the use is non-commercial. See: <http://creativecommons.org/licenses/by-nc/4.0/>.

#### ORCID iDs

Svenja Specovius <http://orcid.org/0000-0002-4572-4059>

Philipp Albrecht <http://orcid.org/0000-0001-7987-658X>

Ivan Maynard Tavares <http://orcid.org/0000-0003-2220-7603>

#### REFERENCES

- Jarius S, Wildemann B, Paul F. Neuromyelitis optica: clinical features, immunopathogenesis and treatment. *Clin Exp Immunol* 2014;176:149–64.
- Sepulveda M, Delgado-García G, Blanco Y, et al. Late-onset neuromyelitis optica spectrum disorder: the importance of autoantibody serostatus. *Neurol Neuroimmunol Neuroinflamm* 2019;6:e607.
- Beekman J, Keisler A, Pedraza O, et al. Neuromyelitis optica spectrum disorder: patient experience and quality of life. *Neurol Neuroimmunol Neuroinflamm* 2019;6:e580.
- D'Souza M, Papadopoulou A, Levy M, et al. Diagnostic procedures in suspected attacks in patients with neuromyelitis optica spectrum disorders: results of an international survey. *Mult Scler Relat Disord* 2020;41:102027.
- Wingerchuk DM, Banwell B, Bennett JL, et al. International consensus diagnostic criteria for neuromyelitis optica spectrum disorders. *Neurology* 2015;85:177–89.
- Zekeridou A, Lennon VA. Aquaporin-4 autoimmunity. *Neurol Neuroimmunol Neuroinflamm* 2015;2:e110.
- Cook LJ, Rose JW, Alvey JS, et al. Collaborative international research in clinical and longitudinal experience study in NMOSD. *Neurol Neuroimmunol Neuroinflamm* 2019;6:e583.
- Kim HJ, Paul F, Lana-Peixoto MA, et al. MRI characteristics of neuromyelitis optica spectrum disorder: an international update. *Neurology* 2015;84:1165–73.
- Kim S-M, Woodhall MR, Kim J-S, et al. Antibodies to MOG in adults with inflammatory demyelinating disease of the CNS. *Neurol Neuroimmunol Neuroinflamm* 2015;2:e163.
- Chalimoukou K, Alexopoulos H, Akrivou S, et al. Anti-MOG antibodies are frequently associated with steroid-sensitive recurrent optic neuritis. *Neurol Neuroimmunol Neuroinflamm* 2015;2:e131.
- Narayan R, Simpson A, Fritsche K, et al. MOG antibody disease: a review of MOG antibody seropositive neuromyelitis optica spectrum disorder. *Mult Scler Relat Disord* 2018;25:66–72.
- Waters P, Woodhall M, O'Connor KC, et al. MOG cell-based assay detects non-MS patients with inflammatory neurologic disease. *Neurol Neuroimmunol Neuroinflamm* 2015;2:e89.
- Zamvil SS, Slavin AJ. Does MOG Ig-positive AQP4-seronegative opticospinal inflammatory disease justify a diagnosis of NMO spectrum disorder? *Neurol Neuroimmunol Neuroinflamm* 2015;2:e62.
- Jarius S, Paul F, Aktas O, et al. MOG encephalomyelitis: international recommendations on diagnosis and antibody testing. *J Neuroinflammation* 2018;15:134.
- Kwon YN, Waters PJ, Kim M, et al. Peripherally derived macrophages as major phagocytes in MOG encephalomyelitis. *Neurol Neuroimmunol Neuroinflamm* 2019;6:e600.
- Wynford-Thomas R, Jacob A, Tomassini V. Neurological update: MOG antibody disease. *J Neurol* 2019;266:1280–6.
- Ramanathan S, Prelog K, Barnes EH, et al. Radiological differentiation of optic neuritis with myelin oligodendrocyte glycoprotein antibodies, aquaporin-4 antibodies, and multiple sclerosis. *Mult Scler* 2016;22:470–82.
- Bennett JL, de Seze J, Lana-Peixoto M, et al. Neuromyelitis optica and multiple sclerosis: seeing differences through optical coherence tomography. *Mult Scler* 2015;21:678–88.
- Schneider E, Zimmermann H, Oberwahrenbrock T, et al. Optical coherence tomography reveals distinct patterns of retinal damage in neuromyelitis optica and multiple sclerosis. *PLoS One* 2013;8:e66151.
- Outteryck O, Majed B, Defoort-Dhellemmes S, et al. A comparative optical coherence tomography study in neuromyelitis optica spectrum disorder and multiple sclerosis. *Mult Scler* 2015;21:1781–93.
- Schmidt F, Zimmermann H, Mikolajczak J, et al. Severe structural and functional visual system damage leads to profound loss of vision-related quality of life in patients with neuromyelitis optica spectrum disorders. *Mult Scler Relat Disord* 2017;11:45–50.
- Oertel FC, Zimmermann H, Paul F, et al. Optical coherence tomography in neuromyelitis optica spectrum disorders: potential advantages for individualized monitoring of progression and therapy. *Epma J* 2018;9:21–33.
- Oertel FC, Zimmermann HG, Brandt AU, et al. Novel uses of retinal imaging with optical coherence tomography in multiple sclerosis. *Expert Rev Neurother* 2019;19:31–43.
- Oberwahrenbrock T, Traber GL, Lukas S, et al. Multicenter reliability of semiautomatic retinal layer segmentation using OCT. *Neurol Neuroimmunol Neuroinflamm* 2018;5:e449.
- Brandt AU, Specovius S, Oberwahrenbrock T, et al. Frequent retinal ganglion cell damage after acute optic neuritis. *Mult Scler Relat Disord* 2018;22:141–7.
- Costello F, Pan Yi, Yeh EA, et al. The temporal evolution of structural and functional measures after acute optic neuritis. *J Neurol Neurosurg Psychiatry* 2015;86:1369–73.
- Stiebel-Kalish H, Hellmann MA, Mimouni M, et al. Does time equal vision in the acute treatment of a cohort of AQP4 and MOG optic neuritis? *Neurol Neuroimmunol Neuroinflamm* 2019;6:e572.

- 28 Soelberg K, Specovius S, Zimmermann HG, et al. Optical coherence tomography in acute optic neuritis: a population-based study. *Acta Neurol Scand* 2018;138:566–73.
- 29 Akaishi T, Sato DK, Nakashima I, et al. MRI and retinal abnormalities in isolated optic neuritis with myelin oligodendrocyte glycoprotein and aquaporin-4 antibodies: a comparative study. *J Neurol Neurosurg Psychiatry* 2016;87:446–8.
- 30 Sotirchos ES, Filippatou A, Fitzgerald KC, et al. Aquaporin-4 IgG seropositivity is associated with worse visual outcomes after optic neuritis than MOG-IgG seropositivity and multiple sclerosis, independent of macular ganglion cell layer thinning. *Mult Scler* 2019;135245851986492.
- 31 Pache F, Zimmermann H, Mikolajczak J, et al. MOG-IgG in NMO and related disorders: a multicenter study of 50 patients. Part 4: afferent visual system damage after optic neuritis in MOG-IgG-seropositive versus AQP4-IgG-seropositive patients. *J Neuroinflammation* 2016;13:282.
- 32 Borisow N, Mori M, Kuwabara S, et al. Diagnosis and treatment of NMO spectrum disorder and MOG-Encephalomyelitis. *Front Neurol* 2018;9:888.
- 33 Havla J, Kumpfel T, Schinner R, et al. Myelin-oligodendrocyte-glycoprotein (MOG) autoantibodies as potential markers of severe optic neuritis and subclinical retinal axonal degeneration. *J Neurol* 2017;264:139–51.
- 34 Petzold A, de Boer JF, Schippling S, et al. Optical coherence tomography in multiple sclerosis: a systematic review and meta-analysis. *Lancet Neurol* 2010;9:921–32.
- 35 Petzold A, Balcer LJ, Calabresi PA, et al. Retinal layer segmentation in multiple sclerosis: a systematic review and meta-analysis. *Lancet Neurol* 2017;16:797–812.
- 36 Storoni M, Davagnanam I, Radon M, et al. Distinguishing optic neuritis in neuromyelitis optica spectrum disease from multiple sclerosis: a novel magnetic resonance imaging scoring system. *J Neuroophthalmol* 2013;33:123–7.
- 37 Khanna S, Sharma A, Huecker J, et al. Magnetic resonance imaging of optic neuritis in patients with neuromyelitis optica versus multiple sclerosis. *Journal of Neuro-Ophthalmology* 2012;32:216–20.
- 38 Oertel FC, Kuchling J, Zimmermann H, et al. Microstructural visual system changes in AQP4-antibody-seropositive NMOSD. *Neurol Neuroimmunol Neuroinflamm* 2017;4:e334.
- 39 Jeong IH, Kim HJ, Kim N-H, et al. Subclinical primary retinal pathology in neuromyelitis optica spectrum disorder. *J Neurol* 2016;263:1343–8.
- 40 Yamamura T, Nakashima I. Foveal thinning in neuromyelitis optica: a sign of retinal astrocytopathy? *Neurol Neuroimmunol Neuroinflamm* 2017;4:e347.
- 41 Motamedi S, Oertel FC, Yadav SK, et al. Altered fovea in AQP4-IgG-seropositive neuromyelitis optica spectrum disorders. *Neurol Neuroimmunol Neuroinflamm* 2020;7:e805.
- 42 Oertel FC, Havla J, Roca-Fernández A, et al. Retinal ganglion cell loss in neuromyelitis optica: a longitudinal study. *J Neurol Neurosurg Psychiatry* 2018;89:1259–65.
- 43 Pisa M, Ratti F, Vabanesi M, et al. Subclinical neurodegeneration in multiple sclerosis and neuromyelitis optica spectrum disorder revealed by optical coherence tomography. *Mult Scler* 2020;26:1197–206.
- 44 Oertel FC, Outteryck O, Knier B, et al. Optical coherence tomography in myelin-oligodendrocyte-glycoprotein antibody-seropositive patients: a longitudinal study. *J Neuroinflammation* 2019;16:154.
- 45 Kaufhold F, Zimmermann H, Schneider E, et al. Optic neuritis is associated with inner nuclear layer thickening and microcystic macular edema independently of multiple sclerosis. *PLoS One* 2013;8:e71145.
- 46 Sotirchos ES, Saidha S, Byraiah G, et al. In vivo identification of morphologic retinal abnormalities in neuromyelitis optica. *Neurology* 2013;80:1406–14.
- 47 Gelfand JM, Cree BA, Nolan R, et al. Microcystic inner nuclear layer abnormalities and neuromyelitis optica. *JAMA Neurol* 2013;70:629.
- 48 Brandt AU, Oberwahrenbrock T, Kadas EM, et al. Dynamic formation of macular microcysts independent of vitreous traction changes. *Neurology* 2014;83:73–7.
- 49 Mori M, Kuwabara S, Paul F. Worldwide prevalence of neuromyelitis optica spectrum disorders. *J Neurol Neurosurg Psychiatry* 2018;89:555–6.
- 50 Harris PA, Taylor R, Thielke R, et al. Research electronic data capture (REDCap)—a metadata-driven methodology and workflow process for providing translational research informatics support. *J Biomed Inform* 2009;42:377–81.
- 51 Kurtzke JF. Rating neurologic impairment in multiple sclerosis: an expanded disability status scale (EDSS). *Neurology* 1983;33:1444–52.
- 52 Trebst C, Jarius S, Berthele A, et al. Update on the diagnosis and treatment of neuromyelitis optica: recommendations of the neuromyelitis optica Study Group (NEMOS). *J Neurol* 2014;261:1–16.
- 53 Tewarie P, Balk L, Costello F, et al. The OSCAR-IB consensus criteria for retinal OCT quality assessment. *PLoS One* 2012;7:e34823.
- 54 Schippling S, Balk LJ, Costello F, et al. Quality control for retinal OCT in multiple sclerosis: validation of the OSCAR-IB criteria. *Mult Scler* 2015;21:163–70.
- 55 Motamedi S, Gawlik K, Ayadi N, et al. Normative data and minimally detectable change for inner retinal layer thicknesses using a semi-automated OCT image segmentation pipeline. *Front Neurol* 2019;10:1117.
- 56 R Core Team (2017). *R: A language and environment for statistical computing*. Vienna, Austria: R Foundation for Statistical Computing, 2017. <https://www.R-project.org/>
- 57 Pandit L, Asgari N, Apiwatanakul M, et al. Demographic and clinical features of neuromyelitis optica: a review. *Mult Scler* 2015;21:845–53.
- 58 Jarius S, Ruprecht K, Wildemann B, et al. Contrasting disease patterns in seropositive and seronegative neuromyelitis optica: a multicentre study of 175 patients. *J Neuroinflammation* 2012;9:503.
- 59 Borisow N, Kleiter I, Gahlen A, et al. Influence of female sex and fertile age on neuromyelitis optica spectrum disorders. *Mult Scler* 2017;23:1092–103.
- 60 Lang A, Carass A, Hauser M, et al. Retinal layer segmentation of macular OCT images using boundary classification. *Biomed Opt Express* 2013;4:1133.
- 61 Waters P, Reindl M, Saiz A, et al. Multicentre comparison of a diagnostic assay: aquaporin-4 antibodies in neuromyelitis optica. *J Neurol Neurosurg Psychiatry* 2016;87:1005–15.
- 62 Heidelberg Engineering G. SPECTRALIS imaging platform technical specifications, 2020. Available: [https://www.heidelbergengineering.com/download.php?https://media.heidelbergengineering.com/uploads/Products-Downloads/200279-002-INT-AE18\\_SPECTRALIS-Technical-Data-Sheet\\_EN.pdf](https://www.heidelbergengineering.com/download.php?https://media.heidelbergengineering.com/uploads/Products-Downloads/200279-002-INT-AE18_SPECTRALIS-Technical-Data-Sheet_EN.pdf)
- 63 Carl Zeiss Meditec I. Cirrus HD-OCT brochure, 2007. Available: [http://www.eyecarealliance.com/wp-content/uploads/2018/08/Cirrus-OCT-4000-Brochure\\_ECA.pdf](http://www.eyecarealliance.com/wp-content/uploads/2018/08/Cirrus-OCT-4000-Brochure_ECA.pdf)
- 64 TOPCON Medical Systems I. 3D Oct-1 MAESTRO optical coherence tomography brochure, 2017. Available: [https://west.visionexpo.com/\\_novadocuments/491865?v=636682302031730000](https://west.visionexpo.com/_novadocuments/491865?v=636682302031730000)

### **11.1.2.5. Contrasting the brain imaging features of MOG-antibody disease, with AQP4-antibody NMOSD and multiple sclerosis.**

Citation: Messina, S., Mariano, R., **Roca-Fernández, A.**, Cavey, A., Jurynczyk, M., Leite, M. I., Calabrese, M., Jenkinson, M., & Palace, J. (2021). *Contrasting the brain imaging features of MOG-antibody disease, with AQP4-antibody NMOSD and multiple sclerosis*. Multiple Sclerosis Journal (Houndmills, Basingstoke, England), May 28; 13524585211018988. IF:6.312

# Contrasting the brain imaging features of MOG-antibody disease, with AQP4-antibody NMOSD and multiple sclerosis

Silvia Messina , Romina Mariano, Adriana Roca-Fernandez, Ana Cavey, Maciej Jurynczyk, Maria Isabel Leite, Massimiliano Calabrese, Mark Jenkinson and Jacqueline Palace

Multiple Sclerosis Journal

2022, Vol. 28(2) 217–227

DOI: 10.1177/  
13524585211018987

© The Author(s), 2021.



Article reuse guidelines:  
sagepub.com/journals-  
permissions

## Abstract

**Background:** Identifying magnetic resonance imaging (MRI) markers in myelin-oligodendrocytes-glycoprotein antibody-associated disease (MOGAD), neuromyelitis optica spectrum disorder-aquaporin-4 positive (NMOSD-AQP4) and multiple sclerosis (MS) is essential for establishing objective outcome measures.

**Objectives:** To quantify imaging patterns of central nervous system (CNS) damage in MOGAD during the remission stage, and to compare it with NMOSD-AQP4 and MS.

**Methods:** 20 MOGAD, 19 NMOSD-AQP4, 18 MS in remission with brain or spinal cord involvement and 18 healthy controls (HC) were recruited. Volumetrics, lesions and cortical lesions, diffusion-imaging measures, were analysed.

**Results:** Deep grey matter volumes were lower in MOGAD ( $p=0.02$ ) and MS ( $p=0.0001$ ), compared to HC and were strongly correlated with current lesion volume (MOGAD  $R=-0.93$ ,  $p<0.001$ , MS  $R=-0.65$ ,  $p=0.0034$ ). Cortical/juxtacortical lesions were seen in a minority of MOGAD, in a majority of MS and in none of NMOSD-AQP4. Non-lesional tissue fractional anisotropy (FA) was only reduced in MS ( $p=0.01$ ), although focal reductions were noted in NMOSD-AQP4, reflecting mainly optic nerve and corticospinal tract pathways.

**Conclusion:** MOGAD patients are left with grey matter damage, and this may be related to persistent white matter lesions. NMOSD-AQP4 patients showed a relative sparing of deep grey matter volumes, but reduced non-lesional tissue FA. Observations from our study can be used to identify new markers of damage for future multicentre studies.

**Keywords:** Multiple sclerosis, neuromyelitis optica with AQP4-Ab, MOG-Ab disease, MRI, non-conventional MRI

Date received: 28 December 2020; revised: 13 March 2021; accepted: 15 April 2021.

## Introduction

Recently, two new antibody-mediated central nervous system (CNS) diseases, previously been thought to be multiple sclerosis (MS) variants, have been identified. The first, aquaporin-4-antibody (AQP4-Ab) disease,<sup>1</sup> is a primary astrocytopathy and is recognised to be the major cause of the neuromyelitis optica spectrum disorders (NMOSD).<sup>2,3</sup> Myelin oligodendrocyte glycoprotein (MOG) antibody, targeting myelin, is associated with a wider clinical phenotype.<sup>4,5</sup>

Brain lesions, reported in up to 60% of NMOSD-AQP4 patients,<sup>6</sup> can be difficult to distinguish from MOG antibody-associated disease (MOGAD);<sup>7</sup> however, using conventional magnetic resonance imaging (MRI), the presence of typical MS lesions, may help in differentiating it from the antibody disorders.<sup>7</sup>

The presence of occult white and grey matter damage in MS, detected using non-conventional MRI, is well-known, while opinion varies as to whether

Correspondence to:

**J Palace**  
Nuffield Department of  
Clinical Neurosciences,  
John Radcliffe Hospital,  
University of Oxford,  
Level 3, West Wing,  
Headley Way, Oxford OX3  
9DU, UK  
jacqueline.palace@ndcn.  
ox.ac.uk

**Silvia Messina**  
**Maria Isabel Leite**  
**Jacqueline Palace**  
Nuffield Department of  
Clinical Neurosciences,  
John Radcliffe Hospital,  
University of Oxford,  
Oxford, UK/Oxford  
University Hospital NHS  
Foundation Trust, Oxford,  
UK

**Romina Mariano**  
**Adriana Roca-Fernandez**  
**Ana Cavey**  
Nuffield Department of  
Clinical Neurosciences,  
John Radcliffe Hospital,  
University of Oxford,  
Oxford, UK

**Maciej Jurynczyk**  
Nuffield Department of  
Clinical Neurosciences,  
John Radcliffe Hospital,  
University of Oxford,  
Oxford, UK/Laboratory  
of Brain Imaging, Nencki  
Institute of Experimental  
Biology, Polish Academy of  
Sciences, Warsaw, Poland

**Massimiliano Calabrese**  
Multiple Sclerosis Centre,  
Neurology Department of  
Neurosciences, Biomedicine  
and Movement, University  
Hospital of Verona, Verona,  
Italy

**Mark Jenkinson**  
Nuffield Department of  
Clinical Neurosciences,  
John Radcliffe Hospital,  
University of Oxford,  
Oxford, UK/University of  
Adelaide, Adelaide, SA,  
Australia

**Table 1.** Baseline clinical and demographic characteristics of the enrolled participants.

	NMOSD-AQP4	MOGAD	MS	HC	<i>p</i> -value
Participants, <i>n</i>	19	20	18	18	N/A
Mean age at onset $\pm$ SD	55.6 $\pm$ 13.2	41.8 $\pm$ 11.0	44.1 $\pm$ 6.6	38.9 $\pm$ 13.4	< 0.001*
Female, %	68.4	50	55.5	55.5	0.695
Caucasian, %	52.6	100	100	83	0.001
Median disease duration, years (range)	11 (0–24)	2 (0–24)	11.5 (1–24)	N/A	0.018
Median number of relapse (range)	2 (1–11)	2 (1–11)	3 (1–13)	N/A	0.347
Median EDSS (range)	3 (0–7)	1.5 (0–7)	2.0 (0–6)	N/A	0.025
Mean EDSS $\pm$ SD	3.0 $\pm$ 1.9	1.7 $\pm$ 1.6	2.8 $\pm$ 1.7	N/A	0.055
Mean LogMAR VA (average OD and OS) $\pm$ SD	0.4 $\pm$ 0.9	–0.03 $\pm$ 0.6	–0.08 $\pm$ 0.1	N/A	0.022

NMOSD-AQP4: neuromyelitis optica spectrum disorder-aquaporin-4 positive; MOGAD: myelin-oligodendrocytes-glycoprotein antibody-associated disease; MS: multiple sclerosis; HC: healthy control; N/A: not applicable; SD: standard deviation; EDSS: Expanded Disability Status Scale; VA: visual acuity; OD: right eye (*oculus dexter*); OS: left eye (*oculus sinister*).

\*After Bonferroni comparison: NMOSD-AQP4 versus HC,  $p=0.002$ ; MS versus HC,  $p=1.0$ ; MOGAD versus HC,  $p=1.0$ .

NMOSD-AQP4 causes normal-appearing white and grey matter abnormalities and atrophy<sup>8–12</sup> Non-conventional volumetric and diffusion imaging data in MOGAD are scarce.<sup>13</sup>

Furthermore, in contrast to MS, MOGAD and NMOSD-AQP4 do not have a progressive stage; therefore, identifying differences between antibody-mediated conditions and MS may provide clues as to what is driving the progressive neurodegenerative process in MS.

The main aims of our study are to use volumetrics, lesion analysis and DTI measures to: (a) to identify different pattern of CNS damage in the three diseases and (b) to quantify the damage during the remission stage.

### Materials and methods

Further details of patients' enrolment, clinical assessment, MRI imaging analysis are in Supplementary Materials and Methods.

### Patients

A total of 20 MOGAD, 19 NMOSD-AQP4, 18 relapsing remitting MS and 18 healthy controls (HC) over the age of 18 consented to the study (REC 17/EE/0246; Table 1). Patients were recruited if they were at least 6 months downstream of an acute attack and had a brain or spinal cord involvement, with or without optic neuritis (ON). All patients with NMOSD-AQP4 and MOGAD had positive antibodies.

### MRI imaging protocol

Brain MRI was performed at 3T (Siemens Magnetom Prisma, Erlangen, Germany) including T1-weighted, fluid attenuated inversion recovery (FLAIR), proton density (PD), double inversion recovery (DIR) T2-weighted and diffusion-weighted sequences (see Supplementary Material and Methods).

### Statistical analysis

RStudio version 1.1.447 for non-imaging data was used. Differences were evaluated by analysis of variance (ANOVA to test means) and  $\chi^2$  (to test proportion), non-parametric tests were performed when the variables were not normally distributed. Linear models with disease group, sex and age as independent variables (volumetric scaling factor in case of volumetric measures) and the specific MRI measure as the dependent variable were fit, then for pairwise-comparison between groups, the estimated marginal means and standard error (SE) with Bonferroni correction across groups were calculated. Pearson's correlation was used to test the relationship between MRI findings.

In addition, a multivariable linear regression model with a stepwise variable selection based on the Akaike information criterion (AIC), was fitted in every disease group using age and sex, and MRI measures (that show differences across groups) as independent variables, and Expanded Disability Status Scale (EDSS) as the dependent variable.

For visual acuity (mean LogMAR), we use the same demographic variables and only two a priori MRI measures as independent variables (optic chiasm and



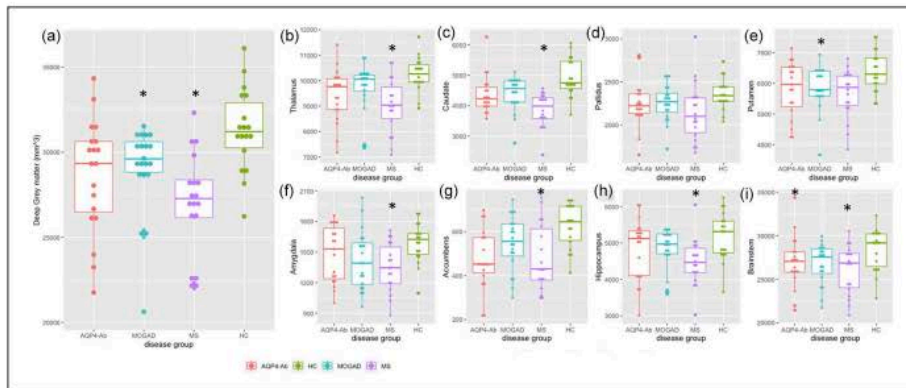


**Figure 1.** Total deep grey matter volumes (a), basal ganglia, hippocampus and brainstem volumes (b-I) between disease groups. The graphs represent the median and the 25th and 75th percentile; \* $p < 0.05$  when compared to HC, on the linear model adjusted for age, sex and volume scaling factors; AQP4-Ab = NMOSD-AQP4.

thalamus volume due to their connection to the anterior visual pathways) in the multivariable linear regression model.

For all analyses,  $p < 0.05$  was considered statistically significant. Graphs were created using ggplot and ggpvr packages, Rstudio.

### Results

The clinical and demographic characteristics of the four groups are represented in Table 1. Age in NMOSD-AQP4 was significantly different from HC, thus, was included in all regression models, together with sex.

All the non-significant results described below are shown in detail in Supplementary Results.

#### Volumetric analysis

Non-normalised volumes are shown in Supplementary Table 1. Results are shown as difference of volume estimates between groups in cubic millimetres, standard error (SE),  $p$ -value; when compared to HC a negative value indicates a lower volume in the disease group; when describing disease comparisons, the negative value indicates a lower volume in the disease group first mentioned in the comparison).

Total brain volume, white/grey matter fraction and third/fourth ventricular volumes: no significant differences were found in global measures (see Supplementary Results).

Grey matter volumes: when considering the total deep grey matter volumes, both MOGAD and MS showed lower volumes when compared to HC (MOGAD:  $-2609 \text{ mm}^3$  (880)  $p = 0.02$ ; MS:  $-4092 \text{ mm}^3$  (891)  $p = 0.0001$ ; Figure 1(a)) driven predominantly by significant putamen atrophy in MOGAD ( $-615.4 \text{ mm}^3$  (226)  $p = 0.05$ ) and more diffuse atrophy across the individual grey matter structures in MS (see Figure 1(b-i)). Only the brainstem was smaller in NMOSD-AQP4 ( $-2575.8 \text{ mm}^3$  (933)  $p = 0.04$ ) when compared to HC. Compared to NMOSD-AQP4, the caudate was significantly smaller in MS ( $-650 \text{ mm}^3$  (202)  $p = 0.01$ ). The remaining comparisons were not statistically significant (see Supplementary Results). The deep grey matter volume was not significantly correlated with the number of relapses (see Supplementary Results).

Cortical thickness and volumes: cortical thickness ( $\text{mm}^2$ ) and volumes ( $\text{mm}^3$ ) were not significantly different between groups (see Supplementary Results).

White matter region of interest volumes: given that visual function is often involved in the antibody-mediated diseases, and association fibres can be abnormal in MS, we selected the optic chiasm and corpus callosum as regions of interest for volume analysis. No significant difference in optic chiasm volumes were seen, but when including only those with at least one attack of ON, NMOSD-AQP4-ON had significantly lower chiasmatic volumes when compared to the other groups (NMOSD-AQP4:  $-153.54 \text{ mm}^3$  (23.8)  $p < 0.001$ ; HC:  $-121.43 \text{ mm}^3$  (23.3)  $p < 0.001$ , MOGAD-ON:  $-80.05 \text{ mm}^3$  (24.8)

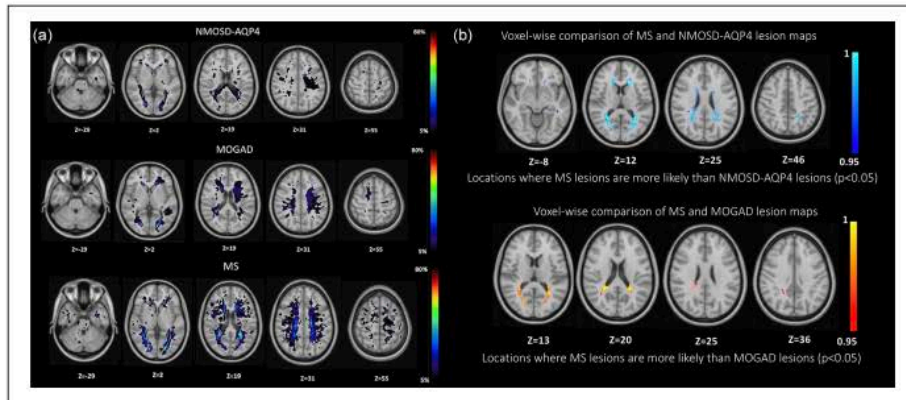


**Figure 2.** (a) Lesion probability map in NMOSD-AQP4, MOGAD and MS (b) voxel-wise comparison between MS and NMOSD-AQP4, MS and MOGAD. Lesions were identified on the lesion map with cluster tool (part of FSL) and using the Talairach Atlas. (a) The colour scale (from 5% to 80%) represents the minimum to maximum probability of a lesion occurring in a particular spatial location. Montreal Neurological Institute (MNI) standard space template Z coordinate is shown in millimetres. In the NMOSD-AQP4 group, the lesion map showed a widespread distribution, with the highest percentage of patients having lesions in the lateral ventricle anterior horns (31.5%), and in the right lingual gyrus of the occipital lobe (42%) and 10.5% in the corpus callosum. In the MOGAD group, the lesion map showed a widespread distribution, with the highest percentage of patients having lesions in the lingual gyrus bilaterally (50% right and 57.1% left), 42.8% have small lesions in the anterior horns of the right and left lateral ventricles, 14.3% in the superior frontal gyrus and 14.3% in the medial frontal gyrus. In the MS group, the lesion map showed a more focal distribution, with the highest percentage of patients having lesions in the periventricular anterior horns area (88.8% on the right and 94.4% on the left lateral ventricles), 16.6% in the brainstem, 11.1% cerebellum and 55.5% in the corpus callosum. (b) Statistically significant voxel locations (values represent 1-p-value, TFCE corrected) are represented in blue-light blue (MS vs NMOSD-AQP4) and red-yellow (MS vs MOGAD).

$p=0.04$ , MS-ON:  $-95.51 \text{ mm}^3$  (28.1)  $p=0.02$  likely reflecting the recognised posterior location of NMOSD-AQP4-ON and its severity (see Table 1). This effect was not seen in the MOGAD-ON groups and, additionally, there were no significant differences of the corpus callosum across groups (see Supplementary Results).

#### Lesion analysis

Lesion volume: 14 out of 20 (70%) MOGAD patients had brain lesions at the time of the scan and 17 (85%) of MOGAD patients had brain lesions acutely. All MS and NMOSD-AQP4 had acute brain lesions with persistent lesions at the time of the research scan. Only two HC had brain lesions, one had two punctiform small lesions normal for ageing brain and another had a few small punctiform non-specific lesions. The MS patients had a higher lesion volume when compared to NMOSD-AQP4 disease ( $1.326 \text{ mm}^3$  (0.503)  $p=0.03$ ) and MOGAD patients ( $2.219 \text{ mm}^3$  (0.545)  $p=0.0005$ ). Lesion volume was positively correlated with disease duration in MS (Pearson's correlation  $R=0.46$ ,  $p=0.05$ ) and MOGAD patients ( $R=0.81$ ,  $p<0.001$ ). Lesion

volume also showed a moderate correlation with the number of relapses in NMOSD-AQP4 ( $R=0.53$ ,  $p=0.02$ ) but this was not significant in MOGAD ( $R=0.26$ ,  $p=0.37$ ) and MS ( $R=0.48$ ,  $p=0.06$ ).

Lesion probability maps: the voxel-wise analysis between MOGAD and NMOSD-AQP4 was not significant, while the MS analysis showed that lesions are statistically more frequent in the periventricular areas than NMOSD-AQP4 and MOGAD ( $p<0.05$  TFCE (threshold-free cluster enhancement) corrected; see Figure 2(a) and (b)).

Cortical lesions analysis: a total of 69 DIR sequences were available for the cortical lesions' analysis (16 HC, 16 NMOSD-AQP4, 19 MOGAD and 17 MS). We defined cortical lesions as those lesions within the cortex or extending from the cortex to the adjacent white matter and juxtacortical lesions as white matter lesions in direct contact with the cortex.<sup>14</sup> Three MOGAD patients (15.7%) showed cortical/juxtacortical lesions (type I; one with one curvilinear and one with one ovoid lesion, and one participant with three curvilinear lesions), while 11 (65%) MS patients had identifiable cortical/juxtacortical (leukocortical)

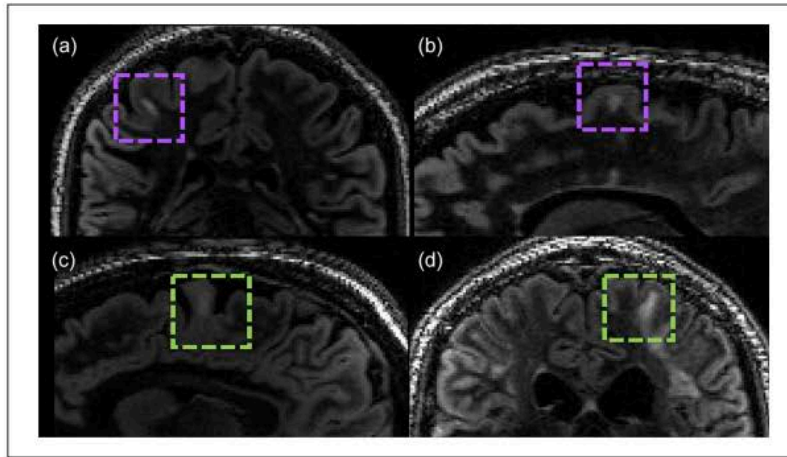


**Figure 3.** Cortical/juxtacortical lesions in (a and b) MS and (c and d) MOGAD. The inter-rater agreement was  $k=0.78$  ( $p < 0.001$ ) with 95% confidence interval (CI) 0.59–0.97. (a) Ovoid cortical lesion in MS participant; (b) ovoid cortical/juxtacortical lesion in MS participant; (c and d) curvilinear juxtacortical lesions in two MOGAD participants.

lesions, with three patients presenting at least one pure cortical lesion (type II; see Figure 3(a)–(d)) and one an extensive subpial lesion (see Table 2 with  $p$ -value).

#### Diffusion-weighted imaging analysis

Diffusion measures across the groups are shown in Supplementary Table 2 (16 MS, 19 MOGAD, 17 NMOSD-AQP4 and 17 HC scans were available for the analysis). All group comparisons used linear regression with Bonferroni correction and were adjusted for age and sex (results are shown as difference of diffusion measures estimates between groups, standard error (SE)  $p$ -value).

White matter diffusion metrics: fractional anisotropy (FA) and mean diffusivity (MD in  $10^{-3} \text{ mm}^2 \text{ s}^{-1}$ ), axial diffusivity (AD in  $10^{-3} \text{ mm}^2 \text{ s}^{-1}$ ) and radial diffusivity (RD in  $10^{-3} \text{ mm}^2 \text{ s}^{-1}$ ) were calculated (see Supplementary Table 3) within the lesions voxels (lesion-FA) using the FLAIR lesion masks, and also in the normal-appearing white matter (NAWM).

Lesion-FA was lower, and lesion-MD and -RD were higher when compared to the NAWM within all the three diseases ( $p < 0.001$ ; see Figure 4(a)–(d)), and also compared to HC (lesion-FA NMOSD-AQP4:  $-0.16$  (0.02), MOGAD:  $-0.16$  (0.02), MS:  $-0.15$  (0.02),  $p < 0.001$  in each group; lesion-MD NMOSD-AQP4:  $0.11$  (0.03),  $p = 0.002$ , MOGAD:  $0.13$  (0.03), MS:  $0.17$  (0.03)  $p < 0.001$  in each group; lesion-RD

NMOSD-AQP4:  $0.16$  (0.03), MOGAD:  $0.15$  (0.02), MS:  $0.17$  (0.02),  $p < 0.001$  in each group), but no differences were found in AD values. NAWM-FA in MOGAD and NMOSD-AQP4 was similar to HC and only in MS was lower compared to both HC and MOGAD ( $-0.03$  (0.01),  $p = 0.01$ ;  $-0.03$  (0.01),  $p = 0.03$ ; see Figure 4(a)–(d)).

Tract-based spatial statistics (TBSS) of NAWM FA: although 85% of MOGAD had brain lesions acutely, the TBSS voxel-wise analysis of FA-NAWM did not show significantly low FA as compared to HC. NAWM-FA was abnormal in NMOSD-AQP4 and MS when compared with HC, with lower FA in NMOSD-AQP4 affecting mainly corticospinal, brainstem and visual tracts and in MS focussed particularly on the corpus callosum (Figure 4(e)).

Grey matter diffusion metrics: MD values analysed in the cortical and deep grey matter structures did not show significant differences (see Supplementary Results).

#### Correlations between lesion volume and grey matter volumes in NMOSD-AQP4, MOGAD and MS

Because the predominant differences in non-lesional volumes in MOGAD were in grey matter structures, we looked at the relationship between lesion volume and total deep grey matter volume and found significant negative correlations in MOGAD and MS for

**Table 2.** Cortical/juxtacortical lesions in the three disease groups.

	NMOSD-AQP4	MOGAD	MS	Chi-square <i>p</i> -value
Patients, <i>n</i>	16	19	17	–
Patients with at least one cortical/juxtacortical lesion, <i>n</i> (%)	0	3 (15.8)	11 (64.7)	0.005
Patients with one cortical/juxtacortical lesion, <i>n</i> (%)	–	2 (10.5)	3 (17.6)	0.650
Patients with > 1 cortical/juxtacortical lesion, <i>n</i> (%)	–	1 (5.3)	8 (47)	0.006
Number of cortical/juxtacortical lesions, median (range)	–	0 (0–3)	1 (0–12)	–

NMOSD-AQP4: neuromyelitis optica spectrum disorder-aquaporin-4 positive; MOGAD: myelin-oligodendrocytes-glycoprotein antibody-associated disease; MS: multiple sclerosis.

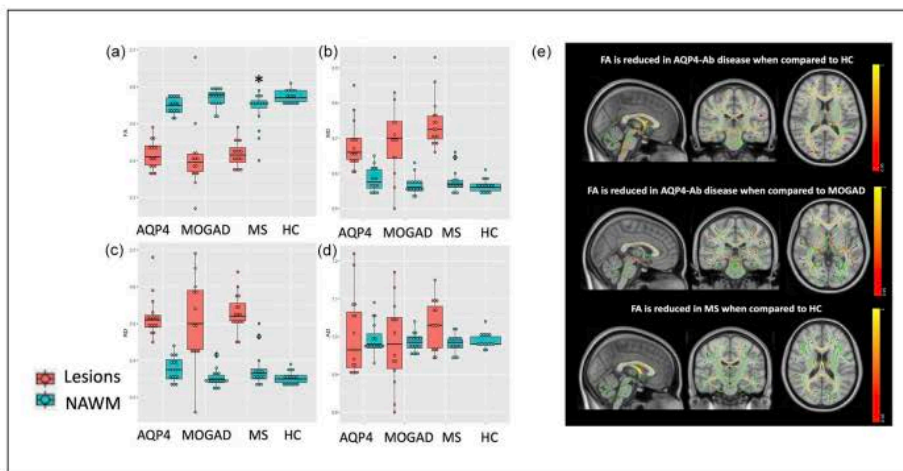


**Figure 4.** FA, MD, RD and AD lesions and NAWM comparison in the four groups (a–d); tract-based spatial statistics (TBSS) FA in NMOSD-AQP4 versus HC, NMOSD-AQP4 versus MOGAD, and MS versus HC (e). (a–d)  $*p < 0.05$  when compared to HC, on the linear model adjusted for age and sex. NAWM: normal-appearing white matter, AQP4: NMOSD-AQP4. (e) The FA skeleton is shown in green with a threshold of 0.2, tracts with lower FA are shown in red–yellow (values represent  $1-p$ -value, TFCE corrected). TBSS voxel-wise analysis of FA NAWM showed a significant reduction in NMOSD-AQP4 when compared with HC in the external capsule, corona radiata, the anterior limb of the internal capsule, posterior limb of the internal capsule (including fibres of the optic radiation), retrolenticular internal capsule, corpus callosum, posterior thalamic radiation (including the optic radiation); in the brainstem, the cerebral peduncle, the middle cerebellar peduncles, medial lemniscus, the pontine crossing tracts (corticospinal tracts) and the inferior cerebellar peduncles. FA NAWM in NMOSD-AQP4 when compared to MOGAD, showed a more widespread significant reduction. MS compared to HC, showed a significant reduction of the FA in the corpus callosum, corona radiata and posterior thalamic radiation, and not significant when compared to MOGAD. The TBSS voxel-wise analysis in the MOGAD did not show any significant difference when compared with HC.

deep grey matter volumes (Pearson's correlation coefficients; MOGAD:  $R = -0.93$ ,  $p < 0.001$ ; MS:  $R = -0.65$ ,  $p = 0.0034$ ) and also for cortical thickness (MOGAD:  $R = -0.71$ ,  $p = 0.005$ ; MS:  $R = -0.64$ ,  $p = 0.0042$ ). No significant correlations were found

with cortical volume. Due to the above correlation, we looked at the deep grey matter lesion volume correlation with deep grey matter volume but there was no significant correlation (although the numbers of lesions here were low; see Supplementary Results).

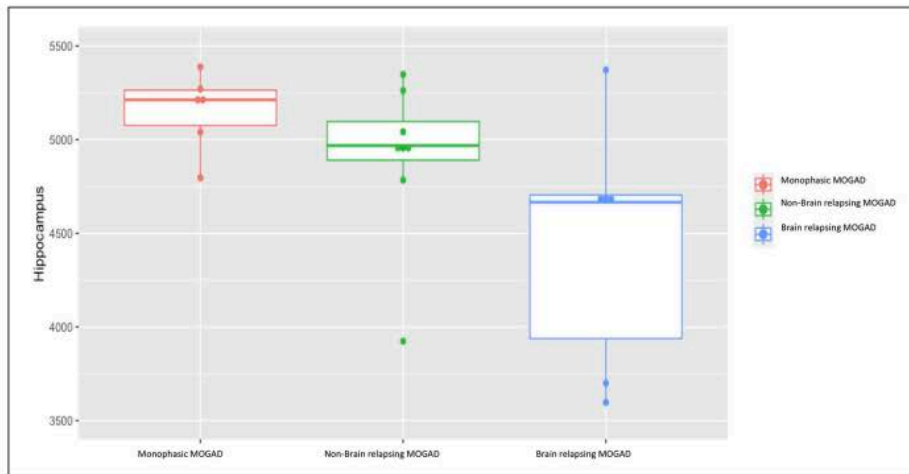


**Figure 5.** Comparison of hippocampus volumetric measures for patients with MOGAD and either a monophasic, relapsing with a brain relapse or relapsing with a non-brain relapse phenotype. The graphs represent the median, the 25th and 75th percentile.

#### Monophasic and relapsing MOGAD

MOGAD can be monophasic or relapsing and thus may be associated with different pathological mechanisms. We compared deep grey matter volumes (where abnormalities were most apparent) in the monophasic group ( $n=6$ ) to those with relapses not affecting the brain/brainstem ( $n=8$ ) to remove a dose effect of repeated brain damage. Hippocampal volumes were lower but not significant (see Figure 5), and caudate volumes were significantly higher in this relapsing group compared to monophasic group (hippocampus:  $-411 \text{ mm}^3$  (218)  $p=0.09$ ; caudate:  $-471 \text{ mm}^3$  (118)  $p=0.03$ ). However, only the hippocampal volume difference was plausible as this pattern was mirrored by a lower volume in the relapsing with brain/brainstem attacks.

#### Clinical outcomes and their association with the imaging findings

**Disability – EDSS.** We explored the association of MRI findings with EDSS, within each disease group, using a stepwise multivariable regression model, which showed that lower NAWM FA in NMOSD-AQP4 ( $R^2=0.49$ ; slope =  $-61.67$ ,  $p<0.001$ ), lower deep grey matter volumes and female sex in MS ( $R^2=0.47$ ; deep grey matter volume slope =  $-0.0002$ ,  $p=0.05$ ; beta value for sex =  $2.09$ ,  $p=0.005$ ) and lower brainstem volume in MOGAD ( $R^2=0.23$ ; slope =  $-0.0003$ ,  $p=0.03$ ) were associated with worse EDSS (see Supplementary Results for further details).

**Disability – visual acuity.** We found that lower optic chiasm in NMOSD-AQP4 ( $R^2=0.63$ ; slope =  $-0.007$ ,  $p<0.001$ ), and lower thalamic volume and female sex in MOGAD ( $R^2=0.42$ ; slope =  $-0.0004$ ,  $p=0.006$ ; beta value for sex =  $0.48$ ,  $p=0.04$ ) were associated with worse visual outcome. We did not find any significant predictor in MS.

#### Discussion

This is the first study using quantitative and non-conventional MRI to compare and contrast MOGAD to NMOSD-AQP4, MS and HC and showed different patterns across the three diseases (Table 3). We noted significant volume loss in the deep grey matter structures in MOGAD, as well as in MS, but not in NMOSD-AQP4, despite the greatest disability being seen in NMOSD-AQP4 and least in MOGAD. Abnormal deep grey matter and cortical thickness in MOGAD, showed a high correlation of 93% and 71%, respectively, with persistent brain lesions. In the white matter, optic chiasm volume was lower only in NMOSD-AQP4-ON patients. Although majority of the MOGAD patients had brain involvement in the acute phase, and FA was lower in the lesional tissue, NAWM-FA was not affected. Non-lesional FA was only found to be low in MS, although focal reductions in FA were noted in NMOSD-AQP4 patients, reflecting mainly the optic nerve, brainstem and corticospinal tract pathways. Cortical/juxtacortical (type I) fluffy, curvilinear lesions were seen in a minority of MOGAD, while cortical/

**Table 3.** Summary of the main findings.

	NMOSD-AQP4	MOGAD	MS
Global volume measures			
Brain volume	↓	↔	↓
White matter volume	↓	↔	↓
Grey matter volume	↓	↔	↓
Third ventricle volume	↑	↑	↑
Fourth ventricle volume	↔	↔	↔
Grey matter measures			
Deep grey matter volume	↓	↓↓	↓↓
Brainstem volume	↓↓	↓↓†	↓↓
Cortex volumes	↓↓†	↔	↔
Cortex thickness	↓	↔	↓
Cortical lesions*	↔	↑	↑↑
Cortex MD	↔	↔	↑
Basal ganglia MD	↔	↔	↔
White matter measures			
Optic chiasm volume in ON	↓↓	↔	↔
Corpus callosum volume	↔	↔	↓
Lesions volume*	↑	↑	↑↑
Lesion FA	↓↓	↓↓	↓↓
Lesion MD	↑↑	↑↑	↑↑
Lesion RD	↑↑	↑↑	↑↑
Lesion AD	↔	↔	↔
Normal-appearing white matter FA	↓	↔	↓↓
Normal-appearing white matter MD	↑	↔	↑
Normal-appearing white matter RD	↑	↔	↑
Normal-appearing white matter AD	↔	↔	↔

NMOSD-AQP4: neuromyelitis optica spectrum disorder-aquaporin-4 positive; MOGAD: myelin-oligodendrocytes-glycoprotein antibody-associated disease; MS: multiple sclerosis; MD: mean diffusivity; ON: optic neuritis; FA: fractional anisotropy; RD: radial diffusivity; AD: axial diffusivity. Compared to HC: ↔ no difference, ↓ lower but not significant, ↓↓ non-significantly lower, ↓↓↓ significantly lower, ↑ higher but not significant, ↑↑ significantly higher; \*comparison across disease groups.

juxtacortical and purely cortical (type II) ovoid lesions were identified in majority of MS patients and in none of the NMOSD-AQP4 patients.

Our study identified that deep grey matter structures are the only region of atrophy in MOGAD and this associated significantly with the current lesion volume. Overall, the grey matter was most sensitive to atrophy in MS, supporting previous studies.<sup>15,16</sup> Deep grey matter volume was lower, but not significantly in NMOSD-AQP4 as compared to HC. Despite poorer outcomes and older age, it appears this measure is less sensitive in NMOSD-AQP4, in keeping with other published papers.<sup>9,12,17</sup> This finding supports the growing evidence for grey matter involvement in MOGAD: grey matter lesions have been described in acute disseminated encephalomyelitis (ADEM) and over half of the children with ADEM have MOG-antibodies,<sup>18,19</sup> and grey matter atrophy has also been shown in the

spinal cord in MOGAD.<sup>20</sup> Further analysis showed that the lesions in both MOGAD and MS, but not in NMOSD-AQP4, correlated negatively with deep grey matter volume suggesting current lesion volume could be driving the atrophy by disruption of the white matter bundles projecting into the deep grey matter structures. The lack of correlation when using deep grey matter lesions alone suggests that lesions in tracts beyond the deep grey matter may contribute to its atrophy. It would be interesting in future studies to assess whether relapsing patients with greater residual lesion load might predict a worse outcome, and thus require more aggressive therapy than those with recovery of lesions.

Optic chiasm volumetric analysis, showed a significant low volume in NMOSD-AQP4 patients who have had an ON attack. This is in keeping with the clinical residual severity of ON associated with AQP4 antibodies and the observed optic radiation damage

may, therefore, be a consequence of the anterograde trans-synaptic degeneration, due to the axonal loss in the optic chiasm.<sup>21</sup> The lack of abnormality in the optic chiasm in MS and MOGAD with ON reflects the better recovery and the lack of posterior involvement, which is typically seen in NMOSD-AQP4.<sup>22</sup>

Ovoid, and some purely cortical (type II) lesions were (as expected) identified in a majority of MS patients. We found none in NMOSD-AQP4. Of note, we found curvilinear and fluffy cortical lesions involving adjacent juxtacortical regions (type I) in three MOGAD patients. This is intriguing, considering MS and MOGAD may have similar predominantly white matter targets (i.e. myelin) but cortical involvement is now well-described in MS,<sup>23</sup> and cortical signal changes associated with seizure have been reported as a rarer isolated phenotype in MOGAD.<sup>5</sup> In addition, cortical/juxtacortical lesions have been described in a clinical MRI study of MOGAD.<sup>24</sup> Cortical/juxtacortical lesions have been reported as absent in NMOSD<sup>25</sup> or have been identified in only a minority of NMOSD-AQP4 patients during the acute phase.<sup>26</sup> Although the cortex is rich in AQP4 water channels, we did not find lesions. Lower cortical thickness has been described in MS patients. In our cohort, it was not significantly lower when compared to the other disease groups, possibly due to the low sample size and low disability of the studied cohort.

We did not show a specific lesion pattern distribution in MOGAD and this is in line with previous findings where a disperse lesion distribution was identified.<sup>27</sup> Although infratentorial lesions are common in the acute phase, we did not find them in our MOGAD cohort as, in contrast to previous retrospective studies,<sup>27</sup> we only included patients in the remission phase. The location of lesions outside of the acute phase, that is, persistent lesions, is likely to be more useful in associating them with long-term disability.

FA changes were not found in MOGAD NAWM, even though MOGAD attacks are equally severe at nadir<sup>4</sup> and 17 out of 20 of the MOGAD cohort had acute brain lesions with 8 out of 20 having large acute lesions. Of interest is that the lesions themselves across all diseases, including MOGAD, appeared similarly affected on diffusion metrics and were abnormal when compared to the NAWM measures. Total NAWM-FA was found to be significantly abnormal in MS, and this could represent widespread lesion related damage (related to remote lesions or 'resolved' lesions) and/or non-lesional pathology. Tract-based analysis also identified damage in NMOSD-AQP4 but predominantly affecting the visual and pyramidal

pathways, supporting remote lesional damage in areas commonly affected in this disease. This predominance of visual and pyramidal pathway tract remote involvement is supported by other studies.<sup>11,12</sup> Thus recovery, as measured by this metric, was best in MOGAD than the other diseases.

Different MRI predictors of disability within the individual disease groups could suggest that different pathological mechanisms contribute to the tissue damage across these diseases. It is not surprising that NAWM FA was associated with EDSS in NMOSD-AQP4 disease, because the regional changes we identified were in those tracts mainly associated with the optic nerve and corticospinal tract and might relate to remote damage from attacks of ON and transverse myelitis. Lower deep grey-matter volume and female sex, associated to worse EDSS in MS, possibly reflecting the widespread atrophy of the deep grey matter structures noted in MS. Brainstem volume was the only MRI measure associated with EDSS in MOGAD, and this may reflect its eloquent site for ambulatory disability and is in line with our observation that the presence of brainstem lesions is associated with a worse recovery from transverse myelitis attacks.<sup>28</sup>

In the NMOSD-AQP4 group, lower optic chiasm volumes could explain reduced visual acuity, in line with previous observations of a preferential involvement of the chiasm in NMOSD-AQP4,<sup>22</sup> reflecting the recognised lack of chiasmatic involvement in MOGAD.<sup>29</sup> Only lower thalamic volume was associated with poorer mean visual acuity in MOGAD.

The main limitation of our study is the small sample size per disease group, related to our including two rare disease groups made even rarer by enriching them with patients with brain/cord involvement, and excluding those with the common phenotype of anatomically limited optic nerve involvement. The use of four different groups gives interesting insights into pathological differences, reflected in non-conventional, quantitative imaging measures. In addition, the homogeneity of a single-centre study, using the same scanner and protocol, along with reliable diagnostic ability (using the same expert clinicians and highly accurate assays) is an advantage and will reduce 'noise' and improve power. All group comparisons were adjusted for multiple comparisons with a Bonferroni correction across groups. No further adjustments for multiple comparisons were made and thus, the significant results, where novel or not studied previously, will need to be replicated in future studies. Observations from our study can then be used to build hypotheses and design future multicentre studies.

### Conclusion

Our study shows for the first time in MOGAD that deep grey matter atrophy can occur and that only lesional and not NAWM tissue damage can be detected using FA. It also highlights the relative sparing of deep grey matter in NMOSD-AQP4 disease, despite being associated with greater disability, and notes focal NAWM white matter changes. Future studies should focus on the association of 'invisible' symptoms (i.e. cognitive impairment and fatigue) with deep grey matter changes in MOGAD. Longitudinal studies in greater numbers may determine if non-conventional MRI measures could predict relapsing disease and may help identify who should be immunosuppressed from onset.

### Acknowledgements

We gratefully acknowledge all patients, relatives and healthy volunteers who participated in this study. We thank the radiographers Michael Sanders, Jon Campbell, David Parker and all the staff at the Wellcome Centre for Integrative Neuroimaging. We thank Dr Ludovica Griffanti for her insight on the MRI analysis, Dr Michael Cottar and Dr Hanna Nowicka for their support on diffusion analysis and Dr Fidel Alvaro Almagro for his insight on the FreeSurfer software.

### Author contributions

J.P. had full access to all of the data in the study and takes responsibility for the integrity of the data and the accuracy of the data analysis. Concept and design were the work of S.M., J.P. and R.M. Acquisition, analysis or interpretation of data were done by all authors. Drafting of the manuscript was done by S.M. and J.P. Critical revision of the manuscript for important intellectual content was done by R.M., A.R.-F., M.Ju., M.Je., M.I.L. and M.C. Statistical analysis was done by S.M. Administrative, technical or material support was provided by A.C. Supervision was done by J.P. and M.Je.

### Declaration of Conflicting Interests


The author(s) declared the following potential conflicts of interest with respect to the research, authorship and/or publication of this article: S.M. has received travel grants from Biogen, Novartis, Bayer, Merck, Almirall, Roche and honorarium for advisory work from Biogen. R.M. is undertaking graduate studies funded by the Rhodes Trust and the Oppenheimer Memorial Trust. A.R.-F. reports no disclosures. A.C. reports no disclosures. M.J. reports no disclosures. M.I.L. reported being involved in aquaporin 4 testing, receiving support from the National Health Service National Specialised Commissioning

Group for Neuromyelitis Optica and the National Institute for Health Research Oxford Biomedical Research Centre, receiving speaking honoraria from Biogen Idec, and receiving travel grant from Novartis. J.P. is partly funded by highly specialised services to run a national congenital myasthenia service and a neuromyelitis service. She has received support for scientific meetings and honorariums for advisory work from Merck Serono, Biogen Idec, Novartis, Teva, Chugai Pharma and Bayer Schering, Alexion, Roche, Genzyme, MedImmune, EuroImmun, MedDay, Abide and ARGENX, and grants from Merck Serono, Novartis, Biogen Idec, Teva, Abide and Bayer Schering. Her hospital trust received funds for her role as clinical lead for the RSS, and she has received grants from the MS society and Guthrie Jackson Foundation for research studies. M.C. has served on scientific advisory boards for Biogen Idec, Genzyme, Merck Serono, Novartis and Roche and has received grants from Genzyme, Merck Serono, Novartis and Roche and travel and/or speaker honoraria from Merck Serono, Roche, Biogen Idec, Novartis and Genzyme. M.J. receives royalties from licensing of FSL to non-academic, commercial parties.

### Funding

The author(s) disclosed receipt of the following financial support for the research, authorship and/or publication of this article: We thank the NHS Highly Specialised Commissioning Team for funding the Neuromyelitis Optica service in Oxford. MRI scans were funded by a Research and Development Fund belonging to the principal investigator, Professor J.P.

### ORCID iD

Silvia Messina  <https://orcid.org/0000-0002-1134-5771>

### Supplemental material

Supplemental material for this article is available online.

### References

1. Lennon VA, Kryzer TJ, Pittock SJ, et al. IgG marker of optic-spinal multiple sclerosis binds to the aquaporin-4 water channel. *J Exp Med* 2005; 202: 473–477.
2. Weinshenker BG, Wingerchuk DM, Pittock SJ, et al. NMO-IgG: A specific biomarker for neuromyelitis optica. *Dis Markers* 2006; 22(4): 197–206.
3. Wingerchuk DM, Banwell B, Bennett JL, et al. International consensus diagnostic criteria for



- neuromyelitis optica spectrum disorders. *Neurology* 2015; 85: 177–189.
4. Jurynczyk M, Messina S, Woodhall MR, et al. Clinical presentation and prognosis in MOG-antibody disease: A UK study. *Brain* 2017; 140: 3128–3138.
  5. Ogawa R, Nakashima I, Takahashi T, et al. MOG antibody-positive, benign, unilateral, cerebral cortical encephalitis with epilepsy. *Neurol Neuroimmunol Neuroinflamm* 2017; 4(2): e322.
  6. Pittock SJ, Lennon VA, Krecke K, et al. Brain abnormalities in neuromyelitis optica. *Arch Neurol* 2006; 63: 390–396.
  7. Jurynczyk M, Gerales R, Probert F, et al. Distinct brain imaging characteristics of autoantibody-mediated CNS conditions and multiple sclerosis. *Brain* 2017; 140: 617–627.
  8. Chanson JB, Lamy J, Rousseau F, et al. White matter volume is decreased in the brain of patients with neuromyelitis optica. *Eur J Neurol* 2013; 20(2): 361–367.
  9. Duan Y, Liu Y, Liang P, et al. Comparison of grey matter atrophy between patients with neuromyelitis optica and multiple sclerosis: A voxel-based morphometry study. *Eur J Radiol* 2012; 81(2): e110–114.
  10. Rocca MA, Agosta F, Mezzapesa DM, et al. Magnetization transfer and diffusion tensor MRI show gray matter damage in neuromyelitis optica. *Neurology* 2004; 62: 476–478.
  11. Kim SH, Kwak K, Hyun JW, et al. Diffusion tensor imaging of normal-appearing white matter in patients with neuromyelitis optica spectrum disorder and multiple sclerosis. *Eur J Neurol* 2017; 24(7): 966–973.
  12. Matthews L, Kolind S, Brazier A, et al. Imaging surrogates of disease activity in neuromyelitis optica allow distinction from multiple sclerosis. *PLoS ONE* 2015; 10(9): e0137715.
  13. Zhuo Z, Duan Y, Tian D, et al. Brain structural and functional alterations in MOG antibody disease. *Mult Scler*. Epub ahead of print 15 October 2020. DOI: 10.1177/1352458520964415.
  14. Filippi M, Preziosa P, Banwell BL, et al. Assessment of lesions on magnetic resonance imaging in multiple sclerosis: Practical guidelines. *Brain* 2019; 142: 1858–1875.
  15. Zhang J, Giorgio A, Vinciguerra C, et al. Gray matter atrophy cannot be fully explained by white matter damage in patients with MS. *Mult Scler* 2020; 27: 39–51.
  16. Messina S and Patti F. Gray matters in multiple sclerosis: Cognitive impairment and structural MRI. *Mult Scler Int* 2014; 2014: 609694.
  17. Eshaghi A, Wotschel V, Cortese R, et al. Gray matter MRI differentiates neuromyelitis optica from multiple sclerosis using random forest. *Neurology* 2016; 87: 2463–2470.
  18. Salama S, Khan M, Pardo S, et al. MOG antibody-associated encephalomyelitis/encephalitis. *Mult Scler* 2019; 25(11): 1427–1433.
  19. Hacoen Y, Mankad K, Chong WK, et al. Diagnostic algorithm for relapsing acquired demyelinating syndromes in children. *Neurology* 2017; 89: 269–278.
  20. Mariano R, Messina S, Roca-Fernandez A, et al. Quantitative spinal cord MRI in MOG-antibody disease, neuromyelitis optica and multiple sclerosis. *Brain* 2020; 144: 198–212.
  21. Juenger V, Cooper G, Chien C, et al. Optic chiasm measurements may be useful markers of anterior optic pathway degeneration in neuromyelitis optica spectrum disorders. *Eur Radiol* 2020; 30: 5048–5058.
  22. Khanna S, Sharma A, Huecker J, et al. Magnetic resonance imaging of optic neuritis in patients with neuromyelitis optica versus multiple sclerosis. *J Neuroophthalmol* 2012; 32(3): 216–220.
  23. Calabrese M, Battaglini M, Giorgio A, et al. Imaging distribution and frequency of cortical lesions in patients with multiple sclerosis. *Neurology* 2010; 75: 1234–1240.
  24. Salama S, Khan M, Levy M, et al. Radiological characteristics of myelin oligodendrocyte glycoprotein antibody disease. *Mult Scler Relat Disord* 2019; 29: 15–22.
  25. Calabrese M, Oh MS, Favaretto A, et al. No MRI evidence of cortical lesions in neuromyelitis optica. *Neurology* 2012; 79: 1671–1676.
  26. Kim W, Lee JE, Kim SH, et al. Cerebral cortex involvement in neuromyelitis optica spectrum disorder. *J Clin Neurol* 2016; 12(2): 188–193.
  27. Yang L, Li H, Xia W, et al. Quantitative brain lesion distribution may distinguish MOG-ab and AQP4-ab neuromyelitis optica spectrum disorders. *Eur Radiol* 2020; 30(3): 1470–1479.
  28. Mariano R, Messina S, Kumar K, et al. Comparison of clinical outcomes of transverse myelitis among adults with myelin oligodendrocyte glycoprotein antibody vs aquaporin-4 antibody disease. *JAMA Netw Open* 2019; 2: e1912732.
  29. Kupfer C, Chumbley L and Downer JC. Quantitative histology of optic nerve, optic tract and lateral geniculate nucleus of man. *J Anat* 1967; 101(Pt. 3): 393–401.

### 11.1.2.6. Retinal Optical Coherence Tomography in Neuromyelitis Optica

Citation: Oertel, F.C., Specovius, S., Zimmermann, H.G. Chien, C., Motamedi, S., Bereuter, C., Cook, C., Lana-Peixoto, M.A., Andrade-Fontanelle, M., Kim, H.J., Hyun, J-W., Palace, J., **Roca-Fernández, A.**, ... Brandt, A.U., and Paul, F. (2021). *Retinal Optical Coherence Tomography in Neuromyelitis Optica*. *Neurol Neuroimmunol Neuroinflammation*. 2021 Nov;8(6): e1068. IF: 8.485

# Retinal Optical Coherence Tomography in Neuromyelitis Optica

Frederike Cosima Oertel, MD/PhD, Svenja Specovius, MSc, Hanna G. Zimmermann, PhD, Claudia Chien, PhD, Seyedamirhosein Motamedi, PhD, Charlotte Bereuter, BSc, Lawrence Cook, PhD, Marco Aurélio Lana Peixoto, MD, PhD, Mariana Andrade Fontanelle, MD, Ho Jin Kim, MD, PhD, Jae-Won Hyun, MD, PhD, Jacqueline Palace, MD, Adriana Roca-Fernandez, MSc, Maria Isabel Leite, MD, PhD, Sriakshmi Sharma, MD, PhD, Fereshteh Ashtari, MD, Rahele Kafieh, PhD, Alireza Dehghani, PhD, Mohsen Pourazizi, PhD, Lekha Pandit, MD, PhD, Anitha D'Cunha, PhD, Orhan Aktas, MD, Marius Ringelstein, MD, Philipp Albrecht, MD, Eugene May, MD, Caryl Tongco, Letizia Leocani, MD, PhD, Marco Pisa, MD, Marta Radaelli, MD, PhD, Elena H. Martinez-Lapiscina, MD, PhD, Hadas Stiebel-Kalish, MD, Sasitorn Siritho, MD, Jérôme de Seze, MD, PhD, Thomas Senger, MD, Joachim Havla, MD, Romain Marignier, MD, PhD, Alvaro Cobo Calvo, MD, PhD, Denis Bichuetti, MD, PhD, Ivan Maynard Tavares, MD, PhD, Nasrin Asgari, MD, PhD, Kerstin Soelberg, MD, Ayse Altintas, MD, Rengin Yildirim, MD, Uygur Tanriverdi, MD, Anu Jacob, MD, Saif Huda, MD, PhD, Zoe Rimler, BSc, Allyson Reid, MD, Yang Mao-Draayer, MD, PhD, Ibis Soto de Castillo, MD, Axel Petzold, MD, PhD, Ari J. Green, MD, Michael R. Yeaman, MD, PhD, Terry Smith, MD, Alexander U. Brandt, MD,\* and Friedemann Paul, MD\*

## Correspondence

Dr. Paul  
friedemann.paul@charite.de

*Neurol Neuroimmunol Neuroinflamm* 2021;8:e1068. doi:10.1212/NXI.0000000000001068

## Abstract

### Background and Objectives

To determine optic nerve and retinal damage in aquaporin-4 antibody (AQP4-IgG)-seropositive neuromyelitis optica spectrum disorders (NMOSD) in a large international cohort after previous studies have been limited by small and heterogeneous cohorts.

### Methods

The cross-sectional Collaborative Retrospective Study on retinal optical coherence tomography (OCT) in neuromyelitis optica collected retrospective data from 22 centers. Of 653 screened participants, we included 283 AQP4-IgG-seropositive patients with NMOSD and 72 healthy controls (HCs). Participants underwent OCT with central reading including quality

\*These authors contributed equally to this work.

From the Experimental and Clinical Research Center (F.C.O., Svenja Specovius, H.G.Z., C.C., S.M., C.B., A.U.B., F.P.), Max Delbrück Center for Molecular Medicine and Charité-Universitätsmedizin Berlin, Corporate Member of Freie Universität Berlin and Humboldt-Universität zu Berlin, Germany; NeuroCure Clinical Research Center (F.C.O., Svenja Specovius, H.G.Z., C.C., S.M., C.B., A.U.B., F.P.), Charité-Universitätsmedizin Berlin, Corporate Member of Freie Universität Berlin, Humboldt-Universität zu Berlin, Germany; Department of Neurology (F.C.O., A.J.G.), University of California San Francisco, CA; Department of Pediatrics (L.C.), University of Utah, Salt Lake City; CIEM MS Research Center (M.A.L.P., M.A.F.), University of Minas Gerais, Medical School, Belo Horizonte, Brazil; Department of Neurology (H.J.K., J.-W.H.), National Cancer Center, Goyang, Republic of Korea; Department of Neurology (J.P., A.R.-F., M.I.L.), and Department of Ophthalmology (Sriakshmi Sharma), and Department of Ophthalmology (Sriakshmi Sharma), Oxford University Hospitals, National Health Service Trust, UK; Kashani MS Center (F.A.), School of Advanced Technologies in Medicine and Medical Image and Signal Processing Research Center (R.K.), Department of Ophthalmology, Isfahan Eye Research Center (A.D., Mohsen Pourazizi), Isfahan University of Medical Sciences, Iran; Department of Neurology (L.P., A.D.C.), KS Hegde Medical Academy, Nitte University, Mangalore, India; Department of Neurology (O.A., Marius Ringelstein, P.A.), Medical Faculty, Heinrich Heine University Düsseldorf, Germany; Swedish Neuroscience Institute Neuro-Ophthalmology (E.M., C.T.), Seattle, WA; Experimental Neurophysiology Unit (L.L., Marco Pisa, Marta Radaelli), Institute of Experimental Neurology (INSPE) Scientific Institute Hospital San Raffaele and University Vita-Salute San Raffaele, Milan, Italy; Hospital Clinic of Barcelona-Institut d'Investigacions (E.H.M.-L.), Biomèdiques August Pi Sunyer, (IDIBAPS), Spain; Sackler School of Medicine (H.S.-K.), Tel Aviv University, Israel; Neuro-Ophthalmology Division (H.S.-K.), Department of Ophthalmology, Rabin Medical Center, Petah Tikva, Israel; Division of Neurology (Sasitorn Siritho), Department of Medicine, Siriraj Hospital and Bumrungrad International Hospital, Bangkok, Thailand; Neurology Service (J.d.S., Thomas Senger), University Hospital of Strasbourg, France; Institute of Clinical Neuroimmunology (J.H.), Biomedical Center and University Hospital, Ludwig-Maximilians-Universität München, Munich, Germany; Neurology (R.M., A.C.C.), Multiple Sclerosis, Myelin Disorders and Neuroinflammation, Pierre Wertheimer Neurological Hospital, Hospices Civils de Lyon, France; Centre d'Esclerosi Múltiple de Catalunya (Cemcat) (A.C.C.), Department of Neurology/Neuroimmunology, Hospital Universitari Vall d'Hebron, Universitat Autònoma de Barcelona, Spain; Department of Neurology and Neurosurgery (D.B., I.M.T.), Escola Paulista de Medicina, Universidade Federal de São Paulo, Brazil; Departments of Neurology (N.A.), Slagelse Hospitals, Institute of Regional Health Research, University of Southern Denmark, Odense; Institute of Regional Health Research (N.A., K.S.), University of Southern Denmark, Odense; Department of Neurology (A.A., U.T.), and Department of Ophthalmology (R.Y.), Cerrahpasa Medical Faculty, Istanbul University, Turkey; The Walton Centre for Neurology and Neurosurgery (A.J., S.H.), Liverpool, UK; The Cleveland Clinic Abu Dhabi (A.J.), United Arab Emirates; NYU Multiple Sclerosis Comprehensive Care Center (Z.R., A.R.), Department of Neurology, NYU School of Medicine, New York; Department of Neurology (Y.M.-D.), University of Michigan Medical School, Ann Arbor; Department of Neurology (I.S.C.), Hospital Clínico de Maracaibo, Venezuela; Moorfields Eye Hospital (A.P.), University College London, UK; Department of Medicine (M.R.Y.), Los Angeles Biomedical Research Institute at Harbor-UCLA Medical Center, Los Angeles, CA, United States of America; Department of Medicine (M.R.Y.), David Geffen School of Medicine at UCLA, Los Angeles, CA, United States of America; Departments of Ophthalmology and Visual Sciences (Terry Smith), Kellogg Eye Center, University of Michigan Medical School, Ann Arbor, United States of America; Division of Metabolism (Terry Smith), Endocrine and Diabetes, Department of Internal Medicine, University of Michigan Medical School, Ann Arbor; Department of Neurology (A.U.B.), University of California, Irvine; and Department of Neurology (F.P.), Charité-Universitätsmedizin Berlin, Corporate Member of Freie Universität Berlin and Humboldt-Universität zu Berlin, Germany.

Go to [Neurology.org/NN](https://www.neurology.org/NN) for full disclosures. Funding information is provided at the end of the article.

The Article Processing Charge was funded by the authors.

This is an open access article distributed under the terms of the Creative Commons Attribution-NonCommercial-NoDerivatives License 4.0 (CC BY-NC-ND), which permits downloading and sharing the work provided it is properly cited. The work cannot be changed in any way or used commercially without permission from the journal.

Copyright © 2021 The Author(s). Published by Wolters Kluwer Health, Inc. on behalf of the American Academy of Neurology.

1

## Glossary

**AQP4-IgG** = aquaporin-4 IgG; **CROCTINO** = Collaborative Retrospective Study on retinal OCT in Neuromyelitis Optica; **EDSS** = Expanded Disability Status Scale; **GCIP** = ganglion cell and inner plexiform; **HC** = healthy control; **HC-VA** = high-contrast visual acuity; **INL** = inner nuclear layer; **MME** = microcystic macular edema; **MS** = multiple sclerosis; **MOG-IgG** = myelin oligodendrocyte glycoprotein IgG; **NMOSD** = neuromyelitis optica spectrum disorder; **NMOSD-NON** = NMOSD eyes without a history of ON; **OCT** = optical coherence tomography; **ON** = optic neuritis; **pRNFL** = peripapillary retinal nerve fiber layer; **SE** = standard error; **VA** = visual acuity; **VEP** = visually evoked potential.

control and intraretinal segmentation. The primary outcome was thickness of combined ganglion cell and inner plexiform (GCIP) layer; secondary outcomes were thickness of peripapillary retinal nerve fiber layer (pRNFL) and visual acuity (VA).

## Results

Eyes with ON (NMOSD-ON,  $N = 260$ ) or without ON (NMOSD-NON,  $N = 241$ ) were assessed compared with HCs ( $N = 136$ ). In NMOSD-ON, GCIP layer ( $57.4 \pm 12.2 \mu\text{m}$ ) was reduced compared with HC (GCIP layer:  $81.4 \pm 5.7 \mu\text{m}$ ,  $p < 0.001$ ). GCIP layer loss ( $-22.7 \mu\text{m}$ ) after the first ON was higher than after the next ( $-3.5 \mu\text{m}$ ) and subsequent episodes. pRNFL observations were similar. NMOSD-NON exhibited reduced GCIP layer but not pRNFL compared with HC. VA was greatly reduced in NMOSD-ON compared with HC eyes, but did not differ between NMOSD-NON and HC.

## Discussion

Our results emphasize that attack prevention is key to avoid severe neuroaxonal damage and vision loss caused by ON in NMOSD. Therapies ameliorating attack-related damage, especially during a first attack, are an unmet clinical need. Mild signs of neuroaxonal changes without apparent vision loss in ON-unaffected eyes might be solely due to contralateral ON attacks and do not suggest clinically relevant progression but need further investigation.

Patients with neuromyelitis optica spectrum disorder (NMOSD) experience recurrent optic neuritis (ON),<sup>1</sup> resulting in vision loss and decreased quality of life.<sup>1-4</sup> According to our understanding, there are at least 3 subtypes based on serostatus: Up to 3 of 4 patients manifest as anti-aquaporin-4 IgG (AQP4-IgG) seropositive. Approximately half of the AQP4-IgG-seronegative patients manifest as anti-myelin oligodendrocyte glycoprotein IgG (MOG-IgG) seropositive, and half are double seronegative.<sup>5</sup> Yet, clinical correlates of serologic phenotypes, including subclinical or clinical retinal degeneration and vision loss, remain unclear.<sup>6,7</sup>

Optical coherence tomography (OCT) is an interferometric technique producing high-resolution retinal images.<sup>1,8</sup> OCT has become a reliable tool for diagnosing and monitoring neurologic and neuro-ophthalmologic diseases, especially for quantifying neurodegeneration after ON.<sup>1</sup> Because of limited samples and varying methods, existing OCT studies in NMOSD are inconsistent regarding the amount of retinal neurodegeneration with and without ON. Previous studies also failed to address the influence of retinal neurodegeneration on microcystic macular edema (MME) and function.<sup>2,6,7</sup> These issues together with heterogeneities and the often monocentric character of previous cohorts limit the relevance of meta-analyses.

To overcome these limitations, we performed an OCT analysis of AQP4-IgG-seropositive patients with NMOSD in an international multicenter study, termed Collaborative Retrospective Study on retinal OCT in Neuromyelitis Optica (CROCTINO).<sup>9</sup>

It represents the largest NMOSD OCT data set and additionally validated an OCT postprocessing approach to circumvent differences in acquisition and imaging processing protocols inherent to pooled analyses.<sup>10</sup> Outcomes include: (1) distinguishing retinal neurodegeneration after ON from subtle damage in clinically unaffected eyes, (2) defining frequency of MME, and (3) deriving structure-function correlations.

## Methods

### Study Design

This cross-sectional international multicenter study was performed under the aegis of the CROCTINO study, which was a collaborative effort within the Guthy-Jackson Charitable Foundation network.<sup>9</sup> Participating centers contributed OCT data (acquired between 2008 and 2018) and clinical metadata (acquired between 2000 and 2018, eTable 1, [links.lww.com/NXI/A557](https://links.lww.com/NXI/A557)).

### Cohort Selection

Inclusion criteria for this analysis were (1) patients diagnosed with NMOSD per the 2015 International Panel of NMOSD diagnosis criteria<sup>11</sup> and (2) having confirmed serum AQP4-IgG. Exclusion criteria were (1) comorbidities potentially confounding interpretation of OCT results (e.g., macular degeneration, glaucoma, and intracranial hypertension); (2) > 3 months distance between clinical and OCT data acquisition; (3) < 6 months between OCT imaging and most recent ON, or (4) an uncertain history of ON. The inclusion and

**Table 1** Cohort Description for AQP4-IgG-Seropositive Patients With NMOSD and HCs

	AQP4-IgG-seropositive NMOSD	HC
Subjects (N)	283	72
Eyes (N)	501	136
Sex (male/female, N/N [%/%])	28/255 (9.9/90.1)	26/46 (36.1/63.9)
Age (y, mean ± SD)	44.1 ± 14.2	30.9 ± 7.7
Ethnicity (N [%])		
Asian	77 (27.2)	16 (22.2)
Black/African American	13 (4.6)	0 (0)
White, Hispanic/Latino	4 (1.4)	1 (1.4)
White, Non-Hispanic	159 (56.2)	55 (76.4)
Other/nonreported	30 (10.6)	0 (0)
Disease-modifying therapy (N [%])		
Rituximab	73 (25.8)	
Azathioprine	67 (23.7)	
Oral prednisolone	53 (18.7)	
Mycophenolate mofetil	48 (17.0)	
Methotrexate	8 (2.8)	
Time since onset (y, mean ± SD)	7.2 ± 6.7	
EDSS score (median [IQR])	3.5 (2.0–4.5)	
Patients with a clinical history of ON (N [%])	204 (72.1)	
Eyes with a clinical history of ON (N [%])	260 (52)	
No. of ON episodes/eye (N, median [min–max])	1 (1–6)	
Time since last ON (mo, mean ± SD)	71 ± 57	

Abbreviations: AQP4-IgG = aquaporin-4 antibodies; NMOSD = neuromyelitis optica spectrum disorder; HC = healthy control; N = number; OCT = optical coherence tomography; ON = optic neuritis episode. Age ( $p < 0.0001$ ) and sex ( $p < 0.0001$ ) were not matched.

exclusion criteria are depicted in eFigure 1, [links.lww.com/NXI/A556](https://links.lww.com/NXI/A556). AQP4-IgG testing was performed at the discretion of each investigator.

### Standard Protocol Approvals, Registrations, and Patient Consents

All participants gave written informed consent, and the study was approved by local ethics committees and conducted in accordance with the applicable laws and the current version of the Declaration of Helsinki. Data are reported according to STROBE reporting guidelines.<sup>12</sup>

### OCT

High-resolution imaging data were acquired using 3 different spectral domain OCT devices: Spectralis SD-OCT (Heidelberg Engineering, Heidelberg, Germany) at 15 centers (194 patients/358 eyes; 72 healthy controls [HCs]/136 eyes); Cirrus HD-OCT (Carl Zeiss Meditec, Dublin, CA) at 6 centers (58 patients/87 eyes); or Topcon 3D OCT-1 (Topcon, Tokyo, Japan) at 1 center (31 patients/56 eyes). All reading of OCT data was performed at Charité–Universitätsmedizin Berlin Translational Neuroimaging Group by 5 graders. Image quality was assessed using modified OSCAR-IB criteria by one of the graders, respectively.<sup>13,14</sup> OCT segmentation for the combined ganglion cell and inner plexiform (GCIP) layer and inner nuclear layer (INL) thicknesses was corrected semi-automatically using an in-house software.<sup>10,15</sup> In brief, GCIP layer and INL thicknesses were calculated from a 5-mm diameter cylinder around the fovea excluding the central 1-mm diameter cylinder from a macular volume scan.<sup>10</sup> The peripapillary retinal nerve fiber layer (pRNFL) thickness was measured and corrected according to the device protocol (Spectralis: peripapillary ring scan with 12° or approximately 3.4 mm diameter around the optic disc; Topcon and Cirrus: extraction from optic disc volume scan). For the current analysis, eyes were excluded from the analysis if neither ring nor macular scan passed quality control. We further excluded data from the less common instrument for 1 center. The final cohort included 364 macular and 481 peripapillary scans of 501 eyes from 283 patients and 136 eyes from 72 HCs. Lower numbers of macular scans compared with peripapillary scans were due to both lower submission of macular data and more exclusions based on quality concerns.

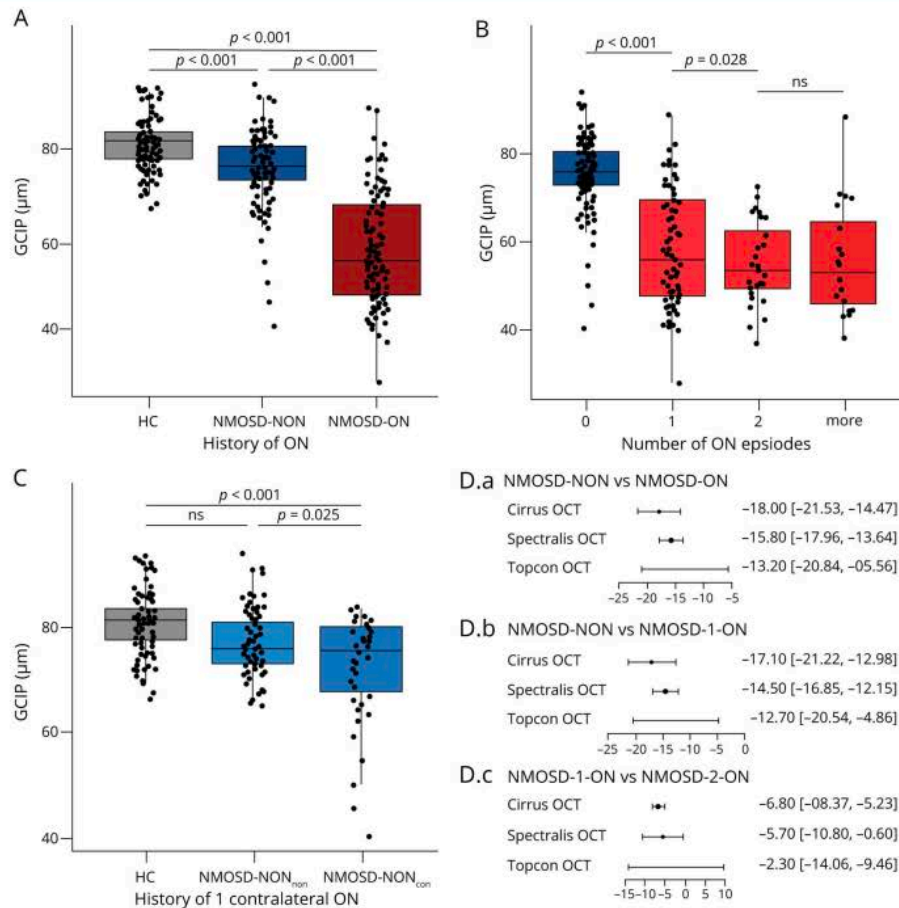
### Visual and Global Function Testing

High-contrast visual acuity (HC-VA) was available for 497 (99.2%) patient and 10 (13.9%) HC eyes. HC-VA was best corrected for 212 (42.3%) patient and 56 (41.2%) HC eyes, habitually corrected for 145 (28.9%) patient and 2 (<0.1%) HC eyes, and without correction for 140 (27.9%) patient eyes and 17 (1.3%) HC eyes. All VA data are reported as logMAR. VA measurement method was decided on discretion of each center. Visually evoked potentials (VEPs) were available for 167 (33.3%) patient eyes and 40 (29.4%) HC eyes, with P100 latency recorded as a binary value (normal/prolonged). Expanded Disability Status Scale (EDSS) scores were determined at the discretion of each center with data available for 180 (63.6%) patients.

### Statistical Analysis

Statistical analyses were performed with R version 3.6.1 using RStudio and R Markdown (RStudio Inc., Boston, MA).<sup>16</sup>  $p$  Values less than 0.05 were considered significant. We considered  $p$  values less than 0.10 a trend. Group matching by age and sex for confirmatory analyses was performed using automatic matching by R package MatchIt (method: exact). Group comparisons and correlations of OCT and VA values were performed using linear mixed-

**Figure 1** Group Comparisons of GCIPL Layer Thickness



Boxplots of GCIPL layer thicknesses ( $\mu\text{m}$ ) acquired by Heidelberg SD-OCT with values of individual eyes (jitter) for (A) HC (gray/left), NMOSD-NON (dark blue/middle), NMOSD-ON (dark red/right); for (B) number of ON episodes (NMOSD-NON dark blue/left, NMOSD-1-ON light red/left-middle, NMOSD-2-ON medium-red/right-middle, NMOSD- $\geq$ 3-ON medium-dark red/right); and for (C) HC (gray/left), NMOSD-NON<sub>con</sub> (light blue/middle), NMOSD-NON<sub>con</sub> (blue/right). (D) Forest plots for results from different OCT devices for (D.a) NMOSD-NON vs NMOSD-ON, (D.b) NMOSD-NON vs NMOSD-1-ON, and (D.c) NMOSD-1-ON vs NMOSD-2-ON (eFigure 2 and eTable 2, [links.lww.com/NXI/A556](https://links.lww.com/NXI/A556) and [links.lww.com/NXI/A557](https://links.lww.com/NXI/A557)). GCIPL = ganglion cell and inner plexiform; HC = eyes of HCs; NMOSD-NON = eyes of patients with neuromyelitis optica without a history of ON; NMOSD-NON<sub>con</sub> = eyes of patients with neuromyelitis optica without a history of ON but a history of contralateral ON; NMOSD-NON<sub>non</sub> = eyes of patients with neuromyelitis optica without a history of ipsilateral or contralateral ON; NMOSD-ON = eyes of patients with neuromyelitis optica with a history of ON; NMOSD-1-ON = eyes of patients with neuromyelitis optica with a history of 1 ON episode; NMOSD-2-ON = eyes of patients with neuromyelitis optica with a history of 2 ON episodes; ON = optic neuritis.

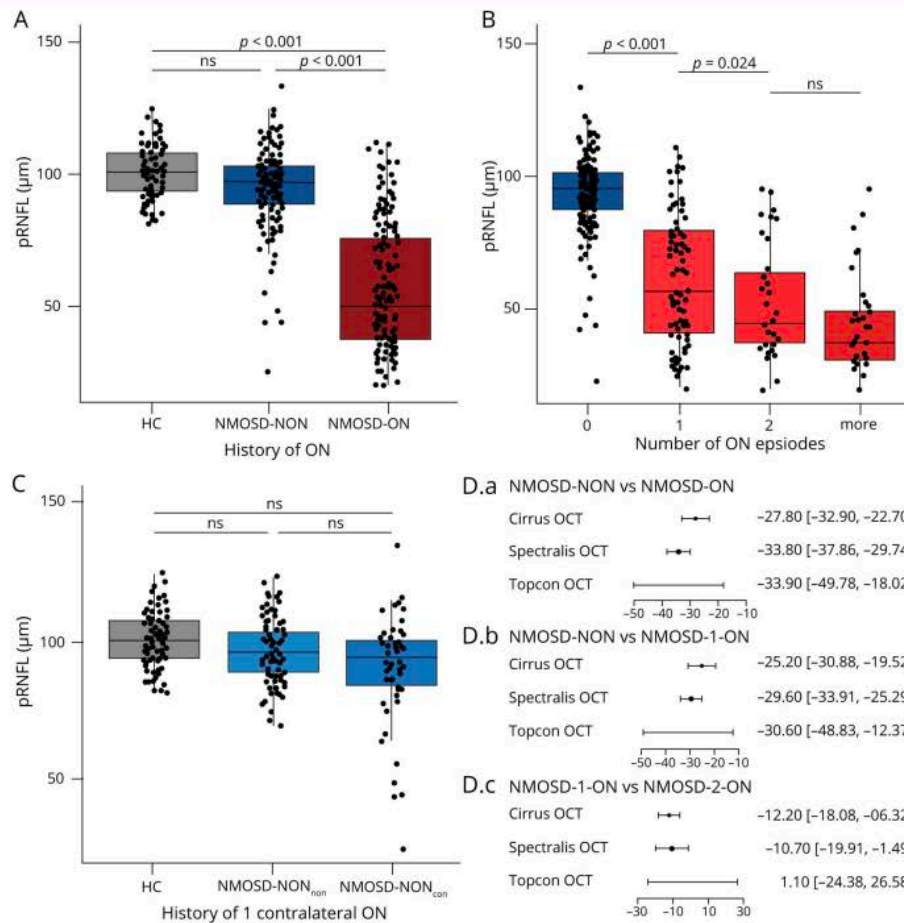
effect models. Intereye within-subject effects and effects of the center were included as random effects. Sex, ethnicity, and age were included as fixed effects for the analyses in the entire cohort. Age and sex were not included for the matched subset. For OCT parameters, the model was used for data from all devices separately and combined by Fisher combined probability test. The marginal and conditional coefficients of determination of the linear models were calculated with pseudo R-squared. All results are reported

combined and individually for Spectralis SD-OCT; the analyses of data acquired by Cirrus HD-OCT or Topcon 3D OCT-1 and for the matched subset are reported as online-only supplement.

#### Data Availability

The data supporting the findings of this study are available within the article and from the corresponding author by reasonable request.

**Figure 2** Group Comparisons of pRNFL Thickness



Boxplots of pRNFL thicknesses acquired by Heidelberg SD-OCT [ $\mu\text{m}$ ] with values of individual eyes (jitter) for (A) HC (gray/left), NMOSD-NON (dark blue/middle), and NMOSD-ON (dark red/right); for (B) number of ON episodes (NMOSD-NON dark blue/left, NMOSD-1-ON light red/left-middle, NMOSD-2-ON medium-red/right-middle, and NMOSD- $\geq$ 3-ON medium-dark red/right); and for (C) HC (gray/left), NMOSD-NON<sub>non</sub> (light blue/middle), and NMOSD-NON<sub>con</sub> (blue/right). (D) Forest plots for results from different OCT devices for (D.a) NMOSD-NON vs NMOSD-ON, (D.b) NMOSD-NON vs NMOSD-1-ON, and (D.c) NMOSD-1-ON vs NMOSD-2-ON (eFigure 3 and eTable 3, [links.lww.com/NXI/A556](https://links.lww.com/NXI/A556) and [links.lww.com/NXI/A557](https://links.lww.com/NXI/A557)). HC = eyes of HCs; NMOSD-NON = eyes of patients with neuromyelitis optica without a history of optic neuritis; NMOSD-NON<sub>non</sub> = eyes of patients with neuromyelitis optica without a history of optic neuritis but a history of contralateral optic neuritis; NMOSD-NON<sub>con</sub> = eyes of patients with neuromyelitis optica without a history of ipsilateral or contralateral optic neuritis; NMOSD-ON = eyes of patients with neuromyelitis optica with a history of optic neuritis; NMOSD-1-ON = eyes of patients with neuromyelitis optica with a history of 1 optic neuritis episode; NMOSD-2-ON = eyes of patients with neuromyelitis optica with a history of 2 optic neuritis episodes; ON = optic neuritis; pRNFL = peripapillary retinal nerve fiber layer.

## Results

Five hundred one eyes of 283 AQP4-IgG-seropositive patients and 136 eyes of 72 HCs were included in the analysis (Table 1).

### Neuroaxonal Damage After ON

GCIP layer and pRNFL were reduced in NMOSD-ON compared with NMOSD eyes without a history of ON

(NMOSD-NON) and HC (GCIP layer:  $81.4 \pm 5.7 \mu\text{m}$ , pRNFL:  $101.1 \pm 9.0 \mu\text{m}$ ) (Figures 1A and 2A; Tables 2 and 3). The absolute (GCIP layer:  $-22.7 \mu\text{m}$ ; pRNFL:  $-38.5 \mu\text{m}$ ) and relative (GCIP layer:  $-38.8\%$ ; pRNFL:  $-61.6\%$ ) loss in eyes with 1 ON episode (NMOSD-1-ON) compared with NMOSD-NON was higher than in eyes with 2 ON episodes (NMOSD-2-ON) compared with NMOSD-1-ON (GCIP layer absolute loss:  $-3.5 \mu\text{m}$ , relative loss:  $-6.0\%$ ; pRNFL absolute loss:  $-9.1 \mu\text{m}$ , relative loss:  $-14.5\%$ , n.s.). The loss in

**Table 2** Group Comparisons of GCIP Layer Thickness for Heidelberg SD-OCT

	No. of eyes	Thickness ( $\mu\text{m}$ , mean $\pm$ SD)	Comparison to	Absolute difference ( $\mu\text{m}$ , mean)	Relative difference (% mean)	B	SE	p Value	R <sup>2</sup> <sub>marg</sub>	R <sup>2</sup> <sub>cond</sub>	Combined p value
NMOSD	268	67.3 $\pm$ 13.6	HCS	-14.0	-20.8	15.6	2.0	<0.0001	0.143	0.690	—
NMOSD-ON	124	57.4 $\pm$ 12.2		-24.0	-41.8	25.0	2.0	<0.0001	0.482	0.839	—
NMOSD-NON	144	75.9 $\pm$ 7.7		-5.4	-7.2	5.8	1.4	<0.0001	0.088	0.947	—
NMOSD-NON <sub>non</sub>	99	77.3 $\pm$ 5.9		-4.0	-5.0	2.69	1.42	0.061	0.189	0.924	—
NMOSD-NON <sub>con</sub>	45	72.9 $\pm$ 10.2		-8.5	-10.4	8.44	1.77	<0.0001	0.260	0.985	—
NMOSD-ON	124	57.4 $\pm$ 12.2	NMOSD-NON	-18.5	-24.4	-15.8	1.1	<0.0001	0.430	0.795	5.9e <sup>-45</sup>
NMOSD-1-ON	76	58.6 $\pm$ 12.9		-17.3	-22.8	-14.5	1.2	<0.0001	0.417	0.803	1.4e <sup>-33</sup>
NMOSD-2-ON	28	55.1 $\pm$ 9.4	NMOSD-1-ON	-3.5	-6.0	-5.7	2.6	0.028	0.143	0.729	0.038
NMOSD- $\geq$ 3-ON	20	55.9 $\pm$ 12.8	NMOSD-2-ON	0.8	1.4	4.9	2.6	0.070	0.311	0.781	0.222
NMOSD-NON <sub>con</sub>	45	72.9 $\pm$ 10.2	NMOSD-NON <sub>non</sub>	-4.4	-6.1	-3.8	1.7	0.025	0.111	0.701	0.004
NMOSD-NON <sub>1-con</sub>	37	73.6 $\pm$ 9.4		-3.7	-5.1	-3.5	1.6	0.037	0.149	0.906	0.154

Abbreviations: AQP4-IgG = aquaporin-4 IgG; B = estimate; GCIP = ganglion cell and inner plexiform; NMOSD = AQP4-IgG-seropositive NMOSD; NMOSD-NON = AQP4-IgG-seropositive NMOSD eyes without a history of ON; NMOSD-NON<sub>non</sub> = AQP4-IgG-seropositive NMOSD eyes without a history of ON or contralateral ON; NMOSD-NON<sub>con</sub> = AQP4-IgG-seropositive NMOSD eyes without a history of ON but with a history of contralateral ON; NMOSD-NON<sub>1-con</sub> = AQP4-IgG-seropositive NMOSD eyes without a history of ON but with a history of 1 contralateral ON; NMOSD-ON = AQP4-IgG-seropositive NMOSD eyes with a history of ON; NMOSD-1-ON = AQP4-IgG-seropositive NMOSD eyes with a history of 1 ON; NMO-2-ON = AQP4-IgG-seropositive NMOSD eyes with a history of 2 ONs; NMOSD- $\geq$ 3-ON = AQP4-IgG-seropositive NMOSD eyes with a history of 3 or more ONs; NMOSD = neuromyelitis optica spectrum disorder; NMOSD-NON = NMOSD eyes without a history of ON; OCT = optical coherence tomography; ON = optic neuritis episode; Rcon = conditional R-squared; Rmarg = marginal R-squared; SE = standard error.

eyes with  $\geq$ 3-ON episodes (NMOSD-3-ON) was lower compared with NMOSD-2-ON (n.s.) (Figures 1B and 2B). Five NMOSD-NON eyes had pRNFL values < 60  $\mu\text{m}$ ; these patients had no relevant comorbidities but a history of contralateral ON.<sup>17,18</sup> In sensitivity analyses to account for device differences, all significant analyses within the NMOSD cohort were confirmed for data acquired by Cirrus and Topcon OCT devices (eFigures 2 and 3; eTables 3 and 4, links.lww.com/NXI/A556; links.lww.com/NXI/A557).

### Neuroaxonal Damage Without ON

NMOSD-NON eyes had a reduced GCIP layer (75.9  $\pm$  7.7  $\mu\text{m}$ ,  $p < 0.001$ ), but not pRNFL (95.3  $\pm$  14.4  $\mu\text{m}$ ) compared with HC (GCIP layer: 81.4  $\pm$  5.7  $\mu\text{m}$ , pRNFL: 101.1  $\pm$  9.0  $\mu\text{m}$ ; Figures 1A and 2A; Tables 2 and 3). By comparison, only 28 NMOSD-NON eyes (5.1%) had a GCIP layer  $\leq$  the 5th percentile of HC. GCIP layer was also reduced in NMOSD-NON with a history of contralateral ON (72.9  $\pm$  10.2  $\mu\text{m}$ ) compared with NMOSD-NON without a history of contralateral ON (77.3  $\pm$  5.9  $\mu\text{m}$ ,  $p = 0.025$ , NMOSD-NON<sub>non</sub>). This effect vanished when only considering NMOSD-NON<sub>con</sub> with a history of 1 contralateral ON (73.6  $\pm$  9.4  $\mu\text{m}$ ). However, only NMOSD-NON<sub>con</sub> ( $p <$

0.001) but not NMOSD-NON<sub>non</sub> ( $p = 0.061$ ) had thinned GCIP layer compared with HC (Figures 1C and 2C).

### INL Changes

INL was thicker in NMOSD-ON compared with HC (39.4  $\pm$  2.6  $\mu\text{m}$ ) and NMOSD-NON (eTable 4, links.lww.com/NXI/A557). Specifically, INL was thicker in eyes with 1 ON episode compared with NMOSD-NON but did not differ between eyes with different numbers of ON episodes. Also, INL did not differ between NMOSD-NON<sub>con</sub> (38.9  $\pm$  3.2  $\mu\text{m}$ ) and NMOSD-NON<sub>non</sub> (38.5  $\pm$  3.2  $\mu\text{m}$ ,  $p = 0.931$ ). In all patients, INL thickness (as the dependent variable in the linear mixed model described above) was correlated with thinner GCIP layer ( $B = -0.11$ , standard error [SE] = 0.01,  $p < 0.001$ ) and pRNFL ( $B = -0.06$ , SE = 0.01,  $p < 0.001$ ). This correlation existed in NMOSD-ON (GCIP layer:  $B = -0.08$ , SE = 0.03,  $p = 0.005$ ; pRNFL:  $B = -0.06$ , SE = 0.01,  $p < 0.001$ ) and not present in NMOSD-NON (eFigure 4, links.lww.com/NXI/A556).

Scans of 363 NMOSD eyes were clearly suitable for MME investigations (high quality, eFigure 4C, links.lww.com/NXI/A556). MMEs were visible in 24 (6.6%) eyes of 21 patients.



**Table 3** Group Comparisons of pRNFL Thickness With (A) Spectralis SD-OCT Data for Comparisons vs HC (B) Data From All Devices for Inpatient Cohort Comparisons

	No. of eyes	Thickness ( $\mu\text{m}$ , mean $\pm$ SD)	Comparison to	Absolute difference ( $\mu\text{m}$ , mean)	Relative difference (% mean)	B	SE	p Value	R <sup>2</sup> <sub>marg</sub>	R <sup>2</sup> <sub>cond</sub>	Combined p value
NMOSD	344	76.3 $\pm$ 27.4	HCS	-14.0	-32.6	24.2	4.3	<0.0001	0.143	0.690	—
NMOSD-ON	170	56.9 $\pm$ 23.7		-44.3	-77.9	43.1	4.1	<0.0001	0.482	0.839	—
NMOSD-NON	174	95.3 $\pm$ 14.4		-5.9	-6.2	4.6	3.0	0.129	0.088	0.947	—
NMOSD-NON <sub>non</sub>	116	97.4 $\pm$ 10.9		-3.7	-3.7	-2.9	2.2	0.204	0.107	0.893	—
NMOSD-NON <sub>con</sub>	58	91.0 $\pm$ 19.1		-4.7	-4.6	7.1	4.2	0.097	0.100	0.975	—
NMOSD-ON	170	56.9 $\pm$ 23.7	NMOSD-NON	-38.4	-40.3	-33.8	2.1	<0.0001	0.436	0.741	4.4e <sup>-60</sup>
NMOSD-1-ON	97	62.6 $\pm$ 24.9		-32.7	-34.3	-29.6	2.2	<0.0001	0.379	0.712	4.6e <sup>-40</sup>
NMOSD-2-ON	35	53.5 $\pm$ 21.3	NMOSD-1-ON	-9.1	-14.5	-10.7	4.7	0.024	0.087	0.528	0.010
NMOSD- $\geq$ 3-ON	38	45.2 $\pm$ 17.8	NMOSD-2-ON	-8.3	-15.5	-0.4	4.3	0.924	0.087	0.719	0.838
NMOSD-NON <sub>con</sub>	58	91.0 $\pm$ 19.1	NMOSD-NON <sub>non</sub>	-6.5	-7.1	-4.0	2.9	0.173	0.061	0.939	0.157
NMOSD-NON <sub>1-con</sub>	47	93.2 $\pm$ 18.1		-4.2	-4.6	-3.2	2.9	0.276	0.056	0.925	0.616

Abbreviations: AQP4-IgG = aquaporin-4 IgG; NMOSD = AQP4-IgG-seropositive NMOSD; NMOSD-NON = AQP4-IgG-seropositive NMOSD eyes without a history of ON; NMOSD-NON<sub>non</sub> = AQP4-IgG-seropositive NMOSD eyes without a history of ON or contralateral ON; NMOSD-NON<sub>con</sub> = AQP4-IgG-seropositive NMOSD eyes without a history of ON but with a history of contralateral ON; NMOSD-NON<sub>con</sub> = AQP4-IgG-seropositive NMOSD eyes without a history of ON but with a history of 1 contralateral ON; NMOSD-ON = AQP4-IgG-seropositive NMOSD eyes with a history of ON; NMOSD-1-ON = AQP4-IgG-seropositive NMOSD eyes with a history of 1 ON; NMOSD-2-ON = AQP4-IgG-seropositive NMOSD eyes with a history of 2 ONs; NMOSD- $\geq$ 3-ON = AQP4-IgG-seropositive NMOSD eyes with a history of 3 or more ONs; NMOSD = neuromyelitis optica spectrum disorder; NMOSD-NON = NMOSD eyes without a history of ON; OCT = optical coherence tomography; ON = optic neuritis episode; pRNFL = peripapillary retinal nerve fiber layer; VEP = visually evoked potential.

Twenty-three eyes (13.1%) of NMOSD-ON and 1 eye (0.5%) of NMOSD-NON (with a history of contralateral ON) were affected. The number of ON episodes did not influence the incidence of MMEs (NMOSD-1-ON N = 16 (14%), NMOSD-2-ON N = 4 (11.4%), NMOSD- $\geq$ 3-ON N = 3 (11.1%).

Including only the most frequent ethnicities in our data set (Asian and non-Hispanic White), results did not differ, and no ethnicity was singled out regarding its pattern of injury (data not shown).

### OCT and Vision Loss

HC-VA was numerically reduced in NMOSD (0.25  $\pm$  0.48) compared with HC (-0.01  $\pm$  0.08) and known healthy reference values. NMOSD-ON also had reduced HC-VA (0.44  $\pm$  0.58) compared with NMOSD-NON (0.04  $\pm$  0.20,  $p < 0.001$ ,  $p = 0.401$ ) and HC/healthy reference populations. HC-VA was correlated with GCIP layer ( $B = -0.016$ ,  $SE = 0.002$ ,  $p < 0.001$ ) and pRNFL thicknesses ( $B = -0.010$ ,  $SE = 0.001$ ,  $p < 0.001$ ) in AQP4-IgG-seropositive NMOSD. AQP4-IgG-seropositive NMOSD eyes with prolonged VEP latency had a thinned GCIP

layer ( $B = -11.647$ ,  $SE = 3.628$ ,  $p = 0.002$ ) and pRNFL ( $B = -21.965$ ,  $SE = 3.724$ ,  $p < 0.001$ ). EDSS score as a metric of global disability was inversely correlated with GCIP layer ( $B = -1.370$ ,  $SE = 0.566$ ,  $p = 0.017$ ) and pRNFL thicknesses ( $B = -3.148$ ,  $SE = 1.080$ ,  $p = 0.004$ ).

## Discussion

Our study specifies a severe and functionally relevant decrease of GCIP layer and pRNFL in NMOSD-ON compared with NMOSD-NON and HCs in AQP4-IgG-seropositive patients. Neuroaxonal damage is particularly large from the first episode of ON, where contribution to retinal damage in subsequent episodes of ON is still considerable but smaller. In contrast to previous smaller studies, the current study ascertains GCIP layer but not pRNFL thinning in NMOSD-NON compared with HC.<sup>6,19</sup> This effect was driven by eyes with contralateral ON and not statistically significant in eyes without a history of ON. INL was thicker in NMOSD-ON and was inversely correlated with GCIP layer. Of note, 13.1%

of NMOSD-ON eyes showed MME indicative of secondary inflammatory changes.<sup>20,21</sup> This investigation overcame limits of small samples and OCT data heterogeneity of earlier studies through use of an international consortium of NMOSD specialists. This framework substantiated the CROCTINO study—a large, multicenter, retrospective evaluation of retinal pathology in NMOSD using OCT.

The neuroaxonal degeneration in NMOSD-ON demonstrated here is substantially greater than reported changes in multiple sclerosis (MS), a common differential diagnosis.<sup>2,22</sup> In a meta-analysis, an average pRNFL loss of 20  $\mu\text{m}$  was estimated in MS after ON, which is nearly 2-fold higher in our NMOSD-ON cohort ( $-38.4 \mu\text{m}$ ).<sup>22</sup> For GCIP layer, our data suggested approximately 1.5-fold higher loss in NMOSD ( $-24.0 \mu\text{m}$ ) compared with MS.<sup>22</sup> These differences not only result from a higher ON frequency, but may also be caused by more severe retinal damage in NMOSD after a singular ON.<sup>23</sup> It is intriguing that the damage is particularly large after the first ON episode with smaller losses after subsequent episodes, which might be due to less neuroaxonal content in subsequent episodes.<sup>2,24</sup> Alternatively, although the analysis of treatment effects exceeds the scope of this study, it is possible that the longer time to effective anti-inflammatory therapy and the typical choice of less effective therapies (e.g., steroids instead of plasma exchange) at the first attack compared with following attacks may significantly contribute to this difference. Independent of the number of ONs, the percent loss is smaller in GCIP layer compared with pRNFL—pointing toward either (1) stronger loss of retinal nerve fibers than retinal ganglion cells, (2) impairment of ganglion cells not leading to extinction but axonal loss; (3) a larger amount of non-neuronal tissue in GCIP layer, or (4) RNFL loss in the periphery beyond the macular area measured by GCIP layer. These hypotheses are not mutually exclusive, and each might contribute to the effect. Consistent with these concepts, excessive vision loss relative to neuroaxonal content and VEP latency in AQP4-IgG-seropositive patients compared with MOG-IgG-seropositive and MS patients implies damage of the peripheral retina and optic nerve tissues, which are not reflected in the macula and pattern VEP measurements.<sup>4</sup>

Whether attack-independent neurodegeneration in AQP4-IgG-seropositive NMOSD occurs has been controversial.<sup>2,6,7,25-28</sup> The current study identifies decreased GCIP layer in NMOSD-NON compared with HC, but not pRNFL. Such subclinical changes could be caused by contralateral involvement after unilateral ON.<sup>17,18</sup> Indeed, our cohort suggests pronounced neurodegeneration in eyes with contralateral ON. However, eyes of patients without ON also exhibit a trend for thinner GCIP layer compared with HCs. Underscored by longitudinal studies showing ON-independent neurodegeneration and VEP latency prolongation,<sup>7,29</sup> such patterns suggest at least 2 mechanisms of injury: (1) a primary retinopathy or optic neuropathy in context of an astrocytopathy or caused by direct damage to AQP4-expressing cells such as astrocytes

and Müller cells by either AQP4-IgG or AQP4-specific T cells or (2) a global or afferent visual system specific chronic or episodic neurodegenerative process. Because lesions often spare the brain, and most studies outside of predisposed areas such as optic nerve and spinal cord failed to detect effects,<sup>30</sup> a constant global involvement seems unlikely. Several studies described changes affecting AQP4 expression and astrocytic end feet,<sup>31</sup> parafoveal changes in agreement with an involvement of AQP4-expressing Müller cell,<sup>6,26,27,32</sup> and attack-independent spinal cord atrophy.<sup>33</sup> These findings are consistent with tissue infiltration by AQP4-IgG-specific T cells<sup>34</sup> and the attack-independent loss of retinal ganglion cells<sup>7</sup>—further supporting the existence of an ON-independent pathology, which might be restricted to the main disease foci. The latter hypotheses could be addressed by region-specific pathology or advanced imaging studies.

INL changes have been suggested as a marker of neuroinflammation and potential treatment response in MS.<sup>21,35,36</sup> MME may develop as a consequence of neurodegeneration or other—non-disease-specific—processes.<sup>35</sup> Patients with NMOSD were described to have INL thickening and MME.<sup>20,37</sup> In our cohort, 13.1% of NMOSD-ON eyes were affected by MME, which is higher than the 2%–5% described in MS but comparable to incidences in NMOSD described before by Gelfand and colleagues.<sup>35,37</sup> However, INL thickening itself remained comparable to changes reported in MS.<sup>35</sup> This disparity could reflect a disrupted fluid homeostasis due to Müller cell involvement or loss of content of the INL with a parallel inflammatory reaction and development of MME. The limited accessibility of MMEs, especially in severely affected eyes due to limited image quality, has hindered their detailed assessments and most likely leads to underestimation of their incidence.<sup>38</sup> We demonstrate that the INL thickness is inversely correlated with neuroaxonal content and could be a valuable marker of disease severity also in NMOSD.

Our study cohort was representative of patients with AQP4-IgG-seropositive NMOSD with respect to a female predominance and ON history.<sup>11,39</sup> This OCT study included multiple ethnicity backgrounds, although the distribution was shifted toward Caucasian/White patients and other ethnicities were underrepresented (e.g., Hispanic White and Black), limiting the generalizability of results.<sup>40</sup> Patients from different heritages presented similar findings.

The current study was based on source data instead of a meta-analysis. Using the Guthy-Jackson Charitable Foundation network, this multicentric study was conducted without investigator reimbursement and illustrated how collaboration integrating international perspectives can produce meaningful results. To overcome technical challenges of heterogeneous source data, we developed novel OCT postprocessing techniques allowing us to perform standardized analyses and enabling the uniform analysis of the largest OCT image data set in NMOSD to date.<sup>10</sup> Thus, the strengths of CROCTINO include its established

infrastructure, large international network of experts representing multiple ethnicities and geographic regions, and the use of state-of-the-art OCT postprocessing techniques.<sup>41</sup>

We recognize limitations of the current investigation: The retrospective and heterogeneous data acquisition might have led to biases and impreciseness beyond the ability of our quality control. We addressed this by excluding uncertain cases. HCs were only included from a limited number of centers. The unbalanced data set limited some analyses, such as the influence of ethnicities or acute and disease-modifying treatments. Case-control matching was impossible, particularly with respect to subclinical progression dependent or independent of ON and to ethnicity. Similarly, comparisons with other NMOSD subtypes or MS were beyond the scope of this study. Longitudinal data, acute ON data, and AQP4-IgG-seronegative and MOG-IgG-seropositive patient data are part of the CROCTINO data set and will be analyzed in the future. Also, OCT data processing was performed by multiple raters potentially introducing interrater variability. MRI data and posterior visual pathway involvement were not investigated in this study. However, the current study achieved an unprecedented worldwide assessment of retinal damage in AQP4-IgG-seropositive NMOSD.

To conclude, AQP4-IgG-seropositive NMOSD is characterized by a severe, functionally relevant retinal neurodegeneration as a consequence of ON. Although the majority of damage occurs during the first episode, there is cumulative loss with each succeeding relapse. The ON-associated damage is not limited to the neuroaxonal content but can also induce—likely inflammation-mediated—INL increase and occurrence of MME. Our data also suggest attack-independent retinal damage in AQP4-IgG-seropositive NMOSD. Our study supports that attack prevention is key in avoiding neuroaxonal damage and vision loss in patients with NMOSD. It further suggests that the first ON episode causes the most damage, where only some patients with then established diagnosis will be on immunosuppressive therapy. This highlights the need for effective therapies that can ameliorate an ongoing attack or regenerate attack-generated damage, which is an unmet clinical need. Last, the study emphasizes the utility of OCT as a sensitive structural metric and its potential for monitoring progression and even treatment response in AQP4-IgG-seropositive NMOSD. The international CROCTINO program provides an unprecedented opportunity to apply OCT in a standardized manner to assess pathophysiology, clinical course, and therapeutic efficacy in NMOSD.

### Study Funding

Guthy-Jackson Charitable Foundation (GJCF) and German Research Foundation (DFG).

### Disclosure

F.C. Oertel was employee of Nocturne GmbH and receives research support by the American Academy of Neurology and the National Multiple Sclerosis Society, unrelated to this work.

S. Specovius reports no disclosures. H.G. Zimmerman reports research grants from Novartis and speaking honoraria from Bayer Healthcare, unrelated to this study. C. Chien reports speaking honoraria from Bayer Healthcare, unrelated to this work. S. Motamedi and C. Bereuter report no disclosures. L. Cook reports grants from Guthy Jackson Charitable Foundation, during the conduct of the study. E.H. Martinez-Lapiscina is employed by the European Medicines Agency (Human Medicines) since 16 April 2019. This article is related with her activity under Hospital Clinic of Barcelona/IDIBAPS affiliation and consequently, as external activity, it does not represent the views of the Agency, its Committees or working parties. Before enrolling EMA, Dr. Martinez-Lapiscina reports grants from Instituto de Salud Carlos III (Spain) & Fondo Europeo de Desarrollo Regional, grants from MS Innovation GMSI, other from Fundació Privada Cellex, and personal fees from Novartis, Roche, Sanofi-Genzyme, outside the submitted work. M.A. Lana Peixoto and M.A. Fontanelle report no disclosures. H.J. Kim reports grants from the National Research Foundation of Korea, personal fees from Alexion Pharmaceuticals, Aprilbio, Biogen, Celltrion, Eisai, HanAll BioPharma, MDImmune, Merck Serono, Novartis, Sanofi Genzyme, Teva-Handok, and Viela Bio, other from Viela Bio (formerly MedImmune), Multiple Sclerosis Journal, and Journal of Clinical Neurology, outside the submitted work. J.-W. Hyun reports grants from the National Research Foundation of Korea, outside the submitted work. J. Palace reports personal fees from Abide Therapeutics, Alexion Pharmaceuticals, ARGENX, Bayer Schering, Biogen Idec, Chugai Pharma, EuroImmun, Genzyme, MedDay, MedImmune, Merck Serono, Novartis, Roche, Teva, UCB, and Viela Bio; grants from Abide Therapeutics, Alexion Pharmaceuticals, Bayer Schering, Biogen Idec, Chugai Pharma, Genzyme, MedImmune, Merck Serono, Novartis, and Teva, grants from Merck Serono, Novartis, Biogen Idec, Teva, Abide, MedImmune, Bayer Schering, Genzyme, Chugai and Alexion; Eugène Devic European Network, the Grant for Multiple Sclerosis Innovation, the John Fell Fund, the Medical Research Council, the MS Society, Myaware, the UK National Institute for Health Research, Oxford Health Services Research Committee, and the Guthy-Jackson Charitable Foundation AMPLO and SPARKS Great Ormond Street, for research studies outside the submitted work. M.I. Leite and S. Sharma report no disclosures. A. Roca-Fernandez is sponsored by Abide Therapeutic outside of the submitted work and reports no potential conflicts of interest. R. Kafieh, A. Dehghani, M. Pourazizi, L. Pandit and A. D’Cunha report no disclosures. O. Aktas reports grants from German Research Foundation (DFG) and German Ministry of Education and Research (BMBF); personal fees from Alexion and Almirall; grants and personal fees from Biogen, personal fees from Merck, grants and personal fees from Novartis, grants and personal fees from Roche, personal fees from Sanofi, personal fees from Teva, personal fees from Viela Bio, outside the submitted work. M. Ringelstein received speaker honoraria from Novartis, Bayer Vital GmbH, Roche, Alexion and Ipsen and travel reimbursement from Bayer Schering, Biogen Idec, Merz, Genzyme, Teva, Roche, and Merck, none related to this study. P. Albrecht reports grants,

personal fees and non-financial support from Allergan, Biogen, Merck, Merz Pharmaceuticals, Novartis, Ipsen, Celgene, Roche, and personal fees and non-financial support from Teva outside the submitted work. E. May and C. Tongco report no disclosures. L. Leocani reports personal fees from Roche, Merck, Bristol Myers Squibb, and Med-ex learning, outside the submitted work. M. Pisa reports no disclosures. M. Radaelli reports personal fees from Merck Serono, Sanofi-Genzyme, Novartis, and Biogen, outside the submitted work. H. Stiebel-Kalish reports no disclosures. S. Siritho reports personal fees from Novartis, Thailand, Biogen Idec, Eisai Thailand marketing co. Ltd., Merck Serono, Teva Thailand, and Menarini, outside the submitted work. J. de Seze and T. Senger report no disclosures. J. Havla reports grants, personal fees and non-financial support from Merck, personal fees from Novartis, Celgene, Roche, Santhera, Biogen, Alexion, Sanofi, non-financial support from Guthy-Jackson Charitable Foundation, and grants from Friedrich Baur Foundation, outside the submitted work. R. Marignier, A.C. Calvo, D. Bichueti, I.M. Tavares, N. Asgari, K. Soelberg, A. Altintas, R. Yildirim, U. Tanriverdi, A. Jacob, S. Huda, Z. Rimler and A. Reid report no disclosures. Y. Mao-Draayer reports grants from NIH NIAID, grants and personal fees from Genzyme, grants from Chugai, personal fees from Biogen and EMD Serono, grants and personal fees from Genentech and Novartis, during the conduct of the study; grants from NIH NIAID, grants and personal fees from Genzyme, grants from Chugai, personal fees from Biogen and EMD Serono, grants and personal fees from Genentech and Novartis, outside the submitted work. I. Soto de Castillo reports no disclosures. A. Petzold reports personal fees and grants from Novartis, outside the submitted work, and is part of the steering committee of the OCTIMS study which is sponsored by Novartis. He has not received honoraria for this activity. A.J. Green reports other from Bionure, grants, personal fees and other from Inception Sciences, grants from Sherak Foundation, personal fees and other from Pipeline Pharmaceuticals, grants from Hilton Foundation, Adelson Foundation, and National MS Society, personal fees from JAMA Neurology, personal fees and other from Mediimmune/Viela, outside the submitted work. In addition, Dr. Green has a patent Small Molecule drug for Remyelination pending and has worked on testing off label compounds for remyelination. M.R. Yeaman serves as an advisor to the Guthy-Jackson Charitable Foundation. T. Smith reports no disclosures. A.U. Brandt reports grants from the Guthy Jackson Charitable Foundation during the conduct of the study; shares from Motognosis GmbH and shares from Nocturne GmbH outside the submitted work. In addition, Dr. Brandt has a patent pending describing Foveal Morphometry. F. Paul reports grants from the Guthy Jackson Charitable Foundation, during the conduct of the study; grants from the German Research Foundation and German Federal Ministry of Education and research, grants, and other from Novartis, grants and other from Bayer, Novartis, Biogen Idec, Teva, Sanofi-Aventis/Genzyme, Merck Serono, Chugai, other from PLoS ONE, other from *Neurology*<sup>®</sup> *Neuroimmunology & Neuroinflammation*, other from Sanofi-Genzyme, Biogen Idec, grants from German Research Council, Werth Stiftung of the City of

Cologne, German Ministry of Education and Research, Arthur Arnstein Stiftung Berlin, EU FP7 Framework Program, Arthur Arnstein Foundation Berlin, National Multiple Sclerosis (USA), other from MedImmune, Shire, Alexion, outside the submitted work. In addition, Dr. Paul has a patent Foveal Morphometry pending to Nocturne GmbH. Go to [Neurology.org/NN](https://www.neurology.org/NN) for full disclosures.

## Publication History

Received by *Neurology: Neuroimmunology & Neuroinflammation* March 23, 2021. Accepted in final form June 15, 2021.

## Appendix Authors

Name	Location	Contribution
<b>Frederike Cosima Oertel, MD/PhD</b>	Experimental and Clinical Research Center, Max Delbrück Center for Molecular Medicine and Charité-Universitätsmedizin, Corporate Member of Freie Universität Berlin and Humboldt-Universität zu Berlin, Germany	Acquisition and analysis of data and drafting a significant portion of the manuscript or figures; conception and design of the study
<b>Svenja Specovius, MSc</b>	Experimental and Clinical Research Center, Max Delbrück Center for Molecular Medicine and Charité-Universitätsmedizin, Corporate Member of Freie Universität Berlin and Humboldt-Universität zu Berlin, Germany	Acquisition and analysis of data; conception and design of the study
<b>Hanna G Zimmermann, PhD</b>	Experimental and Clinical Research Center, Max Delbrück Center for Molecular Medicine and Charité-Universitätsmedizin, Corporate Member of Freie Universität Berlin and Humboldt-Universität zu Berlin, Germany	Acquisition and analysis of data; conception and design of the study
<b>Claudia Chien, PhD</b>	Experimental and Clinical Research Center, Max Delbrück Center for Molecular Medicine and Charité-Universitätsmedizin, Corporate Member of Freie Universität Berlin and Humboldt-Universität zu Berlin, Germany	Acquisition and analysis of data
<b>Seyedamirhosein Motamedi, PhD</b>	Experimental and Clinical Research Center, Max Delbrück Center for Molecular Medicine and Charité-Universitätsmedizin, Corporate Member of Freie Universität Berlin and Humboldt-Universität zu Berlin, Germany	Acquisition and analysis of data
<b>Charlotte Bereuter, BSc</b>	Experimental and Clinical Research Center, Max Delbrück Center for Molecular Medicine and Charité-Universitätsmedizin, Corporate Member of Freie Universität Berlin and Humboldt-Universität zu Berlin, Germany	Acquisition and analysis of data

**Appendix** (continued)

Name	Location	Contribution
<b>Lawrence Cook, PhD</b>	University of Utah, Salt Lake City, UT	Acquisition and analysis of data and conception and design of the study
<b>Marco Aurélio Lana Peixoto, MD, PhD</b>	University of Minas Gerais, Medical School, Belo Horizonte, Brazil	Acquisition and analysis of data
<b>Mariana Andrade Fontanelle, MD</b>	University of Minas Gerais, Medical School, Belo Horizonte, Brazil	Acquisition and analysis of data
<b>Ho Jin Kim, MD, PhD</b>	National Cancer Center, Goyang, Republic of Korea	Acquisition and analysis of data
<b>Jae-Won Hyun, MD, PhD</b>	University of Minas Gerais, Medical School, Belo Horizonte, Brazil	Acquisition and analysis of data
<b>Jacqueline Palace, MD</b>	Oxford University Hospitals, National Health Service Trust, Oxford, United Kingdom	Acquisition and analysis of data
<b>Adriana Roca-Fernandez, MSc</b>	Oxford University Hospitals, National Health Service Trust, Oxford, United Kingdom	Acquisition and analysis of data
<b>Maria Isabel Leite, MD, PhD</b>	Oxford University Hospitals, National Health Service Trust, Oxford, United Kingdom	Acquisition and analysis of data
<b>Srilakshmi Sharma, MD, PhD</b>	Oxford University Hospitals, National Health Service Trust, Oxford, United Kingdom	Acquisition and analysis of data
<b>Fereshteh Ashtari, MD</b>	Isfahan University of Medical Sciences, Isfahan, Iran	Acquisition and analysis of data
<b>Rahele Kafieh, PhD</b>	Isfahan University of Medical Sciences, Isfahan, Iran	Acquisition and analysis of data
<b>Alireza Dehghani, PhD</b>	Isfahan University of Medical Sciences, Isfahan, Iran	Acquisition and analysis of data
<b>Mohsen Pourazizi, PhD</b>	Isfahan University of Medical Sciences, Isfahan, Iran	Acquisition and analysis of data
<b>Lekha Pandit, MD, PhD</b>	KS Hegde Medical Academy, Nitte University, Mangalore, India	Acquisition and analysis of data
<b>Anitha D'Cunha, PhD</b>	KS Hegde Medical Academy, Nitte University, Mangalore, India	Acquisition and analysis of data
<b>Orhan Aktas, MD</b>	Heinrich Heine University Düsseldorf, Düsseldorf, Germany	Acquisition and analysis of data
<b>Marius Ringelstein, MD</b>	Heinrich Heine University Düsseldorf, Düsseldorf, Germany	Acquisition and analysis of data
<b>Philipp Albrecht, MD</b>	Heinrich Heine University Düsseldorf, Düsseldorf, Germany	Acquisition and analysis of data
<b>Eugene May, MD</b>	Swedish Neuroscience Institute Neuro-Ophthalmology, Seattle, WA	Acquisition and analysis of data
<b>Caryl Tongco</b>	Swedish Neuroscience Institute Neuro-Ophthalmology, Seattle, WA	Acquisition and analysis of data

**Appendix** (continued)

Name	Location	Contribution
<b>Letizia Leocani, MD, PhD</b>	Institute of Experimental Neurology, Scientific Institute Hospital San Raffaele and University Vita-Salute San Raffaele, Milan, Italy	Acquisition and analysis of data
<b>Marco Pisa, MD</b>	Institute of Experimental Neurology, Scientific Institute Hospital San Raffaele and University Vita-Salute San Raffaele, Milan, Italy	Acquisition and analysis of data
<b>Marta Radaelli, MD, PhD</b>	Institute of Experimental Neurology, Scientific Institute Hospital San Raffaele and University Vita-Salute San Raffaele, Milan, Italy	Acquisition and analysis of data
<b>Elena H Martinez-Lapiscina, MD, PhD</b>	Hospital Clinic of Barcelona-Institut d'Investigacions, Biomediques August Pi Sunyer, Barcelona, Spain	Acquisition and analysis of data
<b>Hadas Stiebel-Kalish, MD</b>	Sackler School of Medicine, Tel Aviv University, Tel Aviv, Israel	Acquisition and analysis of data
<b>Sasitorn Siritho, MD</b>	Siriraj Hospital and Bumrungrad International Hospital, Bangkok, Thailand	Acquisition and analysis of data
<b>Jérôme de Seze, MD, PhD</b>	University Hospital of Strasbourg, France	Acquisition and analysis of data
<b>Thomas Senger, MD</b>	University Hospital of Strasbourg, France	Acquisition and analysis of data
<b>Joachim Havla, MD</b>	Ludwig-Maximilians Universität Muenchen, Munich, Germany	Acquisition and analysis of data
<b>Romain Marignier, MD, PhD</b>	Pierre Wertheimer Neurological Hospital, Hospices Civils de Lyon, France	Acquisition and analysis of data
<b>Alvaro Cobo Calvo, MD, PhD</b>	Pierre Wertheimer Neurological Hospital, Hospices Civils de Lyon, France; Hospital Universitari Vall d'Hebron, Universitat Autònoma de Barcelona, Spain	Acquisition and analysis of data
<b>Denis Bichuetti, MD, PhD</b>	Escola Paulista de Medicina, Universidade Federal de São Paulo, São Paulo, Brazil	Acquisition and analysis of data
<b>Ivan Maynart Tavares, MD, PhD</b>	Escola Paulista de Medicina, Universidade Federal de São Paulo, São Paulo, Brazil	Acquisition and analysis of data
<b>Nasrin Asgari, MD, PhD</b>	University of Southern Denmark, Odense, Denmark	Acquisition and analysis of data
<b>Kerstin Soelberg, MD</b>	University of Southern Denmark, Odense, Denmark	Acquisition and analysis of data
<b>Ayse Altintas, MD</b>	Cerrahpasa Medical Faculty, Istanbul University, Cerrahpasa, Turkey	Acquisition and analysis of data
<b>Regin Yildirim, MD</b>	Cerrahpasa Medical Faculty, Istanbul University, Cerrahpasa, Turkey	Acquisition and analysis of data

Continued

## Appendix (continued)

Name	Location	Contribution
<b>Uygur Tanriverdi, MD</b>	Cerrahpasa Medical Faculty, Istanbul University, Cerrahpasa, Turkey	Acquisition and analysis of data
<b>Anu Jacob, MD</b>	The Walton Centre for Neurology and Neurosurgery, Liverpool, United Kingdom	Acquisition and analysis of data
<b>Saif Huda, MD, PhD</b>	The Walton Centre for Neurology and Neurosurgery, Liverpool, United Kingdom	Acquisition and analysis of data
<b>Zoe Rimler, BSc</b>	NYU School of Medicine, New York, NY	Acquisition and analysis of data
<b>Allyson Reid, MD</b>	NYU School of Medicine, New York, NY	Acquisition and analysis of data
<b>Yang Mao-Draayer, MD, PhD</b>	University of Michigan Medical School, Ann Arbor, MI	Acquisition and analysis of data
<b>Ibis Soto de Castillo, MD</b>	Hospital Clínico de Maracaibo, Maracaibo, Venezuela	Acquisition and analysis of data
<b>Axel Petzold, MD, PhD</b>	University College London, London, UK	Conception and design of the study
<b>Ari J Green, MD</b>	University of California San Francisco, CA	Conception and design of the study
<b>Michael R Yeaman, MD, PhD</b>	University of California Los Angeles, CA	Conception and design of the study
<b>Terry Smith, MD</b>	University of Michigan Medical School, Ann Arbor, MI	Conception and design of the study
<b>Alexander U Brandt, MD</b>	Experimental and Clinical Research Center, Max Delbrück Center for Molecular Medicine and Charité-Universitätsmedizin Berlin, Berlin, Germany	Acquisition and analysis of data, conception and design of the study, and drafting a significant portion of the manuscript or figures
<b>Friedemann Paul, MD</b>	Charité-Universitätsmedizin Berlin, Corporate Member of Freie Universität Berlin and Humboldt-Universität zu Berlin	Acquisition and analysis of data and conception and design of the study

## References

- Oertel FC, Zimmermann H, Paul F, Brandt AU. Optical coherence tomography in neuromyelitis optica spectrum disorders: potential advantages for individualized monitoring of progression and therapy. *EPMA J*. 2018;9(1):21-33.
- Schneider E, Zimmermann H, Oberwahrenbrock T, et al. Optical coherence tomography reveals distinct patterns of retinal damage in neuromyelitis optica and multiple sclerosis. *PLoS One*. 2013;8(6):e66151.
- Bouyon M, Collongues N, Zéphir H, et al. Longitudinal follow-up of vision in a neuromyelitis optica cohort. *Mult Scler*. 2013;19(10):1320-1322.
- Sotirchos ES, Filippatou A, Fitzgerald KC, et al. Aquaporin-4 IgG seropositivity is associated with worse visual outcomes after optic neuritis than MOG-IgG seropositivity and multiple sclerosis, independent of macular ganglion cell layer thinning. *Mult Scler*. 2019;26(11):1360-1371.
- Hamid SHM, Whittam D, Mutch K, et al. What proportion of AQP4-IgG-negative NMO spectrum disorder patients are MOG-IgG positive? A cross sectional study of 132 patients. *J Neurol*. 2017;264(10):2088-2094.
- Oertel FC, Kuchling J, Zimmermann H, et al. Microstructural visual system changes in AQP4-antibody-seropositive NMOSD. *Neurol Neuroimmunol Neuroinflamm*. 2017;4(3):e334.
- Oertel FC, Havla J, Roca-Fernández A, et al. Retinal ganglion cell loss in neuromyelitis optica: a longitudinal study. *J Neurol Neurosurg Psychiatry*. 2018;89(12):1259-1265.
- Huang D, Swanson EA, Lin CP, et al. Optical coherence tomography. *Science*. 1991;254(5035):1178-1181.
- Specovius S, Zimmermann HG, Oertel FC, et al. Cohort profile: a collaborative multicentre study of retinal optical coherence tomography in 539 patients with neuromyelitis optica spectrum disorders (CROCTINO). *BMJ Open*. 2020;10(10):e035397.
- Motamedi S, Gawlik K, Ayadi N, et al. Normative data and minimally detectable change for inner retinal layer thicknesses using a semi-automated OCT image segmentation pipeline. *Front Neurol*. 2019;10:1117.
- Wingerchuk DM, Banwell B, Bennett JL, et al. International consensus diagnostic criteria for neuromyelitis optica spectrum disorders. *Neurology*. 2015;85(2):177-189.
- von Elm E, Altman DG, Egger M, et al. The strengthening of reporting of observational studies in epidemiology (STROBE) statement: guidelines for reporting observational studies. *Int J Surg*. 2014;12(12):1495-1499.
- Tewarie P, Balk L, Costello F, et al. The OSCAR-IB consensus criteria for retinal OCT quality assessment. *PLoS One*. 2012;7(4):e34823.
- Schipping S, Balk LJ, Costello F, et al. Quality control for retinal OCT in multiple sclerosis: validation of the OSCAR-IB criteria. *Mult Scler*. 2015;21(2):163-170.
- Lang A, Carass A, Hauser M, et al. Retinal layer segmentation of macular OCT images using boundary classification. *Biomed Opt Express*. 2013;4(7):1133-1152.
- R Development Core Team. *R: A Language and Environment for Statistical Computing [online]*. R Foundation for Statistical Computing; 2008. R-project.org.
- Akaishi T, Kaneko K, Himori N, et al. Subclinical retinal atrophy in the unaffected fellow eyes of multiple sclerosis and neuromyelitis optica [online serial]. *J Neuroimmunol*. 2017;313:10-15. Accessed October 8, 2017. jni-journal.com/article/S0165-5728(17)30319-3/fulltext
- Alshowaeir D, Yiannikas C, Fraser C, Klistorner A. Mechanism of delayed conduction of fellow eyes in patients with optic neuritis. *Int J Ophthalmol*. 2018;11(2):329-332.
- Manogaran P, Trabouise AL, Lange AP. Longitudinal study of retinal nerve fiber layer thickness and macular volume in patients with neuromyelitis optica spectrum disorder. *J Neuroophthalmol*. 2016;36(4):363-368.
- Kaufhold F, Zimmermann H, Schneider E, et al. Optic neuritis is associated with inner nuclear layer thickening and microcystic macular edema independently of multiple sclerosis. *PLoS One*. 2013;8(8):e71145.
- Knier B, Schmidt P, Aly L, et al. Retinal inner nuclear layer volume reflects response to immunotherapy in multiple sclerosis. *Brain*. 2016;139(11):2855-2863.
- Petzold A, Balcer LJ, Calabresi PA, et al. Retinal layer segmentation in multiple sclerosis: a systematic review and meta-analysis. *Lancet Neurol*. 2017;16(10):797-812.
- Pawlitzi M, Horbrügger M, Loewe K, et al. MS optic neuritis-induced long-term structural changes within the visual pathway. *Neurol Neuroimmunol Neuroinflamm*. 2020;7(2):e665.
- Pache F, Zimmermann H, Mikolajczak J, et al. MOG-IgG in NMO and related disorders: a multicenter study of 50 patients. Part 4: afferent visual system damage after optic neuritis in MOG-IgG-seropositive versus AQP4-IgG-seropositive patients. *J Neuroinflammation*. 2016;13(1):282.
- Filippatou AG, Vasileiou ES, He Y, et al. Evidence of subclinical quantitative retinal layer abnormalities in AQP4-IgG seropositive NMOSD. *Mult Scler*. 2020 Dec 14;1352458520977771. doi: 10.1177/1352458520977771.
- Motamedi S, Oertel FC, Yadav SK, et al. Altered fovea in AQP4-IgG-seropositive neuromyelitis optica spectrum disorders. *Neurol Neuroimmunol Neuroinflamm*. 2020;7(5):e805.
- Roca-Fernández A, Oertel FC, Yeo T, et al. Foveal changes in AQP4-Ab seropositive NMOSD are independent of optic neuritis and not overtly progressive. *Eur J Neurol*. 2021;28(7):2280-2293.
- Papadopoulou A, Oertel FC, Chien C, et al. Lateral geniculate nucleus volume changes after optic neuritis in neuromyelitis optica: a longitudinal study. *Neuroimage Clin*. 2021;30:102608.
- Ringelstein M, Harmel J, Zimmermann H, et al. Longitudinal optic neuritis-unrelated visual evoked potential changes in NMO spectrum disorders. *Neurology*. 2020;94(4):e407-e418.
- Pache F, Zimmermann H, Finke C, et al. Brain parenchymal damage in neuromyelitis optica spectrum disorder—a multimodal MRI study. *Eur Radiol*. 2016;26(12):4413-4422.
- Hokari M, Yokoseki A, Arakawa M, et al. Clinicopathological features in anterior visual pathway in neuromyelitis optica. *Ann Neurol*. 2016;79(4):605-624.
- You Y, Zhu L, Zhang T, et al. Evidence of müller glial dysfunction in patients with aquaporin-4 immunoglobulin G-positive neuromyelitis optica spectrum disorder. *Ophthalmology*. 2019;126(6):801-810. Elsevier.
- Chien C, Scheel M, Schmitz-Hübsch T, et al. Spinal cord lesions and atrophy in NMOSD with AQP4-IgG and MOG-IgG associated autoimmunity. *Mult Scler*. 2019;25(14):1926-1936.
- Felix CM, Levin MH, Verkman AS. Complement-independent retinal pathology produced by intravitreal injection of neuromyelitis optica immunoglobulin G. *J Neuroinflammation*. 2016;13(1):275.
- Balk LJ, Coric D, Knier B, et al. Retinal inner nuclear layer volume reflects inflammatory disease activity in multiple sclerosis: a longitudinal OCT study. *Mult Scler J Exp Transl Clin*. 2019;5(3):2055217319871582.
- Gelfand JM, Nolan R, Schwartz DM, Graves J, Green AJ. Microcystic macular oedema in multiple sclerosis is associated with disease severity. *Brain*. 2012;135(pt 6):1786-1793.

37. Gelfand JM, Cree BA, Nolan R, Arnow S, Green AJ. Microcystic inner nuclear layer abnormalities and neuromyelitis optica. *JAMA Neurol.* 2013;70(5):629-633.
38. Oberwahrenbrock T, Weinhold M, Mikolajczyk J, et al. Reliability of intra-retinal layer thickness estimates. *PLoS One.* 2015;10(9):e0137316.
39. Borisow N, Kleiter I, Gahlen A, et al. Influence of female sex and fertile age on neuromyelitis optica spectrum disorders. *Multi Scler.* 2017;23(8):1092-1103.
40. Mori M, Kuwabara S, Paul F. Worldwide prevalence of neuromyelitis optica spectrum disorders. *J Neurol Neurosurg Psychiatry.* 2018;89(6):555-556.
41. Oertel FC, Paul F. Accelerating clinical research in neuromyelitis optica spectrum disorders [online serial]. *Clin Exp Neuroimmunol.* 2021;12(2):89-91. Accessed March 28, 2021. [pericles.pericles-prod.literatumonline.com/doi/abs/10.1111/cen3.12637](https://doi.org/10.1111/cen3.12637).

### **11.1.2.7. Astrocytic outer retinal layer thinning is not a feature in AQP4-IgG seropositive neuromyelitis optica spectrum disorders.**

Citation: Lu, A., Zimmermann, H.G., Specovius, S., Motamedi, S., Chien, C., Bereuter, C., Lana-Peixoto, M.A., Andrade-Fontenelle, M., Ashtari, F., Kafieh, R., Dehghani, A., Pourazizi, M., Pandit, L., Saldanha, A., Kim, H.J., Hyun, J-W., Leocani, L., Pisa, M., Radaelli, M., Siritho, S., May, A.F., Tongco, C., de Seze, J., Senger, T., Palace, J., **Roca-Fernández, A.**, ... Brandt, A.U., & Oertel, F.C.\* on behalf of the GJCF International Clinical Consortium for NMOSD. (2021). *Astrocytic outer retinal layer thinning is not a feature in AQP4-IgG seropositive neuromyelitis optica spectrum disorders*. J Neurol Neurosurg Psychiatry. 2021 Oct 28; jnnp-2021-327412. IF: 10.





Original research

# Astrocytic outer retinal layer thinning is not a feature in AQP4-IgG seropositive neuromyelitis optica spectrum disorders

Angelo Lu ,<sup>1,2</sup> Hanna G Zimmermann,<sup>1,2</sup> Svenja Specovius,<sup>1,2</sup> Seyedamirhosein Motamedi,<sup>1,2</sup> Claudia Chien ,<sup>1,2</sup> Charlotte Bereuter,<sup>1,2</sup> Marco A Lana-Peixoto,<sup>3</sup> Mariana Andrade Fontenelle,<sup>3</sup> Fereshteh Ashtari,<sup>4</sup> Rahele Kafieh,<sup>5</sup> Alireza Dehghani,<sup>6</sup> Mohsen Pourazizi,<sup>6</sup> Lekha Pandit,<sup>7</sup> Anitha D'Cunha,<sup>7</sup> Ho Jin Kim ,<sup>8</sup> Jae-Won Hyun,<sup>8</sup> Su-Kyung Jung,<sup>9</sup> Letizia Leocani,<sup>10</sup> Marco Pisa,<sup>10</sup> Marta Radaelli,<sup>10</sup> Sasitorn Siritho,<sup>11</sup> Eugene F May,<sup>12</sup> Caryl Tongco,<sup>12</sup> Jérôme De Sèze,<sup>13</sup> Thomas Senger,<sup>13</sup> Jacqueline Palace,<sup>14</sup> Adriana Roca-Fernández ,<sup>14</sup> Maria Isabel Leite,<sup>14</sup> Srilakshmi M Sharma,<sup>15</sup> Hadas Stiebel-Kalish ,<sup>16,17</sup> Nasrin Asgari,<sup>18</sup> Kerstin Kathrine Soelberg,<sup>19</sup> Elena H Martinez-Lapiscina ,<sup>20</sup> Joachim Havla ,<sup>21</sup> Yang Mao-Draayer,<sup>22</sup> Zoe Rimler,<sup>23</sup> Allyson Reid,<sup>23</sup> Romain Marignier,<sup>24</sup> Alvaro Cobo-Calvo,<sup>24,25</sup> Ayse Altintas,<sup>26</sup> Uygur Tanriverdi,<sup>27</sup> Rengin Yildirim,<sup>28</sup> Orhan Aktas,<sup>29</sup> Marius Ringelstein ,<sup>29,30</sup> Philipp Albrecht ,<sup>29</sup> Ivan Maynard Tavares,<sup>31</sup> Denis Bernardi Bichueti ,<sup>32</sup> Anu Jacob,<sup>33</sup> Saif Huda,<sup>33</sup> Ibis Soto de Castillo,<sup>34</sup> Axel Petzold ,<sup>35</sup> Ari J Green,<sup>36</sup> Michael R Yeaman,<sup>37,38</sup> Terry J Smith,<sup>39,40</sup> Lawrence Cook,<sup>41</sup> Friedemann Paul,<sup>1,2,42</sup> Alexander U Brandt,<sup>1,2,43</sup> Frederike Cosima Oertel ,<sup>1,2,36</sup> GJCF International Clinical Consortium for NMOSD

► Additional supplemental material is published online only. To view, please visit the journal online (<http://dx.doi.org/10.1136/jnnp-2021-327412>).

For numbered affiliations see end of article.

**Correspondence to** Professor Friedemann Paul, Experimental and Clinical Research Center, Charité Universitätsmedizin Berlin, 10117 Berlin, Germany; [friedemann.paul@charite.de](mailto:friedemann.paul@charite.de)

AB and FCO contributed equally.

Received 24 June 2021  
Accepted 26 September 2021  
Published Online First 28 October 2021



► <http://dx.doi.org/10.1136/jnnp-2021-327412>



© Author(s) (or their employer(s)) 2022. Re-use permitted under CC BY-NC. No commercial re-use. See rights and permissions. Published by BMJ.

**To cite:** Lu A, Zimmermann HG, Specovius S, et al. *J Neurol Neurosurg Psychiatry* 2022;**93**:188–195.

## ABSTRACT

**Background** Patients with anti-aquaporin-4 antibody seropositive (AQP4-IgG+) neuromyelitis optica spectrum disorders (NMOSDs) frequently suffer from optic neuritis (ON) leading to severe retinal neuroaxonal damage. Further, the relationship of this retinal damage to a primary astrocytopathy in NMOSD is uncertain. Primary astrocytopathy has been suggested to cause ON-independent retinal damage and contribute to changes particularly in the outer plexiform layer (OPL) and outer nuclear layer (ONL), as reported in some earlier studies. However, these were limited in their sample size and contradictory as to the localisation. This study assesses outer retinal layer changes using optical coherence tomography (OCT) in a multicentre cross-sectional cohort.

**Method** 197 patients who were AQP4-IgG+ and 32 myelin-oligodendrocyte-glycoprotein antibody seropositive (MOG-IgG+) patients were enrolled in this study along with 75 healthy controls. Participants underwent neurological examination and OCT with central postprocessing conducted at a single site.

**Results** No significant thinning of OPL ( $25.02 \pm 2.03 \mu\text{m}$ ) or ONL ( $61.63 \pm 7.04 \mu\text{m}$ ) were observed in patients who were AQP4-IgG+ compared with patients who were MOG-IgG+ with comparable neuroaxonal damage (OPL:  $25.10 \pm 2.00 \mu\text{m}$ ; ONL:  $64.71 \pm 7.87 \mu\text{m}$ ) or healthy controls (OPL:  $24.58 \pm 1.64 \mu\text{m}$ ; ONL:  $63.59 \pm 5.78 \mu\text{m}$ ). Eyes of patients who were AQP4-IgG+ ( $19.84 \pm 5.09 \mu\text{m}$ ,

$p=0.027$ ) and MOG-IgG+ ( $19.82 \pm 4.78 \mu\text{m}$ ,  $p=0.004$ ) with a history of ON showed parafoveal OPL thinning compared with healthy controls ( $20.99 \pm 5.14 \mu\text{m}$ ); this was not observed elsewhere.

**Conclusion** The results suggest that outer retinal layer loss is not a consistent component of retinal astrocytic damage in AQP4-IgG+ NMOSD. Longitudinal studies are necessary to determine if OPL and ONL are damaged in late disease due to retrograde trans-synaptic axonal degeneration and whether outer retinal dysfunction occurs despite any measurable structural correlates.

## INTRODUCTION

Neuromyelitis optica spectrum disorders (NMOSDs) are relapsing autoimmune disorders affecting the central nervous system (CNS).<sup>1</sup> Common clinical attacks in NMOSD include optic neuritis (ON), acute myelitis and area postrema syndrome.<sup>2</sup> Serum autoantibodies to aquaporin-4 (AQP4-IgG) are detectable in 60%–80% of patients with NMOSD.<sup>3,4</sup>

AQP4 is an astrocytic water channel in the CNS.<sup>5</sup> In the retina, astrocytes are mainly located in the inner neuroaxonal layers of the retina, but AQP4 is additionally highly expressed in retinal Müller cells.<sup>6</sup> These glial cells have diverse functions, such as regulation of water homeostasis and neurotransmitter recycling, and are located around the fovea

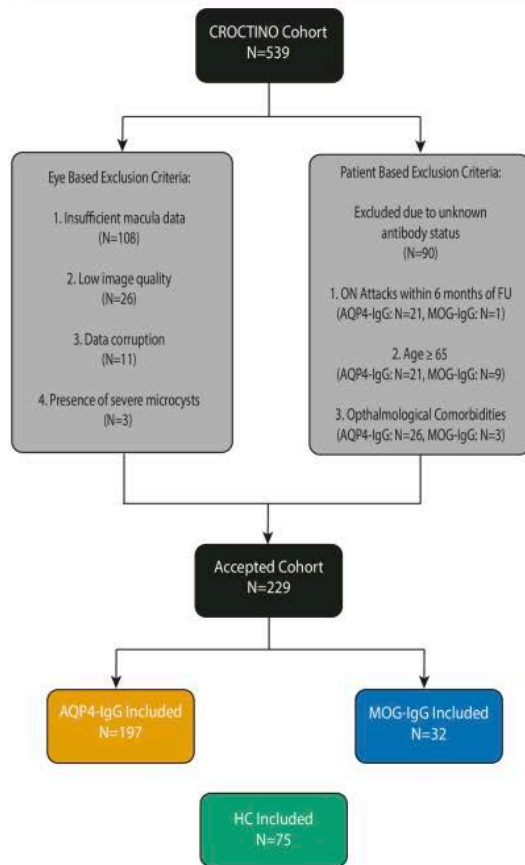


**Figure 1** Cohort design and exclusion criteria: from the original 539 patients recruited in the CROCTINO cohort, 108 patients were excluded due to missing macular data. Of the remaining 431 patients in the segmentation cohort, a further 40 patients were excluded due to anomalies in their OCT scans (OSCAR-IB criteria; primarily due to low image quality (26 patients) or the presence of microcysts (3 patients) or other pathologies) or due to data corruption (11 patients). We also excluded patients with unknown antibody status (90 patients). Of the remaining 301 patients, the cohort was split based on AQP4-IgG or MOG-IgG seropositivity and a further set of exclusion criteria were applied based on age (being  $\geq 65$  years), ophthalmological comorbidities (eg, glaucoma) and in instances where follow-ups occurred within 6 months of an ON attack. AQP4-IgG, anti-aquaporin-4 antibody; HC, healthy control; MOG-IgG, anti-myelin-oligodendrocyte-glycoprotein antibody; OCT, optical coherence tomography; ON, optic neuritis.

spanning the entire thickness of the retina.<sup>7</sup> Of particular interest is also the Henle Fibre outer nuclear layer (ONL) boundary of the parafovea where AQP4 channels are highly expressed.<sup>8</sup>

A primary and attack-independent astrocytopathy in NMOSD has been suggested to contribute to retinal neurodegeneration and to Müller cell-associated parafoveal changes.<sup>9–13</sup> Recent studies suggested potential astrocytopathy-related outer retinal layer (ORL) thinning in AQP4-IgG seropositive NMOSD but were limited in their sample size and in parts contradictory

on the exact layers in which these changes occur.<sup>8–11</sup> It thereby remains unclear if ORLs, especially the ONL are also potentially affected by primary retinal astrocytopathy in AQP4-IgG seropositive NMOSD.

Representing the largest international NMOSD dataset collected so far, the CROCTINO study (*Collaborative Retrospective Study on retinal optical coherence tomography (OCT) in Neuromyelitis Optica*) overcomes one of the common weaknesses of NMOSD studies—being limited to small and homogeneous sample populations.<sup>14–15</sup> Using OCT data from over 20 centres worldwide, reliable quantitative and qualitative retinal assessment becomes possible, and controversial questions such as ORL changes in AQP4-IgG seropositive NMOSD can be clarified. Apart from patients who were AQP4-IgG seropositive, the CROCTINO cohort also includes patients with antibodies to myelin-oligodendrocyte-glycoprotein (MOG-IgG); a group that is now believed to be a distinct disease entity.<sup>14–18</sup> While clinically similar and undergoing comparable retinal neurodegeneration after ON, MOG-IgG-associated disease (MOGAD) lacks an identifiable astrocytopathy component and is thereby an appropriate diseased control group for patients who were AQP4-IgG seropositive when investigating astrocytic changes.<sup>10–19</sup>

In this study, we investigated if ORL thinning, specifically in the foveal and macular ONL, occurs in patients who were AQP4-IgG seropositive compared with healthy controls (HCs) and with patients with MOGAD as a diseased control group.

## METHODS

### Cohort design

A total of 539 patients with NMOSD were recruited between 2000 and 2018 as part of CROCTINO (stratified data of centres by device type and number of patients are summarised in the online supplemental file 1).<sup>14</sup> Patients with (1) diseases potentially confounding OCT analyses (including glaucoma, diabetic retinopathy, retinal surgery and ametropia greater than  $\pm 6$  diopters), (2) a history of ON within the last 6 months before baseline, (3) no evidence of seropositivity for AQP4-IgG or MOG-IgG<sup>20–21</sup> and (4) no macular OCT data were excluded. Cell-based assays were used for the detection of AQP4-IgG and MOG-IgG antibodies in serum samples from all patients. Clinical data (antibody serology, disease duration, frequency of ON, location of ON, date of ON, Expanded Disability Standard Scale and treatment received) were collected from all patients. We also included 75 HCs (recruited from Barcelona, Isfahan, Mangalore and Berlin), who were neither age nor sex matched to either cohort.

### Optical coherence Tomography

Retinal examinations were conducted at each centre using the following OCT devices: Spectralis SD-OCT, Heidelberg Engineering, Heidelberg, Germany (Spectralis), Cirrus HD-OCT, Carl Zeiss Meditec Inc, Dublin, California, USA (Cirrus) and Topcon 3D-OCT, Topcon Corp, Tokyo, Japan (Topcon). With respect to each device and each centre, two scans were collected: (1) a 3.4 mm diameter peripapillary ring scan around the optic nerve head for Spectralis SD-OCT (for Cirrus and Topcon devices: extracted from optic disc volume scans), and (2) a macular volume scans, centred on the fovea.<sup>14</sup> Scans were categorised and uploaded onto a central server to be accessed for further processing.

All OCT images fulfilled the OSCAR-IB criteria<sup>22–23</sup> (see figure 1—images from 29 patients not fulfilling these criteria were excluded) and results were presented in line with the

## Neuro-inflammation

**Table 1** Demographic overview

	HC	AQP4-IgG	MOG-IgG
Subjects (N)	75	197	32
Number of eyes (N)	148	317	55
Age (years, mean±SD)	32.3±9.6	41.8±12.1	36.5±13.7
Sex (male, N (%))	25 (33.8)	24 (12.2)	10 (31.2)
EDSS (median (IQR))	–	3.5 (2.0–5.0)	2.0 (1.5–2.5)
Average age at onset (years, median (IQR))	–	32.9 (24.9–42.4)	30.0 (17.6–42.5)
Patients with a history of ON (N (%))	–	142 (72.1)	24 (75.0)
Median number of ON episodes (median, IQR)	–	1.00 (0.00–3.00)	2.00 (1.00–4.00)
Disease duration (years, mean±SD)	–	7.1±6.7	4.8±7.8
Ethnicity (N (%))	White (57 (76.1)) Asian (16 (21.3)) Hispanic (1 (1.3)) Other (1 (1.3))	White (105 (53.3)) Asian (56 (28.4)) African American (11 (5.6)) Other (25 (12.7))	White (19 (59.4)) Asian (13 (40.6))
Current treatment (N (%))	–	Rituximab (51 (25.9)) Azathioprine (42 (21.3)) Mycophenolate Mofetil (31 (15.7)) Methotrexate (4 (2.0)) Other or missing (69 (35.0))	Rituximab (6 (18.8)) Azathioprine (6 (18.8)) Prednisone (6 (18.8)) Mycophenolate mofetil (5 (15.6)) Other or missing (9 (28.1))
OCT device (N (%))	Spectralis (75 (100))	Spectralis (139 (70.6)) Cirrus (38 (19.3)) Topcon (20 (10.2))	Spectralis (25 (78.1)) Cirrus (3 (9.4)) Topcon (4 (12.5))

Cirrus: Cirrus HD-OCT, Carl Zeiss Meditec Inc, Dublin, California, USA; Spectralis: SD-OCT, Heidelberg Engineering, Heidelberg, Germany; Topcon: Topcon 3D-OCT, Topcon Corp, Tokyo Japan.  
AQP4-IgG, anti-aquaporin-4 antibody; EDSS, Expanded Disability Standard Scale; HCs, healthy controls; MOG-IgG, anti-myelin-oligodendrocyte-glycoprotein antibody; N, number of subjects; ON, optic neuritis.

APOSTEL V.2.0 recommendations.<sup>24</sup> Peripapillary retinal nerve fibre layer (pRNFL) thickness was derived using a device-specific protocol and centred around the optic nerve head. Segmentation of all layers in macular volume scans were performed semiautomatically and processed with an in-house proprietary software (SAMIRIX).<sup>25</sup> For the purposes of this study, the macular retinal

layers were segmented in the following layers: macular retinal nerve fibre layer (mRNFL), ganglion cell and inner plexiform layer (GCIP), inner nuclear layer (INL), outer plexiform layer (OPL), ONL, the outer plexiform and nuclear layer (OPNL), photoreceptor layer (PR, inner photoreceptor segments to Bruch's membrane) and the total retinal thickness (RT, calculated as the thickness consisting of the RNFL (defined as layer no. 3 per Staurenghi *et al*<sup>26</sup>) to the Bruch's membrane (layer no. 14). All scans were checked and, where necessary, manual correction of the automatic segmentation was conducted using SAMIRIX by experienced raters (FCO, CB and SS for ring scans, HZ, FCO and AL for macular scans) at a single site at the Charité—Universitätsmedizin Berlin. To assure comparability with previously published data on ORL changes in NMOSD, the macular volume data were further segregated into one of three export protocols: (1) a 5 mm diameter cylinder omitting a 1 mm diameter around the fovea (5 mm study), (2) a 3 mm diameter cylinder omitting a 1 mm diameter around the fovea (3 mm study) and (3) a 1 mm mean thickness around the fovea (1 mm study). Results are reported for the 5 mm study on Spectralis devices; confirmatory results based on the 3 mm and 1 mm study as well as for Cirrus and Topcon devices are set out in the online supplemental file 1.

### Statistical methods

Data were stratified in cohorts by (1) antibody status and (2) ON history (contralateral eyes of patients with a history of unilateral ON are classified not fulfilling the ON history criteria). The data were further bifurcated by OCT device (Spectralis, Cirrus or Topcon) to mitigate any device-specific aberrations. For continuous cohort data (age, average age at onset and disease duration) on each of the AQP4-IgG, MOG-IgG and HC cohorts, the Student's t-test was employed. Cross-sectional group comparisons of the OCT values were conducted using linear mixed-effect models with age and sex as fixed and centre and patient-ID as random effects; where necessary, models were corrected for age and sex. Marginal and conditional coefficients of determination for the models were estimated by pseudo-R<sup>2</sup> for mixed-effect models. Significance was established at p<0.05. Statistical

**Table 2** Group comparison between HC and patients who were AQP4-IgG and MOG-IgG seropositive at baseline (Spectralis devices only)

	HC	AQP4-IgG	MOG-IgG	AQP4-IgG vs HC			AQP4-IgG vs MOG-IgG			MOG-IgG vs HC		
				B	SE	P	B	SE	P	B	SE	P
Number of eyes	148	317	55									
pRNFL in µm (mean±SD)	99.17±9.76	78.46±24.13	74.33±23.44	-20.22	2.86	<0.001	0.34	4.33	0.937	-29.40	2.75	<0.001
mRNFL in µm (mean±SD)	35.25±3.13	28.09±6.60	27.62±5.43	-6.12	0.69	<0.001	-0.15	1.38	0.913	-6.98	0.66	<0.001
GCIP in µm (mean±SD)	80.62±6.14	65.81±13.03	66.16±11.85	-14.74	1.45	<0.001	-2.18	2.95	0.461	-15.16	1.33	<0.001
INL in µm (mean±SD)	39.64±2.51	39.85±3.57	41.55±4.14	0.34	0.39	0.384	-1.93	0.87	0.028	1.79	0.53	0.001
OPL in µm (mean±SD)	24.58±1.64	25.02±2.03	25.10±2.00	0.28	0.24	0.241	-0.21	0.44	0.634	-0.01	0.29	0.986
ONL in µm (mean±SD)	63.59±5.78	61.63±7.04	64.71±7.87	-0.01	0.83	0.993	-1.77	1.80	0.327	0.69	0.93	0.457
OPNL in µm (mean±SD)	89.23±6.95	86.65±7.21	89.81±8.61	-0.41	0.85	0.634	-1.54	1.85	0.406	-0.14	0.93	0.878
PR in µm (mean±SD)	80.80±2.38	80.35±2.94	81.49±3.59	-0.30	0.33	0.363	-0.07	0.68	0.923	0.20	0.39	0.610
RT in µm (mean±SD)	324.47±13.24	300.76±20.11	306.6±17.99	-20.16	2.37	<0.001	-6.61	4.77	0.169	-18.91	2.49	<0.001

AQP4-IgG, anti-aquaporin-4 antibody; B, estimate; GCIP, ganglion cell and inner plexiform layer; HC, healthy control; INL, inner nuclear layer; MOG-IgG, anti-myelin-oligodendrocyte-glycoprotein antibody; mRNFL, macular retinal nerve fibre layer; ONL, outer nuclear layer; OPL, outer plexiform layer; OPNL, outer plexiform and nuclear layer; PR, photoreceptor layer; pRNFL, peripapillary retinal nerve fibre layer; RT, total retinal thickness.

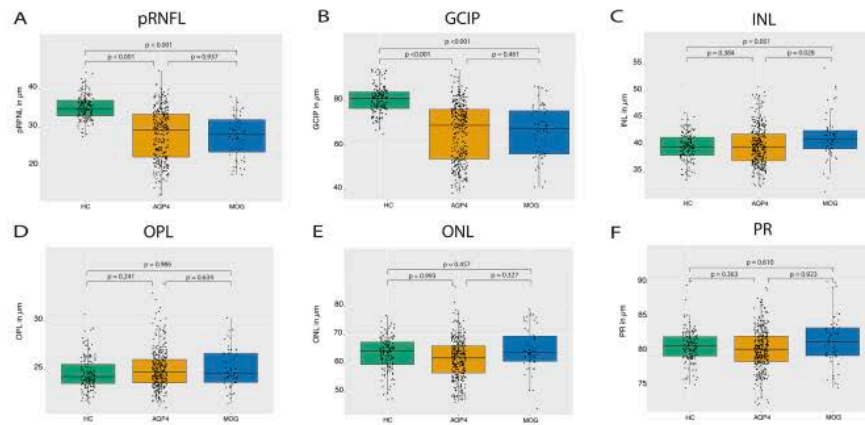


**Figure 2** Group comparison of HC and patients who were AQP4-IgG and MOG-IgG seropositive at baseline: boxplots of mean OCT values with individual eyes (jitter) in HC (left, green), patients with AQP4-IgG (middle, yellow) and patients with MOG-IgG (right, blue). (A) pRNFL; (B) GCIP; (C) INL; (D) OPL; (E) ONL; and (F) PR. AQP4, aquaporin-4; HC, healthy control; GCIP, ganglion cell and inner plexiform layer; INL, inner nuclear layer; MOG, myelin-oligodendrocyte-glycoprotein; OCT, optical coherence tomography; ONL, outer nuclear layer; OPL, outer plexiform layer; PR, photoreceptive layer; pRNFL, peripapillary retinal nerve fibre layer

analyses were conducted using R (V4.0.0) (RStudio Inc, Boston, Massachusetts, USA).<sup>27</sup>

## RESULTS

### Cohort description

In total, 197 patients who were AQP4-IgG seropositive fulfilled the inclusion criteria (figure 1, table 1). We also included 75 unmatched HCs and 32 patients who were MOG-IgG seropositive as control groups.

Neuroaxonal damage measured by pRNFL, mRNFL and GCIP was comparable in patients who were AQP4-IgG seropositive (pRNFL:  $78.46 \pm 24.13 \mu\text{m}$ , mRNFL:  $28.09 \pm 6.60 \mu\text{m}$ , GCIP:  $65.81 \pm 13.03 \mu\text{m}$ ) and MOG-IgG seropositive (pRNFL:  $74.33 \pm 23.44 \mu\text{m}$ , mRNFL:  $27.62 \pm 5.43 \mu\text{m}$ , GCIP:  $66.16 \pm 11.85 \mu\text{m}$ ) making MOGAD a highly relevant comparative disease control group for our investigation of ORLs (table 2).

### Limited outer retinal changes in AQP4-IgG seropositive NMOSD

No significant thinning of macular OPL and ONL in patients who were AQP4-IgG seropositive (irrespective of ON status) were observed compared with HC or patients who were MOG-IgG seropositive using the 5 mm diameter macular data (table 2, figure 2). No significant changes were observed when the OPL and ONL values were analysed as the combined OPNL. Previous studies described ORL thinning only in the foveal and parafoveal area as a sign of AQP4-IgG-induced Müller cell damage.<sup>8,11</sup> We therefore repeated our analyses in both 3 mm and the 1 mm diameter volumes around the fovea, but these narrower volumes showed again no relevant OPL or ONL thinning in patients who were AQP4-IgG seropositive compared with HC or patients who were MOG-IgG seropositive (see online supplemental data). Additionally, while these previous studies reported changes in the inner segment layer of the photoreceptors, this was not seen in our study.<sup>8,11</sup>

After a previous description<sup>11</sup> of ORL changes in patients who were AQP4-IgG seropositive with a history of ON, we also examined ORL differences separately in eyes with a history of ON.

AQP4-IgG seropositive eyes with a history of ON (AQP4-ON) did not display any thinning of ONL and OPL compared with patients without a history of ON (AQP4-NON) or HC, despite severe neuroaxonal loss measured by pRNFL and GCIP layer (table 3, figure 3). Comparing patients who were AQP4-IgG and MOG-IgG seropositive, both groups had a comparable neuroaxonal loss (pRNFL, GCIP)—in the whole group as well as in respect of ON and non-ON eyes (table 2, figure 2). AQP4-ON ( $B = -1.54$ ,  $SE = 0.69 \mu\text{m}$ ,  $p = 0.027$ ) as well as MOG-ON ( $B = -2.51$ ,  $SE = 0.87 \mu\text{m}$ ,  $p = 0.004$ ) showed an OPL thinning in the fovea (1 mm diameter) compared with HC, but no difference was observed between AQP4-ON and MOG-ON ( $p = 0.100$ ). Also, no significant correlation between ethnicity and current therapies on outer retinal thickness was found (data not shown).

## DISCUSSION

Our study suggests that neither macular OPL nor ONL loss occurs in AQP4-IgG seropositive NMOSD, regardless of ON phenotype, as compared with HC and patients who were MOG-IgG seropositive. The MOG-IgG cohort presented a unique opportunity to contrast our AQP4-IgG seropositive cohort with a highly relevant comparator group, which most likely has no astrocytopathy-component.<sup>28</sup>

Our results differ from those published by You *et al* in 2019<sup>8</sup> and Filippatou *et al* in 2020.<sup>11</sup> In both studies, thinning was observed in the ONL and the inner segment of the photoreceptor layers. In the case of You *et al*, who utilised Spectralis SD-OCT devices for the image acquisition, foveal thinning was observed along with a reduction in b-wave amplitudes in full-field electroretinography (ERG) suggestive of Müller cell dysfunction.<sup>8</sup> Filippatou *et al*, who employed Cirrus-SD-OCT for the image acquisition, also described thinning of the fovea in the 5 mm diameter macular area around the fovea.<sup>11</sup> Both studies suggested the ORL changes to be caused by a primary retinal astrocytopathy with AQP4-IgG associated glial dysfunction in Müller cells.<sup>29</sup> These pathological responses could account for the associated thinning observed in the ONL in these studies. However, other exogenous factors

**Table 3** OCT results in patients who were AQP4-IgG seropositive stratified by history of on (Spectralis devices only)

Number of eyes	AQP4-ON			AQP4-NON			MOG-ON			MOG-NON			AQP4-ON vs AQP4-NON			AQP4-ON vs HC			AQP4-ON vs MOG-ON			AQP4-ON vs MOG-NON		
	B	SE	P	B	SE	P	B	SE	P	B	SE	P	B	SE	P	B	SE	P	B	SE	P	B	SE	P
pRNFL in $\mu\text{m}$ (mean $\pm$ SD)	72.84 $\pm$ 24.47	72.84 $\pm$ 24.47	96.09 $\pm$ 12.99	68.03 $\pm$ 22.95	95.33 $\pm$ 7.32	<0.001	-25.18	3.93	<0.001	-29.56	3.57	<0.001	-9.29	5.15	0.07	2.63	6.12	0.667	6.03	5.44	0.75	6.03	5.44	0.75
GCIPL in $\mu\text{m}$ (mean $\pm$ SD)	62.94 $\pm$ 12.73	62.94 $\pm$ 12.73	77.11 $\pm$ 7.56	63.45 $\pm$ 11.96	75.88 $\pm$ 6.01	<0.001	-14.74	2.06	<0.001	-19.60	1.49	<0.001	-0.50	1.48	0.735	-4.00	3.20	0.215	3.22	3.36	0.344	3.22	3.36	0.344
OPL in $\mu\text{m}$ (mean $\pm$ SD)	25.06 $\pm$ 2.01	25.06 $\pm$ 2.01	24.71 $\pm$ 1.79	25.28 $\pm$ 2.08	24.45 $\pm$ 1.55	0.26	0.38	0.498	0.34	0.26	0.184	0.09	0.38	0.804	0.34	0.51	0.509	-0.12	0.56	0.899	-0.12	0.56	0.899	0.446
ONL in $\mu\text{m}$ (mean $\pm$ SD)	62.53 $\pm$ 7.45	62.53 $\pm$ 7.45	63.14 $\pm$ 6.62	66.09 $\pm$ 8.08	59.76 $\pm$ 4.58	-0.19	1.49	0.901	-0.18	0.92	0.847	-0.82	1.40	0.560	-2.84	2.12	0.183	2.76	3.58	0.446	2.76	3.58	0.446	0.446
OPL in $\mu\text{m}$ (mean $\pm$ SD)	87.58 $\pm$ 7.67	87.58 $\pm$ 7.67	87.85 $\pm$ 6.78	84.21 $\pm$ 5.68	91.37 $\pm$ 8.69	0.00	1.53	0.879	0.27	0.95	0.775	0.37	1.42	0.794	-2.51	2.21	0.259	2.67	3.51	0.50	2.67	3.51	0.50	
PR in $\mu\text{m}$ (mean $\pm$ SD)	80.89 $\pm$ 2.93	80.89 $\pm$ 2.93	79.80 $\pm$ 2.94	82.01 $\pm$ 3.45	79.62 $\pm$ 3.58	0.75	0.57	0.187	-0.19	0.36	0.595	-1.08	0.59	0.071	-0.58	0.77	0.454	1.36	1.44	0.348	1.36	1.44	0.348	

AQP4, aquaporin-4; B, best-fit; GCIPL, ganglion cell and inner plexiform layer; HC, healthy control; MOG, myelin-oligodendrocyte-glycoprotein; NON, non-optic neuritis; ONL, outer nuclear layer; OPL, outer plexiform layer; ONL, outer nuclear layer; PR, photoreceptor layer; pRNFL, peripapillary retinal nerve fibre layer.

cannot be ruled out as contributory, such as cohort composition and study methodologies.

On a cohort level, our population is larger (197 patients who were AQP4-IgG seropositive vs 22 and 51 by You *et al* and Filippatou *et al*, respectively)<sup>8,11</sup> and more diverse than prior studies, which minimises potential type I errors. While You *et al* did not specify the ethnic composition of their cohort, the cohort in Filippatou *et al* had a relatively even distribution between Caucasian Americans (43%) and African Americans (53%) with a minor subset of Asian Americans (4%)—describing a pronounced ONL thinning in African Americans. African American patients with multiple sclerosis (MS) are also known to suffer from faster and often more aggressive disease course in general, which could also be true for other neuroinflammatory diseases like NMOSD.<sup>30,31</sup> Our AQP4-IgG seropositive cohort included an ethnically diverse dataset acquired worldwide with a lower African American patient composition (5.6%), which might have contributed to the less profound foveal ONL changes.<sup>11,32</sup>

Recently, it has been hypothesised that the neuroplastic characteristics of the INL may act as a barrier to retrograde (but not anterograde) trans-synaptic axonal degeneration—rectified to the ORLs—in patients with MS following ON.<sup>33</sup> This limited neuroplastic ability is hypothesised to rest with the bipolar, amacrine and horizontal cells, which feed into the synaptic tree at the level of the INL, and raises questions as to whether such protective mechanisms may also play a limited part in NMOSD and whether it remains so as we age.<sup>33</sup> The average age of participants in the two other studies were relatively older (mean age for both being 47 years), whereas for our AQP4-IgG cohort it was 42 years. Previously reported studies concerning cohorts of similar demographic distribution to ours reported no significant correlation between age and retinal thickness.<sup>34,35</sup> However, age-related changes in the retina cannot be ruled out and ORLs may be more susceptible to change with increasing age and/or disease duration. It is well-known that the plasticity of the CNS markedly reduces over time, and as a corollary, the regenerative properties of the INL may also be affected thereby diminishing its protective effects in reducing retrograde (trans-synaptic) axonal degeneration.<sup>36</sup> The retina is also a vascularised organ, particularly at the interface between inner and outer retina, where the deep vascular plexus intercepts the boundary between the INL and OPL.<sup>37</sup> Should the blood-retina barrier be compromised in the boundary between the INL and OPL, it is conceivable that the protective abilities of the INL may be circumvented and thereby mediating glial dysfunction in the Müller cells. This may have been what was observed in the OPL from the 1 mm AQP4-ON and MOG-ON cohort given the relative location of the OPL to the INL. To that end, while disease duration did not reveal to any correlates with OPL (p=0.805) or ONL (p=0.835) values, we cannot exclude time-dependent effects in a cross-sectional analysis. We believe that this area warrants more research to quantify if (1) age is a factor, (2) ON damages the barrier function and (3) the INL does indeed play a role as a dam to retrograde axonal degeneration in NMOSD.

A strength of our study rests on its cohort size and composition, which mirrors that of a global population. This result derives from a consortium of expert NMOSD researchers enabling the enrolment of participants through a multicentre strategy. This approach was designed to overcome many of the earlier NMOSD study limitations, for example small and homogeneous sample populations. Additionally, the use of differing OCT devices compounds complexities in OCT comparisons and a high degree of caution is needed in order to rely on differing platforms interchangeably.<sup>38</sup> Thus, our study focuses on use of

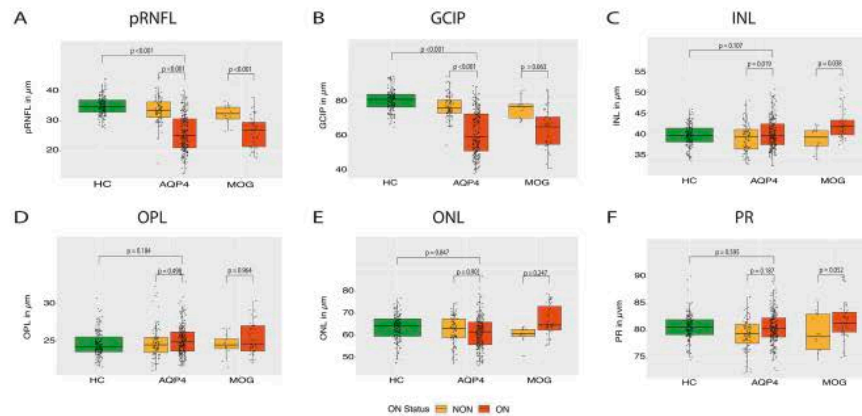


**Figure 3** OCT results stratified by ON status (tested with Spectralis devices): boxplots of mean OCT values with individual eyes (jitter) in HC (left, green), AQP4-IgG cohort (middle) and MOG-IgG cohort (right). Seropositive patients with a history of ON are highlighted with light yellow and seropositive patients without a history of ON are highlighted in orange. (A) pRNFL; (B) GCIP; (C) INL; (D) OPL; (E) ONL; and (F) PR. AQP4, aquaporin-4; GCIP, ganglion cell and inner plexiform layer; INL, inner nuclear layer; MOG, myelin-oligodendrocyte-glycoprotein; OCT, optical coherence tomography; ONL, outer nuclear layer; OPL, outer plexiform layer; PR, photoreceptive layer; pRNFL, peripapillary retinal nerve fibre layer.

three widely available OCT devices, and obtained confirmatory results with each of them; of these, two were also employed respectively in the studies by You *et al*<sup>8</sup> and Filipatou *et al*.<sup>11</sup>

Limitations of the current study should also be considered. First, the HCs and patients with MOGAD were not matched, which makes it difficult to rule out age-related and gender-related affects. Notably, retinal thickness decreases with age and males generally exhibit higher GCIP and RT.<sup>25</sup> Also, no ERG or functional visual pathway assessments were conducted, which could have potentially shown more subtle functional impairment of ORLs without associated tissue loss. Outer retinal studies are additionally complicated by Henle Fibre morphologies as OCT beam placement plays a major role in how this layer is depicted; the high level of irregularity and variability in these morphologies add a level of subjectiveness in the quantification and correction of outer layer segmentation and analyses.<sup>39</sup> Finally, Cirrus and Topcon measurements could not be utilised as confirmatory cohorts as there lacked sufficient HCs examined with these devices. Nonetheless, the current findings provide insights into relationships between retinal layer changes and axonal damage that have not previously been recognised; as no ORL changes can be observed on account of a primary astrocytopathy in NMO, it potentially alleviates the burden of monitoring the ORLs when tracking disease progression and reinforces the need to focus primarily on the inner layers, particularly the RNFL and the GCIP layer.

**CONCLUSION**

Our results show no evidence of macular ORL changes as a major component of retinal damage in patients who were seropositive AQP4-IgG NMO and patients with MOGAD. Further studies will be necessary to clarify (1) if OPL and ONL are damaged in late disease stages due to retrograde trans-synaptic axonal degeneration across the damaged INL barrier and (2) if outer retinal dysfunction without a measurable structural correlate occurs. Longitudinal studies could help quantify changes in the ORLs alongside disease progression.

**Author affiliations**

- <sup>1</sup>Experimental and Clinical Research Center, Max Delbrück Center for Molecular Medicine and Charité – Universitätsmedizin Berlin, corporate member of Freie Universität Berlin and Humboldt-Universität zu Berlin, Berlin, Germany
- <sup>2</sup>NeuroCure Clinical Research Center, Charité – Universitätsmedizin Berlin, corporate member of Freie Universität Berlin and Humboldt-Universität zu Berlin, Berlin, Germany
- <sup>3</sup>CIEM MS Research Center, University of Minas Gerais State, Medical School, Belo Horizonte, Brazil
- <sup>4</sup>Kashani MS Center, Isfahan University of Medical Sciences, Isfahan, Iran (the Islamic Republic of)
- <sup>5</sup>School of Advanced Technologies in Medicine, Medical Image and Signal Processing Research Center, Isfahan University of Medical Sciences, Isfahan, Iran (the Islamic Republic of)
- <sup>6</sup>Isfahan Eye Research Center, Department of Ophthalmology, Isfahan University of Medical Sciences, Isfahan, Iran (the Islamic Republic of)
- <sup>7</sup>Center for Advanced Neurological Research, Nitte University, Mangalore, Karnataka, India
- <sup>8</sup>Department of Neurology, National Cancer Center Korea, Goyang-si, Korea (the Republic of)
- <sup>9</sup>Department of Ophthalmology, Research Institute and Hospital of National Cancer Center, Goyang, Korea (the Republic of)
- <sup>10</sup>Experimental Neurophysiology Unit, Institute of Experimental Neurology (INSPE) Scientific Institute, Hospital San Raffaele and University Vita-Salute San Raffaele, Milano, Italy
- <sup>11</sup>Division of Neurology, Department of Medicine, Siriraj Hospital and Bumrungrad International Hospital, Bangkok, Thailand
- <sup>12</sup>Swedish Neuroscience Institute Neuro-Ophthalmology, Seattle, Washington, USA
- <sup>13</sup>Department of Neurology, Neurology Service, University Hospital of Strasbourg, Strasbourg, France
- <sup>14</sup>Department of Neurology, Oxford University Hospitals NHS Trust, Oxford, UK
- <sup>15</sup>Department of Ophthalmology, Oxford University Hospitals NHS Trust, Oxford, UK
- <sup>16</sup>Neuro-Ophthalmology Division, Department of Ophthalmology, Rabin Medical Center, Petah Tikva, Israel
- <sup>17</sup>Sackler School of Medicine, Tel Aviv University, Tel Aviv, Israel
- <sup>18</sup>Department of Neurology Slagelse, Institutes of Regional Health Research and Molecular Medicine, University of Southern Denmark, Odense, Syddanmark, Denmark
- <sup>19</sup>Institute of Regional Health Research, University of Southern Denmark, Odense, Denmark
- <sup>20</sup>Hospital Clinic of Barcelona-Institut d'Investigacions Biomèdiques August Pi Sunyer, University of Barcelona, Barcelona, Spain
- <sup>21</sup>Institute of Clinical Neuroimmunology, LMU Hospital, Ludwig-Maximilians-Universität München, Munich, Germany
- <sup>22</sup>Department of Neurology, University of Michigan Medical School, Ann Arbor, Michigan, USA

## Neuro-inflammation

- <sup>23</sup>NYU Multiple Sclerosis Comprehensive Care Center, Department of Neurology, NYU, New York, New York, USA
- <sup>24</sup>Neurology, Multiple Sclerosis, Myelin Disorders and Neuroinflammation, Hospital for Neurology Pierre Wertheimer, Lyon, France
- <sup>25</sup>Centre d'Esclerosi Múltiple de Catalunya (Cemcat). Department of Neurology/Neuroimmunology, Universitat Autònoma de Barcelona, Barcelona, Spain
- <sup>26</sup>Department of Neurology, Koc University Research Center for Translational Medicine (KUTTAM), Koc University School of Medicine, Istanbul, Turkey
- <sup>27</sup>Cerrahpaşa Faculty of Medicine, Department of Neurology, Istanbul University-Cerrahpaşa, Istanbul, Turkey
- <sup>28</sup>Department of Ophthalmology, Cerrahpaşa Medical Faculty, Istanbul Universitesi, Fatih, Turkey
- <sup>29</sup>Department of Neurology, Medical Faculty, Heinrich-Heine-Universität Düsseldorf, Düsseldorf, Nordrhein-Westfalen, Germany
- <sup>30</sup>Department of Neurology, Center for Neurology and Neuropsychiatry, LVR-Klinikum, Heinrich-Heine-Universität Düsseldorf, Düsseldorf, Germany
- <sup>31</sup>Department of Ophthalmology and Visual Sciences, Escola Paulista de Medicina, Universidade Federal de São Paulo, São Paulo, Brazil
- <sup>32</sup>Department of Neurology and Neurosurgery, Escola Paulista de Medicina, Universidade Federal de São Paulo, Sao Paulo, Brazil
- <sup>33</sup>The Walton Centre NHS Foundation Trust, Liverpool, UK
- <sup>34</sup>Department of Neurology, Hospital Clínico de Maracaibo, Maracaibo, Venezuela, Bolivarian Republic of
- <sup>35</sup>Moorfield's Eye Hospital, The National Hospital for Neurology and Neurosurgery, Queen Square Institute of Neurology, University College London, London, UK
- <sup>36</sup>Department of Neurology, University of California San Francisco, San Francisco, California, USA
- <sup>37</sup>Department of Medicine, Harbor-University of California at Los Angeles (UCLA) Medical Center, and Lundquist Institute for Biomedical Innovation, Torrance, California, USA
- <sup>38</sup>Department of Medicine, David Geffen School of Medicine, UCLA, Los Angeles, California, USA
- <sup>39</sup>Departments of Ophthalmology and Visual Sciences, Kellogg Eye Center, Ann Arbor, Michigan, USA
- <sup>40</sup>Department of Metabolism, Endocrine and Diabetes, Department of Internal Medicine, University of Michigan Medical School, Ann Arbor, Michigan, USA
- <sup>41</sup>Department of Pediatrics, University of Utah Health, Salt Lake City, Utah, USA
- <sup>42</sup>Department of Neurology, Charité – Universitätsmedizin Berlin, corporate member of Freie Universität Berlin and Humboldt-Universität zu Berlin, Berlin, Germany
- <sup>43</sup>Department of Neurology, University of California Irvine, Irvine, California, USA

**Twitter** Elena H Martinez-Lapiscina @elenahlapiscina@ and Joachim Havla @NeuroVisionLab

**Contributors** The study was conceived and designed by AL, HZ, FCO, AB and FP. AL, HZ, FCO, CB, SM and SvS collected and analysed data for the study. HZ, FCO, AB and FP contributed to the scientific design and conduct of the study. AL and FCO performed biostatistical analyses to the study, were responsible for literature research and wrote the manuscript. AP, AJG, MRY, LC and TJS contributed to the conception and design of the study. All other authors contributed to the acquisition and analysis of data. All authors approved the final version of the manuscript.

**Funding** The authors acknowledge support from the Guthy Jackson Charitable Foundation (GJCF) and the German Research Foundation (DFG) pertaining to the CROCTINO project.

**Competing interests** HZ reports grants from Novartis and speaking honoraria from Bayer Healthcare, unrelated to this study. EHM-L received funding from the Instituto de Salud Carlos III (Spain) and Fondo Europeo de Desarrollo Regional (FEDER-JR16/00006), Grant for MS Innovation, Fundació Privada Cellex and Marató TV3 Charitable Foundation and is a researcher in the OCTIMS study, an observational study (that involves no specific drugs) to validate SD-OCT as a biomarker for MS, sponsored by Novartis and has received honoraria and travel support for international and national meetings over the last 3 years from from Biogen, Novartis, Roche, Genzyme. She is a member of the working committee of International Multiple Sclerosis Visual System (IMSVISUAL) Consortium. MAL-P has received funding for travel and speaker honoraria from Novartis, Sanofi-Genzyme and Roche. MAF has nothing to disclose. *Jacqueline Palace has received support for scientific meetings and honorariums for advisory work from Merck Serono, Novartis, Chugai, Alexion, Roche, MedImmune, Argenx, UCB, Mitsubishi, Ampro, Janssen. Grants from Alexion, Ampro biotechnology. Shares in AstraZenica. Acknowledges Partial funding by Highly specialised services NHS England.* MIL reported being involved in aquaporin 4 testing, receiving salary from the National Health Service National Highly Specialised Commissioning Group for Neuromyelitis Optica, UK, being supported by the National Institute for Health Research Oxford Biomedical Research Centre, UK, and receiving speaking honoraria and travel grants from Biogen Idec, and travel grant from Novartis. SMS has nothing to disclose. AR-F is sponsored by Abide Therapeutic outside of the submitted work and reports no potential conflicts of interest. SSiritho received funding for travel

and speaker honoraria from Merck Serono, Pacific Healthcare (Thailand), Menarini (Thailand), Biogen Idec, UCB (Thailand), and Novartis. AA reports personal fees from received honoraria for giving educational presentations on multiple sclerosis and neuroimmunology at several national congresses or symposia from Teva Turkey, Merck-Serono, Biogen Idec-Gen Pharma of Turkey, Roche, Novartis, Bayer, Sanofi-Genzyme. She has received travel and registration coverage for attending several national and international congresses or symposia from Merck-Serono, Biogen Idec-Gen Pharma of Turkey, Roche, Sanofi-Genzyme and Bayer. AJ has received compensation for advisory board, consulting, meeting attendance and speaking from Biogen, Terumo-BCT, Genentech, Shire and Chugai Pharmaceuticals. SH has received funding from the NMO Spectrum-UK charity and was previously funded by an MGA/Watney/NIHR Oxford Biomedical research grant. RM serves on scientific advisory board for MedImmune and has received funding for travel and honoraria from Biogen, Merck Serono, Novartis, Sanofi-Genzyme, Roche and Teva. EN has nothing to disclose. ACC received funding from the Instituto de Salud Carlos III (Spain) JR19/00007 unrelated to this manuscript. DB has received speaking/consulting honoraria from Bayer Health Care, Biogen Idec, Merck, Sanofi-Genzyme, TEVA and Roche and had travel expenses to scientific meetings sponsored by Bayer Health Care, Merck Serono, TEVA and Roche. JH reports grants for OCT research from the Friedrich-Baur-Stiftung and Merck, personal fees and non-financial support from Celgene, Merck, Alexion, Novartis, Roche, Santhera, Biogen, Heidelberg Engineering, Sanofi Genzyme and non-financial support of the Guthy-Jackson Charitable Foundation, all outside the submitted work. JH is partially funded by the German Federal Ministry of Education and Research (DIFUTURE), Grant Numbers 01ZZ1603[A-D] and 01ZZ1804[A-H]. LL received honoraria for consulting services from Merck, Roche, Biogen and for speaking activities from Teva; research support from Merck, Biogen, Novartis; travel support from Merck, Roche, Biogen, Almiral. MP has nothing to disclose. OA has received honoraria for speaking/consultation and travel grants from Bayer Healthcare, Biogen Idec, Chugai, Novartis, MedImmune, Merck Serono, and Teva and research grants from Bayer Healthcare, Biogen Idec, Novartis, and Teva. MR received speaker honoraria from Novartis, Bayer, Roche, Alexion and Ipsen and travel reimbursement from Bayer, Biogen, Merz, Genzyme, Teva, Roche and Merck, none related to this study. PA reports grants, personal fees and non-financial support from Allergan, Biogen, Ipsen, Merz Pharmaceuticals, Novartis, and Roche, personal fees and non-financial support from Bayer Healthcare, and Merck, and non-financial support from Sanofi-Aventis/Genzyme. HJK reports speaking and/or consulting: Bayer Schering Pharma, Biogen, Celltrion, Eisai, HanAll BioPharma, MedImmune, Merck Serono, Novartis, Sanofi Genzyme, Teva-Handok, and UCB; research support: Ministry of Science & ICT, Sanofi Genzyme, Teva-Handok, and UCB; steering committee member: MedImmune; co-editor/associated editor: MS Journal-Experimental, Translational and Clinical; and Journal of Clinical Neurology. J-WH has received a grant from the National Research Foundation of Korea. YM-D has served as a consultant and/or received grant support from: Acorda, Bayer Pharmaceutical, Biogen Idec, Celgene, EMD Serono, Genzyme, Novartis, Questor, Chugai, and Teva Neuroscience and is currently supported by grants from NIH NIAID Autoimmune Center of Excellence: UM1-AI110557; NIH NINDS R01-NS080821. HSK has nothing to disclose. IK served on scientific advisory board for Biogen Idec and Genentech and received research support from Guthy-Jackson Charitable Foundation, National Multiple Sclerosis Society, Biogen-Idec, Serono, Genzyme and Novartis. ZR has nothing to disclose. AR has nothing to disclose. MRY is founder and a shareholder of NovaDigm Therapeutics, Inc; he receives funding from the United States National Institutes of Health and United States Department of Defense; he holds US and international patents on immunotherapeutic and anti-infective technologies, is a member of the Genentech-Roche Scientific Advisory Committee and adviser to The Guthy-Jackson Charitable Foundation. TJS was issued US patents covering the therapeutic targeting of IGF-I receptor in autoimmune diseases. He is a paid consultant for Horizon Thera and Immunovant and is a scientific advisor to the Guthy-Jackson Charitable Foundation. He receives research funding from the National Institutes of Health. AP is supported by the National Institute for Health Research (NIHR) Biomedical Research Centre based at Moorfields Eye Hospital National Health Service (NHS) Foundation Trust and University College London Institute of Ophthalmology. AB is cofounder and shareholder of Motognosis and Nocturne. He is named as inventor on several patent applications regarding MS serum biomarkers, OCT image analysis and perceptual visual computing. FP reports research grants and speaker honoraria from Bayer, Teva, Genzyme, Merck, Novartis, MedImmune and is member of the steering committee of the OCTIMS study (Novartis), all unrelated to this work. FCO was employee of Nocturne GmbH and receives research support by the American Academy of Neurology and National Multiple Sclerosis Society (US), unrelated to this work as well as funding by the German Association of Neurology (Deutsche Gesellschaft für Neurologie) in context of this project. CC has received a speaking honorarium from Bayer and research funding from Novartis unrelated to this publication. All other authors have nothing to disclose.

**Patient consent for publication** Consent obtained directly from patient(s).

**Ethics approval** Written informed consent was obtained from all patients prior to the commencement of the study and institutional review board approvals for retrospective data use were obtained or waived from each centre in accordance with

the Declaration of Helsinki (1964) in its currently applicable version at their own discretion and in accordance with relevant local laws. The study also conformed to all relevant best practice guidelines and ethical standards of each centre.

**Provenance and peer review** Not commissioned; externally peer reviewed.

**Data availability statement** Data are available upon reasonable request.

**Supplemental material** This content has been supplied by the author(s). It has not been vetted by BMJ Publishing Group Limited (BMJ) and may not have been peer-reviewed. Any opinions or recommendations discussed are solely those of the author(s) and are not endorsed by BMJ. BMJ disclaims all liability and responsibility arising from any reliance placed on the content. Where the content includes any translated material, BMJ does not warrant the accuracy and reliability of the translations (including but not limited to local regulations, clinical guidelines, terminology, drug names and drug dosages), and is not responsible for any error and/or omissions arising from translation and adaptation or otherwise.

**Open access** This is an open access article distributed in accordance with the Creative Commons Attribution Non Commercial (CC BY-NC 4.0) license, which permits others to distribute, remix, adapt, build upon this work non-commercially, and license their derivative works on different terms, provided the original work is properly cited, appropriate credit is given, any changes made indicated, and the use is non-commercial. See: <http://creativecommons.org/licenses/by-nc/4.0/>.

#### ORCID iDs

Angelo Lu <http://orcid.org/0000-0002-7897-6498>  
 Claudia Chien <http://orcid.org/0000-0001-8280-9513>  
 Ho Jin Kim <http://orcid.org/0000-0002-8672-8419>  
 Adriana Roca-Fernández <http://orcid.org/0000-0002-8720-9397>  
 Hadas Stiebel-Kalish <http://orcid.org/0000-0001-7715-6706>  
 Elena H Martinez-Lapiscina <http://orcid.org/0000-0003-4272-0826>  
 Joachim Havla <http://orcid.org/0000-0002-4386-1340>  
 Marius Ringelstein <http://orcid.org/0000-0003-3618-8407>  
 Philipp Albrecht <http://orcid.org/0000-0001-7987-658X>  
 Denis Bernardi Bichueti <http://orcid.org/0000-0002-4011-3734>  
 Axel Petzold <http://orcid.org/0000-0002-0344-9749>  
 Frederike Cosima Oertel <http://orcid.org/0000-0003-4906-5983>

#### REFERENCES

- Jarius S, Paul F, Weinschenker BG, et al. Neuromyelitis optica. *Nat Rev Dis Primers* 2020;6:85.
- Wingerchuk DM, Lennon VA, Lucchinetti CF, et al. The spectrum of neuromyelitis optica. *Lancet Neurol* 2007;6:805–15.
- Oertel FC, Kuchling J, Zimmermann H, et al. Microstructural visual system changes in AQP4-antibody-seropositive NMOSD. *Neurol Neuroimmunol Neuroinflamm* 2017;4:e334.
- Uzawa A, Mori M, Kuwabara S. Neuromyelitis optica: concept, immunology and treatment. *J Clin Neurosci* 2014;21:12–21.
- Papadopoulos MC, Verkman AS. Aquaporin 4 and neuromyelitis optica. *Lancet Neurol* 2012;11:535–44.
- Nagelhus EA, Ottersen OP. Physiological roles of aquaporin-4 in brain. *Physiol Rev* 2013;93:1543–62.
- Bringmann A, Pannicke T, Grosche J, et al. Müller cells in the healthy and diseased retina. *Prog Retin Eye Res* 2006;25:397–424.
- You Y, Zhu L, Zhang T, et al. Evidence of Müller glial dysfunction in patients with aquaporin-4 immunoglobulin G-Positive neuromyelitis optica spectrum disorder. *Ophthalmology* 2019;126:801–10.
- Jeong IH, Kim HJ, Kim N-H, et al. Subclinical primary retinal pathology in neuromyelitis optica spectrum disorder. *J Neurol* 2016;263:1343–8.
- Oertel FC, Outteryck O, Knier B, et al. Optical coherence tomography in myelin-oligodendrocyte-glycoprotein antibody-seropositive patients: a longitudinal study. *J Neuroinflammation* 2019;16:154.
- Filippatou AG, Vasileiou ES, He Y, et al. Evidence of subclinical quantitative retinal layer abnormalities in AQP4-IgG seropositive NMOSD. *Mult Scler* 2021;27:1738–48.
- Oertel FC, Havla J, Roca-Fernández A, et al. Retinal ganglion cell loss in neuromyelitis optica: a longitudinal study. *J Neurol Neurosurg Psychiatry* 2018;89:1259–65.
- Motamedi S, Oertel FC, Yadav SK, et al. Altered fovea in AQP4-IgG-seropositive neuromyelitis optica spectrum disorders. *Neurol Neuroimmunol Neuroinflamm* 2020;7. doi:10.1212/NXI.0000000000000805. [Epub ahead of print: 23 Jun 2020].
- Specovius S, Zimmermann HG, Oertel FC, et al. Cohort profile: a collaborative multicentre study of retinal optical coherence tomography in 539 patients with neuromyelitis optica spectrum disorders (CROCTINO). *BMJ Open* 2020;10:e035397.
- Oertel FC, Specovius S, Zimmermann HG, et al. Retinal optical coherence tomography in neuromyelitis optica. *Neurol Neuroimmunol Neuroinflamm* 2021;8. doi:10.1212/NXI.000000000001068. [Epub ahead of print: 15 Sep 2021].
- Bruijstens AL, Wong YJM, van Pelt DE, et al. Hla association in MOG-IgG- and AQP4-IgG-related disorders of the CNS in the Dutch population. *Neurol Neuroimmunol Neuroinflamm* 2020;7. doi:10.1212/NXI.000000000000702. [Epub ahead of print: 20 Mar 2020].
- Kim H, Lee E-J, Kim S, et al. Serum biomarkers in myelin oligodendrocyte glycoprotein antibody-associated disease. *Neurol Neuroimmunol Neuroinflamm* 2020;7. doi:10.1212/NXI.000000000000708. [Epub ahead of print: 17 Mar 2020].
- Narayan R, Simpson A, Fritsche K, et al. Mog antibody disease: a review of MOG antibody seropositive neuromyelitis optica spectrum disorder. *Mult Scler Relat Disord* 2018;25:66–72.
- Havla J, Kämpfel T, Schinner R, et al. Myelin-oligodendrocyte-glycoprotein (MOG) autoantibodies as potential markers of severe optic neuritis and subclinical retinal axonal degeneration. *J Neurol* 2017;264:139–51.
- Reindl M, Schanda K, Woodhall M, et al. International multicenter examination of MOG antibody assays. *Neurol Neuroimmunol Neuroinflamm* 2020;7:e674.
- Waters P, Reindl M, Saiz A, et al. Multicentre comparison of a diagnostic assay: aquaporin-4 antibodies in neuromyelitis optica. *J Neurol Neurosurg Psychiatry* 2016;87:1005–15.
- Tewarie P, Balk L, Costello F, et al. The OSCAR-IB consensus criteria for retinal OCT quality assessment. *PLoS One* 2012;7:e34823.
- Schippeling S, Balk LJ, Costello F, et al. Quality control for retinal OCT in multiple sclerosis: validation of the OSCAR-IB criteria. *Mult Scler* 2015;21:163–70.
- Aytulun A, Cruz-Herranz A, Aktas O, et al. Apostel 2.0 recommendations for reporting quantitative optical coherence tomography studies. *Neurology* 2021;97:68–79.
- Motamedi S, Gawlik K, Ayadi N, et al. Normative data and minimally detectable change for inner retinal layer thicknesses using a semi-automated OCT image segmentation pipeline. *Front Neurol* 2019;10:1117.
- Staufering G, Sadda S, Chakravarthy U, et al. Proposed lexicon for anatomic landmarks in normal posterior segment spectral-domain optical coherence tomography: the IN-OCT consensus. *Ophthalmology* 2014;121:1572–8.
- R Core Team. *R: a language and environment for statistical computing*. Vienna, Austria: R Foundation for Statistical Computing, 2017. <https://www.R-project.org/>
- Höftberger R, Guo Y, Flanagan EP, et al. The pathology of central nervous system inflammatory demyelinating disease accompanying myelin oligodendrocyte glycoprotein autoantibody. *Acta Neuropathol* 2020;139:875–92.
- Goodyear MJ, Crewther SG, Junghans BM. A role for aquaporin-4 in fluid regulation in the inner retina. *Vis Neurosci* 2009;26:159–65.
- Caldito NG, Saidha S, Sotirchos ES, et al. Brain and retinal atrophy in African-Americans versus Caucasian-Americans with multiple sclerosis: a longitudinal study. *Brain* 2018;141:3115–29.
- Mealy MA, Kessler RA, Rimler Z, et al. Mortality in neuromyelitis optica is strongly associated with African ancestry. *Neurol Neuroimmunol Neuroinflamm* 2018;5:e468.
- Liu J, Mori M, Zimmermann H, et al. Anti-Mog antibody-associated disorders: differences in clinical profiles and prognosis in Japan and Germany. *J Neurol Neurosurg Psychiatry* 2021;92:377–83.
- Panneman EL, Coric D, Tran LMD, et al. Progression of anterograde trans-synaptic degeneration in the human retina is modulated by axonal convergence and divergence. *Neuroophthalmology* 2019;43:382–90.
- Tian G, Li Z, Zhao G, et al. Evaluation of retinal nerve fiber layer and ganglion cell complex in patients with optic neuritis or neuromyelitis optica spectrum disorders using optical coherence tomography in a Chinese cohort. *J Ophthalmol* 2015;2015:1–6.
- Martinez-Lapiscina EH, Sepulveda M, Torres-Torres R, et al. Usefulness of optical coherence tomography to distinguish optic neuritis associated with AQP4 or MOG in neuromyelitis optica spectrum disorders. *Ther Adv Neurol Disord* 2016;9:436–40.
- Balk LJ, Coric D, Knier B, et al. Retinal inner nuclear layer volume reflects inflammatory disease activity in multiple sclerosis: a longitudinal OCT study. *Mult Scler J Exp Transl Clin* 2019;5:205521731987158.
- Campbell JP, Zhang M, Hwang TS, et al. Detailed vascular anatomy of the human retina by Projection-Resolved optical coherence tomography angiography. *Sci Rep* 2017;7:42201.
- Bhargava P, Lang A, Al-Louzi O, et al. Applying an open-source segmentation algorithm to different OCT devices in multiple sclerosis patients and healthy controls: implications for clinical trials. *Mult Scler Int* 2015;20:15:1–10.
- Gonzalez Caldito N, Antony B, He Y, et al. Analysis of agreement of Retinal-Layer thickness measures derived from the segmentation of horizontal and vertical spectralis OCT macular scans. *Curr Eye Res* 2018;43:415–23.